Lijie Grace Zhang · David L. Kaplan
Editors

Neural Engineering

From Advanced Biomaterials to 3D Fabrication Techniques

Springer

Neural Engineering

Lijie Grace Zhang • David L. Kaplan
Editors

Neural Engineering

From Advanced Biomaterials to 3D Fabrication Techniques

Springer

Editors
Lijie Grace Zhang
Department of Mechanical and Aerospace
The George Washington University
Washington, DC, USA

Department of Biomedical Engineering
The George Washington University
Washington, DC, USA

Department of Medicine
The George Washington University
Washington, DC, USA

David L. Kaplan
Department of Biomedical Engineering
Tufts University
Medford, MA, USA

ISBN 978-3-319-31431-0 ISBN 978-3-319-31433-4 (eBook)
DOI 10.1007/978-3-319-31433-4

Library of Congress Control Number: 2016940092

Printed on acid-free paper

This Springer imprint is published by Springer Nature
The registered company is Springer International Publishing AG Switzerland

Preface

The frontiers of medical technology that are currently being explored are unparalleled. Scientists, engineers, and clinicians are pushing the boundaries of our understanding of the underlying mechanisms of human neurobiology and applying this new knowledge in truly innovative ways. All of these explorations and advances have been focused toward solving some of medicine's most intractable problems. Nowhere has the rapid growth and advancement of high tech solutions been more prevalent than in the use of advanced engineering techniques for the study of neural tissue repair, stimulation, and disease. This premier edition of *Neural Engineering: From Advanced Biomaterials to 3D Fabrication Techniques* encompasses an extensive body of knowledge including various cutting-edge topics related to neural engineering. Specifically, the contributions detail the state of the art in the use of advanced 3D bioprinting, stem cells, conductive materials, nanomaterials, neural modeling, and brain machine interfaces as applied to solving prevalent clinical issues related to neurology.

The majority of this book focuses on highly controllable 3D fabrication methods, stem cells, and materials for neural regeneration. Relevant chapters span a variety of areas, including 3D bioprinting, microfluidics, stem cell signaling and differentiation, bioactive 3D scaffolds, surface patterning and the influence of nanotopography, controlled neural growth, and the use of electrically conductive materials, among many related topics. As the collective understanding grows pertaining to neuronal tissue extracellular matrix components and their interactions with native cells, new approaches to seamlessly integrate micro- to nano-architectural characteristics, biochemical signaling, and other key influencing features for controlling stem cell biology have taken center stage as a prevailing methodology for treating complex neurological conditions. The text is meant to provide a resource for biomedical engineers, neuroscientists, neurophysiologists, and industry professionals for both comprehensive and cutting-edge themes in the practice of neural engineering. This book contains contributions from some of the world's leading authorities on advanced approaches to neuronal engineering. Their work and perspectives combine to create a powerful resource for informing the activities of other researchers

and clinicians, as well as creating a unique window into the state of the art in areas of micro/nanotechnology, biomaterials, stem cell biology, and neural tissue engineering.

This book has a particular focus on the important progress that has been made in the manipulation of materials and controlled fabrication techniques which can direct neural tissue formation. A unique set of environmental and functional characteristics unique to stem cells and neuronal cells for development and function are linked to the precise design of biomimetic systems. None of the advances in these areas would be possible without the scientists, medical practitioners, and individuals who have dedicated themselves to developing cutting-edge neural engineering techniques. Special recognition should be made to the formative minds who have contributed to this book. This book should be viewed not only as a thorough review of the current state of the field but also to document some of the incredible accomplishments made in recent years that will lead us into the future.

Washington, DC, USA — Lijie Grace Zhang
Medford, MA, USA — David L. Kaplan

Contents

Chapter 1
Biomaterials and 3D Printing Techniques for Neural Tissue Regeneration

Se-Jun Lee, Wei Zhu, Nathan Castro, and Lijie Grace Zhang

1.1 Introduction

Nervous system is the most vital system in the human body affecting the sensory and motor functions (Jeans et al. 2007; Anon. 2011; Khaing and Schmidt 2012; Kiernan and Rajakumar 2013) which is broadly divided into the central nervous system (CNS) and the peripheral nervous system (PNS). The CNS consists of the two major structures: brain and spinal cord, whereas the PNS involves nerves located throughout the rest of the body. Injuries to the CNS affect two million people in the United States each year (Ai et al. 2013) often leading to very serious complications including neurodegenerative diseases and physical damage to regions of brain and spinal cord. Unfortunately, injuries to these sites are largely intractable. Associating with post brain trauma, astrocytes will be activated, proliferate, and form an inhibitory glial scar. Although this process prevents the spread of injuries to nearby tissues, permanent damage is present at the injury site. In addition to traumatic brain injuries, the annual incidence of spinal cord injuries (SCI) is estimated to be approximately 12,000 new cases each year leading to a total of ~273,000

S.-J. Lee • W. Zhu • N. Castro
Department of Mechanical and Aerospace Engineering, The George Washington University, 3590 Science and Engineering Hall, 800 22nd Street NW, Washington, DC 20052, USA

L.G. Zhang (✉)
Department of Mechanical and Aerospace Engineering, The George Washington University, 3590 Science and Engineering Hall, 800 22nd Street NW, Washington, DC 20052, USA

Department of Biomedical Engineering, The George Washington University, 3590 Science and Engineering Hall, 800 22nd Street NW, Washington, DC 20052, USA

Department of Medicine, The George Washington University, 3590 Science and Engineering Hall, 800 22nd Street NW, Washington, DC 20052, USA
e-mail: lgzhang@gwu.edu

L.G. Zhang, D.L. Kaplan (eds.), *Neural Engineering*,
DOI 10.1007/978-3-319-31433-4_1

persons in the United states (Daly et al. 2011). Successful therapeutics for full neural functional recovery has been difficult to achieve due to the complexity of the CNS and an inhospitable environment around the lesion site for cell translation (Tam et al. 2013). After the swelling from the injury subsides, patients begin a long period of rehabilitation during which time they train the remaining nerves to compensate for the loss of function (Meaney and Smith 2014; Perry and Teeling 2013). Unfortunately, there is currently no treatment available to fully restore nerve function.

Although the PNS has a greater capacity for axonal regeneration after injury than CNS, spontaneous peripheral nerve repair is still always incomplete with poor functional recovery (Schmidt and Leach 2003; Sulaiman and Gordon 2013). When a severe peripheral nerve injury occurs, scar tissue begins to form between the proximal and distal segments. If the cell body is intact within the proximal segment, the cell will begin to sprout out axons (Calvo and Bennett 2012; Gaudet et al. 2011). On the other side, the disconnected distal segment undergoes demyelination and degradation within hours of injury. For the greatest chance of success, surgical interventions must occur as soon as possible to the time of injury. The goal of surgical repair is to guide regenerating sensory, motor, and autonomic axons to the distal nerve stump to increase the chance of target regeneration. Currently, transplantation of autografts is the most common used method to bridge the lesion site (Lin et al. 2013). However, there remain many inherent drawbacks to autologous transplantation including pain and donor site morbidity, mismatch of donor nerve size, and fascicular inconsistency between the autograft and the proximal and the distal stumps of the injured site (Hasirci et al. 2014). Alternatively, neural tissue engineering is being explored in an effort to develop artificial nerve scaffolds to overcome these limitations.

Neural tissue engineering approach utilizes an artificial neural scaffold to replace the defective sites and eventually restore nerve function. In the last few decades, many nerve scaffold fabrication techniques have been explored. Among them, 3D printing techniques have recently drawn great interest because they can fabricate scaffolds with highly controlled spatial architecture to meet patient-specific requirements. Many natural and synthetic biomaterials have been investigated in creating 3D-printed nerve scaffolds. Naturally derived materials share similar characteristics to human native tissue, which enhance their biocompatibility for neural tissue engineering applications. However, the intrinsic poor mechanical properties of many natural polymers limit its wide use in 3D printing technologies. In contrast, synthetic biomaterials have great chemical and mechanical properties that can be easily tailored to meet the specifications necessary for 3D printing. Therefore, they are very popular to construct 3D-printed nerve scaffolds. A major drawback of synthetic biomaterials is their poor cell adhesive properties. Thus, utilization of combined synthetic and natural polymers with unique characteristics can be an appropriate solution to repair damaged nerve tissues. In the following, we will focus on the current progress in advanced biomaterials and 3D printing techniques for neural tissue regeneration.

1.2 Neural Tissue Engineering

Neural tissue engineering integrates cells, biomaterials, and 3D fabrication techniques to treat nerve injuries. Fortunately, advances in both tissue engineering and neuroscience have provided a very optimistic outlook for nerve injury treatments.

1.2.1 Criteria for Ideal Tissue-Engineered Neural Scaffolds

The development of biomimetic scaffolds is very important in guiding native cells to adhere and proliferate within native extracellular matrix (ECM). Nervous system ECM contains a myriad of biological constituents such as various glycoproteins which are essential in guiding neuronal outgrowth (Barros et al. 2011; Zimmermann and Dours-Zimmermann 2008; Rutka et al. 1998). Therefore, when the ECM in the nervous system is disrupted because of injury, the implanted scaffold is required to have analogous functions of native ECM to support axonal regeneration. Ideally, scaffolds for neural tissue engineering should meet several design criteria: (1) the surface of scaffold should allow excellent cell adhesion and proliferation; (2) the scaffolds should be biocompatible with very low cytotoxicity and inflammation in vivo; (3) the scaffolds should degrade in vivo with producing cytocompatible metabolites; (4) high porosity is desirable to allow sufficient gas and nutrient exchange and promote cell adhesion and migration; and (5) the scaffolds should have mechanically stable three-dimensional structures. Figure 1.1 shows these ideal characteristics of nerve scaffolds. Next, we will discuss the biomaterials and 3D printing for the fabrication of ideal nerve scaffolds.

1.2.2 Biomaterials for Nerve Scaffold

Both natural polymers [i.e., chitosan, collagen, gelatin, alginate, hyaluronic acid) and synthetic polymers (i.e., polycaprolactone (PCL), poly(lactic-co-glycolic acid) (PLGA), and poly(L-lactic acid) (PLLA)] have been used in clinical practice for various biomedical applications for more than 30 years and have been developed for neural tissue regeneration (Zorlutuna et al. 2013). In addition to these conventional natural/synthetic polymers, electrically conductive polymers and carbon-based nanomaterials have been found as promising candidate materials for enhancing neural cells-scaffold interaction. Each biomaterial will be discussed for its potential uses in neural interfaces.

1.2.2.1 Natural Biomaterials

A wide range of natural biomaterials possessing great biocompatibility have been studied for use in nerve regeneration (Khaing and Schmidt 2012; Tarun et al. 2012; Anon. 2011; Subramanian et al. 2009; Tam et al. 2013; Huang and Huang 2006;

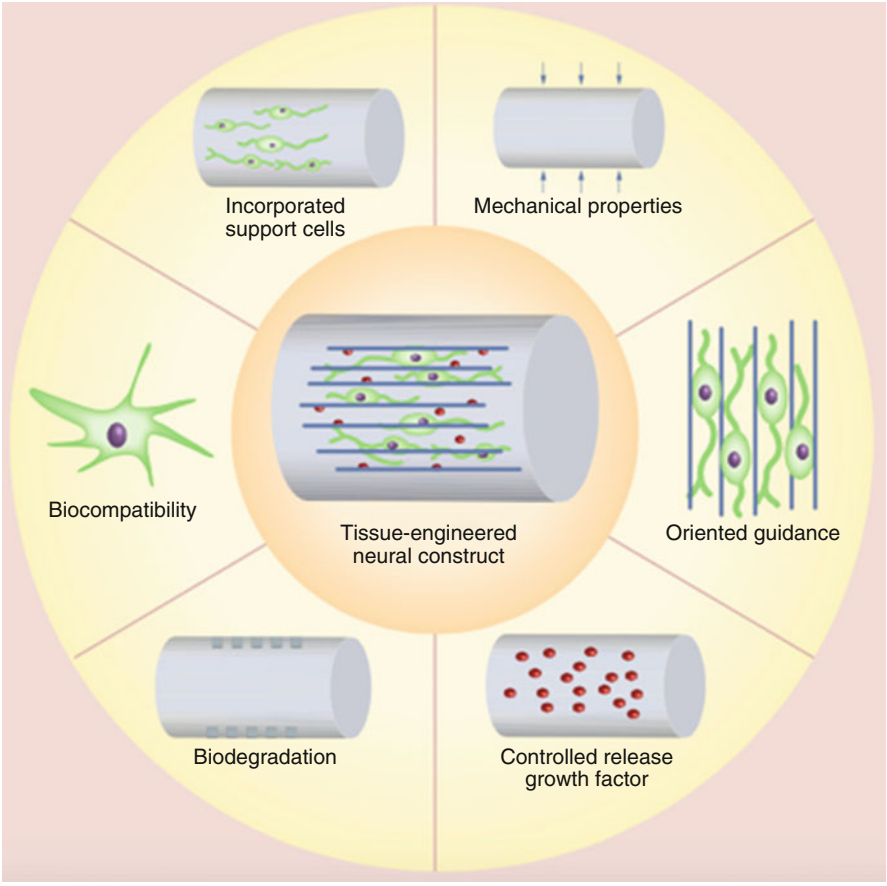

Fig. 1.1 Schematic illustration of an ideal tissue-engineered neural scaffold

Nectow et al. 2012; Daly et al. 2011; Hodde 2002). They also closely mimic the natural tissue ECM. The common natural polymers for neural tissue engineering include alginate, collagen, gelatin, chitosan, hyaluronic acid (HA), and fibrin. Currently, many approved and commercially available nerve conduits are made from natural biomaterials such as collagen type I-based NeuroFlex and NeuroMax. In the following discussion, we will explore some of the most popular neural-related natural biomaterials.

Collagen is the most abundant mammalian protein comprising the majority of connective tissue (Glowacki and Mizuno 2008; Miyata et al. 1992; Cen et al. 2008; Walker et al. 2009). The indigenous nature of collagen and potential ability to supply both structural and nutritive support make it an attractive material for nerve scaffold fabrication (Li et al. 1992; Archibald et al. 1991; 1995; Mackinnon and Dellon 1990; Ceballos et al. 1999; Hodde 2002). Mollers et al. described the cytocompatibility of a micro-structured porcine collagen scaffold for nerve tissue repair

(Mollers et al. 2009). They found that the highly orientated and porous microstructure of the porcine collagen scaffold supported excellent glial cell attachment, proliferation, and orientated migration, as well as directed axonal outgrowth. The excellent biocompatibility of collagen and the maintained 3D geometry of such scaffolds may provide the orientational cues that are important for the efficient repair of nerve injuries.

Alginate is another naturally occurring polymer obtained from the brown algae of seaweed. Due to the ability to cast the material at room/body temperature for producing a porous construct, alginate is an attractive material for scaffold fabrication. Many studies have successfully used alginate-based conduit for nerve regeneration (Pfister et al. 2007; 2008; Ohta et al. 2004; Sufan et al. 2001; Mosahebi et al. 2003; Suzuki et al. 1999). Implantation of neural stem cells (NSCs)-laden alginate scaffolds into a spinal cord defect of rat model has shown axonal elongation and progenitor cell differentiation toward astrocyte lineage (Wu et al. 2001). Additionally, preliminary research has shown the ability of alginate scaffolds to promote angiogenesis as well as progenitor cell viability, maturation, and differentiation, thus warranting further investigation into nerve injuries.

Normally, many natural biomaterials have poor mechanical properties, disadvantage of variability among batches, short supply, and difficulty in processing. Hence, in order to meet the requirements for preparing an optimal scaffold, several studies have used combinations of two or more natural materials to enhance scaffold chemical and mechanical properties. Wang et al. reported that HA/collagen composite scaffolds exhibited suitable mechanical properties for CNS regeneration (Wang et al. 2012). In vitro experiments showed that NSCs cultured upon HA/collagen scaffolds enhanced neuronal differentiation. In addition, Amado et al. have tested mechanically modified chitosan nerve scaffolds in animal transplants, which demonstrated improved nerve fiber regeneration and functional recovery in the sciatic nerve when compared to normal control nerve (Amado et al. 2008).

1.2.2.2 Synthetic Biomaterials

A number of synthetic biomaterials such as polymers have been investigated for use in tissue-engineered scaffolds for both peripheral and central nerve regeneration (Reid et al. 2013; Lee et al. 2012; Hanna and Dempsey 2013; Sivak et al. 2014; Niu et al. 2014; Khatri and Peerzada 2014; Mobasseri et al. 2015; Matsumine et al. 2014; Liu et al. 2011). Many of the synthetic polymers are biodegradable and can be designed with inherent porosity which directly influences adhesion, proliferation, and migration of neural cells (Gunatillake and Adhikari 2003; Bajaj et al. 2014; Daly et al. 2011; Zhu and Che 2013). The most widely used synthetic polymers as a scaffold material including PLGA, PCL, polyglycolide (PGA) and PLLA will be introduced next.

PLGA has been extensively investigated as a scaffold material for various tissue regenerations (Krämer et al. 2011; Zamani et al. 2014; Lee et al. 2009). It has been approved by FDA for many other medical devices owing to its excellent biocompat-

ibility and biodegradability in the human body. Kramer et al. created a PLGA nanofiber matrix with incorporated poly-L-lysine and observed neurite outgrowth of NSCs on the scaffold (Krämer et al. 2011). In addition, numerous surface modification approaches on PLGA and many other polymer materials including incorporation of ECM proteins such as laminin, fibronectin, and collagen or other specific adhesion peptide sequences like RGD have been investigated (Subramanian et al. 2009). For example, Huang et al. showed that laminin-modified PLGA films had a significant effect on the Schwann cells' attachment and affinity compared to that of control PLGA film (Huang et al. 2007). Overall, these surface modifications produce a hydrophilic and biomimetic surface which leads to increased cell adhesion upon the scaffold.

PCL is another popular biodegradable synthetic polymer for use in peripheral nerve regeneration. Sun et al. used microporous biodegradable PCL and PCL/PLA films to test biocompatibility with primary Schwann cells (Sun et al. 2010). The in vivo result demonstrated that PCL conduits exceeded the performance of the widely studied polyhydroxybutyrate (PHB) conduit in bridging up a 10-mm gap in rat sciatic nerve in 2 weeks. Furthermore, long-term peripheral nerve regeneration was examined using a novel PCL nerve conduit (Reid et al. 2013). The result demonstrated that similar volume of regenerating axons was found within the nerve autograft and PCL conduit samples. In addition, similar numbers of myelinated axons were found in the distal stump of both groups at 18 weeks post surgical repair. This study illustrated the potential use of synthetic biodegradable PCL nerve conduit in a clinical setting.

Several studies have attempted to optimize the porosity and mechanical strength of synthetic materials as a nerve scaffold (Yang et al. 2004; Plikk et al. 2009; Sundback et al. 2003; Vleggeert-Lankamp et al. 2007). Vleggeert-Lankamp et al. have examined the effect of pore size of synthetic nerve scaffold on nerve regeneration (Vleggeert-Lankamp et al. 2007). The group used nonporous, macroporous, and microporous PCL nerve grafts to bridge a 6-mm gap in the rat sciatic nerve. The microporous PCL nerve graft performed much better than any other groups due to a higher electrophysiological response rate producing more regenerated nerve fibers distal to the graft.

1.2.2.3 Electrically Conductive Biomaterials

One of the main functions of the nervous systems involves electrical signaling in order for cells to communicate with other cell bodies. This implies that an ideal neural scaffold should possess electrical properties to enhance proliferation and migration of neural cells (Subramanian et al. 2009; Brushart et al. 2005; Mozafari et al. 2012; Jin and Li 2014; Balint et al. 2014; Richardson-Burns et al. 2007). In this regard, an electrically conductive polymer is highly desirable in reconstructing neural connections. Conductive polymers have loosely held electrons along their backbones. Each atom along the backbone is involved in a pi bond, which is much weaker than sigma bonds which hold the atoms in the polymer chain together

(Kumar and Sharma 1998; MacDiarmid 2001). In order to exhibit the electrical properties, all conductive polymers undergo a process known as doping. The doping process allows a neutral chain to be oxidized or reduced to become either positively or negatively charged (Ghasemi-Mobarakeh et al. 2011; Green et al. 2012). The doping process transfers charge from a dopant molecule to the polymer chain within an overall neutral system. During the process, charge carriers like polarons and bioplarons are introduced into the conjugated chain (Ghasemi-Mobarakeh et al. 2011). The main drawback of conductive polymers for in vivo applications is their inherent inability to degrade, which may induce chronic inflammation and require surgical removal (Huang and Huang 2006). To overcome this issue, many efforts have been made to blend conductive materials with more favorable biodegradable polymers. In the following section, the most widely used conductive biomaterials will be discussed for use in neural interfaces.

Many studies have reported that polypyrrole (PPY), one of the common conductive polymers, enhances nerve regeneration (Mihardja et al. 2008; Xie et al. 2009; Runge et al. 2010; Jin et al. 2012; Cui et al. 2001; Green et al. 2008; Lee et al. 2009; George et al. 2005; Richardson-Burns et al. 2007; Nickels and Schmidt 2012). For example, Schmidt et al. found that electrical stimulation through PPY polymer scaffolds promoted cell proliferation and axon regeneration (Nickels and Schmidt 2012). Many researchers have used PPY and other synthetic polymers to tailor an optimal conductive composite. For instance, PPY/PDLLA/PCL composite scaffolds have been implanted in a rat sciatic nerve model to bridge a gap of 8 mm (Subramanian et al. 2009). The nerve scaffold successfully promoted nerve cell proliferation and axon regeneration in the presence of electrical stimulation (Subramanian et al. 2009).

Polyaniline (PANI) is another popular conductive polymer. PANI has several advantages to include low cost, good environmental stability, and ease of synthesis. In order to improve its biocompatibility and biodegradability, one study has combined PANI with PCL and gelatin to create a scaffold for supporting neural stem proliferation and neurite outgrowth (Ghasemi-Mobarakeh et al. 2011). Also, it was noted that collagen-coated PANI constructs greatly enhanced its biocompatibility and cell adhesion (Cullen et al. 2008) as well.

1.2.2.4 Carbon-Based Nanomaterials

Carbon-based nanomaterials with unique electrical, mechanical, and biological properties have also been investigated for tissue engineering applications (Harrison and Atala 2007; MacDonald et al. 2005; Abarrategi et al. 2008; Shi et al. 2007; Boccaccini et al. 2007; Keefer et al. 2008; Tran et al. 2009). Graphene and carbon nanotubes (CNTs) are among the most widely used nanomaterials in neural tissue engineering. Graphene is a flat monolayer of carbon atoms, arranged in a two-dimensional hexagonal structure (Bressan et al. 2014). The carbon atom is able to form covalent bonds between carbon atoms within a molecule. Graphene is highly biocompatible with low cell toxicity and a large dosage loading capacity, making it a

potential efficient carrier for therapeutic delivery. Another important characteristic of graphene is its capacity to form a functional neural network. For instance, Park et al. have shown that human neural stem cells can differentiate into neurons rather than glia cells on a graphene substrate (Park et al. 2011). Differentiated neurons exhibited elongated cell shapes with neurite outgrowths that resemble neural network formations. Furthermore, the research group observed the electrical neural activity of the differentiated cells using underlying graphene films as a stimulating electrode.

Li et al. developed a graphene-based 3D structure scaffold to guide NSC differentiation. The authors demonstrated that 3D graphene scaffolds exhibit a greater capacity for electrical stimulation when compared to a 2D graphene structure (Li et al. 2013). In addition, studies by Song et al. have revealed that most carbon-based nanomaterials may initiate some form of inflammation (Song et al. 2014). 3D graphene elicited milder neuroinflammation in the microglia after lipopolysaccharide (LPS) activation when compared to 2D graphene, suggesting that topographical structures of the materials might affect inflammatory behavior.

Carbon nanotubes are rolled graphene sheets with excellent electrical and mechanical properties and can be synthesized to a wide variety of lumen structures from singled-walled (SWCNTs) to multi-walled (MWCNTs) (Fig. 1.2). CNTs are similar in size to ECM biomolecules such as collagen and laminin and have been reported to promote neuronal growth. Tzu-I Chao et al. developed a CNT-modified polymer 2D film and demonstrated that human embryonic stem cells can differentiate toward a neuronal lineage while maintaining excellent viability (Chao et al. 2009). The group has also shown that CNT-coated electrodes have improved electrochemical and functional properties of cultured neurons of the rat motor cortex and monkey visual cortex (Keefer et al. 2008). Both in vitro and in vivo experiments have investigated the cytotoxicity and biocompatibility of CNTs for potential use in neural regenerative applications.

In addition, Aldinucci et al. studied the immunomodulatory action of human dendritic cells on MWCNTs in vitro (Aldinucci et al. 2013). Based on their findings, differentiated and activated dendritic cells exhibited a lower immunogenic profile when interfaced with MWCNTs and the immune reaction modulation was related to topographical and physical features of the growth surface. It was also found that neuronal viability of postnatal mouse dorsal root ganglia was reduced when exposed to higher concentrations of MWCNTs containing culture media (Gladwin et al. 2013). In this work, 250 μg/mL of MWCNT-containing media exhibited neuronal death and abnormal neurite morphology while 5 μg/mL of MWCNT-containing media presented no cytotoxicity over 14-day culture. Although there have been cytotoxicity concerns raised about CNTs, thus far the exact mechanisms of CNT's effects on cells are still not fully known. But the results described previously show that nanotubes are cytocompatible under certain conditions, e.g., certain tube lengths, high concentration, hydrophobicity of bare nanomaterial, and dispersion of nanotubes. It was suggested that CNTs can serve as an excellent nanobiomaterial for neural regeneration through surface and structural modifications for enhanced biocompatibility and cell growth.

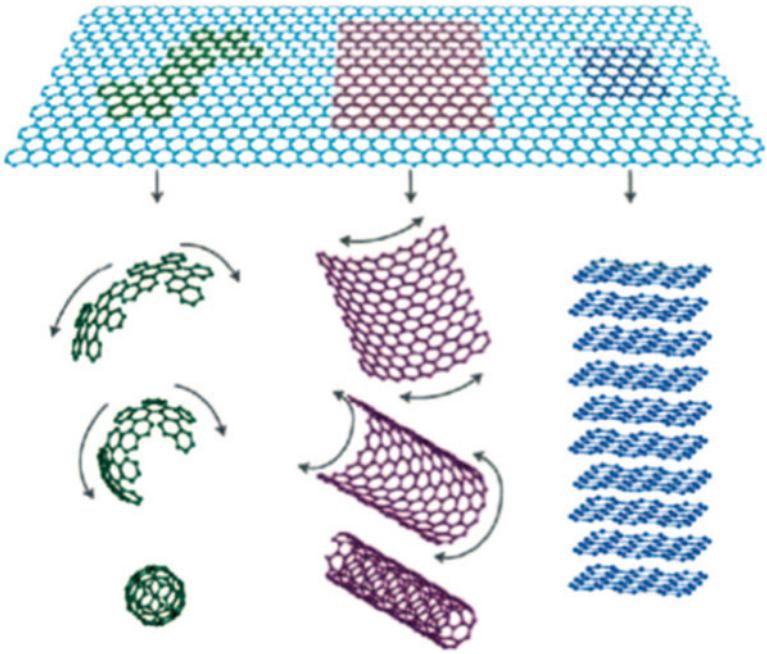

Fig. 1.2 Graphene forms: fullerenes, carbon nanotubes, and graphite. Images are adapted from Geim et al. (2007)

1.3 3D Printing Techniques for Nerve Regeneration

In this section, we will introduce some of the most popular 3D printing methods to configure 3D scaffolds for neural tissue engineering. In contrast to 2D printing methods, 3D printing has garnered considerable attention in tissue engineering as a means of fabricating tunable 3D biomimetic scaffolds. The outstanding advantage of 3D printing techniques is their capacity to directly produce complex tissue scaffolds with precise spatial distribution and biomimetic architecture. Many studies have used these techniques to print cell-free scaffolds or scaffolds encapsulating living cells.

1.3.1 Inkjet Bioprinting

Inkjet bioprinting has been the most popular 3D fabrication technology for neural tissue engineering. Most inkjet printers used for bioprinting applications were modified versions of commercially available 2D ink-based printers (Xu et al. 2013). The ink in the cartridge was replaced with a cell-containing bioink, and the paper was replaced with controllable platform stage with z-axis. Inkjet bioprinting is capable of dispensing and handling biological and polymer solutions in highly

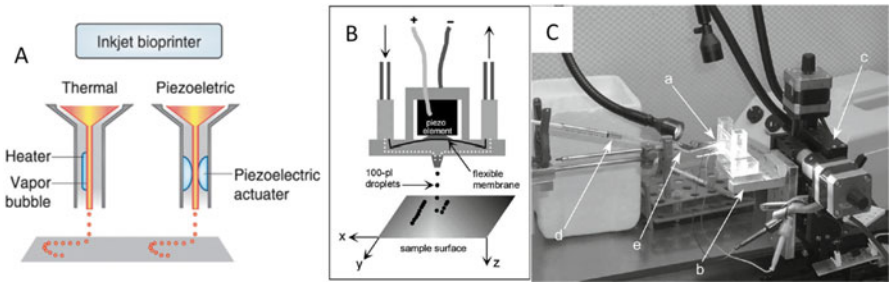

Fig. 1.3 (**a**) Diagram of the operation of a thermal and piezoelectric head in inkjet bioprinting. Image adapted from Murphy et al. (2014). (**b**, **c**) Scheme of customized piezoelectric head and the setup of the inkjet printer. Images are adapted from Turcu et al. (2003)

controlled manner. There are two types of inkjet printing: thermal and piezoelectric (Fig. 1.3). Thermal inkjet printers electrically heat the print head to produce air-pressure pulses which force droplets from the nozzle. Piezoelectric inkjet generates pulses by piezoelectric and forces printing materials from the nozzle (Zheng et al. 2011). The primary advantage of piezoelectric inkjet over thermal printer is that it can increase cell viability by eliminating heat.

Many researchers have used inkjet bioprinting technologies in developing novel patterned scaffolds (Weng et al. 2012; Roth et al. 2004; Ilkhanizadeh et al. 2007; Zheng et al. 2011; Choi et al. 2011). For example, Turcu et al. have utilized a piezo-based microdispenser in conjunction with inkjet bioprinting to create a line pattern scaffold with resolution of 100 μm (Turcu et al. 2003) (Fig. 1.4a, b). They used a commercially available polymeric matrix for laminin coating to increase adhesion and outgrowth of embryonic neurons (Fig. 1.4c, d). Another study from Xu et al. successfully used commercially available inkjet technology to print primary embryonic hippocampal and cortical neurons in a controlled pattern (Xu et al. 2009). They showed that printed fibrin-based neural scaffolds are suitable for maintaining a cell-favorable microenvironment for neural cell adhesion. In addition, the results indicated that cellular properties and functional fidelity of neurons after being ejected through the nozzles of a thermal inkjet printer were retained after the printing.

Moreover, inkjet bioprinting has also provided a means for the incorporation of electrically conductive materials within neural scaffolds. Weng et al. have successfully used inkjet technology to print a conductive polymer composite PPY/collagen scaffold with incorporated electrical stimulation (Weng et al. 2012). In this study, PPY and collagen were micro-structured on a polyarylate film by inkjet printing for electrical stimulation of a spatially controlled system. The PPY/collagen track was illustrated to guide PC-12 adherence and growth, while electrical stimulation showed the ability to promote neurite outgrowth and orientation. In addition, biomimetic materials and ECM proteins could be printed on a traditional scaffolds' surface to obtain more cell-favorable features. Sanjana et al. revealed inkjet-printed collagen/poly-D-lysine (PDL) on a poly(ethylene) glycol surface can support rat hippocampal neurons and glial growth in defined patterns when compared to collagen/PDL absent regions (Sanjana and Fuller 2004).

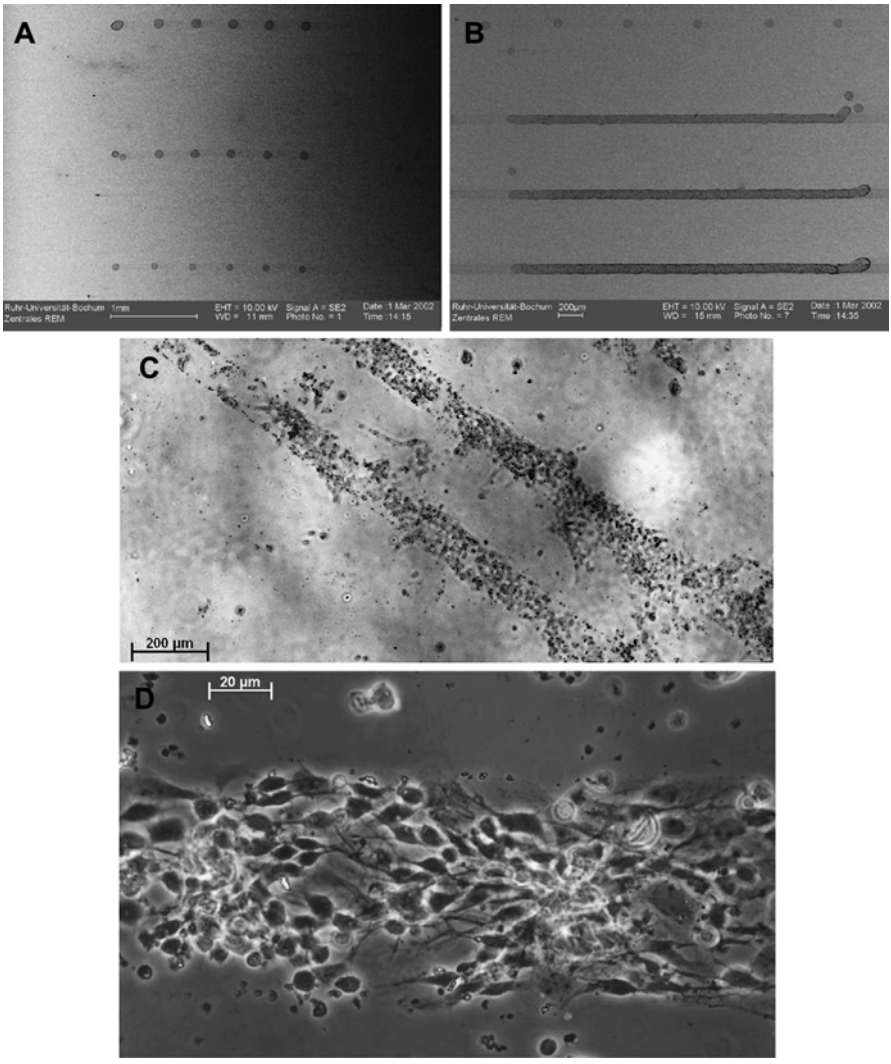

Fig. 1.4 (**a**, **b**) Patterns of dots and lines made from vinyl acetate-ethylene copolymer using inkjet printing. (**c**, **d**) Examples of neurons cultured on (**b**) line pattern with laminin coating. All images are adapted from Turcu et al. (2003)

1.3.2 Stereolithography

Stereolithography (SL) is a laser-based printing system, which was first commercially available in the late 1980s (Jacobs 1992). Figure 1.5a shows a schematic diagram of SL printing. A typical SL apparatus consists of a build platform, UV laser source, and printing materials containing a photo initiator (Fig. 1.5a). With the

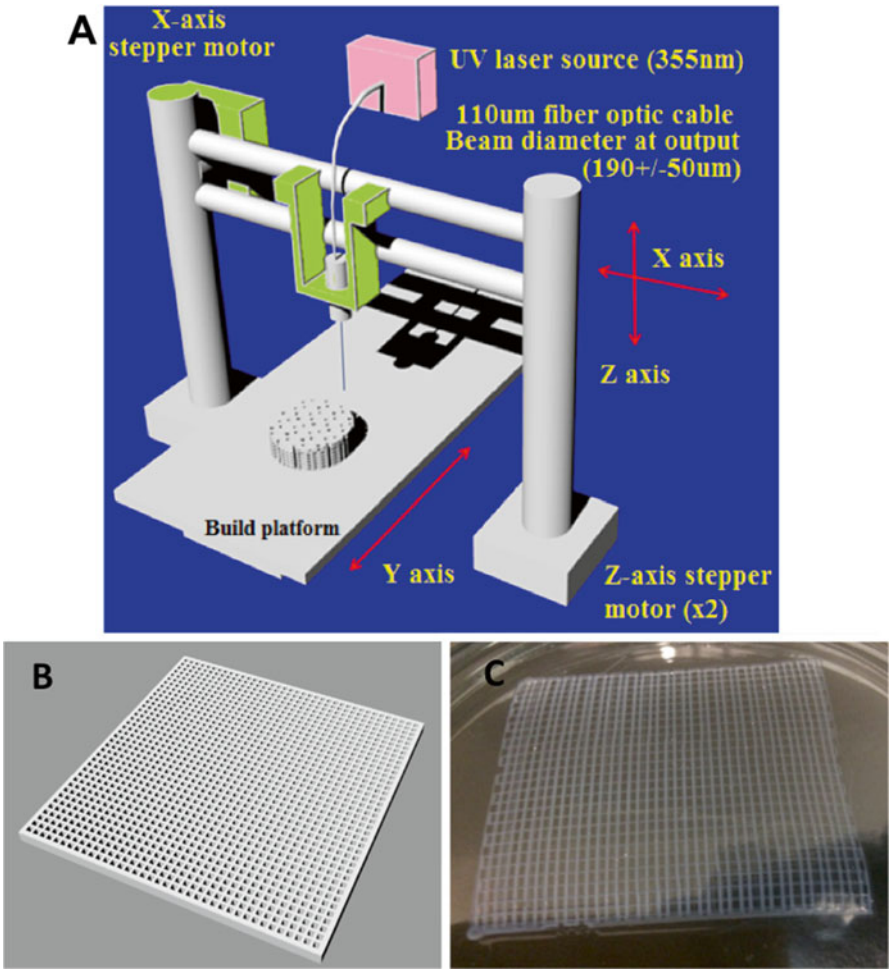

Fig. 1.5 (**a**) Overview of the process for fabricating structures using the SL. (**b**) CAD model of one square pattern scaffold. (**c**) SL printed scaffold using previous CAD model.

aid of modeling software, a micro-macro size 3D construct is achieved using a layer-by-layer approach. Figure 1.5b, c represents the computer-aided design (CAD) model of one square pattern scaffold and SL printed scaffold using previous CAD model, respectively.

Several studies have fabricated tissue-engineered scaffold with various patterns particularly square and hexagonal, using SL printing technique (Skoog et al. 2013; Chan et al. 2010; Arcaute et al. 2006). For example, Arcaute et al. successfully used a commercial SL system to fabricate three-dimensional, multilayered, and multimaterial nerve guidance conduits (NGC) (Arcaute et al. 2010) (Fig. 1.6a, b). In their study, multiple material conduits were printed by varying the build solution during the layering process. Results demonstrated that SL is a promising technology for the fabrication of bioactive NGCs using PEG hydrogels. Since overall lengths of the

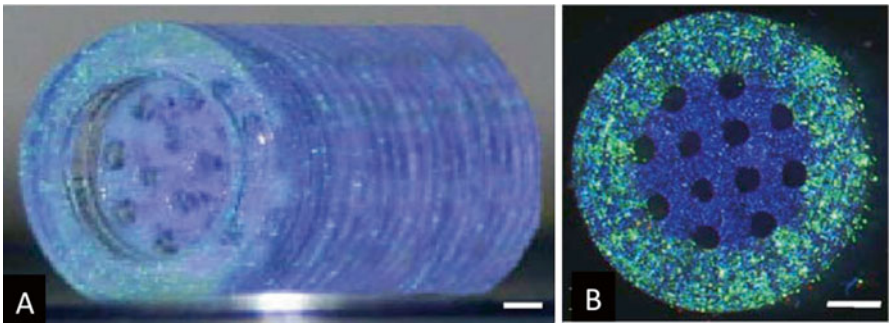

Fig. 1.6 (**a**, **b**) Multi-lumen PEG hydrogel conduit with fluorescent particles having an outer diameter of 5 mm and an inner diameter of 3 mm (*left*, isometric view; *right*, top view) Images adapted from Arcaute et al. (2006)

NGCs were constrained by the ability of the conduit to self-support, further observations showed that NGCs having a multi-lumen design have better resistance to compression than a single-lumen design with an equivalent surface area (Arcaute et al. 2010).

Hanson Shepherd, J.N. et al. created 3D microperiodic poly(2-hydroxyethyl methacrylate) (pHEMA) neural scaffolds via photolithography (Hanson Shepherd, J.N. et al. 2011). In the study, 3D pHEMA scaffolds of varying microperiodicity are patterned and cultured with primary rat hippocampal neurons. The development of primary rat hippocampal neurons on this 3D scaffold was carefully monitored with confocal laser scanning microscopy. Their results showed that scaffold architecture can be controlled precisely and the structure influenced both, cell distribution and aligned extension of neurons (Fig. 1.7). In addition, Zorlutuna co-encapsulated hippocampus neurons and skeletal muscle myoblast cells on 3D hydrogel matrix fabricated by SL technique (Zorlutuna et al. 2011). The results showed that muscle cells spread extensively throughout the scaffold and formed tube-like structures, while neurons extended their processes throughout the hydrogel. Moreover, 3D coculture of these two cell types resulted in significantly enhanced functionality of hippocampus neurons, quantified by their choline acetyltransferase (ChAT) activity. Their findings show that SL system can precisely control spatial organization of cells and can be used for the fabrication of multicellular biological systems.

Another promising method among SL techniques is Directed Mirror Device (DMD) SL printing. The DMD microfabrication system employs a dynamic mask for photopolymerization of an entire polymer layer simultaneously. Further, the DMD system provides flexible manufacturing solution that allows to create patient-specific scaffolds. For example, Shalu Suri et al. fabricated micro- and macroarchitecture scaffolds composed of HA exhibiting different geometries using the DMD technique (Suri et al. 2011). Their results showed that Schwann cells adhere and undergo normal spreading on laminin-coated HA scaffolds. In addition, they successfully used DMD system to create two gradients of biomolecules running in

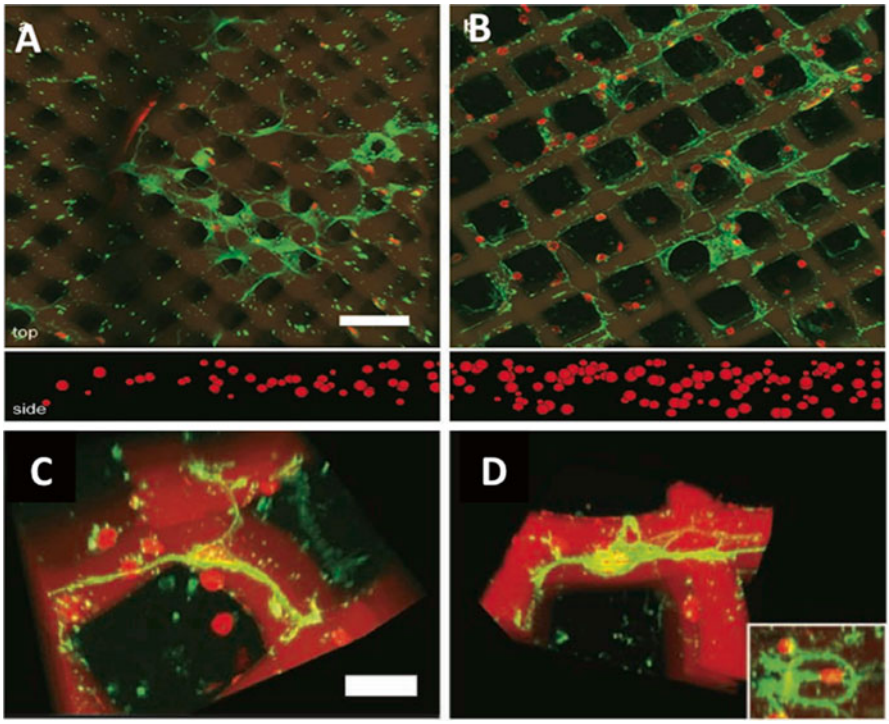

Fig. 1.7 (**a**, **b**) Confocal images of primary rat hippocampal cells distributed within pHEMA scaffolds of different porosity. (**c**, **d**) 3D confocal images of neuronal cell growth and spreading on the scaffolds. All images are adapted from Hanson Shepherd, J.N. et al. (2011)

opposite direction on the hydrogel scaffolds. This might be beneficial for neural cell adhesion and proliferation, as some studies have shown that cells can respond better to multiple bimolecular gradients (Chan et al. 2010).

In our lab, we have fabricated a novel 3D biomimetic scaffold, which has tunable porous structure, and embedded core-shell nanoparticles as a neurogenic factor delivery system using SL-based 3D printing and core-shell electrospraying techniques. Our results indicated that scaffolds with higher porosity significantly improve PC-12 neural cell adhesion compared to less porous scaffolds. Furthermore, scaffolds with embedded bovine serum albumin containing nanoparticles showed an enhancement in cell proliferation relative to bare control scaffolds. In addition, confocal microscopy images illustrated that scaffolds with nerve growth factor (NGF) nanoparticles increased the length of neurites and directed neurite extension of PC-12 cells along the fiber (Fig. 1.8). The results of this study demonstrate the potential of this 3D scaffold in improving neural cell function and nerve growth.

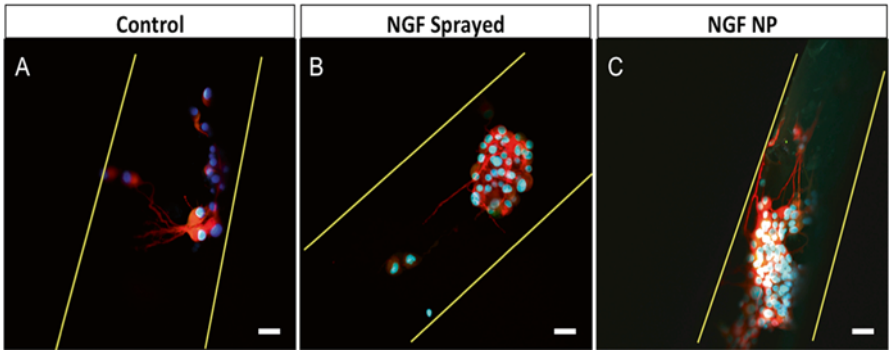

Fig. 1.8 Confocal microscopy images of PC-12 cell growth and spreading on 3D printed scaffold at day 7. (**a**–**c**) Double staining of MAP2 and TuJ1 to detect PC-12 differentiation on various scaffolds after 7 days of culture. Scale bar = 50 μm. NGF NP represents scaffold embedded with NGF nanoparticles.

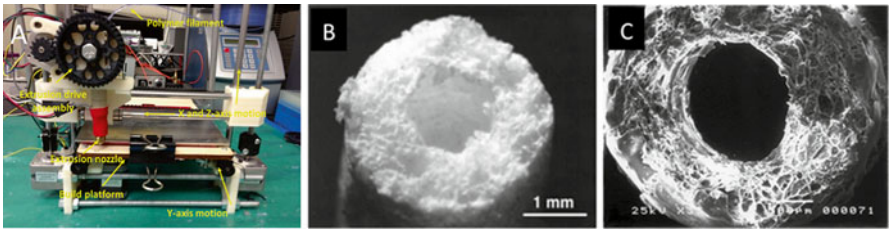

Fig. 1.9 (**a**) Fused deposition modeling printer. (**b**, **c**) Optical micrographs and SEM image of a conduit fabricated from PLGA using a combined solvent casting and extrusion technique. Images are adapted from Widmer et al. (1998)

1.3.3 Extrusion-Based Printing

Extrusion-based printing is developed depending on the deposition of heated thermoplastics. Figure 1.9a represents a fused deposition modeling based 3D printer. This strategy is capable of producing complex with highly interconnected porous structures. However, the melt process involves elevated temperature, which is not suitable for cell encapsulation. Therefore, extrusion-based printing is only ideal for fabricating cell-free scaffolds. Several researchers have applied melt extrusion methods to produce polymeric scaffold for neural tissue engineering applications (Widmer et al. 1998; Evans et al. 1999; Verreck et al. 2005). They have examined the effect of processing conditions with regard to the chemical-physical properties and biocompatibility of the processed polymeric material (Domingos et al. 2009).

Widmer et al. described the use of melt extrusion as well as melt compression for the preparation of nerve guides made of PLLA and PLGA (Widmer et al. 1998) (Fig. 1.9b, c). In addition to these melt processing techniques, they have combined leaching and casting methods to increase porosity of the nerve conduits. Optical

micrographs and SEM images showed extensive pores which were roughly spherical in shape and evenly distributed throughout. Furthermore, both PLGA and PLLA conduits maintained their shape and did not collapse after degradation for 8 weeks. Then later study evaluated the number of axons per unit area and nerve fiber density in the distal sciatic nerve for the PLLA conduit. The results confirmed that the PLLA conduits fabricated by extrusion technique performed similar to the control isograft after 16 weeks of implantation (Evans et al. 1999).

Verreck et al. have further confirmed the feasibility of melt extrusion techniques to prepare PGA/PCL nerve conduits. The purpose of their work was to optimize methods of incorporating sabeluzole, a nerve growth factor, into a biodegradable polymeric system as well as evaluate the physicochemical and release characteristics of the drug-loaded nerve guides. The in vitro release measurements showed absence of crystalline sabeluzole, indicating the formation of an amorphous dispersion. In addition, authors demonstrated that the drug release is complete, reproducible, and can be controlled by the proper selection of the polymer. These findings help to illustrate the potential of melt extrusion system as an easy fabrication method to produce biocompatible and bioresorbable nerve conduits.

1.3.4 Bioplotting

3D bioplotting is another type of nozzle-based printing similar to extrusion printing. Landers and Mülhaupt introduced this 3D dispensing process in 2000 at the Freiburg Research Centre for the first time (Landers and Mülhaupt 2000). This technique was specifically developed to produce scaffolds for soft tissue engineering purposes and to simplify hydrogel manufacturing. The three-dimensional construction of objects occurs in a laminar fashion by computer-aided deposition of materials on a surface. The dispensing head moves in three dimensions, while the fabrication platform remains stationary (Fig. 1.10). The biggest advantage of this technique is that it is applicable in various studies. Wang et al. used 3D-bioplotting techniques to construct alginate/HA hydrogel scaffolds for nerve tissue repair (Wang et al. 2013) (Fig. 1.11). Their results showed that Schwann cells survived and grew on the alginate/HA hydrogel scaffolds in vitro for 5 days. This provides a basis for continuing development of 3D bioplotter system for neural scaffold fabrication.

In a more recent study, Shim et al. used a 3-D bioplotter to design and construct poly(caprolactone-*co*-lactide) (PCLA) and small intestine submucosa (SIS) conduits for peripheral nerve regeneration (Shim et al. 2015). After in vivo implantation, the results indicated that regenerated nerves grew from the SIS- and PCLA-NGC through the sciatic nerve-injured gap and connected from the proximal to distal direction along the nerve guiding conduit axis. This result indicates the feasibility of clinical nerve regeneration with PCLA-SIS nerve conduit prepared through bioplotter system using promising biomaterials.

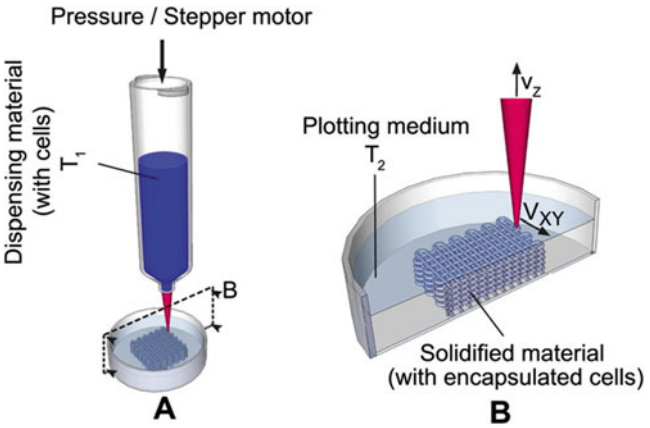

Fig. 1.10 (**a**, **b**) Scheme of 3D-Bioplotter dispensing principle. In the 3D-Bioplotter system, the nozzle works pneumatically or via volume-driven injection. This also illustrates the principle of nozzle-based systems in general, where a nozzle is used for the deposition of material. Image is adapted from Billiet et al. (2012)

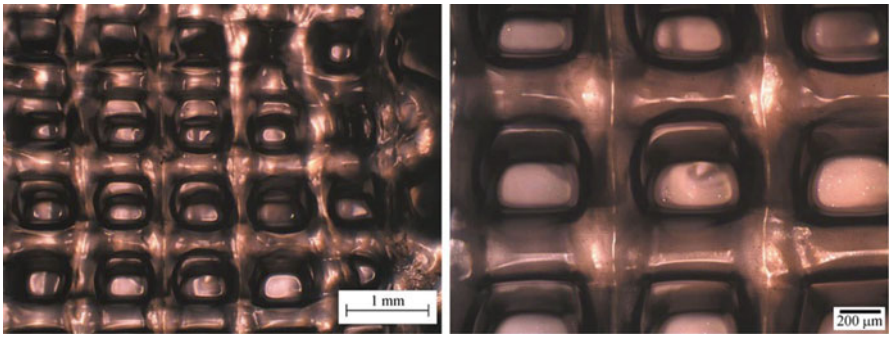

Fig. 1.11 An example of the multilayer scaffolds fabricated from 1.5 % alginate/0.75 % HA using the 3D Bioplotter system. Image is adapted from Wang et al. (2013)

1.3.5 Emerging Novel 3D Printing Technologies

In recent years, a group of researchers at University of North Carolina developed a novel 3D printing process called continuous liquid interface production (CLIP) (Tumbleston et al. 2015). This technique uses photopolymerization to create smooth surface 3D objects with less than 100 µm resolution. Furthermore, unlike the traditional SL system which relies on layer by layer printing process, CLIP is continuous and can create objects up to 100 times faster than commercial 3D printings. In addition, CLIP process is compatible with producing 3D models from soft elastic materials as well as biological materials (Tumbleston et al. 2015). Considering these

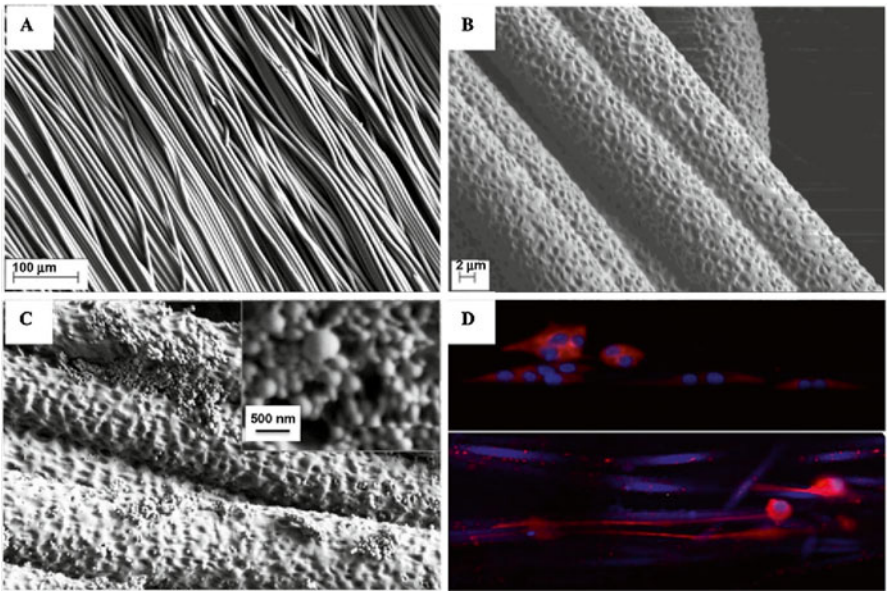

Fig. 1.12 SEM images of (**a**) an aligned electrospun neural scaffold fabricated in our lab; (**b**) random nanopores created on the surface of the electrospun fibers via solvent evaporation; (**c**) electrosprayed core-shell nanospheres incorporated aligned scaffold; and (**d**) confocal images of axons extension along the direction of aligned fibers (*red* represents the cell skeleton and axons)

advantageous features of CLIP, this new technology is very promising for use in neural tissue engineering.

Many current 3D bioprinting techniques exhibit difficulty in achieving a nano resolution for fabricating nanostructured tissue constructs. As a well-established nanofabrication technique, electrospinning has been employed to produce nanofibrous scaffolds that closely mimic native ECM for neural engineering. A recent study conducted in our lab investigated the effects of a highly aligned fibrous neural scaffold using electrospinning in conjunction with electrosprayed growth factor-encapsulated nanoparticles (Zhu et al. 2015) (Fig. 1.12). However, the electrospinning techniques often offer limited control over constructive geometry and porosity. To date, one interesting trend in the field is to combine the electrospinning technique and 3D printing system to fabricate a novel tissue scaffold with both nano and well-designed micro architecture (Centola et al. 2010; Lee et al. 2015). For example, Centola et al. have successfully combined electrospinning and FDM to fabricate artificial vascular graft. Such scaffold showed better mechanical properties compared to electrospun graft and induced endothelial differentiation. This implies that nano size features of electrospun fiber can improve the specificity and accuracy of 3D printed scaffolds for a number of tissue engineering applications including fabrication of neural scaffold.

1.4 Conclusion and Future Directions

Neural tissue engineering has successfully emerged as a promising field to address current complications in nerve injuries. Natural, synthetic, and conductive polymers are currently being most popularly investigated for uses as neural scaffold materials. Surface modification of scaffolds is also crucial to closely mimic the native ECM and to improve material biocompatibility. In addition, various 3D printing techniques were discussed as a tool to customize neural scaffolds for particular cells of interest. Many reports have shown that 3D printed scaffolds have highly flexible design and greatly enhanced neural cell functions, thus holding great promise for future neural regeneration applications. It is important to note that 3D printing is still in early phase for neural tissue regeneration. Currently, 3D printing is hindered by lack of available biomimetic materials as printing "inks" and advanced 3D printing platform for improved nano resolution and cell viability. In order to fabricate an ideal neural scaffold, development of novel biomimetic materials and sophisticated 3D printer is highly desirable.

Acknowledgments This work is supported by March of Dimes Foundation's Gene Discovery and Translational Research Grant and NIH Director's New Innovator Award 1DP2EB020549-01.

References

Abarrategi, A., et al. 2008. Multiwall Carbon Nanotube Scaffolds for Tissue Engineering Purposes. *Biomaterials* 29(1): 94–102.

Ai, J., et al. 2013. Polymeric Scaffolds in Neural Tissue Engineering: A Review. *Archives of Neuroscience* 1(1): 15–20.Aldinucci, Alessandra, et al. 2013. Carbon nanotube scaffolds instruct human dendritic cells: modulating immune responses by contacts at the nanoscale. *Nano letters* 13(12): 6098-6105.

Amado, S., et al. 2008. Use of hybrid chitosan membranes and N1E-115 cells for promoting nerve regeneration in an axonotmesis rat model. *Biomaterials* 29(33): 4409–4419.

Anon. 2011. Advances in Bioengineered Conduits for Peripheral Nerve Regeneration. *Atlas of the Oral and Maxillofacial Surgery Clinics of North America* 19(1): 119–130.

Arcaute, K., B.K. Mann, and R.B. Wicker. 2006. Stereolithography of Three-Dimensional Bioactive Poly(Ethylene Glycol) Constructs with Encapsulated Cells. *Annals of Biomedical Engineering* 34(9): 1429–1441.

Arcaute, K., B. Mann, and R. Wicker. 2010. Stereolithography of spatially controlled multi-material bioactive poly(ethylene glycol) scaffolds. *Acta Biomaterialia* 6(3): 1047–1054.

Archibald, S.J., et al. 1991. A Collagen-Based Nerve Guide Conduit for Peripheral Nerve Repair: An Electrophysiological Study of Nerve Regeneration in Rodents and Nonhuman Primates. *Journal of Comparative Neurology* 306(4): 685–696.

Archibald, S.J., et al. 1995. Monkey Median Nerve Repaired by Nerve Graft or Collagen Nerve Guide Tube. *The Journal of Neuroscience* 15(5): 4109–4123.

Bajaj, P., et al. 2014. 3D Biofabrication Strategies for Tissue Engineering and Regenerative Medicine. *Annual Review of Biomedical Engineering* 16(1): 247–276.

Balint, R., N.J. Cassidy, and S.H. Cartmell. 2014. Conductive Polymers: Towards a Smart Biomaterial for Tissue Engineering. *Acta Biomaterialia* 10(6): 2341–2353.

Barros, C.S., S.J. Franco, and U. Muller. 2011. Extracellular Matrix: Functions in the Nervous System. *Cold Spring Harbor Perspectives in Biology* 3(1): a005108.Billiet, T., et al. 2012. A review of trends and limitations in hydrogel-rapid prototyping for tissue engineering. *Biomaterials* 33(26): 6020-6041.

Boccaccini, A.R., et al. 2007. Carbon Nanotube Coatings on Bioglass-Based Tissue Engineering Scaffolds. *Advanced Functional Materials* 17(15): 2815–2822.

Bressan, E., et al. 2014. Graphene Based Scaffolds Effects on Stem Cells Commitment. *Journal of Translational Medicine* 12: 296.

Brushart, T.M., et al. 2005. Electrical Stimulation Restores the Specificity of Sensory Axon Regeneration. *Experimental Neurology* 194(1): 221–229.

Calvo, M., and D.L. Bennett. 2012. The Mechanisms of Microgliosis and Pain Following Peripheral Nerve Injury. *Experimental Neurology* 234(2): 271–282.

Ceballos, D., et al. 1999. Magnetically Aligned Collagen Gel Filling a Collagen Nerve Guide Improves Peripheral Nerve Regeneration. *Experimental Neurology* 158(2): 290–300.

Cen, L., et al. 2008. Collagen Tissue Engineering: Development of Novel Biomaterials and Applications. *Pediatric Research* 63(5): 492–496.

Centola, M., et al. 2010. Combining electrospinning and fused deposition modeling for the fabrication of a hybrid vascular graft. *Biofabrication* 2(1): 014102.

Chan, V., et al. 2010. Three-dimensional photopatterning of hydrogels using stereolithography for long-term cell encapsulation. *Lab on a Chip* 10(16): 2062–2070.

Chao, T.-I., et al. 2009. Carbon Nanotubes Promote Neuron Differentiation from Human Embryonic Stem Cells. *Biochemical and Biophysical Research Communications* 384(4): 426–430.

Choi, W.S., et al. 2011. Synthetic Multicellular Cell-to-Cell Communication in Inkjet Printed Bacterial Cell Systems. *Biomaterials* 32(10): 2500–2507.

Cui, X., et al. 2001. Electrochemical Deposition and Characterization of Conducting Polymer Polypyrrole/PSS on Multichannel Neural Probes. *Sensors and Actuators A: Physical* 93(1): 8–18.

Cullen, D.K., et al. 2008. Developing a Tissue-Engineered Neural-Electrical Relay Using Encapsulated Neuronal Constructs on Conducting Polymer Fibers. *Journal of Neural Engineering* 5(4): 374–384.

Daly, W., et al. 2011. A Biomaterials Approach to Peripheral Nerve Regeneration: Bridging the Peripheral Nerve Gap and Enhancing Functional Recovery. *Journal of the Royal Society Interface* 9(67): 202–221.

Domingos, M., et al. 2009. Polycaprolactone Scaffolds Fabricated Via Bioextrusion for Tissue Engineering Applications. *International Journal of Biomaterials* 2009(5): 1–9.

Evans, G.R.D., et al. 1999. In Vivo Evaluation of Poly(L-Lactic Acid) Porous Conduits for Peripheral Nerve Regeneration. *Biomaterials* 20: 1109–1115.

Gaudet, A.D., P.G. Popovich, and M.S. Ramer. 2011. Wallerian Degeneration: Gaining Perspective on Inflammatory Events After Peripheral Nerve Injury. *Journal of Neuroinflammation* 8(1): 110.Geim, A.K., and K.S. Novoselov. 2007. The rise of graphene. *Nature materials* 6(3): 183-191.

George, P.M., et al. 2005. Fabrication and Biocompatibility of Polypyrrole Implants Suitable for Neural Prosthetics. *Biomaterials* 26(17): 3511–3519.

Ghasemi-Mobarakeh, L., et al. 2011. Application of Conductive Polymers, Scaffolds and Electrical Stimulation for Nerve Tissue Engineering. *Journal of Tissue Engineering and Regenerative Medicine* 5(4): e17–e35.Gladwin, Karen M., et al. 2013. In vitro biocompatibility of multi-walled carbon nanotubes with sensory neurons. *Advanced healthcare materials* 2.5: 728-735.

Glowacki, J., and S. Mizuno. 2008. Collagen Scaffolds for Tissue Engineering. *Biopolymers* 89(5): 338–344.

Green, R.A., et al. 2008. Novel Neural Interface for Implant Electrodes: Improving Electroactivity of Polypyrrole Through MWNT Incorporation. *Journal of Materials Science: Materials in Medicine* 19(4): 1625–1629.

Green, R.A., et al. 2012. Conductive Hydrogels: Mechanically Robust Hybrids for Use as Biomaterials. *Macromolecular Bioscience* 12(4): 494–501.

Gunatillake, P.A., and R. Adhikari. 2003. Biodegradable Synthetic Polymers for Tissue Engineering. *European Cells and Materials* 5: 1–16.

Hanna, A., and R. Dempsey. 2013. Nerve Conduits Used for End-to-Side Grafting After Nerve Injury. *Neurosurgery* 72(2): N15–N16.Hanson Shepherd, J.N., et al. 2011. 3D microperiodic hydrogel scaffolds for robust neuronal cultures. *Advanced functional materials* 21.1: 47-54.

Harrison, B.S., and A. Atala. 2007. Carbon Nanotube Applications for Tissue Engineering. *Biomaterials* 28(2): 344–353.

Hasirci, V., et al. 2014. Peripheral Nerve Conduits: Technology Update. *Medical Devices: Evidence and Research* 7: 405–420.

Hodde, J. 2002. Naturally Occurring Scaffolds for Soft Tissue Repair and Regeneration. *Tissue Engineering* 8(2): 295–308.

Huang, Y.C., and Y.Y. Huang. 2006. Biomaterials and Strategies for Nerve Regeneration. *Artificial Organs* 30(7): 514–522.

Huang, Y.C., et al. 2007. Surface Modification and Characterization of Chitosan or PLGA Membrane with Laminin by Chemical and Oxygen Plasma Treatment for Neural Regeneration. *Journal of Biomedical Materials Research. Part A* 82(4): 842–851.

Ilkhanizadeh, S., A. Teixeira, and O. Hermanson. 2007. Inkjet Printing of Macromolecules on Hydrogels to Steer Neural Stem Cell Differentiation. *Biomaterials* 28(27): 3936–3943.

Jacobs, P.F., and D.T. Reid. 1992. *Rapid Prototyping & Manufacturing: Fundamentals of Stereolithography*. Dearborn: Society of Manufacturing Engineers in Cooperation with the Computer and Automated Systems Association of SME.

Jeans, L.A., T. Gilchrist, and D. Healy. 2007. Peripheral Nerve Repair by Means of a Flexible Biodegradable Glass Fibre Wrap: A Comparison with Microsurgical Epineurial Repair. *Journal of Plastic, Reconstructive & Aesthetic Surgery* 60(12): 1302–1308.

Jin, G., and K. Li. 2014. The Electrically Conductive Scaffold as the Skeleton of Stem Cell Niche in Regenerative Medicine. *Materials Science and Engineering: C* 45: 671–681.

Jin, L., et al. 2012. A Novel Fluffy Conductive Polypyrrole Nano-Layer Coated Plla Fibrous Scaffold for Nerve Tissue Engineering. *Journal of Biomedical Nanotechnology* 8(5): 779–785.

Keefer, E.W., et al. 2008. Carbon Nanotube Coating Improves Neuronal Recordings. *Nature Nanotechnology* 3(7): 434–439.

Khaing, Z.Z., and C.E. Schmidt. 2012. Advances in Natural Biomaterials for Nerve Tissue Repair. *Neuroscience Letters* 519(2): 103–114.

Khatri, Z., and M.H. Peerzada. 2014. Electrospun Polycaprolactone/Polylactic Acid Nanofibers as an Artificial Nerve Conduit. *Mehran University Research Journal of Engineering and Technology* 33: 304–308.

Kiernan, J., and R. Rajakumar. 2013. *Barr's the Human Nervous System: An Anatomical Viewpoint*. Baltimore: Lippincott Williams and Wilkins.

Krämer, M., et al. 2011. Aligned Neurite Outgrowth on Electrospun PLGA Nanofibres. *European Cells and Materials* 22(Suppl 2): 59.

Kumar, D., and R.C. Sharma. 1998. Advances in Conductive Polymers. *European Polymer Journal* 34(8): 1053–1060.

Landers, R., and R. Mülhaupt. 2000. Desktop Manufacturing of Complex Objects, Prototypes and Biomedical Scaffolds by Means Of Computer-Assisted Design Combined with Computer-Guided 3D Plotting of Polymers and Reactive Oligomers. *Macromolecular Materials and Engineering* 282(1): 17–21.

Lee, J.Y., et al. 2009. Polypyrrole-Coated Electrospun PLGA Nanofibers for Neural Tissue Applications. *Biomaterials* 30(26): 4325–4335.

Lee, B.K., et al. 2012. End-to-Side Neurorrhaphy Using an Electrospun PCL/Collagen Nerve Conduit for Complex Peripheral Motor Nerve Regeneration. *Biomaterials* 33(35): 9027–9036.

Lee, S.J., et al. 2015. Characterization and Preparation of Bio-tubular Scaffolds for Fabricating Artificial Vascular Grafts by Combining Electrospinning and a 3D Printing System. *Physical Chemistry Chemical Physics* 17: 2996–2999.Li, Ning, et al. 2013. Three-dimensional graphene foam as a biocompatible and conductive scaffold for neural stem cells. *Scientific reports,* 3.

Li, S.T., et al. 1992. Peripheral nerve repair with collagen conduits. *Clinical Materials* 9(3): 195–200.

Lin, M.Y., G. Manzano, and R. Gupta. 2013. Nerve Allografts and Conduits in Peripheral Nerve Repair. *Hand Clinics* 29(3): 331–348.

Liu, J.J., et al. 2011. Peripheral Nerve Regeneration Using Composite Poly(Lactic Acid-Caprolactone)/Nerve Growth Factor Conduits Prepared by Coaxial Electrospinning. *Journal of Biomedical Materials Research. Part A* 96(1): 13–20.

MacDiarmid, A.G. 2001. "Synthetic Metals": A Novel Role for Organic Polymers (Nobel Lecture). *Angewandte Chemie International Edition* 40(14): 2581–2590.

MacDonald, R.A., et al. 2005. Collagen–Carbon Nanotube Composite Materials as Scaffolds in Tissue Engineering. *Journal of Biomedical Materials Research. Part A* 74(3): 489–496.

Mackinnon, S.E., and A.L. Dellon. 1990. A Study of Nerve Regeneration Across Synthetic (Maxon) and Biologic (Collagen) Nerve Conduits for Nerve Gaps up to 5 cm in the Primate. *Journal of Reconstructive Microsurgery* 6(2): 117–121.

Matsumine, H., et al. 2014. A Polylactic Acid Non-woven Nerve Conduit for Facial Nerve Regeneration in Rats. *Journal of Tissue Engineering and Regenerative Medicine* 8(6): 454–462.

Meaney, D.F., and D.H. Smith. 2014. Cellular Biomechanics of Central Nervous System Injury. *Handbook of Clinical Neurology* 127: 105–114.

Mihardja, S.S., R.E. Sievers, and R.J. Lee. 2008. The Effect of Polypyrrole on Arteriogenesis in an Acute Rat Infarct Model. *Biomaterials* 29(31): 4205–4210.

Miyata, T., T. Taira, and Y. Noishiki. 1992. Collagen Engineering for Biomaterial Use. *Clinical Materials* 9(3): 139–148.

Mobasseri, A., et al. 2015. Polymer Scaffolds with Preferential Parallel Grooves Enhance Nerve Regeneration. *Tissue Engineering Part A* 21: 1152–1162.

Mollers, S., et al. 2009. Cytocompatibility of a Novel, Longitudinally Microstructured Collagen Scaffold Intended for Nerve Tissue Repair. *Tissue Engineering. Part A* 15: 1–13.

Mosahebi, A., M. Wiberg, and G. Terenghi. 2003. Addition of Fibronectin to Alginate Matrix Improves Peripheral Nerve Regeneration in Tissue-Engineered Conduits. *Tissue Engineering* 9(2): 209–218.

Mozafari, M., et al. 2012. Electroconductive Nanocomposite Scaffolds: A New Strategy into Tissue Engineering and Regenerative Medicine. In *Nanocomposites—New Trends and Developments*. InTech.Murphy, S.V., and A. Atala. 2014. 3D bioprinting of tissues and organs. *Nature biotechnology* 32(8): 773-785.

Nectow, A.R., K.G. Marra, and D.L. Kaplan. 2012. Biomaterials for the Development of Peripheral Nerve Guidance Conduits. *Tissue Engineering, Part B: Reviews* 18(1): 40–50.

Nickels, J.D., and C.E. Schmidt. 2012. Surface Modification of the Conducting Polymer, Polypyrrole, Via Affinity Peptide. *Journal of Biomedical Materials Research. Part A* 101A(5): 1464–1471.

Niu, Y., et al. 2014. Scaffolds from Block Polyurethanes Based on Poly(ε-Caprolactone) (PCL) and Poly(Ethylene Glycol) (PEG) for Peripheral Nerve Regeneration. *Biomaterials* 35(14): 4266–4277.

Ohta, M., et al. 2004. Novel Heparin/Alginate Gel Combined with Basic Fibroblast Growth Factor Promotes Nerve Regeneration in Rat Sciatic Nerve. *Journal of Biomedical Materials Research. Part A* 71(4): 661–668.

Park, S.Y., et al. 2011. Enhanced Differentiation of Human Neural Stem Cells into Neurons on Graphene. *Advanced Materials* 23(36): H263–H267.

Perry, V.H., and J. Teeling. 2013. Microglia and Macrophages of the Central Nervous System: The Contribution of Microglia Priming and Systemic Inflammation to Chronic Neurodegeneration. *Seminars in Immunopathology* 35(5): 601–612.

Pfister, L.A., et al. 2007. Hydrogel Nerve Conduits Produced from Alginate/Chitosan Complexes. *Journal of Biomedical Materials Research. Part A* 80(4): 932–937.

Pfister, L.A., et al. 2008. Controlled Nerve Growth Factor Release from Multi-Ply Alginate/ Chitosan-Based Nerve Conduits. *European Journal of Pharmaceutics and Biopharmaceutics* 69(2): 563–572.

Plikk, P., S. Målberg, and A.C. Albertsson. 2009. Design of Resorbable Porous Tubular Copolyester Scaffolds for Use in Nerve Regeneration. *Biomacromolecules* 10(5): 1259–1264.

Reid, A.J., et al. 2013. Long term peripheral nerve regeneration using a novel PCL nerve conduit. *Neuroscience Letters* 544: 125–130.

Richardson-Burns, S.M., et al. 2007. Polymerization of the Conducting Polymer Poly(3, 4-Ethylenedioxythiophene) (PEDOT) Around Living Neural Cells. *Biomaterials* 28(8): 1539–1552.

Roth, E.A., et al. 2004. Inkjet Printing for High-Throughput Cell Patterning. *Biomaterials* 25(17): 3707–3715.

Runge, M.B., et al. 2010. The Development of Electrically Conductive Polycaprolactone Fumarate–Polypyrrole Composite Materials for Nerve Regeneration. *Biomaterials* 31(23): 5916–5926.

Rutka, J.T., et al. 1998. The Extracellular Matrix of the Central and Peripheral Nervous Systems: Structure and Function. *Journal of Neurosurgery* 69: 1–16.

Sanjana, N.E., and S.B. Fuller. 2004. A Fast Flexible Ink-Jet Printing Method for Patterning Dissociated Neurons in Culture. *Journal of Neuroscience Methods* 136(2): 151–163.

Schmidt, C.E., and J.B. Leach. 2003. Neural Tissue Engineering: Strategies for Repair and Regeneration. *Annual Review of Biomedical Engineering* 5(1): 293–347.

Shi, X., et al. 2007. Fabrication of Porous Ultra-Short Single-Walled Carbon Nanotube Nanocomposite Scaffolds for Bone Tissue Engineering. *Biomaterials* 28(28): 4078–4090.

Shim, S.W., et al. 2015. Evaluation of Small Intestine Submucosa and Poly(Caprolactone-Co-Lactide) Conduits for Peripheral Nerve Regeneration. *Tissue Engineering Part A*. 21(5–6): 1142–1151.

Sivak, W.N., J.M. Bliley, and K.G. Marra. 2014. In *Polymeric Biomaterials for Nerve Regeneration: Fabrication and Implantation of a Biodegradable Nerve Guide A*, vol. 1162, ed. J. Murray, 139–148.

Skoog, S.A., P.L. Goering, and R.J. Narayan. 2013. Stereolithography in Tissue Engineering. *Journal of Materials Science: Materials in Medicine* 25(3): 845–856.

Song, Q., et al. 2014. Anti-inflammatory Effects of Three-Dimensional Graphene Foams Cultured with Microglial Cells. *Biomaterials* 35(25): 6930–6940.

Subramanian, A., U. Krishnan, and S. Sethuraman. 2009. Development of Biomaterial Scaffold for Nerve Tissue Engineering: Biomaterial Mediated Neural Regeneration. *Journal of Biomedical Science* 16(1): 108.

Sufan, W., et al. 2001. Sciatic Nerve Regeneration Through Alginate with Tubulation or Nontubulation Repair in Cat. *Journal of Neurotrauma* 18(3): 329–338.

Sulaiman, W., and T. Gordon. 2013. Neurobiology of Peripheral Nerve Injury, Regeneration, and Functional Recovery: From Bench Top Research to Bedside Application. *The Ochsner Journal* 13(1): 100–108.

Sun, M., et al. 2010. In Vitro and In Vivo Testing of Novel Ultrathin PCL and PCL/PLA Blend Films as Peripheral Nerve Conduit. *Journal of Biomedical Materials Research. Part A* 93(4): 1470–1481.

Sundback, C., et al. 2003. Manufacture of Porous Polymer Nerve Conduits by a Novel Low-Pressure Injection Molding Process. *Biomaterials* 24(5): 819–830.Suri, S., et al. 2011. Solid freeform fabrication of designer scaffolds of hyaluronic acid for nerve tissue engineering. *Biomedical microdevices* 13(6): 983-993.

Suzuki, Y., et al. 1999. Cat Peripheral Nerve Regeneration Across 50 mm Gap Repaired with a Novel Nerve Guide Composed of Freeze-Dried Alginate Gel. *Neuroscience Letters* 259(2): 75–78.

Tam, R.Y., et al. 2013. Regenerative Therapies for Central Nervous System Diseases: A Biomaterials Approach. *Neuropsychopharmacology* 39(1): 169–188.

Tarun, G., et al. 2012. Biomaterials Review. *International Research Journal of Pharmacy* 1–6.

Tran, P.A., L. Zhang, and T.J. Webster. 2009. Carbon Nanofibers and Carbon Nanotubes in Regenerative Medicine. *Advanced Drug Delivery Reviews* 61(12): 1097–1114.

Tumbleston, J.R., et al. 2015. Continuous Liquid Interface Production of 3D Objects. *Science* 347(6228): 1349–1352.

Turcu, F., et al. 2003. Ink-Jet Printing for Micropattern Generation of Laminin for Neuronal Adhesion. *Journal of Neuroscience Methods* 131(1–2): 141–148.

Verreck, G., et al. 2005. Preparation and Physicochemical Characterization of Biodegradable Nerve Guides Containing the Nerve Growth Agent Sabeluzole. *Biomaterials* 26(11): 1307–1315.

Vleggeert-Lankamp, C.L.A.M., et al. 2007. Pores In Synthetic Nerve Conduits Are Beneficial to Regeneration. *Journal of Biomedical Materials Research. Part A* 80A(4): 965–982.

Walker, P.A., et al. 2009. Advances in Progenitor Cell Therapy Using Scaffolding Constructs for Central Nervous System Injury. *Stem Cell Reviews and Reports* 5(3): 283–300.

Wang, X., et al. 2012. Hyaluronic Acid-Based Scaffold for Central Neural Tissue Engineering. *Interface Focus* 2(3): 278–291.

Wang, M.-D., et al. 2013. Novel Crosslinked Alginate/Hyaluronic Acid Hydrogels for Nerve Tissue Engineering. *Frontiers of Materials Science* 7(3): 269–284.

Weng, B., et al. 2012. Inkjet Printed Polypyrrole/Collagen Scaffold: A Combination of Spatial Control and Electrical Stimulation of PC12 Cells. *Synthetic Metals* 162(15): 1375–1380.

Widmer, M.S., et al. 1998. Manufacture of Porous Biodegradable Polymer Conduits by an Extrusion Process for Guided Tissue Regeneration. *Biomaterials* 19: 1945–1955.

Zhu, W., et al. 2015. Highly Aligned Nanocomposite Scaffolds by Electrospinning and Electrospraying for Neural Tissue Regeneration. *Nanomedicine: Nanotechnology, Biology, and Medicine* 11(3): 693–704.

Wu, S., et al. 2001. Migration, Integration, and Differentiation of Hippocampus-Derived Neurosphere Cells After Transplantation into Injured Rat Spinal Cord. *Neuroscience Letters* 312(3): 173–176.

Xie, J., et al. 2009. Conductive Core–Sheath Nanofibers and Their Potential Application in Neural Tissue Engineering. *Advanced Functional Materials* 19(14): 2312–2318.

Xu, T., et al. 2009. Electrophysiological Characterization of Embryonic Hippocampal Neurons Cultured in a 3D Collagen Hydrogel. *Biomaterials* 30(26): 4377–4383.

Xu, T., et al. 2013. Complex Heterogeneous Tissue Constructs Containing Multiple Cell Types Prepared by Inkjet Printing Technology. *Biomaterials* 34(1): 130–139.

Yang, F., et al. 2004. Fabrication of Nano-Structured Porous PLLA Scaffold Intended for Nerve Tissue Engineering. *Biomaterials* 25(10): 1891–1900.

Zamani, F., et al. 2013. The influence of surface nanoroughness of electrospun PLGA nanfibrous scaffold on nerve cell adhesion and proliferation. *Journal of Materials Science: Materials in Medicine* 24: 1551–1560.

Zheng, Q., et al. 2011. Application of inkjet printing technique for biological material delivery and antimicrobial assays. *Analytical Biochemistry* 410(2): 171–176.

Zhu, N., and X. Che. 2013. Biofabrication of tissue scaffolds. In *Advances in Biomaterials Science and Biomedical Applications*. InTech.

Zimmermann, D.R., and M.T. Dours-Zimmermann. 2008. Extracellular matrix of the central nervous system: from neglect to challenge. *Histochemistry and Cell Biology* 130(4): 635–653. Zorlutuna, P., et al. 2011. Stereolithography-Based Hydrogel Microenvironments to Examine Cellular Interactions. *Advanced Functional Materials* 21(19): 3642-3651.

Zorlutuna, P., N.E. Vrana, and A. Khademhosseini. 2013. The Expanding World of Tissue Engineering: The Building Blocks and New Applications of Tissue Engineered Constructs. *IEEE Reviews in Biomedical Engineering* 6: 47–62.

Chapter 2
Stem Cells, Bioengineering, and 3-D Scaffolds for Nervous System Repair and Regeneration

Elizabeth J. Sandquist, Metin Uz, Anup D. Sharma, Bhavika B. Patel, Surya K. Mallapragada, and Donald S. Sakaguchi

Abbreviations

ADSCs	Adipose-derived stem cells
BBB	Blood–brain barrier
BDNF	Brain-derived neurotrophic factor
bFGF	Basic fibroblast growth factor
c-Myc	V-Myc avian myelocytomatosis viral oncogene homolog
CNS	Central nervous system
CNTF	Ciliary-neurotrophic factor
CNTs	Carbon nanotubes
DNA	Deoxyribonucleic acid
DPSCs	Dental pulp stem cells
DRG	Dorsal root ganglia

E.J. Sandquist
Department of Genetics, Development and Cell Biology, Iowa State University, Ames, IA 50011, USA

M. Uz
Department of Chemical and Biological Engineering, Iowa State University, Ames, IA 50011, USA

A.D. Sharma • S.K. Mallapragada
Department of Chemical and Biological Engineering, Iowa State University, Ames, IA 50011, USA

Neuroscience Program, Iowa State University, Ames, IA 50011, USA

B.B. Patel • D.S. Sakaguchi (✉)
Department of Genetics, Development and Cell Biology, Iowa State University, Ames, IA 50011, USA

Neuroscience Program, Iowa State University, Ames, IA 50011, USA
e-mail: dssakagu@iastate.edu

L.G. Zhang, D.L. Kaplan (eds.), *Neural Engineering*,
DOI 10.1007/978-3-319-31433-4_2

ECM	Extracellular matrix
EGF	Epidermal growth factor
En1	Engrailed homeobox 1
ERK	Extracellular signal-regulated kinases
ESCs	Embryonic stem cells
FGF-2	Fibroblast growth factor-2
GABAergic	Gamma-aminobutyric acid-ergic
GDNF	Glial cell line-derived neurotrophic factor
GFP	Green fluorescent protein
hdpPSCs	Human decidua parietalis placental stem cells
HUVECs	Human umbilical vein endothelial cells
iPSCs	Induced pluripotent stem cells
Klf4	Kruppel-like factor 4
MAP2	Microtubule-associated protein 2
mm	Millimeters
MNPs	Magnetic nanoparticles
MSCs	Mesenchymal stem cells
NANOG	Nanog Homeobox
NGF	Nerve growth factor
nm	Nanometers
NPCs	Neural progenitor cells
NSCs	Neural stem cells
NT-3	Neurotrophin-3
Nurr1	Nuclear receptor related 1
Oct4	Octamer-binding transcription factor 4
OECs	Olfactory ensheathing cells
PBCA	Polybutylcyanoacrylate
PCL	Poly(ε-caprolactone)
PCLEEP	ε-Caprolactone and ethyl ethylene phosphate copolymer
PD	Parkinson's disease
PEG	Polyethylene glycol
PEI	Polyethylenimine
PHT	Poly(3-hexylthiophene)
PLA	Poly(lactic acid)
PLGA	Poly(D,L-lactide-co-glycolide)
PLLA	Poly(L-lactic acid)
PNS	Peripheral nervous system
PPC	Poly(propylene carbonate)
PPE	Poly(phosphoester)
Ppy	Polypyrrol
PVA	Poly(vinyl alcohol)
RA	Retinoic acid
RGCs	Retinal ganglion cells
RhoG	Ras homology growth-related
RNA	Ribonucleic acid

RPCs	Retinal progenitor cells
SCs	Stem cells
SF	Silk fibroin
SHEDs	Stem cells from human exfoliated deciduous teeth
siRNA	Small interfering RNA
Sox2	Sex determining region Y-box 2
TuJ1	Class III β-tubulin
VEGF	Vascular endothelial growth factor
Wnt1	Wingless-type MMTV integration site family, member 1
β-NGF	β-Nerve growth factor
β-TCP	β-Tricalcium phosphate

2.1 Introduction

A fundamental issue in biology concerns how cells establish and maintain their identity during early embryogenesis. Gaining a better understanding of these rules is key to future development of experimental therapeutics and is an important foundation of tissue engineering and regenerative medicine. With the successful isolation of embryonic stem cells and the emergence of induced pluripotent stem cell technologies, it has become achievable to recapitulate developmental processes of early development. Furthermore, the advent of cellular reprogramming and transdifferentiation technologies has made it possible to implement rational strategies to generate specific cell types in order to model neurodegenerative diseases and develop cell-based therapies for nervous system disorders. Moreover, with advances in biomaterials and in 3-D scaffold fabrication techniques, it is becoming possible to mimic the neural stem cell niche. In this chapter, we provide an overview of approaches merging stem cells, polymeric scaffolds, drug delivery systems, gene therapy, cellular engineering, and biomaterials to develop experimental strategies for neural tissue engineering. Combined, these enabling technologies are likely to be beneficial for development of therapeutic interventions for translation to the clinic. A summary of a number of current clinical trials is also presented at the end to illustrate how combination of these technologies is helping nervous system rescue and repair.

2.2 Stem Cells

Multipotent stem cells were first identified in the hematopoietic system, identified by their ability to self-renew and differentiate into multiple cell types (Till and Mc 1961; Siminovitch et al. 1963). Stem cells undergo asymmetric cell division, in which progeny include one cell identical to the stem cell and another, unique cell type that undergoes differentiation. These properties are attractive to the field of

regenerative biology, which seeks to replace cells lost to disease or damage. Stem cells from a variety of sources have been used in the field of developmental neuroscience as well as in search of therapeutic treatment for neurodegenerative diseases including Alzheimer's and Parkinson's, and damage such as that from stroke and traumatic brain injury. Stem cells are broadly categorized by their differentiation potential, from totipotent cells, which are able to recapitulate all cells in an organism, to multipotent cells, which differentiate into a limited number of cell types(s).

2.2.1 Pluripotent Stem Cells

Pluripotent stem cells create progeny that differentiate into cells from all three germ layers. Expression of the transcription factors Oct4, Sox2, and NANOG are indicative of pluripotency (Chambers and Smith 2004; Chambers et al. 2003; Masui et al. 2007). Proof of cell pluripotency is evidenced by the formation of teratomas, tumors containing cells of ecto-, meso-, and endodermal origin, when injected into an animal model (Kleinsmith and Pierce 1964). Pluripotency is also confirmed by the ability to generate chimeric mice, in which the original embryonic stem cells are successfully replaced by stem cells of another origin (Gardner 1968).

2.2.1.1 Pluripotent Embryonic Stem Cells

Embryonic stem cells (ESCs) were first isolated in 1966 from the inner cell mass of the blastocyst, a population of cells which gives rise to the embryo (Cole et al. 1966; Evans and Kaufman 1981). Implantation of mouse embryonic stem cells into blastocysts of another strain generated chimeric mice, proving their pluripotency (Gardner 1968). The first successful graft of ESCs was to the hematopoietic system, in which transplanted cells repopulated the bone marrow of irradiated mice (Hollands 1987). In 1998, Thomson and colleagues were the first to derive ESCs from human blastocysts (Thomson et al. 1998).

Embryonic stem cells can be induced toward neuronal lineages through the application of retinoic acid (RA) (Bain et al. 1995; Mujtaba et al. 1999; Schuldiner et al. 2001). Additionally, ESCs proliferate in the presence of basic fibroblast growth factor (bFGF), while withdrawal of bFGF promotes neural and glial differentiation (Okabe et al. 1996). After removal of self-renewing factors, human ESCs differentiate naturally into neuroepithelia (Zhang et al. 2001). Glial precursor cells that develop into oligodendrocytes and astrocytes have also been derived from ESCs (Brüstle et al. 1999). Embryonic stem cells have been successfully differentiated into a number of neural types, including dopaminergic and serotonergic neurons (Lee et al. 2000), GABAergic neurons (Westmoreland et al. 2001), motor neurons (Wichterle et al. 2002), telencephalic neurons (Li et al. 2009), cholinergic neurons (Bissonnette et al. 2011), and cortical neurons (Gaspard et al. 2008). Embryonic stem cells have also been differentiated into cells of the eye (Fig. 2.1), including

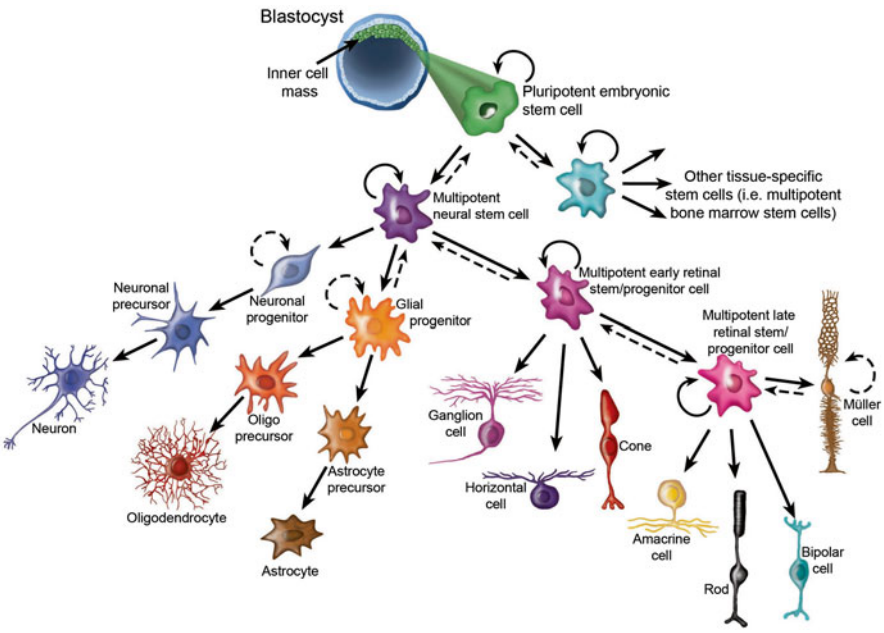

Fig. 2.1 Stem cell hierarchy and multipotency of neural and retinal stem cells. Pluripotent embryonic stem cells (ESC) are derived from the inner cell mass of a blastocyst (in humans the blastocyst stage is about 4–5 days post fertilization). Under appropriate culture conditions, the ESC can produce multipotent tissue specific stem cells from all three germ layers (ectoderm, mesoderm and endoderm). This illustration depicts the generation of differentiated cell types from multipotent neural and retinal stem cells. Multipotent neural stem cells generate the three major neural cell types present within the central nervous system (CNS): neurons, oligodendrocytes and astrocytes. Multipotent retinal stem cells produce the seven major cell types found within the vertebrate retina including: ganglion cells, horizontal cells, cone and rod photoreceptors, amacrine cells, bipolar cells, and Müller glial cells. *Arrows* curling back onto the same cell represent the ability for self-renewal, while *reversed arrows* represent possible reprogramming events

retinal progenitors (Lamba et al. 2009; Meyer et al. 2009), photoreceptor precursors (Gonzalez-Cordero et al. 2013), and retinal pigment epithelial cells (Klimanskaya et al. 2004).

Embryonic stem cells have been tested for their therapeutic application in numerous neurodegenerative diseases and injuries; including Huntington's, Alzheimer's, and Parkinson's disease, as well as spinal cord injury, traumatic brain injury and stroke, with varying success. In rodent models of Parkinson's disease, transplantation of undifferentiated ESCs, dopaminergic precursor cells, and dopaminergic neurons derived from ESCs recovered motor function (Bjorklund et al. 2002; Kim et al. 2002; Kriks et al. 2011; Yang et al. 2008). Implantation of ESCs has also improved behavioral deficits in models of Huntington's disease (Song et al. 2007). Rodent models of Alzheimer's disease have shown cognitive improvement following transplantation of ESC-derived neural stem cells in the cortex (Wang et al. 2006).

Embryonic stem cells and ESC-derived neural stem cells demonstrated functional engraftment in models of stroke (Daadi et al. 2008; Yanagisawa et al. 2006), as well. Implantation of ESC-derived GABAergic interneurons for treatment of epilepsy have also been positive, with reduced seizures and abnormal behavior in epileptic mice (Cunningham et al. 2014). Transplantation of ESC-derived retinal pigment epithelial cells to the eye has proved quite successful for the treatment of degenerative eye diseases, with promising clinical trials for age-related macular degeneration and Stargardt's macular dystrophy (Schwartz et al. 2012).

Embryonic stem cells have also been tested for central nervous system (CNS) injury. Undifferentiated ESCs, ES-derived motor neurons, and ESCs differentiated into neural progenitors improved motor function following transplantation in spinal cord injured mice (Bottai et al. 2010; McDonald et al. 1999; Deshpande et al. 2006; Marques et al. 2010). Neural and glial precursors differentiated from ESCs implanted following traumatic brain injury recovered sensorimotor function, but not cognitive function (Hoane et al. 2004).

While the therapeutic use of ESCs is promising, it comes with considerable ethical and political challenges. The isolation of ESCs causes the destruction of a human embryo. While many feel the potential benefits of human ES research outweigh these ethical objections it still remains a significant moral dilemma. As such, it is essential that a critical analysis of these issues continue as policies are established to regulate this biomedical research.

2.2.1.2 Induced Pluripotent Stem Cells

The ability to derive pluripotent stem cells from adult tissues has reduced many of the ethical barriers associated with stem cell research. Induced pluripotent stem cells, or iPSCs, are created by de-differentiating adult somatic cells such as skin fibroblasts in vitro, allowing for direct transplantation or further re-differentiation into other cell types. Another advantage of iPSCs is the potential to generate patient-specific stem cells, reducing graft-host reactions. The first evidence that somatic cells could be reverted to a pluripotent state was demonstrated by nuclear transfer in 1966, in which transplantation of adult intestinal nuclei into enucleated frog eggs resulted in the development of normal, fertile adult frogs (Gurdon and Uehlinger 1966).

Cellular reprogramming to a pluripotent state can be initiated through three mechanisms: nuclear transfer, cell fusion, and transcription-factor transduction. Somatic cell nuclear transfer was successfully achieved in mice in 1998, utilizing enucleated oocytes rather than eggs (Wakayama et al. 1998). From a therapeutic standpoint, this approach has the appeal of the ability to generate patient specific-pluripotent stem cells that would be compatible for autologous transplantation (Fig. 2.2). Nuclear fusion is another way to generate pluripotent cells, through the fusion of one ES and one somatic cell. This technique has proven particularly useful for the study of regulatory mechanisms of pluripotency, in which regulators of pluripotency override those for differentiation (Tada et al. 2001). The method that has gained the most attention is transcription factor transduction, in which the

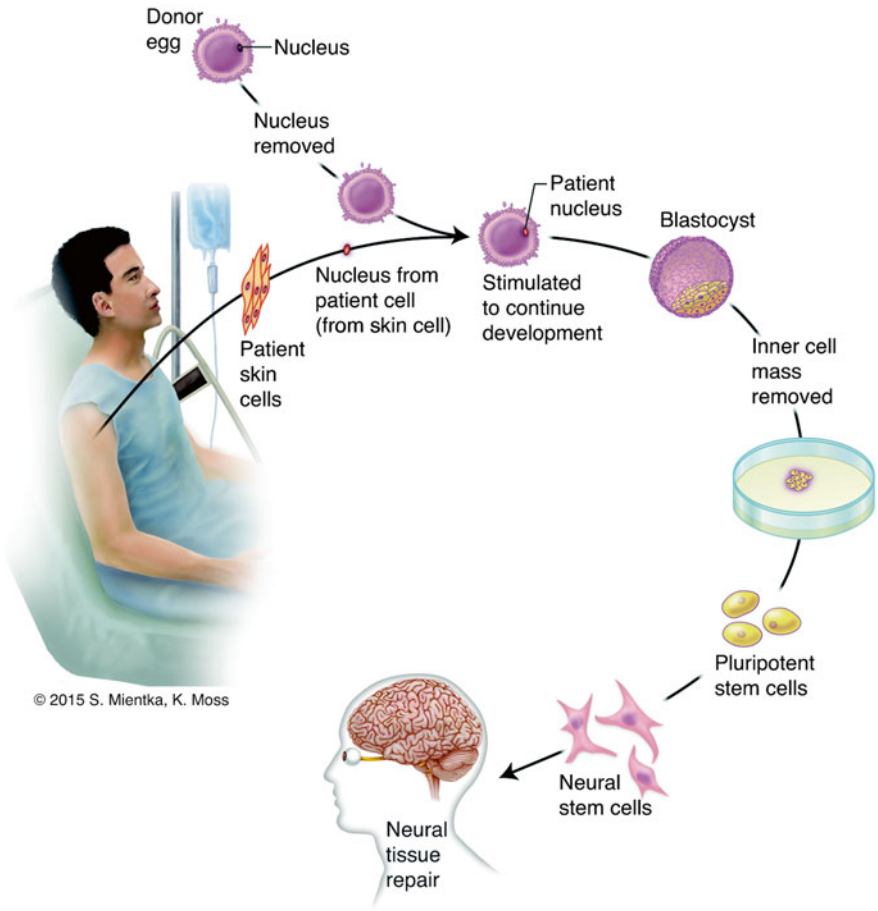

Fig. 2.2 Somatic cell nuclear transfer would provide a means to generate patient–specific pluripotent cells that could then be used for disease research or therapeutics. Eggs are procured from consenting donors and the nucleus of the donor egg cell is removed. Somatic cells from the patient (such as skin cells, fat cells, or other differentiated cells) are isolated and the nucleus of a somatic cell is collected and then transferred into the enucleated donor egg. The egg, containing the somatic cell's nucleus, is stimulated to divide and develops in vitro into a blastocyst. At that point, the cells of the inner cell mass are isolated and grown as pluripotent stem cells. These pluripotent stem cells can then be differentiated toward neural lineages that may be used for treating the patient suffering from the neurological disorder

introduction of four transcription factors is sufficient to induce a pluripotent state. These four factors, coined as the "Yamanaka factors," include Oct4, Sox2, Klf4, and c-Myc and were established by S. Yamanaka and colleagues in 2006 and continue to play an important part in cellular therapies (Takahashi and Yamanaka 2006).

Induced pluripotent stem cells have been differentiated into neural precursors (Zhou et al. 2010), oligodendrocyte precursors (Wang et al. 2013), dopaminergic

neurons (Kriks et al. 2011), cortical neurons (Shi et al. 2012), motor neurons (Karumbayaram et al. 2009; Chambers et al. 2009), and retinal cells (Hirami et al. 2009). Neuronal differentiation from iPSCs is commonly achieved through a combination of embryoid body culture, retinoic acid application, and Sonic Hedgehog pathway agonists. Synthetic small molecules for neural differentiation are being used to alter these signaling pathways in order to promote differentiation into specific cell lineages (Skalova et al. 2015).

Neurons originating from iPSCs are currently being tested for their therapeutic applications. Induced pluripotent stem cell-derived dopaminergic neurons transplanted into animal models of Parkinson's disease have resulted in improved functional recovery (Kriks et al. 2011; Wernig et al. 2008). Oligodendrocyte precursors derived from iPSCs demonstrated functional improvement in congenital hypomyelination disorder (Wang et al. 2013). Additionally, animal models of multiple sclerosis have ameliorated clinical features following transplant of iPSC-derived neural precursors (Laterza et al. 2013). In amyotrophic lateral sclerosis (ALS), implants of iPSC-derived neural stem cells improved neuromuscular function and significantly increased life span (Nizzardo et al. 2014). Neural stem cells from iPSCs have also shown benefits for stroke (Yuan et al. 2013). Multiple studies of spinal cord injury have seen functional improvement following transplant of iPSC-derived neural precursors. In a recent study, hindlimb locomotor recovery was observed following implantation (Romanyuk et al. 2015).

The development of neural cells from differentiated somatic cells is very time consuming, with several stages and incubation periods. Further, any remaining undifferentiated cells increase the risk of tumorigenesis. The direct induction of somatic cells to neural cells, skipping the pluripotent state, is now possible. Direct conversion typically proceeds by one of two protocols: the forced expression of genes for differentiated neurons, or a reprogramming to a partially pluripotent state followed by culture with the appropriate growth factors for neuronal differentiation (Matsui et al. 2014). Expandable neural stem cells have been directly converted from mouse fibroblasts through the constitutive activation of Sox2, Klf4, and c-Myc, and Oct4 (Thier et al. 2012). Differentiated neurons, astrocytes, and oligodendrocytes have also been directly converted from somatic cells. Of the neuronal subtypes, dopaminergic neurons (Caiazzo et al. 2011; Pfiesterer et al. 2011), motor neurons (Son et al. 2011), cholinergic neurons (Liu et al. 2013), and peripheral sensory neurons (Blanchard et al. 2015) have been directly induced from mouse and human fibroblasts. Induced dopaminergic neurons were able to functionally integrate and ameliorate symptoms in a mouse model of Parkinson's disease (Kim et al. 2011a).

While ESCs and iPSCs retain many similarities in differentiation potential, it cannot be concluded that the two cell types are identical at the molecular level. Induced pluripotent stem cells generated by transcription factor-based reprogramming maintain residual epigenetic signatures from their somatic origins, which must be "reset" (Kim et al. 2010). Additionally, some iPSC lines are closer than others to ESCs in terms of gene expression (Ghosh et al. 2010). Comparison of gene expression profiles between iPSCs and ESCs revealed that unique microRNA

expression is observed in iPSCs, implicating differences regulatory control (Chin et al. 2009; Wilson et al. 2009). The impacts of the differences between ES and iPSCs are seen in cloned animals generated from somatic cell nuclear transfer. These animals often suffer from incomplete epigenetic reprogramming and permanent genetic changes occurring during development or the reprogramming process, demonstrating that much is yet to be understood about cellular reprogramming (Wilmut et al. 2002). While the formation of chimeric animals is the definitive test of pluripotency, a small percentage of iPSCs generate strong chimeras relative to ESCs, and even fewer produce viable animals through tetraploid complementation (Zhao et al. 2009). Further, iPSC-derived chimeric mice are prone to cancer due to the expression of the transgene c-Myc during reprogramming (Okita et al. 2007), and teratocarcinomas formed from iPSCs are more aggressive than those from ESCs (Gutierrez-Aranda et al. 2010).

Pluripotent stem cells are an ideal source for cell replacement in a variety of diseases; however, the pluripotent nature of the cells makes them prone to tumor formation following transplant. For example, undifferentiated ESCs and iPSCs transplanted into ischemic mouse brains as a model of stroke did not migrate and differentiate into neurons, but formed teratomas and highly malignant teratocarcinomas (Erdo et al. 2003; Kawai et al. 2010). Embryonic stem cell-derived neural progenitor cells have also proven tumorigenic, particularly after syngeneic transplantation (Erdo et al. 2003). In a mouse model of Alzheimer's disease, transplantation of ESCs also resulted in teratocarcinoma formation (Wang et al. 2006). As such, it has been recommended that pluripotent stem cells and neural progenitors be predifferentiated and the remaining pluripotent cells removed prior to transplantation (Wernig et al. 2008; Erdo et al. 2003; Dihne et al. 2006; Doi et al. 2012; Brederlau et al. 2006). Reprogramming of somatic cells into iPSCs must also be performed with caution, as viral delivery of transgenes has a high risk of mutagenesis and tumorigenicity. Alternative strategies with lower risk for tumor formation include excision systems such as cre-lox, or use of non-integrating delivery systems including episomal vectors, plasmid DNA, or the use of specific proteins (Lee-Kubli and Lu 2015).

2.2.2 Multipotent Stem Cells for Neural Repair Strategies

Multipotent stem cells, also known as somatic stem cells, have the capacity for self-renewal and possess the ability to develop into multiple specialized cell types. However, unlike pluripotent stem cells, they possess a limited differentiation capacity, giving rise to a restricted range of cells within a specific tissue. Multipotent stem cells are found in juvenile and adult animals and have been isolated from many organs and tissues, including brain, retina, bone marrow, peripheral blood, blood vessels, skeletal muscle, skin, teeth, heart, gut, liver, adipose tissue, and testis (Fig. 2.3). They are thought to reside in a specific area of each tissue referred to as a "stem cell niche." Multipotent stem cells from a variety of tissues have been used for

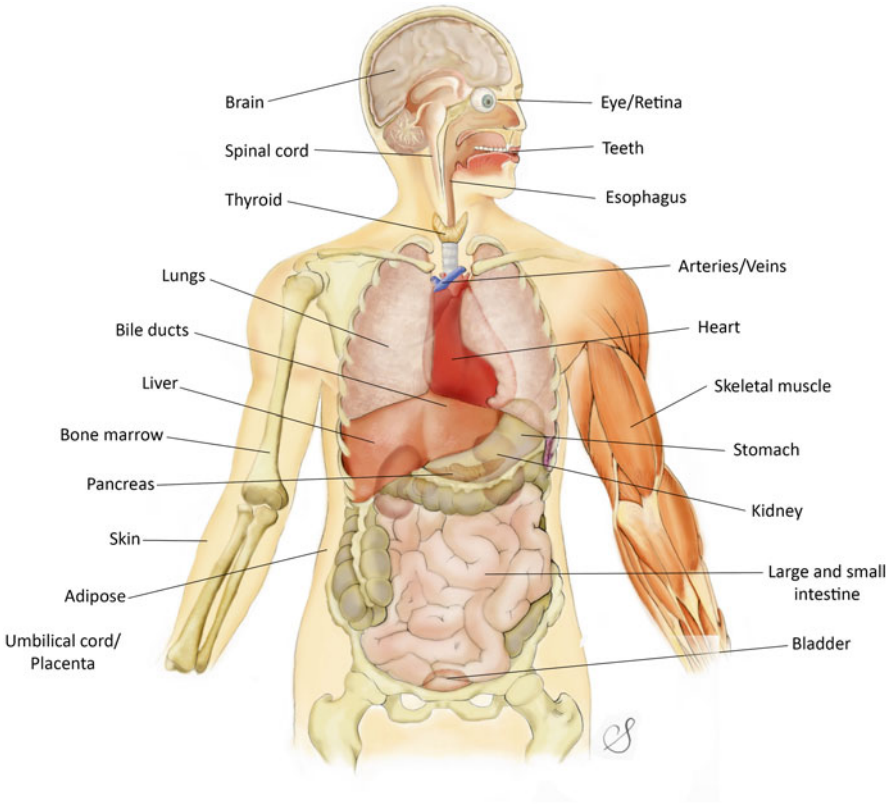

Fig. 2.3 Adult stem cells (also called somatic stem cells) are naturally present throughout the body and have been identified in a number of different tissues and organs. They are self-renewing and typically reside in a specialized region of the tissue often referred to as a "stem cell niche." They can differentiate yielding some, or all the specific cell types within a particular tissue (e.g., tissue specific adult stem cells). In general, the function of adult stem cells is to maintain and repair the tissue in which they reside. This illustration depicts different tissue sources in which adult stem cells have thus far been isolated. In some cases, cellular reprogramming or transdifferentiation experiments have demonstrated that certain adult stem cells have differentiated into cell types other than those of their predicted lineal relationship

neural repair strategies with varying degrees of success. In some cases the use of adult stem cells is considered less controversial and also has the potential advantage for autologous transplantation, thus minimizing immune rejection complications.

2.2.2.1 Neural Stem Cells

Neural stem cells (NSCs) have been proposed as a unique source of transplantable multipotent cells to replace damaged and diseased neurons and glia in the CNS and peripheral nervous system (PNS). They are defined by their ability to differentiate

into cells of all neural lineages (e.g., neurons, oligodendroglia, and astroglia); to self-renew (to give rise to new NSCs with similar potential); to populate the developing and/or degenerating nervous system and have been isolated from the developing and adult nervous system (Fig. 2.1). In addition, they have also been produced in vitro by differentiation of pluripotent stem cells (ESCs and iPSCs) toward a neuroepithelial fate. Under defined conditions, NSCs can generate a complement of more specialized cells found within specific regions of the CNS, PNS, as well as the retina. While, NSC transplants have been proposed as a method of neurorepair and replacement, it is important to note that studies examining the transplantation of "neural stem cells," are often grafting mixed populations of cells, some of which may be "true" neural stem cells, but that also contain cells that are at a more differentiated state. These cells are best-termed neural progenitor cells or precursor cells (Klassen et al. 2004).

Neural stem cells and neural progenitor cells (NPCs) possess a number of characteristics that make them ideal vectors for brain rescue and repair. Novel therapeutic strategies are being developed to take advantage of the ability of NPCs to proliferate in culture and survive following transplantation into the nervous system, where they may integrate and stably express foreign genes, or repopulate the damaged or diseased nervous system. They can be clonally expanded in culture, providing a renewable supply of distinct cellular populations for transplantation. In addition, they may be genetically modified for expression of exogenous genes encoding neurotrophic factors, neurotransmitters, or enzymes that may provide neuroprotection and facilitate regeneration. Thus, NPCs are capable of functionally integrating into host neural circuitry and/or may serve as cellular sources for delivery of trophic, or other factors to facilitate cell survival and neuroprotection, as well as stimulate regenerative events. Neural progenitor cells have been isolated from various regions of the nervous system, including the hippocampus, subventricular zone, cerebellum, olfactory bulbs, spinal cord, retina as well as neural crest (Temple 2001), and in vitro studies show that they can adopt a variety of cellular fates. The discovery of NPCs in the adult brain as well as retina has encouraged research into their role during neurogenesis in the normal mature nervous system and following traumatic injury. Gaining a more thorough understanding of adult neurogenesis can contribute greatly to our knowledge of neurodegenerative diseases and their treatments.

2.2.2.2 Non-neural Adult Stem Cells

Experimental strategies for cellular therapy in the CNS consist primarily of heterologous transplantation. Although the CNS (and the retina) are immunologically privileged sites, immune rejection of heterologous cell transplants remains an important consideration that may limit the routine use of NPCs (or retinal progenitors) for transplantation. Furthermore, the use of immunosuppressive drugs (e.g., cyclosporine) is a major constraint associated with transplantations and may compromise the effectiveness of the transplanted cells. Thus, autologous transplantation

is widely viewed as the model of choice for cellular therapy. Furthermore, depending on the source of cells, if derived from embryonic stem cells or fetal-derived tissue moral and ethical objections may be present. As such, a number of other cell populations are also being considered for cell-based therapies for nervous system disorders.

In this section, we describe the potential of alternative sources of somatic stem cells, including mesenchymal stem cells, umbilical cord (blood) stem cells, adipose stem cells, and dental pulp stem cells, sources that normally do not generate neural cell types. However, these non-neural adult stem cell populations in some cases appear to be capable of inducing endogenous neurogenesis. In addition to the neurogenic influence, these cell types may also have trophic effects that exert neuroprotective benefits when used to treat neurodegenerative conditions.

Mesenchymal stem cells (MSCs) derived and expanded from different sources of connective tissue (e.g., bone marrow, adipose tissue, placenta, umbilical cord blood) hold considerable potential for cell-based therapeutics in the nervous system. In addition to their self-renewal capacity, these multipotent stem cells also display paracrine activity having the capacity to secrete bioactive molecules capable of stimulating neuroprotection and reducing inflammation (reviewed in Liang et al. 2012). Their differentiation can be induced by multiple factors within their microenvironment including biological, chemical, and physical cues. A number of studies suggest that adult bone marrow-derived mesenchymal stem cells (MSCs) possess the ability to transdifferentiate into neuronal-like cells (Fig. 2.4) (Prockop et al. 2000; Tomita et al. 2002; Woodbury et al. 2000). However, this potentially extraordinary ability to generate neural lineages is not without controversy. Other studies suggest some of these findings may be due to cell fusion events (Terada et al. 2002) or a type of injury/stress response. Nevertheless, the multipotent nature of MSCs and their lack of ethical constraints for their isolation and derivation make them attractive candidates for cell-based therapies using autologous transplantation.

In a number of animal models, transplantation of MSCs has been used to treat CNS disease, cerebral ischemia, traumatic brain injury, retinal degeneration, spinal cord injury, and peripheral nerve damage. Numerous benefits have been reported including promotion of axonal regeneration, reduced lesion size, enhanced neuronal survival, and improved functional outcomes (Harper et al. 2011; Johnson et al. 2010; Kocsis 2009; Kurozumi et al. 2005; Li and Chopp 2009; Sasaki et al. 2009; Zhao et al. 2002; Zheng et al. 2010). Genetically engineered MSCs are commonly used in therapies for CNS diseases (see cellular reprogramming below) in order to increase cell survival and integration into various brain regions. Although MSCs offer considerable hope for treatment of neurodegenerative conditions, there are still challenges to overcome before their widespread clinical application.

Adipose-derived stem cells (ADSCs) are also a potential therapeutic option for neural repair strategies. Multipotent ADSCs have the capacity to differentiate into adipocytes, osteoblasts, chondrocytes, and muscle cells (Zuk et al. 2002). In addition, they are an easily obtained, self-renewing, and rapidly expanding cell population. A number of studies have demonstrated that ADSCs can be induced to differentiate into neural progenitor cells using neuronal induction techniques that

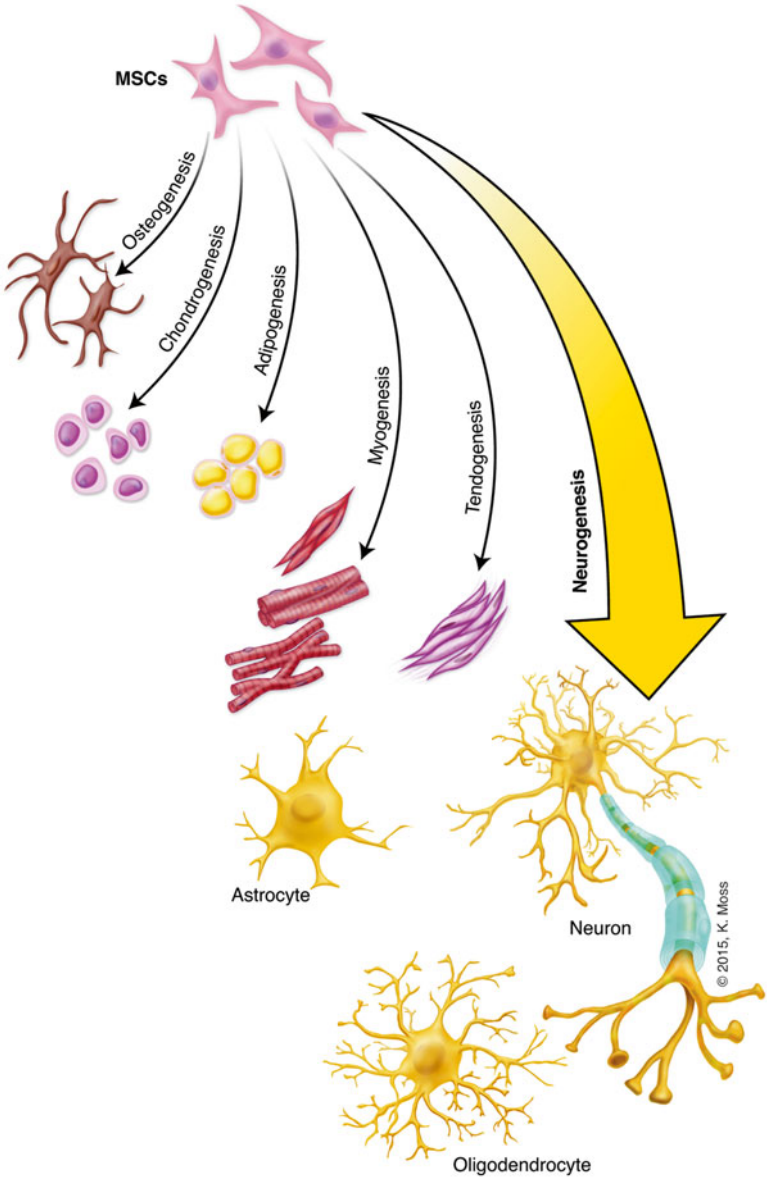

Fig. 2.4 Differentiation potential of multipotent mesenchymal stem cells (MSCs). In addition, MSCs can also be transdifferentiated or reprogrammed toward neural fates including neurons and glial cells (astrocytes, oligodendrocytes, and Schwann cells)

include using specific factors in order to promote cells to a neuronal lineage. These and other studies have found that induced and transdifferentiated ADSCs can express a variety of neuronal markers including Nestin, NeuN, TuJ1, MAP2, as well as the glial markers, glial fibrillary acidic protein (GFAP) and CNPase (Safford et al. 2002; Jang et al. 2010). When studying ADSCs for transplantation, it was found that injecting the ADSCs into the brain promoted increased movement and cognitive function in aged animals, as well as levels of the neurotransmitter acetylcholine, in various parts of the brain (Park et al. 2013). Furthermore, ADSCs have been used as targeted therapies for Parkinson's disease; when ADSCs were injected into Parkinson's disease model mice, it was found that dopaminergic neurons were more likely to survive and exhibited lower behavioral problems than mice without the transplantation (Choi et al. 2015). Other studies have also used ADSCs to facilitate peripheral nerve injury repair. Implantation of ADSCs or of Schwann-like cells transdifferentiated from ADSCs within nerve regeneration conduits has resulted in enhanced nerve regeneration (Lopatina et al. 2011; Shen et al. 2012).

Dental pulp stem cells (DPSCs) are self-renewing and reside within the perivascular niche of the dental pulp. They appear to originate from the cranial neural crest and possess MSC-like properties, differentiating into adipocytes, chondrocytes, osteoblasts as well as endothelial cells under appropriate conditions. In humans, unlike other sources of MSCs, isolation of this population of maturing/adult stem cells is noninvasive as they can be routinely isolated from discarded wisdom teeth and human exfoliated deciduous teeth (SHEDs). In addition to their ability to generate mesodermal lineages, through induction methods, DPSCs can be directed toward a neural lineage, generating neuronal and glial/Schwann-like cells (Arthur et al. 2008; Martens et al. 2014). Human DPSCs have recently been induced toward dopaminergic neuronal phenotypes and have been transplanted into a rat model of Parkinson's disease. Results showed that certain factors including epidermal growth factor (EGF) and bFGF help convert SHED stem cells to an induced cell state with the addition of neurotrophic factors. Overall, studies have shown that using DPSCs can aid in neuroprotection of Parkinson's disease. Sakai and colleagues showed that human DPSCs transplanted into the transected spinal cord in adult rats produced a marked recovery of locomotor function in hind limbs (Sakai et al. 2012). In contrast, human bone-derived MSCs or skin fibroblasts produced substantially less recovery of locomotor function. In this study, the DPSCs appear to have inhibited apoptosis of endogenous neural cells within the damaged area and promoted regeneration of transected axons likely due to paracrine mechanisms.

The hair follicle within mammalian skin harbors a population of multipotent stem cells known as dermal papilla (DP) stem cells (Hunt et al. 2008). These stem cells can be obtained less invasively and can be isolated from the hair follicle. Dermal papilla stem cells have the ability to differentiate into various lineages including smooth muscle, fibroblasts, osteoblasts, neurons or glial, and adipocytes (Driskell et al. 2011). Induced pluripotent stem cells have been derived using DP stem cells along with the use of two transcription factors, Oct4 and Klf4 with high

efficiency (Tsai et al. 2010). Their ability to form spheres further enhances their differentiation into neuronal and glial cell types (Hunt et al. 2008). Hair follicle pluripotent stem cells have been generated and studied in vitro for their ability to differentiate into neuronal and glial lineages. In addition, these cells were transplanted into the severed sciatic nerve of the mouse, where they differentiated into Schwann-like cells and promoted nerve regeneration (Amoh et al. 2009).

Olfactory ensheathing cells (OECs) are a source of multipotent stem cells that can be derived from the olfactory bulb of the forebrain and the olfactory mucosa. Studies characterizing OECs have demonstrated their capacity to secrete neurotrophic factors including brain-derived neurotrophic factor (BDNF) and nerve growth factor (NGF) along with ECM molecules like fibronectin, making them a potential source for neural repair strategies. These phenotypic properties are similar to those of Schwann cells and as such, OECs have been utilized for peripheral nerve repair. Co-culture of OECs derived from the olfactory bulb and the olfactory mucosa showed positive effects on axonal regrowth in a peripheral nerve lesion model (Guerout et al. 2011). Additionally, co-culture of bone marrow stromal cells with OECs increased neural differentiation in vitro (Ni et al. 2010). In some studies, NSC transplants into the brain as a method of cellular therapy display minimal survival of the grafted cells. However, OECs have been shown to increase the survival of NSCs when co-implanted into Parkinson's mice (Shukla et al. 2009). Overall, OECs have a synergistic effect when transplanted with other heterologous sources of stem cells, in part likely due to their ability to secrete trophic factors.

Human cord blood-derived multipotent stem cells have also been identified to express characteristics of embryonic stem cells. By using these stem cells and treating with all-trans retinoic acid, they were found to express pertinent proteins that are found in dopaminergic neurons, Nurr1, Wnt1, and En1 (Li et al. 2012a). These results show that human cord blood-derived multipotent stem cells have the potential to differentiate into neuronal cells, and can be specifically targeted for Parkinson's disease therapy.

Haile and colleagues have investigated the use of human umbilical vein endothelial cells (HUVECs) and their potential to differentiate into neurons and astrocytes by utilizing a direct differentiation protocol (Haile et al. 2015). HUVECs were converted to an iPSC state and then later differentiated into cells of the CNS through the use of lentiviral vectors, encoding Lin28, c-Myc, Klf4, NANOG, Sox2, and Oct4. This type of strategy may help improve the development of new drugs and cellular-based therapies for neurodegenerative diseases including Parkinson's disease, Alzheimer's disease, and Huntington's disease.

Adult somatic stem cells remain an important class of stem cells for further investigation. In general, these cell types possess a number of significant advantages with respect to technical (isolation procedures), ethical (embryonic/fetal/adult), and immunological (autologous grafting) issues concerning cell transplantation strategies for neurological disorders. However, the mechanism/s through which they promote functional recovery remain to be definitively elucidated.

2.2.2.3 Cellular Reprogramming Strategies

The discovery of the ability to generate iPSCs produced considerable excitement in the fields of developmental biology and regenerative medicine (Takahashi and Yamanaka 2006; Takahashi et al. 2007). However, the technology is not without limitations. The reprogramming technology is sometimes inefficient and often very time intensive. In addition, the pluripotent state can result in genetic instability and tumorigenesis when these cells are implanted in animal models. As such, there is a critical need to develop alternative (or complementary) approaches toward cellular reprogramming.

Direct Conversion Using Transcription Factors or Small Molecules

During normal embryonic development cellular differentiation processes are guided by an assortment of specific extracellular soluble factors such as gradients of chemical cues and cell-to-cell contact signals that ultimately lead to induction and activation of specific combinations of lineage-determining transcription factor pathways. An emerging research frontier of epigenetic reprogramming employs small molecules from key developmental pathways and cell differentiation factors to directly convert somatic cells from one fate/lineage to another (Zhang et al. 2012).

These strategies usually first subject the somatic cells to conditions known to enhance reversion toward a more "primitive" state by making the cells more susceptible to cell-fate changes, a process often referred to as transdifferentiation (Tursun et al. 2011). In addition to gene delivery techniques, compounds such as valproic acid or other histone deacetylase inhibitors are known to enhance this reprogramming process. Next, potent neural inducing signals are generally used to drive the cells toward proliferating neural progenitor cells, and finally inducing them toward specific neural cell fates. In this strategy, the selection of small molecules is usually guided by developmental signaling molecules known to be involved in generation of the particular cells. This gene-free approach was recently used to generate induced Schwann cells from neonatal human foreskin fibroblasts that may potentially be used to treat severe peripheral nerve injuries (Thoma et al. 2014).

Recently, the direct conversion of somatic cells to neural stem/progenitor cells has been demonstrated using viral delivery of transcription factors (Thier et al. 2012; Han et al. 2012). Fibroblasts have been directly reprogrammed into induced neural stem cells through the insertion of genes for reprogramming factors such as Oct4 and NANOG (Hockemeyer et al. 2008). With these factors, fibroblasts were converted to a partially reprogrammed state with the potential to further differentiate into various neural cell types. Studies have also shown that a single reprogramming factor, Oct4, is able to reprogram human neural stem cells into a pluripotent stage (Kim et al. 2009). The use of small molecules or fusion protein transduction over genetic manipulation reduces the risks of genetic instability and tumor formation. As such, there are some genetic material-free approaches that have successfully resulted in induced neurons and neural progenitor cells. In such studies the

forced growth of somatic cells within 3-D microenvironments has resulted in a more direct pathway to reprogramming (Kulangara et al. 2014; Su et al. 2013).

Ex Vivo Gene Therapy Approaches for Neuroprotection

Perhaps an even more powerful strategy toward brain repair comprises a multifactorial approach addressing a number of important issues, including optimization of survival and function of remaining neural elements and modulation of trophic (as well as inhibitory/repellent) influences in order to promote neuroregeneration. Neurotrophic/growth factors have emerged as promising candidates to augment neurorepair. Neurotrophic factors are essential for neuronal development and plasticity, and also can prevent cellular atrophy, enhance neuronal survival, and facilitate axon regeneration in the developing and adult nervous system. A cell-based approach for neuroprotection is to genetically engineer stem cells as delivery vehicles for neurotrophic factors. Ex vivo gene transfer to NSCs, MSCs, Schwann cells, fibroblasts, OECs, as well as other somatic cells prior to transplantation holds promise as cellular platforms for delivery of therapeutic factors. A number of viral vectors are available for ex vivo gene delivery, including, adeno-associated viral, adenoviral, retroviral, and lentiviral vectors, each with their own advantages and disadvantages (reviewed in Hendriks et al. 2004). Cao and colleagues used OECs that were genetically modified to secrete glial cell line-derived neurotrophic factor (GDNF) in order to facilitate spinal cord repair through regeneration of axons (Cao et al. 2004). A strategy to target Huntington's disease (HD) employed genetically engineered MSCs. In this study, BDNF was genetically overexpressed in MSCs that were then transplanted into the striatum of HD model mice. Findings showed that those mice that were injected with BDNF-engineered MSCs had a decrease in behavioral symptoms typically associated with HD (Dey et al. 2010). Furthermore, Harper and colleagues used neurotrophic factor-engineered MSCs to deliver a constant, low level of BDNF and demonstrated that this approach had potential for functional and structural neuroprotection in chronic ocular hypertension, an experimental model used for glaucoma (Harper et al. 2011).

Genetically engineered cells have also been used to promote dopaminergic neuron survival through the use of GDNF (Behrstock et al. 2006) as well as using fibroblasts engineered to secrete BDNF (Frim et al. 1994) also enhanced the survival of retinal ganglion cells (RGCs) (Castillo et al. 1994). Mesenchymal stem cells were also genetically modified to express the neurotrophic factor BDNF to support neuroprotection in a retinal cell line (RGC-5) when exposed to toxic cellular stressors such as glutamate or hydrogen peroxide (Harper et al. 2009). An important step in implementing cell-based delivery of neuroprotective compounds is to determine the health of the engineered cells. Employing cellular image-based high content screening is a powerful approach to rapidly assess multiple cell parameters (Sharma et al. 2015). Promising results with potential therapeutic relevance have been obtained by cellular reprogramming and by genetic modification of cells to secrete neurotrophic

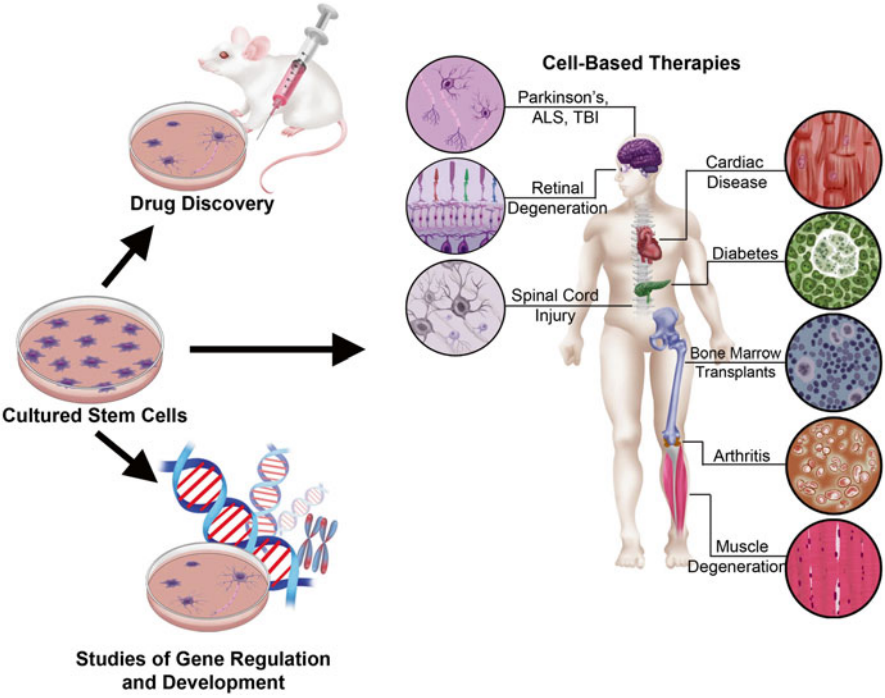

Fig. 2.5 Stem cell research. Recent advances in stem cell biology have revolutionized research opportunities in drug discovery. The ability to isolate and generate stem cell and somatic cell lines associated with specific diseases is providing effective in vitro models for pre-clinical testing. Stem cell research is also providing powerful tools to help decipher the molecular mechanisms of gene regulation and development. Another important goal of stem cell research is to elucidate the pathways for generating specific cell types that can be used for cell transplantation to treat a variety of degenerative diseases and injuries

factors; combining biomaterials to develop bio-mimetic strategies can lead to further advancement in regenerative therapies.

Stem cell research provides a powerful approach to gain a more thorough understanding of the molecular mechanisms of gene regulation and cell fate determination in normal, as well as in diseased states (Fig. 2.5). In addition, specific cell types differentiated from pluripotent or multipotent stem cells are proving to be useful as models for understanding the biology of diseases, for drug discovery, and for toxicological bioassays. This is particularly significant, where there may be no animal models for the disease under study and for preclinical testing. An especially promising area is cell-based transplantation therapies, whereby stem cells can be used to generate specific cell types in order to replace those cells compromised by disease or injury (Fig. 2.5). Coupling these approaches with biocompatible nano/micromaterials will be an especially powerful tactic for development and implementation of experimental strategies for neural tissue engineering and therapeutics (Fig. 2.6).

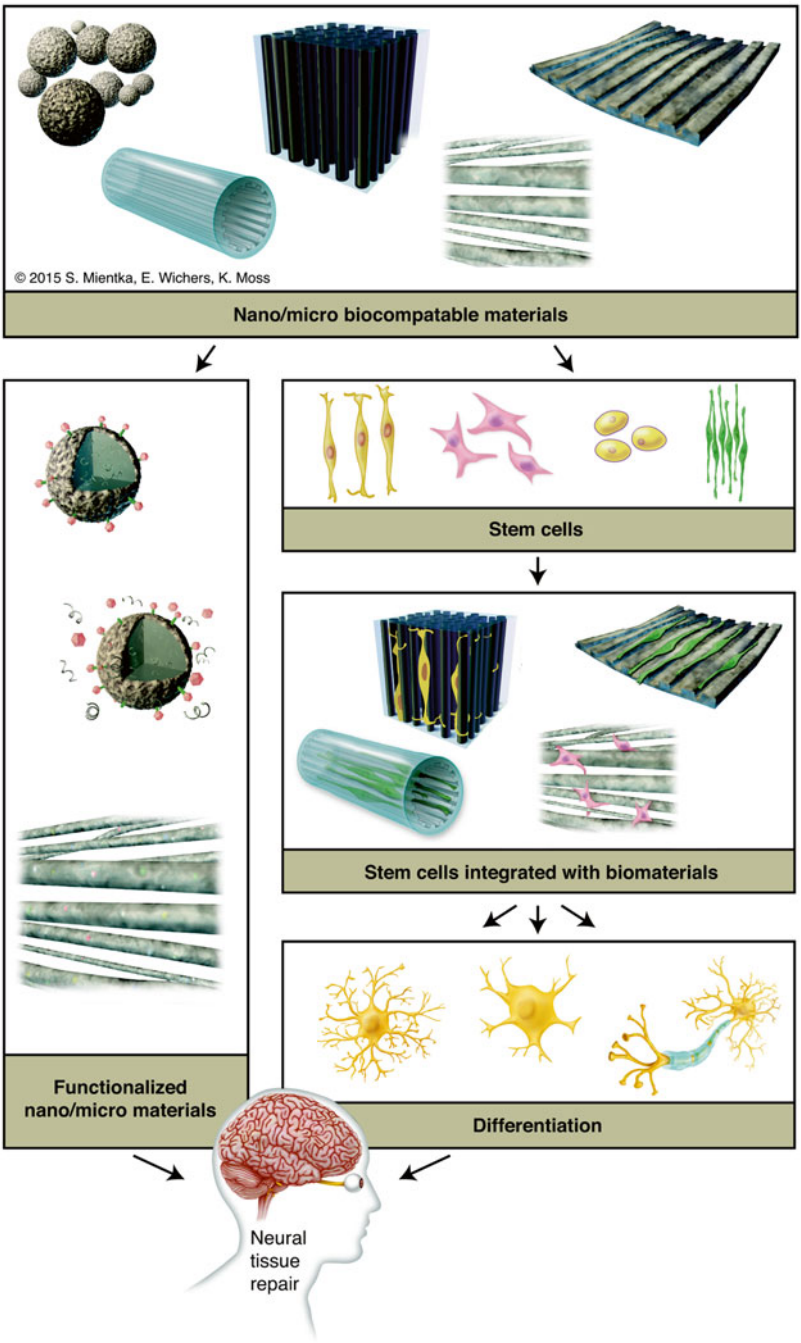

Fig. 2.6 Overview of approaches merging stem cells, polymeric scaffolds, drug delivery systems, gene therapy, cellular engineering, and biomaterials to develop experimental strategies for neural tissue engineering and repair

2.3 3-D Scaffolds for Neural Tissue Engineering

Polymeric materials fabricated from natural and synthetic polymers have been successfully used in the recent past for fabrication of biomimetic 3-D scaffolding environments analogous to the extracellular matrix (ECM) microenvironment and tissue architecture that support the growth and differentiation of native and transplanted cells. Before using a material for development of a 3-D-scaffold, various properties of the polymers are important to take into consideration such as biodegradability, biocompatibility, biological activity, mechanical properties, surface chemistry, cytotoxicity, and growth factor binding capabilities (Dhandayuthapani et al. 2011; Sell et al. 2010; Zhu and Marchant 2011; Kumbar et al. 2014).

Biodegradable synthetic materials with controllable degradation rates, surface, mechanical, and structural properties have been favored for neural regeneration applications. The adjustable features of synthetic materials make them promising candidates to design 3-D scaffolds that overcome challenges in neural regeneration such as biocompatibility, mimicking of the ECM, appropriate immunomodulation response and fast degradation (Cunha et al. 2011; Elliott Donaghue et al. 2014; GhoshMitra et al. 2012). Synthetic material-based 3-D scaffolds possessing particular features can be produced in various sizes ranging from nano to microscales using different techniques such as electrospinning, self-assembly, and phase separation among others. Several synthetic material-based scaffolds have been used for neural tissue engineering applications composed of poly(glycolic acid) (PGA) (Keeley et al. 1991), poly(lactic acid) (PLA) (Corey et al. 2007), poly(L-lactic acid) (PLLA) (Patel et al. 2007; Yang et al. 2005a), or of a blend of the above such as poly(L-lactic acid)-caprolactone (PLLA-PCL) (Ghasemi-Mobarakeh et al. 2008; Schnell et al. 2007) and poly(D,L-lactide-co-glycolide) with poly(εcaprolactone) (PLGA/PCL) (Panseri et al. 2008). However, a number of potential drawbacks to the use of synthetic materials include insufficient similarity to the ECM and possible release of cytotoxic chemicals upon degradation, which have raised concerns and resulted in efforts to identify other biodegradable, biocompatible, and nontoxic natural materials as alternatives (Table 2.1).

Natural polymers are readily available and can be processed and extracted from naturally occurring sources. Most commonly used natural polymers for tissue engineering and regenerative medicine are polysaccharides, various ECM molecules, polypeptides, proteins, and DNA (Dhandayuthapani et al. 2011; Ko et al. 2010; Yoon and Fisher 2009). Natural polymers such as collagen, fibronectin, laminin, chitosan, heparin, dextran, alginate, albumin, hyaluronic acid, and gelatin have been used for preparing scaffolds sizing from nanometers to several centimeters, which can be applied to diverse applications such as tissue engineering, cell encapsulation, cell differentiation, gene delivery, and drug delivery (Dang and Leong 2006; Abraham et al. 2009; Chai and Leong 2007; Liechty et al. 2010; Gasperini et al. 2014; de Vos et al. 2014). Throughout this section, we provide an overview of the application of synthetic and natural material-based scaffolds with varying nano- and microstructures in neural regeneration strategies.

Table 2.1 Classification of biomaterials used for neural regeneration

Biomaterials	Type	Structure	Purpose/application	Outcomes	Ref.
Polybutyl-cyanoacrylate	Synthetic	Nano/microparticle	Transport across BBB	Enhanced transport across BBB, provide controlled release. Premature release is the con	Abraham et al. (2009), Kreuter (2013), Graff and Pollack (2005), Kreuter et al. (1997), Gulyaev et al. (1999), Steiniger et al. (2004), Alyautdin et al. (1997), Alyautdin et al. (1998), Hasadsri et al. (2009)
Polyanhydrides	Synthetic	Nano/microparticle	Alzheimer's diseases and brain cancer	Provide controlled release through surface erosion	Wu et al. (1994), Howard et al. (1989), Brem et al. (1989), Jampel et al. (1991), Lesniak et al. (2005), Tamada and Langer (1993), Gao et al. (1998), Torres et al. (2006), Chavez-Santoscoy et al. (2012), Burkersroda et al. (2002)
				Hydrolytic degradation is the con	
PLGA	Synthetic	Nano/microparticle	Alzheimer's, Parkinson diseases and retinal degeneration	Provide easy copolymerization, controlled release with low toxicity and rapid degradation into metabolites. Can be modified through backbone chemistry, molecular weight and hydrophobic surface coating	Garbayo et al. (2009), Andrieu-Soler et al. (2005), Jollivet et al. (2004a, b), Péan et al. (2000), Grozdanic et al. (2010), Kyhn et al. (2009)
				Bulk erosion and difficult dispersion are the cons	

(continued)

Table 2.1 (continued)

Biomaterials	Type	Structure	Purpose/application	Outcomes	Ref.
PLGA	Synthetic	Nano/microparticle	Spinal cord injury	Provide controlled release, axonal growth and functional improvement after spinal cord injury	Lowry et al. (2012), Wang et al. (2008), Johnson et al. (2008)
PLGA	Synthetic	Nano/microparticle	Mobilization and migration of NSCs	Provide enhanced mobilization and migration of human NSCs	Li et al. (2012b)
PEG-PEI	Synthetic	Nanospheres	Neural regeneration therapy	Depict the potential for controlled release of siRNA for neural regeneration	Liang et al. (2012)
PEI	Synthetic	Nano/microparticle	Differentiation of subventricular zone NSCs	PEI electrostatically complexed with RA and dextran sulfate through electrostatic interactions provided controlled release and the differentiation	Santos et al. (2012)
PLGA	Synthetic	Nano/microparticle	Stroke-injured brain	Co-delivery of cells and growth factors improved the particle adhesion of human neural stem/progenitor cells promoting vascularization into the graft site and forming of primary neuro-vascular networks	Bible et al. (2012)

Laminin and poly-D-lysine coated PLGA microspheres	Synthetic	Nano/microparticle	Hemi-Parkinsonian rats	Co-delivery of mesenchymal stromal cells (MSCs) and growth factors improved MSC survival and behavioral improvements	Delcroix et al. (2011)
PLGA/ collagen	Natural	Nano/microparticle	Differentiation of neural progenitor cells	Provide differentiation of neural progenitor cells into microtubule-associated protein 2 (MAP2)-expressing mature neurons	Gujral et al. (2013)
Collagen	Natural	Nano/microparticle	Differentiation of oligodendrocyte progenitor cells	Enhance differentiation of oligodendrocyte progenitor cells	Yao et al. (2013)
Collagen	Natural	Hollow microspheres	Neural regeneration	Provide controlled release of neurotropic factors	Kraskiewicz et al. (2013)
Chitosan	Natural	Microspheres	Growth and survivability of NSCs	Provide enhanced growth and survivability of NSCs	Skop et al. (2013)
Alginate	Natural	Microspheres	Survival, growth, proliferation and differentiation of NSCs	Provide sustained delivery 3-D structure for survival, growth, proliferation and differentiation of NSCs	

(continued)

Table 2.1 (continued)

Biomaterials	Type	Structure	Purpose/application	Outcomes	Ref.
Iron oxide	Metal	Magnetic Nano/microparticle	Guidance for regenerating axons and directed neurite outgrowth	Synergetic effect of external magnetic field and controlled release on enhanced nerve regeneration and guidance for regenerating axons directed neurite outgrowth. Need polymeric coating for enhanced intracellular uptake and targeting	Aqil et al. (2008), Herrera et al. (2008), Rubio-Retama et al. (2007), Bakandritsos et al. (2010), Lutz et al. (2006), Hu et al. (2006), Kim et al. (2011b), Riggio et al. (2012), Calatayud et al. (2013)
Quantum dots	Synthetic	Nanaoparticle	Neurite outgrowth and neuronal differentiation. Labeling of neurons and glia	Provide neurite outgrowth and neuronal differentiation. Enhanced labeling of neurons and glia	Dahan et al. (2003), Pathak et al. (2006), Vu et al. (2005)
PLA-PEG-PLA Hydrogel and PLGA microparticles	Synthetic	Hydrogel/microparticle system	Survival of transplanted neural stem cells and neurite outgrowth for CNS	Sustained release enhanced survival of transplanted neural stem cells neurite outgrowth for CNS	Burdick et al. (2006), Lampe et al. (2011)
PLGA conduit and PLGA/PVA microspheres	Synthetic	Conduit/microparticle system	Survival of transplanted neural stem cells and neurite outgrowth for PNS	Sustained release enhanced survival of transplanted neural stem cells neurite outgrowth for PNS	de Boer et al. (2012)

Silicone or PPE conduits and PPE microspheres	Synthetic	Conduit/microparticle system	10 mm gap in a rat sciatic nerve model	Provide prolonged, site-specific NGF delivery with long-term effect on regeneration of peripheral nerves	Xu et al. (2003)
Ppy film and MSN	Synthetic	Conduit/microparticle system	Axon extension	Provide synergetic effect of controlled release and electrical stimuli on PC12 cells	Cho et al. (2009)
Collagen-chitosan scaffolds and Chitosan microspheres	Natural	Scaffold/microparticle system	1.5 cm long sciatic nerve repair model	Sustained delivery of NGF along with longitudinal channels enhanced nerve regeneration process	Zeng et al. (2014)
Silicone tube and Gelatin microspheres	Natural	Tube/ microparticle system	1 mm long facial nerve transection injury model	Improved rate of nerve regeneration and number of matured axons	Matsumine et al. (2014)
PCL	Synthetic	Nano/microfiber	Differentiation of neural stem/progenitor cells upon transplantation into the rat brain	Synergetic effect of co-delivery of cells and growth factors enhanced neuronal differentiation of neural stem/progenitor cells upon transplantation into the rat brain	Wang et al. (2012)
PLLA	Synthetic	Nano/microfiber	Directed outgrowth of sensory and motor neurons	Enhanced directed outgrowth of sensory and motor neurons	Leach et al. (2011)
PLGA	Synthetic	Nano/microfiber	Orient the direction of Schwann cells	Oriented the direction of Schwann cells	Subramanian et al. (2011)

(continued)

Table 2.1 (continued)

Biomaterials	Type	Structure	Purpose/application	Outcomes	Ref.
PPC	Synthetic	Nano/microfiber	Nurite outgrowth and Schwann cells migration	Enhanced nurite outgrowth and Schwann cells migration	Wang et al. (2011)
PCL	Synthetic	Nano/microfiber	Elongated contact guidance of Schwann cells	Provide elongated contact guidance of Schwann cells	Chew et al. (2008)
PLA	Synthetic	Nano/microfiber	Directed growth of retinal ganglion cells	Cell delivery vehicle for transplanting RGCs axially directed the growth of retinal ganglion cells.	Kador et al. (2013)
ε-capro-lactone and ethyl ethylene phosphate copolymer (PCLEEP)	Synthetic	Neurotropic factor incorporated Nano/microfiber	Neurite outgrowth	The synergistic effect of sustained β-NGF release and alignment of nanofibers enhanced neurite outgrowth of PC12 cells	Chew et al. (2005)
Silk fibroin (SF)/ P(LLA-CL) blended nanofibers	Synthetic	Neurotropic factor incorporated Nano/microfiber	Peripheral nerve regeneration	NGF release and alignment enhanced nerve regeneration	Zhang et al. (2014)
P(LLA-CL)/ NGF	Synthetic	Neurotropic factor incorporated Nano/microfiber	Sciatic nerve regeneration in rats	NGF release and alignment enhanced sciatic nerve regeneration in rats	Liu et al. (2011)

PLLA	Synthetic	Neurotropic factor conjugated Nano/microfiber	Neurite extension	Covalently attached neurotropic factors in micro/nanofiber enhanced neurite extension through controlled release	Patel et al. (2007), Lam et al. (2010)
PLLA and polyaniline blend	Synthetic	Electrically conductive nano/ microfibers	Neurite outgrowth of neural stem cells	Enhanced neurite outgrowth of neural stem cells through applied electrical field	Prabhakaran et al. (2011)
PLGA/ PHT	Synthetic	Electrically conductive nano/ microfibers	Adhesion and proliferation of Schwann cells	Enhanced adhesion and proliferation of Schwann cells under an electrical field	Subramanian et al. 2012)
Polypyrrole-coated PLGA	Synthetic	Electrically conductive nano/ microfibers	Differentiation of PC12	Enhanced the differentiation of PC12 cells with electrical field stimuli	Lee et al. (2009)
Rose bengal photoinitiated-acetic acid electrospun collagen nanofibers	Natural	Nano/microfiber	Neural stem cell grow, proliferation and neurite outgrowth	Enhanced neural stem cell grow, proliferation and neurite outgrowth	Liu et al. (2010b)
Collagen-silk composite microfibers	Natural	Nano/microfiber	Human decidua parietalis placental stem cells (hdpPSCs)	Differentiation of hdpPSCs into neural-like cells	Yin et al. (2014)

(continued)

Table 2.1 (continued)

Biomaterials	Type	Structure	Purpose/application	Outcomes	Ref.
Collagen nanofibers	Natural	Nano/microfiber	Maturation of synapses in spinal cord-derived NSCs	Increased the maturation of synapses in spinal cord-derived NSCs by MAPK/ERK1/2 pathway	Yin et al. (2014)
3-D chitosan nanofibers	Natural	Nano/microfiber	Differentiation of PC12 cells and human neural stem cells	Enhanced proliferation and differentiation of PC12 cells and human neural stem cells	Du et al. (2014)
Micropatterned poly(D,L-lactic acid) films	Synthetic	Micro/nanopatterning	Alignment of SCs and orientation of DRGs	Enhanced the alignment of SCs and orientation of DRGs	Miller et al. (2001a), Miller et al. (2001b)
Micropatterned polystyrene films	Synthetic	Micro/nanopatterning	Alignment of Rat type-I astrocytes orientation and selectively different-iation of adult hippocampal progenitor cells into neuronal fate	Enhanced the alignment of Rat type-1 astrocytes orientation and selectively differentiate adult hippocampal progenitor cells into neuronal fate	Recknor et al. (2004, 2006), Oh et al. (2009)

Carbon nanotubes (CNTs)	Synthetic	Nano/microtubes	Neural regeneration activities including neurite branching, outgrowth, attachment of growth cones and cell differentiation	Improved neural regeneration activities through chemical functionalization, controlled release, electrical field stimuli, surface micropatterning or layer by layer assembly. Toxicity is main concern	Tran et al. (2009), Huang et al. (2012), Fabbro et al. (2013), Bosi et al. (2014), Hopley et al. (2014), Bosi et al. (2013)
Silicone tubes filled with collagen or laminin gels	Synthetic	Nano/microtubes	4–6 mm gaps in a mouse sciatic nerve transection injury model	Enhanced repair in 4–6 mm gaps in a mouse sciatic nerve transection injury model	Labrador et al. (1998)

2.3.1 Nano/Microparticle Systems

Very small particles ranging in size from one nm to a few microns are classified in the category of nano/microparticle systems (Marti et al. 2013; Mallapragada et al. 2015; Auffan et al. 2009; Soppimath et al. 2001; He et al. 2010). The main difference in the properties of nano/microparticles compared to their bulk counterparts is due to their high surface area to volume ratio. These particulate systems capable of delivering and releasing therapeutic molecules and drugs have revolutionized the area of drug delivery. Before the advent of such sub-micron delivery vehicles, researchers working on controlled release devices had to address various limitations such as rapid degradation of the drug after injection, drug clearance time, cytotoxicity caused by drug injected in bulk amounts, and targeting specific regions of the body (Kohane 2007; Kumar 2000; Gaharwar et al. 2013; Zimmer and Kreuter 1995). Polymers, both natural and synthetic, have been used for fabrication of polymeric nano/microparticles for drug release due to their numerous advantages including improved stability of the drugs, high drug encapsulation capacity, less toxicity, fewer number of drug administration time points, ability to incorporate both hydrophobic and hydrophilic drugs, sustained release of drugs, cellular uptake potential, and ability to cross the blood–brain barrier (BBB) (Gelperina et al. 2005; De Jong and Borm 2008; Singh and Lillard 2009). Drug encapsulated biodegradable nano/microparticles are capable of overcoming many biomedical challenges and have been extensively used for drug and gene delivery, stem cell differentiation, imaging of live cells, and also for encapsulating genetically engineered live cells for release of therapeutic proteins (Mudshinge et al. 2011; Norizadeh-Abbariki et al. 2014; Brustle et al. 2015; Ilie et al. 2012; Lee et al. 2012; Wang et al. 2009).

The site-specific and efficient delivery of neurotropic agents aimed at targeting neurodegenerative conditions including injuries to the nervous system can be achieved by manipulating the properties of the particles such as size, surface charge, and chemistry. Several classes of biodegradable polymers, including polyalkyl cyanoacrylates, polyanhydrides, polyesters, etc., with varying modified surface chemistry, degradation, and sustained payload release profiles have been used for neural tissue engineering (GhoshMitra et al. 2012; Cho and Ben Borgens 2012; Mallapragada et al. 2015).

Polybutylcyanoacrylate (PBCA) nanoparticles coated with surfactant polysorbate 80 have been shown to provide significant transport of therapeutics across the blood–brain barrier (Kreuter 2013; Graff and Pollack 2005). These particles have been loaded with various active compounds including hexapeptide dalargin (Kreuter et al. 1997), doxorubicin (Gulyaev et al. 1999; Steiniger et al. 2004), loperamide (Alyautdin et al. 1997), and tubocurarine (Alyautdin et al. 1998) in order to overcome the BBB and provide efficient release properties. Recently, the potential use of PBCA nanoparticles in neurons and neuron-like PC12 cells has been evaluated by Hasadsri and coworkers demonstrating the differentiation of PC12 cells after exposure through intracellular delivery to PBCA nanoparticles loaded with the small guanine nucleotide triphosphatase RhoG (Hasadsri et al. 2009). Although

promising, the premature release of therapeutics from the surface of PBCA nanoparticles restricts the degradation dependency and obstruct the controlled release properties. To our knowledge, the performance of PBCA-based particles have not yet been evaluated for axon regeneration in different types of neurons (Ghosh Mitra et al. 2012; Mallapragada et al. 2015).

Biocompatible polyanhydrides are another class of degradable material with drug delivery potential, and have been used in the CNS for treatment of Alzheimer's disease (Wu et al. 1994; Howard et al. 1989) and brain cancer (Brem et al. 1989; Jampel et al. 1991; Lesniak et al. 2005). The drug release from loaded polyanhydride particles was controlled through surface or bulk erosion depending on the type of chemistry (Tamada and Langer 1993; Gao et al. 1998; Torres et al. 2006; Chavez-Santoscoy et al. 2012; Burkersroda et al. 2002). Although the surface erosion property is the most significant advantage of polyanhydrides, their susceptibility to hydrolytic degradation is the main drawback limiting their translational potential (Burkersroda et al. 2002).

Considering the constraints of the previously mentioned synthetic polymer-based particles, the degradable polyesters, such as poly(lactic acid) (PLA) and poly(lactic-co-glycolic acid) (PLGA), have been extensively used for nerve tissue engineering applications due to their low toxicity and rapid degradation into metabolites (Gunatillake and Adhikari 2003). Although these polymers undergo bulk erosion (Tamada and Langer 1993; Burkersroda et al. 2002) causing burst and rapid drug release (Wang et al. 2004; Kashi et al. 2012; Musumeci et al. 2006), the erosion rate and, hence, the drug release can be easily controlled by backbone chemistry (Wang et al. 2004; Musumeci et al. 2006), molecular weight (Kashi et al. 2012; Musumeci et al. 2006), and hydrophobic surface coating (Budhian et al. 2008). In addition, they can be easily copolymerized with PCL, which possesses mechanical strength and slow degradation rate, in order to manipulate the payload release and polymer degradation (Ghasemi-Mobarakeh et al. 2008; Schnell et al. 2007; Panseri et al. 2008).

A number of studies have investigated delivery of neurotrophic growth factors including NGF and GDNF-encapsulated PLGA microparticles as a therapeutic approach for Alzheimer's, Parkinson's disease, and retinal degeneration (Garbayo et al. 2009; Andrieu-Soler et al. 2005; Jollivet et al. 2004a, b; Péan et al. 2000; Grozdanic et al. 2010; Kyhn et al. 2009). Exposure to NGF or GDNF microparticles resulted in functional improvements and tissue regeneration as a result of high burst release followed by long-term sustained release. However, the use of high concentrations of surfactants to disperse the microparticles was a disadvantage of their system. Poly-lactic co-glycolic acid nano/microparticles have also been studied for CNS regeneration. For example, sonic hedgehog (SHH)-encapsulated PLGA microparticles were shown to promote both axonal growth and functional improvement after spinal cord injury (Lowry et al. 2012). Another study indicated that GDNF encapsulated PLGA nanoparticles of 20 nm size were transported by axons and induced the growth of neuronal fibers and promoted functional improvement, whereas 100 nm nanoparticles remained at the injection site (Wang et al. 2008). Johnson and coworkers co-lyophilized NGF with polyethylene glycol (PEG) and

encapsulated them in PLGA microspheres to retain NGF activity and control the release rate. The results suggested that PEG can act both as a pore-forming agent to control release and as a stabilizer for the retention of NGF activity (Johnson et al. 2008).

In addition to various neurotrophic factors, the regulation of gene expression using small interfering RNA (siRNA) can be an alternative approach toward neural regeneration therapies. For this purpose, Liang and colleagues developed siRNA-loaded polyethylene glycol-polyethyleneimine (PEG-PEI)-based nanospheres and demonstrated the potential of this system for neural regeneration therapy (Liang et al. 2012). Additionally, RA-loaded nanoparticles using PEI complexed with RA and dextran sulfate through electrostatic interactions were used for controlling the differentiation of subventricular zone NSCs (Santos et al. 2012). A similar strategy was used for controlling mobilization and migration of human NSCs by using hepatocyte growth factor and leukemia inhibitory factor-loaded PLGA nanoparticles (Li et al. 2012b).

Magnetic nanoparticles (MNPs) can also be used to induce directed neurite outgrowth by applying an external magnetic field. To enhance intracellular uptake and improve targeting and efficacy for neural regeneration applications, these nanoparticles have been surface modified with various polymers (Aqil et al. 2008; Herrera et al. 2008; Rubio-Retama et al. 2007; Bakandritsos et al. 2010; Lutz et al. 2006; Hu et al. 2006). In the work of Kim et al., PEG-coated and NGF-loaded iron oxide nanoparticles were used to enhance neurite growth in PC12 cells. The results demonstrated the synergetic effect of NGF and iron oxide nanoparticles enhanced neurite outgrowth in PC12 cells at low NGF concentrations (Kim et al. 2011b). Riggio et al. designed iron oxide magnetic nanoparticles coated by PLL as magnetic actuators for neural guidance, demonstrating enhanced nerve regeneration and guidance for regenerating axons in the human neuroblastoma SH-SY5Y cell line and primary Schwann cell cultures of the peripheral nervous system (Riggio et al. 2012). Similarly, Calatayud et al. developed PEI-coated MNPs to investigate their effect on neuronal-like models such as PC12 or SH-SY5Y cell lines (Calatayud et al. 2013). In addition to the above-mentioned materials, surface-modified quantum dots have also been used in targeting neurons to investigate specific neurophysiological processes (Dahan et al. 2003), labeling of neurons and glia (Pathak et al. 2006), neurite outgrowth, and neuronal differentiation (Vu et al. 2005).

The incorporation of micro/nanoparticles within a polymer scaffold or hydrogel has been employed as a combined strategy allowing for better localization, sustained release, and slower clearance in vivo. Burdick et al. designed a combined system by dispersing neurotrophin-3 (NT-3)-loaded PLGA microparticles and ciliary-neurotrophic factor (CNTF) in a photopolymerized PLA-PEG-PLA hydrogel. The simultaneous in vitro release results indicated rapid release of CNTF from the hydrogel matrix and extended release of NT-3 from the macroparticles, leading to significant neurite outgrowth from retinal explants (Burdick et al. 2006). In a similar way, Lampe et al. used BDNF- and GDNF-loaded PLGA microparticles and incorporated them into the PLA-PEG-PLA hydrogel for the treatment of Parkinson's disease. GDNF-loaded microparticles were used to promote the survival of

transplanted NSCs, while the BDNF-loaded microparticles were selected to stimulate neurite outgrowth. In these rat models, BDNF was detected for up to 56 days, whereas GDNF was completely released within 28 days indicating the potential of this microparticle/hydrogel system in the delivery of neurotrophic factors (Lampe et al. 2011). Besides the neurotrophic factors, the delivery of both hydrophobic and hydrophilic drugs to the CNS via blend of hyaluronan and methylcellulose (HAMC) coupled with PLGA micro/nanoparticles has been investigated in various studies (Kang et al. 2013; Caicco et al. 2013; Stanwick et al. 2012a, b).

Although the combined strategies mentioned above may involve challenges for CNS regeneration such as the maintenance of biomolecule activity and the delivery of an effective dose, this strategy is also preferable for the PNS. For instance, De Boer et al. developed NGF- and GDNF-encapsulated PLGA/ poly(vinyl alcohol) (PVA) microspheres through a double emulsion solvent evaporation technique. They subsequently distributed these particles in a PLGA conduit matrix to facilitate peripheral nerve regeneration in a rat sciatic nerve gap model. The results showed that histomorphometric values reached their maximum by 6 weeks due to the booster effect of NGF- and GDNF-loaded microspheres (de Boer et al. 2012). Xu et al. developed NGF-loaded poly(phosphoester) (PPE) microspheres dispersed into silicone or PPE conduits to provide prolonged, site-specific NGF delivery to bridge a 10 mm gap in a rat sciatic nerve model for peripheral nerve regeneration. The results indicated a long-term effect of NGF on morphological regeneration of peripheral nerves (Xu et al. 2003). Yang et al. used NGF blended or encapsulated PLGA microspheres with a porogen to develop conduits by gas foaming. The release was controlled for 42 days by manipulating the method of incorporation and polymer molecular weight. The released NGF enhanced neurite outgrowth from primary dorsal root ganglia (DRG) (Yang et al. 2005b). Others have designed an NGF encapsulated mesoporous silica nanoparticle (MSN) delivery system incorporated in electroactive polypyrrol (Ppy) conductive polymer film to enhance axon extension through the synergetic effect of both controlled NGF release and electrical stimuli in PC12 cells (Cho et al. 2009).

Co-delivery of cells and growth factors in immobilized or encapsulated form with scaffolds or particles has been proposed as a promising strategy for neural regeneration. Wang et al. reported that the direct immobilization of GDNF to a fibrous PCL scaffold increased neuronal differentiation of NPCs upon transplantation into the rat brain compared to cells delivered alone, while the presence of immobilized GDNF increased neurite outgrowth compared to PCL alone (Wang et al. 2012). In addition, the encapsulation of growth factors into microparticles and coating of particles with ECM proteins, such as fibronectin or laminin, to promote cell adsorption has also been used for sustained release and delivery. In this context, Bible et al. demonstrated that fibronectin-coated vascular endothelial growth factor (VEGF)-encapsulated PLGA particles improved the particle adhesion of human NPCs. These particles, transplanted into the stroke-injured brain, enabled dual functionality in that the VEGF was able to promote vascularization into the graft site and the formation of primary neurovascular networks (Bible et al. 2012). Similarly, Delcroix et al. coated NT-3-encapsulated PLGA microspheres with laminin and

poly-D-lysine in order to deliver MSCs into hemi-Parkinsonian rats. Following the transplantation, MSCs delivered in PLGA particles in the presence of NT-3 increased MSC survival and rats showed significant behavioral improvements (Delcroix et al. 2011).

The possible drawbacks of synthetic materials such as the lack of ECM mimicking and possible release of cytotoxic degradation byproducts have driven the exploration of using biodegradable, biocompatible, and noncytotoxic natural polymers alone, or in combination with synthetic materials for neural regeneration applications. Accordingly, microparticles composed of collagen binding peptide fused with GDNF encapsulated in a PLGA shell promoted differentiation of NPCs into MAP2-expressing mature neurons (Gujral et al. 2013). Yao et al. (2013) differentiated oligodendrocyte progenitor cells on collagen microspheres and showed that these differentiated cells were capable of myelinating dorsal root ganglion cells in culture. In another study, collagen-based high capacity hollow microspheres prepared by a template method to encapsulate NGF, resulting in highly crosslinked collagen particles that released NGF for a prolonged time period (Kraskiewicz et al. 2013). Such microspheres showed bioactivity in PC12 and DRG cell culture and could be directly used for injection at the site of nerve injuries to stimulate regeneration.

Fibroblast growth factor-2 (FGF-2) bound to heparin crosslinked with chitosan microspheres improved the growth and survivability of neural stem cell line GFP+RG3.6 as compared to normal culture conditions (Skop et al. 2013). These chitosan spheres were used as a growth factor delivery device to facilitate survival of native or transplanted neural stem cells. Zeng et al. (2014) showed that NGF-loaded chitosan microspheres, along with collagen-chitosan scaffolds having longitudinal channels, produced better outcomes in a 1.5 cm long sciatic nerve repair model as compared to just collagen-chitosan scaffolds. Thus concluding that sustained delivery of NGF from chitosan microspheres enhances the nerve regeneration process (Zeng et al. 2014). Chitosan nanoparticles improved the functional outcome (nerve impulse transmission) in a crushed adult guinea pig spinal cord as compared to control silica particles when injected subcutaneously in the nape of the neck of within 30 min following spinal cord injury (Chen et al. 2013).

Many groups have also shown that alginate microspheres can be used as an effective 3-D structure for survival, growth, proliferation, and even differentiation of NSCs (Li et al. 2006; Lin et al. 2012; Meli et al. 2014). Such micron-sized NSC-encapsulated alginate beads can be injected at the site of nerve injury. Alginate microparticles with a magnetite core and encapsulated NGF have been designed to deliver NGF are hypothesized as an effective therapeutic device for enhancing nerve regeneration (Ciofani et al. 2009). Acidic gelatin microspheres containing FGF-2 were transplanted inside a silicone tube to treat a one mm long facial nerve transection injury model and demonstrated a significantly improved rate of nerve regeneration and also the number of matured axons (Matsumine et al. 2014).

2.3.2 *Nano/Microfiber Scaffolds*

Synthetic or natural fibers with dimensions from a few nm to microns in diameter are classified as nano/microfibers. Nano/microfibers have high surface area to volume ratio aiding in the fabrication of scaffolds that not only mimic the normal tissue architecture, but also increases cell adhesion, migration, and even differentiation (Huang et al. 2003; Vasita and Katti 2006; Zhang et al. 2005). The most common methods for fabrication of nano/microfibers are electrospinning (Huang et al. 2003; Li and Xia 2004; Subbiah et al. 2005), self-assembly (Rolandi and Rolandi 2014; Salmon et al. 2005; Hartgerink et al. 2001) and phase separation (Fashandi et al. 2015; Zhao et al. 2011).

Synthetic polymer-based aligned electrospun nano/microfibers (such as PLLA, PLGA, PCL etc.) have been extensively used to direct neural regeneration. Yang and colleagues produced aligned PLLA nano–microfibrous scaffolds through an electrospinning technique for use with NSCs. The results indicated that the aligned nanofibers improved neurite outgrowth without affecting cell orientation and enhanced NSC differentiation as compared to a microsized counterpart regardless of the effect of fiber alignment (Yang et al. 2005a). Leach et al. used highly aligned electrospun PLLA nanofibers to achieve directed outgrowth of sensory and motor neurons (Leach et al. 2011). In a similar way, Subramanian et al. used uniaxially aligned electrospun PLGA nanofibrous scaffolds to orient the direction of Schwann cells (Subramanian et al. 2011), while Wang and coworkers used poly(propylene carbonate)-based electrospun-aligned nanofibrous scaffolds to demonstrate neurite outgrowth and Schwann cell migration (Wang et al. 2011). Similarly, Chew and colleagues observed that Schwann cells elongated and aligned along the axes of the electrospun PCL fibers through contact guidance (Chew et al. 2008). Kador et al. (2013) prepared a biodegradable electrospun PLA scaffold to axially direct the growth of RGCs and showed that this scaffold can be used as an effective cell delivery vehicle for transplanting ganglion cells in order to form the nerve fiber layer (Kador et al. 2013). A number of other studies have investigated the effect of different aligned electrospun polymeric fibrous materials such as poly(methyl methacrylate), poly(ethersulfone), polypyrrole (PPy)/poly(styrene-b-isobutylene-b-styrene), and PCL/PLGA, on the directed growth of different nerve cells (Li et al. 2015; Liu et al. 2010a; Ren et al. 2013; Xia et al. 2014).

Besides the advantages of directed growth and alignment, the nano/microfibers can be loaded with neurotrophic factors to promote neural regeneration. With this idea, Chew et al. encapsulated β-nerve growth factor (β-NGF) in ε-caprolactone and ethyl ethylene phosphate copolymer (PCLEEP)-based electrospun nanofibers. The synergistic effect of sustained β-NGF release and alignment of nanofibers were observed on neurite outgrowth from PC12 cells (Chew et al. 2005). Liu et al. developed novel NGF-encapsulated core shell nanofiber composite P(LLA-CL)/NGF conduits with favorable mechanical properties and biocompatibility effectively enhancing sciatic nerve regeneration in rats (Liu et al. 2011). Zhang et al. showed the significant efficiency of NGF-encapsulated aligned silk fibroin (SF)/P(LLA-CL)-blended nanofibers in promoting peripheral nerve regeneration to

demonstrate the combined use of natural and synthetic polymers (Zhang et al. 2014). As an alternative to direct incorporation of the neurotrophic agents to the fiber matrix, the covalent attachment of the active agents to the fiber structure has also been investigated. Through this approach, diffusion induced drug loss can be prevented, achieving controlled and sustained release. Patel et al. conjugated bFGF and laminin onto PLLA nanofibers through 1-ethyl-3-(3-dimethylaminopropyl) carbodiimide hydrochloride, N-hydroxysulfosuccinimide and heparin click chemistry. With this system, they managed to achieve significant neurite extension by using small amounts of bFGF without activity loss during the synthesis (Patel et al. 2007). In the work of Lam et al., bFGF and EGF were attached to the nanofibrous PLLA conduits through heparin conjugation, thus significantly promoting axon growth as compared to its counterparts in which bFGF and EGF were loaded by physical adsorption (Lam et al. 2010). Besides neurotrophic factors, the use of laminin chemically attached or physically encapsulated in aligned electrospun nano/microfibrous conduits has gained attention due to its ability to facilitate regeneration speed and functional recovery (Junka et al. 2013; Neal et al. 2012).

The use of electrically conductive nano/microfibers for neural regeneration has been proposed as another strategy. Prabhakaran et al. developed conductive nanofibers by blending PLLA and polyaniline, enhancing neurite outgrowth of NSCs through applied electrical fields (Prabhakaran et al. 2011). With a similar strategy, Subramanian et al. produced electrically conductive PLGA/ poly(3-hexylthiophene) nanofibers showing significant influence on adhesion and proliferation of Schwann cells under an electrical field (Subramanian et al. 2012). In contrast to the above mentioned approaches, Lee and coworkers coated PLGA electrospun nanofibers with polypyrrole to form electrically conductive nanoscaffolds enhancing the differentiation of PC12 cells with electrical field stimuli (Lee et al. 2009).

Some studies have also incorporated naturally existing materials to develop nano/microfibrous platforms for nerve regeneration. Liu et al. used a novel cross-linking method to prepare rose bengal photoinitiated-acetic acid electrospun collagen nanofibers, demonstrating that the neural stem cell line C17.2 can grow and proliferate on these fibers for about 7 days before reaching confluence (Liu et al. 2010b). Also, these neural stem cells showed significant cellular processes indicating neurite outgrowth. In another study by Zhu and coworkers, in order to improve the mechanical properties of collagen fibers such as tensile strength and elasticity, silk protein was incorporated while fabricating electrospun aligned collagen-silk composite microfibers (Zhu et al. 2014). Human decidua parietalis placental stem cells (hdpPSCs) developed long processes while growing on these fibers and also showed positive immunostaining for β-III-tubulin and Nestin suggesting that hdpPSCs differentiated into neural-like cells under these growth conditions. Collagen nanofibers were also shown to increase the maturation of synapses in spinal cord-derived NSCs by the mitogen-activated protein kinase/extracellular signaling-regulated kinase MAPK/ERK1/2 pathway (Yin et al. 2014). Spinal cord NSCs differentiated into neurons on these random, as well as aligned collagen nanofibers at a higher percentage as compared to collagen-coated controls (Yin et al. 2014). In a comparative study, 3-D chitosan nanofibers produced higher pro-

liferation and differentiation of PC12 cells and human NSCs predominantly to neurons as compared to 2-D chitosan substrates showing that a 3-D environment may influence the growth properties of NSCs and thus can be effectively used for neural tissue engineering (Du et al. 2014). Gelain et al. attached several cell adhesion, differentiation, and homing motifs to a self-assembling peptide RADA16 (Ac-RADARADARADARADA-COHN2) to obtain 3-D nanofiber scaffolds that were found to be comparative to Matrigel in terms of NSC adhesion and differentiation (Gelain et al. 2006). β-Tricalcium phosphate (β-TCP) immobilized on a chitosan nanofiber mesh tube and polarized to store electric charge improved the immunofluorescence, axon density, and axon area as compared to non-polarized tubes and was found to be comparable to an isograft in a rat sciatic nerve defect model, suggesting that charged β-TCP immobilized chitosan nanofiber mesh tubes can be used as an effective tool for nerve regeneration (Wang et al. 2010).

2.3.3 Other Types of Scaffolds

Various types of 3-D scaffolds and combination therapies other than nanoparticles and nanofibers are also being used for neural tissue engineering, including films, nanotubes, gels, and porous materials (Spivey et al. 2012; McCreedy and Sakiyama-Elbert 2012). For instance, polymer-based porous films physically or chemically loaded with neurotrophic factors with surface gradients and surface nano/micropatterning have been used as conduits for neural regeneration (Tang et al. 2013; Kim et al. 2015). The different types of scaffolds bearing surface nano/micropatterning have also been shown to provide topographic guidance cues to create regenerative platforms for cells (Roberts et al. 2014; Ho et al. 2015; McMurtrey 2014; Houchin-Ray et al. 2007; Rutkowski et al. 2004). Miller and coworkers (Miller et al. 2001a, b) prepared biodegradable micropatterned poly(D,L-lactic acid) films using solvent casting and showed that such films are capable of enhancing the alignment of Schwann cells, indirectly increasing neurite length and orientation of DRG cells growing along with the aligned Schwann cells. Micropatterned polystyrene films prepared using a similar method were used to promote alignment of rat type-1 astrocytes (Recknor et al. 2004) and were also shown to enhance orientation and selectively differentiate adult hippocampal progenitor cells to a neuronal fate when co-cultured with astrocytes (Recknor et al. 2006; Oh et al. 2009). Similarly, micropatterned films fabricated from PLA supported the oriented growth and transdifferentiation of MSCs toward a Schwann cell fate (Sharma et al. 2016). Qi et al. showed that linear and circular micropatterns significantly enhanced NSC differentiation to neurons via the MAPK/ERK signaling pathway (Qi et al. 2013). Coupling stem cells and cellular reprogramming, along with scaffolds (i.e., nerve regeneration conduits) is a significant strategy to facilitate nerve regeneration (Fig. 2.7).

Synthetic and natural-based polymer scaffolds may lack the required properties of neural regeneration applications such as appropriate tensile strength and electrical conductivity. In this case, carbon nanotubes (CNTs) can provide conductive proper-

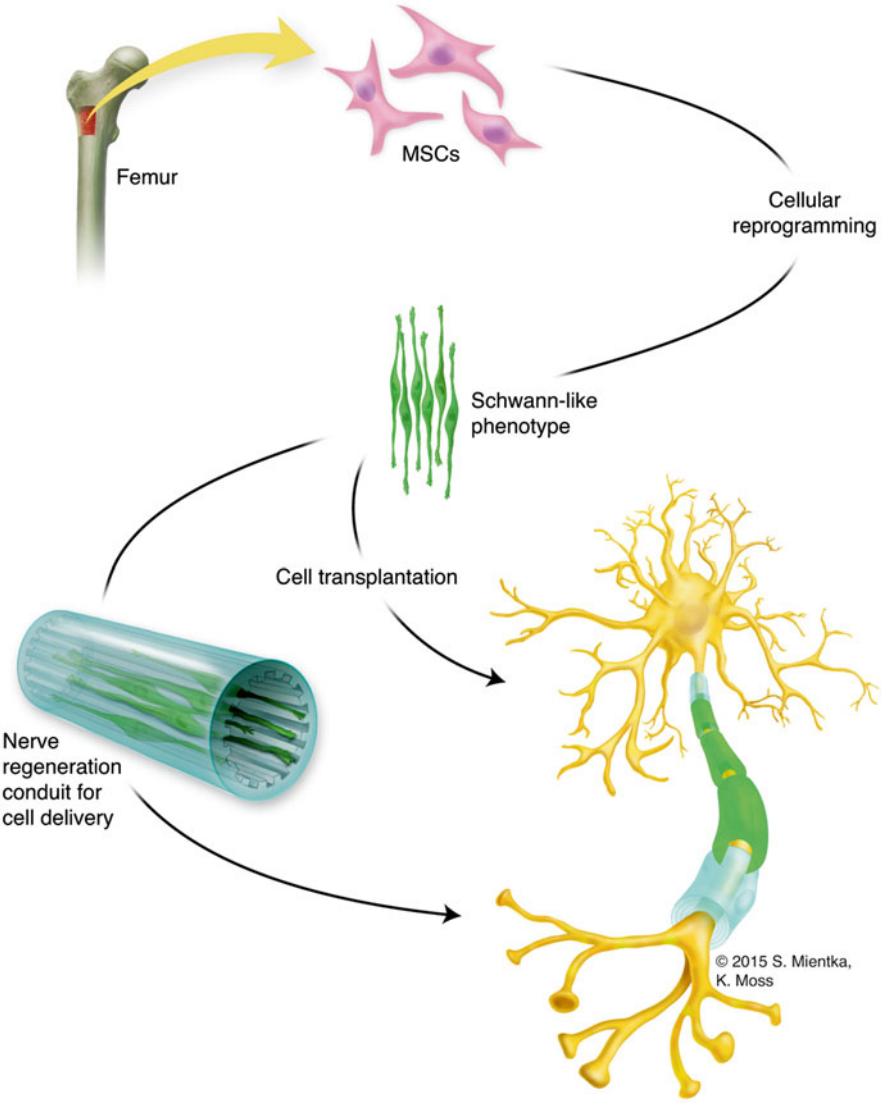

Fig. 2.7 Nerve regeneration strategy employing stem cells and nerve regeneration conduits. Reprogramming bone marrow-derived stem cells into Schwann-like cells is an important approach for peripheral nerve regeneration. Coupling stem cells and cellular reprogramming with scaffolds (i.e., nerve regeneration conduits) is likely to provide a powerful approach to facilitate nerve regeneration

ties along with mechanical and tensile scaffold enhancements. A number of studies have shown that multi or single wall CNTs chemically functionalized with various polymers or bioactive molecules can improve neural regeneration activities including neurite branching, outgrowth, attachment of growth cones, and cell dif-

ferentiation through the release of neurotrophic factors, electrical field stimuli, surface micropatterning, or layer by layer assembly (Tran et al. 2009; Huang et al. 2012; Fabbro et al. 2013; Hopley et al. 2014; Bosi et al. 2013, 2014).

Integrating hydrogels with scaffolds has also shown promise in neuroregenerative studies. Labrador et al. used silicone tubes filled with collagen or laminin gel to repair 4–6 mm gaps in a mouse sciatic nerve transection injury model and found that lower concentrations of collagen and laminin gels provided better functional outcomes as compared to higher concentration gels and the saline control (Labrador et al. 1998). Laminin gels promoted slightly better functional recovery than collagen gels. In another study, biodegradable collagen tubes were filled with a magnetically aligned collagen type I gel and non-aligned gels as control (Ceballos et al. 1999). It was found that magnetically aligned gels supported regenerated axon growth to the distal end in four out of four mice as compared to just one out of six mice in the control, non-aligned collagen gels. Choi and coworkers used a vein graft filled with collagen gel to bridge a 15 mm rabbit peroneal nerve defect injury and found that the number of myelinated fibers was significantly greater than the control vein transplanted rabbits at weeks 4, 8, and 12, suggesting that collagen is an effective matrix to fill tubes that support neural regeneration (Choi et al. 2005). In a similar fashion, several studies used fibrin gels (Nakayama et al. 2007a, b; Wood et al. 2013; Sakiyama et al. 1999; Lee et al. 2014; Schense et al. 2000) or chitosan gels (Ishikawa et al. 2007; Ishikawa et al. 2009) for filling tubes/conduits along with other regenerative cues and showed that fibrin gels promoted nerve regeneration.

In addition to the use of porous scaffolds to promote exchange of nutrients and waste products, cells may be transplanted within scaffolds to promote cell survival. Using blends of PLA and PLGA, 3-D scaffolds were prepared with pores normal to the plane of the scaffold. These scaffolds enhanced the orientation and upregulated markers of differentiation in retinal progenitor cells (RPCs) growing inside the pores of the scaffold demonstrating that such scaffolds can be used for enhancing the differentiation of RPCs into photoreceptor-like cells and also can be transplanted into the sub-retinal space (Lavik et al. 2005). PLLA/PLGA polymer composite grafts prepared by a modified solid–liquid-phase separation technique (Tomita et al. 2005) and microfabricated poly(glycerol-sebacate) scaffolds (Neeley et al. 2008; Redenti et al. 2009) using a replica molding technique were also prepared as RPC delivery devices for transplantation into the sub-retinal space. Recently, human stem cell-derived neural tissue constructs that included vascular networks and microglia were produced by combining precursor cell-types on synthetic hydrogels (Schwartz et al. 2015). Other types of 3-D scaffolds for neural tissue engineering have also been prepared by using methods such as inkjet printing (Xu et al. 2006), microarray printing (Meli et al. 2014), microstereolithography (Pateman et al. 2015), 3-D hydrogels (Nisbet et al. 2008; Suri and Schmidt 2010; Stabenfeldt et al. 2006; Crompton et al. 2007), multiphoton polymerization (Melissinaki et al. 2011), and freeze drying (Yang et al. 2004; Kang et al. 1999; Flynn et al. 2003; Suzuki et al. 1999).

2.4 Stem Cell-Based Approaches Coupled with Bioengineering for Translational Applications

Numerous clinical trials employing bioengineering strategies are underway for the treatment of spinal cord injury. One study is currently in the recruitment phase for autologous transplantation of NSCs for traumatic spinal cord injury (NCT0232666) (Federal Research Clinical Center of Federal Medical & Biological Agency 2015). The cells are transplanted with RMx Biomatrix, a biocompatible matrix containing neural stem cells derived from the patient's own bone marrow stem cells. Conducted by the Federal Research Clinical Center of Federal Medical and Biological Agency, Russia, in collaboration with the Novagenesis Foundation and Ophiuchus Technologies, the goal is to expand the cell replacement technique to other diseases including Primary Progressive Multiple Sclerosis, ALS, and traumatic brain injury. Another company, InVivo Therapeutics, is recruiting participants to test the safety and feasibility of its Neuro-Spinal Scaffold, a PLGA poly-L-lysine scaffold for the treatment of complete thoracic traumatic acute spinal cord injury (NCT02138110). When transplanted in patients with acute spinal cord injury, the Neuro-Spinal Scaffold provided biocompatible and cellular-adhesive support to promote appositional healing, relieving tissue pressure, hemorrhage, and edema at the contusion. Following successful clinical trials with the scaffold alone, trials will be performed using the scaffold seeded with neural stem cells. The Chinese Academy of Sciences is administering a trial of a functional collagen scaffold for transplantation in acute spinal cord injury patients (NCT02510365). The same institute is also sponsoring a trial for the use of a collagen scaffold containing mesenchymal stem cells for transplantation in spinal cord injury (NCT02352077).

Biomaterials for the treatment of peripheral nerve damage are also undergoing clinical trials. The company Axogen has developed the Avance® nerve graft, in which donor nerve tissue is processed to clear cells and cellular debris, providing an open scaffold. Chondroitin sulfate proteoglycans, inhibitors of axonal growth, are also removed with the Avance® process. Used for peripheral nerve injury, the grafts were able to integrate efficiently in nerve gaps 5–50 mm in length (Cho et al. 2012; Karabekmez et al. 2009). NeuraGen bovine type I collagen conduits of varying caliber provided by Integra LifeSciences have shown in clinical trials to recover sensation by 35–45 %. However, empty conduits of this type do not perform well with nerve gaps greater than 5 mm (Wangensteen and Kalliainen 2010; Schmauss et al. 2014).

Macular degeneration and other degenerative eye conditions are being tested for the safety and efficacy of transplanted cells coupled with biomaterials. Clinical trials are ongoing for treatment of age-related macular degeneration, led by M. Takahashi of the RIKEN Center for Developmental Biology in collaboration with Y. Kurimoto of the Institute for Biomedical Research and Innovation Hospital. Autologous iPSCs derived from patient's skin cells are transdifferentiated into retinal pigment epithelial cells, which are cultured as a monolayer sheet. This sheet of cells is then transplanted behind the retina. A similar clinical trial is also being

performed by Pfizer using human ESC-derived retinal pigment epithelial cells (NCT01691261). The cells are provided as a monolayer cultured upon a polyester membrane, which is rolled up and placed at the back of the eye. A recent Phase I safety trial was successful for the intraocular delivery of CNTF with an encapsulated cell implant for the treatment of macular telangiectasia type 2 (Chew et al. 2015). Phase II multicenter randomized clinical trials are now ongoing for macular telangiecgtasia and retinitis pigmentosa, sponsored by Neurotech Pharmaceuticals (NCT01949324, NCT01530659). Phase II clinical trials are also ongoing for the use of encapsulated cell technology for the delivery of VEGF for treatment of recurrent choroidal neovascularization secondary to age-related macular degeneration (NCT02228304).

2.5 Conclusions and Future Directions

The vast complexity of the human brain presents amazing challenges when developing treatment strategies for neurodegenerative disease and injuries sustained by the nervous system. Stem cells along with cellular reprogramming technologies provide a promising resource for studies of neurodevelopment, disease modeling, development of experimental strategies for neural repair, and also for drug discovery. The field of cellular reprogramming has undergone rapid development in recent years. It is becoming routine to convert differentiated mature cells into a variety of other cell types using genetic or small molecule approaches. For example, the ability to convert skin fibroblasts directly into neurons or glia has dramatically altered strategies in regenerative medicine. Cellular reprogramming is becoming a standard approach in our biological toolboxes necessary to study complex diseases, especially when cells and tissues are difficult to isolate, in short supply or otherwise not available. Furthermore, ethical constraints as well as immune rejection associated with heterologous transplants make cellular reprogramming strategies even more appealing.

Combining stem cells with bioengineering technologies has created a new era in regenerative medicine. In order to obtain specific cell types for transplantation, stem cell bioengineering provides a means for manipulating microenvironmental signals that regulate cell proliferation, survival, and differentiation. Enabling stem cell-based therapies for treatment of neurological conditions requires an understanding of how to re-create local microenvironments that sustain cell survival and promote recovery of function. Considerable research effort has helped elucidate these complex microenvironments. It is clear that a myriad of soluble and surface-associated signaling molecules, cell-to-cell contacts, cell-to-ECM, and local mechanical/physical cues interacting in complex ways are involved in regulating not only cell fate, but also cell behavior. Developing nano/microscale engineering platforms that reliably mimic the stem cell microenvironment is becoming a powerful approach for development of therapeutic strategies targeting the nervous system. With advances in scaffold designs must come rigorous interrogation of their functionality. Proof of

principle studies conducted in vitro and subsequently in rodents will need to be followed with studies in larger animal models before clinical application. Implementation of human stem cell-based in vitro model systems that combine biomaterials and that have the ability to mimic human physiology will have considerable potential for drug development and screening and is likely to offer a cost-effective approach for assessing safety and efficacy before moving to clinical trials.

As we move to the future, bioinformatics and systems-level approaches will help guide the field of stem cell bioengineering. Gaining a clear understanding of regulatory networks and neural connectomes will play key roles in development of novel neurotherapeutics and successful transplantation strategies. In addition, the emerging trend of using combinatorial methods coupled with high-throughput characterization will serve as powerful approaches to engineer and explore stem cells and their plasticity and utility for neural repair.

Acknowledgements The authors would like to acknowledge the US Army Medical Research and Materiel Command under contract W81XWH-11-1-0700 and the Stem Cell Biology Fund for funding. Illustrations were prepared by faculty and undergraduate students from the Biological and Pre-Medical Illustration Program (BPMI) at Iowa State University (Professor K.E. Moss, E.L. Wichers, S.D. Mientka, H. Sinsel, C. Swanberg, and R. Rossiter).

References

Abraham, S., N. Eroshenko, and R.R. Rao. 2009. Role of Bioinspired Polymers in Determination of Pluripotent Stem Cell Fate. *Regenerative Medicine* 4(4): 561–578.

Alyautdin, R., et al. 1997. Delivery of Loperamide Across the Blood–Brain Barrier with Polysorbate 80-Coated Polybutylcyanoacrylate Nanoparticles. *Pharmaceutical Research* 14(3): 325–328.

Alyautdin, R.N., et al. 1998. Significant Entry of Tubocurarine into the Brain of Rats by Adsorption to Polysorbate 80-Coated Polybutylcyanoacrylate Nanoparticles: An In Situ Brain Perfusion Study. *Journal of Microencapsulation* 15(1): 67–74.

Amoh, Y., et al. 2009. Human Hair Follicle Pluripotent Stem (hfPS) Cells Promote Regeneration of Peripheral-Nerve Injury: An Advantageous Alternative to ES and iPS Cells. *Journal of Cellular Biochemistry* 107(5): 1016–1020.

Andrieu-Soler, C., et al. 2005. Intravitreous Injection of PLGA Microspheres Encapsulating GDNF Promotes the Survival of Photoreceptors in the rd1/rd1 Mouse. *Molecular Vision* 11: 1002–1011.

Aqil, A., et al. 2008. Magnetic Nanoparticles Coated by Temperature Responsive Copolymers for Hyperthermia. *Journal of Materials Chemistry* 18(28): 3352–3360.

Arthur, A., et al. 2008. Adult Human Dental Pulp Stem Cells Differentiate Toward Functionally Active Neurons Under Appropriate Environmental Cues. *Stem Cells* 26(7): 1787–1795.

Auffan, M., et al. 2009. Towards a Definition of Inorganic Nanoparticles from an Environmental, Health and Safety Perspective. *Nature Nanotechnology* 4(10): 634–641.

Bain, G., et al. 1995. Embryonic Stem Cells Express Neuronal Properties In Vitro. *Developmental Biology* 168(2): 342–357.

Bakandritsos, A., et al. 2010. Preparation, Stability and Cytocompatibility of Magnetic/PLA-PEG Hybrids. *Nanoscale* 2(4): 564–572.

Behrstock, S., et al. 2006. Human Neural Progenitors Deliver Glial Cell Line-Derived Neurotrophic Factor to Parkinsonian Rodents and Aged Primates. *Gene Therapy* 13(5): 379–388.

Bible, E., et al. 2012. Neo-vascularization of the Stroke Cavity by Implantation of Human Neural Stem Cells on VEGF-Releasing PLGA Microparticles. *Biomaterials* 33(30): 7435–7446.

Bissonnette, C.J., et al. 2011. The Controlled Generation of Functional Basal Forebrain Cholinergic Neurons from Human Embryonic Stem Cells. *Stem Cells* 29(5): 802–811.

Bjorklund, L.M., et al. 2002. Embryonic Stem Cells Develop into Functional Dopaminergic Neurons After Transplantation in a Parkinson Rat Model. *Proceedings of the National Academy of Sciences of the United States of America* 99(4): 2344–2349.

Blanchard, J.W., et al. 2015. Selective Conversion of Fibroblasts into Peripheral Sensory Neurons. *Nature Neuroscience* 18(1): 25–35.

Bosi, S., et al. 2013. Carbon Nanotubes: A Promise for Nerve Tissue Engineering? *Nanotechnology Reviews* 2(1): 47–57.

Bosi, S., L. Ballerini, and M. Prato. 2014. Carbon Nanotubes in Tissue Engineering. In *Making and Exploiting Fullerenes, Graphene, and Carbon Nanotubes*, eds. M. Marcaccio and F. Paolucci, 181–204.

Bottai, D., et al. 2010. Embryonic Stem Cells Promote Motor Recovery and Affect Inflammatory Cell Infiltration in Spinal Cord Injured Mice. *Experimental Neurology* 223(2): 452–463.

Brederlau, A., et al. 2006. Transplantation of Human Embryonic Stem Cell-Derived Cells to a Rat Model of Parkinson's Disease: Effect of In Vitro Differentiation on Graft Survival and Teratoma Formation. *Stem Cells* 24(6): 1433–1440.

Brem, H., et al. 1989. Biocompatibility of a Biodegradable, Controlled-Release Polymer in the Rabbit Brain. *Selective Cancer Therapeutics* 5(2): 55–65.

Brustle, O., et al. 1999. Embryonic Stem Cell-Derived Glial Precursors: A Source of Myelinating Transplants. *Science* 285: 754–756.

Brustle, I., et al. 2015. Hematopoietic and Mesenchymal Stem Cells: Polymeric Nanoparticle Uptake and Lineage Differentiation. *Beilstein Journal of Nanotechnology* 6: 383–395.

Budhian, A., S.J. Siegel, and K.I. Winey. 2008. Controlling the In Vitro Release Profiles for a System of Haloperidol-Loaded PLGA Nanoparticles. *International Journal of Pharmaceutics* 346(1–2): 151–159.

Burdick, J.A., et al. 2006. Stimulation of Neurite Outgrowth by Neurotrophins Delivered from Degradable Hydrogels. *Biomaterials* 27(3): 452–459.

Burkersroda, F.V., L. Schedl, and A. Göpferich. 2002. Why Degradable Polymers Undergo Surface Erosion or Bulk Erosion. *Biomaterials* 23(21): 4221–4231.

Caiazzo, M., et al. 2011. Direct Generation of Functional Dopaminergic Neurons from Mouse and Human Fibroblasts. *Nature* 476(7359): 224–227.

Caicco, M.J., et al. 2013. A Hydrogel Composite System for Sustained Epi-Cortical Delivery of Cyclosporin A to the Brain for Treatment of Stroke. *Journal of Controlled Release* 166(3): 197–202.

Calatayud, M.P., et al. 2013. Neuronal Cells Loaded with PEI-Coated Fe_3O_4 Nanoparticles for Magnetically Guided Nerve Regeneration. *Journal of Materials Chemistry B* 1(29): 3607–3616.

Cao, L., et al. 2004. Olfactory Ensheathing Cells Genetically Modified to Secrete GDNF to Promote Spinal Cord Repair. *Brain* 127(Pt 3): 535–549.

Castillo, B., et al. 1994. Retinal Ganglion-Cell Survival Is Promoted by Genetically-Modified Astrocytes Designed to Secrete Brain-Derived Neurotrophic Factor (BDNF). *Brain Research* 647(1): 30–36.

Ceballos, D., et al. 1999. Magnetically Aligned Collagen Gel Filling a Collagen Nerve Guide Improves Peripheral Nerve Regeneration. *Experimental Neurology* 158(2): 290–300.

Chai, C., and K.W. Leong. 2007. Biomaterials Approach to Expand and Direct Differentiation of Stem Cells. *Molecular Therapy* 15(3): 467–480.

Chambers, I., and A. Smith. 2004. Self-Renewal of Teratocarcinoma and Embryonic Stem Cells. *Oncogene* 23(43): 7150–7160.

Chambers, I., et al. 2003. Functional Expression Cloning of Nanog, a Pluripotency Sustaining Factor in Embryonic Stem Cells. *Cell* 113: 643–655.

Chambers, S.M., et al. 2009. Highly Efficient Neural Conversion of Human ES and iPS Cells by Dual Inhibition of SMAD Signaling. *Nature Biotechnology* 27(3): 275–280.

Chavez-Santoscoy, A.V., et al. 2012. Tailoring the Immune Response by Targeting C-Type Lectin Receptors on Alveolar Macrophages Using "Pathogen-Like" Amphiphilic Polyanhydride Nanoparticles. *Biomaterials* 33(18): 4762–4772.

Chen, B., et al. 2013. Pushing the Science Forward: Chitosan Nanoparticles and Functional Repair of CNS Tissue After Spinal Cord Injury. *Journal of Biological Engineering* 7(1): 1–9.

Chew, S.Y., et al. 2005. Sustained Release of Proteins from Electrospun Biodegradable Fibers. *Biomacromolecules* 6(4): 2017–2024.

Chew, S.Y., et al. 2008. The Effect of the Alignment of Electrospun Fibrous Scaffolds on Schwann Cell Maturation. *Biomaterials* 29(6): 653–661.

Chew, E.Y., et al. 2015. Ciliary Neurotrophic Factor for Macular Telangiectasia Type 2: Results From a Phase 1 Safety Trial. *American Journal of Ophthalmology* 159(4): 659–666. e1.

Chin, M.H., et al. 2009. Induced Pluripotent Stem Cells and Embryonic Stem Cells Are Distinguished by Gene Expression Signatures. *Cell Stem Cell* 5(1): 111–123.

Cho, Y., and R. Ben Borgens. 2012. Polymer and Nano-Technology Applications for Repair and Reconstruction of the Central Nervous System. *Experimental Neurology* 233(1): 126–144.

Cho, Y., et al. 2009. A Mesoporous Silica Nanosphere-Based Drug Delivery System Using an Electrically Conducting Polymer. *Nanotechnology* 20(27): 275102.

Cho, M.S., et al. 2012. Functional Outcome Following Nerve Repair in the Upper Extremity Using Processed Nerve Allograft. *Journal of Hand Surgery. American Volume* 37(11): 2340–2349.

Choi, B.H., et al. 2005. Nerve Repair Using a Vein Graft Filled with Collagen Gel. *Journal of Reconstructive Microsurgery* 21(4): 267–272.

Choi, H.S., et al. 2015. Therapeutic Potentials of Human Adipose-Derived Stem Cells on the Mouse Model of Parkinson's Disease. *Neurobiol Aging* 36(10): 2885–2892.

Ciofani, G., et al. 2009. Magnetic Alginate Microspheres: System for the Position Controlled Delivery of Nerve Growth Factor. *Biomedical Microdevices* 11(2): 517–527.

Cole, R.J., R.G. Edwards, and J. Paul. 1966. Cytodifferentiation and Embryogenesis in Cell Colonies and Tissue Cultures Derived from Ova and Blastocysts of the Rabbit. *Developmental Biology* 13: 385–407.

Corey, J.M., et al. 2007. Aligned Electrospun Nanofibers Specify the Direction of Dorsal Root Ganglia Neurite Growth. *Journal of Biomedical Materials Research. Part A* 83(3): 636–645.

Crompton, K.E., et al. 2007. Polylysine-Functionalised Thermoresponsive Chitosan Hydrogel for Neural Tissue Engineering. *Biomaterials* 28(3): 441–449.

Cunha, C., S. Panseri, and S. Antonini. 2011. Emerging Nanotechnology Approaches in Tissue Engineering for Peripheral Nerve Regeneration. *Nanomedicine: Nanotechnology Biology and Medicine* 7(1): 50–59.

Cunningham, M., et al. 2014. hPSC-Derived Maturing GABAergic Interneurons Ameliorate Seizures and Abnormal Behavior in Epileptic Mice. *Cell Stem Cell* 15(5): 559–573.

Daadi, M.M., A.L. Maag, and G.K. Steinberg. 2008. Adherent Self-Renewable Human Embryonic Stem Cell-Derived Neural Stem Cell Line: Functional Engraftment in Experimental Stroke Model. *PLoS One* 3(2): e1644.

Dahan, M., et al. 2003. Diffusion Dynamics of Glycine Receptors Revealed by Single-Quantum Dot Tracking. *Science* 302(5644): 442–445.

Dang, J.M., and K.W. Leong. 2006. Natural Polymers for Gene Delivery and Tissue Engineering. *Advanced Drug Delivery Reviews* 58(4): 487–499.

de Boer, R., et al. 2012. Short- and Long-Term Peripheral Nerve Regeneration Using a Poly-Lactic-Co-Glycolic-Acid Scaffold Containing Nerve Growth Factor and Glial Cell Line-Derived Neurotrophic Factor Releasing Microspheres. *Journal of Biomedical Materials Research. Part A* 100A(8): 2139–2146.

De Jong, W.H., and P.J.A. Borm. 2008. Drug Delivery and Nanoparticles: Applications and Hazards. *International Journal of Nanomedicine* 3(2): 133–149.

de Vos, P., et al. 2014. Polymers in Cell Encapsulation from an Enveloped Cell Perspective. *Advanced Drug Delivery Reviews* 67–68: 15–34.

Delcroix, G.J.R., et al. 2011. The Therapeutic Potential of Human Multipotent Mesenchymal Stromal Cells Combined with Pharmacologically Active Microcarriers Transplanted in Hemi-Parkinsonian Rats. *Biomaterials* 32(6): 1560–1573.

Deshpande, D.M., et al. 2006. Recovery from Paralysis in Adult Rats Using Embryonic Stem Cells. *Annals of Neurology* 60(1): 32–44.

Dey, N.D., et al. 2010. Genetically Engineered Mesenchymal Stem Cells Reduce Behavioral Deficits in the YAC 128 Mouse Model of Huntington's Disease. *Behavioural Brain Research* 214(2): 193–200.

Dhandayuthapani, B., et al. 2011. Polymeric Scaffolds in Tissue Engineering Application: A Review. *International Journal of Polymer Science* 2011: 1–19.

Dihne, M., et al. 2006. Embryonic Stem Cell-Derived Neuronally Committed Precursor Cells with Reduced Teratoma Formation After Transplantation into the Lesioned Adult Mouse Brain. *Stem Cells* 24(6): 1458–1466.

Doi, D., et al. 2012. Prolonged Maturation Culture Favors a Reduction in the Tumorigenicity and the Dopaminergic Function of Human ESC-Derived Neural Cells in a Primate Model of Parkinson's Disease. *Stem Cells* 30(5): 935–945.

Driskell, R.R., et al. 2011. Hair Follicle Dermal Papilla Cells at a Glance. *Journal of Cell Science* 124(Pt 8): 1179–1182.

Du, J., et al. 2014. Comparative Evaluation of Chitosan, Cellulose Acetate, and Polyethersulfone Nanofiber Scaffolds for Neural Differentiation. *Carbohydrate Polymers* 99: 483–490.

Elliott Donaghue, I., et al. 2014. Cell and Biomolecule Delivery for Tissue Repair and Regeneration in the Central Nervous System. *Journal of Controlled Release: Official Journal of the Controlled Release Society* 190: 219–227.

Erdo, F., et al. 2003. Host-Dependent Tumorigenesis of Embryonic Stem Cell Transplantation in Experimental Stroke. *Journal of Cerebral Blood Flow and Metabolism* 23(7): 780–785.

Evans, M.J., and M.H. Kaufman. 1981. Establishment in Culture of Pluripotent Cells from Mouse Embryos. *Nature* 292: 154–156.

Fabbro, A., M. Prato, and L. Ballerini. 2013. Carbon Nanotubes in Neuroregeneration and Repair. *Advanced Drug Delivery Reviews* 65(15): 2034–2044.

Fashandi, H., A. Yegane, and M.M. Abolhasani. 2015. Interplay of Liquid-Liquid and Solid–liquid Phase Separation Mechanisms in Porosity and Polymorphism Evolution Within Poly(Vinylidene Fluoride) Nanofibers. *Fibers and Polymers* 16(2): 326–344.

Federal Research Clinical Center of Federal Medical & Biological Agency, R. *Neural Stem Cell Transplantation in Traumatic Spinal Cord Injury*. Clinicaltrials.gov 10 October 2015]. https://clinicaltrials.gov/ct2/show/NCT02326662?term=spinal+cord+injury+chronic&rank=20

Flynn, L., P.D. Dalton, and M.S. Shoichet. 2003. Fiber Templating of Poly(2-Hydroxyethyl Methacrylate) for Neural Tissue Engineering. *Biomaterials* 24(23): 4265–4272.

Frim, D.M., et al. 1994. Implanted Fibroblasts Genetically Engineered to Produce Brain-Derived Neurotrophic Factor Prevent 1-Methyl-4-Phenylpyridinium Toxicity to Dopaminergic Neurons in the Rat. *Proceedings of the National Academy of Sciences of the United States of America* 91(11): 5104–5108.

Gaharwar, A.K., et al. 2013. *Nanomaterials in Tissue Engineering: Fabrication and Applications*, vol. 56, 1–444. Oxford: Woodhead Publishing.

Gao, J., et al. 1998. Surface Modification of Polyanhydride Microspheres. *Journal of Pharmaceutical Sciences* 87(2): 246–248.

Garbayo, E., et al. 2009. Effective GDNF Brain Delivery Using Microspheres—A Promising Strategy for Parkinson's Disease. *Journal of Controlled Release* 135(2): 119–126.

Gardner, R.L. 1968. Mouse Chimaeras Obtained by the Injection of Cells into the Blastocyst. *Nature* 220: 596–597.

Gaspard, N., et al. 2008. An Intrinsic Mechanism of Corticogenesis from Embryonic Stem Cells. *Nature* 455(7211): 351–357.

Gasperini, L., J.F. Mano, and R.L. Reis. 2014. Natural Polymers for the Microencapsulation of Cells. *Journal of the Royal Society Interface* 11(100): 20140817.

Gelain, F., et al. 2006. Designer Self-Assembling Peptide Nanofiber Scaffolds for Adult Mouse Neural Stem Cell 3-Dimensional Cultures. *PLoS One* 1: e119.

Gelperina, S., et al. 2005. The Potential Advantages of Nanoparticle Drug Delivery Systems in Chemotherapy of Tuberculosis. *American Journal of Respiratory and Critical Care Medicine* 172(12): 1487–1490.

Ghasemi-Mobarakeh, L., et al. 2008. Electrospun Poly(ε-Caprolactone)/Gelatin Nanofibrous Scaffolds for Nerve Tissue Engineering. *Biomaterials* 29(34): 4532–4539.

Ghosh, Z., et al. 2010. Persistent Donor Cell Gene Expression Among Human Induced Pluripotent Stem Cells Contributes to Differences with Human Embryonic Stem Cells. *PLoS One* 5(2): e8975.

GhoshMitra, S., et al. 2012. Role of Engineered Nanocarriers for Axon Regeneration and Guidance: Current Status and Future Trends. *Advanced Drug Delivery Reviews* 64(1): 110–125.

Gonzalez-Cordero, A., et al. 2013. Photoreceptor Precursors Derived from Three-Dimensional Embryonic Stem Cell Cultures Integrate and Mature Within Adult Degenerate Retina. *Nature Biotechnology* 31(8): 741–747.

Graff, C.L., and G.M. Pollack. 2005. Nasal Drug Administration: Potential for Targeted Central Nervous System Delivery. *Journal of Pharmaceutical Sciences* 94(6): 1187–1195.

Grozdanic, S.D., et al. 2010. Exogenous Modulation of Intrinsic Optic Nerve Neuroprotective Activity. *Graefes Archive for Clinical and Experimental Ophthalmology* 248(8): 1105–1116.

Guerout, N., et al. 2011. Co-transplantation of Olfactory Ensheathing Cells from Mucosa and Bulb Origin Enhances Functional Recovery After Peripheral Nerve Lesion. *PLoS One* 6(8): e22816.

Gujral, C., et al. 2013. Biodegradable Microparticles for Strictly Regulating the Release of Neurotrophic Factors. *Journal of Controlled Release* 168(3): 307–316.

Gulyaev, A.E., et al. 1999. Significant Transport of Doxorubicin into the Brain with Polysorbate 80-Coated Nanoparticles. *Pharmaceutical Research* 16(10): 1564–1569.

Gunatillake, P.A., and R. Adhikari. 2003. Biodegradable Synthetic Polymers for Tissue Engineering. *European Cells and Materials* 5: 1–16; discussion 16.

Gurdon, J.B., and V. Uehlinger. 1966. "Fertile" Intestine Nuclei. *Nature* 210: 1240–1241.

Gutierrez-Aranda, I., et al. 2010. Human Induced Pluripotent Stem Cells Develop Teratoma More Efficiently and Faster Than Human Embryonic Stem Cells Regardless the Site of Injection. *Stem Cells* 28(9): 1568–1570.

Haile, Y., et al. 2015. Reprogramming of HUVECs into Induced Pluripotent Stem Cells (HiPSCs), Generation and Characterization of HiPSC-Derived Neurons and Astrocytes. *PLoS One* 10(3): e0119617.

Han, D.W., et al. 2012. Direct Reprogramming of Fibroblasts into Neural Stem Cells by Defined Factors. *Cell Stem Cell* 10(4): 465–472.

Harper, M.M., et al. 2009. Brain-Derived Neurotrophic Factor Released from Engineered Mesenchymal Stem Cells Attenuates Glutamate- and Hydrogen Peroxide-Mediated Death of Staurosporine-Differentiated RGC-5 Cells. *Experimental Eye Research* 89(4): 538–548.

Harper, M.M., et al. 2011. Transplantation of BDNF-Secreting Mesenchymal Stem Cells Provides Neuroprotection in Chronically Hypertensive Rat Eyes. *Investigative Ophthalmology and Visual Science* 52(7): 4506–4515.

Hartgerink, J.D., E. Beniash, and S.I. Stupp. 2001. Self-Assembly and Mineralization of Peptide-Amphiphile Nanofibers. *Science* 294(5547): 1684–1688.

Hasadsri, L., et al. 2009. Functional Protein Delivery into Neurons Using Polymeric Nanoparticles. *Journal of Biological Chemistry* 284(11): 6972–6981.

He, C., et al. 2010. Effects of Particle Size and Surface Charge on Cellular Uptake And Biodistribution of Polymeric Nanoparticles. *Biomaterials* 31(13): 3657–3666.

Hendriks, W.T., et al. 2004. Viral Vector-Mediated Gene Transfer of Neurotrophins to Promote Regeneration of the Injured Spinal Cord. *Progress in Brain Research* 146: 451–476.

Herrera, A.P., et al. 2008. Multifunctional Magnetite Nanoparticles Coated with Fluorescent Thermo-Responsive Polymeric Shells. *Journal of Materials Chemistry* 18(8): 855–858.

Hirami, Y., et al. 2009. Generation of Retinal Cells from Mouse and Human Induced Pluripotent Stem Cells. *Neuroscience Letters* 458(3): 126–131.

Ho, D., et al. 2015. Hierarchical Patterning of Multifunctional Conducting Polymer Nanoparticles as a Bionic Platform for Topographic Contact Guidance. *ACS Nano* 9(2): 1767–1774.

Hoane, M.R., et al. 2004. Transplantation of Neuronal and Glial Precursors Dramatically Improves Sensorimotor Function but Not Cognitive Function in the Traumatically Injured Brain. *Journal of Neurotrauma* 21: 163–174.

Hockemeyer, D., et al. 2008. A Drug-Inducible System for Direct Reprogramming of Human Somatic Cells to Pluripotency. *Cell Stem Cell* 3(3): 346–353.

Hollands, P. 1987. Differentiation and Grafting of Haemopoietic Stem Cells from Early Postimplantation Mouse Embryos. *Development* 99(1): 69–76.

Hopley, E.L., et al. 2014. Carbon Nanotubes Leading the Way Forward in New Generation 3D Tissue Engineering. *Biotechnology Advances* 32(5): 1000–1014.

Houchin-Ray, T., et al. 2007. Patterned PLG Substrates for Localized DNA Delivery and Directed Neurite Extension. *Biomaterials* 28(16): 2603–2611.

Howard 3rd, M.A., et al. 1989. Intracerebral Drug Delivery in Rats with Lesion-Induced Memory Deficits. *Journal of Neurosurgery* 71(1): 105–112.

Hu, F., et al. 2006. Cellular Response to Magnetic Nanoparticles "PEGylated" Via Surface-Initiated Atom Transfer Radical Polymerization. *Biomacromolecules* 7(3): 809–816.

Huang, Z.-M., et al. 2003. A Review on Polymer Nanofibers by Electrospinning and Their Applications in Nanocomposites. *Composites Science and Technology* 63(15): 2223–2253.

Huang, Y.-J., et al. 2012. Carbon Nanotube Rope with Electrical Stimulation Promotes the Differentiation and Maturity of Neural Stem Cells. *Small* 8(18): 2869–2877.

Hunt, D.P., et al. 2008. A Highly Enriched Niche of Precursor Cells with Neuronal And Glial Potential Within the Hair Follicle Dermal Papilla of Adult Skin. *Stem Cells* 26(1): 163–172.

Ilie, I., et al. 2012. Influence of Nanomaterials on Stem Cell Differentiation: Designing an Appropriate Nanobiointerface. *International Journal of Nanomedicine* 7: 3011–3025.

Ishikawa, N., et al. 2007. Peripheral Nerve Regeneration Through the Space Formed by a Chitosan Gel Sponge. *Journal of Biomedical Materials Research. Part A* 83(1): 33–40.

Ishikawa, N., et al. 2009. Peripheral Nerve Regeneration by Transplantation of BMSC-Derived Schwann Cells as Chitosan Gel Sponge Scaffolds. *Journal of Biomedical Materials Research. Part A* 89(4): 1118–1124.

Jampel, H.D., et al. 1991. In Vitro Release of Hydrophobic Drugs from Polyanhydride Disks. *Ophthalmic Surgery* 22(11): 676–680.

Jang, S., et al. 2010. Functional Neural Differentiation of Human Adipose Tissue-Derived Stem Cells Using BFGF and Forskolin. *BMC Cell Biology* 11: 25.

Johnson, P.J., et al. 2008. Maintaining Bioactivity of NGF for Controlled Release from PLGA Using PEG. *Journal of Biomedical Materials Research. Part A* 86A(2): 420–427.

Johnson, T.V., et al. 2010. Neuroprotective Effects of Intravitreal Mesenchymal Stem Cell Transplantation in Experimental Glaucoma. *Investigative Ophthalmology and Visual Science* 51(4): 2051–2059.

Jollivet, C., et al. 2004a. Long-Term Effect of Intra-Striatal Glial Cell Line-Derived Neurotrophic Factor-Releasing Microspheres in a Partial Rat Model of Parkinson's Disease. *Neuroscience Letters* 356(3): 207–210.

Jollivet, C., et al. 2004b. Striatal Implantation of GDNF Releasing Biodegradable Microspheres Promotes Recovery of Motor Function in a Partial Model of Parkinson's Disease. *Biomaterials* 25(5): 933–942.

Junka, R., et al. 2013. Laminin Functionalized Biomimetic Nanofibers for Nerve Tissue Engineering. *Journal of Biomaterials and Tissue Engineering* 3(4): 494–502.

Kador, K.E., et al. 2013. Tissue Engineering the Retinal Ganglion Cell Nerve Fiber Layer. *Biomaterials* 34(17): 4242–4250.

Kang, H.W., Y. Tabata, and Y. Ikada. 1999. Fabrication of Porous Gelatin Scaffolds for Tissue Engineering. *Biomaterials* 20(14): 1339–1344.

Kang, C.E., et al. 2013. Localized and Sustained Delivery of Fibroblast Growth Factor-2 from a Nanoparticle-Hydrogel Composite for Treatment of Spinal Cord Injury. *Cells, Tissues, Organs* 197(1): 55–63.

Karabekmez, F.E., A. Duymaz, and S.L. Moran. 2009. Early Clinical Outcomes with the Use of Decellularized Nerve Allograft for Repair of Sensory Defects Within the Hand. *Hand (N Y)* 4(3): 245–249.

Karumbayaram, S., et al. 2009. Directed Differentiation of Human-Induced Pluripotent Stem Cells Generates Active Motor Neurons. *Stem Cells* 27(4): 806–811.

Kashi, T.S., et al. 2012. Improved Drug Loading and Antibacterial Activity of Minocycline-Loaded PLGA Nanoparticles Prepared by Solid/Oil/Water Ion Pairing Method. *International Journal of Nanomedicine* 7: 221–234.

Kawai, H., et al. 2010. Tridermal Tumorigenesis of Induced Pluripotent Stem Cells Transplanted in Ischemic Brain. *Journal of Cerebral Blood Flow and Metabolism* 30(8): 1487–1493.

Keeley, R.D., et al. 1991. The Artificial Nerve Graft: A Comparison of Blended Elastomer-Hydrogel with Polyglycolic Acid Conduits. *Journal of Reconstructive Microsurgery* 7(2): 93–100.

Kim, J.H., et al. 2002. Dopamine Neurons Derived from Embryonic Stem Cells Function in an Animal Model of Parkinson's Disease. *Nature* 418: 50–56.

Kim, J.B., et al. 2009. Direct Reprogramming of Human Neural Stem Cells by OCT4. *Nature* 461(7264): 643–649.

Kim, K., et al. 2010. Epigenetic Memory in Induced Pluripotent Stem Cells. *Nature* 467(7313): 285–290.

Kim, J., et al. 2011a. Functional Integration of Dopaminergic Neurons Directly Converted from Mouse Fibroblasts. *Cell Stem Cell* 9(5): 413–419.

Kim, J.A., et al. 2011b. Enhancement of Neurite Outgrowth in PC12 Cells by Iron Oxide Nanoparticles. *Biomaterials* 32(11): 2871–2877.

Kim, S.-E., et al. 2015. Coextruded, Aligned, and Gradient-Modified Poly(Epsilon-Caprolactone) Fibers as Platforms for Neural Growth. *Biomacromolecules* 16(3): 860–867.

Klassen, H., D.S. Sakaguchi, and M.J. Young. 2004. Stem Cells and Retinal Repair. *Progress in Retinal and Eye Research* 23(2): 149–181.

Kleinsmith, L.J., and G.B. Pierce Jr. 1964. Multipotentiality of Single Embryonal Carcinoma Cells. *Cancer Research* 24: 1544–1551.

Klimanskaya, I., et al. 2004. Derivation and Comparative Assessment of Retinal Pigment Epithelium from Human Embryonic Stem Cells Using Transcriptomics. *Cloning and Stem Cells* 6: 217–245.

Ko, H.F., C. Sfeir, and P.N. Kumta. 2010. Novel Synthesis Strategies for Natural Polymer and Composite Biomaterials as Potential Scaffolds for Tissue Engineering. *Philosophical Transactions. Series A, Mathematical, Physical, and Engineering Sciences* 368(1917): 1981–1997.

Kocsis, J.D. 2009. Neuroprotection and Immunomodulation by Cell Transplantation Are Becoming Central Themes in Potential Therapeutic Approaches for Cell-Based Therapies. *Neuroscience Letters* 456(3): 99.

Kohane, D.S. 2007. Microparticles and Nanoparticles for Drug Delivery. *Biotechnology and Bioengineering* 96(2): 203–209.

Kraskiewicz, H., et al. 2013. Assembly of Protein-Based Hollow Spheres Encapsulating a Therapeutic Factor. *ACS Chemical Neuroscience* 4(9): 1297–1304.

Kreuter, J. 2013. Mechanism of Polymeric Nanoparticle-Based Drug Transport Across the Blood–Brain Barrier (BBB). *Journal of Microencapsulation* 30(1): 49–54.

Kreuter, J., et al. 1997. Influence of the Type of Surfactant on the Analgesic Effects Induced by the Peptide Dalargin After Its Delivery Across the Blood–Brain Barrier Using Surfactant-Coated Nanoparticles. *Journal of Controlled Release* 49(1): 81–87.

Kriks, S., et al. 2011. Dopamine Neurons Derived from Human ES Cells Efficiently Engraft in Animal Models of Parkinson's Disease. *Nature* 480(7378): 547–551.

Kulangara, K., et al. 2014. The Effect of Substrate Topography on Direct Reprogramming of Fibroblasts to Induced Neurons. *Biomaterials* 35(20): 5327–5336.

Kumar, M.N.V.R. 2000. Nano and Microparticles as Controlled Drug Delivery Devices. *Journal of Pharmacy and Pharmaceutical Sciences* 3(2): 234–258.

Kumbar, S.G., C.T. Laurencin, and M. Deng. 2014. *Natural and Synthetic Biomedical Polymers*, 1–402. Elsevier B.V.

Kurozumi, K., et al. 2005. Mesenchymal Stem Cells That Produce Neurotrophic Factors Reduce Ischemic Damage in the Rat Middle Cerebral Artery Occlusion Model. *Molecular Therapy* 11(1): 96–104.

Kyhn, M.V., et al. 2009. Delayed Administration of Glial Cell Line-Derived Neurotrophic Factor (GDNF) Protects Retinal Ganglion Cells in a Pig Model of Acute Retinal Ischemia. *Experimental Eye Research* 89(6): 1012–1020.

Labrador, R.O., M. Butí, and X. Navarro. 1998. Influence of Collagen and Laminin Gels Concentration on Nerve Regeneration After Resection and Tube Repair. *Experimental Neurology* 149(1): 243–252.

Lam, H.J., et al. 2010. In Vitro Regulation of Neural Differentiation and Axon Growth by Growth Factors and Bioactive Nanofibers. *Tissue Engineering. Part A* 16(8): 2641–2648.

Lamba, D.A., J. Gust, and T.A. Reh. 2009. Transplantation of Human Embryonic Stem Cell-Derived Photoreceptors Restores Some Visual Function in Crx-Deficient Mice. *Cell Stem Cell* 4(1): 73–79.

Lampe, K.J., et al. 2011. The Administration of BDNF and GDNF to the Brain Via PLGA Microparticles Patterned Within a Degradable PEG-Based Hydrogel: Protein Distribution and the Glial Response. *Journal of Biomedical Materials Research. Part A* 96A(3): 595–607.

Laterza, C., et al. 2013. iPSC-Derived Neural Precursors Exert a Neuroprotective Role in Immune-Mediated Demyelination Via the Secretion of LIF. *Nature Communications* 4: 2597.

Lavik, E.B., et al. 2005. Fabrication of Degradable Polymer Scaffolds to Direct the Integration and Differentiation of Retinal Progenitors. *Biomaterials* 26(16): 3187–3196.

Leach, M.K., et al. 2011. The Culture of Primary Motor and Sensory Neurons in Defined Media on Electrospun Poly-L-Lactide Nanofiber Scaffolds. *Journal of Visualised Experiments* 48. http://www.jove.com/details.php?id=2389, doi:10.3791/2389.

Lee, S.H., et al. 2000. Efficient Generation of Midbrain and Hindbrain Neurons from Mouse Embryonic Stem Cells. *Nature Biotechnology* 18: 675–679.

Lee, J.Y., et al. 2009. Polypyrrole-Coated Electrospun PLGA Nanofibers for Neural Tissue Applications. *Biomaterials* 30(26): 4325–4335.

Lee, J.M., et al. 2012. In Vivo Tracking of Mesechymal Stem Cells Using Fluorescent Nanoparticles in an Osteochondral Repair Model. *Molecular Therapy* 20(7): 1434–1442.

Lee, J.Y., et al. 2014. Controlled Release of Nerve Growth Factor from Heparin-Conjugated Fibrin Gel Within the Nerve Growth Factor-Delivering Implant. *Journal of the Korean Association of Oral and Maxillofacial Surgeons* 40(1): 3–10.

Lee-Kubli, C.A., and P. Lu. 2015. Induced Pluripotent Stem Cell-Derived Neural Stem Cell Therapies for Spinal Cord Injury. *Neural Regeneration Research* 10(1): 10–16.

Lesniak, M.S., et al. 2005. Local Delivery of Doxorubicin for the Treatment of Malignant Brain Tumors in Rats. *Anticancer Research* 25(6B): 3825–3831.

Li, Y., and M. Chopp. 2009. Marrow Stromal Cell Transplantation in Stroke and Traumatic Brain Injury. *Neuroscience Letters* 456(3): 120–123.

Li, D., and Y.N. Xia. 2004. Electrospinning of Nanofibers: Reinventing the Wheel? *Advanced Materials* 16(14): 1151–1170.

Li, X., et al. 2006. Culture of Neural Stem Cells in Calcium Alginate Beads. *Biotechnology Progress* 22(6): 1683–1689.

Li, X.J., et al. 2009. Coordination of Sonic Hedgehog and Wnt Signaling Determines Ventral and Dorsal Telencephalic Neuron Types from Human Embryonic Stem Cells. *Development* 136(23): 4055–4063.

Li, X., et al. 2012a. Human Cord Blood-Derived Multipotent Stem Cells (CB-SCs) Treated with All-Trans-Retinoic Acid (ATRA) Give Rise to Dopamine Neurons. *Biochemical and Biophysical Research Communications* 419(1): 110–116.

Li, X., et al. 2012b. Manipulating Neural-Stem-Cell Mobilization and Migration In Vitro. *Acta Biomaterialia* 8(6): 2087–2095.

Li, X., et al. 2015. A Therapeutic Strategy for Spinal Cord Defect: Human Dental Follicle Cells Combined with Aligned PCL/PLGA Electrospun Material. *BioMed Research International* 2015: Article ID 197183, 12 p

Liang, Y., et al. 2012. Delivery of Cationic Polymer-siRNA Nanoparticles for Gene Therapies in Neural Regeneration. *Biochemical and Biophysical Research Communications* 421(4): 690–695.

Liechty, W.B., et al. 2010. Polymers for Drug Delivery Systems. *Annual Review of Chemical and Biomolecular Engineering* 1: 149–173.

Lin, T.-C., I.-M. Chiu, and S.-H. Hsu. 2012. Biodegradable Alginate Microspheres as the Carriers for Neural Stem Cells. *Journal of Neuroscience and Neuroengineering* 1(1): 97–104.

Liu, X., et al. 2010a. Guidance of Neurite Outgrowth on Aligned Electrospun Polypyrrole/Poly(Styrene-Beta-Isobutylene-Beta-Styrene) Fiber Platforms. *Journal of Biomedical Materials Research. Part A* 94A(4): 1004–1011.

Liu, T., et al. 2010b. Photochemical Crosslinked Electrospun Collagen Nanofibers: Synthesis, Characterization and Neural Stem Cell Interactions. *Journal of Biomedical Materials Research. Part A* 95(1): 276–282.

Liu, J.-J., et al. 2011. Peripheral Nerve Regeneration Using Composite Poly(Lactic Acid-Caprolactone)/Nerve Growth Factor Conduits Prepared by Coaxial Electrospinning. *Journal of Biomedical Materials Research. Part A* 96A(1): 13–20.

Liu, M.L., et al. 2013. Small Molecules Enable Neurogenin 2 to Efficiently Convert Human Fibroblasts into Cholinergic Neurons. *Nature Communications* 4: 2183.

Lopatina, T., et al. 2011. Adipose-Derived Stem Cells Stimulate Regeneration of Peripheral Nerves: BDNF Secreted by These Cells Promotes Nerve Healing and Axon Growth De Novo. *PLoS One* 6(3): e17899.

Lowry, N., et al. 2012. The Effect of Long-Term Release of SHH from Implanted Biodegradable Microspheres on Recovery from Spinal Cord Injury in Mice. *Biomaterials* 33(10): 2892–2901.

Lutz, J.-F., et al. 2006. One-Pot Synthesis of PEGylated Ultrasmall Iron-Oxide Nanoparticles and Their In Vivo Evaluation as Magnetic Resonance Imaging Contrast Agents. *Biomacromolecules* 7(11): 3132–3138.

Mallapragada, S.K., et al. 2015. Enabling Nanomaterial, Nanofabrication and Cellular Technologies for Nanoneuromedicines. *Nanomedicine* 11(3): 715–729.

Marques, S.A., et al. 2010. Predifferentiated Embryonic Stem Cells Promote Functional Recovery After Spinal Cord Compressive Injury. *Brain Research* 1349: 115–128.

Martens, W., et al. 2014. Human Dental Pulp Stem Cells Can Differentiate into Schwann Cells and Promote and Guide Neurite Outgrowth in an Aligned Tissue-Engineered Collagen Construct In Vitro. *FASEB Journal* 28(4): 1634–1643.

Marti, M.E., et al. 2013. Nanomaterials for Neural Tissue Engineering. In *Nanomaterials in Tissue Engineering*, ed. A.K. Gaharwar, et al., 275–301. Woodhead Publishing.

Masui, S., et al. 2007. Pluripotency Governed by Sox2 Via Regulation of Oct3/4 Expression in Mouse Embryonic Stem Cells. *Nature Cell Biology* 9(6): 625–635.

Matsui, T., et al. 2014. Regeneration of the Damaged Central Nervous System Through Reprogramming Technology: Basic Concepts and Potential Application for Cell Replacement Therapy. *Experimental Neurology* 260: 12–18.

Matsumine, H., et al. 2014. Facial Nerve Regeneration Using Basic Fibroblast Growth Factor-Impregnated Gelatin Microspheres in a Rat Model. *Journal of Tissue Engineering and Regenerative Medicine* doi: 10.1002/term.1884.

McCreedy, D.A., and S.E. Sakiyama-Elbert. 2012. Combination Therapies in the CNS: Engineering the Environment. *Neuroscience Letters* 519(2): 115–121.

McDonald, J.W., et al. 1999. Transplanted Embryonic Stem Cells Survive, Differentiate and Promote Recovery in Injured Rat Spinal Cord. *Nature Medicine* 5: 1410–1412.

McMurtrey, R.J. 2014. Patterned and Functionalized Nanofiber Scaffolds in Three-Dimensional Hydrogel Constructs Enhance Neurite Outgrowth and Directional Control. *Journal of Neural Engineering* 11(6): 066009.

Meli, L., et al. 2014. Three Dimensional Cellular Microarray Platform for Human Neural Stem Cell Differentiation and Toxicology. *Stem Cell Research* 13(1): 36–47.

Melissinaki, V., et al. 2011. Direct Laser Writing of 3D Scaffolds for Neural Tissue Engineering Applications. *Biofabrication* 3(4): 045005.

Meyer, J.S., et al. 2009. Modeling Early Retinal Development with Human Embryonic and Induced Pluripotent Stem Cells. *Proceedings of the National Academy of Sciences of the United States of America* 106(39): 16698–16703.

Miller, C., et al. 2001a. Oriented Schwann Cell Growth on Micropatterned Biodegradable Polymer Substrates. *Biomaterials* 22(11): 1263–1269.

Miller, C., S. Jeftinija, and S. Mallapragada. 2001b. Micropatterned Schwann Cell-Seeded Biodegradable Polymer Substrates Significantly Enhance Neurite Alignment and Outgrowth. *Tissue Engineering* 7(6): 705–715.

Mudshinge, S.R., et al. 2011. Nanoparticles: Emerging Carriers for Drug Delivery. *Saudi Pharmaceutical Journal* 19(3): 129–141.

Mujtaba, T., et al. 1999. Lineage-Restricted Neural Precursors Can Be Isolated from Both the Mouse Neural Tube and Cultured ES Cells. *Developmental Biology* 214: 113–127.

Musumeci, T., et al. 2006. PLA/PLGA Nanoparticles for Sustained Release of Docetaxel. *International Journal of Pharmaceutics* 325(1–2): 172–179.

Nakayama, K., et al. 2007a. Enhancement of Peripheral Nerve Regeneration Using Bioabsorbable Polymer Tubes Packed with Fibrin Gel. *Artificial Organs* 31(7): 500–508.

Nakayama, K., et al. 2007b. Regeneration of Peripheral Nerves by Bioabsorbable Polymer Tubes with Fibrin Gel. *Journal of Nanoscience and Nanotechnology* 7(3): 730–733.

Neal, R.A., et al. 2012. Alignment and Composition of Laminin-Polycaprolactone Nanofiber Blends Enhance Peripheral Nerve Regeneration. *Journal of Biomedical Materials Research. Part A* 100A(2): 406–423.

Neeley, W.L., et al. 2008. A Microfabricated Scaffold for Retinal Progenitor Cell Grafting. *Biomaterials* 29(4): 418–426.

Nerve Regeneration-Guided Collagen Scaffold and Mesenchymal Stem Cells Transplantation in Spinal Cord Injury Patients. Clinicaltrials.gov 3 October 2015]. https://clinicaltrials.gov/ct2/show/NCT02352077?term=scaffold&rank=17

Ni, W.F., et al. 2010. In Vitro Neural Differentiation of Bone Marrow Stromal Cells Induced by Cocultured Olfactory Ensheathing Cells. *Neuroscience Letters* 475(2): 99–103.

Nisbet, D.R., et al. 2008. Neural Tissue Engineering of the CNS Using Hydrogels. *Journal of Biomedical Materials Research Part B—Applied Biomaterial* 87b(1): 251–263.

Nizzardo, M., et al. 2014. Minimally Invasive Transplantation of iPSC-Derived ALDHhiSSCloVLA4+ Neural Stem Cells Effectively Improves the Phenotype of an Amyotrophic Lateral Sclerosis Model. *Human Molecular Genetics* 23(2): 342–354.

Norizadeh-Abbariki, T., et al. 2014. Superparamagnetic Nanoparticles Direct Differentiation of Embryonic Stem Cells into Skeletal Muscle Cells. *Journal of Biomaterials and Tissue Engineering* 4(7): 579–585.

Oh, J., et al. 2009. Soluble Factors from Neocortical Astrocytes Enhance Neuronal Differentiation of Neural Progenitor Cells from Adult Rat Hippocampus on Micropatterned Polymer Substrates. *Journal of Biomedical Materials Research. Part A* 91(2): 575–585.

Okabe, S., et al. 1996. Development of Neuronal Precursor Cells and Functional Postmitotic Neurons from Embryonic Stem Cells In Vitro. *Mechanisms of Development* 59(1): 89–102.

Okita, K., T. Ichisaka, and S. Yamanaka. 2007. Generation of Germline-Competent Induced Pluripotent Stem Cells. *Nature* 448(7151): 313–317.

Panseri, S., et al. 2008. Electrospun Micro- and Nanofiber Tubes for Functional Nervous Regeneration in Sciatic Nerve Transections. *BMC Biotechnology* 8: 39.

Park, D., et al. 2013. Human Adipose Tissue-Derived Mesenchymal Stem Cells Improve Cognitive Function and Physical Activity in Ageing Mice. *Journal of Neuroscience Research* 91(5): 660–670.

Patel, S., et al. 2007. Bioactive Nanofibers: Synergistic Effects of Nanotopography and Chemical Signaling on Cell Guidance. *Nano Letters* 7(7): 2122–2128.

Pateman, C.J., et al. 2015. Nerve Guides Manufactured from Photocurable Polymers to Aid Peripheral Nerve Repair. *Biomaterials* 49: 77–89.

Pathak, S., et al. 2006. Quantum Dot Applications to Neuroscience: New Tools for Probing Neurons and Glia. *The Journal of Neuroscience* 26(7): 1893–1895.

Péan, J.-M., et al. 2000. Intraseptal Implantation of NGF-Releasing Microspheres Promote the Survival of Axotomized Cholinergic Neurons. *Biomaterials* 21(20): 2097–2101.

Pfiesterer, U., et al. 2011. Direct Conversion of Human Fibroblasts to Dopaminergic Neurons. *PNAS* 25: 10343–10348.

Pfizer. *A Study of Implantation of Retinal Pigment Epithelium in Subjects with Acute Wet Age Related Macular Degeneration*. Clinicaltrials.gov 3 October 2015]. https://www.clinicaltrials.gov/ct2/show/NCT01691261?term=embryonic+stem+cells+AMD&rank=4

Pharmaceuticals, N. *A Phase 2 Multicenter Randomized Clinical Trial of CNTF for MacTel*. Clinicaltrials.gov 3 October 2015]. https://clinicaltrials.gov/ct2/show/NCT01949324?term=neurotech&rank=18

Pharmaceuticals, N. *Retinal Imaging of Subjects Implanted with Ciliary Neurotrophic Factor (CNTF)-Releasing Encapsulated Cell Implant for Early-Stage Retinitis Pigmentosa*. Clinicaltrials.gov 3 October 2015]. https://clinicaltrials.gov/ct2/show/NCT01530659?term=neurotech&rank=19

Pharmaceuticals, N. *Study of the Intravitreal Implantation of NT-503-3 Encapsulated Cell Technology (ECT) for the Treatment of Recurrent Choroidal Neovascularization (CNV) Secondary to Age-related Macular Degeneration (AMD)*. Clinicaltrials.gov 3 October 2015]. https://clinicaltrials.gov/ct2/show/NCT02228304?term=neurotech&rank=14

Prabhakaran, M.P., et al. 2011. Electrospun Conducting Polymer Nanofibers and Electrical Stimulation of Nerve Stem Cells. *Journal of Bioscience and Bioengineering* 112(5): 501–507.

Prockop, D.J., et al. 2000. Potential Use of Marrow Stromal Cells as Therapeutic Vectors for Diseases of the Central Nervous System. *Progress in Brain Research* 128: 293–297.

Qi, L., et al. 2013. The Effects of Topographical Patterns and Sizes on Neural Stem Cell Behavior. *PLoS One* 8(3): e59022.

Recknor, J.B., et al. 2004. Oriented Astroglial Cell Growth on Micropatterned Polystyrene Substrates. *Biomaterials* 25(14): 2753–2767.

Recknor, J.B., D.S. Sakaguchi, and S.K. Mallapragada. 2006. Directed Growth and Selective Differentiation of Neural Progenitor Cells on Micropatterned Polymer Substrates. *Biomaterials* 27(22): 4098–4108.

Redenti, S., et al. 2009. Engineering Retinal Progenitor Cell and Scrollable Poly(Glycerol-Sebacate) Composites for Expansion and Subretinal Transplantation. *Biomaterials* 30(20): 3405–3414.

Ren, Y.-J., et al. 2013. Enhanced Differentiation of Human Neural Crest Stem Cells Towards the Schwann Cell Lineage by Aligned Electrospun Fiber Matrix. *Acta Biomaterialia* 9(8): 7727–7736.

Riggio, C., et al. 2012. Poly-L-Lysine-Coated Magnetic Nanoparticles as Intracellular Actuators for Neural Guidance. *International Journal of Nanomedicine* 7: 3155–3166.

Roberts, M.J., et al. 2014. Growth of Primary Motor Neurons on Horizontally Aligned Carbon Nanotube Thin Films and Striped Patterns. *Journal of Neural Engineering* 11(3): 036013.

Rolandi, M., and R. Rolandi. 2014. Self-Assembled Chitin Nanofibers and Applications. *Advances in Colloid and Interface Science* 207: 216–222.

Romanyuk, N., et al. 2015. Beneficial Effect of Human Induced Pluripotent Stem Cell-Derived Neural Precursors in Spinal Cord Injury Repair. *Cell Transplant* 24(9): 1781–1797.

Rubio-Retama, J., et al. 2007. Synthesis and Characterization of Thermosensitive PNIPAM Microgels Covered with Superparamagnetic γ-Fe_2O_3 Nanoparticles. *Langmuir* 23(20): 10280–10285.

Rutkowski, G.E., et al. 2004. Synergistic Effects of Micropatterned Biodegradable Conduits and Schwann Cells on Sciatic Nerve Regeneration. *Journal of Neural Engineering* 1(3): 151–157.

Safford, K.M., et al. 2002. Neurogenic Differentiation of Murine and Human Adipose-Derived Stromal Cells. *Biochemical and Biophysical Research Communications* 294(2): 371–379.

Sakai, K., et al. 2012. Human Dental Pulp-Derived Stem Cells Promote Locomotor Recovery After Complete Transection of the Rat Spinal Cord by Multiple Neuro-Regenerative Mechanisms. *The Journal of Clinical Investigation* 122(1): 80–90.

Sakiyama, S.E., J.C. Schense, and J.A. Hubbell. 1999. Incorporation of Heparin-Binding Peptides into Fibrin Gels Enhances Neurite Extension: An Example of Designer Matrices in Tissue Engineering. *The FASEB Journal* 13(15): 2214–2224.

Salmon, M.E., P.E. Russell, and E.B. Troughton. 2005. Growth and Characterization of Self-Assembled Nanofibers. *Microscopy and Microanalysis* 11(S02): 372–373.

Santos, T., et al. 2012. Polymeric Nanoparticles to Control the Differentiation of Neural Stem Cells in the Subventricular Zone of the Brain. *ACS Nano* 6(12): 10463–10474.

Sasaki, M., et al. 2009. BDNF-Hypersecreting Human Mesenchymal Stem Cells Promote Functional Recovery, Axonal Sprouting, and Protection of Corticospinal Neurons After Spinal Cord Injury. *The Journal of Neuroscience* 29(47): 14932–14941.

Schense, J.C., et al. 2000. Enzymatic Incorporation of Bioactive Peptides into Fibrin Matrices Enhances Neurite Extension. *Nature Biotechnology* 18(4): 415–419.

Schmauss, D., et al. 2014. Is Nerve Regeneration After Reconstruction with Collagen Nerve Conduits Terminated After 12 Months? The Long-Term Follow-Up of Two Prospective Clinical Studies. *Journal of Reconstructive Microsurgery* 30(8): 561–568.

Schnell, E., et al. 2007. Guidance of Glial Cell Migration and Axonal Growth on Electrospun Nanofibers of Poly-Epsilon-Caprolactone and a Collagen/Poly-Epsilon-Caprolactone Blend. *Biomaterials* 28(19): 3012–3025.

Schuldiner, M., et al. 2001. Induced Neuronal Differentiation of Human Embryonic Stem Cells. *Brain Research* 913: 201–205.

Schwartz, S.D., et al. 2012. Embryonic Stem Cell Trials for Macular Degeneration: A Preliminary Report. *The Lancet* 379(9817): 713–720.

Schwartz, M.P., et al. 2015. Human Pluripotent Stem Cell-Derived Neural Constructs for Predicting Neural Toxicity. *Proceedings of the National Academy of Sciences of the United States of America* 112: 12516–12521.

Sciences, C.A.o. *Functional Neural Regeneration Collagen Scaffold Transplantation in Acute Spinal Cord Injury Patients*. Clinicaltrials.gov 3 October 2016]. https://clinicaltrials.gov/ct2/show/NCT02510365?term=scaffold&rank=16

Sell, S.A., et al. 2010. The Use of Natural Polymers in Tissue Engineering: A Focus on Electrospun Extracellular Matrix Analogues. *Polymers* 2(4): 522–553.

Sharma, A.D., et al. 2015. High Throughput Characterization of Adult Stem Cells Engineered for Delivery of Therapeutic Factors for Neuroprotective Strategies. *Journal of Visualised Experiments* 95: e52242.

Sharma, A.D., et al. 2016. Oriented Growth and Transdifferentiation of Mesenchymal Stem Cells Towards a Schwann cell Fate on Micropatterned Substrates. *Journal of Bioscience and Bioengineering* 121(3): 325–335.

Shen, C.C., Y.C. Yang, and B.S. Liu. 2012. Peripheral Nerve Repair of Transplanted Undifferentiated Adipose Tissue-Derived Stem Cells in a Biodegradable Reinforced Nerve Conduit. *Journal of Biomedical Materials Research. Part A* 100(1): 48–63.

Shi, Y., P. Kirwan, and F.J. Livesey. 2012. Directed Differentiation of Human Pluripotent Stem Cells to Cerebral Cortex Neurons and Neural Networks. *Nature Protocols* 7(10): 1836–1846.

Shukla, S., et al. 2009. Enhanced Survival and Function of Neural Stem Cells-Derived Dopaminergic Neurons Under Influence of Olfactory Ensheathing Cells in Parkinsonian Rats. *Journal of Neurochemistry* 109(2): 436–451.

Siminovitch, L., E.A. McCulloch, and J.E. Till. 1963. The Distribution of Colony-Forming Cells Among Spleen Colonies. *Journal of Cellular and Comparative Physiology* 62(3): 327–336.

Singh, R., and J.W. Lillard Jr. 2009. Nanoparticle-Based Targeted Drug Delivery. *Experimental and Molecular Pathology* 86(3): 215–223.

Skalova, S., et al. 2015. Induced Pluripotent Stem Cells and Their Use in Cardiac and Neural Regenerative Medicine. *International Journal of Molecular Sciences* 16(2): 4043–4067.

Skop, N.B., et al. 2013. Heparin Crosslinked Chitosan Microspheres for the Delivery of Neural Stem Cells and Growth Factors for Central Nervous System Repair. *Acta Biomaterialia* 9(6): 6834–6843.

Son, E.Y., et al. 2011. Conversion of Mouse and Human Fibroblasts into Functional Spinal Motor Neurons. *Cell Stem Cell* 9(3): 205–218.

Song, J., et al. 2007. Human Embryonic Stem Cell-Derived Neural Precursor Transplants Attenuate Apomorphine-Induced Rotational Behavior in Rats with Unilateral Quinolinic Acid Lesions. *Neuroscience Letters* 423(1): 58–61.

Soppimath, K.S., et al. 2001. Biodegradable Polymeric Nanoparticles as Drug Delivery Devices. *Journal of Controlled Release* 70(1–2): 1–20.

Spivey, E.C., et al. 2012. The Fundamental Role of Subcellular Topography in Peripheral Nerve Repair Therapies. *Biomaterials* 33(17): 4264–4276.

Stabenfeldt, S.E., A.J. Garcia, and M.C. LaPlaca. 2006. Thermoreversible Laminin-Functionalized Hydrogel for Neural Tissue Engineering. *Journal of Biomedical Materials Research Part A* 77a(4): 718–725.

Stanwick, J.C., M.D. Baumann, and M.S. Shoichet. 2012a. Enhanced Neurotrophin-3 Bioactivity and Release from a Nanoparticle-Loaded Composite Hydrogel. *Journal of Controlled Release* 160(3): 666–675.

Stanwick, J.C., M.D. Baumann, and M.S. Shoichet. 2012b. In Vitro Sustained Release of Bioactive Anti-NogoA, a Molecule in Clinical Development for Treatment of Spinal Cord Injury. *International Journal of Pharmaceutics* 426(1–2): 284–290.

Steiniger, S.C., et al. 2004. Chemotherapy of Glioblastoma in Rats Using Doxorubicin-Loaded Nanoparticles. *International Journal of Cancer* 109(5): 759–767.

Su, G., et al. 2013. Direct Conversion of Fibroblasts into Neural Progenitor-Like Cells by Forced Growth into 3D Spheres on Low Attachment Surfaces. *Biomaterials* 34(24): 5897–5906.

Subbiah, T., et al. 2005. Electrospinning of Nanofibers. *Journal of Applied Polymer Science* 96(2): 557–569.

Subramanian, A., U.M. Krishnan, and S. Sethuraman. 2011. Fabrication of uniaxially aligned 3D electrospun scaffolds for neural regeneration. *Biomedical Materials* 6(2): 025004.

Subramanian, A., U.M. Krishnan, and S. Sethuraman. 2012. Axially Aligned Electrically Conducting Biodegradable Nanofibers for Neural Regeneration. *Journal of Materials Science: Materials in Medicine* 23(7): 1797–1809.

Suri, S., and C.E. Schmidt. 2010. Cell-Laden Hydrogel Constructs of Hyaluronic Acid, Collagen, and Laminin for Neural Tissue Engineering. *Tissue Engineering. Part A* 16(5): 1703–1716.

Suzuki, K., et al. 1999. Regeneration of Transected Spinal Cord in Young Adult Rats Using Freeze-Dried Alginate Gel. *NeuroReport* 10(14): 2891–2894.

Tada, M., et al. 2001. Nuclear Reprogramming of Somatic Cells by In Vitro Hybridization with ES Cells. *Current Biology* 11: 1553–1558.

Takahashi, K., and S. Yamanaka. 2006. Induction of Pluripotent Stem Cells from Mouse Embryonic and Adult Fibroblast Cultures by Defined Factors. *Cell* 126(4): 663–676.

Takahashi, K., et al. 2007. Induction of Pluripotent Stem Cells from Adult Human Fibroblasts by Defined Factors. *Cell* 131(5): 861–872.

Tamada, J.A., and R. Langer. 1993. Erosion Kinetics of Hydrolytically Degradable Polymers. *Proceedings of the National Academy of Sciences* 90(2): 552–556.

Tang, S., et al. 2013. The Effects of Gradients of Nerve Growth Factor Immobilized PCLA Scaffolds on Neurite Outgrowth In Vitro and Peripheral Nerve Regeneration in Rats. *Biomaterials* 34(29): 7086–7096.

Temple, S. 2001. The Development of Neural Stem Cells. *Nature* 414(6859): 112–117.
Terada, N., et al. 2002. Bone Marrow Cells Adopt the Phenotype of Other Cells by Spontaneous Cell Fusion. *Nature* 416(6880): 542–545.
Therapeutics, I. *Pilot Study of Clinical Safety and Feasibility of the PLGA Poly-L-Lysine Scaffold for the Treatment of Complete (AIS A) Traumatic Acute Spinal Cord Injury*. Clinicaltrials.gov 3 October 2015]. https://clinicaltrials.gov/ct2/show/NCT02138110?spons=invivo&rank=1
Thier, M., et al. 2012. Direct Conversion of Fibroblasts into Stably Expandable Neural Stem Cells. *Cell Stem Cell* 10(4): 473–479.
Thoma, E.C., et al. 2014. Chemical Conversion of Human Fibroblasts into Functional Schwann Cells. *Stem Cell Reports* 3(4): 539–547.
Thomson, J.A., et al. 1998. Embryonic Stem Cell Lines Derived from Human Blastocysts. *Science* 282: 1145–1147.
Till, J.E., and C.E. Mc. 1961. A Direct Measurement of the Radiation Sensitivity of Normal Mouse Bone Marrow Cells. *Radiation Research* 14: 213–222.
Tomita, M., et al. 2002. Bone Marrow-Derived Stem Cells Can Differentiate into Retinal Cells in Injured Rat Retina. *Stem Cells* 20(4): 279–283.
Tomita, M., et al. 2005. Biodegradable Polymer Composite Grafts Promote the Survival and Differentiation of Retinal Progenitor Cells. *Stem Cells* 23(10): 1579–1588.
Torres, M.P., et al. 2006. Synthesis and Characterization of Novel Polyanhydrides with Tailored Erosion Mechanisms. *Journal of Biomedical Materials Research. Part A* 76(1): 102–110.
Tran, P.A., L. Zhang, and T.J. Webster. 2009. Carbon Nanofibers and Carbon Nanotubes in Regenerative Medicine. *Advanced Drug Delivery Reviews* 61(12): 1097–1114.
Tsai, S.Y., et al. 2010. Oct4 and klf4 Reprogram Dermal Papilla Cells into Induced Pluripotent Stem Cells. *Stem Cells* 28(2): 221–228.
Tursun, B., et al. 2011. Direct Conversion of C. elegans Germ Cells into Specific Neuron Types. *Science* 331(6015): 304–308.
Vasita, R., and D.S. Katti. 2006. Nanofibers and Their Applications in Tissue Engineering. *International Journal of Nanomedicine* 1(1): 15–30.
Vu, T.Q., et al. 2005. Peptide-Conjugated Quantum Dots Activate Neuronal Receptors and Initiate Downstream Signaling of Neurite Growth. *Nano Letters* 5(4): 603–607.
Wakayama, T., et al. 1998. Full-Term Development of Mice From Enucleated Oocytes Injected with Cumulus Cell Nuclei. *Nature* 394: 369–374.
Wang, Y., et al. 2004. Controlled Release of Ethacrynic Acid from Poly(Lactide-Co-Glycolide) Films for Glaucoma Treatment. *Biomaterials* 25(18): 4279–4285.
Wang, Q., et al. 2006. Neural Stem Cells Transplantation in Cortex in a Mouse Model of Alzheimer's Disease. *Journal of Medical Investigation* 53: 61–69.
Wang, Y.-C., et al. 2008. Sustained Intraspinal Delivery of Neurotrophic Factor Encapsulated in Biodegradable Nanoparticles Following Contusive Spinal Cord Injury. *Biomaterials* 29(34): 4546–4553.
Wang, N., et al. 2009. Alginate Encapsulation Technology Supports Embryonic Stem Cells Differentiation into Insulin-Producing Cells. *Journal of Biotechnology* 144(4): 304–312.
Wang, W., et al. 2010. Enhancement of Nerve Regeneration Along a Chitosan Nanofiber Mesh Tube on Which Electrically Polarized Beta-Tricalcium Phosphate Particles Are Immobilized. *Acta Biomaterialia* 6(10): 4027–4033.
Wang, Y., et al. 2011. Biocompatibility Evaluation of Electrospun Aligned Poly (Propylene Carbonate) Nanofibrous Scaffolds with Peripheral Nerve Tissues and Cells In Vitro. *Chinese Medical Journal* 124(15): 2361–2366.
Wang, T.-Y., et al. 2012. Promoting Engraftment of Transplanted Neural Stem Cells/Progenitors Using Biofunctionalised Electrospun Scaffolds. *Biomaterials* 33(36): 9188–9197.
Wang, S., et al. 2013. Human iPSC-Derived Oligodendrocyte Progenitor Cells Can Myelinate and Rescue a Mouse Model of Congenital Hypomyelination. *Cell Stem Cell* 12(2): 252–264.
Wangensteen, K.J., and L.K. Kalliainen. 2010. Collagen Tube Conduits in Peripheral Nerve Repair: A Retrospective Analysis. *Hand (N Y)* 5(3): 273–277.

Wernig, M., et al. 2008. Neurons Derived from Reprogrammed Fibroblasts Functionally Integrate into the Fetal Brain and Improve Symptoms of Rats with Parkinson's Disease. *Proceedings of the National Academy of Sciences of the United States of America* 105(15): 5856–5861.

Westmoreland, J.J., C.R. Hancock, and B.G. Condie. 2001. Neuronal Development of Embryonic Stem Cells: A Model of GABAergic Neuron Differentiation. *Biochemical and Biophysical Research Communications* 284(3): 674–680.

Wichterle, H., et al. 2002. Directed Differentiation of Embryonic Stem Cells into Motor Neurons. *Cell* 110: 385–397.

Wilmut, I., et al. 2002. Somatic Cell Nuclear Transfer. *Nature* 419: 583–586.

Wilson, K.D., et al. 2009. MicroRNA Profiling of Human-Induced Pluripotent Stem Cells. *Stem Cells and Development* 18(5): 749–758.

Wood, M.D., et al. 2013. Fibrin Gels Containing GDNF Microspheres Increase Axonal Regeneration After Delayed Peripheral Nerve Repair. *Regenerative Medicine* 8(1): 27–37.

Woodbury, D., et al. 2000. Adult Rat and Human Bone Marrow Stromal Cells Differentiate into Neurons. *Journal of Neuroscience Research* 61(4): 364–370.

Wu, M.P., et al. 1994. In Vivo Versus In Vitro Degradation of Controlled Release Polymers for Intracranial Surgical Therapy. *Journal of Biomedical Materials Research* 28(3): 387–395.

Xia, H., et al. 2014. Directed Neurite Growth of Rat Dorsal Root Ganglion Neurons and Increased Colocalization with Schwann Cells on Aligned Poly(Methyl Methacrylate) Electrospun Nanofibers. *Brain Research* 1565: 18–27.

Xu, X.Y., et al. 2003. Peripheral Nerve Regeneration with Sustained Release of Poly(Phosphoester) Microencapsulated Nerve Growth Factor Within Nerve Guide Conduits. *Biomaterials* 24(13): 2405–2412.

Xu, T., et al. 2006. Viability and Electrophysiology of Neural Cell Structures Generated by the Inkjet Printing Method. *Biomaterials* 27(19): 3580–3588.

Yanagisawa, D., et al. 2006. Improvement of Focal Ischemia-Induced Rat Dopaminergic Dysfunction by Striatal Transplantation of Mouse Embryonic Stem Cells. *Neuroscience Letters* 407(1): 74–79.

Yang, F., et al. 2004. Fabrication of Nano-Structured Porous PLLA Scaffold Intended for Nerve Tissue Engineering. *Biomaterials* 25(10): 1891–1900.

Yang, F., et al. 2005a. Electrospinning of Nano/Micro Scale Poly(L-Lactic Acid) Aligned Fibers and Their Potential in Neural Tissue Engineering. *Biomaterials* 26(15): 2603–2610.

Yang, Y., et al. 2005b. Neurotrophin Releasing Single and Multiple Lumen Nerve Conduits. *Journal of Controlled Release* 104(3): 433–446.

Yang, D., et al. 2008. Human Embryonic Stem Cell-Derived Dopaminergic Neurons Reverse Functional Deficit in Parkinsonian Rats. *Stem Cells* 26(1): 55–63.

Yao, L., F. Phan, and Y.C. Li. 2013. Collagen Microsphere Serving as a Cell Carrier Supports Oligodendrocyte Progenitor Cell Growth and Differentiation for Neurite Myelination In Vitro. *Stem Cell Research and Therapy* 4: 109.

Yin, Y., et al. 2014. Collagen Nanofibers Facilitated Presynaptic Maturation in Differentiated Neurons from Spinal-Cord-Derived Neural Stem Cells Through MAPK/ERK1/2-Synapsin I Signaling Pathway. *Biomacromolecules* 15(7): 2449–2460.

Yoon, D.M., and J.P. Fisher. 2009. Natural and Synthetic Polymer Scaffolds. In *Biomedical Materials*, ed. Narayan, 415–442. New York: Springer.

Yuan, T., et al. 2013. Human Induced Pluripotent Stem Cell-Derived Neural Stem Cells Survive, Migrate, Differentiate, and Improve Neurologic Function in a Rat Model of Middle Cerebral Artery Occlusion. *Stem Cell Research and Therapy* 4: 73–83.

Zeng, W., et al. 2014. Incorporation of Chitosan Microspheres into Collagen-Chitosan Scaffolds for the Controlled Release of Nerve Growth Factor. *PLoS One* 9(7): e101300.

Zhang, S.C., et al. 2001. In Vitro Differentiation of Transplantable Neural Precursors from Human Embryonic Stem Cells. *Nature Biotechnology* 19: 1129–1133.

Zhang, Y., et al. 2005. Recent Development of Polymer Nanofibers for Biomedical and Biotechnological Applications. *Journal of Materials Science: Materials in Medicine* 16(10): 933–946.

Zhang, Y., et al. 2012. Small Molecules, Big Roles—The Chemical Manipulation of Stem Cell Fate and Somatic Cell Reprogramming. *Journal of Cell Science* 125(Pt 23): 5609–5620.

Zhang, K., et al. 2014. Aligned SF/P(LLA-CL)-Blended Nanofibers Encapsulating Nerve Growth Factor for Peripheral Nerve Regeneration. *Journal of Biomedical Materials Research. Part A* 102(8): 2680–2691.

Zhao, L.R., et al. 2002. Human Bone Marrow Stem Cells Exhibit Neural Phenotypes and Ameliorate Neurological Deficits After Grafting into the Ischemic Brain of Rats. *Experimental Neurology* 174(1): 11–20.

Zhao, X.Y., et al. 2009. iPS Cells Produce Viable Mice Through Tetraploid Complementation. *Nature* 461(7260): 86–90.

Zhao, J.H., et al. 2011. Preparation, Structure and Crystallinity of Chitosan Nano-Fibers by a Solid–Liquid Phase Separation Technique. *Carbohydrate Polymers* 83(4): 1541–1546.

Zheng, W., et al. 2010. Therapeutic Benefits of Human Mesenchymal Stem Cells Derived from Bone Marrow After Global Cerebral Ischemia. *Brain Research* 1310: 8–16.

Zhou, J., et al. 2010. High-Efficiency Induction of Neural Conversion in Human ESCs and Human Induced Pluripotent Stem Cells with a Single Chemical Inhibitor of Transforming Growth Factor Beta Superfamily Receptors. *Stem Cells* 28(10): 1741–1750.

Zhu, J., and R.E. Marchant. 2011. Design Properties of Hydrogel Tissue-Engineering Scaffolds. *Expert Review of Medical Devices* 8(5): 607–626.

Zhu, B., et al. 2014. A Study of Unidirectionally Aligned Collagen-Silk Composite Fibers and the Application in hdpPSC Neural Differentiation. *Microscopy and Microanalysis* 20(Suppl. S3): 1436–1437.

Zimmer, A., and J. Kreuter. 1995. Microspheres and Nanoparticles Used in Ocular Delivery Systems. *Advanced Drug Delivery Reviews* 16(1): 61–73.

Zuk, P.A., et al. 2002. Human Adipose Tissue Is a Source of Multipotent Stem Cells. *Molecular Biology of the Cell* 13(12): 4279–4295.

Chapter 3
Engineering Neuronal Patterning and Defined Axonal Elongation In Vitro

Devon A. Bowser and Michael J. Moore

3.1 Introduction

During growth and development, the human body naturally forms complex neural connections and networks. These patterns define communication pathways and ultimately contribute to eliciting the necessary functionality of the nervous system. This process relies heavily on growth cones located at the leading edge of extending neurites that can sense their environment and respond appropriately. Growth cones can interpret both contact-guidance mediated cues such as physical barriers and surface topography as well as chemoattractants and chemorepellents (Kolodkin and Tessier-Lavigne 2011). Upon interaction with a guidance cue, neurons undergo reorganization of their microtubules and actin filaments to reorient neurite elongation. By preferentially increasing or decreasing the rate of creation of these cytoskeletal components within different regions of the growth cone, the cell effectively alters the direction of neurite outgrowth (Lowery and Van Vactor 2009; Dent et al. 2011).

The desire to manipulate neuronal location, axonal elongation and network connectivity stems from three primary areas of scientific inquiry. The first is increasing our knowledge base of general neuroscience concepts. While the basic processes involved in simple neuronal connections have been well characterized, the guidance cue combinations that effect the formation of complex neuronal structures, such as the brain, are still not fully understood. As investigators seek to unravel these unknowns, the use of simpler networks that still accurately replicate the in vivo

D.A. Bowser
Interdisciplinary Bioinnovation PhD Program, Tulane University, New Orleans, LA, USA

M.J. Moore (✉)
Department of Biomedical Engineering, Tulane University, New Orleans, LA, USA

Neuroscience Program, Tulane University, New Orleans, LA, USA
e-mail: mooremj@tulane.edu

L.G. Zhang, D.L. Kaplan (eds.), *Neural Engineering*,
DOI 10.1007/978-3-319-31433-4_3

environment allow for control over potentially confounding variables and make data interpretation easier.

The second area of research benefiting from neuronal guidance is medical devices. This can range from neural guidance conduits for directing the regeneration of severed nerves (Zhang et al. 2014a) to neural interfaces (Tankus et al. 2014). Neuronal guidance is important in these applications as failure to appropriately reconnect could lead to loss of functionality or formation of painful neuromas. Well-defined in vitro cellular networks that give investigators the opportunity to discover what cues best direct neuronal outgrowth can lead to better devices and higher quality of life for patients. Ultimately, it is hoped that the development of medical devices will progress to include tissue engineered neural structures that could improve regeneration or serve as replacements for damaged or diseased neural tissues (Schmidt and Leach 2003).

High-throughput screening (HTS) of neuroactive compounds is the third area of study that will benefit from a more complete understanding of neuronal growth and axonal elongation. HTS platforms are readily used by pharmaceutical companies seeking to elicit the bioactivity of potential drug compounds as well as foresee any undesirable side effects prior to proceeding into expensive clinical trials. While random 2D neuron cultures have been used to this end, the data does not correlate well with in vivo responses, and electrophysiology data is difficult to collect. If neuronal networks could be engineered to more accurately represent the in vivo environment, then these HTS systems have the potential to serve as preclinical screening devices, effectively reducing the time and money required to get drugs to market and, in turn, the costs for the end user (Astashkina and Grainger 2014). Another interesting use for HTS platforms is the determination of the mechanisms of action for toxic compounds used in biological warfare. Only after the mechanism of action is understood is the creation of an antidrug possible.

With these applications in mind, investigators have undertaken the job of creating simple, well-defined in vitro neuronal structures and networks. They seek to control all aspects of neuronal architecture including soma placement, outgrowth direction, neuron polarization, and cell–cell interactions. To this end, the general approach to achieve this goal is to deposit cell bodies in a defined location then provide specific areas that are permissive to migration, outgrowth, and axonal extension. Many different techniques have been employed to generate these types of patterns with varying levels of success.

This chapter explores methods of defining neuronal growth and axonal elongation including topography, printing applications, photolithography techniques, microfluidics, subtractive fabrication, optical cues, and magnetic and electric fields. These fabrication techniques allow the investigator control over environmental culture parameters such as: dimensionality [two-dimensional (2D) vs. three-dimensional (3D)], presentation of cues (chemical, physical, and optical), method of presenting cues (anchored vs. soluble and static vs. dynamic), and level of control (individual cell vs. population). The determination of required parameters for desired outcome can inform the investigator's decision as to which method to employ.

3.2 A Survey of Approaches

The overall objective of engineering neural outgrowth and axon elongation is to create a highly defined culture system that approaches the in vivo neural environment. There are three main parameters typically manipulated during neuronal engineering to achieve this goal: controlling somal placement, influencing the direction of neurite outgrowth, and dictating network connectivity. Somal placement is important in vitro as it allows the investigator to isolate individual neurons for study, control each cell's local microenvironment including the type and number of neighboring cells, and make necessary endpoint measurements such as electrophysiological data easier to capture. When choosing an approach for somal placement, it is essential to consider the required spacing accuracy, the needed cell viability, and the desired dimensionality. Appropriate placement can be achieved by directly depositing the cell body to the desired location or by the creation of a cell adhesive region that favors cell migration and attachment within the cell culture substrate.

The capacity to manipulate neurite outgrowth in vitro enables one to guide neurons toward forming the proper electrical connections as well as elucidates the guidance effects of a variety of stimuli. Method selection depends on the type of cue, the presentation of the cue, the required culture dimensionality, and whether the guidance is desired on a population or individual cell level. There are many types of stimuli that can be introduced into the neuron culture environment including chemical, physical, optical, fluidic, electrical, and magnetic.

The formation of specified neural networks is beneficial for in vitro work in that it allows for the definition of the pathway along which electrical signals can be transferred. Such organized, specific connections facilitate the interpretation of resulting electrical impulses on a scale that is not feasible using the random neural networks. When selecting an appropriate method for guiding network formation, compatibility with microelectrode arrays (MEAs), the required dimensions for the culture environment, and the desired resolution must be considered. Such neural networks are generally formed by creating a growth-permissive region via ablation or the deposition of a cell adhesive material in a guidance pattern.

This chapter seeks to categorize the different approaches for engineering neuronal growth and axonal elongation based on their fundamental fabrication strategy. This grouping was selected because often the manipulated parameter is intrinsically linked to the underlying fabrication principle. For example, all three printing techniques are used to direct soma placement albeit through slightly different setups. It should be noted though that many techniques are capable of affecting several of the environmental parameters. As such, the basic process and a brief overview of results for methods that rely on topography, printing, photolithography, fluids, light sources, material removal, magnetic fields, and electric fields are presented below. From perusing the chapter, the reader should develop a stronger sense of the level to which different techniques allow control over the three aspects of engineering in vitro neural environments. It should also become apparent that a multiplicity of methods are capable of yielding similar outcomes, and the specifics of each experiment will help dictate which method offers the most appropriate approach.

3.3 Physical Topography

The use of physical microstructures to align cells and influence their growth has been performed extensively and as such will only be briefly discussed here. The fabrication methods used to achieve a desired topography depend greatly on the minimum feature size and type of material. Generally speaking, photolithography and e-beam lithography create structures in the micrometer (μm) range, whereas chemical etching, nanoimprint lithography, and chemical vapor deposition are used for nanometer (nm)-sized features. Common materials for physical microstructure manipulation include polymers, silicon, metals, and carbon nanofibers (Khan and Newaz 2010).

When presented with anisotropic microstructures, neuron adhesion and extensions will typically show preference for residing on or along the features. This has been demonstrated for grooves and ridges of varying widths (Clark et al. 1990; Britland et al. 1996; Rajnicek et al. 1997; Zhu et al. 2004; Goldner et al. 2006; Johansson et al. 2006; Tsuruma et al. 2006), microchannels (Gomez et al. 2007a, b), arrays of pillars and wells (Turner et al. 2000; Dowell-Mesfin et al. 2004), fibers (Sorkin et al. 2006; Rahjouei et al. 2011), and areas of increased roughness (Turner et al. 1997; Fan et al. 2002a, b). Neuronal guidance perpendicular to the microstructure has also been reported for cortical neurons cultured on wider microchannels (Tsuruma et al. 2006) and hippocampal neurons cultured on narrow, shallow grooves (Rajnicek et al. 1997).

One unique application of topography utilizes a PMDS cast of aligned Schwann cells to serve as the substrate in a cell culture system. This effectively replicates the Schwann cell structure to create a more physiologically relevant culture environment. The Schwann cell-based micropattern increased dorsal root ganglion (DRG) cell adhesion 95 % over flat surfaces, and DRG growth was seen to align with the underlying structure (Bruder et al. 2007). Additionally, when extending growth parallel to the aligned substrate, the outgrowth was found to occur 48 % faster than on unpatterned replicas and 110 % faster than growth perpendicular to the replica pattern (Richardson et al. 2011).

3.4 Printing Processes

3.4.1 Microcontact Printing

Microcontact printing has been used extensively as a method for constraining and directing neuron placement and neurite outgrowth. The process typically relies on photolithography followed by molding to create a stamp for depositing a bioink onto a substrate. Briefly, a silicon wafer is spincoated with a photoresist then exposed to ultraviolet (UV) light through a chrome mask to form a mold of the desired inking pattern. Polydimethylsiloxane (PDMS) is cured in the mold to create a physical stamp which is subsequently coated in a bioink during an incubation step. The stamp is then "inked" (i.e., the bioink is transferred) by being placed in contact with the

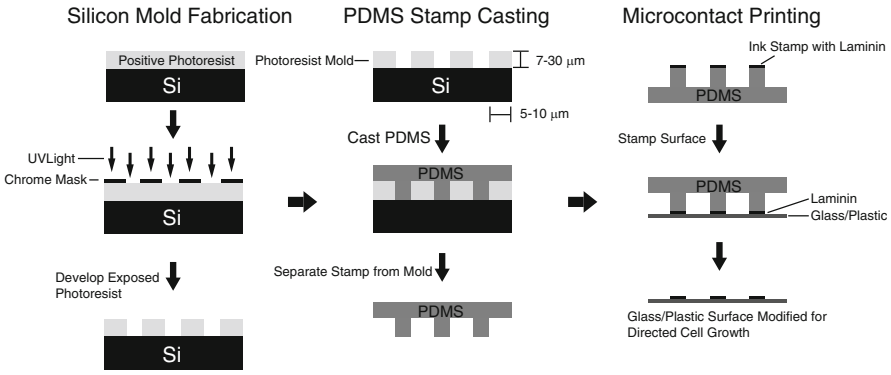

Fig. 3.1 A summary of the fabrication steps required to create a PDMS stamp and then use the stamp for microcontact printing (Leng et al. 2004)

culture substrate (Fig. 3.1) (Fritz and Bastmeyer 2013). The bioink solution is typically deposited onto a hydrophobic material, such as polystyrene, which intrinsically discourages cell adhesion, although backfilling the pattern with a growth-restrictive material such as polyethylene glycol (PEG) is also possible. Additional substrate activation steps are sometimes required to allow appropriate adherence of the bioink to the substrate. As the quantity of ink deposited can affect the quality of cell adhesion and direction, release layers may be added to the stamp to improve transfer (Chang et al. 2003).

Successful microcontact printing of growth-permissive materials has been demonstrated with laminin (Lauer et al. 2001, 2002; Schmalenberg et al. 2004), polylysine (Branch et al. 1998, 2000; Choi et al. 2013), adhesion peptide PA22-2 (Klein et al. 1999; Scholl et al. 2000; Heller et al. 2005), recombinant human IgM12 (Xu et al. 2013), ECM-gel (Vogt et al. 2005a, c), Matrigel (Liazoghli et al. 2012), chondroitin sulfates (A, B, and E) (Swarup et al. 2013), polydopamine plus poly(ethylene imine) (Chien and Tsai 2012), and polylysine-conjugated laminin (Kam et al. 2001). Studies have demonstrated that soma adhesion and neurite outgrowth generally follows the printed patterns, can be maintained for extended periods of time, and exhibits no adverse alterations in morphology or biological activity. Additional levels of guidance can be induced by printing cell-restrictive materials in conjunction with cell-permissive materials. Myelin (Belkaid et al. 2013), chondroitin sulfate C (Swarup et al. 2013), and fibronectin (Fereol et al. 2011) have been used to this end.

With microcontact printing, the pattern of neurite outgrowth directly correlates to that of the stamp and is therefore only limited by fabrication constraints. The most common patterns for engineering neuronal networks include lines and grids, sometimes containing wider nodes for cell body adhesion. Optimal grid and line adhesion has been shown with 4 μm wide lines, and 20 μm nodes (Lauer et al. 2002), and 10 μm gridline spacing (Lauer et al. 2001). Electrophysiological examination of neurons cultured on a grid pattern revealed the formation of a variety of synaptic circuitry including linear connections, branching and converging pathways, and feedback loops of different sizes (Vogt et al. 2005b).

More complex patterns of neuronal cues that allow advanced control over the culture environment are achieved through multiple microcontact printing steps. A grid containing polylysine nodes connected by proteins L1 and N-cadherin, which support axonal and dendritic growth respectively, has been used to direct neuronal polarization in culture (Shi et al. 2007). Alternatively, microislands isolated by backfilling the printed pattern with growth-restrictive PEG allow the observation of natural, nonengineered network formation on a small number of sequestered neurons (Ricoult et al. 2012).

While typically printed on firm, solid substrates, microcontract printing has been employed on hydrogel surfaces for neurite guidance. Biotinylated fibronectin, laminin, and the peptide sequence IKVAV were all transferred onto acrylamide-based hydrogels to form cell-adhesive wide bars and noded lines. Cells selectively adhered to the printed proteins and peptides, showing viability for 4 weeks as neurite outgrowth and synapse formation were observed (Hynd et al. 2007).

Microcontact printing can also be used to fabricate discontinuous guidance gradients. Printed lines, rectangles, and dots can all be manipulated by altering spacing and shape dimensions to create gradients of assorted slopes. Polylysine gradients with a width of 4 μm and a slope of 0.04 were found to direct 84 % of axons toward higher concentrations of polylysine. Combining polylysine with laminin achieves similar results at a less steep slope (Fricke et al. 2011). In another study, temporal retinal axons were shown to extend up a printed concentration gradient of ephrinA5 until they reached a cellularly defined "stop zone." The distance to the "stop zone" could be shortened using a steeper gradient or higher concentration of substrate-bound printing ink (von Philipsborn et al. 2006).

Microcontact printing has also been used to investigate network formation and resulting electrical activity, which is critical for uncovering the dynamics that drive neuronal growth and development. This is done in conjunction with MEAs, which are commonly used to record electrical activity of neurons cultured in vitro. While standard culture conditions are limited to random network formation which fails to position cells that are conducive to recording, microcontact printing has been proven to be a powerful tool for placing cells and guiding their network formation on MEAs to give strong recordings (James et al. 2000; Leng et al. 2004; Mehenti et al. 2006; Nam et al. 2006; Jun et al. 2007a; Jungblut et al. 2009).

3.4.2 Inkjet Printing

The adaptation of standard office printers to allow for the deposition of alternative bioinks has opened a new field of patterning the connectivity and placement of neurons. These systems are typically composed of commercially available printer parts: the ink cartridge/reservoir, the printhead, and a movable receiving substrate. Both piezoelectric and thermal inkjet printers have been utilized; each releases a controlled fluid volume that gets deposited on the substrate, albeit via different

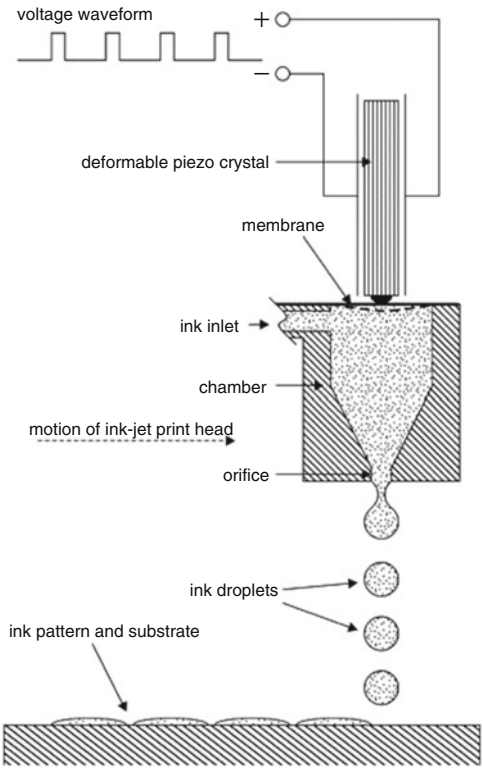

Fig. 3.2 A depiction of the piezoelectric inkjet printing process (Sanjana and Fuller 2004)

mechanisms. Piezoelectric printers rely on a voltage pulse to contract the reservoir dispensing a jet (Fig. 3.2), whereas thermal printers utilize a heating element to generate a bubble that propels a jet from the printhead nozzle (Ringeisen et al. 2006). In-house modifications of printer systems are common to prevent damage to cells and materials.

The first successful application of inkjet printing for the deposition of delicate nervous system cells yielded embryonic motor neurons that visibly retained their printed pattern and exhibited polarized morphology after 5 days (Xu et al. 2005). Later, work on primary embryonic hippocampal and cortical neurons exhibited good neurite outgrowth and maintenance of neuronal morphology postprinting with 74 % cell viability. Electrophysiological evaluations of these printed cells confirmed that their electrical behavior was not statistically different than controls; printed cells maintained normal membrane properties, were excitable, and capable of firing

action potentials, thereby verifying the development of mature sodium and potassium voltage-gated channels (Xu et al. 2006). Printed retinal ganglion cells showed similar results with 69 % viability and neurite outgrowth and survival equivalent to control cells. Close-up visual analysis of the forces experienced by these cells at the area of highest shear stress, the printhead nozzle, further confirmed that the printing process does not result in any significant cell distortion (Lorber et al. 2014).

Inkjet printers can also be used to define neural outgrowth by depositing patterns of cell adhesive materials. Printed poly-L-lysine (Sanjana and Fuller 2004), collagen (Roth et al. 2004), and a mixture of Vinnapas and laminin (Turcu et al. 2003) have all been demonstrated as effective adhesive material bioinks for neuronal cell types. Most impressively, strict pattern adhesion out to 25 days was seen with poly-L-lysine printed on a PEG substrate with no detriment to the electrophysiological properties or synaptic distribution of printed hippocampal neurons (Sanjana and Fuller 2004). While deposition pattern is initially defined by the automated movement of the substrate, additional control over cell adhesive material patterning can be instigated by altering bioink viscosity, the properties of the receiving substrate, and the spatial density of ink drop deposition.

Three-dimensional structures can be constructed using a layer-by-layer, bottom-up approach. In one study, a collagen precursor layer was deposited followed by a patterned layer of neurons and glial cells applied in the desired pattern. A nebulized aerosol form of sodium bicarbonate was then applied to initiate collagen crosslinking and gelation. This process was repeated for several layers. Imaging of the fabricated structure revealed distinct layers of patterned neuronal cells that exhibited neurite outgrowth and connectivity in three dimensions. Although still viable, the astrocytes did not exhibit their standard star-shaped morphology after undergoing the 3D printing process (Lee et al. 2009). A second approach exploited the natural relationship between fibrinogen and thrombin to form layers of fibrin gel upon which NT2 neurons were subsequently printed. The NT2 cells spread across the fibrin and extended neurites after being cultured for 12 days (Xu et al. 2006).

3.4.3 Matrix-Assisted Pulsed Laser Evaporation-Direct Write Printing

Matrix-assisted pulsed laser evaporation-direct write (MAPLE DW) printing is a method of selectively transferring a cell suspension onto a receiving substrate in a user-defined transfer pattern. The underside of a laser transparent print ribbon is coated with a basement membrane matrix, allowing adherence of the cells to be printed. When a pulse of near-UV or UV laser light interacts with the print ribbon, the matrix coating evaporates in the localized area, and gravity and kinetic energy propels the matrix and adhered cells onto the receiving substrate (Fig. 3.3). The incorporation of CAD control and a camera facilitates easy translation of the substrate and real-time viewing of the print transfers (Phamduy et al. 2010; Schiele et al. 2010). Moving the printing ribbon allows for the selective transfer of cells,

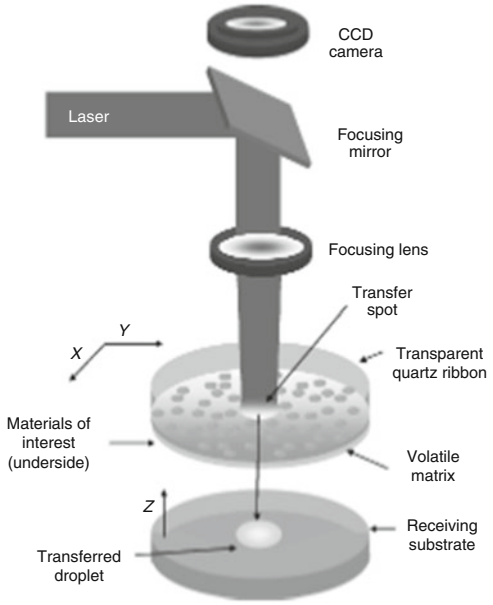

Fig. 3.3 The setup for MAPLE DW printing (Phamduy et al. 2010)

whereas moving the substrate controls the printed pattern. An incubation period allows the cells on the receiving substrate to adhere to the culture surface, and excess printing matrix is removed during media changes.

In one series of experiments, B35 neuronal cells were successfully positioned using MAPLE DW printing technology with 97 % viability at 96 h posttransfer. Cell morphology was unaffected by the deposition process with no significant difference in axonal growth between transferred and control cells. The number of live cells and axonal projections exhibited by transferred cells increased over time, and some transferred cells formed small two-dimensional neuronal networks.

The investigators manipulated the depth of penetration into the receiving substrate by altering the laser fluence thereby creating 3D cell-seeded scaffolds. Increasing the laser fluence was found to lead to greater depth penetration but decreased cell viability. The maximum depth achieved using this method was 75 μm with no discernable difference in axonal extension or cell morphology between cells on the substrate surface and those within the volume. In addition, cells seeded in different planes formed processes that extended to one another yielding a 3D neural network (Patz et al. 2006).

In a separate study, an intermediate triazene absorbing layer was added to the printing ribbon to enable the transfer of B35 neuronal cells at decreased laser fluences. The cells exhibited neuronal extensions at 48 h with similar growth profiles to those cells deposited without the triazene layer. This alteration of the MAPLE DW system opens up the technology for use with more sensitive cells and biomolecules (Doraiswamy et al. 2006).

Neural stem cells have also been printed with MAPLE DW technology and found to be viable posttransfer. It is anticipated that this technology can be used to pattern neural stem cells in order to provide insight into the innate cellular proliferation and differentiation processes of the nervous system (Schiele et al. 2009).

A recent study demonstrated the capacity of MAPLE DW to transfer dissociated dorsal root ganglion cells into defined nodal arrays. The investigators effectively created islands of neurons and their support cells which were viable in culture posttransfer. By day 7 in culture, neurite extensions connected these islands and the expression of synaptic marker, VGLUT2, was visible. However, the cells were not constrained to the area of their printed islands, so the nodal organization induced by printing has begun to degrade by day 7 (Curley et al., 2016).

3.5 Photolithography

3.5.1 Photopatterning Two-Dimensional Substrates

UV light exposure through a photomask can be applied to 2D cell culture substrates to define patterns of bioactive molecules for guiding soma placement and neuronal growth. Typically, cellular adhesion proteins or positively charged molecules are patterned as cell-permissive regions. This is achieved either by applying UV light directly to the cell-permissive material or by patterning a photoresist.

Direct UV light exposure is thought to alter the activity of the substrate protein thereby preventing cells from properly adhering and growing on irradiated portions. Grid patterns of laminin fashioned via this direct exposure were able to guide growth cone motility (Hammarback et al. 1985). Any growth cones that contacted irradiated laminin extended on it momentarily before retracting and continuing on the patterned laminin. If the time of irradiation was increased, the cell exhibited greater adherence to the pattern and increased guidance. Fibrinogen patterned with the same method did not elicit neurite guidance (Hammarback et al. 1988).

UV light can be used to conjugate *N*-(2-mercaptoethyl)-3-(3-methyl-3*H*-diazirine-3-yl) propanamide to chitosan films which then enables the covalent and noncovalent interaction of applied maleimide–streptavidin. Biotinylated-fusion proteins, nerve growth factor (NGF) and semaphorin3A (Sema3A), can then be tethered in the areas where maleimide–streptavidin resides. This immobilization strategy had a greater influence over neurite extension than their simply adsorbed counterparts; NGF encouraged axon extension while Sema3A repulsed axon extension (McCormick et al. 2013). Coimmobilization of ratios of NGF and Sema3A can be used to create a variety of guidance effects (McCormick et al. 2015).

Direct UV light irradiation can also be used to alter the hydrophobicity of a material, making it more hydrophilic and therefore favoring protein adhesion on nonirradiated regions. This was demonstrated using a hydrophilic copolymer of azidostyrene and *N*,*N*-dimethylacrylamide and Type I collagen; neural cells selectively adhered to collagen-coated regions that were patterned by UV exposure (Matsuda et al. 1992).

The photoresist method for selectively depositing materials requires several sequential steps to fully achieve the desired pattern. First, the substrate is coated with a photoresist that is covered with a mask and exposed to UV light. Any exposed areas of the photoresist are then removed in a development bath. The desired bioactive molecule is then applied to the substrate, adhering to the voids in the photoresist. Finally, the remainder of the photoresist is washed off to reveal the final pattern of bioactive molecules (Fig. 3.4). Note that additional grafting and activation steps may be required throughout the process depending on the substrate and bioactive molecule used. This method has been used to pattern polylysine grids (Wyart et al. 2002) and diamine and triamine grids and lines (Kleinfeld et al. 1988). Neurite extension was selectively prescribed to both of the patterned materials and cell maturation was supported both morphologically and electrically. This same method can be used to selectively remove irradiated regions of a self-assembled PEG monolayer which can then be coated with cell-adhesive polylysine. This process in particular has demonstrated compatibility with MEA culture and recordings of neuronal networks (Cheng et al. 2013).

Gradients of immobilized cues can also be created by altering the intensity or duration of UV light exposure over a specified area. Both linear and step gradients can be fabricated. Neurites were found to preferentially grow up gradients of IKVAV (Adams et al. 2005) and down gradients of –COOH (Li et al. 2005).

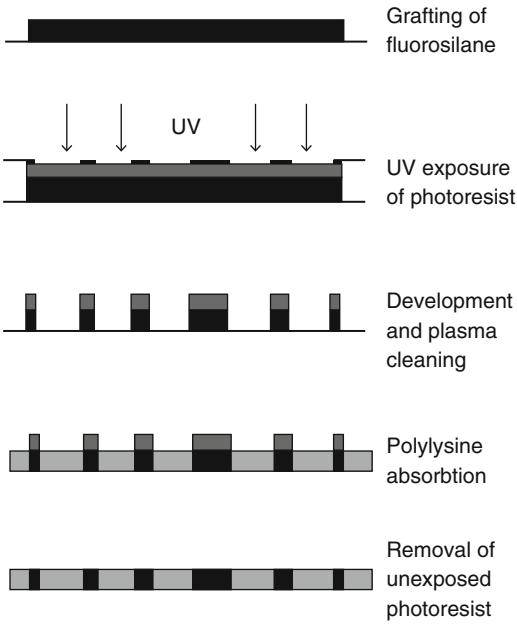

Fig. 3.4 Fabrication steps representing the process for creating a surface modified pattern. Adapted from Wyart et al. (2002)

3.5.2 *Three-Dimensional Photoimmobilization of Guidance Cues*

Hydrogels, which more closely mimic the physiological environment, are commonly implemented as cell culture environments. While hydrogels are capable of supporting robust cell growth, they do not typically provide neurons with specific guidance cues in the absence of additional chemical modifications. Chemically modified hydrogels can be manipulated using UV light to provide chemical cues that can influence neuronal response.

Some hydrogels undergo localized chemical modifications when they are exposed to UV light. This property is commonly exploited in the lab to photoimmobilize adhesion peptides to create defined channels for guiding neurite growth. Agarose modified with photolabile S-(2-nitrobenzyl)cysteine readily forms a hydrogel via thermal cooling. When irradiated with UV light, the 2-nitrobenzyl groups incorporated within the gel are lost and free sulfhydryl groups are exposed. These sulfhydryl groups are susceptible to biomolecule coupling with either maleimidyl or acrylyl-activated peptides. This process was used to effectively immobilize GRGDS peptides within a hydrogel, which supported both cell adhesion and neurite extension. The length of neuronal extension was found to be related to time of irradiation; a longer irradiation time resulted in greater neurite density and length (Luo and Shoichet 2004b).

The formation of vertical guidance channels was instigated by a focused laser beam. By moving the focal plane vertically, a gradient of adhesive peptide was formed in the *xy* plane with the highest concentration located at the center point of the beam. DRG cells that were seeded on top of the hydrogel migrated 600 μm into the hydrogel and those located within 250 μm of a peptide channel would extend neurites preferentially toward the higher peptide concentration. This guidance was not exhibited for the scrambled peptide, GRDGS (Luo and Shoichet 2004a; Musoke-Zawedde and Shoichet 2006).

More complex guidance channels within hydrogels can be formed through slightly different fabrication and coupling process. By incubating a hyaluronic acid hydrogel in a crosslinkable protein solution and applying UV light, geometrically intricate channels are created. The UV light can be directed into the appropriate patterns using two different methods. The first utilizes a three-axis piezoelectric translator to scan the hydrogel sample and create arbitrary pathways at the focal fabrication voxel of the laser (Fig. 3.5). Alternatively, a digital micromirror device in combination with a series of progressive photomasks, vertical increments induced by stage motion, and UV light can pattern channels throughout the hydrogel depth. Spiral channels constructed with these methods were shown to support neuron migration into the hydrogel as well as neurite growth which was preceded by Schwann cell outgrowth. Cellular processes directly aligned with the channels, demonstrating contact-mediated guidance with immobilized IKVAV peptides (Seidlits et al. 2009).

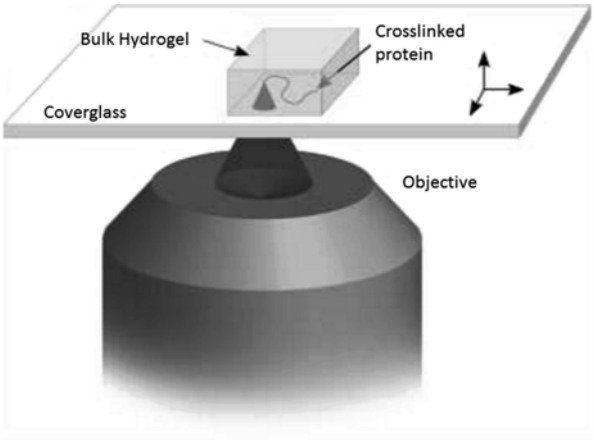

Fig. 3.5 The formation of guidance structures within a hydrogel using UV light to immobilize peptides. Adapted from Seidlits et al. (2009)

3.5.3 Stereolithography of Hydrogel Guidance Structures

Sometimes the physical structure of the hydrogel alone is enough to effectively influence neuron culture. The simplest approach for using stereolithography to effect neuronal outgrowth is to implement standard mask and photoresist photolithographic techniques to pattern 3D voids. This method was executed on silicon wafers with laminin to improve cell adherence to the substrate. Square voids exhibited confining effects on DRG outgrowth that correlated with chamber size. This effect was not demonstrated with rectangular channels (Francisco et al. 2007).

Alternatively, two photon polymerization (2PP) can be used to create guidance structures. 2PP is a method of curing resins whose mechanism is based on the simultaneous adsorption of two photons of light. Microstructures are formed by crosslinking at the depth of the laser focus as the laser scans across the volume of a photosensitive resin as instructed by an uploaded CAD-like file. After completing the first iteration of the pattern, the laser focus plane is altered by stepping vertically then repeating the pattern to create the 3D structure layer by layer. Microwell arrays and suspended guidewires have been fabricated from photopolymerizable polylactic acid using 2PP. Neural cells were viable within these microwell structures (Koroleva et al. 2012); they filled the microwells and extended neurites, which were significantly shorter in length than those of control cells, both inside and outside the niches (Gill et al. 2015). The suspended guidewires were able to support neuron attachment and projections continued along the axis of the wire (Melissinaki et al. 2011).

Stereolithography can be employed to restrict the placement of neurons within the hydrogel, which is particularly beneficial for tissue engineering applications. By using a series of masks with microscale control, cortical neurons suspended in

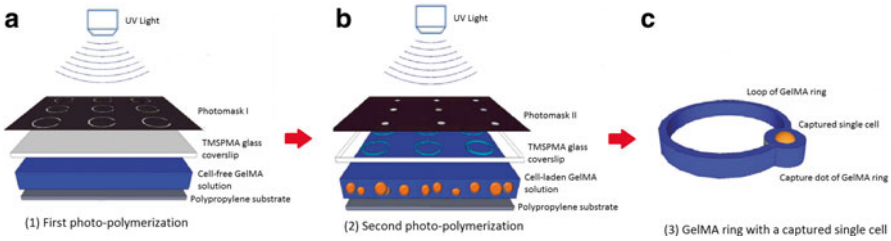

Fig. 3.6 The multiple fabrication steps used to create a microscale hydrogel for neuron capture. (**a**) Creation of ring structure; (**b**) creation of capture dot; and (**c**) depiction of final hydrogel structure with captured neuron. Adapted from Fan et al. (2012)

photocrosslinkable hydrogel solutions were spatially placed in relation to other cell types demonstrating the fundamentally necessary ability to construct cellularly diverse structures (Gurkan et al. 2013). Spatial control can be achieved in the *z*-direction as well by forming individual hydrogel layers that encapsulate the desired cell types using a soft lithography apparatus. By layering hippocampal neurons then myoblast cells encapsulated in an alginate-PEG hydrogel, distinct layers could be formed. The layers maintained their separation throughout the cell culture period. Culture of hippocampal neurons and myoblast cells within the same layer showed a 2.5 time increase of neuronal choline acetyltransferase activity denoting a synergistic effect within the coculture (Zorlutuna et al. 2011).

The geometry of a growth-permissive hydrogel can be used to provide a guidance substrate for extending neurites. This was exhibited by a 3D gelatin methacrylate hydrogel that was fabricated to capture a single neuron through two photolithography steps used to create a looped structure (Fig. 3.6). Within 3 weeks, the neurons grew axons that extended around their hydrogel loop structure to autosynapse with their own soma, which remained localized in the capture dot. Axonal growth occurred in 3D but did not extend beyond the hydrogel structure (Fan et al. 2012).

3.5.4 Laser-Assisted Protein Adsorption by Photobleaching

Laser-assisted protein adsorption by photobleaching (LAPAP) is a technique that creates patterns of substrate-bound proteins using low-power visible lasers and standardly available reagents. It relies on the photobleaching of biotin conjugated fluorophores as a mechanism to covalently link protein molecules to the substrate in a predefined pattern via the production of free radicals. Typically, biotin-4-fluoroscein is photobleached to create the initial pattern followed by incubations of streptavidin, biotinylated antibodies, and desired bioactive protein (Fig. 3.7) (Belisle et al. 2014). LAPAP can be used to establish substrate-bound protein gradients as well as to create patterns of several different proteins simultaneously (Belisle et al. 2009).

This technique was used to create gradients of established guidance molecules to direct neuronal outgrowth. When placed on an LAPAP deposited laminin fragment (IKVAV) gradient, axonal extension from DRGs was found to preferentially travel

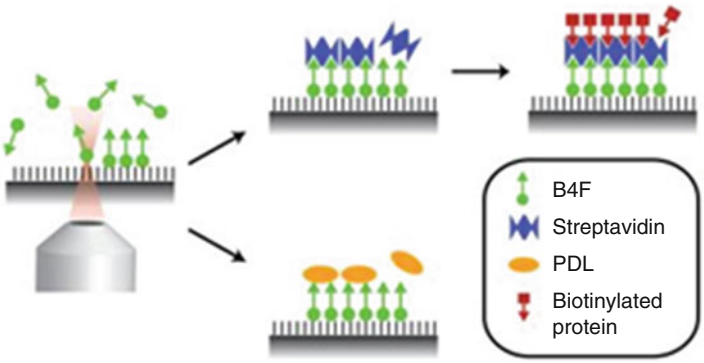

Fig. 3.7 Series of incubation steps used to immobilize proteins during LAPAP. Adapted from Scott et al. (2012)

up the gradient at a three time higher rate than down the laminin gradient (Belisle et al. 2008). This guidance has been attributed to the influence of the laminin gradient on the initiation angle of the axon rather than to actual turning events of axons as they grow (Belisle et al. 2012).

LAPAP has also been used to generate protein patterns atop long-chain acrylated PEG monolayers. Arrays of patterned triangles presenting poly-D-lysine (PDL) to hippocampal neurons resulted in directed polarization, by impeding reverse-projecting and permitting forward projecting neurites. Smaller triangles, approaching the size of the growth cone, exhibited longer neurite extensions than their larger triangle counterparts. Larger triangles could be manipulated to encourage longer neurite outgrowth by reducing the density of PDL (Scott et al. 2012).

3.5.5 Digital Projection Photolithography

Digital projection photolithography, like other photolithography techniques, can be used to create patterns of immobilized guidance cues (Wang et al. 2009), topographical micropatterns (McCormick et al. 2014), as well as defined hydrogel structures (Curley et al. 2011). However, this photolithography method differentiates itself in that it does not implement a physical mask. Using a digital micromirror device, masks developed on a computer can be uploaded and projected directly onto a photolabile hydrogel precursor or protein solution, which is crosslinked in a specified pattern (Fig. 3.8a, b). Distinct regions of gelation or immobilization are created using black and white images while gradients can be formed by using grayscale images or out of focus masks. This method has advantages over traditional photolithography techniques in that it enables the rapid alteration of masks without the need for additional manufacturing steps and the types of patterns that can be created are only limited by the optical resolution. Additionally, the mask does not contact the surface during patterning, which prevents structural damage of the substrate from occurring.

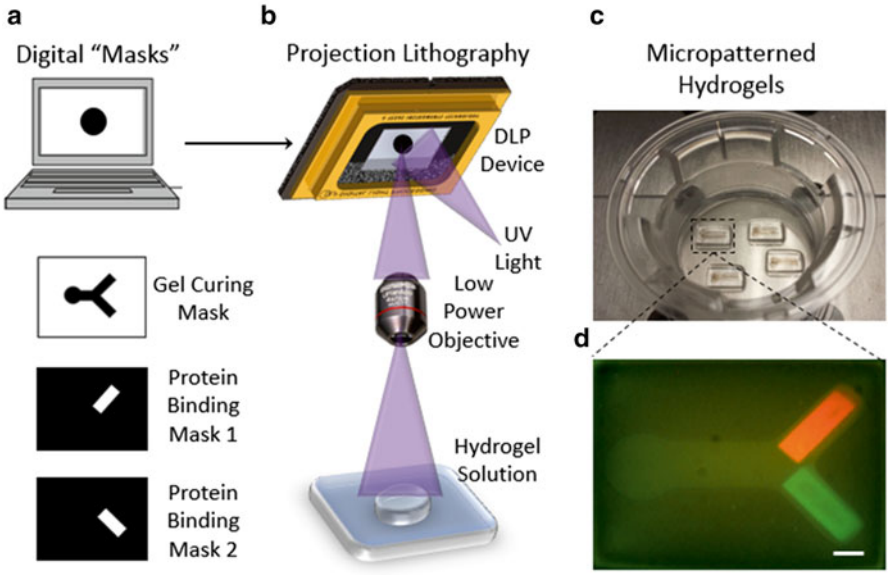

Fig. 3.8 (**a**) Examples of digital projection lithography masks created on the computer, (**b**) setup for digital micromirror device for digital projection lithography, (**c**) image of dual hydrogel culture constructs, and (**d**) example of selectively immobilized biomolecules for guiding neurite outgrowth. Adapted from Curley and Moore (2011) and Horn-Ranney et al. (2013)

One unique application of digital projection photolithography is the fabrication of dual hydrogel systems for culturing embryonic rat DRG tissue explants. Typically, the external cell-restrictive hydrogel, made of a 10 % PEG solution, is patterned first. A cell-permissive gel is then added to the void to create a constrained channel along which neurite growth can extend (Fig. 3.8c) (Curley et al. 2011). DRG explants are either adhered to the permeable substrate prior to hydrogel gelation or pushed into the cell-permissive hydrogel postcrosslinking. A hydrogel thickness of ~500 μm is standard as it provides the appropriate balance between void size resolution and pattern fidelity. After 7 days of culture, it was observed that neurite growth remained confined within the PEG mold; it extended down the channel, throughout the depth of the cell-permissive gel and was highly fasciculated (Curley and Moore 2011).

The design of the dual hydrogel construct and the use of digital projection lithography allows for a variety of different cues to be easily incorporated in the system. This includes immobilized guidance cues (Curley et al. 2014; Horn-Ranney et al. 2014), soluble guidance cues (Horn-Ranney et al. 2013; Curley et al. 2014; Catig et al. 2015), and hydrogel stiffness (Khoshakhlagh and Moore 2015).

Additional photolithography fabrication steps along with more advanced conjugation chemistry involving UV uncageable thiol groups can be utilized to present immobilized guidance cues within the construct (Fig. 3.8d). Immobilized neurotrophin-3 and semaphorin 3A were shown to produce a moderate attractive response and a strong repulsive response to extending neurites, respectively (Horn-Ranney

et al. 2014). The presentation of immobilized semaphorin 6A elicited a repulsive response from lumbosacral DRG explants while ephrin-B3 instigated no guidance effect (Curley et al. 2014).

Soluble guidance cues can be integrated, as transient concentration gradients, into the construct system by including a circular loading well on the initial DMD mask, typically positioned asymmetrically so as to bias the presentation of soluble factors to one section of the channel. The proximity of the loading well to the construct channels as well as the concentration of PEG can be adjusted to achieve the desired concentration profile and duration (Horn-Ranney et al. 2013). Applying NGF into the loading well resulted in a linear NGF gradient in one channel of a bifurcating choice point. NGF gradients function as chemoattractive cues for neurites grown in the system and can help to partially overcome the repulsive effects of immobilized semaphorin 6A in a dose-dependent manner (Curley et al. 2014; Catig et al. 2015).

Additionally, the transparency of the hydrogels typically used in this system lend themselves well to the application of electrophysiology. Field recordings show that the neural tracts are capable of producing compound action potentials that resemble those exhibited by intact nerves (Huval et al. 2015).

3.6 Microfluidic Applications

3.6.1 Material Deposition

This application of microfluidics yields patterns of substrate-bound cues that are reminiscent of those generated by microcontact printing. Typically, soft lithography techniques are implemented to form a PDMS stamp that contains a series of microchannel voids. The stamp is placed in contact with the substrate to form microchannels through which a solution is injected. Once these voids are full, an incubation period allows the solution to adhere to the substrate. Because the solution is constrained by the channels, it is only able to interact with the substrate, and therefore adhere, in the pattern defined by the PDMS stamp. Solutions usually contain cell adhesion proteins or polymers.

Combinations of alternating stripes of poly-L-lysine, laminin, or NgCAM were fabricated using a microfluidic device. Axons preferentially extended on laminin and NgCAM when each was patterned with poly-L-lysine. When laminin and NgCAM were patterned together, on the other hand, the axon was found to initiate on the opposite substrate from where its soma attached. This denotes that the change in substrate is influential in triggering axon polarity (Esch et al. 1999). Additionally, poly-L/D-lysine and collagen IV have both been deposited onto culture substrates in predefined patterns. Neurons selectively adhered to and were guided by patterned laminin to form neuronal connections (Martinoia et al. 1999; Degenaar et al. 2001). These neurons maintained their electrical activity as demonstrated by their negative membrane potentials and the capacity to produce action potentials (Romanova et al. 2004).

Interestingly, polyelectrolytes that have been patterned using microfluidics have been shown to preferentially adhere rat retinal neurons. The polyelectrolytes used, polyallylamine hydrochloride (PAH) and polyethyleneimine (PEI), have an associated positive charge that attracts cells which are negatively charged due to their glycocalyx. Neurons aligned along the prescribed pattern demonstrating favor of PAH and PAI over substrate PDMS, but would still extended neurites over the PDMS surface in order to connect with cells on different regions of the pattern (Reyes et al. 2004).

3.6.2 Gradient Formation

Microfluidics can be used to form both soluble- and substrate-bound gradients to which neurons can interpret and react. Microfluidic devices are fabricated as described above but typically utilize merging and branching channels to mix multiple input solutions to form a gradient (Fig. 3.9). A fluid stream emerges from the end of the channel that either reacts with the substrate becoming immobilized or is utilized as a soluble cue.

Immobilized gradients of several known inhibitory and permissive molecules have been investigated. Neurons have been shown to extend neurites preferentially toward higher concentrations of laminin (Dertinger et al. 2002; Li et al. 2008; Millet et al. 2010), netrin-1, and low-density BDNF (Mai et al. 2009). Gradients of chondroitin sulfate proteoglycans (CSPG) (Li et al. 2008) and high-density BDNF (Mai et al. 2009) repulsed extending neurites causing them to grow in the opposite direction. As would be expected, the use of a laminin-CSPG double gradient could either

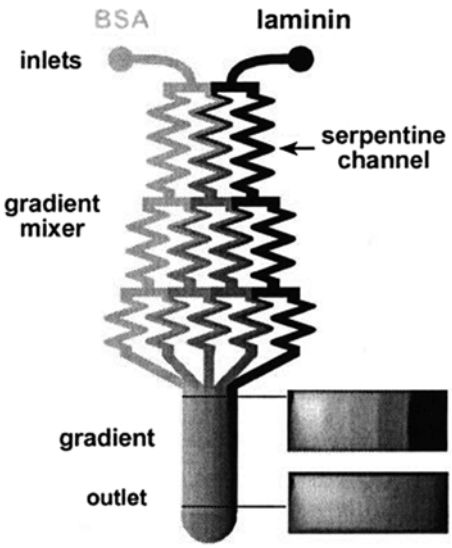

Fig. 3.9 Two inputs, BSA and laminin, are formed into a gradient by flowing through a microfluidic gradient mixer. Adapted from Dertinger et al. (2002)

strongly direct or inhibit guidance when gradients were in opposite directions or parallel, respectively (Li et al. 2008).

Soluble gradients of neurotrophin 3 (Ryan et al. 2006) and netrin-1 (Bhattacharjee et al. 2010) were found to be attractive cues to cultured neurons. Conversely, a soluble linear BDNF gradient serves as a repulsive stimulus to extending axons. However, when a soluble BNDF gradient is combined with an immobilized laminin gradient, the guidance response of the neurite can be manipulated by altering the mean concentration of BNDF in the localized area; for example, higher levels of soluble BNDF overcomes decreasing levels of bound laminin to cause neurites growth down the laminin gradient (Joanne Wang et al. 2008).

3.6.3 Fluid Flow

The force of fluid flow on extending axons can reorient their direction of growth. This has been demonstrated using two different sources of fluid flow: microsyringe nanopump and photon-driven micromotors. The microsyringe nanopump simply ejects fluid through microtubing placed perpendicular to the direction of original neural outgrowth. Thirty-five percent of axons responded to the fluid flow stimuli with 78 % of responsive neurons reorienting to align with the direction of fluid flow. The average induced turning angle was 40° (Gu et al. 2014).

Alternatively, fluid flow in cell culture has been generated by a micromotor. Circularly polarized light is applied to vaterite beads. The photon's angular momentum causes the beads to spin, which creates localized microfluidic flow that is sensed by the extending axons. Counterclockwise rotation turns extending axons to the left, whereas clockwise rotation turns extending axons to the right with average turning angles of 30° and 27°, respectively. Redirected growth was exhibited for 42 % of neurons (Wu et al. 2012).

3.6.4 Block Cell Printing

Block cell printing is a newer technique that allows the creation of patterned cell arrays. Using standard photolithography techniques, a photoresist is patterned into an appropriate mold. Polydimethylsiloxane (PMDS) is cured within the photoresist mold resulting in a BloC-mold with the inverse of the photoresist pattern. This final BloC-mold consists of narrow channels with small hooks that protrude at regular intervals. The BloC-mold is then laid onto a culture dish to allow a cell solution to flow through the channels. Cells get trapped by the hook structures and immobilized at specific locations then an incubation period without fluid flow allows these cells to adhere to the culture dish. The BloC-mold can then be removed, leaving behind a patterned array of cells (Fig. 3.10).

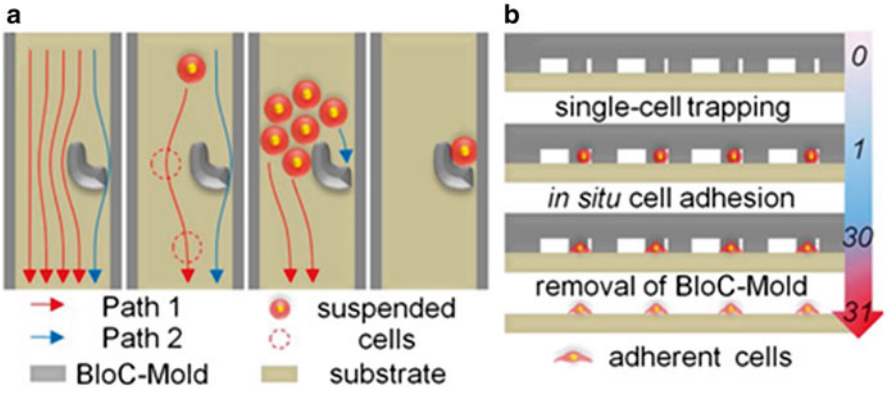

Fig. 3.10 (**a**) Visualization of fluid flow and cell trapping process within BloC printing microfluidic chambers and (**b**) process of BloC printing including cell trapping for 1 min, cell incubation allowing adhesion to substrate for 30 min, and finally removal of microfluidic mold. Adapted from Zhang et al. (2014b)

Individual primary cortical neurons have successfully been patterned using this method. After 14 days of culture in vitro, the cells exhibited normal morphology and neurite extension. Altering the spacing and number of hooks allowed for the patterning of single and paired neurons that demonstrated highly branched dendrites by 7 days in vitro (DIV) (Zhang et al. 2014b).

3.7 Subtractive Fabrication

3.7.1 Photoablation

Photoablation is employed to selectively remove areas of deposited material via UV light exposure in order to present either positive or negative cues for controlling neuronal placement and extension. The light can be broadly applied to the substrate through a mask to yield a specified pattern. Alternatively, the light can be employed as a focused beam that is directly maneuvered to remove patterned sections of materials.

Several materials have been used in photoablation applications for 2D culture environments that were patterned using a mask. Poly-N-isopropylacrylamide (PNIPAM), which resists cell adhesion, was photoablated into parallel stripes. Cells were found to grow, spread, and extend neurites on glass substrates within the confines of the patterned PNIPAM (Bohanon et al. 1996). Laminin-coated coverslips were ablated into grid patterns with wider nodes at line intersections. Seeded hippocampal neurons were found to adhere preferentially to the unablated laminin, to migrate toward larger areas of supportive laminin, and to extend neurites down the patterned pathways. The maximum migration was found for 5 μm lines with 20 μm nodes and 80 μm intersection spacing

(Corey et al. 1991). Similarly, a layer of diethylenetriaminepropyltrimethoxysilane was patterned into a growth-permissive grid pattern with higher laser energies, which resulted in better pattern compliance (Corey et al. 1996). Finally, poly-lactic-co-glycolic acid (PLGA) was patterned into microgrooves of 5- and 10 μm-widths then coated with collagen type I or a laminin peptide. Neurites extended parallel to the microgrooves with the smaller grooves resulting in statistically higher and straighter alignment (Yao et al. 2009).

Focused beam-based photoablation has been used to create guidance channels in 3D PEG-based hydrogels for extending DRG neurites. In this case, the laser was manipulated via the 3-axis motions of a mechanical microscope stage. The exposed PEG underwent optical breakdown and plasma formation forming complex guidance channels. The resulting channels had elliptical cross sections and their size was controlled by laser power. DRG cells extended neurites unidirectionally within the PEGylated fibrinogen hydrogel guidance channels, filling the entire channel volume. Nonneural cells contained within the DRG also migrated into the channels (Sarig-Nadir et al. 2009). Photoablation could also be used to form guidance channels in PEGylated gelatin and PEGylated albumin hydrogels. However, neither gel supported rapid infiltration into the guidance channels like the fibrinogen-based hydrogel. This was attributed to the contact guidance and opportunities for cellular adhesion associated with fibrinogen (Berkovitch et al. 2015).

Similarly, a PEG hydrogel system with an incorporated nitrobenzyl ether moiety, which can be cleaved using two-photon laser light, enables real-time degradation to create guidance channels. Hydrogel encapsulated embryonic stem cell-derived motor neurons were able to extend axons along the degraded portions of the hydrogel, following the prescribed pathways (McKinnon et al. 2014).

3.7.2 Photothermal Etching

Photothermal etching allows the creation of wells, microchannels, and microtunnels for constraining neurite network formation by capitalizing on the physical properties of agar gels. Agar resists cell adhesion and has a low melting point. Using lasers, defined patterns are melted into specific sections of an agar gel. The melted agar diffuses away into the surrounding solid agar gel, leaving a defined void. The wavelength of the laser affects the type of patterning that can be performed; 1480 nm lasers ablate through the depth of the gel giving wells and microchannels (Fig. 3.11a–c), whereas 1064 nm lasers cause heating of the chromium layer which results in localized melting giving microtunnels (Fig. 3.11d–f) (Hattori et al. 2004). The thickness of the microtunnels and the laser power exhibited a linear relationship. A typical pattern consists of a series of wells connected by either microchannels or microtunnels. Individual cells are seeded into and confined within the wells, whereas neurites extend down the narrow connecting structures (Moriguchi et al. 2004). Such intercellular connections can develop within 48 h (Moriguchi et al. 2002). Even after cell culture has been initiated and network formation has begun,

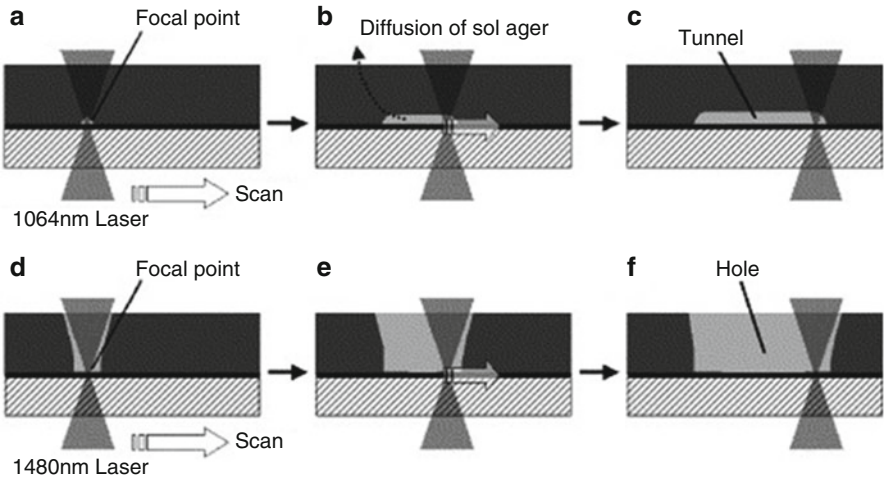

Fig. 3.11 (**a–c**) The fabrication of tunnels during photothermal ablation using 1064 nm laser light; (**d–f**) the creation of voids during photothermal ablation using 1480 nm laser light (Hattori et al. 2004)

gels can be further manipulated by photothermal etching to redirect neurite growth or alter neural connectivity thereby ensuring unidirectional connections (Suzuki et al. 2004c). No detrimental effects on the cultured neurons have been observed from additional irradiation as evidenced by new fiber growth and extension down newly added channels and tunnels (Sugio et al. 2004; Moriguchi et al. 2004).

Photothermal etching is compatible with MEAs for patterning cells (Suzuki et al. 2004a, b, 2005). Wells designated to house the soma are patterned directly on top of electrodes, and further patterning is incorporated to control the neural network that forms. Spontaneous firing was observed among cells at 7 DIV followed by synchronized electrical activity at 9 DIV. Synapse formation was confirmed by immunocytochemistry (Suzuki and Kenji 2007).

Photothermal etching is not limited to 2D applications. This technique was used for the culture of rat hippocampal neurons seeded in a 3D collagen gel. Using a 1064 nm laser beam, specific areas of a collagen gel were effectively melted to create nonadherent (etched) zones and growth permissive (unetched) regions. In order to guide outgrowth, the area around individual neurons was melted with the exception of an "unetched bridge" that connected the newly isolated neuron to another cell. This "unetched bridge" provided the only acceptable adherent substrate onto which neurites could extend processes. Using this procedure, neuronal networks with axo-axonic connections were fabricated after 5 days of culture that achieved spontaneous firing patterns and synaptic transmissions. This method may also be utilized to isolate two different cells together, such as neurons and glial cells, in order to gain insight into their interactions (Odawara et al. 2013).

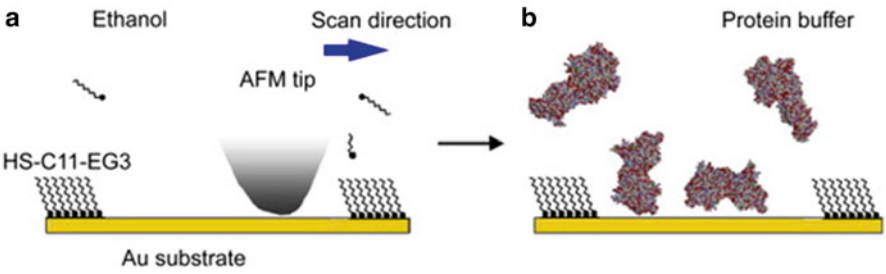

Fig. 3.12 (**a**) The removal of PEG via the force applied by an AFM tip and (**b**) the adsorption of the protein of interest to the nanoshaved surface (Staii et al. 2009)

3.7.3 Nanoshaving

Nanoshaving is a form of Atomic Force Microscopy (AFM) nanolithography. The AFM tip is scanned across a self-assembling monolayer (SAM) of PEG in a defined pattern at high forces, removing the PEG from the gold surface in these regions. This removal is performed in a solvent to prevent shaved PEG from reattaching to the surface. The shaved pattern is then submersed in a solvent containing adhesive proteins for supporting neuronal growth (Fig. 3.12). The protein adheres to the shaved areas only since PEG intrinsically resists protein adhesion.

When the patterns were coated with poly-D-lysine (PDL) or laminin, neuron somas were found to adhere to larger square areas and to extend a single dominant process, the axon, down the thin line that connected the squares until it contacted the next cell. These axons grew to lengths greater than 40 μm on patterned PDL and more than 50 μm on patterned laminin. Shorter processes, the dendrites, were seen to extend from the cell body but remained localized on the square area (Staii et al. 2009). Additional experiments showed that axonal extensions followed the patterned PDL regardless of directional changes within the pattern. However, there was some limitation to PEG's ability to constrain neuronal overgrowth; if 10 μm squares were located within 35 μm of each other, neurons were able to connect to each other by extending over the intact PEG SAM (Staii et al. 2011).

3.8 Optical Guidance

3.8.1 Laser Micromanipulation

Laser micromanipulation utilizes weak optical forces to guide the direction of growth cone advancement. A light beam is steered such that half of the laser spot remains localized on the edge of the lamellipodium while the other half extends in the direction of desired neurite extension allowing the user direct control over the

trajectory of neuronal growth. It is thought that the gradient forces of the infrared light beam cause lamellipodia extension by actin polymerization to become biased in the direction of the applied laser spot (Koch et al. 2004). A variety of different wavelengths can be implemented during the laser micromanipulation process without any appreciable effect on the guidance outcome (Stevenson et al. 2006). In addition, the development and integration of programs that are capable of real-time shape detection and feedback mechanisms enables the automation of the laser micromanipulation steering process (Stuhrmann et al. 2005; Carnegie et al. 2009).

This technique has shown an 85 % success rate in instigating guided turns of actively extending growth cones. The lamellipodia extension rate temporarily increased from 7 to 37.5 μm/h denoting an enhanced rate of outgrowth. While the effects of the applied light beam were localized and temporary, the overall change in cellular morphology was permanent (Ehrlicher et al. 2002, 2007).

Laser micromanipulation is not limited to two-dimensional environments. PC12 cells seeded in a 3D collagen matrix were successfully reoriented with an 80 % success rate. The neurites changed their trajectory by an average of 52° and exhibited an increased growth rate, moving at 0.74 μm/min compared to 0.37 μm/min for control cells. These observable trends were achieved within 30 min of light stimulus application (Graves et al. 2009).

3.8.2 Optical Tweezers

Similar to laser micromanipulation, optical tweezers rely on the application of a beam of light to a neural structure; however, optical tweezers require a more tightly focused beam and increased gradient forces within their optical trap. This technique induces cellular detachment from the substrate and translocation by directing the motion of the laser beam's focal point (Fig. 3.13). Essential to transfer success is the

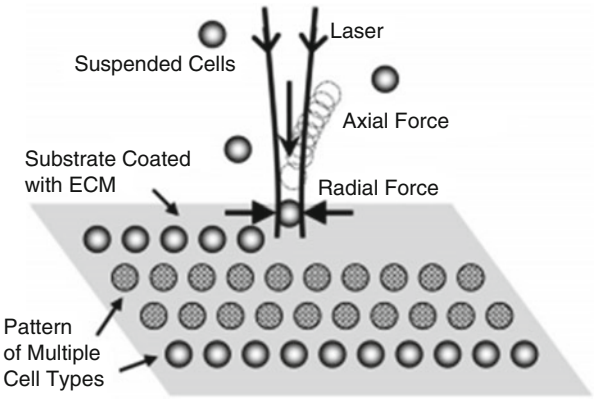

Fig. 3.13 A depiction of the forces utilized in optical tweezing to deposit cells out of suspension to a specific substrate locations (Pirlo et al. 2006)

initial seeding of neurons on a nonadhesive substrate, as the optical forces produced by the tweezers are insufficient to overcome significant cellular focal adhesions (Townes-Anderson et al. 1998).

Experiments performed on embryonic chick forebrain neurons confirmed the validity of optical tweezers for manipulating delicate cell types. Cell viability was unaffected by the duration and laser power required for transportation (Rosenbalm et al. 2006). Neuron cell morphology exhibited no adverse reaction to the process as normal neurite extension occurred for over 7 days (Pirlo et al. 2006). Results from optical tweezing of retinal neurons showed similar success in maintaining viability and morphology. Electron microscopy confirmed that organelle structure remained intact after manipulation (Townes-Anderson et al. 1998). Evaluation of laser parameters on hippocampal neurons elucidated a linear relationship between beam power and speed of translation and determined that shorter wavelength irradiation is less damaging to the cell. Optical tweezers were also used to move neurons into plastic "cages" denoting that translation in the z-direction is possible (Pine and Chow 2009).

3.8.3 Ultrafast Laser Microbeams

Ultrafast laser microbeams use pulsed light as an attractive cue to advancing axons. Cortical neurons exposed to near infrared light at a distance of 15 μm from their growth cone exhibited varied response depending on the stimulus: 45 % demonstrated an attraction to a pulsed microbeam whereas only 8.3 % were attracted to the sham and 13.5 % to continuous wave conditions. Attracted filopodia would change their path trajectory until they neared the beam spot at which point they would halt and continuously sample the beam spot environment (Mathew et al. 2010). It is proposed that neurons interpret the pulsing light as nearby cells with which they desire to interact.

3.8.4 Neuronal Beacon

The neuronal beacon method utilizes a spot of low power, near infrared light as a noncontacting repulsive cue to extending axons. The beam is placed asymmetrically in the path of an advancing axon approximately 5 μm from the filopodia and is held static during each turning event. As the axon senses the repulsive cue, it deviates from its initial path to avoid the light (Fig. 3.14) (Black et al. 2013). It is believed that this is a photothermal phenomenon in which filopodia sense and respond to a laser induced thermal gradient.

When a neuronal beacon was applied to goldfish retinal ganglion cells, the axonal directionality was altered by an average of 51.1°. The directionality shift occurred most rapidly during the first 5–10 min of stimulus application and satu-

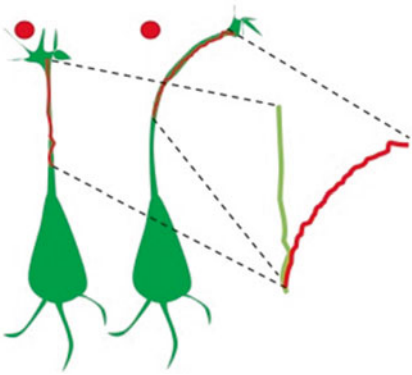

Fig. 3.14 A visualization of the repulsive nature of the neuronal beacon. Adapted from Black et al. (2014)

rated after 15 min. After removal of the light source, axons proceeded to extend in a straight line along their new path with growth rates similar to their pre-exposure speed. Multiple manual repositionings of the laser spot allowed dynamic control over the axon's path; turning angles of up to 120° and over 90 μm were achieved (Black et al. 2014). Neuronal beacons have also been applied to rat cortical neurons to induce axonal loop formation and self-fasciculation. Loops with radii of curvature smaller than typically seen naturally were successfully fabricated. Laser spots with a line profile as well as repetitive application of light stimuli maintained effectiveness as a repulsive cue (Mondal et al. 2014).

3.9 Magnetic Applications

3.9.1 Magnetic Fields

Externally applied magnetic fields have been utilized to induce axonal extension from neurons in culture with contradictory results. For example, a pulsed magnetic field was shown to induce increased neurite outgrowth from DRG explants in a direction parallel to the applied field (Macias et al. 2000). Contrarily, human neuronal SH-SY5Y and PC12 cells exhibited dystrophic neurite outgrowth parallel to the magnetic field while outgrowth perpendicular to the applied field was enhanced (Kim et al. 2008).

3.9.2 Magnetic Fiber Alignment

Magnetic fields can cause the fibers of a gel to align parallel to the applied force. Neurons cultured in gels that are undergoing fibrillogenesis will standardly extend neurites in the same direction. Magnetic fields have been applied to both

collagen and fibrin gels to align their fibers for guidance of cellular processes. DRG neurite extensions within such gels was found to have biased growth in a direction that correlated with the axial direction of the underlying fibers as well as an increased rate of elongation (Dubey et al. 1999). Similarly, fibrin could be used to orient neurite outgrowth but only at fibril diameters greater than 460 nm (Dubey et al. 2001). Alternatively, nickel nanowires suspended in a solution have been applied to a substrate then aligned using a magnetic field. DRGs cultured on these substrates exhibit contact guidance along the wires (Johansson et al. 2010).

3.9.3 Magnetic Nanoparticles

Iron oxide nanoparticles included in culture media can be taken up by neuronal cells via an endocytotic-like pathway and become trapped in the cellular cytoplasm. Under the influence of a magnetic field, these nanoparticles provide tension to specific areas inside the cell that encourages growth along the axis of the magnetic field (Riggio et al. 2014). Nanoparticles doped with cell adhesion molecules, which can be localized to the cell membrane, have been used to apply tension to the surface of a cell. The application of 3–6 pNs of force was shown to be significant enough to direct initiation of filopodia elongation parallel to the magnetic field (Pita-Thomas et al. 2015). Magnetic nanoparticles coated with poly-L-lysine are less cytotoxic to cells than their iron oxide counterparts and are capable of promoting neural cell migration toward a magnetic source (Riggio et al. 2012).

3.10 Electric Fields

Electric fields can be applied to neuronal cultures to alter the direction of neurite outgrowth as well as to cause cell migration. Experiments performed on *Xenopus larvis* neurons consistently show a cathodal growth preference for neurite outgrowth (Patel and Poo 1982; McCaig 1986), regardless of filopodial presence (McCaig 1989) or type of electrical source (Patel and Poo 1984; Graves et al. 2011). Embryonic chick DRG neurons (Jaffe and Poo 1979) and neurons from frog embryos (Hinkle et al. 1981) also exhibit primarily cathodal growth. However, this trend does not hold true for all neuronal cell types. Rat hippocampal neurons (Rajnicek et al. 1992) and embryonic chick sympathetic neurons (Pan and Borgens 2010, 2012; Pan et al. 2012) orient themselves perpendicularly to the applied field. Embryonic zebrafish neurons are not affected by an electric stimulus (Cormie and Robinson 2007). It is apparent from the discrepancy within the literature that the use of an electric field for specific neuronal guidance depends both on the cell type and the mode of electric field application.

The combination of electric fields with other stimuli can enhance and alter the effect on neurite outgrowth. The use of chondroitin sulfate proteoglycans (Erskine and McCaig 1997), brain-derived neurotropic factor, and neurotrophin-4 in culture medium can enhance axonal reorientation toward the cathode. Interestingly, neurotrophin-3 has a dual effect on neurites; it will induce anodal turning at low electric field strength and cathodal turning at higher electric field strength (McCaig et al. 2000). Another factor to consider is the charge of the substrate, which can play a role in the effect of the electric field: positively charged substrates encouraged growth toward the anode while negatively charged substrates enhanced growth toward the cathode (Rajnicek et al. 1998). For example, the coculture of astrocytes and DRGs under an electric field induced a specific orientation of the astrocytes and subsequent alignment of extending neurites (Alexander et al. 2006). Meanwhile, the combination of electric fields and electrospun fibers (Koppes et al. 2014) or Schwann cells (Koppes et al. 2011) gives increased outgrowth but did not affect directional guidance. Electric fields have also been shown to be incapable of overcoming the neurite guidance provided by microcontact-printed laminin (Britland and McCaig 1996).

Hippocampal neurons will respond to a DC electric field by migrating toward the cathode. This directed motion occurs above 120 mV/mm, a physiologically relevant value, with cell directedness increasing in conjunction with the strength of the applied electric field. Switching the polarity of the field reverses the migratory direction of the cell population (Yao et al. 2008). MEAs have been used to induce the electrical stimuli, resulting in cell migration and clustering around the stimulating electrode. This effect was exhibited after 3 weeks in culture alone (Jun et al. 2007b) or after 1 week in coculture of neurons with astrocytes (Jeong et al. 2009).

3.11 Comparison of Methods

Table 3.1 provides an overview of the methods presented herein for manipulation of neuronal location and network formation. Those methods marked with "Ease of Pattern Alteration" denote techniques in which the engineered pattern was controlled manually or could be changed without additional mask or stamp fabrication steps.

By perusing the table, it should be evident that no single method has successfully recapitulated a neuronal network to meet all of the design constraints of the in vivo neural environment. As such, future investigations of neurite guidance should look not only to newly proposed guidance methods but also incorporate aspects of those methods already in use in a way that harnesses their strengths while circumventing their individual shortcomings. The design requirements, as defined by the desired outcome, will ultimately influence which methods can be implemented in an experiment. Therefore, it is important for an investigator to fully understand the final goal before selecting and pursuing a specific fabrication technique.

Table 3.1 A comparison of the characteristics for the discussed in vitro neural engineering techniques

	2D culture	3D culture	Soma Placement	Neurite Guidance	Affect Individual Cell	Affect Population of Cells	Physical Cue	Soluble Cue	Immobilized Cue	Force Cue	Compatible with MEAs	Ease of Pattern Alteration	Use Multiple Cell Types Simultaneously	Feature Parameters
Topography	×			×		×	×							2 nm
Microcontact Printing	×		×	×	×	×			×		×			300 nm
Ink-jet Printing	×	×	×	×	×				×	×		×	×	85-600 μm
MAPLE DW	×	×	×		×					×		×	×	2-300 μm
Photopatterning 2D Substrates	×		×	×	×				×		×			2 μm
3D Photoimmobilization of Guidance Cues		×	×	×	×		×		×			×		~0.5 μm
Stereolithography of Hydrogel Guidance Structures		×	×	×	×	×	×					×	×	~ 1 μm
LAPAP	×			×	×				×			×		~600 nm - 1 μm
Digital Projection Photolithography	×	×	×	×		×	×	×	×			×	×	~2 μm
Microfluidic Material Deposition	×		×	×	×				×					1 μm
Microfluidic Gradient Formation	×			×		×		×	×			×		---
Fluid Flow	×			×	×					×		×		---
Block Cell Printing	×		×		×		×						×	5 μm
Photoablation	×	×		×	×		×		×					3 μm
Photothermal Etching	×	×	×	×	×		×				×	×	×	2-50 μm
Nanoshaving	×		×	×	×		×		×			×		~50 nm
Laser Micromanipulation	×	×		×	×					×		×		---
Ultrafast Laser Microbeams	×			×	×					×		×		---
Neuronal Beacon	×			×	×					×		×		---
Magnetic Field	×			×		×				×		×		---
Magnetic Fiber Alignment	×	×		×		×	×					×		---
Magnetic Nanoparticles	×			×		×				×		×		---
Electric Fields	×		×	×		×				×	×			---

Engineering neuronal connectivity in vitro provides investigators with the opportunity to simplify experimental parameters for general scientific gain, make advances in tissue engineering and neural medical devices, and improve HTS platforms. Methods utilizing topography, printing procedures, photolithography, microfluidics, subtractive fabrication techniques, optical cues, and magnetic and electric fields have all been demonstrated as viable options for creating desired patterns of soma placement and neurite outgrowth, though each comes with its specific advantages and disadvantages as well as fabrication constraints.

References

Adams, D.N., E.Y. Kao, C.L. Hypolite, M.D. Distefano, W.S. Hu, and P.C. Letourneau. 2005. Growth Cones Turn and Migrate up an Immobilized Gradient of the Laminin IKVAV peptide. *Journal of Neurobiology* 62: 134–147.

Alexander, J.K., B. Fuss, and R.J. Colello. 2006. Electric Field-Induced Astrocyte Alignment Directs Neurite Outgrowth. *Neuron Glia Biology* 2: 93–103.

Astashkina, A., and D.W. Grainger. 2014. Critical Analysis of 3-D Organoid In Vitro Cell Culture Models for High-Throughput Drug Candidate Toxicity Assessments. *Advanced Drug Delivery Reviews* 69–70: 1–18.

Belisle, J.M., J.P. Correia, P.W. Wiseman, T.E. Kennedy, and S. Costantino. 2008. Patterning Protein Concentration Using Laser-Assisted Adsorption by Photobleaching, LAPAP. *Lab on a Chip* 8: 2164–2167.

Belisle, J.M., D. Kunik, and S. Costantino. 2009. Rapid Multicomponent Optical Protein Patterning. *Lab on a Chip* 9: 3580–3585.

Belisle, J.M., L.A. Levin, and S. Costantino. 2012. High-Content Neurite Development Study Using Optically Patterned Substrates. *PLoS One* 7: e35911.

Belisle, J.M., J. Mazzaferri, and S. Costantino. 2014. Laser-Assisted Adsorption by Photobleaching. *Methods in Cell Biology* 119: 125–140.

Belkaid, W., P. Thostrup, P.T. Yam, C.A. Juzwik, E.S. Ruthazer, A.S. Dhaunchak, and D.R. Colman. 2013. Cellular Response to Micropatterned Growth Promoting and Inhibitory Substrates. *BMC Biotechnology* 13: 86.

Berkovitch, Y., D. Yelin, and D. Seliktar. 2015. Photo-Patterning PEG-Based Hydrogels for Neuronal Engineering. *European Polymer Journal* 72: 473–483.

Bhattacharjee, N., N. Li, T.M. Keenan, and A. Folch. 2010. A Neuron-Benign Microfluidic Gradient Generator for Studying the Response of Mammalian Neurons Towards Axon Guidance Factors. *Integrative Biology (Cambridge)* 2: 669–679.

Black, B., A. Mondal, Y. Kim, and S.K. Mohanty. 2013. Neuronal Beacon. *Optics Letters* 38: 2174–2176.

Black, B.J., L. Gu, and S.K. Mohanty. 2014. Highly Effective Photonic Cue for Repulsive Axonal Guidance. *PLoS One* 9: e86292.

Bohanon, T., G. Elender, W. Knoll, P. Koberle, J.S. Lee, A. Offenhausser, H. Ringsdorf, E. Sackmann, J. Simon, G. Tovar, and F.M. Winnik. 1996. Neural Cell Pattern Formation on Glass and Oxidized Silicon Surfaces Modified with Poly(N-Isopropylacrylamide). *Journal of Biomaterials Science Polymer Edition* 8: 19–39.

Branch, D.W., J.M. Corey, J.A. Weyhenmeyer, G.J. Brewer, and B.C. Wheeler. 1998. Microstamp Patterns of Biomolecules for High-Resolution Neuronal Networks. *Medical and Biological Engineering and Computing* 36: 135–141.

Branch, D.W., B.C. Wheeler, G.J. Brewer, and D.E. Leckband. 2000. Long-Term Maintenance of Patterns of Hippocampal Pyramidal Cells on Substrates of Polyethylene Glycol and Microstamped Polylysine. *IEEE Transactions on Biomedical Engineering* 47: 290–300.

Britland, S., and C. Mccaig. 1996. Embryonic Xenopus Neurites Integrate and Respond to Simultaneous Electrical and Adhesive Guidance Cues. *Experimental Cell Research* 226: 31–38.

Britland, S., C. Perridge, M. Denyer, H. Morgan, A. Curtis, and C. Wilkinson. 1996. Morphogenetic Guidance Cues Can Interact Synergistically and Hierarchically in Steering Nerve Cell Growth. *Experimental Biology Online* 1: 1–15.

Bruder, J.M., A.P. Lee, and D. Hoffman-Kim. 2007. Biomimetic Materials Replicating Schwann Cell Topography Enhance Neuronal Adhesion and Neurite Alignment In Vitro. *Journal of Biomaterials Science Polymer Edition* 18: 967–982.

Carnegie, D.J., T. Cizmar, J. Baumgartl, F.J. Gunn-Moore, and K. Dholakia. 2009. Automated Laser Guidance of Neuronal Growth Cones Using a Spatial Light Modulator. *Journal of Biophotonics* 2: 682–692.

Catig, G.C., S. Figueroa, and M.J. Moore. 2015. Experimental and Computational Models of Neurite Extension at a Choice Point in Response to Controlled Diffusive Gradients. *Journal of Neural Engineering* 12: 046012.

Chang, J.C., G.J. Brewer, and B.C. Wheeler. 2003. A Modified Microstamping Technique Enhances Polylysine Transfer and Neuronal Cell Patterning. *Biomaterials* 24: 2863–2870.

Cheng, J., G. Zhu, L. Wu, X. Du, H. Zhang, B. Wolfrum, Q. Jin, J. Zhao, A. Offenhausser, and Y. Xu. 2013. Photopatterning of Self-Assembled Poly(Ethylene) Glycol Monolayer for Neuronal Network Fabrication. *Journal of Neuroscience Methods* 213: 196–203.

Chien, H.W., and W.B. Tsai. 2012. Fabrication of Tunable Micropatterned Substrates for Cell Patterning Via Microcontact Printing of Polydopamine with Poly(Ethylene Imine)-Grafted Copolymers. *Acta Biomaterialia* 8: 3678–3686.

Choi, J.H., H. Lee, H.K. Jin, J.S. Bae, and G.M. Kim. 2013. Fabrication of Microengineered Templates and Their Applications into Micropatterned Cell Culture. *Journal of Biomedical Nanotechnology* 9: 377–381.

Clark, P., P. Connolly, A.S. Curtis, J.A. Dow, and C.D. Wilkinson. 1990. Topographical Control of Cell Behaviour: II. Multiple Grooved Substrata. *Development* 108: 635–644.

Corey, J.M., B.C. Wheeler, and G.J. Brewer. 1991. Compliance of Hippocampal Neurons to Patterned Substrate Networks. *Journal of Neuroscience Research* 30: 300–307.

Corey, J.M., B.C. Wheeler, and G.J. Brewer. 1996. Micrometer Resolution Silane-Based Patterning of Hippocampal Neurons: Critical Variables in Photoresist and Laser Ablation Processes for Substrate Fabrication. *IEEE Transactions on Biomedical Engineering* 43: 944–955.

Cormie, P., and K.R. Robinson. 2007. Embryonic Zebrafish Neuronal Growth Is Not Affected by an Applied Electric Field In Vitro. *Neuroscience Letters* 411: 128–132.

Curley, J.L., and M.J. Moore. 2011. Facile Micropatterning of Dual Hydrogel Systems for 3D Models of Neurite Outgrowth. *Journal of Biomedical Materials Research. Part A* 99: 532–543.

Curley, J.L., S.R. Jennings, and M.J. Moore. 2011. Fabrication of Micropatterned Hydrogels for Neural Culture Systems Using Dynamic Mask Projection Photolithography. *Journal of Visualized Experiments* 48: 2636.

Curley, J.L., G.C. Catig, E.L. Horn-Ranney, and M.J. Moore. 2014. Sensory Axon Guidance with Semaphorin 6a and Nerve Growth Factor in a Biomimetic Choice Point Model. *Biofabrication* 6: 035026.

Curley, J.L., S.C. Sklare, D.A. Bowser, J. Saksena, M.J. Moore, and D.B. Chrisey. 2016. Isolated node engineering of neuronal systems using laser direct write. *Biofabrication*, 8: 015013.

Degenaar, P., B.L. Pioufle, L. Griscom, A. Tixier, Y. Akagi, Y. Morita, Y. Murakami, K. Yokoyama, H. Fujita, and E. Tamiya. 2001. A Method for Micrometer Resolution Patterning of Primary Culture Neurons for SPM Analysis. *Journal of Biochemistry* 130: 367–376.

Dent, E.W., S.L. Gupton, and F.B. Gertler. 2011. The Growth Cone Cytoskeleton in Axon Outgrowth and Guidance. *Cold Spring Harbor Perspectives in Biology* 3.

Dertinger, S.K., X. Jiang, Z. Li, V.N. Murthy, and G.M. Whitesides. 2002. Gradients of Substrate-Bound Laminin Orient Axonal Specification of Neurons. *Proceedings of the National Academy of Sciences of the United States of America* 99: 12542–12547.

Doraiswamy, A., R.J. Narayan, T. Lippert, L. Urech, A. Wokaun, M. Nagel, B. Hopp, M. Dinescu, R. Modi, R.C.Y. Auyeung, and D.B. Chrisey. 2006. Excimer Laser Forward Transfer of Mammalian Cells Using a Novel Triazene Absorbing Layer. *Applied Surface Science* 252: 4743–4747.

Dowell-Mesfin, N.M., M.A. Abdul-Karim, A.M. Turner, S. Schanz, H.G. Craighead, B. Roysam, J.N. Turner, and W. Shain. 2004. Topographically Modified Surfaces Affect Orientation and Growth of Hippocampal Neurons. *Journal of Neural Engineering* 1: 78–90.

Dubey, N., P.C. Letourneau, and R.T. Tranquillo. 1999. Guided Neurite Elongation and Schwann Cell Invasion into Magnetically Aligned Collagen in Simulated Peripheral Nerve Regeneration. *Experimental Neurology* 158: 338–350.

Dubey, N., P.C. Letourneau, and R.T. Tranquillo. 2001. Neuronal Contact Guidance in Magnetically Aligned Fibrin Gels: Effect of Variation in Gel Mechano-Structural Properties. *Biomaterials* 22: 1065–1075.

Ehrlicher, A., T. Betz, B. Stuhrmann, D. Koch, V. Milner, M.G. Raizen, and J. Kas. 2002. Guiding Neuronal Growth with Light. *Proceedings of the National Academy of Sciences of the United States of America* 99: 16024–16028.

Ehrlicher, A., T. Betz, B. Stuhrmann, M. Gogler, D. Koch, K. Franze, Y. Lu, and J. Kas. 2007. Optical Neuronal Guidance. *Methods in Cell Biology* 83: 495–520.

Erskine, L., and C.D. Mccaig. 1997. Integrated Interactions Between Chondroitin Sulphate Proteoglycans and Weak DC Electric Fields Regulate Nerve Growth Cone Guidance In Vitro. *Journal of Cell Science* 110(Pt 16): 1957–1965.

Esch, T., V. Lemmon, and G. Banker. 1999. Local Presentation of Substrate Molecules Directs Axon Specification by Cultured Hippocampal Neurons. *Journal of Neuroscience* 19: 6417–6426.

Fan, Y.W., F.Z. Cui, L.N. Chen, Y. Zhai, Q.Y. Xu, and I.S. Lee. 2002a. Adhesion of Neural Cells on Silicon Wafer with Nano-Topographic Surface. *Applied Surface Science* 187: 313–318.

Fan, Y.W., F.Z. Cui, S.P. Hou, Q.Y. Xu, L.N. Chen, and I.S. Lee. 2002b. Culture of Neural Cells on Silicon Wafers with Nano-Scale Surface Topograph. *Journal of Neuroscience Methods* 120: 17–23.

Fan, Y., F. Xu, G. Huang, T.J. Lu, and W. Xing. 2012. Single Neuron Capture and Axonal Development in Three-Dimensional Microscale Hydrogels. *Lab on a Chip* 12: 4724–4731.

Fereol, S., R. Fodil, M. Barnat, V. Georget, U. Milbreta, and F. Nothias. 2011. Micropatterned ECM Substrates Reveal Complementary Contribution of Low and High Affinity Ligands to Neurite Outgrowth. *Cytoskeleton (Hoboken, NJ)* 68: 373–388.

Francisco, H., B.B. Yellen, D.S. Halverson, G. Friedman, and G. Gallo. 2007. Regulation of Axon Guidance and Extension by Three-Dimensional Constraints. *Biomaterials* 28: 3398–3407.

Fricke, R., P.D. Zentis, L.T. Rajappa, B. Hofmann, M. Banzet, A. Offenhausser, and S.H. Meffert. 2011. Axon Guidance of Rat Cortical Neurons by Microcontact Printed Gradients. *Biomaterials* 32: 2070–2076.

Fritz, M., and M. Bastmeyer. 2013. Microcontact Printing of Substrate-Bound Protein Patterns for Cell and Tissue Culture. *Methods in Molecular Biology* 1018: 247–259.

Gill, A.A., I. Ortega, S. Kelly, and F. Claeyssens. 2015. Towards the Fabrication of Artificial 3d Microdevices for Neural Cell Networks. *Biomedical Microdevices* 17: 27.

Goldner, J.S., J.M. Bruder, G. Li, D. Gazzola, and D. Hoffman-Kim. 2006. Neurite Bridging Across Micropatterned Grooves. *Biomaterials* 27: 460–472.

Gomez, N., J.Y. Lee, J.D. Nickels, and C.E. Schmidt. 2007a. Micropatterned Polypyrrole: A Combination of Electrical and Topographical Characteristics for the Stimulation of Cells. *Advanced Functional Materials* 17: 1645–1653.

Gomez, N., Y. Lu, S. Chen, and C.E. Schmidt. 2007b. Immobilized Nerve Growth Factor and Microtopography Have Distinct Effects on Polarization Versus Axon Elongation in Hippocampal Cells in Culture. *Biomaterials* 28: 271–284.

Graves, C.E., R.G. Mcallister, W.J. Rosoff, and J.S. Urbach. 2009. Optical Neuronal Guidance in Three-Dimensional Matrices. *Journal of Neuroscience Methods* 179: 278–283.

Graves, M.S., T. Hassell, B.L. Beier, G.O. Albors, and P.P. Irazoqui. 2011. Electrically Mediated Neuronal Guidance with Applied Alternating Current Electric Fields. *Annals of Biomedical Engineering* 39: 1759–1767.

Gu, L., B. Black, S. Ordonez, A. Mondal, A. Jain, and S. Mohanty. 2014. Microfluidic Control of Axonal Guidance. *Scientific Reports* 4: 6457.

Gurkan, U.A., Y. Fan, F. Xu, B. Erkmen, E.S. Urkac, G. Parlakgul, J. Bernstein, W. Xing, E.S. Boyden, and U. Demirci. 2013. Simple Precision Creation of Digitally Specified, Spatially Heterogeneous, Engineered Tissue Architectures. *Advanced Materials* 25: 1192–1198.

Hammarback, J.A., S.L. Palm, L.T. Furcht, and P.C. Letourneau. 1985. Guidance of Neurite Outgrowth by Pathways of Substratum-Adsorbed Laminin. *Journal of Neuroscience Research* 13: 213–220.

Hammarback, J.A., J.B. Mccarthy, S.L. Palm, L.T. Furcht, and P.C. Letourneau. 1988. Growth Cone Guidance by Substrate-Bound Laminin Pathways Is Correlated with Neuron-to-Pathway Adhesivity. *Developmental Biology* 126: 29–39.

Hattori, A., H. Moriguchi, S.I. Ishiwata, and K. Yasuda. 2004. A 1480/1064 nm Dual Wavelength Photo-Thermal Etching System for Non-Contact Three-Dimensional Microstructure Generation into Agar Microculture Chip. *Sensors and Actuators B: Chemical* 100: 455–462.

Heller, D.A., V. Garga, K.J. Kelleher, T.C. Lee, S. Mahbubani, L.A. Sigworth, T.R. Lee, and M.A. Rea. 2005. Patterned Networks of Mouse Hippocampal Neurons on Peptide-Coated Gold Surfaces. *Biomaterials* 26: 883–889.

Hinkle, L., C.D. Mccaig, and K.R. Robinson. 1981. The Direction of Growth of Differentiating Neurones and Myoblasts from Frog Embryos in an Applied Electric Field. *Journal of Physiology* 314: 121–135.

Horn-Ranney, E.L., J.L. Curley, G.C. Catig, R.M. Huval, and M.J. Moore. 2013. Structural and Molecular Micropatterning of Dual Hydrogel Constructs for Neural Growth Models Using Photochemical Strategies. *Biomedical Microdevices* 15: 49–61.

Horn-Ranney, E.L., P. Khoshakhlagh, J.W. Kaiga, and M.J. Moore. 2014. Light-Reactive Dextran Gels with Immobilized Guidance Cues for Directed Neurite Growth in 3D Models. *Biomaterials Science* 2: 1450–1459.

Huval, R.M., O.H. Miller, J.L. Curley, Y. Fan, B.J. Hall, and M.J. Moore. 2015. Microengineered Peripheral Nerve-on-a-Chip for Preclinical Physiological Testing. *Lab on a Chip* 15(10): 2221–2232.

Hynd, M.R., J.P. Frampton, N. Dowell-Mesfin, J.N. Turner, and W. Shain. 2007. Directed Cell Growth on Protein-Functionalized Hydrogel Surfaces. *Journal of Neuroscience Methods* 162: 255–263.

Jaffe, L.F., and M.M. Poo. 1979. Neurites Grow Faster Towards the Cathode than the Anode in a Steady Field. *Journal of Experimental Zoology* 209: 115–128.

James, C.D., R. Davis, M. Meyer, A. Turner, S. Turner, G. Withers, L. Kam, G. Banker, H. Craighead, M. Isaacson, J. Turner, and W. Shain. 2000. Aligned Microcontact Printing of Micrometer-Scale Poly-L-Lysine Structures for Controlled Growth of Cultured Neurons on Planar Microelectrode Arrays. *IEEE Transactions on Biomedical Engineering* 47: 17–21.

Jeong, S.H., S.B. Jun, J.K. Song, and S.J. Kim. 2009. Activity-Dependent Neuronal Cell Migration Induced by Electrical Stimulation. *Medical and Biological Engineering and Computing* 47: 93–99.

Joanne Wang, C., X. Li, B. Lin, S. Shim, G.L. Ming, and A. Levchenko. 2008. A Microfluidics-Based Turning Assay Reveals Complex Growth Cone Responses to Integrated Gradients of Substrate-Bound ECM Molecules and Diffusible Guidance Cues. *Lab on a Chip* 8: 227–237.

Johansson, F., P. Carlberg, N. Danielsen, L. Montelius, and M. Kanje. 2006. Axonal Outgrowth on Nano-Imprinted Patterns. *Biomaterials* 27: 1251–1258.

Johansson, F., M. Jonsson, K. Alm, and M. Kanje. 2010. Cell Guidance by Magnetic Nanowires. *Experimental Cell Research* 316: 688–694.

Jun, S.B., M.R. Hynd, N. Dowell-Mesfin, K.L. Smith, J.N. Turner, W. Shain, and S.J. Kim. 2007a. Low-Density Neuronal Networks Cultured Using Patterned Poly-L-Lysine on Microelectrode Arrays. *Journal of Neuroscience Methods* 160: 317–326.

Jun, S.B., M.R. Hynd, K.L. Smith, J.K. Song, J.N. Turner, W. Shain, and S.J. Kim. 2007b. Electrical Stimulation-Induced Cell Clustering in Cultured Neural Networks. *Medical and Biological Engineering and Computing* 45: 1015–1021.

Jungblut, M., W. Knoll, C. Thielemann, and M. Pottek. 2009. Triangular Neuronal Networks on Microelectrode Arrays: An Approach to Improve the Properties of Low-Density Networks for Extracellular Recording. *Biomedical Microdevices* 11: 1269–1278.

Kam, L., W. Shain, J.N. Turner, and R. Bizios. 2001. Axonal Outgrowth of Hippocampal Neurons on Micro-Scale Networks of Polylysine-Conjugated Laminin. *Biomaterials* 22: 1049–1054.

Khan, S., and G. Newaz. 2010. A Comprehensive Review of Surface Modification for Neural Cell Adhesion and Patterning. *Journal of Biomedical Materials Research. Part A* 93: 1209–1224.

Khoshakhlagh, P., and M.J. Moore. 2015. Photoreactive Interpenetrating Network of Hyaluronic Acid and Puramatrix as a Selectively Tunable Scaffold for Neurite Growth. *Acta Biomaterialia* 16: 23–34.

Kim, S., W.S. Im, L. Kang, S.T. Lee, K. Chu, and B.I. Kim. 2008. The Application of Magnets Directs the Orientation of Neurite Outgrowth in Cultured Human Neuronal Cells. *Journal of Neuroscience Methods* 174: 91–96.

Klein, C.L., M. Scholl, and A. Maelicke. 1999. Neuronal Networks In Vitro: Formation and Organization on Biofunctionalized Surfaces. *Journal of Materials Science: Materials in Medicine* 10: 721–727.

Kleinfeld, D., K.H. Kahler, and P.E. Hockberger. 1988. Controlled Outgrowth of Dissociated Neurons on Patterned Substrates. *Journal of Neuroscience* 8: 4098–4120.

Koch, D., T. Betz, A. Ehrlicher, M. Gogler, B. Stuhrmann, and J. Kas. 2004. Optical Control of Neuronal Growth. *Proceedings of SPIE* 5514: 428–436.

Kolodkin, A.L., and M. Tessier-Lavigne. 2011. Mechanisms and Molecules of Neuronal Wiring: A Primer. *Cold Spring Harbor Perspectives in Biology* 3(6): 1–14

Koppes, A.N., A.M. Seggio, and D.M. Thompson. 2011. Neurite Outgrowth Is Significantly Increased by the Simultaneous Presentation of Schwann Cells and Moderate Exogenous Electric Fields. *Journal of Neural Engineering* 8: 046023.

Koppes, A.N., N.W. Zaccor, C.J. Rivet, L.A. Williams, J.M. Piselli, R.J. Gilbert, and D.M. Thompson. 2014. Neurite Outgrowth on Electrospun Plla Fibers Is Enhanced by Exogenous Electrical Stimulation. *Journal of Neural Engineering* 11: 046002.

Koroleva, A., A.A. Gill, I. Ortega, J.W. Haycock, S. Schlie, S.D. Gittard, B.N. Chichkov, and F. Claeyssens. 2012. Two-Photon Polymerization-Generated aNd Micromolding-Replicated 3D Scaffolds for Peripheral Neural Tissue Engineering Applications. *Biofabrication* 4: 025005.

Lauer, L., C. Klein, and A. Offenhausser. 2001. Spot Compliant Neuronal Networks by Structure Optimized Micro-contact Printing. *Biomaterials* 22: 1925–1932.

Lauer, L., A. Vogt, C.K. Yeung, W. Knoll, and A. Offenhäusser. 2002. Electrophysiological Recordings of Patterned Rat Brain Stem Slice Neurons. *Biomaterials* 23: 3123–3130.

Lee, W., J. Pinckney, V. Lee, J.H. Lee, K. Fischer, S. Polio, J.K. Park, and S.S. Yoo. 2009. Three-Dimensional Bioprinting of Rat Embryonic Neural Cells. *Neuroreport* 20: 798–803.

Leng, T., P. Wu, N.Z. Mehenti, S.F. Bent, M.F. Marmor, M.S. Blumenkranz, and H.A. Fishman. 2004. Directed Retinal Nerve Cell Growth for Use in a Retinal Prosthesis Interface. *Investigative Ophthalmology and Visual Science* 45: 4132–4137.

Li, B., Y. Ma, S. Wang, and P.M. Moran. 2005. Influence of Carboxyl Group Density on Neuron Cell Attachment and Differentiation Behavior: Gradient-Guided Neurite Outgrowth. *Biomaterials* 26: 4956–4963.

Li, G.N., J. Liu, and D. Hoffman-Kim. 2008. Multi-molecular Gradients of Permissive and Inhibitory Cues Direct Neurite Outgrowth. *Annals of Biomedical Engineering* 36: 889–904.

Liazoghli, D., A.D. Roth, P. Thostrup, and D.R. Colman. 2012. Substrate Micropatterning as a New in Vitro Cell Culture System to Study Myelination. *ACS Chemical Neuroscience* 3: 90–95.

Lorber, B., W.K. Hsiao, I.M. Hutchings, and K.R. Martin. 2014. Adult Rat Retinal Ganglion Cells and Glia Can Be Printed By Piezoelectric Inkjet Printing. *Biofabrication* 6: 015001.

Lowery, L.A., and D. Van Vactor. 2009. The Trip of the Tip: Understanding the Growth Cone Machinery. *Nature Reviews. Molecular Cell Biology* 10: 332–343.

Luo, Y., and M.S. Shoichet. 2004a. A Photolabile Hydrogel for Guided Three-Dimensional Cell Growth and Migration. *Nature Materials* 3: 249–253.

Luo, Y., and M.S. Shoichet. 2004b. Light-Activated Immobilization of Biomolecules to Agarose Hydrogels for Controlled Cellular Response. *Biomacromolecules* 5: 2315–2323.

Macias, M.Y., J.H. Battocletti, C.H. Sutton, F.A. Pintar, and D.J. Maiman. 2000. Directed and Enhanced Neurite Growth with Pulsed Magnetic Field Stimulation. *Bioelectromagnetics* 21: 272–286.

Mai, J., L. Fok, H. Gao, X. Zhang, and M.M. Poo. 2009. Axon Initiation and Growth Cone Turning on Bound Protein Gradients. *Journal of Neuroscience* 29: 7450–7458.

Martinoia, S., M. Bove, M. Tedesco, B. Margesin, and M. Grattarola. 1999. A Simple Microfluidic System for Patterning Populations of Neurons on Silicon Micromachined Substrates. *Journal of Neuroscience Methods* 87: 35–44.

Mathew, M., I. Amat-Roldan, R. Andres, S.I. Santos, D. Artigas, E. Soriano, and P. Loza-Alvarez. 2010. Signalling Effect of Nir Pulsed Lasers on Axonal Growth. *Journal of Neuroscience Methods* 186: 196–201.

Matsuda, T., T. Sugawara, and K. Inoue. 1992. Two-Dimensional Cell Manipulation Technology. An Artificial Neural Circuit Based on Surface Microphotoprocessing. *ASAIO Journal* 38: M243–M247.

Mccaig, C.D. 1986. Electric Fields, Contact Guidance and the Direction of Nerve Growth. *Journal of Embryology and Experimental Morphology* 94: 245–255.

Mccaig, C.D. 1989. Nerve Growth in the Absence of Growth Cone Filopodia and the Effects of a Small Applied Electric Field. *Journal of Cell Science* 93(Pt 4): 715–721.

Mccaig, C.D., L. Sangster, and R. Stewart. 2000. Neurotrophins Enhance Electric Field-Directed Growth Cone Guidance and Directed Nerve Branching. *Developmental Dynamics* 217: 299–308.

Mccormick, A.M., A. Wijekoon, and N.D. Leipzig. 2013. Specific Immobilization of Biotinylated Fusion Proteins NGF and Sema3A Utilizing a Photo-Cross-Linkable Diazirine Compound for Controlling Neurite Extension. *Bioconjugate Chemistry* 24: 1515–1526.

Mccormick, A.M., M.V. Maddipatla, S. Shi, E.A. Chamsaz, H. Yokoyama, A. Joy, and N.D. Leipzig. 2014. Micropatterned Coumarin Polyester Thin Films Direct Neurite Orientation. *ACS Applied Materials & Interfaces* 6: 19655–19667.

Mccormick, A.M., N.A. Jarmusik, and N.D. Leipzig. 2015. Co-immobilization of semaphorin3A and Nerve Growth Factor to Guide and Pattern Axons. *Acta Biomaterialia* 28: 33–44.

Mckinnon, D.D., T.E. Brown, K.A. Kyburz, E. Kiyotake, and K.S. Anseth. 2014. Design and Characterization of a Synthetically Accessible, Photodegradable Hydrogel for User-Directed Formation of Neural Networks. *Biomacromolecules* 15: 2808–2816.

Mehenti, N.Z., G.S. Tsien, T. Leng, H.A. Fishman, and S.F. Bent. 2006. A Model Retinal Interface Based on Directed Neuronal Growth for Single Cell Stimulation. *Biomedical Microdevices* 8: 141–150.

Melissinaki, V., A.A. Gill, I. Ortega, M. Vamvakaki, A. Ranella, J.W. Haycock, C. Fotakis, M. Farsari, and F. Claeyssens. 2011. Direct Laser Writing of 3D Scaffolds for Neural Tissue Engineering Applications. *Biofabrication* 3: 045005.

Millet, L.J., M.E. Stewart, R.G. Nuzzo, and M.U. Gillette. 2010. Guiding Neuron Development with Planar Surface Gradients of Substrate Cues Deposited Using Microfluidic Devices. *Lab on a Chip* 10: 1525–1535.

Mondal, A., B. Black, Y.T. Kim, and S. Mohanty. 2014. Loop Formation and Self-Fasciculation of Cortical Axon Using Photonic Guidance at Long Working Distance. *Scientific Reports* 4: 6902.

Moriguchi, H., Y. Wakamoto, Y. Sugio, K. Takahashi, I. Inoue, and K. Yasuda. 2002. An Agar-Microchamber Cell-Cultivation System: Flexible Change of Microchamber Shapes During Cultivation by Photo-Thermal Etching. *Lab on a Chip* 2: 125–132.

Moriguchi, H., K. Takahashi, Y. Sugio, Y. Wakamoto, I. Inoue, Y. Jimbo, and K. Yasuda. 2004. On-Chip Neural Cell Cultivation using Agarose-Microchamber Array Constructed by a Photothermal Etching Method. *Electrical Engineering in Japan* 146: 37–42.

Musoke-Zawedde, P., and M.S. Shoichet. 2006. Anisotropic Three-Dimensional Peptide Channels Guide Neurite Outgrowth Within a Biodegradable Hydrogel Matrix. *Biomedical Materials* 1: 162–169.

Nam, Y., D.W. Branch, and B.C. Wheeler. 2006. Epoxy-Silane Linking of Biomolecules Is Simple and Effective for Patterning Neuronal Cultures. *Biosensors and Bioelectronics* 22: 589–597.

Odawara, A., M. Gotoh, and I. Suzuki. 2013. Control of Neural Network Patterning Using Collagen Gel Photothermal Etching. *Lab on a Chip* 13: 2040–2046.

Pan, L., and R.B. Borgens. 2010. Perpendicular Organization of Sympathetic Neurons Within a Required Physiological Voltage. *Experimental Neurology* 222: 161–164.

Pan, L., and R.B. Borgens. 2012. Strict Perpendicular Orientation of Neural Crest-Derived Neurons In Vitro Is Dependent on an Extracellular Gradient of Voltage. *Journal of Neuroscience Research* 90: 1335–1346.

Pan, L., J. Cirillo, and R.B. Borgens. 2012. Neuronal Responses to an Asymmetrical Alternating Current Field Can Mimic Those Produced by an Imposed Direct Current Field In Vitro. *Journal of Neuroscience Research* 90: 1522–1532.

Patel, N., and M.M. Poo. 1982. Orientation of Neurite Growth by Extracellular Electric Fields. *Journal of Neuroscience* 2: 483–496.

Patel, N.B., and M.M. Poo. 1984. Perturbation of the Direction of Neurite Growth by Pulsed and Focal Electric Fields. *Journal of Neuroscience* 4: 2939–2947.

Patz, T.M., A. Doraiswamy, R.J. Narayan, W. He, Y. Zhong, R. Bellamkonda, R. Modi, and D.B. Chrisey. 2006. Three-Dimensional Direct Writing of B35 Neuronal Cells. *Journal of Biomedical Materials Research Part B: Applied Biomaterials* 78: 124–130.

Phamduy, T., D. Corr, and D. Chrisey. 2010. Bioprinting. In *Encyclopedia of Industrial Biotechnology: Bioprocess, Bioseparation, and Cell Technology*, ed. M. Flickinger. New York: Wiley.

Pine, J., and G. Chow. 2009. Moving Live Dissociated Neurons with an Optical Tweezer. *IEEE Transactions on Biomedical Engineering* 56: 1184–1188.

Pirlo, R.K., D.M. Dean, D.R. Knapp, and B.Z. Gao. 2006. Cell Deposition System Based on Laser Guidance. *Biotechnology Journal* 1: 1007–1013.

Pita-Thomas, W., M.B. Steketee, S.N. Moysidis, K. Thakor, B. Hampton, and J.L. Goldberg. 2015. Promoting Filopodial Elongation in Neurons by Membrane-Bound Magnetic Nanoparticles. *Nanomedicine* 11: 559–567.

Rahjouei, A., S. Kiani, A. Zahabi, N.Z. Mehrjardi, M. Hashemi, and H. Baharvand. 2011. Interactions of Human Embryonic Stem Cell-Derived Neural Progenitors with an Electrospun Nanofibrillar Surface In Vitro. *International Journal of Artificial Organs* 34: 559–570.

Rajnicek, A.M., N.A. Gow, and C.D. Mccaig. 1992. Electric Field-Induced Orientation of Rat Hippocampal Neurones In Vitro. *Experimental Physiology* 77: 229–232.

Rajnicek, A., S. Britland, and C. Mccaig. 1997. Contact Guidance of Cns Neurites on Grooved Quartz: Influence of Groove Dimensions, Neuronal Age and Cell Type. *Journal of Cell Science* 110(Pt 23): 2905–2913.

Rajnicek, A.M., K.R. Robinson, and C.D. Mccaig. 1998. The Direction of Neurite Growth in a Weak DC Electric Field Depends on the Substratum: Contributions of Adhesivity and Net Surface Charge. *Developmental Biology* 203: 412–423.

Reyes, D.R., E.M. Perruccio, S.P. Becerra, L.E. Locascio, and M. Gaitan. 2004. Micropatterning Neuronal Cells on Polyelectrolyte Multilayers. *Langmuir* 20: 8805–8811.

Richardson, J.A., C.W. Rementer, J.M. Bruder, and D. Hoffman-Kim. 2011. Guidance of Dorsal Root Ganglion Neurites and Schwann Cells by Isolated Schwann Cell Topography on Poly(Dimethyl Siloxane) Conduits and Films. *Journal of Neural Engineering* 8: 046015.

Ricoult, S.G., J.S. Goldman, D. Stellwagen, D. Juncker, and T.E. Kennedy. 2012. Generation of Microisland Cultures Using Microcontact Printing to Pattern Protein Substrates. *Journal of Neuroscience Methods* 208: 10–17.

Riggio, C., M.P. Calatayud, C. Hoskins, J. Pinkernelle, B. Sanz, T.E. Torres, M.R. Ibarra, L. Wang, G. Keilhoff, G.F. Goya, V. Raffa, and A. Cuschieri. 2012. Poly-L-Lysine-Coated Magnetic Nanoparticles as Intracellular Actuators for Neural Guidance. *International Journal of Nanomedicine* 7: 3155–3166.

Riggio, C., M.P. Calatayud, M. Giannaccini, B. Sanz, T.E. Torres, R. Fernandez-Pacheco, A. Ripoli, M.R. Ibarra, L. Dente, A. Cuschieri, G.F. Goya, and V. Raffa. 2014. The Orientation of the neuronal Growth Process Can Be Directed Via Magnetic Nanoparticles Under an Applied Magnetic Field. *Nanomedicine* 10: 1549–1558.

Ringeisen, B.R., C.M. Othon, J.A. Barron, D. Young, and B.J. Spargo. 2006. Jet-Based Methods to Print Living Cells. *Biotechnology Journal* 1: 930–948.

Romanova, E.V., K.A. Fosser, S.S. Rubakhin, R.G. Nuzzo, and J.V. Sweedler. 2004. Engineering the Morphology and Electrophysiological Parameters of Cultured Neurons by Microfluidic Surface Patterning. *Faseb Journal* 18: 1267–1269.

Rosenbalm, T.N., S. Owens, D. Bakken, and B.Z. Gao. 2006. Cell Viability Test After Laser Guidance. *Proceedings of SPIE* 6084: 608418–608418-8.

Roth, E.A., T. Xu, M. Das, C. Gregory, J.J. Hickman, and T. Boland. 2004. Inkjet Printing for High-Throughput Cell Patterning. *Biomaterials* 25: 3707–3715.

Ryan, A.F., J. Wittig, A. Evans, S. Dazert, and L. Mullen. 2006. Environmental Micro-Patterning for the Study of Spiral Ganglion Neurite Guidance. *Audiology and Neuro-Otology* 11: 134–143.

Sanjana, N.E., and S.B. Fuller. 2004. A Fast Flexible Ink-Jet Printing Method for Patterning Dissociated Neurons in Culture. *Journal of Neuroscience Methods* 136: 151–163.

Sarig-Nadir, O., N. Livnat, R. Zajdman, S. Shoham, and D. Seliktar. 2009. Laser Photoablation of Guidance Microchannels into Hydrogels Directs Cell Growth in Three Dimensions. *Biophysical Journal* 96: 4743–4752.

Schiele, N.R., R.A. Koppes, D.T. Corr, K.S. Ellison, D.M. Thompson, L.A. Ligon, T.K.M. Lippert, and D.B. Chrisey. 2009. Laser Direct Writing of Combinatorial Libraries of Idealized Cellular Constructs: Biomedical Applications. *Applied Surface Science* 255: 5444–5447.

Schiele, N.R., D.T. Corr, Y. Huang, N.A. Raof, Y. Xie, and D.B. Chrisey. 2010. Laser-Based Direct-Write Techniques for Cell Printing. *Biofabrication* 2(3): 032001.

Schmalenberg, K.E., H.M. Buettner, and K.E. Uhrich. 2004. Microcontact Printing of Proteins on Oxygen Plasma-Activated Poly(Methyl Methacrylate). *Biomaterials* 25: 1851–1857.

Schmidt, C.E., and J.B. Leach. 2003. Neural Tissue Engineering: Strategies for Repair and Regeneration. *Annual Review of Biomedical Engineering* 5: 293–347.

Scholl, M., C. Sprossler, M. Denyer, M. Krause, K. Nakajima, A. Maelicke, W. Knoll, and A. Offenhausser. 2000. Ordered Networks of Rat Hippocampal Neurons Attached to Silicon Oxide Surfaces. *Journal of Neuroscience Methods* 104: 65–75.

Scott, M.A., Z.D. Wissner-Gross, and M.F. Yanik. 2012. Ultra-Rapid Laser Protein Micropatterning: Screening for Directed Polarization of Single Neurons. *Lab on a Chip* 12: 2265–2276.

Seidlits, S.K., C.E. Schmidt, and J.B. Shear. 2009. High-Resolution Patterning of Hydrogels in Three Dimensions Using Direct-Write Photofabrication for Cell Guidance. *Advanced Functional Materials* 19: 3543–3551.

Shi, P., K. Shen, and L.C. Kam. 2007. Local Presentation of L1 and N-cadherin in Multicomponent, Microscale Patterns Differentially Direct Neuron Function In Vitro. *Developmental Neurobiology* 67: 1765–1776.

Sorkin, R., T. Gabay, P. Blinder, D. Baranes, E. Ben-Jacob, and Y. Hanein. 2006. Compact Self-Wiring in Cultured Neural Networks. *Journal of Neural Engineering* 3: 95–101.

Staii, C., C. Viesselmann, J. Ballweg, L. Shi, G.-Y. Liu, J.C. Williams, E.W. Dent, S.N. Coppersmith, and M.A. Eriksson. 2009. Positioning and Guidance of Neurons on Gold Surfaces by Directed Assembly of Proteins Using Atomic Force Microscopy. *Biomaterials* 30: 3397–3404.

Staii, C., C. Viesselmann, J. Ballweg, J.C. Williams, E.W. Dent, S.N. Coppersmith, and M.A. Eriksson. 2011. Distance Dependence of Neuronal Growth on Nanopatterned Gold Surfaces. *Langmuir* 27: 233–239.

Stevenson, D.J., T.K. Lake, B. Agate, V. Garces-Chavez, K. Dholakia, and F. Gunn-Moore. 2006. Optically Guided Neuronal Growth at Near Infrared Wavelengths. *Optics Express* 14: 9786–9793.

Stuhrmann, B., M. Gögler, T. Betz, A. Ehrlicher, D. Koch, and J. Käs. 2005. Automated Tracking and Laser Micromanipulation of Motile Cells. *Review of Scientific Instruments* 76: 035105.

Sugio, Y., K. Kojima, H. Moriguchi, K. Takahashi, T. Kaneko, and K. Yasuda. 2004. An Agar-Based On-Chip Neural-Cell-Cultivation System for Stepwise Control of Network Pattern Generation During Cultivation. *Sensors and Actuators B: Chemical* 99: 156–162.

Suzuki, Ikurou, and Y. Kenji. 2007. Constructive Formation and Connection of Aligned Micropatterned Neural Networks by Stepwise Photothermal Etching During Cultivation. *Japanese Journal of Applied Physics* 46: 6398.

Suzuki, Ikurou, Yoshihiro Sugio, Yasuhiko Jimbo, and Y. Kenji. 2004a. Individual-Cell-Based Electrophysiological Measurement of a Topographically Controlled Neuronal Network Pattern Using Agarose Architecture with a Multi-electrode Array. *Japanese Journal of Applied Physics* 43: L403.

Suzuki, I., Y. Sugio, H. Moriguchi, A. Hattori, K. Yasuda, and Y. Jimbo. 2004b. Pattern Modification of a Neuronal Network for Individual-Cell-Based Electrophysiological Measurement Using Photothermal Etching of an Agarose Architecture with a Multielectrode Array. *IEE Proceedings: Nanobiotechnology* 151: 116–121.

Suzuki, I., Y. Sugio, H. Moriguchi, Y. Jimbo, and K. Yasuda. 2004c. Modification of a Neuronal Network Direction Using Stepwise Photo-Thermal Etching of an Agarose Architecture. *Journal of Nanobiotechnology* 2: 7.

Suzuki, I., Y. Sugio, Y. Jimbo, and K. Yasuda. 2005. Stepwise Pattern Modification of Neuronal Network in Photo-Thermally-Etched Agarose Architecture on Multi-Electrode Array Chip for Individual-Cell-Based Electrophysiological Measurement. *Lab on a Chip* 5: 241–247.

Swarup, V.P., T.W. Hsiao, J. Zhang, G.D. Prestwich, B. Kuberan, and V. Hlady. 2013. Exploiting Differential Surface Display of Chondroitin Sulfate Variants for Directing Neuronal Outgrowth. *Journal of the American Chemical Society* 135: 13488–13494.

Tankus, A., I. Fried, and S. Shoham. 2014. Cognitive-Motor Brain–Machine Interfaces. *Journal of Physiology, Paris* 108: 38–44.

Townes-Anderson, E., R.S. St Jules, D.M. Sherry, J. Lichtenberger, and M. Hassanain. 1998. Micromanipulation of Retinal Neurons by Optical Tweezers. *Molecular Vision* 4: 12.

Tsuruma, A., M. Tanaka, S. Yamamoto, N. Fukushima, H. Yabu, and M. Shimomura. 2006. Topographical Control of Neurite Extension on Stripe-Patterned Polymer Films. *Colloids and Surfaces, A: Physicochemical and Engineering Aspects* 284–285: 470–474.

Turcu, F., K. Tratsk-Nitz, S. Thanos, W. Schuhmann, and P. Heiduschka. 2003. Ink-Jet Printing for Micropattern Generation of Laminin for Neuronal Adhesion. *Journal of Neuroscience Methods* 131: 141–148.

Turner, S., L. Kam, M. Isaacson, H.G. Craighead, W. Shain, and J. Turner. 1997. Cell Attachment on Silicon Nanostructures. *Journal of Vacuum Science and Technology B* 15: 2848–2854.

Turner, A.M., N. Dowell, S.W. Turner, L. Kam, M. Isaacson, J.N. Turner, H.G. Craighead, and W. Shain. 2000. Attachment of Astroglial Cells to Microfabricated Pillar Arrays of Different Geometries. *Journal of Biomedical Materials Research* 51: 430–441.

Vogt, A.K., G.J. Brewer, T. Decker, S. Bocker-Meffert, V. Jacobsen, M. Kreiter, W. Knoll, and A. Offenhausser. 2005a. Independence of Synaptic Specificity from Neuritic Guidance. *Neuroscience* 134: 783–790.

Vogt, A.K., G.J. Brewer, and A. Offenhausser. 2005b. Connectivity Patterns in Neuronal Networks of Experimentally Defined Geometry. *Tissue Engineering* 11: 1757–1767.

Vogt, A.K., G. Wrobel, W. Meyer, W. Knoll, and A. Offenhausser. 2005c. Synaptic Plasticity in Micropatterned Neuronal Networks. *Biomaterials* 26: 2549–2557.

Von Philipsborn, A.C., S. Lang, J. Loeschinger, A. Bernard, C. David, D. Lehnert, F. Bonhoeffer, and M. Bastmeyer. 2006. Growth Cone Navigation in Substrate-Bound Ephrin Gradients. *Development* 133: 2487–2495.

Wang, S., C. WongPoFoo, A. Warrier, M.M. Poo, S.C. Heilshorn, and X. Zhang. 2009. Gradient Lithography of Engineered Proteins to Fabricate 2D and 3D Cell Culture Microenvironments. *Biomedical Microdevices* 11: 1127–1134.

Wu, T., T.A. Nieminen, S. Mohanty, J. Miotke, R.L. Meyer, H. Rubinsztein-Dunlop, and M.W. Berns. 2012. A Photon-Driven Micromotor Can Direct Nerve Fibre Growth. *Nature Photonics* 6: 62–67.

Wyart, C., C. Ybert, L. Bourdieu, C. Herr, C. Prinz, and D. Chatenay. 2002. Constrained Synaptic Connectivity in Functional Mammalian Neuronal Networks Grown on Patterned Surfaces. *Journal of Neuroscience Methods* 117: 123–131.

Xu, T., J. Jin, C. Gregory, J.J. Hickman, and T. Boland. 2005. Inkjet Printing of Viable Mammalian Cells. *Biomaterials* 26: 93–99.

Xu, T., C.A. Gregory, P. Molnar, X. Cui, S. Jalota, S.B. Bhaduri, and T. Boland. 2006. Viability and Electrophysiology of Neural Cell Structures Generated by the Inkjet Printing Method. *Biomaterials* 27: 3580–3588.

Xu, X., N.J. Wittenberg, L.R. Jordan, S. Kumar, J.O. Watzlawik, A.E. Warrington, S.H. Oh, and M. Rodriguez. 2013. A Patterned Recombinant Human IgM Guides Neurite Outgrowth of CNS NEurons. *Scientific Reports* 3: 2267.

Yao, L., L. Shanley, C. Mccaig, and M. Zhao. 2008. Small Applied Electric Fields Guide Migration of Hippocampal Neurons. *Journal of Cellular Physiology* 216: 527–535.

Yao, L., S. Wang, W. Cui, R. Sherlock, C. O'Connell, G. Damodaran, A. Gorman, A. Windebank, and A. Pandit. 2009. Effect of Functionalized Micropatterned PLGA on Guided Neurite Growth. *Acta Biomaterialia* 5: 580–588.

Zhang, B.G., A.F. Quigley, D.E. Myers, G.G. Wallace, R.M. Kapsa, and P.F. Choong. 2014a. Recent Advances in Nerve Tissue Engineering. *International Journal of Artificial Organs* 37: 277–291.

Zhang, K., C.K. Chou, X. Xia, M.C. Hung, and L. Qin. 2014b. Block-Cell-Printing for Live Single-Cell Printing. *Proceedings of the National Academy of Sciences of the United States of America* 111: 2948–2953.

Zhu, B., Q. Zhang, Q. Lu, Y. Xu, J. Yin, J. Hu, and Z. Wang. 2004. Nanotopographical Guidance of C6 Glioma Cell Alignment and Oriented Growth. *Biomaterials* 25: 4215–4223.

Zorlutuna, P., J.H. Jeong, H. Kong, and R. Bashir. 2011. Stereolithography-Based Hydrogel Microenvironments to Examine Cellular Interactions. *Advanced Functional Materials* 21: 3642–3651.

Chapter 4
Building Blocks for Bottom-Up Neural Tissue Engineering: Tools for In Vitro Assembly and Interrogation of Neural Circuits

Stephanie Knowlton*, Dan Li*, Fulya Ersoy, Yong Ku Cho, and Savas Tasoglu

4.1 Introduction

Bottom-up tissue engineering approaches provide unique opportunities to investigate the formation and dynamics of neural circuits. Given the fact that spatial organization of cells with specific morphological, electrophysiological, and biochemical properties is a defining feature of neural circuits, bottom-up strategies are a promising tool in gaining mechanistic understanding of the role of spatial organization of cell types. Moreover, by controlling the cell density and matrix composition, structures assembled in vitro can have significantly lower light scattering, allowing high-resolution, high-speed optical imaging not possible in intact tissues. These features

*Stephanie Knowlton and Dan Li contributed equally to this work.

S. Knowlton
Department of Biomedical Engineering, University of Connecticut,
260 Glenbrook Road, Storrs, CT 06269, USA

D. Li • Y.K. Cho (✉)
Department of Chemical and Biomolecular Engineering, University of Connecticut,
191 Auditorium Road, Storrs, CT 06269, USA
e-mail: cho@engr.uconn.edu

F. Ersoy
Department of Mechanical Engineering, University of Connecticut,
191 Auditorium Road, Storrs, CT 06269, USA

S. Tasoglu (✉)
Department of Biomedical Engineering, University of Connecticut,
260 Glenbrook Road, Storrs, CT 06269, USA

Department of Mechanical Engineering, University of Connecticut,
191 Auditorium Road, Storrs, CT 06269, USA
e-mail: savas@engr.uconn.edu

L.G. Zhang, D.L. Kaplan (eds.), *Neural Engineering*,
DOI 10.1007/978-3-319-31433-4_4

of bottom-up assembly approaches make them an attractive model system for probing molecular function in disease models, and also potentially in identifying the origin of emergent properties in neural circuits.

The recent emergence of various three-dimensional (3D) models primarily using a mixture of primary cells or single cell types derived from stem cells (Knowlton et al. 2016) suggest the possibility of assembling more sophisticated 3D structures that resemble their cognate state. For example, 3D cultures of human umbilical cord blood-derived neural stem cells formed neural organoids that differentiated into mature neurons and formed functional synaptic connections not found in two-dimensional (2D) cultures (Jurga et al. 2009). Functional synapse formation in 3D neuronal culture systems have been reported in other studies and showed connectivity at similar or earlier time points compared to 2D systems (O'Shaughnessy et al. 2003; van Vliet et al. 2007). 3D cultures of neural stem cells also showed improved cell viability and neuronal differentiation efficiency compared to 2D models (Brannvall et al. 2007; Peretz et al. 2007; Serra et al. 2009). In addition, 3D culture systems have shown great potential for rapidly assessing the impact of compounds or monitoring toxicity in neural cells (Forsby et al. 2009; Gassmann et al. 2012). In order to fully realize these potentials, we need tools to assemble the desired cell types in defined 3D patterns and to monitor and modulate the functional activity in situ. This chapter discusses molecular tools that enable systematic interrogation of neuronal circuits and assembly methods to create 3D structures with complex cell types. Together, these tools will greatly enhance the capabilities of 3D neural models and enable experiments not possible in existing models.

4.2 Molecular Tools for Probing Neuronal Function

4.2.1 Genetically Encoded Tools: Detecting and Controlling Neural Activity in Defined Cell Types

Genetically encoded tools are proteins that, when expressed, act as indicators and actuators of neuronal function (Schmidt and Cho 2015; Emiliani et al. 2015). Proteins encoded by a promoter with the purpose of measuring and controlling physiological functions of neural cells have been extremely powerful in studying the intact brain. This is due to the fact that cell-type-specific promoters can be used to drive their expression, enabling optical imaging and control of specific cell types within the context of the living brain (Cho 2015). Cell-type-specific expression of these tools allows the readout of their activities during cognition and behavior, as well as the causal impact of their activity on these complex brain functions. These genetically encoded tools have several advantages over existing chemical-based detection and modulation reagents. Genetically encoded tools are expressed only in the cell type of interest, reducing background signal. Transgenic model organisms expressing these tools in defined cell types can be generated (Madisen et al. 2012,

2015). Also, their expression may be spatially and temporally regulated, providing ways to detect and control cells based on developmental lineage (Petreanu et al. 2007), axonal projection (Osakada et al. 2011), and potentially synaptic connectivity (Lo and Anderson 2011; Wickersham et al. 2007). Moreover, the expression of genetically encoded tools can be sustained over a period of weeks to months (Ivanova and Pan 2009), while chemicals diffuse and lose signal over time.

4.2.1.1 Genetically Encoded Indicators of Neuronal Activity and Signaling

In general, genetically encoded indicators contain a ligand binding domain or a sensing domain fused to a reporter domain based on fluorescent proteins. The ligand binding or change in biophysical environment (e.g., membrane voltage) is coupled to change in fluorescence intensity or fluorescence resonance energy transfer (FRET) efficiency. Examples include indicators of calcium (Nakai et al. 2001; Chen et al. 2013; Miyawaki et al. 1997), glutamate (Okumoto et al. 2005; Hires et al. 2008), pH (Miesenbock et al. 1998), and chloride (Arosio et al. 2010) (Table 4.1). The measurement of these ions and metabolites allows the detection of various aspects of neuronal function (Table 4.1). Intracellular calcium level in neurons is a good proxy of action potentials, since firing action potentials leads to a large calcium influx through voltage-gated calcium channels (Tank et al. 1988; Muller and Connor 1991). For this reason, calcium indicators are widely used to monitor the activity of neuronal cells. Over the past two decades, genetically encoded calcium indicators (GECI) have been a subject of extensive optimization, resulting in a GECI with signal-to-noise ratio higher than that of widely used chemical calcium indicators (Chen et al. 2013). In addition, GECIs with a wide range of spectral sensitivity have been developed including blue (Zhao et al. 2011) and red (Zhao et al. 2011; Akerboom et al. 2013) fluorescent indicators.

Even though calcium transients in neurons are a widely used proxy for neural activity (i.e., the frequency and duration of action potentials), calcium imaging cannot detect hyperpolarization and subthreshold changes in membrane voltage. An alternative approach is to measure membrane voltage directly. Therefore, an area of intense investigation is the development of genetically encoded voltage indicators (GEVIs). Recent advances in genetically encoded voltage indicators enable high signal-to-noise ratio and fast response rate that enable accurate measurement of membrane potential change as well as subthreshold events (Jin et al. 2012; Hochbaum et al. 2014; St-Pierre et al. 2014) (Table 4.1). These proteins utilize voltage-sensitive transmembrane domains of voltage-gated ion channels or rhodopsins that shift their conformation upon membrane potential change. GEVIs using voltage-sensitive transmembrane domains fused to fluorescent proteins have high signal-to-noise ratios, with variants such as ASAP1 having millisecond timescale response times (St-Pierre et al. 2014). GEVIs based on rhodopsins have orders of magnitude lower quantum yield, requiring high light powers to image, but do not photobleach and have submillisecond response kinetics (Kralj et al. 2012).

Table 4.1 Representative molecular tools for sensing neural activity

Sensing target	Name	Identity	Notable features	References
Calcium	GCaMP	Circularly permuted GFP (cpGFP) fused to calmodulin (CaM)	Monitoring intracellular free calcium level; detection of action potential in neurons using intracellular calcium level as a proxy; single spike detection without averaging trials	Nakai et al. (2001), Chen et al. (2013)
	RCaMP	Circularly permuted mRuby fused to CaM	Red fluorescent variant	Akerboom et al. (2013)
	R-GECI	Circularly permuted mPlum fused to CaM	Red fluorescent variant	Wu et al. (2013)
Membrane voltage	ArcLight	The voltage-sensing domain of *C. intestinalis* voltage-sensitive phosphatase (ci-VSP) fused to super ecliptic pHluorin GFP	Single spike detection without averaging trials; detection of subthreshold events in dendritic segments	Jin et al. (2012)
	ASAP1	cpGFP fused to VSP from *G. gallus*	Single spike detection without averaging trials; detection of subthreshold events and hyperpolarization	St-Pierre et al. (2014)
	QuasAr	Mutant of Archaerhodopsin-3 from *H. sodomense*	Submillisecond kinetics; single spike detection without averaging trials; detection of subthreshold events and hyperpolarization	Hochbaum et al. (2014), Kralj et al. (2012)
Chloride	Clomeleon	Fusion of chloride-sensitive yellow fluorescent protein with a chloride-insensitive cyan fluorescent protein (CFP)	Intracellular chloride level (neuronal excitability)	Kuner and Augustine (2000)
	ClopHensorN	Cl^- and pH-sensitive GFP mutant fused to tdTomato	Assessed in hippocampal slices	Raimondo et al. (2013)

(continued)

Table 4.1 (continued)

Sensing target	Name	Identity	Notable features	References
pH	synaptopHluorin	pH-sensitive mutant of GFP	Monitor vesicle exocytosis and recycling	Miesenbock et al. (1998), Gandhi and Stevens (2003)
Glutamate	SuperGluSnFr	CFP and Citrine fused to glutamate periplasmic binding protein GltI	Time course of synaptic glutamate release, spillover, and reuptake in hippocampal neurons	Hires et al. (2008)

Future development useful in characterizing neural cells include multicolor detection of membrane voltage in distinct cell types, as has been demonstrated for intracellular calcium imaging (Akerboom et al. 2013). Genetically encoded sensors for key metabolites and neurotransmitters such as neuropeptides may enable monitoring and observation of the chemical diversity of neuronal connections.

4.2.1.2 Genetically Encoded Tools for Controlling Neural Circuit Function

A key development in the past decade was the use of light-gated ion channels in neurons to control their membrane potential (Boyden 2011; Boyden et al. 2005). When expressed in neurons, channelrhodopsins, light-gated ion channels originally found in green algae, enable the depolarization of membrane potential over the threshold of voltage-gated sodium channels, initiating action potentials (Boyden et al. 2005). The millisecond timescale kinetics of channel opening and closing enables precise generation of action potentials with single spike resolution (Boyden et al. 2005). On the other hand, light-driven ion pumps, such as halorhodopsins and archaerhodopsins, result in hyperpolarization when illuminated, enabling light-mediated neural silencing (Chow et al. 2010; Han and Boyden 2007). With the discovery and development of new variants of these proteins, it is now possible to use different colors of light to independently activate or silence distinct populations of neurons (Schmidt and Cho 2015; Klapoetke et al. 2014) (Table 4.2). These features will be greatly valuable in assessing the functional connectivity of neurons assembled in cultured model systems (Tonnesen et al. 2011).

4.2.1.3 Simultaneous Control and Imaging Using Genetically Encoded Tools

Traditional electrophysiological characterizations provide rich information on the electrical activity of neural cells. However, the throughput of electrophysiology is restricted to a few cells at a time. High-throughput electrophysiology requires

Table 4.2 Representative molecular tools for controlling neural activity

Function	Name	Identity	Notable features	Reference
Neuronal activation	Channelrhodopsin-2 (ChR2)	Channelrhodopsin-2 from *C. reinhardtii*	Light-gated cation channel	Nagel et al. (2003)
	Chrimson	Channelrhodopsin from *C. noctigama*	Red light sensitive channelrhodopsin	Klapoetke et al. (2014)
	Chronos	Channelrhodopsin from *S. helveticum*	Fast kinetics, high blue light sensitivity	Klapoetke et al. (2014)
	CheRiff	Channelrhodopsin from *S. dubia*	High blue light sensitivity, reduced red cross-activation	Hochbaum et al. (2014)
Neuronal inhibition	eNpHR	Halorhodopsin from *N. pharaonis*	Light-induced inward chloride pump	Zhang et al. (2007)
	Arch	Archaerhodopsin-3 from *H. sodomense*	Light-driven outward proton pumps	Chow et al. (2010)
	Jaws	Cruxhalorhodopsin from *H. salinarum*	Light-induced inward chloride pump with high red sensitivity	Chuong et al. (2014)
	ChloC, iC1C2	Channelrhodopsin mutants conducting chloride	Light-gated inward chloride channel	Wietek et al. (2014), Berndt et al. (2014)

disruptive physical interrogation that may be hard to control, especially in 3D space. Therefore, optical imaging and control methods are highly attractive tools in characterizing in vitro 3D model systems. Given the availability of optogenetic tools for both imaging and controlling neural activity, there is a great interest in combining these tools for simultaneous optical control and modulation.

Several such examples have shown the importance of understanding the biophysical properties of these tools to enable simultaneous optical control and imaging. For example, it was demonstrated that calcium sensors based on red fluorescent proteins such as RCaMP and R-GECI can be coexpressed with channelrhodopsins to allow optical activation while imaging calcium transients in neurons (Akerboom et al. 2013; Wu et al. 2013). These experiments revealed that R-GECI can be transiently photoactivated by blue light, generating an artificial increase in its red fluorescence (Akerboom et al. 2013; Wu et al. 2013). Interestingly, RCaMP did not have this blue-light-mediated photoactivation, enabling reliable measurement of small calcium transients (Akerboom et al. 2013). Another study coexpressed rhodopsin-based GEVIs with channel rhodopsins to enable all-optical electrophysiology in neurons (Hochbaum et al. 2014). This study showed that even though channel rhodopsins have negligible absorbance of red light, intense illumination with 640 nm

light can cause channel opening, leading to depolarization. Through molecular engineering, a channel rhodopsin named CheRiff with high blue sensitivity with minimal red-light-driven activity was developed, allowing simultaneous optical imaging and activation (Hochbaum et al. 2014). Even though these tools have not been tested in 3D in vitro model systems, they are expected to enable high-resolution, high-content imaging that is highly scalable to analyzing large numbers of cells, providing an ideal tool for bottom-up neural tissue engineering.

4.3 Biofabrication Methods

Bottom-up manipulation and assembly strategies hold great promise in creating highly complex tissue architectures. Among these microassembly strategies, the basic physical principles of magnetics (Mirica et al. 2011; Tasoglu et al. 2013a, 2014a, 2015; Xu et al. 2011a; Grzybowski et al. 2000; Snezhko and Aranson 2011), acoustics (Guo et al. 2015; Chen et al. 2014), and self-assembly (Tasoglu et al. 2014a; Bowden et al. 1997, 1999; Grzybowski et al. 2009; Wolfe et al. 2003; Zamanian et al. 2010) have been widely used and studied to form complex tissue constructs (Guven et al. 2015; Gurkan et al. 2012; Tasoglu et al. 2013b). Furthermore, there has been a growing interest in applying 3D bioprinting strategies to develop 3D tissue models (Tasoglu and Demirci 2013; Knowlton et al. 2015). Here, we review emerging bioprinting and microassembly methods which have been or may be applied to neural tissue engineering.

4.3.1 Bioprinting

Bioprinting is a revolutionary biofabrication technique which provides a high level of control over the geometry of the cellular scaffold. This relatively new and rapidly developing technology involves conversion of a virtual computer-aided design (CAD) model into a living tissue by depositing scaffolds or cells in a layer-by-layer fashion. The capability of precise deposition of cell-encapsulating materials makes bioprinting a broadly applicable and versatile biofabrication approach for 3D biological modeling, tissue engineering, and regenerative medicine. Bioprinting has three fundamental goals: biomimicry, creation of tissue building blocks, and self-assembly (Tasoglu and Demirci 2013; Knowlton et al. 2015; Murphy and Atala 2014). Tissue fabrication via bioprinting generally follows sequential design steps including imaging of the native tissue, 3D CAD modeling of the tissue geometry, material and cell type selection, and printing of the tissue structure. Here, we review the most commonly used bioprinting technologies, that is, inkjet, microextrusion, and laser-assisted approaches (Fig. 4.1) (Murphy and Atala 2014).

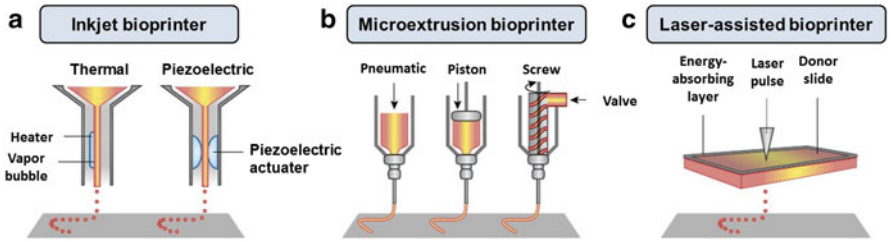

Fig. 4.1 Components of inkjet, microextrusion, and laser-assisted bioprinters. (**a**) To force droplets from the nozzle, thermal inkjet printers use air pressure pulses produced by an electrically heated printhead. On the other hand, acoustic printers use piezoelectric or ultrasound pressure pulses. (**b**) Pneumatic or mechanical (piston or screw) dispensing systems are used in microextrusion printers to eject continuous droplets of material and/or cells. (**c**) In laser-assisted printers, lasers focused on an absorbing substrate create pressure that propels cell-encapsulated materials onto a collector material. Reprinted by permission from Macmillan Publishers Ltd: Nature Biotechnology (Murphy and Atala 2014), copyright 2014.

4.3.1.1 Inkjet Bioprinting

The inkjet printer, which ejects and deposits a controlled volume of liquid onto receiving surfaces, is the most broadly applied bioprinting technology in both biological and nonbiological fields (Tasoglu et al. 2013b, 2010; Tasoglu and Demirci 2013; Knowlton et al. 2015; Muradoglu and Tasoglu 2010). Inkjet bioprinters were first constructed by modifying commercial 2D printers (Xu et al. 2008a, b)—an adjustable stage was positioned to control movement along the *z*-axis, which allows fabrication along a third dimension in addition to the *x*- and *y*-axes. To extend the technology to bioprinting, cartridge inks were replaced with biological materials—either extracellular matrix (ECM) components or cells encapsulated in a fluid material (Xu et al. 2008a, b; Klebe 1988). In two different approaches to inkjet bioprinting, either thermal or acoustic forces are applied to eject liquid droplets onto a substrate. Thermal systems use an electrically heated print head, while acoustic systems use either piezoelectric crystals or an ultrasound field to create acoustic waves which trigger the ejection of droplets (Tekin et al. 2008). The heating used for droplet production in thermal systems is reported to have a negligible effect on the viability and stability of the cells and biological molecules (Murphy and Atala 2014).

Inkjet printers have several advantages over other 3D printing techniques, including low cost, high speed and resolution, wide availability, and high material compatibility (Murphy and Atala 2014; Muradoglu and Tasoglu 2010; Tasoglu et al. 2010). There are some drawbacks associated with the technology such as droplet directionality and size uniformity. Further, the raw printing material must be in a liquid phase with low viscosity (limited to 10 centipoise). However, the main challenge is clogging of the nozzle, which limits the ability to achieve biologically significant cell densities (greater than 10 million cells/mL).

There have been several notable clinical applications of inkjet bioprinting. High-speed printing has been developed into a method to deposit cells directly onto skin

(Skardal et al. 2012) or cartilage (Cui et al. 2012) lesions, promoting functional regeneration in the defected area. Bone constructs have also been fabricated by inkjet printing and matured in an incubator before implanting into a mouse (De Coppi et al. 2007). These applications demonstrate the great potential of inkjet bioprinting to regenerate functional tissue structures.

4.3.1.2 Microextrusion Bioprinting

Similar to the inkjet printer, the microextrusion printer is capable of movement along the *x*, *y*, and *z* axes and layer-by-layer deposition of a material on a substrate. But, in contrast to the liquid droplet formation by inkjet bioprinters, microextrusion printers extrude a continuous efflux of material onto the substrate. The extruder is controlled by CAD–CAM software and moves in two dimensions across a stage where liquid is deposited. Then, either the microextrusion head or the stage moves along the *z* axis to build a 3D structure. The most broadly applied methods to eject biological materials are pneumatic (Khalil and Sun 2007; Chang et al. 2008, 2011; Fedorovich et al. 2009) and mechanical (piston or screw) (Visser et al. 2013; Cohen et al. 2006; Jakab et al. 2006) dispensing systems (Murphy and Atala 2014). Pneumatic dispensing systems are advantageous due to simpler extrusion mechanism elements, but experience a delay due to the compression of gas which is used to eject liquid from the nozzle. On the other hand, mechanical dispensing systems have smaller and more complicated components which bring greater spatial control but have limited maximum force capacities (Murphy and Atala 2014).

A myriad of materials are adaptable to microextrusion printing, including biocompatible hydrogels, cell encapsulating polymer solutions, high viscosity materials, and high cell density solutions (including cell spheroids) (Murphy and Atala 2014; Jones 2012). However, cell viability after fabrication via microextrusion bioprinting is lower than viability following inkjet bioprinting due to the shear stress applied to cells suspended in viscous fluids during the extrusion process (Chang et al. 2008). It is possible to obtain favorable cell viability using low dispensing pressures and large nozzle sizes (though dispersing pressure has a more considerable effect on viability than nozzle diameter) (Chang et al. 2008; Nair et al. 2009). However, altering these parameters can negatively impact the resolution and print speed. A multitude of tissue types have been fabricated successfully via microextrusion bioprinting including branched vascular trees (Norotte et al. 2009), aortic valves (Duan et al. 2013), and in vitro tumor models (Knowlton et al. 2015; Xu et al. 2011b).

4.3.1.3 Laser-Assisted Bioprinting

The laser-assisted bioprinting (LAB) system is based on laser-induced forward transfer—laser pulses are applied to a donor substrate to transfer biological materials to a collector substrate. A typical LAB system has a pulsed laser beam, a

focusing system, a "ribbon" with a donor transport support covered by a laser energy-absorbing layer (e.g., gold or titanium), and a layer of biological material in a liquid solution (Miyawaki et al. 1997; Okumoto et al. 2005). LAB works by applying focused laser pulses through the absorbing layer to produce high-pressure bubbles which push biological material on the opposite side toward the substrate in the form of drops.

This technique has been successfully performed with peptides, DNA, and cells. There is a high acceleration and deceleration during droplet formation, but this has been shown to cause only minimal phenotypic damage and viability loss (Ringeisen et al. 2004; Chrisey 2000). LAB's nozzle-free design remedies the clogging problem associated with inkjet bioprinting and it is compatible with higher viscosity materials (1–300 mPa/s) (Guillotin and Guillemot 2011). LAB is also able to deposit cells at higher densities of up to 10^8 cells/mL (Guillotin and Guillemot 2011) where inkjet printers are limited to below 10^6 cells/mL (Murphy and Atala 2014) and microextrusion printers may use around 5×10^6 cells/mL (Fedorovich et al. 2009; Visser et al. 2013; Cohen et al. 2006). Further, LAB has achieved high-resolution bioprinting with only a single cell per drop (Guillotin et al. 2010). With these features, LAB is a step ahead of inkjet and microextrusion printers in terms of its ability to print mammalian cells, which is critical for solid organ bioprinting. But, this high resolution presents a drawback due to the requirements for rapid gelation kinetics and low overall flow rate. Flexibility is limited since any change in material or cell type requires preparation of a new ribbon. Another complication is metal contamination in the final product due to vaporization of metal laser-absorbing layer; however, this issue can be addressed by using a nonmetallic laser-absorbing layer or designing a printing process which does not require an absorbing layer (Guillotin and Guillemot 2011; Duocastella et al. 2010; Kattamis et al. 2007).

Fabrication of cellularized skin structure (Michael et al. 2013) with a layered tissue architecture comprising three layers of fibroblasts, keratinocytes, and a stabilizing matrix demonstrates the potential of LAB to print clinically relevant cell densities. LAB has also been applied to fill a 3D mouse calvaria defect model with nanohydroxyapatite in vivo, showing promise for application of LAB to medical robotics (Keriquel et al. 2010). However, scaling up this technique for printing larger tissues remains a challenge to be addressed with future technology development.

4.3.2 Microassembly Approaches

The bottom-up tissue engineering approach involves assembling building blocks or cells which mimic native functional units. The assembled structures ultimately form larger tissue structures with a desired geometry and distribution of cells within the structure (Radisic et al. 2004; Khademhosseini and Langer 2007; Khademhosseini et al. 2006; Karoly et al. 2010; Jakab et al. 2008). The goal of research in this area is patterning individual elements of a tissue into a predesigned organization that will assist the maturation of the construct toward a functional tissue (Khademhosseini and Langer 2007; Nichol and Khademhosseini 2009). Bottom-up tissue engineering

addresses two major limitations of top-down tissue engineering: (1) control over mass transfer such as waste removal and nutrient diffusion and (2) fabrication of a functional and controlled histological architecture. However, creating and assembling biomimetic 3D building blocks for tissue regeneration and functionality remain significant challenges, presenting a need for a variety of unique approaches to the assembly of micro-scale hydrogels.

4.3.2.1 Self-Assembly

Self-assembly is an approach which allows the chemical and biological interactions between individual building blocks to form an ordered structure. The process is often driven by the tendency to minimize free energy via organization of these building blocks in a desired spatial arrangement. Due to the minimal need for user input, this technique offers the advantage of high throughput and scalability. The challenge associated with self-assembly is manipulating the properties of the individual hydrogel blocks to facilitate assembly into the desired architecture (Grzybowski et al. 2009).

Capillary force-based self-assembly is an approach where hydrogels assemble due to capillary forces between a liquid interface and the hydrogel units. The assembly process and 3D architecture can be adjusted by changing the geometric shape, size, and wettability of the hydrogel blocks. Capillary self-assembly has been used to develop centimeter-scale hydrogel assemblies with controlled micrometer-scale biological characteristics at an air–liquid interface (Zamanian et al. 2010) and an water–oil interface (Du et al. 2008a). Cell-encapsulating hydrogel building blocks have been successfully assembled using this approach with good cell viability (Fig. 4.2) (Du et al. 2008a).

In another approach utilizing self-assembly mechanisms, complementary molecules which interact and bind with high specificity are used to assemble micrometer-scale hydrogels. One study showed the assembly of multiple microtissue building blocks via orthogonal DNA coding (Li et al. 2011). In this method, complementary single-stranded DNA is conjugated to the microtissues and used as identifier sites; sequence-specific hybridization of the DNA strands onto spotted DNA microarrays enables controllable self-assembly of the hydrogels with high specificity and efficiency. In another approach, host and guest building blocks were engineered to interact with each other by modifying the hydrogels with cyclodextrins and hydrocarbon groups, respectively, as complementary molecular recognition agents (Harada et al. 2011). In this approach, the building blocks can be selectively assembled by controlling the size and shape of the units.

4.3.2.2 Guided Assembly

Guided assembly provides an ordered structure or system through the use of external physical forces. Organization of hydrogel blocks is driven by the minimization of free energy of the system under applied working conditions. In this way, a variety of external forces can be used to control the spatiotemporal distribution of the

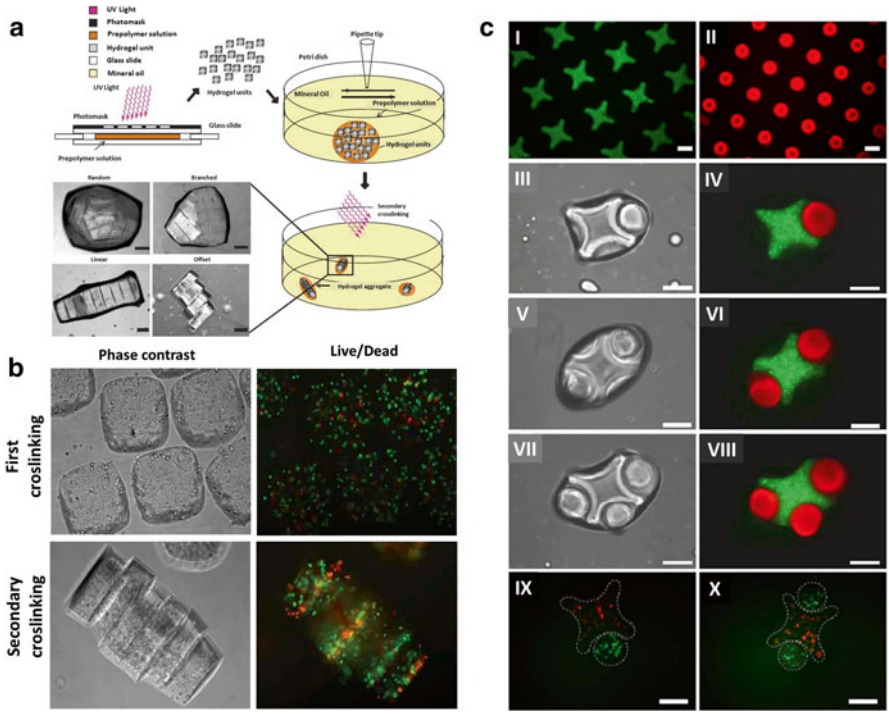

Fig. 4.2 Directed self-assembly. (**a**) Hydrogel assembly process: hydrogel building blocks were fabricated by photolithography and mechanically agitated with a pipette tip in a back-and-forth manner. Linear, branched, random, and offset structures of microgel assemblies were observed. Assemblies were then exposed to UV light to achieve a secondary crosslinking. (Scale bars, 200μm.) (**b**) Phase-contrast and fluorescence images of cell-laden (NIH 3T3) hydrogel assemblies after primary and secondary cross-linking, respectively, demonstrating the cell morphology. (**c**) Directed assembly of lock-and-key-shaped microgels. (*I*) Fluorescence images of cross-shaped microgels stained with FITC-dextran. (*II*) Rod-shaped microgels stained with Nile red. (*III–VIII*) Phase-contrast and fluorescence images of lock-and-key assemblies with 1–3 rods per cross. (*IX–X*) Fluorescence images of microgel assembly composed of cross-shaped microgels containing red stained cells and rod-shaped microgels containing fluorescently stained cells. (Scale bars, 200 μm.) Reproduced with permission from Du et al. (2008a) Copyright (2008) National Academy of Sciences, U.S.A.

building blocks (Mirica et al. 2011; Tasoglu et al. 2013a, 2014a, 2015 Xu et al. 2011a; Gurkan et al. 2012; Demirors et al. 2013; Vanherberghen et al. 2010).

Magnetic Field-Guided Assembly

Magnetic field-guided assembly is an approach where hydrogel blocks are guided by the interaction between the hydrogels and a magnetic field (Tasoglu et al. 2013a). Permanent magnets are widely used to create the magnetic field to enable adaptable,

contact-free, and inexpensive microstructure patterning and assembly strategies (Mirica et al. 2011). In one approach, magnetic nanoparticles are encapsulated in the hydrogels to impart magnetic properties to the building blocks (Xu et al. 2011a). In another approach, the paramagnetic properties of hydrogel building blocks are used to enable assembly of the building blocks without the need for magnetic components (Tasoglu et al. 2013a). Alternatively, a paramagnetic suspension liquid is engineered and, with two magnets with like poles facing each other, cell-seeded building blocks are levitated and assembled (Fig. 4.3) (Tasoglu et al. 2013a, 2015). This approach of using magnets to manipulate and assemble cell-laden hydrogel building blocks has been broadly studied in numerous bottom-up tissue engineering applications (Fig. 4.3) (Tasoglu et al. 2013a, 2014a, 2015; Xu et al. 2011a).

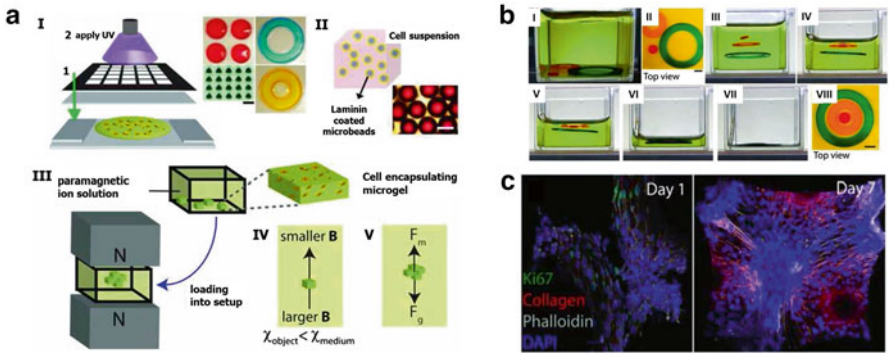

Fig. 4.3 Magnetic field-guided assembly. (**a**) Levitational coding for soft living material fabrication. (*I*) Hydrogel units were manufactured by photolithography with patterned photomasks. Hydrogel prepolymer solution was pipetted onto a glass slide and then exposed to UV light. (Scale bar, 1 mm.) (*II*) Cell-seeded microbead fabrication, showing microbeads coated with laminin prior to incubation in cell suspension. (Scale bar, 500 μm.) (*III*) Levitational self-assembly of cell-encapsulating building blocks in a magnetic setup composed of two NdFeB magnets with the same poles facing each other. (*IV*) If the magnetic susceptibility of the object is lower than magnetic susceptibility of the suspending medium, the object moves from larger magnetic field strength toward the lower magnetic field strength at the centerline between the two magnets. (*V*) Forces acting on levitating objects at equilibrium height include the magnetic force (F_m) and corrected gravitational force (F_g), which is the difference between gravitational force and buoyancy force. (**b**) Concentric assembly of two hollow-disk and a solid-disk PEG hydrogels. (*I–II*) Hydrogels were randomly located at the bottom of reservoir before being subjected to the magnetic setup composed of two NdFeB magnets with like poles facing each other. (*III*) Upon positioning of the reservoir into the magnetic setup, hydrogels were aligned horizontally at the center of the magnets in the region of minimum magnetic field strength and at different vertical equilibrium heights due to differences in densities among hydrogel groups. (*IV–VII*) Draining of the paramagnetic media from the reservoir decreased the height of air–liquid meniscus and caused a concentric deposition of hydrogels. (Scale bars, 1 mm.) (*VIII*) Final shape of assembled hydrogels. (**c**) Immunocytochemistry staining of cells seeded on assembled beads. Cell proliferation (ki67, *green*) and collagen secretion (*red*) are shown one week after fabrication. Reproduced with permission from Tasoglu et al. (2015)

Acoustic Field-Guided Assembly

The interactions between hydrogels and acoustic fields have been applied to 2D assembly and show promising results for future 3D assembly applications. In this approach, bulk acoustic waves or surface acoustic waves are applied to the building blocks (Gurkan et al. 2012). Cells exposed to ultrasound for aggregation and positioning have been shown to remain viable and continue dividing for up to 12 h (Vanherberghen et al. 2010). The combination of acoustic technologies and microfluidics has been applied for various biological approaches such as cell sorting (Chen et al. 2008) and cell patterning (Shi et al. 2009). Acoustic assembly has also been used to assemble microgels with encapsulated cells, maintaining high viability (>93 %) (Gurkan et al. 2012). Single layer assembly of different shape geometries as well as multilayer assembly in a layer-by-layer manner, followed by a secondary crosslinking to stabilize the structure, may be used to assemble complex constructs from microgel building blocks.

Geometric Recognition-Guided Assembly

Geometric pairing between shape-coded hydrogels is also used to create a desired architecture. In this approach, shape-coded micrometer-scale hydrogels bind to shape-matching hydrogel templates on a complementary hydrogel to organize microgels into a desired structure (Eng et al. 2013; Hernandez and Mason 2007; Du et al. 2008b). This assembly strategy is useful for creating repeating patterns such as a microenvironment which includes both cells and biochemical factors. Other strategies, such as acoustic waves, have been used to drive the assembly of complementary geometric shapes (Gurkan et al. 2012). In another study, gravitational forces have been used as a driving force to drive shape-coded assembly of cell-encapsulating hydrogels by docking different shapes into hydrogel templates (Eng et al. 2013). This platform was used to study cell–cell and cell–microenvironment interactions.

Liquid-Based Template Assembly

In liquid-based template assembly, a liquid surface built by standing waves is used as a dynamically tunable template to assemble microscale units into organized 3D networks with controlled architectures. This technique requires an aqueous biocompatible media which has specific criteria for viscosity and density. Liquid-based template assembly is applicable for a range of building blocks, or "floaters," with different materials and sizes ranging from 10 μm to 2 mm (Chen et al. 2014). The assembly of multiple materials has been demonstrated with gelatin methacryloyl (GelMA) hydrogel units, polymethylsiloxane (PDMS) blocks, and silicon chiplets. Using this strategy, neuron-seeded carrier beads were assembled into 3D neuronal networks (Chen et al. 2014). These neuronal networks are promising for future development of in vitro brain models to gain a better understanding of neural circuits.

4.3.2.3 Direct Assembly

Direct assembly is based on a "pick-and-place" strategy in which an organized tissue can be constructed by picking and placing hydrogel blocks one by one. Direct assembly techniques are highly controllable and offer the possibility of developing highly complex structures due to direct temporal and spatial control over single hydrogel building blocks (Nichol and Khademhosseini 2009). Though this strategy may be relatively low throughput, it offers a high level of control and flexibility compared to other assembly approaches.

Digital Patterning

The digital patterning approach to direct assembly involves photolithography fabrication with digitally designed photomasks, which are inherently very simple and precise. Compared to the use of a single photomask for generation of singe hydrogel units, this approach involves precise alignment of multiple photomasks or, alternatively, rotation of a single photomask for sequential hydrogel photocrosslinking steps. The precise heterogeneous arrangement of particular cell types is important for building tissue models with similar organization to the native tissue, which facilitates interactions between different cell types. A simple alignment system has been proposed which allows precise organization of 3D hydrogel blocks, which have been shown to be a suitable environment for primary neuron cells, facilitating cell survival and neurite growth (Gurkan et al. 2013). Further, this study achieved high-throughput, multilayer, heterogeneous patterning of cell-encapsulating tissue constructs with precise, repeatable geometries.

Microrobotics

Robotic assembly is another "pick-and-place" approach using microscale robots to push hydrogels in fluid microenvironments. The microrobot is operated by a real-time computer interface providing spatiotemporal control. This approach allows precise fabrication of complex materials in 3D with a wide variety of structural, morphological, and chemical features. A recently developed microrobotic application allows real-time control over 100 μm to mm scale microrobots to pattern cell-encapsulating hydrogel blocks by pushing them in a fluid microenvironment to form a complex 3D tissue structure (Fig. 4.4) (Tasoglu et al. 2014b). The assembly time varies depending on the number of hydrogel blocks, "pick-and-place" speed, surface friction or stickiness, and drag force (in the case of directed assembly in a liquid medium without surface contact) (Chung et al. 2015; Sitti et al. 2015).

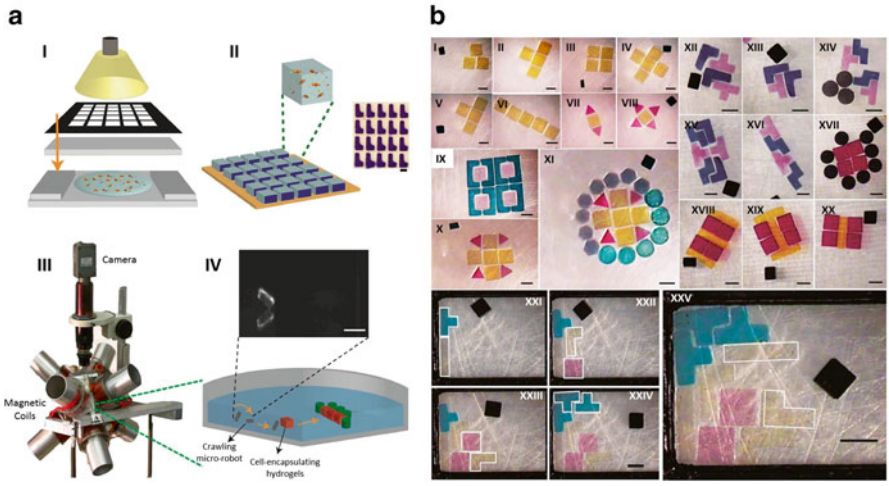

Fig. 4.4 Direct assembly of hydrogels with robotics (**a**) (*I*) Cell-encapsulating hydrogel fabrication via ultraviolet (UV) photocrosslinking. (*II*) Fabricated hydrogels and micrograph of L-shaped hydrogels. (Scale bar, 1 mm.) (*III*) A magnetic coil system is used to manipulate magnetic microrobots remotely. (*IV*) Motion of the unrestrained magnetic microrobot and alignment of building units. (Scale bar, 1 mm.) (**b**) Two-dimensional microrobotic aligning of hydrogel configuration. Microrobotic aligning and reconfiguration of poly(ethylene glycol) dimethacrylate hydrogels (*I–XI*) and gelatin methacrylate hydrogels (*XII–XX*) with different shapes into complex planar architectures. The black object in each image is a top view of a crawling microrobot. All the experiments were performed in a 20 mm × 20 mm × 4 mm chamber in phosphate-buffered saline (PBS). Continuous aligning and reconfiguring sequences are shown. (*XXI–XXV*) Manipulation and placement control in untethered microrobotic alignment of hydrogel composition. Adapted by permission from Macmillan Publishers Ltd: Nature Communications (Tasoglu et al. 2014b), copyright 2014

Conclusions

The natural structure of human tissues is highly organized, involving 3D complexity and precise spatial distribution of multiple cell types. This structure is essential to the proper function of the tissues, which relies heavily on cellular microenvironment and cell–cell interactions. Neural circuits, in particular, are known for their highly complex 3D networks. Therefore, in order to successfully recapitulate the structure and function of natural tissues in vitro, we must develop fabrication techniques which allow for rapid and precise fabrication of biomimetic tissue structures. These techniques can be combined with molecular tools that allow the detection and control of physiological activities of the cells within the constructs. Bottom-up fabrication techniques address the challenge of complex 3D organization of cells by assembling smaller building blocks into desired geometries. Emerging technologies enable high cell viability, repeatability, specificity, and throughput in the complex microscale assembly of cells into desired geometries. Bioprinting uses digital

technology to deposit scaffolds, often mixed with living cells or later seeded with cells, in a layer-by-layer fashion with desired geometries based on a virtual model. Microassembly approaches use a variety of strategies—self-assembly, guided assembly, and direct assembly—to arrange smaller building blocks, often cell-encapsulating hydrogels, into larger tissue constructs with desired geometries. While some of these approaches have already been shown to facilitate survival and growth of neural tissues, each has potential to be applied to fabrication of neural circuits. Molecular tools such as genetically encoded sensors and actuators of neuronal activity have the potential to enable real-time in situ functional analysis of engineered neural tissues. Optical imaging can be combined with optical control approaches to allow scalable analysis of neuronal activities, both at the single cell and circuit level. When combined, these technologies show potential for the creation of spatially complex 3D tissues with in situ monitoring and control capabilities, which may ultimately be used as replacements for damaged or diseased tissues, as models for scientific research, or as platforms for high-throughput pharmaceutical testing. This technology will enable assembly and analysis of a highly complex biomimetic in vitro neural model, which serves as a platform for direct interrogation of neuronal function which is not currently possible in vivo or in traditional 2D neural cell cultures.

References

Akerboom, J., et al. 2013. Genetically Encoded Calcium Indicators for Multi-color Neural Activity Imaging and Combination with Optogenetics. *Frontiers in Molecular Neuroscience* 6: 2.

Arosio, D., et al. 2010. Simultaneous Intracellular Chloride and pH Measurements Using a GFP-Based Sensor. *Nature Methods* 7(7): 516–518.

Berndt, A., et al. 2014. Structure-Guided Transformation of Channelrhodopsin into a Light-Activated Chloride Channel. *Science* 344(6182): 420–424.

Bowden, N., et al. 1997. Self-Assembly of Mesoscale Objects into Ordered Two-Dimensional Arrays. *Science* 276(5310): 233–235.

Bowden, N., et al. 1999. Mesoscale Self-Assembly of Hexagonal Plates Using Lateral Capillary Forces: Synthesis Using the "Capillary Bond". *Journal of the American Chemical Society* 121(23): 5373–5391.

Boyden, E.S., 2011. A History of Optogenetics: The Development of Tools for Controlling Brain Circuits with Light. F1000 Biol Rep 3: 11.

Boyden, E.S., et al. 2005. Millisecond-Timescale, Genetically Targeted Optical Control of Neural Activity. *Nature Neuroscience* 8(9): 1263–1268.

Brannvall, K., et al. 2007. Enhanced Neuronal Differentiation in a Three-Dimensional Collagen-Hyaluronan Matrix. *Journal of Neuroscience Research* 85(10): 2138–2146.

Chang, R., J. Nam, and W. Sun. 2008. Effects of Dispensing Pressure and Nozzle Diameter on Cell Survival from Solid Freeform Fabrication-Based Direct Cell Writing. *Tissue Engineering. Part A* 14(1): 41–48.

Chang, C.C., et al. 2011. Direct-Write Bioprinting Three-Dimensional Biohybrid Systems for Future Regenerative Therapies. *Journal of Biomedical Materials Research. Part B, Applied Biomaterials* 98(1): 160–170.

Chen, P., et al. 2008. Microfluidic Chips for Cell Sorting. *Frontiers in Bioscience* 13: 2464–2483.

Chen, T.W., et al. 2013. Ultrasensitive Fluorescent Proteins for Imaging Neuronal Activity. *Nature* 499(7458): 295–300.
Chen, P., et al. 2014. Microscale Assembly Directed by Liquid-Based Template. *Advanced Materials* 26(34): 5936–5941.
Cho, Y.K. 2015. Genetically Encoded Tools: Bridging the Gap Between Neuronal Identity and Function. *ACS Chemical Neuroscience* 6(1): 14–15.
Chow, B.Y., et al. 2010. High-Performance Genetically Targetable Optical Neural Silencing by Light-Driven Proton Pumps. *Nature* 463(7277): 98–102.
Chrisey, D.B. 2000. Materials Processing: The Power of Direct Writing. *Science* 289(5481): 879–881.
Chung, S.E., X. Dong, and M. Sitti. 2015. Three-Dimensional Heterogeneous Assembly of Coded Microgels Using an Untethered Mobile Microgripper. *Lab on a Chip* 15(7): 1667–1676.
Chuong, A.S., et al. 2014. Noninvasive Optical Inhibition with a Red-Shifted Microbial Rhodopsin. *Nature Neuroscience* 17(8): 1123–1129.
Cohen, D.L., et al. 2006. Direct Freeform Fabrication of Seeded Hydrogels in Arbitrary Geometries. *Tissue Engineering* 12(5): 1325–1335.
Cui, X., et al. 2012. Direct Human Cartilage Repair Using Three-Dimensional Bioprinting Technology. *Tissue Engineering. Part A* 18(11–12): 1304–1312.
De Coppi, P., et al. 2007. Isolation of Amniotic Stem Cell Lines with Potential for Therapy. *Nature Biotechnology* 25(1): 100–106.
Demirors, A.F., et al. 2013. Colloidal Assembly Directed by Virtual Magnetic Moulds. *Nature* 503(7474): 99–103.
Du, Y., et al. 2008a. Directed Assembly of Cell-Laden Microgels for Fabrication of 3D Tissue Constructs. *Proceedings of the National Academy of Sciences of the United States of America* 105(28): 9522–9527.
Du, Y., et al. 2008b. Method of Bottom-Up Directed Assembly of Cell-Laden Microgels. *Cellular and Molecular Bioengineering* 1(2–3): 157–162.
Duan, B., et al. 2013. 3D Bioprinting of Heterogeneous Aortic Valve Conduits with Alginate/Gelatin Hydrogels. *Journal of Biomedical Materials Research. Part A* 101(5): 1255–1264.
Duocastella, M., et al. 2010. Novel Laser Printing Technique for Miniaturized Biosensors Preparation. *Sensors and Actuators B: Chemical* 145(1): 596–600.
Emiliani, V., et al. 2015. All-Optical Interrogation of Neural Circuits. *Journal of Neuroscience* 35(41): 13917–13926.
Eng, G., et al. 2013. Assembly of Complex Cell Microenvironments Using Geometrically Docked Hydrogel Shapes. *Proceedings of the National Academy of Sciences* 110(12): 4551–4556.
Fedorovich, N.E., et al. 2009. Evaluation of Photocrosslinked Lutrol Hydrogel for Tissue Printing Applications. *Biomacromolecules* 10(7): 1689–1696.
Forsby, A., et al. 2009. Neuronal In Vitro Models for the Estimation of Acute Systemic Toxicity. *Toxicology In Vitro* 23(8): 1564–1569.
Gandhi, S.P., and C.F. Stevens. 2003. Three Modes of Synaptic Vesicular Recycling Revealed by Single-Vesicle Imaging. *Nature* 423(6940): 607–613.
Gassmann, K., et al. 2012. Automated Neurosphere Sorting and Plating by the Copas Large Particle Sorter Is a Suitable Method for High-Throughput 3D in Vitro Applications. *Toxicology In Vitro* 26(6): 993–1000.
Grzybowski, B.A., H.A. Stone, and G.M. Whitesides. 2000. Dynamic Self-Assembly of Magnetized, Millimetre-Sized Objects Rotating at a Liquid-Air Interface. *Nature* 405(6790): 1033–1036.
Grzybowski, B.A., et al. 2009. Self-Assembly: From Crystals to Cells. *Soft Matter* 5(6): 1110–1128.
Guillotin, B., and F. Guillemot. 2011. Cell Patterning Technologies for Organotypic Tissue Fabrication. *Trends in Biotechnology* 29(4): 183–190.
Guillotin, B., et al. 2010. Laser Assisted Bioprinting of Engineered Tissue with High Cell Density and Microscale Organization. *Biomaterials* 31(28): 7250–7256.

Guo, F., et al. 2015. Controlling Cell–Cell Interactions Using Surface Acoustic Waves. *Proceedings of the National Academy of Sciences* 112(1): 43–48.

Gurkan, U.A., et al. 2012. Emerging Technologies for Assembly of Microscale Hydrogels. *Advanced Healthcare Materials* 1(2): 149–158.

Gurkan, U.A., et al. 2013. Simple Precision Creation of Digitally Specified, Spatially Heterogeneous. *Engineered Tissue Architectures. Advanced Materials* 25(8): 1192–1198.

Guven, S., et al. 2015. Multiscale Assembly for Tissue Engineering and Regenerative Medicine. *Trends in Biotechnology* 33(5): 269–279.

Han, X., and E.S. Boyden. 2007. Multiple-Color Optical Activation, Silencing, and Desynchronization of Neural Activity, With Single-Spike Temporal Resolution. *PLoS One* 2(3): e299.

Harada, A., et al. 2011. Macroscopic Self-Assembly Through Molecular Recognition. *Nature Chemistry* 3(1): 34–37.

Hernandez, C.J., and T.G. Mason. 2007. Colloidal Alphabet Soup: Monodisperse Dispersions of Shape-Designed LithoParticles. *The Journal of Physical Chemistry C* 111(12): 4477–4480.

Hires, S.A., Y. Zhu, and R.Y. Tsien. 2008. Optical Measurement of Synaptic Glutamate Spillover and Reuptake by Linker Optimized Glutamate-Sensitive Fluorescent Reporters. *Proceedings of the National Academy of Sciences of the United States of America* 105(11): 4411–4416.

Hochbaum, D.R., et al. 2014. All-Optical Electrophysiology in Mammalian Neurons Using Engineered Microbial Rhodopsins. *Nature Methods* 11(8): 825–833.

Ivanova, E., and Z.H. Pan. 2009. Evaluation of the Adeno-Associated Virus Mediated Long-Term Expression of Channelrhodopsin-2 in the Mouse Retina. *Molecular Vision* 15: 1680–1689.

Jakab, K., et al. 2006. Three-Dimensional Tissue Constructs Built by Bioprinting. *Biorheology* 43(3–4): 509–513.

Jakab, K., et al. 2008. Tissue Engineering by Self-Assembly of Cells Printed into Topologically Defined Structures. *Tissue Engineering. Part A* 14(3): 413–421.

Jin, L., et al. 2012. Single Action Potentials and Subthreshold Electrical Events Imaged in Neurons with a Fluorescent Protein Voltage Probe. *Neuron* 75(5): 779–785.

Jones, N. 2012. Science in Three Dimensions: The Print Revolution. *Nature* 487(7405): 22–23.

Jurga, M., et al. 2009. Generation of Functional Neural Artificial Tissue from Human Umbilical Cord Blood Stem Cells. *Tissue Engineering. Part C, Methods* 15(3): 365–372.

Karoly, J., et al. 2010. Tissue Engineering by Self-Assembly and Bio-Printing of Living Cells. *Biofabrication* 2(2): 022001.

Kattamis, N.T., et al. 2007. Thick Film Laser Induced Forward Transfer for Deposition of Thermally and Mechanically Sensitive Materials. *Applied Physics Letters* 91(17): 171120.

Keriquel, V., et al. 2010. In Vivo Bioprinting for Computer- and Robotic-Assisted Medical Intervention: Preliminary Study in Mice. *Biofabrication* 2(1): 014101.

Khademhosseini, A., and R. Langer. 2007. Microengineered Hydrogels for Tissue Engineering. *Biomaterials* 28(34): 5087–5092.

Khademhosseini, A., et al. 2006. Microscale Technologies for Tissue Engineering and Biology. *Proceedings of the National Academy of Sciences of the United States of America* 103(8): 2480–2487.

Khalil, S., and W. Sun. 2007. Biopolymer Deposition for Freeform Fabrication of Hydrogel Tissue Constructs. *Materials Science and Engineering: C* 27(3): 469–478.

Klapoetke, N.C., et al. 2014. Independent Optical Excitation of Distinct Neural Populations. *Nature Methods* 11(3): 338–346.

Klebe, R.J. 1988. Cytoscribing: A Method for Micropositioning Cells and the Construction of Two- and Three-Dimensional Synthetic Tissues. *Experimental Cell Research* 179(2): 362–373.

Knowlton, S., et al. 2015. Bioprinting for Cancer Research. *Trends in Biotechnology* 33(9): 504–513.

Knowlton, S., et al. 2016. Utilizing Stem Cells for Three-Dimensional Neural Tissue Engineering. *Biomaterials Science*, advance article DOI: 10.1039/C5BM00324E.

Kralj, J.M., et al. 2012. Optical Recording of Action Potentials in Mammalian Neurons Using a Microbial Rhodopsin. *Nature Methods* 9(1): 90–95.
Kuner, T., and G.J. Augustine. 2000. A Genetically Encoded Ratiometric Indicator for Chloride: Capturing Chloride Transients In Cultured Hippocampal Neurons. *Neuron* 27(3): 447–459.
Li, C.Y., et al. 2011. DNA-Templated Assembly of Droplet-Derived PEG Microtissues. *Lab on a Chip* 11(17): 2967–2975.
Lo, L., and D.J. Anderson. 2011. A Cre-dependent, Anterograde Transsynaptic Viral Tracer for Mapping Output Pathways of Genetically Marked Neurons. *Neuron* 72(6): 938–950.
Madisen, L., et al. 2012. A Toolbox of Cre-dependent Optogenetic Transgenic Mice for Light-Induced Activation and Silencing. *Nature Neuroscience* 15(5): 793–802.
Madisen, L., et al. 2015. Transgenic Mice for Intersectional Targeting of Neural Sensors and Effectors with High Specificity and Performance. *Neuron* 85(5): 942–958.
Michael, S., et al. 2013. Tissue Engineered Skin Substitutes Created by Laser-Assisted Bioprinting form Skin-Like Structures in the Dorsal Skin Fold Chamber in Mice. *PLoS One* 8(3): e57741.
Miesenbock, G., D.A. De Angelis, and J.E. Rothman. 1998. Visualizing Secretion and Synaptic Transmission with Ph-Sensitive Green Fluorescent Proteins. *Nature* 394(6689): 192–195.
Mirica, K.A., et al. 2011. Using Magnetic Levitation for Three Dimensional Self-Assembly. *Advanced Materials* 23(36): 4134–4140.
Miyawaki, A., et al. 1997. Fluorescent Indicators For Ca2+ Based on Green Fluorescent Proteins and Calmodulin. *Nature* 388(6645): 882–887.
Muller, W., and J.A. Connor. 1991. Dendritic Spines as Individual Neuronal Compartments for Synaptic Ca2+ Responses. *Nature* 354(6348): 73–76.
Muradoglu, M., and S. Tasoglu. 2010. A Front-Tracking Method for Computational Modeling of Impact and Spreading of Viscous Droplets on Solid Walls. *Computers & Fluids* 39(4): 615–625.
Murphy, S.V., and A. Atala. 2014. 3D Bioprinting of Tissues and Organs. *Nature Biotechnology* 32(8): 773–785.
Nagel, G., et al. 2003. Channelrhodopsin-2, a Directly Light-Gated Cation-Selective Membrane Channel. *Proceedings of the National Academy of Sciences of the United States of America* 100(24): 13940–13945.
Nair, K., et al. 2009. Characterization of Cell Viability During Bioprinting Processes. *Biotechnology Journal* 4(8): 1168–1177.
Nakai, J., M. Ohkura, and K. Imoto. 2001. A High Signal-To-Noise Ca(2+) Probe Composed of a Single Green Fluorescent Protein. *Nature Biotechnology* 19(2): 137–141.
Nichol, J.W., and A. Khademhosseini. 2009. Modular Tissue Engineering: Engineering Biological Tissues from the Bottom Up. *Soft Matter* 5(7): 1312–1319.
Norotte, C., et al. 2009. Scaffold-Free Vascular Tissue Engineering Using Bioprinting. *Biomaterials* 30(30): 5910–5917.
O'Shaughnessy, T.J., H.J. Lin, and W. Ma. 2003. Functional Synapse Formation Among Rat Cortical Neurons Grown on Three-Dimensional Collagen Gels. *Neuroscience Letters* 340(3): 169–172.
Okumoto, S., et al. 2005. Detection of Glutamate Release from Neurons by Genetically Encoded Surface-Displayed Fret Nanosensors. *Proceedings of the National Academy of Sciences of the United States of America* 102(24): 8740–8745.
Osakada, F., et al. 2011. New Rabies Virus Variants for Monitoring and Manipulating Activity and Gene Expression in Defined Neural Circuits. *Neuron* 71(4): 617–631.
Peretz, H., et al. 2007. Superior Survival and Durability of Neurons and Astrocytes on 3-Dimensional Aragonite Biomatrices. *Tissue Engineering* 13(3): 461–472.
Petreanu, L., et al. 2007. Channelrhodopsin-2-Assisted Circuit Mapping of Long-Range Callosal Projections. *Nature Neuroscience* 10(5): 663–668.
Radisic, M., et al. 2004. Functional Assembly of Engineered Myocardium by Electrical Stimulation of Cardiac Myocytes Cultured on Scaffolds. *Proceedings of the National Academy of Sciences* 101(52): 18129–18134.

Raimondo, J.V., et al. 2013. A Genetically-Encoded Chloride and pH Sensor for Dissociating Ion Dynamics in the Nervous System. *Frontiers in Cellular Neuroscience* 7: 202.
Ringeisen, B.R., et al. 2004. Laser Printing of Pluripotent Embryonal Carcinoma Cells. *Tissue Engineering* 10(3–4): 483–491.
Schmidt, D., and Y.K. Cho. 2015. Natural Photoreceptors and Their Application to Synthetic Biology. *Trends in Biotechnology* 33(2): 80–91.
Serra, M., et al. 2009. Integrating Human Stem Cell Expansion and Neuronal Differentiation in Bioreactors. *BMC Biotechnology* 9: 82.
Shi, J., et al. 2009. Acoustic Tweezers: Patterning Cells and Microparticles Using Standing Surface Acoustic Waves (SSAW). *Lab on a Chip* 9(20): 2890–2895.
Sitti, M., et al. 2015. Biomedical Applications of Untethered Mobile Milli/Microrobots. *Proceedings of the IEEE* 103(2): 205–224.
Skardal, A., et al. 2012. Bioprinted Amniotic Fluid-Derived Stem Cells Accelerate Healing of Large Skin Wounds. *Stem Cells Translational Medicine* 1(11): 792–802.
Snezhko, A., and I.S. Aranson. 2011. Magnetic Manipulation of Self-Assembled Colloidal Asters. *Nature Materials* 10(9): 698–703.
St-Pierre, F., et al. 2014. High-Fidelity Optical Reporting of Neuronal Electrical Activity with an Ultrafast Fluorescent Voltage Sensor. *Nature Neuroscience* 17(6): 884–889.
Tank, D.W., et al. 1988. Spatially Resolved Calcium Dynamics of Mammalian Purkinje Cells in Cerebellar Slice. *Science* 242(4879): 773–777.
Tasoglu, S., and U. Demirci. 2013. Bioprinting for Stem Cell Research. *Trends in Biotechnology* 31(1): 10–19.
Tasoglu, S., et al. 2010. Impact of a Compound Droplet on a Flat Surface: A Model for Single Cell Epitaxy. *Physics of Fluids* 22(8): 082103.
Tasoglu, S., et al. 2013a. Paramagnetic Levitational Assembly of Hydrogels. *Advanced Materials* 25(8): 1137–1143.
Tasoglu, S., et al. 2013b. Manipulating Biological Agents and Cells in Micro-Scale Volumes for Applications in Medicine. *Chemical Society Reviews* 42(13): 5788–5808.
Tasoglu, S., et al. 2014a. Guided and Magnetic Self-Assembly of Tunable Magnetoceptive Gels. *Nature Communications* 5, 4702.
Tasoglu, S., et al. 2014b. Untethered Micro-Robotic Coding of Three-Dimensional Material Composition. *Nature Communications* 5: 3124.
Tasoglu, S., et al. 2015. Magnetic Levitational Assembly for Living Material Fabrication. *Advanced Healthcare Materials* 4(10): 1469–1476.
Tekin, E., P.J. Smith, and U.S. Schubert. 2008. Inkjet Printing as a Deposition and Patterning Tool for Polymers and Inorganic Particles. *Soft Matter* 4(4): 703–713.
Tonnesen, J., et al. 2011. Functional Integration of Grafted Neural Stem Cell-Derived Dopaminergic Neurons Monitored by Optogenetics in an In Vitro Parkinson Model. *PLoS One* 6(3): e17560.
van Vliet, E., et al. 2007. Electrophysiological Recording of Re-aggregating Brain Cell Cultures on Multi-Electrode Arrays to Detect Acute Neurotoxic Effects. *Neurotoxicology* 28(6): 1136–1146.
Vanherberghen, B., et al. 2010. Ultrasound-Controlled Cell Aggregation in a Multi-Well Chip. *Lab on a Chip* 10(20): 2727–2732.
Visser, J., et al. 2013. Biofabrication of Multi-material Anatomically Shaped Tissue Constructs. *Biofabrication* 5(3): 035007.
Wickersham, I.R., et al. 2007. Retrograde Neuronal Tracing with a Deletion-Mutant Rabies Virus. *Nature Methods* 4(1): 47–49.
Wietek, J., et al. 2014. Conversion of Channelrhodopsin into a Light-Gated Chloride Channel. *Science* 344(6182): 409–412.
Wolfe, D.B., et al. 2003. Mesoscale Self-Assembly: Capillary Interactions When Positive and Negative Menisci Have Similar Amplitudes. *Langmuir* 19(6): 2206–2214.
Wu, J., et al. 2013. Improved Orange and Red Ca(2)+/− Indicators and Photophysical Considerations for Optogenetic Applications. *ACS Chemical Neuroscience* 4(6): 963–972.

Xu, T., et al. 2008a. High-Throughput Production of Single-Cell Microparticles Using an Inkjet Printing Technology. *Journal of Manufacturing Science and Engineering* 130(2): 021017.

Xu, T., et al. 2008b. Characterization of Cell Constructs Generated with Inkjet Printing Technology Using In Vivo Magnetic Resonance Imaging. *Journal of Manufacturing Science and Engineering* 130(2): 021013.

Xu, F., et al. 2011a. Three-Dimensional Magnetic Assembly of Microscale Hydrogels. *Advanced Materials* 23(37): 4254–4260.

Xu, F., et al. 2011b. A Three-Dimensional In Vitro Ovarian Cancer Coculture Model Using a High-Throughput Cell Patterning Platform. *Biotechnology Journal* 6(2): 204–212.

Zamanian, B., et al. 2010. Interface-Directed Self-Assembly of Cell-Laden Microgels. *Small* 6(8): 937–944.

Zhang, F., et al. 2007. Circuit-Breakers: Optical Technologies for Probing Neural Signals and Systems. *Nature Reviews. Neuroscience* 8(8): 577–581.

Zhao, Y., et al. 2011. An Expanded Palette of Genetically Encoded Ca(2)(+) Indicators. *Science* 333(6051): 1888–1891.

Chapter 5
Electrically Conductive Materials for Nerve Regeneration

Elisabeth M. Steel and Harini G. Sundararaghavan

5.1 Introduction

In order to achieve complete functional recovery of an injured neural tissue, approaches seek to develop a material construct that combines several cues to modulate cell behavior, whether it be to guide regenerating axons to reconnect with target tissue or to elicit migration and growth factor release by support cells. Cells respond to cues in the microenvironment. Topographical, chemical, mechanical, and electrical cues have all separately (and in limited combination) been shown to guide and direct these behaviors (Fig. 5.1) (Wrobel 2013; Rodriguez and Schneider 2013). Ideally, multiple cues could be presented spatially and temporally during the regeneration process.

Bioelectricity plays its most notable role in the body in the form of electrical signals throughout tissues in the nervous system, influencing a broad range of active and passive biological functions ranging from movement and thinking to sensory perception and respiration. Mammalian cells maintain a resting electrical potential of −60 to −100 mV across the cell membrane compared to the extracellular side (Ghasemi-Mobarakeh et al. 2011). Maintenance and changes in membrane potential influences cellular functions, particularly as a method of signal transduction in the nervous system (Prabhakaran et al. 2011). The prominent role of bioelectricity in the body makes it an attractive factor to manipulate for accelerating wound healing. External electric fields can influence ion influx through ionic membrane channels to affect intracellular signal transduction pathways through second messengers such as cAMP and Ca^{2+}, which can in turn affect enzyme phosphorylation and alter gene expression (Meng and Zhang 2011). Meng et al. points to several

E.M. Steel (✉) • H.G. Sundararaghavan
Department of Biomedical Engineering, Wayne State University, Detroit, MI, USA
e-mail: hsundara@wayne.edu

L.G. Zhang, D.L. Kaplan (eds.), *Neural Engineering*,
DOI 10.1007/978-3-319-31433-4_5

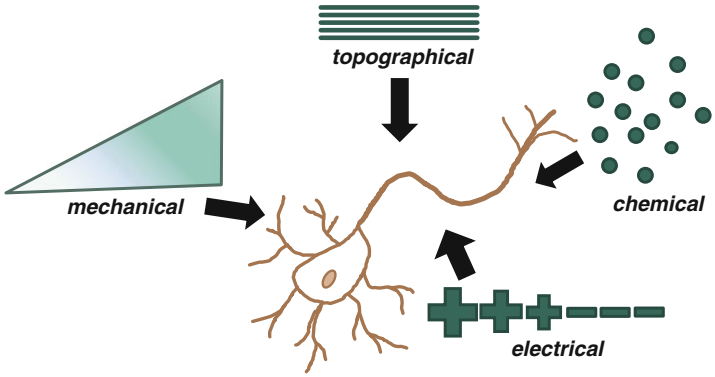

Fig. 5.1 Directed cell behavior from cues in the microenvironment

studies that document electrical stimulation influencing actin assembly and distribution as well as activating transmembrane channels and receptors; components identified to be involved in cell migration and proliferation (Meng and Zhang 2011). From a seminal report in 1982, Patel theorized that electrical stimulation induces the redistribution of components in the cytoplasm, activates transport and proliferative processes, and causes the electrophoretic accumulation of surface molecules that promote neurite adhesion and outgrowth (Wrobel 2013; Ghasemi-Mobarakeh et al. 2011). Application of a range of voltages from 1 to 25 mV/mm using both AC, DC, and pulsed signals have successfully elicited neurite outgrowth in various cell types (Seil and Webster 2010; Royo-Gascon et al. 2013) with Feng et al. calculating a threshold to be 16 mV/mm (Wrobel 2013). While it has been established for over 30 years that neural cells respond to electrical field stimulation, clinical application for restoring function following injury to the nervous system has remained elusive. Given the roles electrical stimulation has played in the clinical success of cochlear and visual prosthetics and in deep brain stimulation for management of disorders ranging from neurological conditions like Parkinson's, epilepsy, and dementia to non-neurological disorders like obesity, the field of neural tissue engineering has the potential to make groundbreaking progress in the near future if conductive materials can be developed that can elicit regenerative behavior and maintain tissue homeostatic mechanisms (Thompson et al. 2014).

Electrical cues can be delivered to target cells and tissues through conductive scaffold materials. Several synthetic and natural organic materials have been studied for their potential application in neural tissue engineering; many reviews highlight the pioneering and significant contributions from earlier studies (Wrobel 2013; Ghasemi-Mobarakeh et al. 2011; Seil and Webster 2010; Balint et al. 2014; Bosi et al. 2014; Hardy et al. 2013; Huang et al. 2014; Kaur et al. 2015; Khaing et al. 2014; Lanmuller et al. 1997; Molino and Wallace 2015; Palermo et al. 2007; Zhang et al. 2014a). Conductive materials that have been investigated for neural tissue engineering (NTE) applications can be generally classified as inherently conductive polymers (ICPs), piezoelectric, and nanostructured carbons. ICPs and nanostructured

carbons have intrinsic conductive properties, but require an external power source (Balint et al. 2014). When piezoelectric materials undergo minute mechanical deformation, they produce transient surface charges which can be harnessed for electrical stimulation (Damaraju et al. 2013). Each material has its benefits and drawbacks; ICPs, piezoelectric, and nanostructured carbon materials and example applications will be discussed in the following sections.

Engineering techniques and clever chemistries have been utilized to modify conductive materials to present simultaneously along with topographical, chemical, and mechanical cues (Hardy et al. 2013). Additionally, advances have been made to engineer conductive materials to be biodegradable to allow for hydrolytic or enzymatic cleavage for degradation into biocompatible waste products that can be cleared by the renal system (Hardy et al. 2013). This is often achieved by synthesizing composites of ICPs, piezoelectric, and/or nanostructured carbons with FDA approved synthetic polymers or those traditionally found within the extracellular matrix (i.e., collagen, hyaluronic acid). Many of these materials could be applied in regenerative therapies beyond neural tissue, including stem cell differentiation and organs in the skin, musculoskeletal, and cardiovascular systems. This review will focus on key studies demonstrating the potential in NTE applications sampled from each of the conductive material classifications. These studies are examples of the investigations that conductive materials can influence neural tissue cell behavior, including stem cell and neural progenitor differentiation, as well as be modified to tailor mechanical, topographical, and chemical cue properties through diverse fabrication techniques such as electrospinning and wet spinning, inkjet and extrusion printing, self and layer-by-layer assembly, and in situ polymerization within acellular tissue constructs (Kaur et al. 2015; Peramo 2008).

5.2 Conductive Materials

5.2.1 Evaluating Electrical Properties

Electrical properties of conductive material constituents such as surface energy, zeta potential, and resistivity or conductivity can influence material surface wetting and adhesion in turn modulating cell attachment, proliferation, differentiation, motility, and outgrowth (Higgins and Wallace 2013). Common techniques to measure surface energy are inverse gas chromatography (IGC) and contact angle. Zeta potential can be calculated from data utilizing dynamic light scattering techniques and measuring dielectric constants. Surface electrical property values for films and 3D scaffolds can be challenging, a variation of atomic force microscopy called kelvin probe force microscopy (KPFM) can provide information on variations of surface potential that correlate with material topography (Higgins and Wallace 2013). KPFM is a powerful though complex tool for evaluating nanometer-scale surface potential; thorough reviews are provided by Melitz et al. (2011) and Palermo et al. (2007).

Demonstrating the influence of surface charge on neurite growth and branching, Hu et al. prepared a series of covalently functionalized multi-walled carbon nanotubes (MWCNTs) with various charges: carboxylic groups to carry a negative charge (MWCNT-COOH), poly-*m*-aminobenzene sulfonic acid to carry a zwitterionic charge (±, MWCNT-PABS), or ethylenediamine to carry a positive charge (MWCNT-EN) (Hu et al. 2004). The group systematically demonstrated that surface charge can modulate the number, branching, and extent of outgrowth of neurites and their growth cones, with positively charged MWCNTs eliciting the most growth over neutral or negatively charged MWCNTs.

Surface conductivity is commonly measured by two-point probe (2PP) (Sudwilai et al. 2014) or four-point probe (4PP) meters (Broda et al. 2011). In 2PP, probes placed in contact with the material are connected to source meters that measure the current following application of a constant voltage. In 4PP, current is passed through the two outer probes (referred to as source and drain) while voltage is measured through the two inner probes (Fig. 5.2). Sheet resistivity (R_s) is calculated by plotting the applied voltage versus the current change (2PP), or voltage change versus applied current (4PP). Electrically conductivity of films and fiber mats can be calculated by (5.1):

$$\sigma = \frac{1}{\rho} = \frac{1}{R_s \times t} = \frac{I}{K \times V \times t} \tag{5.1}$$

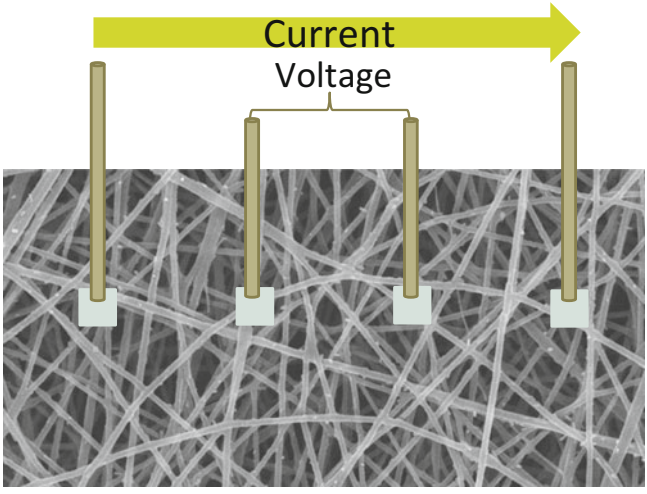

Fig. 5.2 Sheet resistivity can be measured by probing methods such as four-point probe to calculate conductivity. Probes can be applied either directly to the material surface or onto patterned contacts for fragile specimens. Current is passed through the two outer probes, while the voltage is measured through the two inner probes

where σ is defined as specific conductivity (S/cm), ρ as specific resistivity (Ω cm), I as current (A), K as the geometrical correction factor, V as voltage (V), and t as material thickness (cm). The geometrical correction factor, which accounts for effects of probe configuration and spacing, can be determined using a standard material such as silicon oxide that has known resistivity value (Sudwilai et al. 2014).

Two techniques that enable material characterization in dynamic physical and biochemical environments are electrical impedance spectroscopy (EIS) and cyclic voltammetry (CV) (Richardson-Burns et al. 2007a). EIS is a technique that characterizes material impedance over a frequency range, giving real and imaginary components of impedance as a function of frequency. The lower the impedance, electrical stimulation through the conductive material generally will require lower power (Lanmuller et al. 1997). Cyclic voltammetry characterizes charge transfer capacity and identifies redox reactions that occur. The measured current is visualized as current density as a function of the cyclic reference electrode potential during a cyclic voltage sweep (Merrill et al. 2005). The area under the CV curve specifies the material's capability to transfer charge and the effective surface area (Richardson-Burns et al. 2007a). The shape of the curve indicates whether reversible or irreversible Faradaic reactions occur while the potential is cycled (Richardson-Burns et al. 2007a; Merrill et al. 2005). To be effective for electrical stimulation, a material should have a large reversible charge storage capacity in order to be able to transfer that charge to the surrounding tissue but also be able to transfer that charge before an irreversible Faradaic reaction results (Merrill et al. 2005). Irreversible Faradaic reactions have the potential to create oxidative stress in the tissue (Merrill et al. 2005).

5.2.2 Inherently Conductive Polymers

5.2.2.1 Synthesis

To synthesize polymers capable of conducting electrons, the starting material, consisting of a neutral polymer chain with monomers conjugated to one another by π bonds, undergoes a doping procedure (Balint et al. 2014). Doping transfers charge from the dopant molecules, thus oxidizing or reducing the π bonds in the neutral polymer chain so that they become positively or negatively charged (Ghasemi-Mobarakeh et al. 2011). The initial polymer synthesis is commonly performed by electrochemical polymerization of monomers at an electrode surface or in the presence of a catalyst (Hardy et al. 2013). The choice of dopant can influence the resulting polymer's conductivity as well as other factors such as surface energy, degradability, and biocompatibility. Dopants can be introduced during or after polymerization. Low molecular weight dopants that only interact with the polymer by non-covalent interactions leech out of the matrix into the surrounding environment (Svirskis et al. 2010). This leeching effect can be utilized as a means to deliver neurotrophic factors upon application of an external electrical stimulus

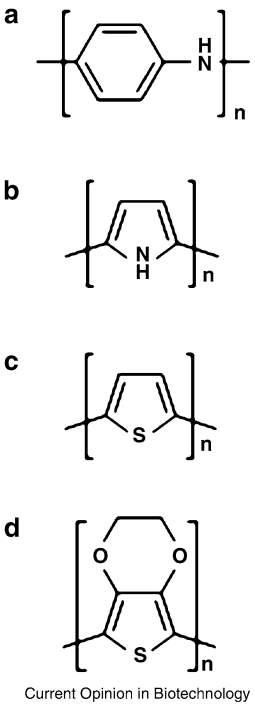

Fig. 5.3 The structures of common conducting polymers. (**a**) Polyaniline. (**b**) Polypyrrole. (**c**) Polythiophene. (**d**) Poly(3,4-ethylenedioxythiophene). Image reprinted with the permission from the authors and publisher of Hardy et al. (2013)

(Svirskis et al. 2010; Thompson et al. 2006, 2010, 2011). The most common conductive polymers used in biological applications are polypyrrole (PPy), polyaniline (PANi), polythiophene (PT), and poly(3,4-ethylenedioxythiphene) (PEDOT), as seen in Fig. 5.3 (Lee 2013). To improve processability, biocompatibility, and stability, these traditional ICPs are often combined with other biomaterials (Ghasemi-Mobarakeh et al. 2011). ICPs are highly processable enabling control over nano- and micro-topography. Fabrication techniques that have been utilized are inkjet printing, extrusion printing, electrospinning, and wet spinning (Molino and Wallace 2015; Zhu et al. 2014; Dhandayuthapani et al. 2011).

Schmidt et al. highlights some of the potential advantages for the use of conducting polymers in NTE applications in a seminal 1997 article: (1) stimulation can be localized to the area around the polymer versus exogenously applied electric fields (EFs) and (2) CPs surface properties can be tailored with biochemical or adhesive cues based on which dopant ions are incorporated into the polymer chain (Schmidt et al. 1997). A drawback of using pure CPs is the lack of degradability. Further work by the Schmidt group produced the first fully biodegradable electrically conductive polymer (BECP) by which PPy-thiophene-PPy oligomers were linked by degradable ester groups using an aliphatic linker which provided flexibility (Rivers et al. 2002). BECP films demonstrated the ability to degrade enzymatically, support neuroblastoma cell attachment and proliferation, and in vivo biocompatibility in rats (Rivers et al. 2002). These studies are just two examples that laid the foundation for

establishing biodegradable conductive materials as attractive candidates for NTE scaffolds with the potential to deliver electrical, chemical, adhesive, mechanical, and topographical cues. Polypyrrole is by far the most extensively studied ICP for neural applications due to its conductivity and biocompatibility and ease of synthesis (Lee et al. 2009a).

5.2.2.2 Polypyrrole

Building on their success, Schmidt's group developed two biodegradable PPy block co-polymers with poly(ε-caprolactone) (PCL) and poly(ethyl cyanoacrylate) (PECA). Notably, the conductivity of PPy-PCL (32 S/cm) was greater than the PPy homopolymer (22 S/cm) while that of PPy-PECA was equivalent (19 S/cm). The group used PC12 cells as one of their cell models for neuron behavior. PC12 cells are a commonly used model cell for neurons. They originate from a cell line isolated from a rat adrenal pheochromocytoma and differentiate into neuronal-like cells upon exposure to nerve growth factor as evidenced by extending neurites (Greene and Tischler 1976). Upon stimulation of PC12 cells cultured on co-polymer films, cell attachment and neurite extension were significantly greater on PPy-PCL in comparison to PPy-PECA. These results were attributed to PECA causing irritation in nervous tissue despite its use in other biomedical applications. The study essentially demonstrated that blocks of PPy could be co-polymerized with "macromonomers," which are comprised of non-conducting polymer oligomers with PPy endcaps that have oxidation potential similar to that of PPy homo-monomers. Using a biocompatible and hydrolytically degradable polymer, like PCL, for the nonconducting oligomer units allows for a uniquely conductive PPy composite.

Recent work headed by Ma's group took another approach to mitigate the low solubility, brittle nature, and poor degradability of the PPy homopolymer by synthesizing a composite with poly(D,L-lactic acid) (PDLLA) (Xu et al. 2014). This FDA approved polymer used in commercially available nerve guide conduits is utilized for its biodegradability, cytocompatibility, and mechanical properties. A PPy/PDLLA emulsion polymerization was performed in chloroform using sodium dodecyl sulfate (SDS) as an emulsifier and $FeCl_3$ as an oxidizer and dopant (Xu et al. 2014). Electrically stimulated composite films containing 5/10/15 % PPy, with respective conductivities of 5.65, 10.4, 15.56 mS/cm, produced significantly increase PC12 attachment and neurite growth and extension compared to their respective unstimulated controls. Remarkably, the neurite length and number of neurite-bearing cells increased with increasing PPy concentration. Further investigation into the molecular mechanisms behind this phenomenon is needed.

Studies have incorporated adhesive cues into scaffold design to enhance the behavior of neural support cells. Electrical stimulation of Schwann cells with a 100 mV DC signal for 4 h on PPy/chitosan membranes significantly increased expression and secretion of NGF and BDNF (Huang et al. 2010a). PPy was polymerized via microemulsion in the presence of $FeCl_3$, and the purified suspension was mixed with a 1.5 % w/v solution of 90 % deacetylated chitosan before casting into films.

Modulating support cell release of neurotrophic factors has immense potential in NTE scaffold fabrication. To this end, Lee and Schmidt functionalized PPy with amine groups to improve material adhesivity demonstrating a significant increase in fibroblast and Schwann cell adhesion to PPy films (Lee and Schmidt 2015). While adhesion was dramatically improved in comparison to native PPy polymer and poly-L-lysine (PLL)-coated PPy, the conductivity of 50 and 100 % amine-functionalized PPy was reduced by 2 and 4 orders of magnitude, respectively. Lee and Schmidt point out that this outcome limits the usage of this material in applications that require high conductivity and electrical sensitivity (Lee and Schmidt 2015). An earlier study from the Schmidt group (Nickels and Schmidt 2013) highlights the ability to control surface adhesive properties of PPy through the use of an affinity peptide without sacrificing bulk material conductivity. After utilizing the phage display technique to identify the affinity peptide, THRTSTLDYFVI (denoted as T59), that could non-covalently bind to chlorine-doped PPy (PPyCl) to be used as a linker, the laminin fragment IKVAV was tethered to PPy via T59. While there was no significant difference in conductivity between the T59-PPyCL and PPyCl following incubation in 10 mM PBS, the IKVAV-T59-PPyCl conductivity was not reported. Aqueous solutions cause de-doping and oxidation of ICPs. While these phenomena have benefits and drawbacks (conductivity stabilization on one hand but signal weakening on the other), the added complexity in tethering a large molecule like IKVAV to the surface potentially introduces a physical barrier to ion transport (Nickels and Schmidt 2013). Despite these potential problems, stimulation of PC12 cells with 100 mV/cm for 2 h on IKVAV-T59-PPyCl films resulted in significantly increased cell attachment, neurite length, and number of neurites per cell compared to the unmodified films. Another strategy employed by Cui and colleagues is to incorporate an adhesive cue during PPy synthesis by using a bioactive anion as the dopant. They have investigated several peptide sequences from laminin, including CDPGYIGSR (p31) and RNIAEIIKDI (p20), as a means to promote cell attachment, migration, and neurite extension from dorsal root ganglia and neuroblastoma cells. More recently, the group used PPy doped with p20, p31, and a mixture of p20 and p31 to grow and differentiate human embryonic and rat neural stem cells (hESCs, rNSCs) to neuronal fates (Zhang et al. 2010a). PPy/p20 improved neuronal differentiation and neurite outgrowth of hESCs and rNSCs. PPy/p31 promoted cell adhesion and spreading. Substrates displaying a mixture of p20 and p31 produced intermediate effects, further demonstrating that PPy doped or modified with adhesive cues can modulate the behavior of a variety of cell types.

PPy can also be doped with neurotrophins allowing for the spatially and temporally controlled release of chemical cues to induce neuroprotective and regenerative activity. Following a successful study in doping PPy with NT-3(Thompson et al. 2006), Thompson et al. simultaneously incorporated brain-derived neurotrophic factor (BDNF) and neurotrophin-3 (NT-3) into PPy films during electrosynthesis from a solution of PPy and sodium *p*-toluenesulfonate (pTS) (Thompson et al. 2010). Release kinetics and in vitro characterization assays were performed by applying a charge balanced 250 Hz, biphasic ±1 mA current waveform with clinically established pulse widths, and interphase open- and short-circuit gaps mimicking cochlear implant settings (Thompson et al. 2010). Interestingly, results

revealed that using both neurotrophins affected each other's release profiles, where the presence of BDNF impeded NT-3 release, and NT-3 amplified BDNF release (Thompson et al. 2010). Stimulation of the PPy/BDNF/NT-3 films resulted in more than doubled auditory neuron survival and outgrowth from cochlear nerve explants compared to either neurotrophin alone. The group reported elsewhere that the choice of dopant during electrochemical PPy synthesis has a dramatic effect on both the biocompatibility of the polymer and its efficacy under electrically stimulated neurotrophic release to enhance nerve survival and outgrowth (Thompson et al. 2011). When characterizing NT-3 release and spiral ganglion neuron behavior, the small anionic dopant pTS outperformed the other common PPy dopants, dodecylbenzene sulfonate (DBS), poly(3-styrenesulfonate) (PSS), poly(2-methoxyaniline-4-sulfonic acid) (PMAS), hyaluronic acid (HA), and chondroitin sulfate (CS) (Thompson et al. 2011). PPy/dopant composite films incorporating these anions have been extensively characterized by the Schmidt and Wallace groups (Hardy et al. 2013; Molino and Wallace 2015; Schmidt et al. 1997; Collier et al. 2000; Liu et al. 2009; Stewart et al. 2015).

Rather than inducing neurotrophic factor release by electrical stimulation, another strategy to present a chemical cue is to immobilize bioactive factors to the ICP. Lee et al. immobilized NGF to PPy by functionalizing PPy with *N*-hydroxyl succinimidyl ester groups (Lee et al. 2009b). NGF remained bioactive and stably conjugated to PPy-NSE functionalized films following electrical stimulation with 1 V (Lee et al. 2009b). To further this work, Lee et al. immobilized NGF to an electrically active fibrous scaffold by a four-step fabrication process (Lee et al. 2012). First, a PLGA fibrous mesh was fabricated by electrospinning, then coated with a layer of PPy via chemical polymerization. Carboxyl groups necessary for NGF conjugation were introduced to the fiber surface by performing a chemical copolymerization with equal molar ratios of pristine pyrrole and 1-(2-carboxyethyl) pyrrole (Py-COOH) (Lee et al. 2012). Upon electrical stimulation of PC12 cells with a 10 mV/cm DC signal, neurite formation and median length significantly increased compared to unstimulated controls (Lee et al. 2012).

Incorporating PPy into electrospun fibers allows for the presentation of a topographical guidance cue as an extracellular matrix mimic. Lee et al. first described coating electrospun PLGA fibers with PPy and stimulating PC12 cells through these nanofibers in a 2009 study (Fig. 5.4) (Lee et al. 2009a). Statistically significant increases in neurite bearing PC12 cells and neurite length were observed on stimulated PPy-PLGA nanofibers, with an additive effect occurring with aligned fibers compared to random (Fig. 5.5) (Lee et al. 2009a). Notably, electrical resistance was observed to be conducted along the fiber axis as evidenced by sheet resistance values of $7.4 \pm 3.2 \times 10^3$ and $1.7 \pm 0.6 \times 10^4\ \Omega$/square for aligned and random fiber mats, respectively (Lee et al. 2009a). Greater conductivity in aligned fibers was also measured in PLA fibers coated with PPy using an admicellar polymerization procedure (Sudwilai et al. 2014). The synergistic effects of electrical and topographical cues were further corroborated by the stimulation of chick dorsal root ganglia (DRG) on aligned core-sheath PCL-PPy nanofibers that resulted in a 1.5-fold increase in neurite length compared to random unstimulated nanofibers (Xie et al. 2009).

A summary of the studies involving PPy is provided in Table 5.1.

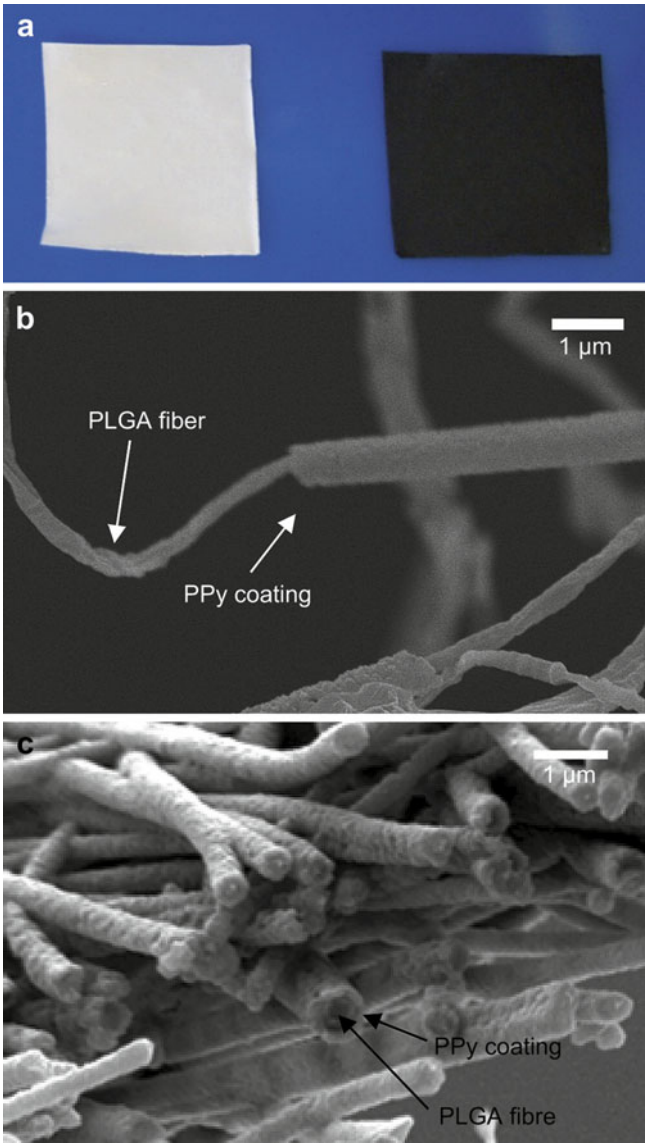

Fig. 5.4 PPy-coated PLGA meshes. (**a**) Photographs of uncoated PLGA meshes (*white*, left) and PPy–PLGA meshes (*black*, right). (**b**) SEM micrograph of single strands of PPy–PLGA fibers. (**c**) SEM image of section of the PPy–PLGA meshes. Images reprinted with permission from the authors and publisher of Lee et al. (2009a)

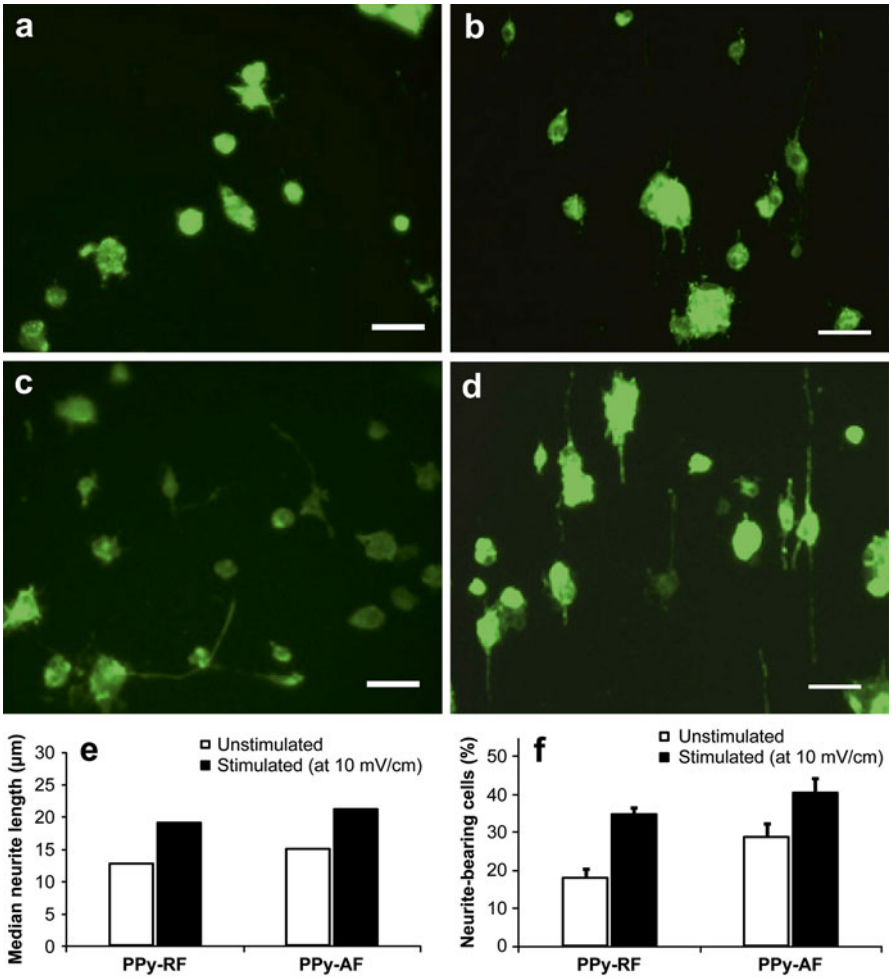

Fig. 5.5 Electrical stimulation of PC12 cells through PPy–PLGA (PPy–RF and PPy–AF) fibers at 0 and 10 mV/cm. Representative fluorescence images of electrically stimulated cells: (**a**) PPy–RF at 0 mV/cm (unstimulated); (**b**) PPy–AF at 0 mV/cm; (**c**) PPy–RF at 10 mV/cm; (**d**) PPy–AF at 10 mV/cm. Scale bars are 50 μm. (**e**) Median neurite lengths, and (**f**) percentages of neurite-bearing PC12 cells when unstimulated and when electrically stimulated (10 mV/cm) on random (PPy–RF) and aligned (PPy–AF) PPy–PLGA fibers. At least 300 neurites were analyzed from four substrates for each condition. Images reprinted with permission from the authors and publisher of Lee et al. (2009a)

Table 5.1 A summary of PPy conductive scaffolds

Material	Conductivity (S/cm)	Cells	Stimulation	Outcome	Reference
PPy	8.1	PC12	–	↑†	Lee et al. (2009b)
PPy-PLGA	[a]7.4–17	PC12; embryonic hippocampal neurons	10 mV/cm or 100 mV/cm for 2 h	↑‡	Lee et al. (2009a)
PPy-PCL, PPy-PECA	19	PC12	100 μA 2 h	↑‡	Durgam et al. (2010)
	32				
PPy-PLGA	[a]64–190	PC12	10 mV/cm 2 h	↑‡	Lee et al. (2012)
PPy		PC12	100 mV/cm 2 h	↑¥, †, ‡	Nickels and Schmidt (2013)
PPy/PDLLA	5.65×10^{-3}–5.56×10^{-4}	PC12	100 mV/cm 2 h	↑†, ‡	(Xu et al. 2014)
PPy	$3.3x10^{-3}$–0.5	F, SC	–	↑¥	Lee and Schmidt (2015)
PPy/chitosan	10^{-3}	SC	100 mV/mm 4 h	↑NGF, BDNF	Huang et al. (2010b)
PCL-PPy	[b]40	Chick DRG	250 μA 4 h/day 6 days	↑‡	Xie et al. (2009)
PPy	–	hESC-derived neurons, rNSCs	–	↑¥, ‡	Zhang et al. (2010a)
PPy-PLGA	–	rNSCs	–[c]	↑ c-fos	Sudwilai et al. (2014)
PPy	–	Cochlear neural explants	–[d]	↑‡	Thompson et al. (2010)
PPy	–	Spiral ganglion neural explants	–[d]	↑†	Thompson et al. (2011))

F Fibroblasts, *SC* Schwann Cells, *m* mouse, *r* rat, *DRGs* dorsal root ganglia
† neurite number, ‡ neurite length, ¥ attachment
[a]Sheet resistance (kΩ/square)
[b]Resistance (kΩ)
[c]100 mV/cm 2 h, biphasic 100 mV/cm 4 h/day for 3 days
[d]Biphasic 1 mA/cm^2 100 μs pulses at 250 Hz 8 h/day

5.2.2.3 PANi

Polyaniline, the chemical structure of which can be seen in Fig. 5.3b, has three oxidation levels: fully oxidized pernigraniline base, half-oxidized emeraldine base, and fully reduced leucoemeraldine base (Balint et al. 2014). Due to its low cost, ease of synthesis, stability, and electrical properties, PANi is the second most studied ICP for NTE applications behind PPy (Balint et al. 2014). The greatest challenges of using PANi in tissue engineering applications are its rigidity, brittleness, and difficulty in processing (Ghasemi-Mobarakeh et al. 2009). Co-polymerizing analine derivatives improves its miscibility with common solvents and other polymers, while blending PANi with other polymers mitigates its brittle and rigid nature in the pure form (Zhang et al. 2014b; Karim 2013; Huang et al. 2008). Ghasemi-Mobarakeh blended 15 wt% PANi with a PCL/gelatin solution to electrospin conductive nanofibers measured to have 0.02 μS conductivity (Ghasemi-Mobarakeh et al. 2009). Nerve stem cells stimulated with a 100 mV/mm stimulus for 60 min exhibited significantly greater proliferation than those stimulated for 15 or 30 min on PANi/PCL/gelatin nanofibers (Ghasemi-Mobarakeh et al. 2009). Similarly, the group blended PANi with PLLA to fabricate electrospun conductive nanofibers for stimulation of neural stem cells (NSCs) (Prabhakaran et al. 2011). Neurite length was measured to be significantly greater for NSCs stimulated on PLLA/PANi nanofibers compared to unstimulated controls (Prabhakaran et al. 2011). PANi composites with PLLA and PCL exhibited low conductivity (3 and 20 nS/cm, respectively). Zhang reported more favorable conductivity and electrical stability of PANi with a 50:50 co-polymer of poly(L-lactic acid-*co*-ε-caprolactone) (P(LLA-CL)) and silk fibroin (PS). Aligned PS/PANi (17 wt%) nanofibers were measured to have a 30 mS/cm conductivity that remained relatively stable over 14 days immersed in serum-free RPMI 1640 medium at 37 °C, with a mild decrease over time likely due to dopant leaching (Zhang et al. 2014b). Further, core–shell PS/PANi nanofibers loaded with NGF supported significantly greater Schwann cell proliferation and significantly greater neurite lengths and number of neurite-bearing PC12 cells after 1 h daily stimulation with a 100 mV/cm stimulus for 5 days (Zhang et al. 2014b). In combination with delivering electrical and topographical guidance cues, these results suggest neurotrophic factors could be released in an electrically controlled manner from conductive core–shell nanofibers (Zhang et al. 2014b).

Another strategy for creating conductive NTE scaffolds is to use PANi as a conductive filler to enhance the weak conductivity of a cationic polyelectrolyte such as chitosan, whose amino groups become partially protonated when hydrated (Baniasadi et al. 2015). A highly conductive polyaniline/graphene nanocomposite (PAG) synthesized by microemulsion and polymerization in the presence of ammonium peroxydisulfate (Baniasadi et al. 2014) was found to be a suitable conductive filler in chitosan/gelatin porous membranes, with conductivities ranging from 2 to 182 mS/cm for 2.5–10 wt% PAG (Baniasadi et al. 2015). Attachment studies revealed the greatest number of Schwann cells on 2.5 wt% PAG chitosan/gelatin scaffolds (Baniasadi et al. 2015).

5.2.2.4 Polythiophenes

Fully bioerodible, electroactive thiophenes have been investigated as layer-by-layer (LBL) systems with polyethyleneimine (PEI) and as hydrogels and evidenced to be biocompatible by promoting L929 fibroblast adhesion and proliferation (Mawad et al. 2011, 2012). The polythiophene derivative poly(3,4-ethylenedioxythiophene) (PEDOT) is the most commonly investigated ICP for use in neural electrodes due to its non-biodegradability, thermal stability, high optical transparency, and low redox potential (Richardson-Burns et al. 2007a, b; Ludwig et al. 2006; Xiao et al. 2004; Cui and Martin 2003; Harris et al. 2013, 2015; Jin et al. 2013). PEDOT has been used as an electroactive coating for nanofibers fabricated from poly(vinyl chloride) and poly(ethylene terephthalate) (PET), exhibiting the ability to support cell adhesion and proliferation of human cancer stem cells and neuroblastoma SH-SY5Y cells (Jin et al. 2013; Bolin et al. 2009). PEDOT composites containing poly(styrene sulfonic acid) PSS are water soluble and bio-erodible over the long term, meaning the molecular weight of erosion products is within the range for renal filtration (30–50 kDa) (Mawad et al. 2011; Pires et al. 2015). The physical stability of PEDOT:PSS can be improved by cross-linking. Electrical stimulation of these substrates can sustain controlled drug release (Esrafilzadeh et al. 2013) and modulate neural stem cell differentiation (Pires et al. 2015). Electrochemical or self-assembly functionalization of PEDOT:PSS films and subsequent electrical stimulation can modulate neural cell adhesion and differentiation (Collazos-Castro et al. 2010). PEDOT/PSS tracks embedded into chitosan and chitosan-hyaluronic acid hydrogels by extrusion printing exhibit high conductivity (17 S cm^{-1}) and demonstrated a versatile fabrication technique for integrating conductive polymers into bio-polymer-based tissue engineering scaffolds for delivery of an electrical signal (Mire et al. 2011). PEDOT has also been chemically polymerized in situ on acellular muscle tissue, providing evidence that it is possible to coat a biological tissue sample with a conductive layer opening up future applications to peripheral nerve repair (Peramo 2008).

5.2.3 Piezoelectric Materials

In piezoelectric materials, electrical charges can be generated by mechanical stress, and vice versa (Rajabi et al. 2015). The most commonly investigated piezoelectric material for biological applications is poly(vinylidene) fluoride (PVDF). During fabrication, the electromechanical properties of PVDF can be induced by mechanical stretching to align the fluorine ions and hydrogen atoms on opposite sides of the carbon backbone in an all-*trans* conformation known as the β-phase (Damaraju et al. 2013; Fine et al. 1991). The material is then rendered piezoelectric in the poling process that applies a high voltage DC field across the polymer to align the otherwise random dipoles in individual crystals (Fine et al. 1991). Poling creates a net dipole moment that, under minute mechanical deformation, results in the

autonomous generation of transient surface charges as an oscillating electrical field (Royo-Gascon et al. 2013). Co-polymerization of PVDF with trifluoroethylene results in the β-phase all-*trans* configuration; the steric hindrance of TrFE groups eliminates the need for mechanical stretching during fabrication thus preserving porous microarchitecture (Fine et al. 1991). Electrospinning is an effective technique to induce β-phase piezoelectricity due to the mechanical stretching that occurs during the fiber formation process, particularly when PVDF is spun with an elastic co-polymer like polyurethane (Guo et al. 2012).

While piezoelectric materials offer the advantage of conducting electricity without external voltage input, the inability to finely regulate and control the waveform characteristics is a disadvantage (Schmidt et al. 1997). PVDF scaffolds have been shown to support a variety of cell types including primary neurons (Royo-Gascon et al. 2013; Lee et al. 2011), human fibroblasts (Guo et al. 2012; Weber et al. 2010), and mesenchymal stem cells (Damaraju et al. 2013). Enhanced nerve regeneration and neurite outgrowth on PVDF-based materials were first reported in a series of studies by Aebischer and Valentini (Fine et al. 1991; Valentini 1992; Valentini et al. 1989; Aebischer et al. 1987). The 1200 Hz resonance frequency of standard incubator shelves in the 1991 Valentini study generated a sinusoidal voltage output with an average peak of 2.5 mV, which resulted in an average substrate charge density of 0.8–1 pC/cm^2 on PVDF films (Valentini 1992). Culture of mouse neuroblastoma cells on poled PVDF films and P(VDF-TrFE) films compared to non-poled films enhanced neurite outgrowth (Valentini 1992). In mouse and rat sciatic nerve injury models, PVDF and P(VDF-TrFE) nerve guidance channels contained significantly greater numbers of myelinated axons (Fine et al. 1991; Aebischer et al. 1987). Piezoelectric charge output was attributed to random animal movements causing mechanical deformations, though actual values were not evaluated.

Other studies have attributed increased neural regeneration to the cell's ability to deform the material thus producing electrical stimulation (Lee et al. 2011; Lee and Arinzeh 2012). Lee et al. electrospun random and aligned nonpiezoelectric PVDF and piezoelectric PVDF-TrFE fibers of nano- and micron-size (Lee et al. 2011). After culturing rat dorsal root ganglia neurons for 4 days on random and aligned, annealed and as-spun fibers. Results showed that annealed, aligned PVDF-TrFE micron-sized fibers exhibited the greatest neurite extension and lowest neurite aspect ratio (Figs. 5.6 and 5.7). Characterization of annealed and as-spun fibers revealed that the former have an increased crystallinity resulting in enhanced piezoelectricity (Lee et al. 2011; Lee and Arinzeh 2012). The annealed fibers, although higher in crystallinity, had a relatively low elastic modulus of 9.4 MPa and supported neuron outgrowth and differentiation (Lee et al. 2011; Lee and Arinzeh 2012). Human neural stem and progenitor cells stimulated on the annealed, micron-sized, aligned PVDF-TrFE fibers differentiated toward neuron-like cells, as evidenced by positive β-III tubulin staining, extended the longest neurites, and also maintained a population of nestin-positive stem cells (Lee and Arinzeh 2012).

Royo-Gascon et al. stimulated primary rat spinal cord neurons for 96 h on polarized PVDF (PZ) and unpolarized PVDF (PV) films at 50 Hz using a custom vibration platform (Royo-Gascon et al. 2013). *Bonfire* (MATLAB scripts), which

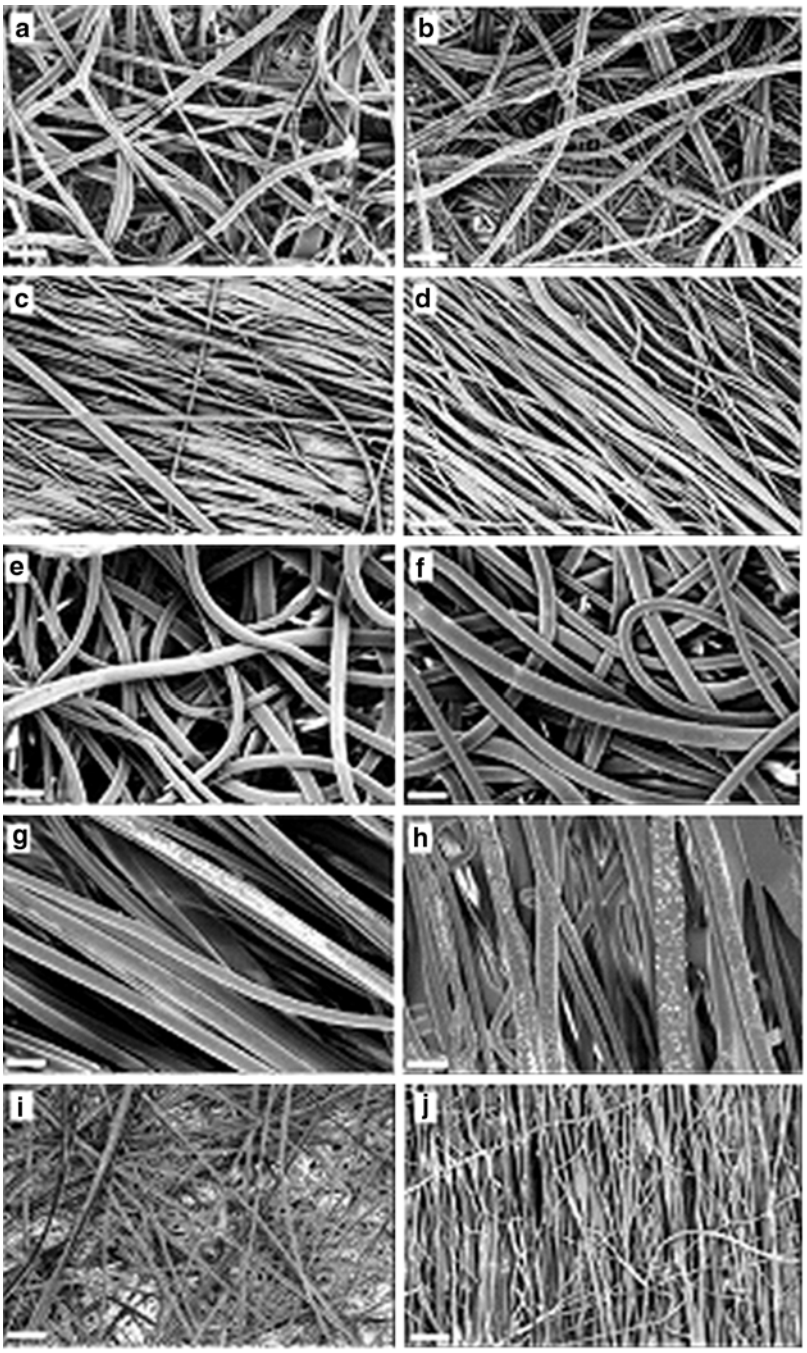

Fig. 5.6 SEM images of electrospun PVDF–TrFE nano-sized random (**a**) as-spun and (**b**) annealed, and aligned (**c**) as-spun and (**d**) annealed, PVDF–TrFE micron-sized random (**e**) as-spun and (**f**) annealed, and aligned (**g**) as-spun and (**h**) annealed, and electrospun PVDF nano-sized (**i**) random and (**j**) aligned scaffolds. Magnification ×3500, scale bar 10 μm. Images reprinted with permission from the authors and publisher of Lee et al. (2011)

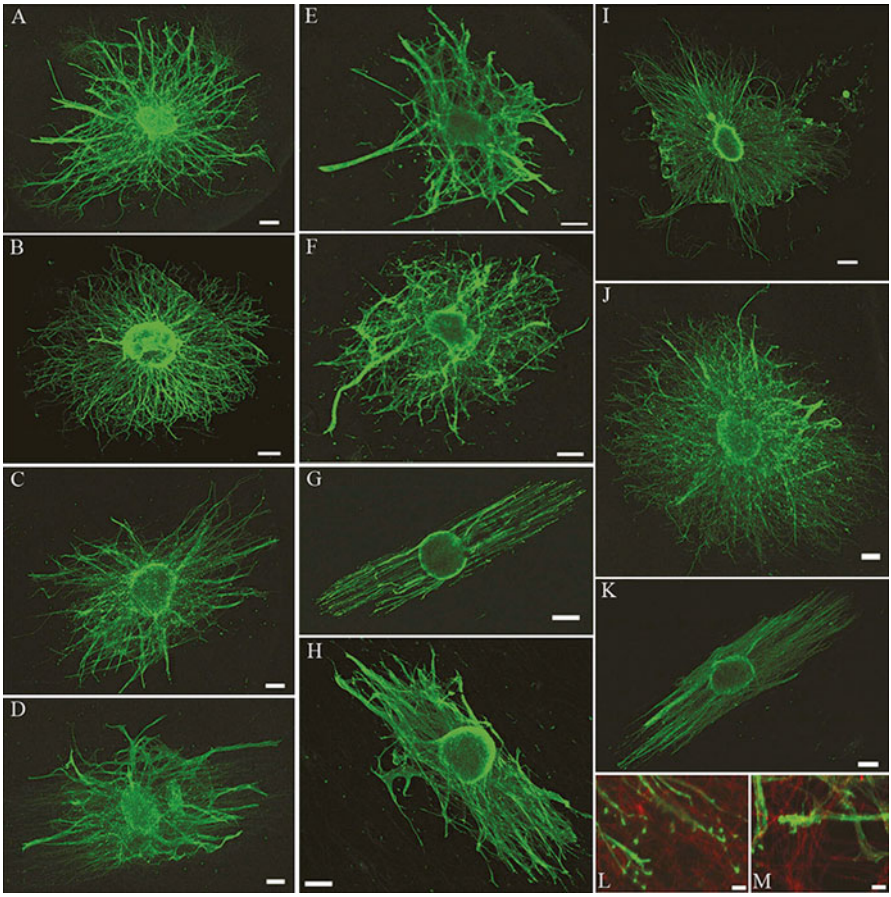

Fig. 5.7 Confocal fluorescent images of DRG stained with phalloidin (actin) on nano-sized as-spun and annealed (**a**, **b**) random and (**c**, **d**) aligned PVDF–TrFE and micron-sized as-spun and annealed (**e**, **f**) random and (**g**, **h**) aligned PVDF–TrFE scaffolds, a collagen-coated surface (**i**), and nano-sized (**j**) random and (**k**) aligned PVDF scaffolds (magnification ×4, scale bar 300 μm). Confocal fluorescent images of DRG neurite tips stained with phalloidin (*green*) attached to PVDF–TrFE micron-sized (**l**) annealed aligned and (**m**) as-spun random fibrous scaffolds (*red*) (magnification ×20, scale bar 50 μm). Images reprinted with permission from the authors and publisher of Lee et al. (2011)

interfaces with *Neuron J* of *Image J*, was used to measure the total number of branch points, terminal points, processes, and branch order. Sholl analysis was used to quantify neurite spreading relative to the soma based on neurites intersecting with superimposed successive concentric circles centered on the soma. Neuronal density was also calculated by immunofluorescently labeled neurons with the microtubule-associated protein 2 (MAP2). All metrics, including branch point and processes, were significantly higher for cells grown on stimulated PZ films. Uniquely, this

study also investigated the effect of mechanical vibration alone by monitoring cells grown on PV films; in all cases, metrics trended toward decreased response compared to cells grown on unstimulated PV films (Royo-Gascon et al. 2013).

Another piezoelectric material, zinc oxide, has demonstrated the ability to support the viability, proliferation, and differentiation of PC12 cells (Ciofani et al. 2012). Although these ZnO nanowire arrays have the potential to deliver electrical stimulation, this was not reported. The ability for an electrical cue to be delivered by bulk mechanical deformation of piezoelectric materials, perhaps by cerebrospinal fluid circulation or body motion, is a compelling property for neural tissue engineering applications (Lee and Arinzeh 2012).

5.3 Nanostructured Carbons

Nanostructured carbons is a general term used to describe carbon-based materials with at least one dimension in the nanoscale, including but not limited to: graphene, single-walled carbon nanotubes (SWCNTs), multi-walled carbon nanotubes (MWCNTs), and amorphous carbon. The electrical, mechanical, chemical, and physical properties of nanostructured carbons make them attractive candidates for incorporation into tissue engineering substrates. In particular, electrical stimulation through nanostructured carbon-containing materials have induced proliferation, differentiation, and neurite extension in neural stem cells and neurons. Further, surface modification of nanostructured carbon allows for delivery of adhesive and trophic cues (Hu et al. 2004; Matsumoto et al. 2007; Jang et al. 2010). However, conflicting reports on carbon-based material toxicity raises concerns of the health risks associated with these materials, requiring researchers to understand the factors that influence the in vitro and in vivo responses to nanostructured carbons (Liu et al. 2012). Factors such as impurities from synthesis, size, surface charge, aspect ratio, layer numbers, agglomeration, and surface topography can induce oxidative stress, inflammation, DNA damage, fibrosis, or tissue transformations (Liu et al. 2012; Bosi et al. 2014; Jain and Pillai 2012). The molecular mechanisms underlying these toxic effects include oxidative stress and apoptosis but have been shown to be concentration and shape dependent (Zhang et al. 2010b). Despite these concerns, there are numerous reports providing evidence supporting neuronal and glial cell growth on nanostructured carbon-based materials, particularly highlighting that aspect ratio, size, and surface modifications improve cytocompatibility (Hu et al. 2004; Liu et al. 2012; Zhang et al. 2010b; Cho and Ben Borgens 2010; Jain et al. 2013a, b; Thompson et al. 2009). Furthermore, several studies have shown the anti-inflammatory effects of graphene foams and SWCNT-PEG hydrogels on microglia and astrocyte cell behavior, respectively (Song et al. 2014; Gottipati et al. 2012, 2013, 2014). Carbon cytocompatibility has been confirmed most recently by an in vivo assessment of chronic CNT fiber implants for electrical stimulation and recording (Vitale et al. 2015). Reduced astrogliosis and microglial and pro-inflammatory macrophage activity was found by immunohistological quantification using CNT fiber electrodes,

while delivering similar neuronal recording efficacy when compared to traditional platinum iridium electrodes (Vitale et al. 2015).

Jain et al. electrospun carbon nanofibers and spin-coated carbon films from polyacrylonitrile solutions in DMF solvent to study neuroblastoma (N2a) and Schwann cell (RT4-D6P2T) fate in response to culture on amorphous carbon structures (Jain et al. 2013a, b). Interestingly, carbon nanofibers and film substrates rendered hydrophilic by oxygen plasma treatment (introduced —COOH groups), supported greater cell viability than UV treated substrates (—OH groups) when tested with the neuroblastoma cell Neuro-2a (N2a). Schwann cells stained for actin after 2 days of culture on carbon nanofibrous substrates showed alignment with the direction of fiber orientation. Flow cytometry analysis revealed there to be no significantly higher degree of apoptosis in Schwann cells after 5 days of culture on carbon nanofibrous substrates, compared to the control cells grown on tissue culture plastic (Jain et al. 2013b).

Since their accidental discovery by Iijima in 1991, carbon nanotubes have inspired researchers to develop conductive composites containing variations of these unique materials for use in biomedical applications (Iijima 1991). Conductive biogels fabricated by drop casting homogeneous dispersions of SWCNTs with DNA, hyaluronic acid (HA), and chitosan (CS) have been reported to have low impedance values suitable for electrical stimulation applications for modulating cell behavior and neurotrophic factors release (Thompson et al. 2009). In a series of studies by Gottipati et al., morphological and functional behavior of astrocytes grown on SWCNT films were found to be mediated by glial fibrillary acidic protein (GFAP) (Gottipati et al. 2012, 2013, 2014). The group attributed the decrease in astrocyte immunoreactivity to a CNT-induced dedifferentiation of astrocytes characterized by morphology and GFAP expression, suggesting similarities to neural stem cells (Gottipati et al. 2013, 2014). Neural stem cells that were stimulated by SWCNTs wound into a ropelike structure differentiated into mature neurons as evidenced by higher MAP2 and β-tubulin III and lower Synapsin I (Syn1) expression (Huang et al. 2012). MAP2 and β-tubulin III serve as neuron-specific markers essential in neurogenesis. MAP2 is involved in microtubule assembly, and the β-tubulin III protein is a microtubule stabilizer (Huang et al. 2012). Syn1 is implicated in the regulation of synapse formation and release of neurotransmitter from synaptic vesicles (Huang et al. 2012).

One study systematically reviewed the effect of MWCNT surface charge on neurite outgrowth from rat hippocampal neurons (Hu et al. 2004). Hu et al. prepared a series of MWCNTs with various charges via chemical functionalization to assess neurite growth and branching. MWCNTs were either functionalized with carboxylic groups to carry a negative charge (MWCNT-COOH), poly-*m*-aminobenzene sulfonic acid to carry a zwitterionic charge (±, MWCNT-PABS), or ethylenediamine to carry a positive charge (MWCNT-EN). Number of neurons, growth cones and neurites, neurite length, and neurite branching were quantified by fluorescence microscopy using calcein for viability or the neuron-specific FITC-conjugated C fragment of tetanus toxin. All three functionalized MWCNTs supported neuronal growth as assessed by positive uptake of calcein. Growth cone number and neurite

length were greatest for the positively charged MWCNT-EN compared to MWCNT-PABS and MWCNT-COOH. Hu et al. concluded that the negatively charged MWCNT-COOH (deprotonated at pH 7.35) are not as effective in promoting initiation of growth cones, whereas the amine groups of the MWCNT-EN are positively charged (Hu et al. 2004).

Results of several studies support the incorporation of MWCNTs in electroactive scaffolds. Cho and Borgens developed MWCNTs/collagen composite films by dispersing HCl-treated MWCNTs in a 1 % w/v collagen solution (Cho and Ben Borgens 2010). The uniform dispersion of the 5 % CNT composite resulted in increased conductivity and lower resistivity (10^5 Ω cm), measured by cyclic voltammetry and four-point probe method. The cyclic voltammograms, the graphical trace output from cyclic voltammetry, for CNT/collagen composite films showed that collagen/CNT composites can transfer electrons to the working electrode surface compared to collagen only. Higher CNT concentration decreased PC12 metabolic activity, regardless of the exposure to 100 mV DC for 6 h. Although 5 % CNT/collagen composites exhibited significantly less viability compared to the 100 % collagen control, it did not appear that the CNT concentration had a negative effect at concentrations of 10 % CNT and below. PC12 cells cultured on 5 % CNT/collagen composites and stimulated with 100 mV for 6 h revealed an increase in neurite extension versus unstimulated cells (Cho and Ben Borgens 2010).

Carboxylated MWCNTs have been successfully electrospun out of an aqueous methacrylated hyaluronic acid solution containing a photoinitiator to form conductive hyaluronic acid nanofibers (CNT-HA) (Fig. 5.8b). Under UV light exposure, and in the presence of a photoinitiator, the HA methacrylate groups crosslink to provide stability (Ifkovits et al. 2009). Electrical stimulation was delivered through the CNT-HA fibers to whole chick DRG cultures for 4 h using a 4 mV/mm peak-to-peak square wave at a 1 kHz frequency. Anti-neurofilament and DAPI staining revealed robust outgrowth on both unstimulated and stimulated CNT-HA nanofibers as seen in Fig. 5.8 parts C and D, respectively.

Aligned electrospun poly (L-lactic acid-co-caprolactone) (PLCL) nanofibers have been coated with MWCNTs following anionic modification with potassium sodium tartrate (Jin et al. 2011a, b). SEM analysis revealed MWCNT-coated PLCL fibers to be generally rougher than the PLCL fibers alone; diameters were measured to be between 1.3 and 1.5 μm. Jin et al. assessed neurite outgrowth of rat dorsal root ganglia neurons cultured on aligned MWCNT-coated PLCL fibers for up to 9 days by fluorescence microscopy after staining with Phalloidin to visualize actin filaments. Compared to control-aligned PLCL fibers, PC12 neurite length on aligned MWCNT-coated PLCL fibers was significantly greater. Notably, PC12 FAK expression, indicative of integrin-mediated signal transduction involved in neurite outgrowth, was assessed on the MWCNT-coated PLCL fibers by western blot band intensity and found to be higher compared to the control (Jin et al. 2011a).

In recent years, graphene has garnered much attention as a potential conductive material in the development of electroactive scaffolds. Graphene deposited via LbL assembly onto PCL films and nanofibers enhanced primary cortical neuron attachment and spreading, and supported branched and elongated neurites compared to

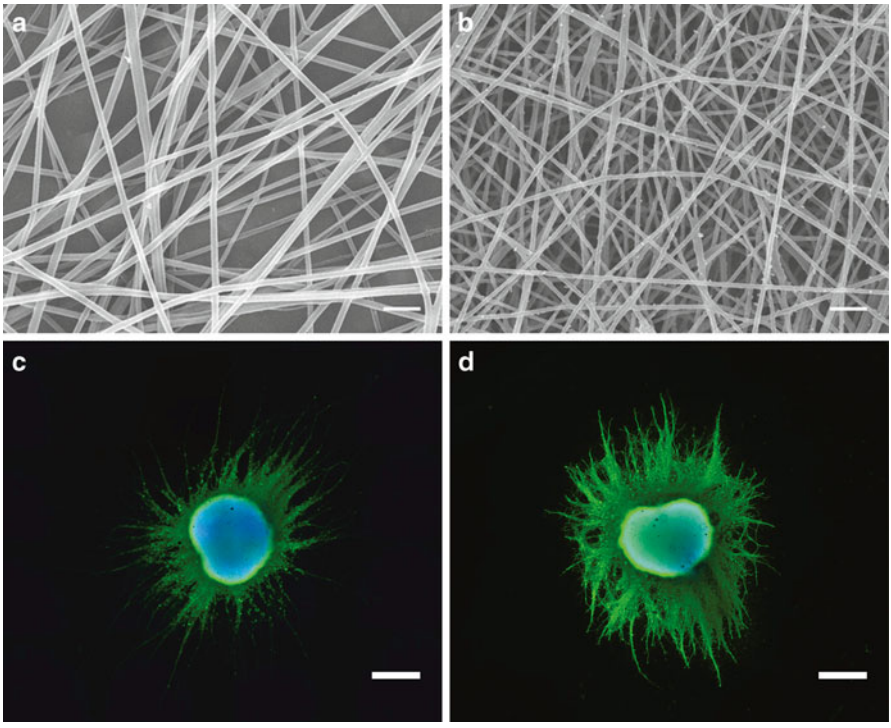

Fig. 5.8 FE-SEM micrographs (scale bar 1 μm) of (**a**) pristine MWCNTs (**b**) HA nanofibers. DRGs grown on 1 % CNT-HA nanofibers after 96 h culture (**a**) unstimulated or (**b**) stimulated (scale bar 500 μm)

unmodified PCL (Zhou et al. 2012). Sherrell and colleagues from the Wallace group were the first to report electrical stimulation of PC12 cells on graphene. Following 8 h of electrical stimulation daily for 3 days, a dramatic increase was observed in neurite length and connectivity compared to unstimulated cells cultured on bilayer graphene-coated 50:50 PLGA substrates (Sherrell et al. 2014). Both of these studies validate the ability to develop biocompatible conductive composites utilizing graphene. The latter study employed drop-casting of the biopolymers over graphene during fabrication. The self-assembly layer-by-layer fabrication technique in the Zhou et al. study could find wider application for incorporating graphene in biopolymer composites for electrical stimulation. In this method, graphene-polyelectrolyte multi-layers (PEMs) were self-assembled onto the substrate after surface activation with polythyleneimine by soaking in alternating solutions of a colloidal suspension of graphene nanosheets in a heparin solution (anionic layer) and a poly-L-lysine (PLL) solution (cationic layer) (Zhou et al. 2012). Elsewhere, the Wallace group has reported successful preparation of stable dispersions of chemically converted graphene (CCG) in dimethylformamide (DMF), which led to the fabrication of covalently linked graphene/polycaprolactone composites

(cPCL-CCG) (Sayyar et al. 2013). Material characterization of the PCL-CCG composites confirmed homogenous dispersion of the graphene nanosheets within the PCL polymer matrix. The conductivities of the cPCL-CCG composites with 0.5 and 5 % CCG were ~10 and ~11 orders of magnitude greater than pristine PCL (Sayyar et al. 2013). Incorporation of CCG into PCL scaffolds did not alter biocompatibility; films robustly supported the attachment and proliferation of 3 different cell types: L929 fibroblasts, C2C12 myoblasts, and PC12 cells (Sayyar et al. 2013).

A summary of the studies involving the other ICPs as well as piezoelectric and nanostructured carbons is provided in Table 5.2.

5.4 In Vivo Studies

Most of the in vivo work with conductive materials completed to date have been assessments of biocompatibility and nerve regeneration without the application of electrical stimulation. Yu et al. electrospun 1 % w/w MWCNT into collagen/PCL nanofibers to form nerve guide conduits (NGCs) to study treatment efficacy as well as the biocompatibility and toxicology of MWCNTs in an in vivo rat sciatic nerve injury model (Yu et al. 2014). The scaffolds demonstrated the abilities to support in vitro Schwann cell adhesion and elongation and to promote in vivo nerve regeneration without inducing inflammation when compared to the negative control (Yu et al. 2014).

PPy-copolymers have also exhibited in vivo biocompatibility. In the 2010 Durgam study, biodegradable composite nerve guidance channels were fabricated by airbrushing a layer of a PPy co-polymer over poly(3-hydroxybutyrate-co-3-hydroxyvalerate) (PHB-HV) films which were then cut and rolled around a 1.2-mm mandrel (Durgam et al. 2010). The PPy block co-polymer was synthesized with either PCL or poly(ethyl cyanoacrylate) (PECA). NGCs were used to repair 10-mm gaps in the sciatic nerve and recovered for histology after 8 weeks. No inflammation was detected as evidenced by the absence of macrophages. All of the NGC treatments using either PPy, PPy-PECA, PHB-V, or PPy-PCL resulted in fiber cables of comparable size with similar density of neurofilament (Durgam et al. 2010). Xu et al. fabricated PPy/PDLLA conduits by a dip coating method in which a cylindrical mandrel was repeatedly submerged into a PPy/PDLLA emulsion (Xu et al. 2014). Five percent PPy/PDLLA nerve conduits bridged 10 mm defects in a rat sciatic nerve model. After 6 months, the functional recovery and nerve regeneration in rats receiving PPy/PDLLA conduits were significantly greater than those with PDLLA conduits and statistically similar to autologous nerve grafts.

Numerous studies from the Gordon group have investigated the application of electrical stimulation to the injured sciatic nerve with electrodes rather than a material intervention. The electrodes consist of looped insulated wires on either side of the nerve stump, with the anode located proximally and the cathode distal to the repair site. The stimulator delivered supramaximal 3 V, 100 μs impulses in a continuous 20 Hz train, the frequency of hindlimb motoneuron discharge, for either 1 h,

Table 5.2 A summary of conductive scaffolds

Material	Conductivity (S/cm)	Cells	Stimulation	Outcome	References
PANi/PCL/gelatin	2×10^{-8}	NSCs	100 mV/mm 1 h	↑§	Ghasemi-Mobarakeh et al. (2009)
PLLA/PANi	3×10^{-9}–20×10^{-9}	NSCs	100 mV/mm 1 h	↑‡	Prabhakaran et al. (2011)
PCL/PANi					
PANi/P(LLA-CL)/ silk fibroin	3×10^{4}	SC, PC12	100 mV/cm 1 h 5 days	↑§	Zhang et al. (2014b)
				↑†, ‡	
PANi/graphene/ chitosan/gelatin	2×10^{-3}–0.182	SC	–	↑¥	Huang et al. (2008)
PEDOT/PSS	–	r eCCN	−3 mC/cm^2 in 15 min	↑¥	Esrafilzadeh et al. (2013)
P(VDF-TrFE)	–	r *n*	0.8–1 pC/cm^2	↑‡	Valentini (1992)
PVDF-TrFE	–	rDRGs	–	↑‡	Lee et al. (2011)
PVDF-TrFE	–	hNSCs	–	±	Lee and Arinzeh (2012)
PVDF	–	rMNs	50 Hz	↑†, ‡, ∫	Royo-Gascon et al. (2013)
MWCNT/collagen	[b]100	PC12	100 mV/cm 6 h	↑†, ‡	Cho and Ben Borgens 2010)
Graphene/PLGA	[a]1	PC12	–[c]	↑‡	Sherrell et al. (2014)
Graphene/PCL	1×10^{-11}–0.001	PC12	–	↑¥, §	Sayyar et al. (2013)

F Fibroblasts, *SC* Schwann cells, *m* mouse, *r* rat, *eCCN* embryonic cerebral cortical neurons, *n* neuroblastoma, *DRGs* dorsal root ganglia, *MN* motoneurons
† neurite number, ‡ neurite length, ∫ neurite branching and density
¥ attachment, § proliferation, ± differentiated to neuron-like cells
[a]Sheet resistance (kΩ/square)
[b]Resistance (kΩ)
[c]Biphasic 1 mA/cm^2 100 μs pulses at 250 Hz 8 h/day

1 day, 1 week, or 2 weeks (Al-Majed et al. 2000a). In the 2000 study, which used neurotracers to backlabel motorneurons that have been cut following regeneration, it was found that 1 h of stimulation was equally as effective as the long-term conditions in accelerating complete regeneration of the nerve from 10 weeks to 3 weeks. Based on the additional findings using an action potential blockade experiment that the effects of electrical stimulation were mediated by the neuron cell bodies, a separate study reported the results of in situ hybridization measurements that electrical stimulation increases the motoneuron expression of BDNF and its receptor trkB (Al-Majed et al. 2000b). Further, accelerated axon growth was associated with an upregulation of the regeneration-associated genes of Tα1-tubulin and GAP-43, a cytoskeleton protein and stabilizer(Al-Majed et al. 2004). Direct application of electrical stimulation to the injured nerve following repair has also resulted in accelerated sensory axon regeneration and functional recovery and modulated spinal cord plasticity by maintaining the expression of substance P in afferent neurons in the dorsal horn (Brushart et al. 2002; Brushart et al. 2005; Geremia et al. 2007; Vivo et al. 2008).

5.5 Conclusions and Future Directions

There are a variety of potential material candidates to serve as scaffold components to deliver an electrical cue. Future work should include systematic characterization of the molecular mechanisms underlying regenerative cell behavior following electrical stimulation. Understanding the conductive material-protein-cell interactions informs material selection during scaffold design and is crucial in developing clinically translational neural tissue engineering treatments.

5.5.1 Electrical Stimulation: Incomplete Mechanistic Evidence

A handful of studies have provided evidence for identifying molecular targets affected by electrical stimulation. A 2012 Guo et al. study observed an increase in the expression of the extracellular matrix proteins collagen I, elastin, and fibronectin I by NIH 3T3 fibroblasts piezoelectrically excited through polyurethane (PU)/PVDF scaffolds affixed to a flexible-bottomed culture plate (Flexcell) by applying an 8 % deformation at 0.5 Hz (Guo et al. 2012). The protein expression from cells cultured on nonpiezoelectric-excited PU/PVDF scaffolds and PU scaffolds under the same deformation conditions were not significantly different from one another (Guo et al. 2012). When PC12 cells were cultured on a CNT-coated PLCL fibrous scaffold, Jin et al. discovered increased expression of focal adhesion kinase (FAK), which plays a role in integrin-mediated binding (Jin et al. 2011a). Although this result suggests that FAK activation due to integrin receptors binding to CNTs may be involved in the pathway responsible for increased neurite outgrowth, further investigation is needed to determine if this observation is repeatable and

quantifiable under electrical stimulation conditions. Using adult rat DRG neurons and PC12 cells, Eva et al. demonstrated that the proteins ARF6 and Rab11 are required for optimal integrin-dependent axon regeneration following injury, due to their roles in trafficking of the integrin subunits, *α9* and *β1* (Eva et al. 2012). These integrins may serve as viable targets to elucidate their involvement in FAK activation in future studies.

Other studies investigating receptor-mediated mechanisms indicate voltage-gated calcium channels to play a role in enhanced neurite outgrowth. Several studies have reported accelerated motoneuron axonal regeneration in response to an AC square wave signal that was associated with an upregulation of BDNF and the receptor trkB (Al-Majed et al. 2000b, 2004). Multiple promoters can be activated to induce BDNF transcription by pathways involving trkB receptors as well as through calcium influx through voltage-gated calcium channels and NMDA receptors. Ca^{2+}-dependent signaling is propagated to calcium responsive elements regulated by calcium-stimulated protein kinases (Zheng et al. 2011). After being released from the post-synaptic membrane, BDNF can act in an autocrine fashion on local trkB receptors triggering the MAPK signaling cascade that downstream increases actin polymerization (Brushart et al. 2002; Hronik-Tupaj et al. 2013; Difato et al. 2011). Calcium influx has also been associated with f-actin polymerization during growth cone formation (Kamber et al. 2009). GAP-43 stabilizes f-actin polymerization and microtubule formation in the growth cone (Aigner and Caroni 1995). Interestingly, the electrical stimulation studies that found increased expression of BDNF and its receptor trk-B associated with accelerated motoneuron growth, also found an increase in GAP-43 expression and the cytoskeletal proteins tubulin and actin (Al-Majed et al. 2004; Hronik-Tupaj et al. 2013).

Wenjin et al. (2011) demonstrated that BDNF expression following electrical stimulation is dependent on calcium influx through voltage-gated calcium channels (VGCC), which activates the extracellular signal regulated kinase (Erk) pathways. Electrical stimulation of spinal cord neuron cultures treated with the L-type VGCC inhibitor nifedipine resulted in a reduction in the upregulation of BDNF expression seen with the stimulated controls (Wenjin et al. 2011). Nifedipine is in the dihydropyridine class of antagonistic molecules that block L-type VGCC activity (Gurkoff et al. 2013). The Erk phosphorylation inhibitor PD98059 eliminated the upregulation of BDNF seen in stimulated controls and reduced expression beyond the basal levels measured in the unstimulated controls. PD98058 specifically blocks the phosphorylation of Erk which then prevents the phosphorylation of the transcription factor CREB required in BDNF transcription (Wenjin et al. 2011).

Calcium channels and two-pore domain potassium (2-PK) channels can be influenced by electrical stimulation serving to activate neurite outgrowth through cytoskeletal protein synthesis (Huang et al. 2012; Mathie et al. 2003). Electric field stimulation may regulate protein kinase A and C phosphorylation, which mediate the activation of the 2-PK channel (Mathie et al. 2003). Two groups have demonstrated that electrical stimulation of Schwann cells activates T-type voltage-gated calcium channels leading to increased intracellular calcium production resulting in calcium-dependent exocytosis of NGF (Huang et al. 2010b; Koppes et al. 2014). Similarly, through the use of calcium imaging, VGCCs have been identified as the

transducers of electrical cues in neural stem cells differentiated into neurons (Park et al. 2011) and embryonic rat hippocampal neurons (Wang et al. 2006), when stimulated through graphene and CNT substrates.

Toward defining electrical cue signal parameters, Shi et al. applied both voltage-defined signals (100 mV/mm) and current-defined signals (2.5, 25, and 250 μA/mm) to human cutaneous fibroblasts cultured on gold-coated Petri dishes (Shi et al. 2008). They found no significant effect of the surface current density on cell adhesion or viability; whereas, the constant 100 mV/mm electrical field significantly increased adhesion and viability. These results taken in accordance with the previous discussion on VGCCs suggest that voltage rather than current modulates the effects of electrical stimulation on cell behavior. One theory suggests that enhanced neurite outgrowth may be due to ionic current in the culture medium or interstitial fluid due to the applied electric field (Schmidt et al. 1997; Patel and Poo 1982).

There is debate concerning the method of electrical stimulation, as to whether the electrodes that are delivering the electrical signal to the conductive material must be separated from the media surrounding the cells during culture (Pires et al. 2015). Schmidt argues that if the stimulus is under the point at which electrolysis of water occurs (1.2 V), then the electrodes can be in contact with the cell media (Schmidt et al. 1997). Results from both Patel and Schmidt provide evidence that field-induced ion transport through the media played no role in the effects elicited by electrical stimulation. The former discovered more growth-controlling membrane glycoproteins in growth cones near the cathode, suggesting an electrophoretic redistribution of charged membrane components (Patel and Poo 1982). When cells are cultured on plastic with an exogenously applied current, Schmidt and colleagues found results similar to the non-stimulated control (Schmidt et al. 1997).

Other studies attribute enhanced cell behavior to be due to the attraction and adsorption of serum proteins to the surface of the stimulated substrate. Kotwal and Schmidt observed enhanced neurite outgrowth in PC12 cells following surface adsorption of fibronectin to PPy films (Kotwal and Schmidt 2001). Interestingly, neurite outgrowth was not increased if stimulation was delayed for 2 h. The group offered altered protein conformation following stimulation to explain enhanced neurite outgrowth. Recently, Schmidt and colleagues have systematically investigated the effects of protein adsorption and electric field strength on Schwann cell behavior. Their results suggest that Schwann cell migration directionality toward the anode is a function of electric-field-mediated phenomenon whereas migration speed is an integrin- or receptor-mediated phenomenon (Forciniti et al. 2014). Factors such as using composite PPy materials or co-culturing Schwann cells with neurons could be effecting the results of previous studies that concluded that migration is electric field mediated. For example, Quigley observed increased migration distance of Schwann cells from DRG explants after electrical stimulation on a PPy platform upon which 75:25 PLA:PLGA fibers had been wet-spun (Quigley et al. 2009). Cell–cell interactions between neurons and Schwann cells as well as the polymer blend may have influenced Schwann cell behavior.

5.5.2 *Future Work*

While there is an ever-growing body of studies indicating benefits of electrical stimulation, future in vitro studies should include data to elucidate the molecular mechanisms behind enhanced neural and glial cell behavior. Experiments utilize quantitative RT-PCR, in-cell western blot analyses, and flow cytometry function to determine the targets and molecular pathways involved. siRNA knockdown studies could help determine signal transduction pathways that may be affected by electrical stimulation. Once more comprehensive evidence of molecular mechanisms has been collected, electrical stimulation of co-cultures of neurons and glial cells could be informative to gain a systems understanding. Further, once molecular pathway targets have been identified, the exact parameters of the electrical stimulus or waveform necessary to elicit desired effects can be defined.

It is critical to drive forward animal testing to gain crucial information regarding long-term physiological response to conductive materials, functional recovery of nerves, and immune response to degradation products. In a review of peripheral nerve regeneration, Bellamkonda emphasizes several key points with regards to evaluating scaffold efficacy in animal models. First, the scaffolds in question should repair nerve defects greater than 15 mm (in rats) and be compared to control autografts. If these repairs are successful, the scaffolds should then be tested in a larger animal model with gap lengths greater than 40 mm. He asserts that in order for these interventions to be clinically translatable, it is equally important to perform electrophysiological studies to assess the functional repair of sensory and motor nerve fibers in addition to histological measurement of neuromuscular junctions (Bellamkonda 2006). Extending these principles to in vivo electrical stimulation studies is essential for characterizing the efficacy of interventions using conductive scaffolds.

From the conductive scaffold design and synthesis side, fabrication techniques utilizing 3D printing and extrusion technologies may become more widespread. Mire et al. embedded conductive PEDOT tracks into chitosan and HA-based substrates using custom-built extrusion printing systems with programmable *xyz*-translation paving the way for future gel matrix-based, integrated structures containing embedded conductive components, cells, and microdevices (Mire et al. 2011). Inkjet printing techniques allow for high resolution for enhanced spatial control over cell behavior when delivering electrical stimulation (Mire et al. 2011; Weng et al. 2012).

5.6 Conclusion

To summarize, studies to date have demonstrated the potential for electrically conductive materials to elicit regenerative behavior in neural tissue cell types. Future success in clinical translation is dependent on:

(1) Characterizing the mechanisms influenced by electrical stimulation that influence cell behavior
(2) Designing conductive materials that meet all of the design criteria
(3) and systematically testing efficacy in functional in vivo studies

The implications of developing effective conductive biomaterials that modulate cell behavior based on mechanistic understanding extend beyond neural tissue into the broader realm of all organ systems in the tissue engineering and regenerative medicine fields.

References

Aebischer, P., R.F. Valentini, P. Dario, C. Domenici, and P.M. Galletti. 1987. Piezoelectric Guidance Channels Enhance Regeneration in the Mouse Sciatic Nerve After Axotomy. *Brain Research* 436(1): 165–168.

Aigner, L., and P. Caroni. 1995. Absence of Persistent Spreading, Branching, and Adhesion in GAP-43-Depleted Growth Cones. *The Journal of Cell Biology* 128(4): 647–660.

Al-Majed, A.A., C.M. Neumann, T.M. Brushart, and T. Gordon. 2000a. Brief Electrical Stimulation Promotes the Speed and Accuracy of Motor Axonal Regeneration. *Journal of Neuroscience* 20(7): 2602–2608.

Al-Majed, A.A., T.M. Brushart, and T. Gordon. 2000b. Electrical Stimulation Accelerates and Increases Expression of BDNF and trKB rnRNA in Regenerating Rat Femoral Motoneurons. *European Journal of Neuroscience* 12(12): 4381–4390. doi:10.1111/j.1460-9568.2000.01341.x.

Al-Majed, A.A., S.L. Tam, and T. Gordon. 2004. Electrical Stimulation Accelerates and Enhances Expression of Regeneration-Associated Genes in Regenerating Rat Femoral Motoneurons. *Cellular and Molecular Neurobiology* 24(3): 379–402. doi:10.1023/B:CEMN.0000022770.66463.f7.

Balint, R., N.J. Cassidy, and S.H. Cartmell. 2014. Conductive Polymers: Towards a Smart Biomaterial for Tissue Engineering. *Acta Biomaterialia* 10(6): 2341–2353. doi:10.1016/j.actbio.2014.02.015.

Baniasadi, H., S.A.A. Ramazani, S. Mashayekhan, and F. Ghaderinezhad. 2014. Preparation of Conductive Polyaniline/Graphene Nanocomposites Via In Situ Emulsion Polymerization and Product Characterization. *Synthetic Metals* 196: 199–205. doi:10.1016/j.synthmet.2014.08.007.

Baniasadi, H., S.A.A. Ramazani, and S. Mashayekhan. 2015. Fabrication and Characterization of Conductive Chitosan/Gelatin-Based Scaffolds for Nerve Tissue Engineering. *International Journal of Biological Macromolecules* 74: 360–366. doi:10.1016/j.ijbiomac.2014.12.014.

Bellamkonda, R.V. 2006. Peripheral Nerve Regeneration: an Opinion on Channels, Scaffolds and Anisotropy. *Biomaterials* 27(19): 3515–3518. http://dx.doi.org/10.1016/j.biomaterials.2006.02.030.

Bolin, M.H., K. Svennersten, X. Wang, I.S. Chronakis, A. Richter-Dahlfors, W.W.H. Jager, and M. Berggren. 2009. Nano-Fiber Scaffold Electrodes Based on PEDOT for Cell Stimulation. *Sensors and Actuators B: Chemical* 142(2): 451–456. http://dx.doi.org/10.1016/j.snb.2009.04.062.

Bosi, S., L. Ballerini, and M. Prato. 2014. Carbon Nanotubes in Tissue Engineering. In: *Making and Exploiting Fullerenes, Graphene, and Carbon Nanotubes*, eds. M. Marcaccio, F. Paolucci, vol. 348. *Topics in Current Chemistry*, 181–204. Springer. doi:10.1007/128_2013_474.

Broda, C.R., J.Y. Lee, S. Sirivisoot, C.E. Schmidt, and B.S. Harrison. 2011. A Chemically Polymerized Electrically Conducting Composite of Polypyrrole Nanoparticles and Polyurethane for Tissue Engineering. *Journal of Biomedical Materials Research. Part A* 98A(4): 509–516. doi:10.1002/jbm.a.33128.

Brushart, T.M., P.N. Hoffman, R.M. Royall, B.B. Murinson, C. Witzel, and T. Gordon. 2002. Electrical Stimulation Promotes Motoneuron Regeneration Without Increasing Its Speed or Conditioning the Neuron. *Journal of Neuroscience* 22(15): 6631–6638.

Brushart, T.M., R. Jari, V. Verge, C. Rohde, and T. Gordon. 2005. Electrical Stimulation Restores the Specificity of Sensory Axon Regeneration. *Experimental Neurology* 194(1): 221–229. doi:10.1016/j.expneuro.2005.02.007.

Cho, Y.N., and R. Ben Borgens. 2010. The Effect of an Electrically Conductive Carbon Nanotube/Collagen Composite on Neurite Outgrowth of Pc12 Cells. *Journal of Biomedical Materials Research. Part A* 95A(2): 510–517. doi:10.1002/jbm.a.32841.

Ciofani, G., G.G. Genchi, and V. Mattoli. 2012. ZnO Nanowire Arrays as Substrates for Cell Proliferation and Differentiation. *Materials Science and Engineering C—Materials for Biological Applications* 32(2): 341–347. doi:10.1016/j.msec.2011.11.001.

Collazos-Castro, J.E., J.L. Polo, G.R. Hernández-Labrado, V. Padial-Cañete, and C. García-Rama. 2010. Bioelectrochemical Control of Neural Cell Development on Conducting Polymers. *Biomaterials* 31(35): 9244–9255.

Collier, J.H., J.P. Camp, T.W. Hudson, and C.E. Schmidt. 2000. Synthesis and Characterization of Polypyrrole-Hyaluronic Acid Composite Biomaterials for Tissue Engineering Applications. *Journal of Biomedial Materials Research* 50(4): 574–584. doi:10.1002/(sici)1097-4636(20000615)50:4<574::aid-jbm13>3.0.co;2-i.

Cui, X., and D.C. Martin. 2003. Electrochemical Deposition and Characterization of Poly (3,4-Ethylenedioxythiophene) on Neural Microelectrode Arrays. *Sensors and Actuators B: Chemical* 89(1): 92–102.

Damaraju, S.M., S.L. Wu, M. Jaffe, and T.L. Arinzeh. 2013. Structural Changes in Pvdf Fibers Due to Electrospinning and its Effect on Biological Function. *Biomedical Materials* 8(4): 11. doi:10.1088/1748-6041/8/4/045007.

Dhandayuthapani, B., Y. Yoshida, T. Maekawa, and D.S. Kumar. 2011. Polymeric Scaffolds in Tissue Engineering Application: A Review. *International Journal of Polymer Science* 2011. doi:10.1155/2011/290602.

Difato, F., H. Tsushima, M. Pesce, F. Benfenati, A. Blau, and E. Chieregatti. 2011. The Formation of Actin Waves During Regeneration After Axonal Lesion Is Enhanced by BDNF. *Scientific Reports* 1: 10. doi:10.1038/srep00183.

Durgam, H., S. Sapp, C. Deister, Z. Khaing, E. Chang, S. Luebben, and C.E. Schmidt. 2010. Novel Degradable Co-polymers of Polypyrrole Support Cell Proliferation and Enhance Neurite Out-Growth with Electrical Stimulation. *Journal of Biomaterials Science—Polymer Edition* 21(10): 1265–1282. doi:10.1163/092050609x12481751806330.

Esrafilzadeh, D., J.M. Razal, S.E. Moulton, E.M. Stewart, and G.G. Wallace. 2013. Multifunctional Conducting Fibres with Electrically Controlled Release of Ciprofloxacin. *Journal of Controlled Release* 169(3): 313–320. doi:10.1016/j.jconrel.2013.01.022.

Eva, R., S. Crisp, J.R. Marland, J.C. Norman, V. Kanamarlapudi, C. Ffrench-Constant, and J.W. Fawcett. 2012. ARF6 Directs Axon Transport and Traffic of Integrins and Regulates Axon Growth in Adult DRG Neurons. *The Journal of Neuroscience: The Official Journal of the Society for Neuroscience* 32(30): 10352–10364. doi:10.1523/jneurosci.1409-12.2012.

Fine, E.G., R.F. Valentini, R. Bellamkonda, and P. Aebischer. 1991. Improved Nerve Regeneration Through Piezoelectric Vinylidenefluoride-Trifluoroethylene Copolymer Guidance Channels. *Biomaterials* 12(8): 775–780.

Forciniti, L., J. Ybarra, M.H. Zaman, and C.E. Schmidt. 2014. Schwann Cell Response on Polypyrrole Substrates Upon Electrical Stimulation. *Acta Biomaterialia* 10(6): 2423–2433. doi:10.1016/j.actbio.2014.01.030.

Geremia, N.M., T. Gordon, T.M. Brushart, A.A. Al-Majed, and V.M.K. Verge. 2007. Electrical Stimulation Promotes Sensory Neuron Regeneration and Growth-Associated Gene Expression. *Experimental Neurology* 205(2): 347–359. doi:10.1016/j.expneurol.2007.01.040.

Ghasemi-Mobarakeh, L., M.P. Prabhakaran, M. Morshed, M.H. Nasr-Esfahani, and S. Ramakrishna. 2009. Electrical Stimulation of Nerve Cells Using Conductive Nanofibrous Scaffolds for Nerve

Tissue Engineering. *Tissue Engineering. Part A* 15(11): 3605–3619. doi:10.1089/ten.tea.2008.0689.

Ghasemi-Mobarakeh, L., M.P. Prabhakaran, M. Morshed, M.H. Nasr-Esfahani, H. Baharvand, S. Kiani, S.S. Al-Deyab, and S. Ramakrishna. 2011. Application of Conductive Polymers, Scaffolds and Electrical Stimulation for Nerve Tissue Engineering. *Journal of Tissue Engineering and Regenerative Medicine* 5(4): e17–e35. doi:10.1002/term.383.

Gottipati, M.K., I. Kalinina, E. Bekyarova, R.C. Haddon, and V. Parpura. 2012. Chemically Functionalized Water-Soluble Single-Walled Carbon Nanotubes Modulate Morpho-Functional Characteristics of Astrocytes. *Nano Letters* 12(9): 4742–4747. doi:10.1021/nl302178s.

Gottipati, M.K., J.J. Samuelson, I. Kalinina, E. Bekyarova, R.C. Haddon, and V. Parpura. 2013. Chemically Functionalized Single-Walled Carbon Nanotube Films Modulate the Morpho-Functional and Proliferative Characteristics of Astrocytes. *Nano Letters* 13(9): 4387–4392. doi:10.1021/nl402226z.

Gottipati, M.K., E. Bekyarova, M. Brenner, R.C. Haddon, and V. Parpura. 2014. Changes in the Morphology and Proliferation of Astrocytes Induced by Two Modalities of Chemically Functionalized Single-Walled Carbon Nanotubes Are Differentially Mediated by Glial Fibrillary Acidic Protein. *Nano Letters* 14(7): 3720–3727. doi:10.1021/nl4048114.

Greene, L.A., and A.S. Tischler. 1976. Establishment of a Noradrenergic Clonal Line of Rat Adrenal Pheochromocytoma Cells Which Respond to Nerve Growth Factor. *Proceedings of the National Academy of Sciences of the United States of America* 73(7): 2424–2428.

Guo, H.F., Z.S. Li, S.W. Dong, W.J. Chen, L. Deng, Y.F. Wang, and D.J. Ying. 2012. Piezoelectric PU/PVDF Electrospun Scaffolds for Wound Healing Applications. *Colloids and Surfaces B: Biointerfaces* 96: 29–36. doi:10.1016/j.colsurfb.2012.03.014.

Gurkoff, G., K. Shahlaie, B. Lyeth, and R. Berman. 2013. Voltage-Gated Calcium Channel Antagonists and Traumatic Brain Injury. *Pharmaceuticals (Basel, Switzerland)* 6(7): 788–812. doi:10.3390/ph6070788.

Hardy, J.G., J.Y. Lee, and C.E. Schmidt. 2013. Biomimetic Conducting Polymer-Based Tissue Scaffolds. *Current Opinion in Biotechnology* 24(5): 847–854. doi:10.1016/j.dopbio.2013.03.011.

Harris, A.R., S.J. Morgan, J. Chen, R.M.I. Kapsa, G.G. Wallace, and A.G. Paolini. 2013. Conducting Polymer Coated Neural Recording Electrodes. *J Neural Eng* 10(1): 016004. doi:10.1088/1741-2560/10/1/016004.

Harris, A.R., P.J. Molino, R.M.I. Kapsa, G.M. Clark, A.G. Paolini, and G.G. Wallace. 2015. Optical and Electrochemical Methods for Determining the Effective Area and Charge Density of Conducting Polymer Modified Electrodes for Neural Stimulation. *Analytical Chemistry* 87(1): 738–746. doi:10.1021/ac503733s.

Higgins, M.J., and G.G. Wallace. 2013. Surface and Biomolecular Forces of Conducting Polymers. *Polymer Reviews* 53(3): 506–526. doi:10.1080/15583724.2013.813856.

Hronik-Tupaj, M., W.K. Raja, M. Tang-Schomer, F.G. Omenetto, and D.L. Kaplan. 2013. Neural Responses to Electrical Stimulation on Patterned Silk Films. *Journal of Biomedical Materials Research. Part A* 101(9): 2559–2572. doi:10.1002/jbm.a.34565.

Hu, H., Y. Ni, V. Montana, R.C. Haddon, and V. Parpura. 2004. Chemically Functionalized Carbon Nanotubes as Substrates for Neuronal Growth. *Nano Letters* 4(3): 507–511. doi:10.1021/nl035193d.

Huang, L., X. Zhuang, J. Hu, L. Lang, P. Zhang, Y. Wang, X. Chen, Y. Wei, and X. Jing. 2008. Synthesis of Biodegradable and Electroactive Multiblock Polylactide and Aniline Pentamer Copolymer for Tissue Engineering Applications. *Biomacromolecules* 9(3): 850–858.

Huang, J., X. Hu, L. Lu, Z. Ye, Q. Zhang, and Z. Luo. 2010a. Electrical Regulation of Schwann Cells Using Conductive Polypyrrole/Chitosan Polymers. *Journal of Biomedical Materials Research. Part A* 93(1): 164–174.

Huang, J., Z. Ye, X. Hu, L. Lu, and Z. Luo. 2010b. Electrical Stimulation Induces Calcium-Dependent Release of NGF from Cultured Schwann Cells. *Glia* 58(5): 622–631. doi:10.1002/glia.20951.

Huang, Y.J., H.C. Wu, N.H. Tai, and T.W. Wang. 2012. Carbon Nanotube Rope with Electrical Stimulation Promotes the Differentiation and Maturity of Neural Stem Cells. *Small* 8(18): 2869–2877. doi:10.1002/smll.201200715.

Huang, Z.-B., G.-F. Yin, X.-M. Liao, and J.-W. Gu. 2014. Conducting Polypyrrole in Tissue Engineering Applications. *Frontiers of Materials Science* 8(1): 39–45.

Ifkovits, J.L., H.G. Sundararaghavan, and J.A. Burdick. 2009. Electrospinning Fibrous Polymer Scaffolds for Tissue Engineering and Cell Culture. *Journal of Visualized Experiments* 32. doi:10.3791/1589.

Iijima, S. 1991. Helical Microtubules of Graphitic Carbon. *Nature* 354(6348): 56–58.

Jain, S.S.S., and S. Pillai. 2012. Toxicity Issues Related to Biomedical Applications of Carbon Nanotubes. *Journal of Nanomedicine and Nanotechnology* 3(5): 140.

Jain, S., A. Sharma, and B. Basu. 2013a. In Vitro Cytocompatibility Assessment of Amorphous Carbon Structures Using Neuroblastoma and Schwann Cells. *Journal of Biomedical Materials Research, Part B: Applied Biomaterials* 101B(4): 520–531. doi:10.1002/jbm.b.32852.

Jain, S., T.J. Webster, A. Sharma, and B. Basu. 2013b. Intracellular Reactive Oxidative Stress, Cell Proliferation and Apoptosis of Schwann Cells on Carbon Nanofibrous Substrates. *Biomaterials* 34(21): 4891–4901.

Jang, M.J., S. Namgung, S. Hong, and Y. Nam. 2010. Directional Neurite Growth Using Carbon Nanotube Patterned Substrates as a Biomimetic Cue. *Nanotechnology* 21(23): 235102.

Jin, G.Z., M. Kim, U.S. Shin, and H.W. Kim. 2011a. Neurite Outgrowth of Dorsal Root Ganglia Neurons Is Enhanced on Aligned Nanofibrous Biopolymer Scaffold with Carbon Nanotube Coating. *Neuroscience Letters* 501(1): 10–14. doi:10.1016/j.neulet.2011.06.023.

Jin, G.Z., M. Kim, U.S. Shin, and H.W. Kim. 2011b. Effect of Carbon Nanotube Coating of Aligned Nanofibrous Polymer Scaffolds on the Neurite Outgrowth of PC-12 Cells. *Cell Biology International* 35(7): 741–745. doi:10.1042/cbi20100705.

Jin, L., T. Wang, Z.-Q. Feng, M.K. Leach, J. Wu, S. Mo, and Q. Jiang. 2013. A Facile Approach for the Fabrication of Core–Shell Pedot Nanofiber Mats with Superior Mechanical Properties and Biocompatibility. *Journal of Materials Chemistry B* 1(13): 1818–1825.

Kamber, D., H. Erez, and M.E. Spira. 2009. Local Calcium-Dependent Mechanisms Determine Whether a Cut Axonal End Assembles a Retarded Endbulb or Competent Growth Cone. *Experimental Neurology* 219(1): 112–125. doi:10.1016/j.expneurol.2009.05.004.

Karim, M.R. 2013. Fabrication of Electrospun Aligned Nanofibers from Conducting Polyaniline Copolymer/Polyvinyl Alcohol/Chitosan Oligossacaride in Aqueous Solutions. *Synthetic Metals* 178: 34–37. doi:10.1016/j.synthmet.2013.06.014.

Kaur, G., R. Adhikari, P. Cass, M. Bown, and P. Gunatillake. 2015. Electrically Conductive Polymers and Composites for Biomedical Applications. *RSC Advances* 5(47): 37553–37567. doi:10.1039/c5ra01851j.

Khaing, Z.Z., R.C. Thomas, S.A. Geissler, and C.E. Schmidt. 2014. Advanced Biomaterials for Repairing the Nervous System: What Can Hydrogels Do for the Brain? *Materials Today* 17(7): 332–340. doi:10.1016/j.mattod.2014.05.011.

Koppes, A.N., A.L. Nordberg, G.M. Paolillo, N.M. Goodsell, H.A. Darwish, L.X. Zhang, and D.M. Thompson. 2014. Electrical Stimulation of Schwann Cells Promotes Sustained Increases in Neurite Outgrowth. *Tissue Engineering. Part A* 20(3–4): 494–506.

Kotwal, A., and C.E. Schmidt. 2001. Electrical Stimulation Alters Protein Adsorption and Nerve Cell Interactions with Electrically Conducting Biomaterials. *Biomaterials* 22(10): 1055–1064. doi:10.1016/s0142-9612(00)00344-6.

Lanmuller, H., M. Bijak, W. Mayr, D. Rafolt, S. Sauermann, and H. Thoma. 1997. Useful Applications and Limits of Battery Powered Implants in Functional Electrical Stimulations. *Artificial Organs* 21(3): 210–212.

Lee, J.Y. 2013. Electrically Conducting Polymer-Based Nanofibrous Scaffolds for Tissue Engineering Applications. *Polymer Reviews* 53(3): 443–459. doi:10.1080/15583724.2013.806544.

Lee, Y.S., and T.L. Arinzeh. 2012. The Influence of Piezoelectric Scaffolds on Neural Differentiation of Human Neural Stem/Progenitor Cells. *Tissue Engineering. Part A* 18(19-20): 2063–2072. doi:10.1089/ten.tea.2011.0540.

Lee, J.Y., and C.E. Schmidt. 2015. Amine-Functionalized Polypyrrole: Inherently Cell Adhesive Conducting Polymer. *Journal of Biomedical Materials Research. Part A* 103(6): 2126–2132. doi:10.1002/jbm.a.35344.

Lee, J.Y., C.A. Bashur, A.S. Goldstein, and C.E. Schmidt. 2009a. Polypyrrole-Coated Electrospun Plga Nanofibers for Neural Tissue Applications. *Biomaterials* 30(26): 4325–4335.

Lee, J.Y., J.W. Lee, and C.E. Schmidt. 2009b. Neuroactive Conducting Scaffolds: Nerve Growth Factor Conjugation on Active Ester-Functionalized Polypyrrole. *Journal of the Royal Society Interface* 6(38): 801–810. doi:10.1098/rsif.2008.0403.

Lee, Y.S., G. Collins, and T.L. Arinzeh. 2011. Neurite Extension of Primary Neurons on Electrospun Piezoelectric Scaffolds. *Acta Biomaterialia* 7(11): 3877–3886. doi:10.1016/j.actbio.2011.07.013.

Lee, J.Y., C.A. Bashur, C.A. Milroy, L. Forciniti, A.S. Goldstein, and C.E. Schmidt. 2012. Nerve Growth Factor-Immobilized Electrically Conducting Fibrous Scaffolds for Potential Use in Neural Engineering Applications. *IEEE Transactions on Nanobioscience* 11(1): 15–21. doi:10.1109/tnb.2011.2159621.

Liu, X.A., K.J. Gilmore, S.E. Moulton, and G.G. Wallace. 2009. Electrical Stimulation Promotes Nerve Cell Differentiation on Polypyrrole/Poly(2-Methoxy-5 Aniline Sulfonic Acid) Composites. *Journal of Neural Engineering* 6(6): 065002. doi:10.1088/1741-2560/6/6/065002.

Liu, Y., Y. Zhao, B. Sun, and C. Chen. 2012. Understanding the Toxicity of Carbon Nanotubes. *Accounts of Chemical Research* 46(3): 702–713.

Ludwig, K.A., J.D. Uram, J. Yang, D.C. Martin, and D.R. Kipke. 2006. Chronic Neural Recordings Using Silicon Microelectrode Arrays Electrochemically Deposited with a Poly(3,4-Ethylenedioxythiophene) (Pedot) Film. *Journal of Neural Engineering* 3(1): 59.

Mathie, A., L.E. Kennard, and E.L. Veale. 2003. Neuronal Ion Channels and Their Sensitivity to Extremely Low Frequency Weak Electric Field Effects. *Radiation Protection Dosimetry* 106(4): 311–316.

Matsumoto K, Sato C, Naka Y, Kitazawa A, Whitby RLD, Shimizu N. 2007. Neurite Outgrowths of Neurons with Neurotrophin-Coated Carbon Nanotubes. *Journal of Bioscience and Bioengineering* 103(3): 216–220. http://dx.doi.org/10.1263/jbb.103.216

Mawad, D., K. Gilmore, P. Molino, K. Wagner, P. Wagner, D.L. Officer, and G.G. Wallace. 2011. An Erodible Polythiophene-Based Composite for Biomedical Applications. *Journal of Materials Chemistry* 21(15): 5555–5560.

Mawad, D., E. Stewart, D.L. Officer, T. Romeo, P. Wagner, K. Wagner, and G.G. Wallace. 2012. A Single Component Conducting Polymer Hydrogel as a Scaffold for Tissue Engineering. *Advanced Functional Materials* 22(13): 2692–2699. doi:10.1002/adfm.201102373.

Melitz, W., J. Shen, A.C. Kummel, and S. Lee. 2011. Kelvin Probe Force Microscopy and Its Application. *Surface Science Reports* 66(1): 1–27.

Meng, S.R.M., and Z. Zhang. 2011. *Applied Biomedical Engineering: Electrical Stimulation in Tissue Regeneration*. Croatia: InTech.

Merrill, D.R., M. Bikson, and J.G. Jefferys. 2005. Electrical Stimulation of Excitable Tissue: Design of Efficacious and Safe Protocols. *Journal of Neuroscience Methods* 141(2): 171–198.

Mire, C.A., A. Agrawal, G.G. Wallace, and P. Calvert. 2011. Inkjet and Extrusion Printing of Conducting Poly(3,4-Ethylenedioxythiophene) Tracks on and Embedded in Biopolymer Materials. *Journal of Materials Chemistry* 21(8): 2671–2678.

Molino, P.J., and G.G. Wallace. 2015. Next Generation Bioelectronics: Advances in Fabrication Coupled with Clever Chemistries Enable the Effective Integration of Biomaterials and Organic Conductors. *APL Materials* 3(1): 12. doi:10.1063/1.4905372.

Nickels, J.D., and C.E. Schmidt. 2013. Surface Modification of the Conducting Polymer, Polypyrrole, Via Affinity Peptide. *Journal of Biomedical Materials Research. Part A* 101A(5): 1464–1471. doi:10.1002/jbm.a.34435.

Palermo, V., A. Liscio, M. Palma, M. Surin, R. Lazzaroni, and P. Samori. 2007. Exploring Nanoscale Electrical and Electronic Properties of Organic and Polymeric Functional Materials by Atomic Force Microscopy Based Approaches. *Chemical Communications* 32: 3326–3337. doi:10.1039/B701015J.

Park, S.Y., J. Park, S.H. Sim, M.G. Sung, K.S. Kim, B.H. Hong, and S. Hong. 2011. Enhanced Differentiation of Human Neural Stem Cells into Neurons on Graphene. *Advanced Materials* 23(36): H263–H267.

Patel, N., and M.M. Poo. 1982. Orientation of Neurite Growth by Extracellular Electric-Fields. *Journal of Neuroscience* 2(4): 483–496.

Peramo, A. 2008. Polymerization of a Conductive Polymer in Acellular Muscle Tissue Constructs. *Tissue Engineering. Part A* 14(3): 423–432. doi:10.1089/tea.2007.0123.

Pires, F., Q. Ferreira, C.A.V. Rodrigues, J. Morgado, and F.C. Ferreira. 2015. Neural Stem Cell Differentiation by Electrical Stimulation Using a Cross-Linked Pedot Substrate: Expanding the Use of Biocompatible Conjugated Conductive Polymers for Neural Tissue Engineering. *Biochimica Et Biophysica Acta—General Subjects* 1850(6): 1158–1168. doi:10.1016/j.bbagen.2015.01.020.

Prabhakaran, M.P., L. Ghasemi-Mobarakeh, G.R. Jin, and S. Ramakrishna. 2011. Electrospun Conducting Polymer Nanofibers and Electrical Stimulation of Nerve Stem Cells. *Journal of Bioscience and Bioengineering* 112(5): 501–507. doi:10.1016/j.jbiosc.2011.07.010.

Quigley, A.F., J.M. Razal, B.C. Thompson, S.E. Moulton, M. Kita, E.L. Kennedy, G.M. Clark, G.G. Wallace, and R.M.I. Kapsa. 2009. A Conducting-Polymer Platform with Biodegradable Fibers for Stimulation and Guidance of Axonal Growth. *Advanced Materials* 21(43): 4393–4397. doi:10.1002/adma.200901165.

Rajabi, A.H, M. Jaffe, T.L. Arinzeh. 2015. Piezoelectric Materials for Tissue Regeneration: A Review. *Acta Biomaterialia* 24: 12–23. http://dx.doi.org/10.1016/j.actbio.2015.07.010

Richardson-Burns, S.M., J.L. Hendricks, and D.C. Martin. 2007a. Electrochemical Polymerization of Conducting Polymers in Living Neural Tissue. *Journal of Neural Engineering* 4(2): L6.

Richardson-Burns, S.M., J.L. Hendricks, B. Foster, L.K. Povlich, D.-H. Kim, and D.C. Martin. 2007b. Polymerization of the Conducting Polymer Poly(3,4-Ethylenedioxythiophene) (Pedot) Around Living Neural Cells. *Biomaterials* 28(8): 1539–1552.

Rivers, T.J., T.W. Hudson, and C.E. Schmidt. 2002. Synthesis of a Novel, Biodegradable Electrically Conducting Polymer for Biomedical Applications. *Advanced Functional Materials* 12(1): 33–37. doi:10.1002/1616-3028(20020101)12:1<33::aid-adfm33>3.0.co;2-e.

Rodriguez, L.L., and I.C. Schneider. 2013. Directed Cell Migration in Multi-Cue Environments. *Integrative Biology* 5(11): 1306–1323. doi:10.1039/c3ib40137e.

Royo-Gascon, N., M. Wininger, J. Scheinbeim, B. Firestein, and W. Craelius. 2013. Piezoelectric Substrates Promote Neurite Growth in Rat Spinal Cord Neurons. *Annals of Biomedical Engineering* 41(1): 112–122. doi:10.1007/s10439-012-0628-y.

Sayyar, S., E. Murray, B.C. Thompson, S. Gambhir, and D.L. Officer. 2013. Covalently Linked Biocompatible Graphene/Polycaprolactone Composites for Tissue Engineering. *Carbon (New York)* 52: 296–304. doi:10.1016/j.carbon.2012.09.031.

Schmidt, C.E., V.R. Shastri, J.P. Vacanti, and R. Langer. 1997. Stimulation of Neurite Outgrowth Using an Electrically Conducting Polymer. *Proceedings of the National Academy of Sciences of the United States of America* 94(17): 8948–8953. doi:10.1073/pnas.94.17.8948.

Seil, J.T., and T.J. Webster. 2010. Electrically Active Nanomaterials as Improved Neural Tissue Regeneration Scaffolds. *Wiley Interdisciplinary Reviews. Nanomedicine and Nanobiotechnology* 2(6): 635–647. doi:10.1002/wnan.109.

Sherrell, P.C., B.C. Thompson, J.K. Wassei, A.A. Gelmi, M.J. Higgins, R.B. Kaner, and G.G. Wallace. 2014. Maintaining Cytocompatibility of Biopolymers Through a Graphene Layer for Electrical Stimulation of Nerve Cells. *Advanced Functional Materials* 24(6): 769–776. doi:10.1002/adfm.201301760.

Shi, G., M. Rouabhia, S. Meng, and Z. Zhang. 2008. Electrical Stimulation Enhances Viability of Human Cutaneous Fibroblasts on Conductive Biodegradable Substrates. *Journal of Biomedical Materials Research. Part A* 84(4): 1026–1037.

Song, Q., Z.Y. Jiang, N. Li, P. Liu, L.W. Liu, M.L. Tang, and G.S. Cheng. 2014. Anti-inflammatory Effects of Three-Dimensional Graphene Foams Cultured with Microglial Cells. *Biomaterials* 35(25): 6930–6940. doi:10.1016/j.biomaterials.2014.05.002.

Stewart, E., N.R. Kobayashi, M.J. Higgins, A.F. Quigley, S. Jamali, S.E. Moulton, R.M. Kapsa, G.G. Wallace, and J.M. Crook. 2015. Electrical Stimulation Using Conductive Polymer Polypyrrole Promotes Differentiation of Human Neural Stem Cells: A Biocompatible Platform for Translational Neural Tissue Engineering. *Tissue Engineering Part C: Methods* 21(4): 385–393. doi:10.1089/ten.tec.2014.0338.

Sudwilai, T., J.J. Ng, C. Boonkrai, N. Israsena, S. Chuangchote, and P. Supaphol. 2014. Polypyrrole-Coated Electrospun Poly(Lactic Acid) Fibrous Scaffold: Effects of Coating on Electrical Conductivity and Neural Cell Growth. *Journal of Biomaterials Science—Polymer Edition* 25(12): 1240–1252. doi:10.1080/09205063.2014.926578.

Svirskis, D., J. Travas-Sejdic, A. Rodgers, and S. Garg. 2010. Electrochemically Controlled Drug Delivery Based on Intrinsically Conducting Polymers. *Journal of Controlled Release* 146(1): 6–15.

Thompson, B.C., S.E. Moulton, J. Ding, R. Richardson, A. Cameron, S. O'Leary, G.G. Wallace, and G.M. Clark. 2006. Optimising the Incorporation and Release of a Neurotrophic Factor Using Conducting Polypyrrole. *Journal of Controlled Release* 116: 285.

Thompson, B.C., S.E. Moulton, K.J. Gilmore, M.J. Higgins, P.G. Whitten, and G.G. Wallace. 2009. Carbon Nanotube Biogels. *Carbon* 47(5): 1282–1291. doi:10.1016/j.carbon.2009.01.013.

Thompson, B.C., R.T. Richardson, S.E. Moulton, A.J. Evans, S. O'Leary, G.M. Clark, and G.G. Wallace. 2010. Conducting Polymers, Dual Neurotrophins and Pulsed Electrical Stimulation—Dramatic Effects on Neurite Outgrowth. *Journal of Controlled Release* 141(2): 161–167. doi:10.1016/j.jconrel.2009.09.016.

Thompson, B.C., S.E. Moulton, R.T. Richardson, and G.G. Wallace. 2011. Effect of the Dopant Ion in Polypyrrole on Nerve Growth and Release of a Neurotrophic Protein. *Biomaterials* 32: 3822.

Thompson, D.M., A.N. Koppes, J.G. Hardy, and C.E. Schmidt. 2014. Electrical Stimuli in the Central Nervous System Microenvironment. *Annual Review of Biomedical Engineering* 16(16): 397–430. doi:10.1146/annurev-bioeng-121813-120655.

Valentini, R. 1992. Electrically Charged Polymeric Substrates Enhance Nerve Fibre Outgrowth In Vitro. *Biomaterials* 13(3): 183–190. doi:10.1016/0142-9612(92)90069-Z.

Valentini, R., A. Sabatini, P. Dario, and P. Aebischer. 1989. Polymer Electret Guidance Channels Enhance Peripheral Nerve Regeneration in Mice. *Brain Research* 480(1): 300–304.

Vitale, F., S.R. Summerson, B. Aazhang, C. Kemere, and M. Pasquali. 2015. Neural Stimulation and Recording with Bidirectional, Soft Carbon Nanotube Fiber Microelectrodes. *ACS Nano* 9(4): 4465–4474. doi:10.1021/acsnano.5b01060.

Vivo, M., A. Puigdemasa, L. Casals, E. Asensio, E. Udina, and X. Navarro. 2008. Immediate Electrical Stimulation Enhances Regeneration and Reinnervation and Modulates Spinal Plastic Changes After Sciatic Nerve Injury and Repair. *Experimental Neurology* 211(1): 180–193. doi:10.1016/j.expneurol.2008.01.020.

Wang, K., H.A. Fishman, H. Dai, and J.S. Harris. 2006. Neural Stimulation with a Carbon Nanotube Microelectrode Array. *Nano Letters* 6(9): 2043–2048. doi:10.1021/nl061241t.

Weber, N., Y.S. Lee, S. Shanmugasundaram, M. Jaffe, and T.L. Arinzeh. 2010. Characterization and In Vitro Cytocompatibility of Piezoelectric Electrospun Scaffolds. *Acta Biomaterialia* 6(9): 3550–3556. doi:10.1016/j.actbio.2010.03.035.

Weng, B., X. Liu, R. Shepherd, and G.G. Wallace. 2012. Inkjet Printed Polypyrrole/Collagen Scaffold: A Combination of Spatial Control and Electrical Stimulation of PC12 Cells. *Synthetic Metals* 162(15–16): 1375–1380. doi:10.1016/j.synthmet.2012.05.022.

Wenjin, W.J., W.C. Liu, H. Zhu, F. Li, Y. Wo, W.D. Shi, X.Q. Fan, and W.L. Ding. 2011. Electrical Stimulation Promotes BDNF Expression in Spinal Cord Neurons Through Ca2+- and Erk-Dependent Signaling Pathways. *Cellular and Molecular Neurobiology* 31(3): 459–467. doi:10.1007/s10571-010-9639-0.

Wrobel, M.S.H. 2013. Directed Migration in Neural Tissue Engineering. *Tissue Engineering Part B* 20(2): 93–105. doi:10.1089/ten.teb.2013.0233.

Xiao, Y., X. Cui, and D.C. Martin. 2004. Electrochemical Polymerization and Properties of Pedot/S-Edot on Neural Microelectrode Arrays. *Journal of Electroanalytical Chemistry* 573(1): 43–48.

Xie, J.W., M.R. MacEwan, S.M. Willerth, X.R. Li, D.W. Moran, S.E. Sakiyama-Elbert, and Y.N. Xia. 2009. Conductive Core-Sheath Nanofibers and Their Potential Application in Neural Tissue Engineering. *Advanced Functional Materials* 19(14): 2312–2318. doi:10.1002/adfm.200801904.

Xu, H.X., J.M. Holzwarth, Y.H. Yan, P.H. Xu, H. Zheng, Y.X. Yin, S.P. Li, and P.X. Ma. 2014. Conductive PPY/PDLLA Conduit for Peripheral Nerve Regeneration. *Biomaterials* 35(1): 225–235. doi:10.1016/j.biomaterials.2013.10.002.

Yu, W.W., X.Q. Jiang, M. Cai, W. Zhao, D.X. Ye, Y. Zhou, C. Zhu, X.L. Zhang, X.F. Lu, and Z.Y. Zhang. 2014. A Novel Electrospun Nerve Conduit Enhanced by Carbon Nanotubes for Peripheral Nerve Regeneration. *Nanotechnology* 25(16): 165102. doi:10.1088/0957-4484/25/16/165102.

Zhang, L., W.R. Stauffer, E.P. Jane, P.J. Sammak, and X.T. Cui. 2010a. Enhanced Differentiation of Embryonic and Neural Stem Cells to Neuronal Fates on Laminin Peptides Doped Polypyrrole. *Macromolecular Bioscience* 10: 1456.

Zhang, Y., S.F. Ali, E. Dervishi, Y. Xu, Z. Li, D. Casciano, and A.S. Biris. 2010b. Cytotoxicity Effects of Graphene and Single-Wall Carbon Nanotubes in Neural Phaeochromocytoma-Derived Pc12 Cells. *ACS Nano* 4(6): 3181–3186.

Zhang, B.G.X., A.F. Quigley, D.E. Myers, G.G. Wallace, R.M.I. Kapsa, and P.F.M. Choong. 2014a. Recent Advances in Nerve Tissue Engineering. *International Journal of Artificial Organs* 37(4): 277–291. doi:10.5301/ijao.5000317.

Zhang, J.G., K.X. Qiu, B.B. Sun, J. Fang, K.H. Zhang, H. Ei-Hamshary, S.S. Al-Deyab, and X.M. Mo. 2014b. The Aligned Core-Sheath Nanofibers with Electrical Conductivity for Neural Tissue Engineering. *Journal of Materials Chemistry B* 2(45): 7945–7954. doi:10.1039/c4tb01185f.

Zheng, F., X. Zhou, Y. Luo, H. Xiao, G. Wayman, and H. Wang. 2011. Regulation of Brain-Derived Neurotrophic Factor Exon IV Transcription Through Calcium Responsive Elements in Cortical Neurons. *PLoS One* 6(12): e28441. doi:10.1371/journal.pone.0028441.

Zhou, K., G.A. Thouas, C.C. Bernard, D.R. Nisbet, D.I. Finkelstein, D. Li, and J.S. Forsythe. 2012. Method to Impart Electro- and Biofunctionality to Neural Scaffolds Using Graphene-Polyelectrolyte Multilayers. *ACS Applied Materials & Interfaces* 4(9): 4524–4531. doi:10.1021/am3007565.

Zhu, W., C. O'Brien, J.R. O'Brien, and L.G. Zhang. 2014. 3D Nano/Microfabrication Techniques and Nanobiomaterials for Neural Tissue Regeneration. *Nanomedicine* 9(6): 859–875. doi:10.2217/nnm.14.36.

Chapter 6
Bioactive Nanomaterials for Neural Engineering

Melike Sever, Idil Uyan, Ayse B. Tekinay, and Mustafa O. Guler

6.1 Introduction

6.1.1 Nerve Regeneration and the Roles of Extracellular Matrix Elements

Nervous system is a highly complex interconnected network and higher organisms including humans have limited neural regeneration capacity. Neurodegenerative diseases result in significant cognitive, sensory, or motor impairments. Following an injury in the neural network, there is a balance between promotion and inhibition of regeneration and this balance is shifted to different directions in central nervous system (CNS) and peripheral nervous system (PNS). More regeneration capacity is observed in the PNS compared to the CNS. Although, several mechanisms play roles in the inhibitory and growth-promoting natures of the CNS and PNS, extracellular matrix (ECM) elements are key players in this process. ECM is a three-dimensional environment where the cells migrate, proliferate, and differentiate (Rutka et al. 1988; Pan et al. 1997). After a comprehensive investigation of the interactions between the ECM proteins and cell receptors, the ECM environment was found to regulate significant cellular processes such as survival, proliferation, differentiation, and migration (Yurchenco and Cheng 1994; Aszodi et al. 2006). Its components have major roles not only in neurogenesis during development of the nervous system but also in normal neural functioning during adulthood (Hubert et al. 2009).

M. Sever • I. Uyan • A.B. Tekinay • M.O. Guler (✉)
Institute of Materials Science and Nanotechnology, National Nanotechnology Research Center (UNAM), Bilkent University, Ankara, Turkey, 06800

L.G. Zhang, D.L. Kaplan (eds.), *Neural Engineering*,
DOI 10.1007/978-3-319-31433-4_6

6.1.1.1 Peripheral Nervous System

In the PNS, neurons (axons) and Schwann cells are the major cellular elements. Endoneurium tissue is the connective tissue that surrounds individual axon-Schwann cell units, whereas perineurium covers a fascicle of axons. Perineurium also acts as a barrier against fluxes of ionic and macromolecular compounds between connective and vascular tissues and endoneurium (Siegel et al. 1999). Epineurium is the outermost connective tissue, which covers the entire nerve (Bunge et al. 1989). In the endoneurium, Schwann cells are abundant, whereas fibroblasts form 10 % of the cell population (Verheijen et al. 2003). Myelination after axonal regeneration has a central role for functional outcomes, and proper ECM formation has strong influence on this process (Bunge 1993).

Basal lamina of PNS contains laminin, fibronectin, entactin, and heparan sulfate proteoglycans (Bunge 1993) and collagens (Shellswell et al. 1979). Laminin is synthesized by the Schwann cells, and it is considered to have the leading bioactivity in terms of growth, adhesion, and migration of these cells (Milner et al. 1997). Laminin has also been shown to have a critical effect on myelination during peripheral nerve regeneration in culture systems (Tsiper and Yurchenco 2002). As another basal lamina element, collagen is the major ECM protein and it is produced mostly by the fibroblasts and Schwann cells in fibrillary and nonfibrillar forms (Koopmans et al. 2009). Fibrous types of collagens: collagen I, III, and V are found in all three ensheathing layers of peripheral nerve tissue. Collagen type-I and III are present in small diameters in the external face of Schwann cell basal lamina, whereas collagen type-V colocalizes with them in addition to enveloping myelinating Schwann cells in the basal lamina (Chernousov et al. 2006). Schwann cells also produce a more glycosylated and nonfibrillar type of collagen, collagen IV, which is a principle component of basal lamina. Collagen IV has a role in integrating laminin, perlecan, nidogen, and other ECM proteins into a supramolecular structure (Hudson et al. 1993) in the basal lamina surrounding Schwann cells, the perineurial cells, and endoneurial capillaries (Koopmans et al. 2009). Fibroblasts produce a fibrillary network of collagens and provide the framework required for Schwann cell ensheathment of regenerating axons (Eather et al. 1986). Fibronectin is another important ECM protein that has a very defined and specific expression pattern to guide neuronal outgrowth (Sheppard et al. 1991). Interaction of fibronectin with collagen, heparin, fibrin, and integrins via its specific domains results in cellular responses including cell adhesion, Schwann cell motility, and growth (Ahmed and Brown 1999). Chondroitin sulfate proteoglycans (CSPG) are also abundant in the Schwann cell ECM; however, they show inhibitory activity in contrast to other ECM elements in the PNS tissue (Braunewell et al. 1995).

Although complete recovery of PNS is not common, especially for large gaps, PNS injury environment is more permissive for regeneration compared to CNS. Nonneuronal cells respond to injury and start a key event called “Wallerian degeneration” (Waller 1850). This process initiates a series of events, which together help clearance of inhibitory myelin debris and promotion of axon regrowth (Griffin et al. 1995). Axon degeneration starts several days after the injury, leaving

the tissues denervated (Gilliatt and Hjorth 1972). When calcium starts to influx from the ECM and internal Ca^{2+} stores to the injured axon (Stirling and Stys 2010), calpain is activated, a protease, which functions in cytoskeletal degradation and axonal degeneration (Wang et al. 2004). Schwann cells and fibroblasts secrete tropic and tropic factors, and detached Schwann cells go through proliferation. The basal lamina remains and guides endoneurium toward the distal site (Fu and Gordon 1997). Schwann cells form Bands of Büngner with the help of fibrin cables, where fibroblasts and blood vessels can also use as a guiding surface (Williams et al. 1983). Fibrin is later replaced by collagens produced by fibroblasts and laminin secreted by Schwann cells. Regeneration fails when the initial fibrin cable cannot be formed due to a large gap (Yannas et al. 2007).

6.1.1.2 Central Nervous System

Apart from the neurons and glial cells, ECM constitutes 10–20 % volume of the CNS (Bignami et al. 1993). While specific pathfinding, migration, and differentiation of the cells are regulated by specific ECM proteins during CNS development (Bandtlow and Zimmermann 2000), ECM components play role in stabilization of the structure, regulation of the synaptic plasticity, and prevention of aberrant synaptic remodeling throughout the adulthood (Dityatev and Schachner 2003). The matrix forms a dense network of proteins and glycans, facilitating the organization of the cells as well as providing structural support to them (Lau et al. 2013). Basal lamina, perineuronal nets, and interstitial matrix form the ECM structurally. Basement membrane is the tissue that covers the entire pial surface of the CNS and it comprises of collagen, laminin, nidogen, fibronectin, dystroglycan, and perlecan. On the contrary, the matrix surrounding the neurons, perineuronal nets, have a network majorly made up of proteoglycans, tenascin R, and other proteins (Kwok et al. 2011), which conserve and maintain synaptic plasticity. Interstitial network is formed by proteoglycans, hyaluronan, tenascins, and other linking proteins (Rauch 2007). Moreover, collagen, elastin, laminin, and fibronectin also participate in the structure of the network, however in smaller amounts (Lau et al. 2013).

Following a damage to the CNS, a series of molecular and cellular events occur resulting in inhibition of regeneration process. Glial scar tissue formation is triggered by the entrance of non-CNS elements to the CNS. Although it leads to inhibition of regeneration, one important beneficial role of glial scar is to preserve the damaged tissue, repair the blood–brain barrier (BBB), and minimize cellular degeneration and inflammatory burden (Silver and Miller 2004; Bush et al. 1999). First, macrophages migrate to the injury site from the blood due to BBB disruption. Then, oligodendrocyte precursors migrate to the injury site in massive numbers. Finally, astrocytes proliferate and migrate to the area to fill in the injury area and become reactive, which is a process called “reactive astrogliosis” (Fawcett and Asher 1999). Reactive astrocytes produce glial fibrillary acidic protein (GFAP) after CNS injury, which can also be used as a marker for glial scar formation. Although GFAP production is similar to collagen fibers, they are important in regeneration process.

ECM of CNS is composed of protein or proteoglycan-based aggregates, whereas native PNS ECM has a fibrous structure (Alovskaya et al. 2007).

Besides producing growth promoting factors, astrocytes also produce four different types of proteoglycans, which are made up of a core protein and sulfated glycosaminoglycan chains attached to the sides that are inhibitory to regeneration: heparan sulfate proteoglycan (HSPG), dermatan sulfate proteoglycan (DSPG), keratan sulfate proteoglycan (KSPG), and CSPG (Larsen et al. 2003). Hyaluronic acid is another carbohydrate, which is also present in the ECM of CNS. It interacts with proteoglycans to form a mesh-like structure in the perineuronal network (Kwok et al. 2010). During development, CSPG plays a role in inhibitory patterning of neuronal pathway (Tang et al. 2003). In healthy adult perineuronal networks, they are involved in stabilization of synaptic plasticity (Hunanyan et al. 2010). However, upregulated levels of CSPGs are known to increase glial scar in the mature spinal cord and brain (Becker and Becker 2002), and they inhibit neurite outgrowth extensively in vitro (Sharma et al. 2012). They are upregulated within 24 h following injury and they remain at the injury site for months (McKeon et al. 1999; Jones et al. 2003). Mechanism of CSPGs inhibition is thought to be both nonspecific, through the contact of negatively charged glycosaminoglycan chains, and specific through signaling mechanisms by interacting with PTP and receptors (Dickendesher et al. 2012; Sharma et al. 2012).

6.1.2 Blood–Brain Barrier and Blood–Spinal Cord Barrier

BBB and blood–spinal cord barrier (BSCB) are mechanisms that act as shields between CNS and blood and they preserve homeostasis in organisms with well-developed CNS (Abbott 2005). Even though they have similar morphological characteristics and functions such as preservation of CNS, BBB and BSCB are considered to be different processes. Both BBB and BSCB are composed of nonfenestrated endothelial cells, basement membrane, pericytes, and astrocytic end processes. Endothelial cells have tight junctions via claudin, occludin, and adherens junction molecules (Abbott et al. 2006). BSCB differs from BBB in terms of permeability of different molecules. Furthermore, there are glycogen deposits in the microvessels, which are not present on the cerebral vascular structure (Sharma 2005) and are thought to serve as an endogenous energy source. Cellular components of BBB are microvascular endothelium, astrocytes, basement membrane, pericytes, and the neurons that are in physical proximity to the microvascular endothelial cells. The neurons in the brain and the spinal cord communicate through chemical signals via neurotransmitters and modulators, and electrical signals via synaptic potentials and action potentials, which form a complex network. Ionic movements across the neuronal membranes are involved in the signaling processes. There are also the ionic fluxes, which maintain the resting membrane potentials stable and the ionic movements involved with electrochemical signals are transmitted on this background of ionic fluxes. In order for signal transmission to be precise, reliable, and consistent,

ionic composition of the brain extracellular milieu needs to be preserved against the rapid fluctuations of ionic composition in the blood caused by physical exercise or food intake. There is evolutionary evidence that ionic movements were the major factor driving barriers between CNS and blood, and the barriers gained other functions subsequently (Abbott 1992).

Brain microvascular endothelial cells (BMVEC) are responsible for regulation of function such as transportation of micro and macronutrients, receptor-mediated signaling, regulation of osmotic pressure, and leukocyte trafficking. They impede free exchange of solutes (Ohtsuki and Terasaki 2007) with the exception of lipid-soluble molecules smaller than 400 Da with less than nine hydrogen bonds, which are able to cross BBB via lipid mediated diffusion (Pardridge 2007). Structurally, the cells are connected to each other via tight junctions (TJs), adherens junctions (AJs) (Hawkins and Davis 2005), and gap junctions (Boulay et al. 2015), which are required for the compact characteristics of the barrier. Their main role is to restrict passage of unwanted molecules between blood and brain by forming a continuous layer of membrane that does not contain fenestrae, which are normally found on the endothelial cells of blood vessels for rapid exchange of molecules. Along with the physical barrier created by junctional elements and low transcytotic activity, endothelial cells also create an enzymatic barrier against potential lipophilic substances, such as lipophilic drugs and toxic substances (El-Bacha and Minn 1999), which provides a metabolic barrier to the brain (El-Bacha and Minn 1999). Neurons at the periphery are connected through astrocytic interactions to the BBB (Abbott et al. 2006) and together with the other neovascular unit elements (astrocytes and pericytes), they provide required paracrine signals to the endothelium (Deane and Zlokovic 2007) and control BBB permeability, structure, and function (Abbott et al. 2006).

The CNS barriers protect nervous system homeostasis and they control molecular traffic, toxins, neuronal signaling, low protein environment in CNS, and neuronal circuits. They reduce cross talk by separation of central and peripheral neurotransmitter pools and ensuring minimal inflammatory response and functional impairment during immune surveillance (Abbott 2013).

6.1.3 Challenges in Engineering Biomaterials for Nervous System Repair

Following a nervous system injury, regeneration capacity usually depends on the extent of the injury, the distance of the injury to the cell body, and biological status of the patient (morbidity, age, etc.) (Faroni et al. 2015). The PNS and CNS respond to injury in their own unique way. In the PNS, Wallerian degeneration occurs in the distal end following a series of pathophysiological events. The distal portion of the nerve is degenerated and the cellular debris is digested by the macrophages and monocytes (Stoll et al. 1989). Schwann cells form the Bands of Büngner in order to guide regenerating axonal sprouts to its synaptic target (Chaudhry et al. 1992;

Schmidt and Leach 2003). During the extension process, bridging the gap between the two ends and optimizing the environment physically, chemically, and biologically is a strategy that has been followed (Schmidt and Leach 2003). In PNS, the challenge is to find a perfect alternative to autologous nerve grafts: eliminating risks of secondary surgeries and precluding secondary damage on the body. Even though structural plasticity is achieved clinically, functional plasticity does not always reach complete state and it still is another principal consideration in PNS regeneration studies. Autologous nerve graft treatment shows 50 % clinical functional recovery (Lee and Wolfe 2000). Furthermore, use of natural proteins for therapeutic purposes can cause immunogenic reactions. Sustained delivery or storage of growth factors are also required in order for effective usage of growth factors (Schmidt and Leach 2003).

CNS has much smaller capacity to regenerate; thus, CNS therapies are more challenging. Embryonic spinal cord and peripheral nerve grafts have been shown to support regeneration of CNS fibers, however failed to successfully grow through the CNS–PNS transition zone (Bernstein and Goldberg 1995) (Carlstedt 1997). CNS does not have a permissive nature for regeneration. There are many reasons behind the obstructive environment of CNS injuries. Regeneration-associated genes are expressed at low levels in the CNS (Bulsara et al. 2002). Following the CNS injury, glial scar is formed and inhibitory molecules are released at the site of injury. Cellular debris and inhibitory myelin components are cleared much slowly compared to the PNS as a result of low infiltration levels of macrophages through the brain–spinal cord barrier (Avellino et al. 1995). Moreover, astrocytes proliferate at the site of injury, in a similar way to Schwann cell proliferation, however, in contrast, creating an inhibitory environment and becoming reactive astrocytes (McKeon et al. 1991). Thus, nerve regeneration studies focus on suppressing the inhibitory nature of the nervous system injuries and future directions in PNS and CNS repair include combining multiple cues at a time to increase the regeneration capacity (Schmidt and Leach 2003). BBB is another obstacle for drug delivery to the brain, considering that intracranial injections are much more invasive than other administration (i.e., intravenous, oral) methods. Another challenge for drug delivery is accurate targeting of the correct population of the cells.

6.2 Biomaterial Design for Peripheral Nerve Repair

PNS injuries most commonly caused by trauma (Ichihara et al. 2008), bone fractures, or joint dislocations (Zumwalt and Wooldridge 2014). They result in partial loss of sense or motor function in the distal segment of the injured axon (Navarro et al. 2007). The potential to achieve functional recovery depends on the severity of the damage at the axon, nerve tube, or connective tissues at the injury site, timing of the surgery, surgical technique used, and postoperational rehabilitation (Lanaras et al. 2009; Barton et al. 2014).

As a clinical strategy, the two ends of the nerve are sutured if the gap between the distal and proximal end is <2 cm. However, other alternatives are considered in

cases of nerve segmental loss with a consequent gap longer than 2 cm because of the tension that emerges when two ends are sutured to each other (Johnson et al. 2005). Nerve grafting or nerve conduits are standard procedure in cases like these (Siemionow and Brzezicki 2009; Pabari et al. 2010). During autograft nerve transplants, a nerve segment is transplanted from another region of the same patient. Clinically, autografts are accepted as the "gold standard" because of being nonimmunogenic and having best possible combination of the natural environment required for nerve regeneration. Autografts provide bridging of two ends, allowing physical adherence guidance and proper support for Schwann cell proliferation. On the other hand, they have some drawbacks such as sensation at the donor site, creating a second incision in the body, and having a limited supply of the donor site. Cadaveric nerve allografts are another option as nerve grafts, which do not require a second incision on the patient, however, compel systemic immunosuppression (Trumble and Shon 2000; Pollard et al. 1971; Mackinnon et al. 1982; Lassner et al. 1989; Gulati and Cole 1990; Gulati 1998). This technique is usually preferred in cases like severely damaged segmental nerve loss (Ray and Mackinnon 2010). Although nerve grafts seem plausible because of their optimal nature for regeneration, only 50 % of patients with autograft nerve transplants regain functional nerve regeneration (Lee and Wolfe 2000) and the drawbacks of these techniques have led to development of synthetic and biological nerve guidance conduits (Fansa et al. 2001; Walsh et al. 2009; Glasby et al. 1986). For this purpose, a primary concern should be mimicking the native environment of the PNS for optimal nerve regeneration. Some of the important points that should be taken into consideration while designing a peripheral construct are supporting axonal migration, promotion of viability, and proliferation of Schwann cells; proper storage of growth factors; and providing multiple cues from the native ECM (Evans 2000). In this regard, biodegradable hollow neural guidance channels can be used with ECM mimicking matrix fillers, coatings, and growth factor storing scaffolds. Schwann cell transplantation is another alternative that can be delivered within these scaffolds (De Luca et al. 2014).

6.2.1 Engineering Topographical and Mechanical Properties for Neural Guidance

Biocompatible and bioactive materials have been utilized in order to mimic physical, chemical, and biological properties of the native neural tissue. Cells are distinctly responsive to every cue in their environment including surface topography, stiffness, and interacting fiber diameter and change their behavior accordingly (Georges and Janmey 2005; Pedersen and Swartz 2005; Khatiwala et al. 2006; Curtis and Riehle 2001). Grooves, micro- and nanofibers, gels, and films have been studied in order to promote and direct neuronal outgrowth and enhance neuronal attachment (Xie et al. 2010; Sun et al. 2010; Mobasseri et al. 2013; Daud et al. 2012; Bell and Haycock 2012). Instead of using hollow guidance tubes that lacks physical

properties of the native nerve structure, studies have focused on developing materials that guide the axons to the distal site of the injury. Lumen filling materials are used for this purpose to provide contact, attachment, and growth of the cells (Chen et al. 2006; Jiang et al. 2010). Naturally, Schwann cell basal lamina is a favorable environment for physical guidance. It consists primarily of laminin and collagen that represent aligned, nanoscale features (Bunge and Bunge 1983). Neurite outgrowth of chick dorsal root ganglia (DRG) neurons was intensely improved on aligned nanofibrous surfaces, which demonstrates the importance of these features (Kim et al. 2008; Corey et al. 2007). Incorporating Schwann cells is also a strategy; aligned collagen poly-E-caprolactone (PCL) filament constructs seeded with Schwann cells have shown that DRG cells had enhanced and oriented neurite outgrowth in vitro (Ribeiro-Resende et al. 2009).

Along with these factors, porosity of the conduit is also important in axonal regeneration. Pores of the conduits enable inward diffusion of ECM proteins and growth factors (Kim et al. 1993), and outward diffusion of waste products. In addition to this, infiltration of connective fibrous tissue should also be prevented (Wang et al. 2009) and regeneration was observed to proceed into microsized pores (Oh et al. 2013). Therefore, the pores of the conduits should be wide enough for growth factor and waste product diffusion and narrow enough to prevent fibrous tissue infiltration and regeneration toward the pore. "Roll and seal" model aligned nanofibrous conduit-derived pores have been shown to trigger greater neurite outgrowth and functional recovery compared to aligned microfibrous conduit-derived pores (Jiang et al. 2014).

Nervous tissue is a soft tissue and is sensitive to the mechanical stiffness of the environment. Natural stiffness of the peripheral neural tissue has stiffness value between 150 and 300 kPa, whereas glial cells and neurons individually have stiffness values ranging from 0.5 to 1.6 kPa (Jalili-Firoozinezhad et al. 2014). Therefore, resemblance of stiffness to the native environment is an important factor that plays role on nerve regeneration. Agarose gel stiffness (density) was showed to have an inversely proportional relationship with neurite extension rate of DRG cultures (Balgude et al. 2001). PEG-based hydrogels have also been studied for nerve regeneration purposes and as the stiffness of the PEG-based hydrogel increased, PC12 cells showed reduced neurite extension. In addition, below a threshold value of stiffness, neurite outgrowth of PC12 cells decreased drastically (Leach et al. 2007), which proves that neurons require a defined range of intermediate stiffness (Hoffman-Kim et al. 2010). These studies indicate the significance of mechanical properties of native nerve tissue in designing biomaterials for peripheral nerve repair.

6.2.2 Surface Chemistry and Biochemical Modifications to Increase Nerve Regeneration

Nerve guidance conduits require some additional properties such as surface modification and some biochemical cues in order to promote axon guidance, Schwann cell proliferation, adhesion, and migration (Gu et al. 2014). These modifications may be

in the form of protein coatings, chemical/physical treatment of the surface, or protein mimetic peptides presented on the biomaterials (Chung and Park 2007). In order to create the native environment of the healthy nerve tissue, ECM proteins are considered to have great potential for functionalization of the conduit surface. Collagen, fibronectin, and laminin are examples of some major components of the ECM that have been used for this purpose (Yu and Bellamkonda 2003; Armstrong et al. 2007; Koh et al. 2010). Laminin, in particular, has been used most frequently for surface modification or ECM mimicking purposes among others due to its ability to improve neurite extension and provide Schwann cell adhesion, proliferation, and migration (Yu and Bellamkonda 2003; Silva et al. 2004; Yu et al. 1999; Itoh et al. 2001; Rangappa et al. 2000; Rutkowski et al. 2004; Toba et al. 2001; Matsumoto et al. 2000; Koh et al. 2010; Bellamkonda et al. 1995). Collagen and fibronectin also have regenerative capacity in terms of Schwann cell adhesion, proliferation, and neurite outgrowth improvement; however, outcomes have shown to be significantly lower than that of laminin in terms of regeneration (Yu and Bellamkonda 2003; Armstrong et al. 2007; Koh et al. 2010). Despite the major impact of ECM protein-based functionalization of the materials on neural regeneration, they are difficult to synthesize due to their large size (~900 kDa) (Santiago et al. 2009; Itoh et al. 2001). An alternative to using large ECM protein modifications is protein mimetic short peptide sequences, which are more stable, less immunogenic, and relatively low molecular weight. These short peptides are usually designed to be recognized by the cellular receptors and they are represented on a surface. Due to their small size, they have a high surface density; thus, there is more interaction for signaling events and cell attachment (Itoh et al. 2001; Chung and Park 2007).

A widely used short peptide sequence is RGD (Arg–Gly–Asp), which is an integrin binding amino acid sequence found in fibronectin, laminin, and other ECM molecules and has been used for inducing cell attachment. IKVAV (Ile–Lys–Val–Ala–Val) (Tashiro et al. 1989) and YIGSR (Tyr–Ile–Gly–Ser–Arg) are found at the laminin b chain and RNIAEIIKDI (Arg–Asn–Ile–Ala–Glu–Ile–Ile–Lys–Asp–Ile) belongs to laminin g chain, which all mimic laminin. HAV (His–Ala–Val) sequence mimics N-cadherin, which is an adhesive and regulatory protein found on both neurons and glial cells (Chung and Park 2007; Itoh et al. 2003; Santiago et al. 2009; Itoh et al. 2001). Functionality of these peptides has been assessed in various applications. Adams et al. showed that DRG neurons, that were grown on gradients of photoimmobilized IKVAV bound polystyrene grids, preferentially directed their neurites toward higher concentration of IKVAV containing surface (Adams et al. 2005). In another study, melt coextruded aligned poly(ε-caprolactone) (PCL) fibers were modified with photochemical gradient of IKVAV peptide, which provided directional cues for neuronal outgrowth of PC-12 cells (Kim et al. 2015).

Schense et al. (2000) evaluated the effects of five ECM mimetic peptides: RGD, IKVAV, YIGSR, RNIAEIIKDI, and HAV within a fibrin matrix. In this study, each peptide-coated matrix showed increased neurite extension than uncoated fibrin matrix in vitro. Moreover, synergistic effect of the four laminin mimetic peptides showed significant increase in terms of neurite outgrowth compared with the single peptide-coated matrices (Schense et al. 2000). In the in vivo studies of the same group, they tested same materials as neural guidance channel fillings for their

regenerative capacity in dorsal root ganglion models. Synergistic effects of four laminin mimetic peptides also showed similar effects to the in vitro studies (Schense et al. 2000). Similarly, PCL scaffolds with RGD peptide functionalization resulted in enhanced Schwann cell adhesion as well as axonal interaction in vivo (Santiago et al. 2009).

Another method to produce nanofibrous scaffolds, while controlling diameter, porosity, and surface morphology, is electrospinning (Pham et al. 2006; Subbiah et al. 2005). A variety of polymers can be electrospun on aluminum surfaces and these polymers are also known to contribute to neural regeneration by their nanofibrous topography. In addition, their surface can be functionalized by bioactive epitopes or chemical groups (Pham et al. 2006; Prabhakaran et al. 2008). Bellamkonda et al. showed that multiple layers of aligned acrylonitrile-methacrylate (PAN-MA) nanofibers stacked within semipermeable nerve guidance tubes showed highly aligned and enhanced neurite extension of DRG cultures and in vivo PNS regeneration studies (Clements et al. 2013). In another study conducted by Ahmed et al., electrospun nanofibers were biofunctionalized by tenascin-C-derived peptides, which increased cell adhesion compared to poly-L-lysine-coated glass surfaces (Ahmed et al. 2006).

Self-assembled peptide amphiphile (PA) nanofibers are used as matrices similar to ECM characteristics. With these nanostructures, the neural microenvironment can be manipulated in a way that ECM mimicking peptides are represented on the surfaces of the nanofibers. These peptide nanofibers are promising materials due to their nonimmunogenic, biodegradable, and bioactive nature (Tan et al. 2012). These materials consist of a hydrophobic alkyl tail, β-sheet forming amino acids, and a hydrophilic bioactive epitope. In aqueous solutions, oppositely charged PA molecules self-assemble into nanofibers and form gels (Cui et al. 2010). Cooperative effect of laminin mimetic IKVAV PAs and heparan sulfate proteoglycan-derived PAs promoted neurite outgrowth of PC-12 cells significantly. Besides, the inhibitory environment caused by chondroitin sulfate was also overcome by these materials (Mammadov et al. 2012). The protein or peptide modification is a significant approach for neural guidance conduit functionalization.

6.2.3 Enhancing Regeneration by Electrical Stimulation via Conductive Biomaterials

Electrical stimulation is a method to accelerate nerve regeneration (Seil and Webster 2010). Since neurons are electroactive cells, they respond to electrical stimulation by neurite extension and differentiation. Both direct and alternating current (DC and AC) within a voltage range is known to promote neurite outgrowth. DC was shown to enhance increased and directed neurite outgrowth (Borgens et al. 1979). One mechanism of promotion of neurite outgrowth by electrical stimulation is by upregulation of growth-associated genes. For instance, cyclic adenosine monophosphate

(cAMP) production was upregulated upon electrical stimulation of DRG cells (Udina et al. 2008). Polyaniline, polypyrrole, polythiophene, and polyacetylene are some known conductive substrates (Marquardt and Sakiyama-Elbert 2013; Schmidt et al. 1997). Poly (D,L-lactide-co-epsilon-caprolactone) (PDLLA/CL) nerve guidance (NGCs) fabricated with polypyrrole enhanced neurite outgrowth compared to PDLLA/CL conduits alone (Zhang et al. 2007). In another study, high-voltage electrical stimulation of PLGA films significantly increased number of total neurites and myelinated axons (Bryan et al. 2004).

Polypyrrole and polyaniline both have excellent conductive and antioxidant properties in terms of cellular stimulation; however, their nonbiodegradable structure limits their usage in nerve regeneration studies (Gu et al. 2014). As an alternative strategy, blending of these materials with other biodegradable biomaterials has been proposed (Ghasemi-Mobarakeh et al. 2011). Rivers et al. were successful in synthesizing a conductive polymer by binding pyrrole oligomers to thiophene via ester linkages, so that ester linkages get cleaved by esterases in vivo (Rivers et al. 2002). In another study, a block copolymer of polyglycolide and aniline pentamer showed electroactivity and degradability (Ding et al. 2007). Several studies show the effect of electrical stimulation on the axis of neural cell division, neuronal polarity, and directed neurite outgrowth (Nguyen et al. 2013; McCaig et al. 2005; Yao et al. 2011). All these studies prove that electrical stimulation has a noteworthy effect on axonal regrowth acceleration.

6.3 Biomaterial Design for Central Nervous System Repair

Any damage to CNS can be destructive due to loss of communication between healthy neurons, and it can cause neuronal degeneration and eventually cell death. Due to the low regeneration capacity of CNS, people with CNS trauma or neurodegenerative disorders suffer from lifelong consequences and there is a significant demand for new strategies to overcome the progressive cell death as well as to induce tissue regeneration. The failure of neurons in the CNS to communicate with each other after injury is mostly due to the lack of supporting environment for regeneration around the damaged neurons rather than characteristics of the cells (Richardson et al. 1980). For regeneration process of CNS neurons, first the survival of injured neuron is required, so that it can connect with its target. However, making contact is not enough for functional recovery; remyelination of the axons and properly functioning synapses on the target neurons are also required. The strategies to generate a biomaterial for central nerve repair should focus on removal of inhibitory environment, axon guidance, manipulation of cell signaling, increasing the local concentration of neurotrophic factors and suitable drugs, and providing artificial microenvironment to fill the gap occurred as a result of injury (Horner and Gage 2000).

6.3.1 *Mimicking Extracellular Matrix of Central Nervous System*

ECM is the surrounding environment of cells composed of proteins such as laminin and fibronectin, glycosaminoglycans, proteoglycans, and different types of soluble factors (Zimmermann and Dours-Zimmermann 2008). It provides structural, biological, and chemical support to the cells through modulating cell adhesion, proliferation, migration, cell-to-cell interaction, and differentiation. Within the scope of tissue engineering, focusing on the development of in vitro cell culture environments, which mimic the natural ECM of specific cell types has received a lot of attention (Holmes 2002; Lutolf and Hubbell 2005). For nervous system applications, synthetic materials are especially attractive, because their chemical, mechanical, and physical properties can be specifically modified to mimic a particular area within the nervous system (Schmidt and Leach 2003).

6.3.1.1 Chemical Signals

ECM proteins regulate cell fate including proliferation, migration, and differentiation through interacting with cell surface receptors. One of the major differences of CNS from other systems is the composition of ECM proteins. Many ECM proteins, including collagen and fibronectin, are abundant in other tissues, whereas there is almost none in CNS. On the other hand, there are different types of proteoglycans present between neurons and glial cells (Li et al. 2012).

While designing a biomaterial, the chemical signals provided by these specific proteins can be introduced into the system by incorporating the bioactive sequence for specific interaction depending on the nature of tissue of interest. For instance, arginine–glycine–aspartate (RGD) peptide sequence derived from fibronectin was found to bind to integrin proteins and function in cell adhesion (Pierschbacher and Ruoslahti 1984; Prowse et al. 2011). Later, several ECM-derived short sequences have been identified and used for the interaction with integrin proteins to take benefit of cell–ECM interactions. Due to the important role of laminin protein in ECM of nervous system, laminin-derived short sequences were identified. Tyrosine–isoleucine–glycine–serine–arginine (YIGSR) peptide sequence was used to promote cell adhesion in in vitro studies (Graf et al. 1987). Another sequence derived from laminin, isoleucine–lysine–valine–alanine–valine (IKVAV), was also discovered and found to promote neurite outgrowth (Tashiro et al. 1989). After the discovery of these small peptide sequences, they were included in nanomaterial surfaces with different forms and used in both in vitro and in vivo studies. These peptides, rather than whole proteins, have become more favorable for tissue engineering studies, since they are more stable and easy to synthesize. While fibronectin-derived synthetic peptide (GRGDS) was used in gellan gum hydrogels to enhance the cell adhesion of neural stem/progenitor cells in in vitro studies (Silva et al. 2012), laminin-derived IKVAV sequence was used in self-assembled peptide nanofibers as

a therapeutic system in a mouse model of spinal cord injury (SCI) (Tysseling-Mattiace et al. 2008).

Many soluble factors have important roles in NSC differentiation into specific lineages. Therefore, they can be incorporated within hydrogels to induce neural differentiation. For instance, through incorporation of neurotrophin-3 (NT-3) into chitosan hydrogels, NSC differentiation toward neurons was achieved (Li et al. 2009). On the other hand, when FGF-2 was incorporated into PEG hydrogels, NSCs preferred to stay at undifferentiated state in spite of the addition of differentiation medium (Freudenberg et al. 2009).

Biomaterial studies have also focused on neurotransmitters, which are important chemicals for transfer of messages between the cells of the brain. Acetylcholine-like biomimetic polymers, including both a bioactive unit (acetylcholine-like unit) and a bioinert unit (PEG unit), were studied with primary hippocampal neurons. These polymers have potential therapeutic use in neural tissue applications related with neurotransmitter-related diseases such as Alzheimer's disease through modulating the growth of hippocampal neurons (Tu et al. 2011).

6.3.1.2 Mechanical and Physical Cues

Besides the chemical signals to induce neural regeneration, mechanical and physical properties of the biomaterial system, such as stiffness and dimensionality, have to be taken into consideration to mimic the natural environment of nervous system. Mechanical properties of the material could contribute to differentiation into different lineages and sometimes, elasticity of the material can override the effect of chemical signals as shown in mesenchymal stem cells, which did not display any response to osteogenic growth factors when plated on soft surfaces (Engler et al. 2006).

The mechanical properties of the substrate show highly selective and specific effects in regenerative studies of central nervous system. Although brain and spinal cord are the softest tissues in human body with elastic moduli around 2 kPa, when glial scar occurs as a consequence of an injury, stiffness of this local area can become higher which forms both physical and chemical obstacles to neurite extension and regeneration in nervous tissue injuries. Soft materials have become more favorable in the studies of CNS tissue due to the selective response of neurons and astrocytes to matrix stiffness (Georges et al. 2006). In addition, gels with low elastic moduli were found to selectively induce neuronal development. It was previously shown that rat adult NSCs primarily differentiated into glial cells when cultured on stiff substrates having elastic moduli between 1 and 10 kPa, whereas soft materials primarily gave rise to neurons. Also, the highest amount of neurons was obtained when culturing on interpenetrating polymer network hydrogel with elastic modulus of 0.5 kPa, which is close to physiological mechanical properties of brain tissue (Saha et al. 2008). While spinal cord and cortical brain neurons favor soft materials to extend their neurites (Balgude et al. 2001; Saha et al. 2008), astrocytes generate stress fibers and they are more activated on the surfaces with high elastic modulus (Georges et al. 2006).

Another important factor about the physical structure of the material is the dimensionality of the substrate. Although two-dimensional (2D) cell culture studies are more commonly preferred because environmental control, cell observation, and manipulation are easy, three-dimensional (3D) studies have great importance as they provide a more realistic model for in vivo studies. In one study, hippocampal neurons were encapsulated into 3D aragonite matrix and compared to ones seeded on 2D surface. The cells showed higher survival rate in 3D cell culture compared to 2D conditions (Peretz et al. 2007). Also, Cunha et al. decorated the 3D biomaterial scaffold with RGD, BMHP1 (bone marrow homing peptide 1), and BMHP2 motifs, for adult NSC culture (Cunha et al. 2011). They provided deeper understanding about the cell behavior in 3D scaffolds which is required for future clinical applications. 3D gel matrices were also studied in injured brain model. Laminin-derived IKVAV motif was linked to self-assembling peptide RADA (16) to form a functional 3D peptide-based scaffold for NSC encapsulation. Beside differentiation of NSCs into neural cell in in vitro conditions, injection of this hydrogel into damaged brain tissue to fill the cavity and form a bridge for the gap eventually led to improvement in brain tissue regeneration (Cheng et al. 2013).

6.3.2 Approaches for Drug Delivery to Central Nervous System

The complexity of the nervous system is an important criterion that should be taken into consideration while designing a system for drug delivery. Biocompatible materials for drug delivery are desired to promote neural regeneration through releasing the cargo in a controlled manner while maintaining the integrity of healthy tissue. However, the presence of BBB and BSCB is the primary problem to deliver drug to CNS and limit the efficacy of drug delivery of therapeutics through forming anatomical, transport, and metabolic barriers. Therefore, different strategies should be considered to enhance drug delivery to CNS, including material properties, drug selection, and delivery method.

6.3.2.1 Material Properties and Methods for Drug Delivery

While designing new materials for neural tissue engineering, it is important to choose appropriate materials for nervous system. The chemical and physical properties of the material must be well evaluated in order to provide controlled release through degradation rate with suitable dimensions for the injected site. Depending on the purpose, you can use different synthetic materials with different mechanical properties and release profile so that the immune response can be modified through altering the composition of the material. For instance, Poly (ethylene glycol) (PEG) has the property to resist cell adhesion and protein adsorption (Alcantar et al. 2000), which contribute to minimize immune response. Further modifications with bioactive epitopes for cell adhesion or mimicking ECM can be used to provide cell

migration into the scaffold, which also contributes to regeneration (Benoit and Anseth 2005; Groll et al. 2005).

Poly (ethylene-covinyl acetate) (pEVA) is another commonly used delivery system used in neural tissue engineering studies since it is a nondegradable and biocompatible scaffold, which makes it a favorable choice. Stability is another important property of pEVA for drug delivery over an extended period. It has been used in nerve growth factor (NGF)- and NT-3-releasing guidance channels to induce regeneration in transected rat dorsal root (Bloch et al. 2001).

To overcome the BBB penetration problem, many different carrier systems have been developed and used in neural tissue engineering studies. The techniques used as delivery system can be classified as systemic and local delivery.

Systemic drug delivery is performed through intravenous or intraperipheral injection, but it requires high dosages to fulfill the therapeutic effect and can influence nontarget tissues due to systemic toxicity. Therefore, while designing systemic drug carriers, it is important to provide properties resisting to long circulation and favorable surface properties for endothelial cell interaction (Misra et al. 2003). For systemic drug delivery, liposomes and polymeric NPs have been extensively studied for brain drug delivery (Garcia-Garcia et al. 2005). Liposomes are biocompatible and biodegradable delivery systems, and their surfaces are generally modified with hydrophilic polymers to deal with plasma clearance of liposomes (Lian and Ho 2001). Generally, poly(ethylene glycol) (PEG) is used for an additional layer, which increases blood circulation time of liposome (Garcia-Garcia et al. 2005). For penetration of liposomes through BBB, the carrier system can be developed by active targeting, which modifies the distribution of liposomes through an antibody or a ligand conjugation that is eventually recognized by the receptor specific to target tissue (Schnyder and Huwyler 2005). Therefore, by combining the effect of PEG on extended circulation time and specificity due to an antibody or a ligand conjugation, delivery can be obtained through the BBB. Liposomes have been used for the treatment of CNS diseases including brain tumors, infection, and ischemia (Zhong and Bellamkonda 2008).

Polymeric nanoparticles (NPs) ranging from 10 to 1000 nm in size can be used as carrier polymers encapsulated or covalently attached to therapeutic drugs (Lockman et al. 2002). Polymeric NPs are more stable against the biological fluids when compared to liposomes. Moreover, their structures are more suitable for controlled and sustained drug release over a period of time after injection. Generally, poly(alkylcyanoacrylates) (PACAs), polyacetates, polysaccharides, and copolymers are used for NP synthesis (Garcia-Garcia et al. 2005). For instance, drugs including dalargin, loperamide, tubocurarine, and doxorubicin have been delivered to the CNS by Polybutylcyanoacrylate (PBCA) NPs (Zhong and Bellamkonda 2008). NPs can also be coated with hydrophilic polymers, such as PEG, to increase their uptake (Brigger et al. 2002).

To manage systemic toxicity of the drugs and increase their effectiveness, local delivery systems are favorable. Local delivery of therapeutic drugs with a biocompatible carrier provides an advantageous method at the target region. This approach also bypasses the BBB penetration problem. For CNS, PLGA and poly-

anhydride poly [bis(p-carboxyphenoxy)] propane-sebacic acid (PCPP-SA) are most commonly used biodegradable polymers for local drug delivery. For instance, PLGA microspheres were used as local delivery for antitumor agents such as 5-fluorouracil and platelet factor 4 fragment to treat brain tumors (Benny et al. 2005; Menei et al. 1996). PLGA microspheres were also used for neurodegenerative diseases. Dopamine and noradrenaline delivery with PLGA microspheres was used as a therapeutic strategy for Parkinson's disease (McRae and Dahlstrom 1994). Also, PLGA microparticles were used as NGF carriers for the protection of neurons from excitotoxin-induced lesions (Benoit et al. 2000).

6.3.2.2 Drug Selection

Depending on the tissue type to be regenerated, a specific therapeutic drug or combination of different drugs can be selected. Within the potential therapeutic drugs for neural tissue engineering, neurotrophins are the most common growth factors used for neural regeneration. Neurotrophins are composed of NGF, brain-derived neurotrophic factor (BDNF), NT-3, and neurotrophin-4/5. For instance, NGF works both in PNS and CNS. It especially enhances survival of cholinergic neurons, which makes it attractive for therapeutic studies against neurodegenerative disorders such as Alzheimer's disease (Siegel and Chauhan 2000). However, while designing a delivery system, it is important to know the right place to inject and dose required, because NGF can cause unwanted sensory neural fiber sprouting which terminally can cause chronic pain (Romero et al. 2001). In addition to NGF, NT-3 functions in neurogenesis through promoting the differentiation of new neurons. Moreover, studies have shown that NT-3 can promote cell survival and neurite outgrowth in motor neurons after spinal cord injury (Bloch et al. 2001; Grill et al. 1997).

Anti-inflammatory drugs can also be used in drug delivery systems to suppress chronic inflammation and immune response caused by implantation. Among these anti-inflammatory drugs, dexamethasone is one of the most commonly used drugs for this purpose. Although it is generally used to treat inflammatory diseases including arthritis and multiple sclerosis, some studies revealed promising results in neural tissue applications (Kim and Martin 2006).

Another drug category used for delivery systems in CNS is chemotherapeutic agents. Since chemotherapeutic agents can also affect nontarget tissues and cause systemic toxicity, targeted delivery of these drugs is quite critical and important. Glioblastoma is one of the most aggressive cancer types with short survival rates. The chemotherapeutic drugs cannot access to the brain by traditional chemotherapy applications because of the presence of BBB. Therefore, therapeutic potential of these drugs can be modified with delivery systems. For example, doxorubicin, one of the most potent antitumor agents, has been attached to the surface of poly(butyl cyanoacrylate) nanoparticles coated with polysorbate 80 and this drug was successfully transported into the brain to treat brain tumors (Gulyaev et al. 1999).

6.4 Concluding Remarks

Nervous system is the most complex system in the body due to the complex interactions of the cells with each other. Also, due to poor regeneration capacity of nervous system, development of new strategies for repair and regeneration of this system is in high demand. Moreover, lack of clinically available successful therapies makes these therapeutic studies more attractive. Biomaterials have been widely studied up to now and they provide highly promising strategies in treatment for disorders of nervous system. They can be tailored at molecular level and their structural and biochemical properties can be tuned, which allows improvement of therapeutic methods according to the purpose of treatment. Looking ahead, a wide range of materials, such as polymers and synthetic self-assembled systems, have already been developed, but it is still essential to generate other biomaterials considering the nature and all requirements of the tissue including physical, chemical, and biological demands.

References

Abbott, N. 1992. *Comparative Physiology of the Blood-Brain Barrier*, Physiology and Pharmacology of the Blood-Brain Barrier. Berlin: Springer.

Abbott, N.J. 2005. Dynamics of CNS Barriers: Evolution, Differentiation, and Modulation. *Cellular and Molecular Neurobiology* 25: 5–23.

———. 2013. Blood-Brain Barrier Structure and Function and the Challenges for CNS Drug Delivery. *Journal of Inherited Metabolic Disease* 36: 437–449.

Abbott, N.J., L. Ronnback, and E. Hansson. 2006. Astrocyte-Endothelial Interactions at the Blood-Brain Barrier. *Nature Reviews Neuroscience* 7: 41–53.

Adams, D.N., E.Y.C. Kao, C.L. Hypolite, M.D. Distefano, W.S. Hu, and P.C. Letourneau. 2005. Growth Cones Turn and Migrate up an Immobilized Gradient of the Laminin IKVAV Peptide. *Journal of Neurobiology* 62: 134–147.

Ahmed, Z., and R.A. Brown. 1999. Adhesion, Alignment, and Migration of Cultured Schwann Cells on Ultrathin Fibronectin Fibres. *Cell Motility and the Cytoskeleton* 42: 331–343.

Ahmed, I., H.Y. Liu, P.C. Mamiya, A.S. Ponery, A.N. Babu, T. Weik, M. Schindler, and S. Meiners. 2006. Three-Dimensional Nanofibrillar Surfaces Covalently Modified With Tenascin-C-Derived Peptides Enhance Neuronal Growth in Vitro. *Journal of Biomedical Materials Research. Part A* 76: 851–860.

Alcantar, N.A., E.S. Aydil, and J.N. Israelachvili. 2000. Polyethylene Glycol-Coated Biocompatible Surfaces. *Journal of Biomedical Materials Research. Part A* 51: 343–351.

Alovskaya, A., T. Alekseeva, J. Phillips, V. King, and R. Brown. 2007. Fibronectin, Collagen, Fibrin-Components of Extracellular Matrix for Nerve Regeneration. *Topics in Tissue Engineering* 3: 1–26.

Armstrong, S.J., M. Wiberg, G. Terenghi, and P.J. Kingham. 2007. ECM Molecules Mediate Both Schwann Cell Proliferation and Activation to Enhance Neurite Outgrowth. *Tissue Engineering* 13: 2863–2870.

Aszodi, A., K.R. Legate, I. Nakchbandi, and R. Fassler. 2006. What Mouse Mutants Teach Us About Extracellular Matrix Function. *Annual Review of Cell and Developmental Biology* 22: 591–621.

Avellino, A.M., D. Hart, A.T. Dailey, M. Mackinnon, D. Ellegala, and M. Kliot. 1995. Differential Macrophage Responses in the Peripheral and Central Nervous System During Wallerian Degeneration of Axons. *Experimental Neurology* 136: 183–198.

Balgude, A., X. Yu, A. Szymanski, and R. Bellamkonda. 2001. Agarose Gel Stiffness Determines Rate of DRG Neurite Extension in 3D Cultures. *Biomaterials* 22: 1077–1084.

Bandtlow, C.E., and D.R. Zimmermann. 2000. Proteoglycans in the Developing Brain: new Conceptual Insights for Old Proteins. *Physiological Reviews* 80: 1267–1290.

Barton, M.J., J.W. Morley, M.A. Stoodley, A. Lauto, and D.A. Mahns. 2014. Nerve Repair: Toward a Sutureless Approach. *Neurosurgical Review* 37: 585–595.

Becker, C.G., and T. Becker. 2002. Repellent Guidance of Regenerating Optic Axons by Chondroitin Sulfate Glycosaminoglycans in Zebrafish. *The Journal of Neuroscience* 22: 842–853.

Bell, J.H., and J.W. Haycock. 2012. Next Generation Nerve Guides: Materials, Fabrication, Growth Factors, and Cell Delivery. *Tissue Engineering. Part B: Reviews* 18: 116–128.

Bellamkonda, R., J. Ranieri, and P. Aebischer. 1995. Laminin Oligopeptide Derivatized Agarose Gels Allow Three-Dimensional Neurite Extension in Vitro. *Journal of Neuroscience Research* 41: 501–509.

Benny, O., M. Duvshani-Eshet, T. Cargioli, L. Bello, A. Bikfalvi, R.S. Carroll, and M. Machluf. 2005. Continuous Delivery of Endogenous Inhibitors from Poly(Lactic-co-Glycolic Acid) Polymeric Microspheres Inhibits Glioma Tumor Growth. *Clinical Cancer Research* 11: 768–776.

Benoit, D.S.W., and K.S. Anseth. 2005. Heparin Functionalized PEG Gels that Modulate Protein Adsorption for hMSC Adhesion and Differentiation. *Acta Biomaterialia* 1: 461–470.

Benoit, J.P., N. Faisant, M.C. Venier-Julienne, and P. Menei. 2000. Development of Microspheres for Neurological Disorders: From Basics to Clinical Applications. *Journal of Controlled Release* 65: 285–296.

Bernstein, J.J., and W.J. Goldberg. 1995. Experimental Spinal Cord Transplantation as a Mechanism of Spinal Cord Regeneration. *Paraplegia* 33: 250–253.

Bignami, A., M. Hosley, and D. Dahl. 1993. Hyaluronic Acid and Hyaluronic Acid-Binding Proteins in Brain Extracellular Matrix. *Anatomy and Embryology* 188: 419–433.

Bloch, J., E.G. Fine, N. Bouche, A.D. Zurn, and P. Aebischer. 2001. Nerve Growth Factor- and Neurotrophin-3-Releasing Guidance Channels Promote Regeneration of the Transected rat Dorsal Root. *Experimental Neurology* 172: 425–432.

Borgens, R.B., J.W. Vanable, and L.F. Jaffe. 1979. Small Artificial Currents Enhance Xenopus Limb Regeneration. *Journal of Experimental Zoology* 207: 217–226.

Boulay, A.C., A. Mazeraud, S. Cisternino, B. Saubamea, P. Mailly, L. Jourdren, C. Blugeon, V. Mignon, M. Smirnova, A. Cavallo, P. Ezan, P. Ave, F. Dingli, D. Loew, P. Vieira, F. Chretien, and M. Cohen-Salmon. 2015. Immune Quiescence of the Brain is set by Astroglial Connexin 43. *Journal of Neuroscience* 35: 4427–4439.

Braunewell, K.H., P. Pesheva, J.B. McCarthy, L.T. Furcht, B. Schmitz, and M. Schachner. 1995. Functional Involvement of Sciatic Nerve-Derived Versican- and Decorin-Like Molecules and Other Chondroitin Sulphate Proteoglycans in ECM-Mediated Cell Adhesion and Neurite Outgrowth. *European Journal of Neuroscience* 7: 805–814.

Brigger, I., C. Dubernet, and P. Couvreur. 2002. Nanoparticles in Cancer Therapy and Diagnosis. *Advanced Drug Delivery Reviews* 54: 631–651.

Bryan, D.J., J.B. Tang, S.A. Doherty, D.D. Hile, D.J. Trantolo, D.L. Wise, and I.C. Summerhayes. 2004. Enhanced Peripheral Nerve Regeneration Through a Poled Bioresorbable Poly (Lactic-co-Glycolic Acid) Guidance Channel. *Journal of Neural Engineering* 1: 91.

Bulsara, K.R., B.J. Iskandar, A.T. Villavicencio, and J.H. Skene. 2002. A new Millenium for Spinal Cord Regeneration: Growth-Associated Genes. *Spine (Phila Pa 1976)* 27: 1946–1949.

Bunge, R.P. 1993. Expanding Roles for the Schwann Cell: Ensheathment, Myelination, Trophism and Regeneration. *Current Opinion in Neurobiology* 3: 805–809.

Bunge, R.P., and M.B. Bunge. 1983. Interrelationship Between Schwann Cell Function and Extracellular Matrix Production. *Trends in Neurosciences* 6: 499–505.

Bunge, M.B., P.M. Wood, L.B. Tynan, and M.L. Bates. 1989. Perineurium Originates from Fibroblasts: Demonstration In Vitro with a Retroviral Marker. *Science* 243: 229–231.

Bush, T.G., N. Puvanachandra, C.H. Horner, A. Polito, T. Ostenfeld, C.N. Svendsen, L. Mucke, M.H. Johnson, and M.V. Sofroniew. 1999. Leukocyte Infiltration, Neuronal Degeneration, and Neurite Outgrowth After Ablation of Scar-Forming, Reactive Astrocytes in Adult Transgenic Mice. *Neuron* 23: 297–308.

Carlstedt, T. 1997. Nerve Fibre Regeneration Across the Peripheral-Central Transitional Zone. *Journal of Anatomy* 190(Pt 1): 51–56.

Chaudhry, V., J.D. Glass, and J.W. Griffin. 1992. Wallerian Degeneration in Peripheral Nerve Disease. *Neurologic Clinics* 10: 613–627.

Chen, M.B., F. Zhang, and W.C. Lineaweaver. 2006. Luminal Fillers in Nerve Conduits for Peripheral Nerve Repair. *Annals of Plastic Surgery* 57: 462–471.

Cheng, T.Y., M.H. Chen, W.H. Chang, M.Y. Huang, and T.W. Wang. 2013. Neural Stem Cells Encapsulated in a Functionalized Self-Assembling Peptide Hydrogel for Brain Tissue Engineering. *Biomaterials* 34: 2005–2016.

Chernousov, M.A., K. Rothblum, R.C. Stahl, A. Evans, L. Prentiss, and D.J. Carey. 2006. Glypican-1 and α4 (V) Collagen Are Required for Schwann Cell Myelination. *The Journal of Neuroscience* 26: 508–517.

Chung, H.J., and T.G. Park. 2007. Surface Engineered and Drug Releasing pre-Fabricated Scaffolds for Tissue Engineering. *Advanced Drug Delivery Reviews* 59: 249–262.

Clements, I.P., V.J. Mukhatyar, A. Srinivasan, J.T. Bentley, D.S. Andreasen, and R.V. Bellamkonda. 2013. Regenerative Scaffold Electrodes for Peripheral Nerve Interfacing. *IEEE Transactions on Neural Systems and Rehabilitation Engineering* 21: 554–566.

Corey, J.M., D.Y. Lin, K.B. Mycek, Q. Chen, S. Samuel, E.L. Feldman, and D.C. Martin. 2007. Aligned Electrospun Nanofibers Specify the Direction of Dorsal Root Ganglia Neurite Growth. *Journal of Biomedical Materials Research. Part A* 83: 636–645.

Cui, H., M.J. Webber, and S.I. Stupp. 2010. Self-Assembly of Peptide Amphiphiles: From Molecules to Nanostructures to Biomaterials. *Peptide Science* 94: 1–18.

Cunha, C., S. Panseri, O. Villa, D. Silva, and F. Gelain. 2011. 3D Culture of Adult Mouse Neural Stem Cells Within Functionalized Self-Assembling Peptide Scaffolds. *International Journal of Nanomedicine* 6: 943–955.

Curtis, A., and M. Riehle. 2001. Tissue Engineering: The Biophysical Background. *Physics in Medicine and Biology* 46: R47–R65.

Daud, M.F., K.C. Pawar, F. Claeyssens, A.J. Ryan, and J.W. Haycock. 2012. An Aligned 3D Neuronal-Glial Co-culture Model for Peripheral Nerve Studies. *Biomaterials* 33: 5901–5913.

De Luca, A.C., S.P. Lacour, W. Raffoul, and P.G. Di Summa. 2014. Extracellular Matrix Components in Peripheral Nerve Repair: how to Affect Neural Cellular Response and Nerve Regeneration? *Neural Regeneration Research* 9: 1943.

Deane, R., and B.V. Zlokovic. 2007. Role of the Blood-Brain Barrier in the Pathogenesis of Alzheimer's Disease. *Current Alzheimer Research* 4: 191–197.

Dickendesher, T.L., K.T. Baldwin, Y.A. Mironova, Y. Koriyama, S.J. Raiker, K.L. Askew, A. Wood, C.G. Geoffroy, B. Zheng, C.D. Liepmann, Y. Katagiri, L.I. Benowitz, H.M. Geller, and R.J. Giger. 2012. NgR1 and NgR3 are Receptors for Chondroitin Sulfate Proteoglycans. *Nature Neuroscience* 15: 703–712.

Ding, C., Y. Wang, and S. Zhang. 2007. Synthesis and Characterization of Degradable Electrically Conducting Copolymer of Aniline Pentamer and Polyglycolide. *European Polymer Journal* 43: 4244–4252.

Dityatev, A., and M. Schachner. 2003. Extracellular Matrix Molecules and Synaptic Plasticity. *Nature Reviews Neuroscience* 4: 456–468.

Eather, T.F., M. Pollock, and D.B. Myers. 1986. Proximal and Distal Changes in Collagen Content of Peripheral Nerve that Follow Transection and Crush Lesions. *Experimental Neurology* 92: 299–310.

El-Bacha, R., and A. Minn. 1999. Drug metabolizing enzymes in cerebrovascular endothelial cells afford a metabolic protection to the brain. *Cellular and Molecular Biology (Noisy-le-Grand, France)* 45: 15–23.

Engler, A.J., S. Sen, H.L. Sweeney, and D.E. Discher. 2006. Matrix Elasticity Directs Stem Cell Lineage Specification. *Cell* 126: 677–689.

Evans, G.R. 2000. Challenges to Nerve Regeneration. *Seminars in Surgical Oncology* 19: 312–318.

Fansa, H., G. Keilhoff, G. Wolf, W. Schneider, and B.G. Gold. 2001. Tissue Engineering of Peripheral Nerves: A Comparison of Venous and Acellular Muscle Grafts with Cultured Schwann Cells. *Plastic and Reconstructive Surgery* 107: 495–496.

Faroni, A., S.A. Mobasseri, P.J. Kingham, and A.J. Reid. 2015. Peripheral Nerve Regeneration: Experimental Strategies and Future Perspectives. *Advanced Drug Delivery Reviews* 82–83: 160–167.

Fawcett, J.W., and R.A. Asher. 1999. The Glial Scar and Central Nervous System Repair. *Brain Research Bulletin* 49: 377–391.

Freudenberg, U., A. Hermann, P.B. Welzel, K. Stirl, S.C. Schwarz, M. Grimmer, A. Zieris, W. Panyanuwat, S. Zschoche, D. Meinhold, A. Storch, and C. Werner. 2009. A Star-PEG-Heparin Hydrogel Platform to aid Cell Replacement Therapies for Neurodegenerative Diseases. *Biomaterials* 30: 5049–5060.

Fu, S.Y., and T. Gordon. 1997. The Cellular and Molecular Basis of Peripheral Nerve Regeneration. *Molecular Neurobiology* 14: 67–116.

Garcia-Garcia, E., K. Andrieux, S. Gil, and P. Couvreur. 2005. Colloidal Carriers and Blood-Brain Barrier (BBB) Translocation: A way to Deliver Drugs to the Brain? *International Journal of Pharmaceutics* 298: 274–292.

Georges, P.C., and P.A. Janmey. 2005. Cell type-specific response to growth on soft materials. *Journal of Applied Physiology (Bethesda, Md.: 1985)* 98: 1547–53.

Georges, P.C., W.J. Miller, D.F. Meaney, E.S. Sawyer, and P.A. Janmey. 2006. Matrices with Compliance Comparable to that of Brain Tissue Select Neuronal Over Glial Growth in Mixed Cortical Cultures. *Biophysical Journal* 90: 3012–3018.

Ghasemi-Mobarakeh, L., M.P. Prabhakaran, M. Morshed, M.H. Nasr-Esfahani, H. Baharvand, S. Kiani, S.S. Al-Deyab, and S. Ramakrishna. 2011. Application of Conductive Polymers, Scaffolds and Electrical Stimulation for Nerve Tissue Engineering. *Journal of Tissue Engineering and Regenerative Medicine* 5: e17–e35.

Gilliatt, R., and R. Hjorth. 1972. Nerve Conduction During Wallerian Degeneration in the Baboon. *Journal of Neurology, Neurosurgery & Psychiatry* 35: 335–341.

Glasby, M., S. Gschmeissner, C.L. Huang, and B. De Souza. 1986. Degenerated Muscle Grafts Used for Peripheral Nerve Repair in Primates. *Journal of Hand Surgery (British and European Volume)* 11: 347–351.

Graf, J., R.C. Ogle, F.A. Robey, M. Sasaki, G.R. Martin, Y. Yamada, and H.K. Kleinman. 1987. A Pentapeptide from the Laminin B1 Chain Mediates Cell Adhesion and Binds the 67,000 Laminin Receptor. *Biochemistry* 26: 6896–6900.

Griffin, J.W., E.B. George, S.-T. Hsieh, and J.D. Glass. 1995. 20 Axonal Degeneration and Disorders of the Axonal Cytoskeleton. *The Axon: Structure, Function, and Pathophysiology* 375.

Grill, R., K. Murai, A. Blesch, F.H. Gage, and M.H. Tuszynski. 1997. Cellular Delivery of Neurotrophin-3 Promotes Corticospinal Axonal Growth and Partial Functional Recovery After Spinal Cord Injury. *Journal of Neuroscience* 17: 5560–5572.

Groll, J., J. Fiedler, E. Engelhard, T. Ameringer, S. Tugulu, H.A. Klok, R.E. Brenner, and M. Moeller. 2005. A Novel Star PEG-Derived Surface Coating for Specific Cell Adhesion. *Journal of Biomedical Materials Research. Part A* 74: 607–617.

Gu, X., F. Ding, and D.F. Williams. 2014. Neural Tissue Engineering Options for Peripheral Nerve Regeneration. *Biomaterials* 35: 6143–6156.

Gulati, A.K. 1998. Immune Response and Neurotrophic Factor Interactions in Peripheral Nerve Transplants. *Acta Haematologica* 99: 171–174.

Gulati, A.K., and G.P. Cole. 1990. Nerve Graft Immunogenicity as a Factor Determining Axonal Regeneration in the Rat. *Journal of Neurosurgery* 72: 114–122.

Gulyaev, A.E., S.E. Gelperina, I.N. Skidan, A.S. Antropov, G.Y. Kivman, and J. Kreuter. 1999. Significant Transport of Doxorubicin into the Brain With Polysorbate 80-Coated Nanoparticles. *Pharmaceutical Research* 16: 1564–1569.

Hawkins, B.T., and T.P. Davis. 2005. The Blood-Brain Barrier/Neurovascular Unit in Health and Disease. *Pharmacological Reviews* 57: 173–185.

Hoffman-Kim, D., J.A. Mitchel, and R.V. Bellamkonda. 2010. Topography, Cell Response, and Nerve Regeneration. *Annual Review of Biomedical Engineering* 12: 203–231.

Holmes, T.C. 2002. Novel Peptide-Based Biomaterial Scaffolds for Tissue Engineering. *Trends in Biotechnology* 20: 16–21.

Horner, P.J., and F.H. Gage. 2000. Regenerating the Damaged Central Nervous System. *Nature* 407: 963–970.

Hubert, T., S. Grimal, P. Carroll, and A. Fichard-Carroll. 2009. Collagens in the Developing and Diseased Nervous System. *Cellular and Molecular Life Sciences* 66: 1223–1238.

Hudson, B.G., S.T. Reeders, and K. Tryggvason. 1993. Type IV Collagen: Structure, Gene Organization, and Role in Human Diseases. Molecular Basis of Goodpasture and Alport Syndromes and Diffuse Leiomyomatosis. *Journal of Biological Chemistry* 268: 26033–26036.

Hunanyan, A.S., G. Garcia-Alias, J.M. Levine, J.W. Fawcett, L.M. Mendell, and V.L. Arvanian. 2010. Role of Chondroitin Sulfate Proteoglycans (CSPGs) in Synaptic Plasticity and Neurotransmission in Mammalian Spinal Cord. *Journal of Neuroscience* 30(23):7761-7769 (23): 7761–7769.

Ichihara, S., Y. Inada, and T. Nakamura. 2008. Artificial Nerve Tubes and Their Application for Repair of Peripheral Nerve Injury: An Update of Current Concepts. *Injury* 39: 29–39.

Itoh, S., K. Takakuda, S. Ichinose, M. Kikuchi, and K. Schinomiya. 2001. A Study of Induction of Nerve Regeneration Using Bioabsorbable Tubes. *Journal of Reconstructive Microsurgery* 17: 115–124.

Itoh, S., I. Yamaguchi, M. Suzuki, S. Ichinose, K. Takakuda, H. Kobayashi, K. Shinomiya, and J. Tanaka. 2003. Hydroxyapatite-Coated Tendon Chitosan Tubes With Adsorbed Laminin Peptides Facilitate Nerve Regeneration in Vivo. *Brain Research* 993: 111–123.

Jalili-Firoozinezhad, S., F. Mirakhori, and H. Baharvand. 2014. Nanotissue Engineering of Neural Cells. *Stem Cell Nanoengineering* 265.

Jiang, B., P. Zhang, and B. Jiang. 2010. Advances in Small gap Sleeve Bridging Peripheral Nerve Injury. *Artificial Cells, Blood Substitutes, and Immobilization Biotechnology* 38: 1–4.

Jiang, X., R. Mi, A. Hoke, and S.Y. Chew. 2014. Nanofibrous Nerve Conduit-Enhanced Peripheral Nerve Regeneration. *Journal of Tissue Engineering and Regenerative Medicine* 8: 377–385.

Johnson, E.O., A.B. Zoubos, and P.N. Soucacos. 2005. Regeneration and Repair of Peripheral Nerves. *Injury* 36(Suppl 4): S24–S29.

Jones, L.L., R.U. Margolis, and M.H. Tuszynski. 2003. The Chondroitin Sulfate Proteoglycans Neurocan, Brevican, Phosphacan, and Versican are Differentially Regulated Following Spinal Cord Injury. *Experimental Neurology* 182: 399–411.

Khatiwala, C.B., S.R. Peyton, and A.J. Putnam. 2006. Intrinsic Mechanical Properties of the Extracellular Matrix Affect the Behavior of pre-Osteoblastic MC3T3-E1 Cells. *American Journal Of Physiology. Cell Physiology* 290: C1640–C1650.

Kim, D.H., and D.C. Martin. 2006. Sustained Release of Dexamethasone from Hydrophilic Matrices Using PLGA Nanoparticles for Neural Drug Delivery. *Biomaterials* 27: 3031–3037.

Kim, D.H., S.E. Connolly, S. Zhao, R.W. Beuerman, R.M. Voorhies, and D.G. Kline. 1993. Comparison of Macropore, Semipermeable, and Nonpermeable Collagen Conduits in Nerve Repair. *Journal of Reconstructive Microsurgery* 9: 415–420.

Kim, Y.-T., V.K. Haftel, S. Kumar, and R.V. Bellamkonda. 2008. The Role of Aligned Polymer Fiber-Based Constructs in the Bridging of Long Peripheral Nerve Gaps. *Biomaterials* 29: 3117–3127.

Kim, S.-E., E.C. Harker, A.C. De Leon, R.C. Advincula, and J.K. Pokorski. 2015. Coextruded, Aligned, and Gradient-Modified Poly (ε-Caprolactone) Fibers as Platforms for Neural Growth. *Biomacromolecules* 16: 860–867.

Koh, H.S., T. Yong, W.E. Teo, C.K. Chan, M.E. Puhaindran, T.C. Tan, A. Lim, B.H. Lim, and S. Ramakrishna. 2010. In Vivo Study of Novel Nanofibrous Intra-Luminal Guidance Channels to Promote Nerve Regeneration. *Journal of Neural Engineering* 7: 046003.

Koopmans, G., B. Hasse, and N. Sinis. 2009. Chapter 19: The Role of Collagen in Peripheral Nerve Repair. *International Review of Neurobiology* 87: 363–379.

Kwok, J.C., D. Carulli, and J.W. Fawcett. 2010. In Vitro Modeling of Perineuronal Nets: Hyaluronan Synthase and Link Protein are Necessary for Their Formation and Integrity. *Journal of Neurochemistry* 114: 1447–1459.

Kwok, J.C., G. Dick, D. Wang, and J.W. Fawcett. 2011. Extracellular Matrix and Perineuronal Nets in CNS Repair. *Developmental Neurobiology* 71: 1073–1089.

Lanaras, T.I., H.E. Schaller, and N. Sinis. 2009. Brachial Plexus Lesions: 10 Years of Experience in a Center for Microsurgery in Germany. *Microsurgery* 29: 87–94.

Larsen, P.H., J.E. Wells, W.B. Stallcup, G. Opdenakker, and V.W. Yong. 2003. Matrix Metalloproteinase-9 Facilitates Remyelination in Part by Processing the Inhibitory NG2 Proteoglycan. *The Journal of Neuroscience* 23: 11127–11135.

Lassner, F., E. Schaller, G. Steinhoff, K. Wonigeit, G.F. Walter, and A. Berger. 1989. Cellular Mechanisms of Rejection and Regeneration in Peripheral Nerve Allografts. *Transplantation* 48: 386–392.

Lau, L.W., R. Cua, M.B. Keough, S. Haylock-Jacobs, and V.W. Yong. 2013. Pathophysiology of the Brain Extracellular Matrix: A new Target for Remyelination. *Nature Reviews Neuroscience* 14: 722–729.

Leach, J.B., X.Q. Brown, J.G. Jacot, P.A. Dimilla, and J.Y. Wong. 2007. Neurite Outgrowth and Branching of PC12 Cells on Very Soft Substrates Sharply Decreases Below a Threshold of Substrate Rigidity. *Journal of Neural Engineering* 4: 26–34.

Lee, S.K., and S.W. Wolfe. 2000. Peripheral Nerve Injury and Repair. *Journal of the American Academy of Orthopaedic Surgeons* 8: 243–252.

Li, X., Z. Yang, and A. Zhang. 2009. The Effect of Neurotrophin-3/Chitosan Carriers on the Proliferation and Differentiation of Neural Stem Cells. *Biomaterials* 30: 4978–4985.

Li, X.W., E. Katsanevakis, X.Y. Liu, N. Zhang, and X.J. Wen. 2012. Engineering Neural Stem Cell Fates With Hydrogel Design for Central Nervous System Regeneration. *Progress in Polymer Science* 37: 1105–1129.

Lian, T., and R.J. Ho. 2001. Trends and Developments in Liposome Drug Delivery Systems. *Journal of Pharmaceutical Sciences* 90: 667–680.

Lockman, P.R., R.J. Mumper, M.A. Khan, and D.D. Allen. 2002. Nanoparticle Technology for Drug Delivery Across the Blood-Brain Barrier. *Drug Development and Industrial Pharmacy* 28: 1–13.

Lutolf, M.P., and J.A. Hubbell. 2005. Synthetic Biomaterials as Instructive Extracellular Microenvironments for Morphogenesis in Tissue Engineering. *Nature Biotechnology* 23: 47–55.

Mackinnon, S., A. Hudson, R. Falk, J. Bilbao, D. Kline, and D. Hunter. 1982. Nerve Allograft Response: A Quantitative Immunological Study. *Neurosurgery* 10: 61–69.

Mammadov, B., R. Mammadov, M.O. Guler, and A.B. Tekinay. 2012. Cooperative Effect of Heparan Sulfate and Laminin Mimetic Peptide Nanofibers on the Promotion of Neurite Outgrowth. *Acta Biomaterialia* 8: 2077–2086.

Marquardt, L.M., and S.E. Sakiyama-Elbert. 2013. Engineering Peripheral Nerve Repair. *Current Opinion in Biotechnology* 24: 887–892.

Matsumoto, K., K. Ohnishi, T. Kiyotani, T. Sekine, H. Ueda, T. Nakamura, K. Endo, and Y. Shimizu. 2000. Peripheral Nerve Regeneration Across an 80-mm gap Bridged by a Polyglycolic Acid (PGA)-Collagen Tube Filled With Laminin-Coated Collagen Fibers: A Histological and Electrophysiological Evaluation of Regenerated Nerves. *Brain Research* 868: 315–328.

McCaig, C.D., A.M. Rajnicek, B. Song, and M. Zhao. 2005. Controlling Cell Behavior Electrically: Current Views and Future Potential. *Physiological Reviews* 85: 943–978.

McKeon, R.J., R.C. Schreiber, J.S. Rudge, and J. Silver. 1991. Reduction of Neurite Outgrowth in a Model of Glial Scarring Following CNS Injury is Correlated With the Expression of Inhibitory Molecules on Reactive Astrocytes. *Journal of Neuroscience* 11: 3398–3411.

Mckeon, R.J., M.J. Jurynec, and C.R. Buck. 1999. The Chondroitin Sulfate Proteoglycans Neurocan and Phosphacan are Expressed by Reactive Astrocytes in the Chronic CNS Glial Scar. *The Journal of Neuroscience* 19: 10778–10788.

McRae, A., and A. Dahlstrom. 1994. Transmitter-Loaded Polymeric Microspheres Induce Regrowth of Dopaminergic Nerve Terminals in Striata of Rats With 6-OH-DA Induced Parkinsonism. *Neurochemistry International* 25: 27–33.

Menei, P., M. Boisdron-Celle, A. Croue, G. Guy, and J.P. Benoit. 1996. Effect of Stereotactic Implantation of Biodegradable 5-Fluorouracil-Loaded Microspheres in Healthy and C6 Glioma-Bearing Rats. *Neurosurgery* 39: 117–123; discussion 123–124.

Milner, R., M. Wilby, S. Nishimura, K. Boylen, G. Edwards, J. Fawcett, C. Streuli, and R. Pytela. 1997. Division of Labor of Schwann Cell Integrins During Migration on Peripheral Nerve Extracellular Matrix Ligands. *Developmental Biology* 185: 215–228.

Misra, A., S. Ganesh, A. Shahiwala, and S.P. Shah. 2003. Drug Delivery to the Central Nervous System: A Review. *Journal of Pharmacy & Pharmaceutical Sciences* 6: 252–273.

Mobasseri, S.A., G. Terenghi, and S. Downes. 2013. Micro-Structural Geometry of Thin Films Intended for the Inner Lumen of Nerve Conduits Affects Nerve Repair. *Journal of Materials Science. Materials in Medicine* 24: 1639–1647.

Navarro, X., M. Vivó, and A. Valero-Cabré. 2007. Neural Plasticity After Peripheral Nerve Injury and Regeneration. *Progress in Neurobiology* 82: 163–201.

Nguyen, H.T., C. Wei, J.K. Chow, L. Nguy, H.K. Nguyen, and C.E. Schmidt. 2013. Electric Field Stimulation Through a Substrate Influences Schwann Cell and Extracellular Matrix Structure. *Journal of Neural Engineering* 10: 046011.

Oh, S.H., J.R. Kim, G.B. Kwon, U. Namgung, K.S. Song, and J.H. Lee. 2013. Effect of Surface Pore Structure of Nerve Guide Conduit on Peripheral Nerve Regeneration. *Tissue Engineering. Part C, Methods* 19: 233–243.

Ohtsuki, S., and T. Terasaki. 2007. Contribution of Carrier-Mediated Transport Systems to the Blood–Brain Barrier as a Supporting and Protecting Interface for the Brain; Importance for CNS Drug Discovery and Development. *Pharmaceutical Research* 24: 1745–1758.

Pabari, A., S.Y. Yang, A.M. Seifalian, and A. Mosahebi. 2010. Modern Surgical Management of Peripheral Nerve gap. *Journal of Plastic, Reconstructive & Aesthetic Surgery* 63: 1941–1948.

Pan, W., W.A. Banks, and A.J. Kastin. 1997. Permeability of the Blood–Brain and Blood–Spinal Cord Barriers to Interferons. *Journal of Neuroimmunology* 76: 105–111.

Pardridge, W.M. 2007. Blood-Brain Barrier Delivery. *Drug Discovery Today* 12: 54–61.

Pedersen, J.A., and M.A. Swartz. 2005. Mechanobiology in the Third Dimension. *Annals of Biomedical Engineering* 33: 1469–1490.

Peretz, H., A.E. Talpalar, R. Vago, and D. Baranes. 2007. Superior Survival and Durability of Neurons and Astrocytes on 3-Dimensional Aragonite Biomatrices. *Tissue Engineering* 13: 461–472.

Pham, Q.P., U. Sharma, and A.G. Mikos. 2006. Electrospinning of Polymeric Nanofibers for Tissue Engineering Applications: A Review. *Tissue Engineering* 12: 1197–1211.

Pierschbacher, M.D., and E. Ruoslahti. 1984. Cell Attachment Activity of Fibronectin can be Duplicated by Small Synthetic Fragments of the Molecule. *Nature* 309: 30–33.

Pollard, J.D., J.G. McLeod, and R.S. Gye. 1971. The use of Immunosuppressive Agents in Peripheral Nerve Homograft Surgery: An Experimental Study. *Proceedings of the Australian Association of Neurologists* 8: 77–83.

Prabhakaran, M.P., J. Venugopal, C.K. Chan, and S. Ramakrishna. 2008. Surface Modified Electrospun Nanofibrous Scaffolds for Nerve Tissue Engineering. *Nanotechnology* 19: 455102.

Prowse, A.B., F. Chong, P.P. Gray, and T.P. Munro. 2011. Stem Cell Integrins: Implications for ex-Vivo Culture and Cellular Therapies. *Stem Cell Research* 6: 1–12.

Rangappa, N., A. Romero, K.D. Nelson, R.C. Eberhart, and G.M. Smith. 2000. Laminin-Coated Poly (L-Lactide) Filaments Induce Robust Neurite Growth While Providing Directional Orientation. *Journal of Biomedical Materials Research* 51: 625–634.

Rauch, U. 2007. Brain Matrix: Structure, Turnover and Necessity. *Biochemical Society Transactions* 35: 656–660.

Ray, W.Z., and S.E. Mackinnon. 2010. Management of Nerve Gaps: Autografts, Allografts, Nerve Transfers, and end-to-Side Neurorrhaphy. *Experimental Neurology* 223: 77–85.

Ribeiro-Resende, V.T., B. Koenig, S. Nichterwitz, S. Oberhoffner, and B. Schlosshauer. 2009. Strategies for Inducing the Formation of Bands of Bungner in Peripheral Nerve Regeneration. *Biomaterials* 30: 5251–5259.

Richardson, P.M., U.M. McGuinness, and A.J. Aguayo. 1980. Axons from CNS Neurons Regenerate into PNS Grafts. *Nature* 284: 264–265.

Rivers, T.J., T.W. Hudson, and C.E. Schmidt. 2002. Synthesis of a Novel, Biodegradable Electrically Conducting Polymer for Biomedical Applications. *Advanced Functional Materials* 12: 33–37.

Romero, M.I., N. Rangappa, M.G. Garry, and G.M. Smith. 2001. Functional Regeneration of Chronically Injured Sensory Afferents into Adult Spinal Cord After Neurotrophin Gene Therapy. *Journal of Neuroscience* 21: 8408–8416.

Rutka, J.T., G. Apodaca, R. Stern, and M. Rosenblum. 1988. The Extracellular Matrix of the Central and Peripheral Nervous Systems: Structure and Function. *Journal of Neurosurgery* 69: 155–170.

Rutkowski, G.E., C.A. Miller, S. Jeftinija, and S.K. Mallapragada. 2004. Synergistic Effects of Micropatterned Biodegradable Conduits and Schwann Cells on Sciatic Nerve Regeneration. *Journal of Neural Engineering* 1: 151.

Saha, K., A.J. Keung, E.F. Irwin, Y. Li, L. Little, D.V. Schaffer, and K.E. Healy. 2008. Substrate Modulus Directs Neural Stem Cell Behavior. *Biophysical Journal* 95: 4426–4438.

Santiago, L.Y., J. Clavijo-Alvarez, C. Brayfield, J.P. Rubin, and K.G. Marra. 2009. Delivery of Adipose-Derived Precursor Cells for Peripheral Nerve Repair. *Cell Transplantation* 18: 145–158.

Schense, J.C., J. Bloch, P. Aebischer, and J.A. Hubbell. 2000. Enzymatic Incorporation of Bioactive Peptides into Fibrin Matrices Enhances Neurite Extension. *Nature Biotechnology* 18: 415–419.

Schmidt, C.E., and J.B. Leach. 2003. Neural Tissue Engineering: Strategies for Repair and Regeneration. *Annual Review of Biomedical Engineering* 5: 293–347.

Schmidt, C.E., V.R. Shastri, J.P. Vacanti, and R. Langer. 1997. Stimulation of neurite outgrowth using an electrically conducting polymer. *Proceedings of the National Academy of Sciences of the United States of America* 94: 8948–8953.

Schnyder, A., and J. Huwyler. 2005. Drug Transport to Brain with Targeted Liposomes. *NeuroRx* 2: 99–107.

Seil, J.T., and T.J. Webster. 2010. Electrically Active Nanomaterials as Improved Neural Tissue Regeneration Scaffolds. *Wiley Interdisciplinary Reviews: Nanomedicine and Nanobiotechnology* 2: 635–647.

Sharma, H.S. 2005. Pathophysiology of Blood-Spinal Cord Barrier in Traumatic Injury and Repair. *Current Pharmaceutical Design* 11: 1353–1389.

Sharma, K., M.E. Selzer, and S. Li. 2012. Scar-Mediated Inhibition and CSPG Receptors in the CNS. *Experimental Neurology* 237: 370–378.

Shellswell, G.B., D.J. Restall, V.C. Duance, and A.J. Bailey. 1979. Identification and Differential Distribution of Collagen Types in the Central and Peripheral Nervous Systems. *FEBS Letters* 106: 305–308.

Sheppard, A.M., S.K. Hamilton, and A.L. Pearlman. 1991. Changes in the Distribution of Extracellular Matrix Components Accompany Early Morphogenetic Events of Mammalian Cortical Development. *The Journal of Neuroscience* 11: 3928–3942.

Siegel, G.J., and N.B. Chauhan. 2000. Neurotrophic Factors in Alzheimer's and Parkinson's Disease Brain. *Brain Research. Brain Research Reviews* 33: 199–227.

Siegel, G.J., B.W. Agranoff, R.W. Albers, S.K. Fisher, M.D. Uhler, and D.E. Pleasure. 1999. *Regeneration in the Central and Peripheral Nervous Systems*.

Siemionow, M., and G. Brzezicki. 2009. Chapter 8: Current Techniques and Concepts in Peripheral Nerve Repair. *International Review of Neurobiology* 87: 141–172.

Silva, G.A., C. Czeisler, K.L. Niece, E. Beniash, D.A. Harrington, J.A. Kessler, and S.I. Stupp. 2004. Selective Differentiation of Neural Progenitor Cells by High-Epitope Density Nanofibers. *Science* 303: 1352–1355.

Silva, N.A., M.J. Cooke, R.Y. Tam, N. Sousa, A.J. Salgado, R.L. Reis, and M.S. Shoichet. 2012. The Effects of Peptide Modified Gellan gum and Olfactory Ensheathing Glia Cells on Neural Stem/Progenitor Cell Fate. *Biomaterials* 33: 6345–6354.

Silver, J., and J.H. Miller. 2004. Regeneration Beyond the Glial Scar. *Nature Reviews Neuroscience* 5: 146–156.

Stirling, D.P., and P.K. Stys. 2010. Mechanisms of Axonal Injury: Internodal Nanocomplexes and Calcium Deregulation. *Trends in Molecular Medicine* 16: 160–170.

Stoll, G., J.W. Griffin, C.Y. Li, and B.D. Trapp. 1989. Wallerian Degeneration in the Peripheral Nervous System: Participation of Both Schwann Cells and Macrophages in Myelin Degradation. *Journal of Neurocytology* 18: 671–683.

Subbiah, T., G. Bhat, R. Tock, S. Parameswaran, and S. Ramkumar. 2005. Electrospinning of Nanofibers. *Journal of Applied Polymer Science* 96: 557–569.

Sun, M., M. McGowan, P.J. Kingham, G. Terenghi, and S. Downes. 2010. Novel Thin-Walled Nerve Conduit With Microgrooved Surface Patterns for Enhanced Peripheral Nerve Repair. *Journal of Materials Science. Materials in Medicine* 21: 2765–2774.

Tan, A., J. Rajadas, and A.M. Seifalian. 2012. Biochemical Engineering Nerve Conduits Using Peptide Amphiphiles. *Journal of Controlled Release* 163: 342–352.

Tang, X., J.E. Davies, and S.J. Davies. 2003. Changes in Distribution, Cell Associations, and Protein Expression Levels of NG2, Neurocan, Phosphacan, Brevican, Versican V2, and Tenascin-C During Acute to Chronic Maturation of Spinal Cord Scar Tissue. *Journal of Neuroscience Research* 71: 427–444.

Tashiro, K.-I., G. Sephel, B. Weeks, M. Sasaki, G. Martin, H.K. Kleinman, and Y. Yamada. 1989. A Synthetic Peptide Containing the IKVAV Sequence from the A Chain of Laminin Mediates Cell Attachment, Migration, and Neurite Outgrowth. *Journal of Biological Chemistry* 264: 16174–16182.

Toba, T., T. Nakamura, Y. Shimizu, K. Matsumoto, K. Ohnishi, S. Fukuda, M. Yoshitani, H. Ueda, Y. Hori, and K. Endo. 2001. Regeneration of Canine Peroneal Nerve With the use of a Polyglycolic Acid–Collagen Tube Filled With Laminin-Soaked Collagen Sponge: A Comparative Study of Collagen Sponge and Collagen Fibers as Filling Materials for Nerve Conduits. *Journal of Biomedical Materials Research* 58: 622–630.

Trumble, T.E., and F.G. Shon. 2000. The Physiology of Nerve Transplantation. *Hand Clinics* 16: 105–122.

Tsiper, M.V., and P.D. Yurchenco. 2002. Laminin Assembles into Separate Basement Membrane and Fibrillar Matrices in Schwann Cells. *Journal of Cell Science* 115: 1005–1015.

Tu, Q., L. Li, Y.R. Zhang, J.C. Wang, R. Liu, M.L. Li, W.M. Liu, X.Q. Wang, L. Ren, and J.Y. Wang. 2011. The Effect of Acetylcholine-Like Biomimetic Polymers on Neuronal Growth. *Biomaterials* 32: 3253–3264.

Tysseling-Mattiace, V.M., V. Sahni, K.L. Niece, D. Birch, C. Czeisler, M.G. Fehlings, S.I. Stupp, and J.A. Kessler. 2008. Self-Assembling Nanofibers Inhibit Glial Scar Formation and Promote Axon Elongation After Spinal Cord Injury. *Journal of Neuroscience* 28: 3814–3823.

Udina, E., M. Furey, S. Busch, J. Silver, T. Gordon, and K. Fouad. 2008. Electrical Stimulation of Intact Peripheral Sensory Axons in Rats Promotes Outgrowth of Their Central Projections. *Experimental Neurology* 210: 238–247.

Verheijen, M.H., R. Chrast, P. Burrola, and G. Lemke. 2003. Local Regulation of fat Metabolism in Peripheral Nerves. *Genes & Development* 17: 2450–2464.

Waller, A. 1850. Experiments on the Section of the Glossopharyngeal and Hypoglossal Nerves of the Frog, and Observations of the Alterations Produced Thereby in the Structure of Their Primitive Fibres. *Philosophical Transactions of the Royal Society of London* 140: 423–429.

Walsh, S., J. Biernaskie, S. Kemp, and R. Midha. 2009. Supplementation of Acellular Nerve Grafts With Skin Derived Precursor Cells Promotes Peripheral Nerve Regeneration. *Neuroscience* 164: 1097–1107.

Wang, M.S., A.A. Davis, D.G. Culver, Q. Wang, J.C. Powers, and J.D. Glass. 2004. Calpain Inhibition Protects Against Taxol-Induced Sensory Neuropathy. *Brain* 127: 671–679.

Wang, X., T. Cui, Y. Yan, and R. Zhang. 2009. Peroneal Nerve Regeneration Using A Unique Bilayer Polyurethane-Collagen Guide Conduit. *Journal of Bioactive and Compatible Polymers* 24: 109–127.

Williams, L.R., F.M. Longo, H.C. Powell, G. Lundborg, and S. Varon. 1983. Spatial-Temporal Progress of Peripheral Nerve Regeneration Within a Silicone Chamber: Parameters for a Bioassay. *Journal of Comparative Neurology* 218: 460–470.

Xie, J., M.R. Macewan, A.G. Schwartz, and Y. Xia. 2010. Electrospun Nanofibers for Neural Tissue Engineering. *Nanoscale* 2: 35–44.

Yannas, I.V., M. Zhang, and M.H. Spilker. 2007. Standardized Criterion to Analyze and Directly Compare Various Materials and Models for Peripheral Nerve Regeneration. *Journal of Biomaterials Science, Polymer Edition* 18: 943–966.

Yao, L., A. Pandit, S. Yao, and C.D. McCaig. 2011. Electric Field-Guided Neuron Migration: A Novel Approach in Neurogenesis. *Tissue Engineering. Part B, Reviews* 17: 143–153.

Yu, X., and R.V. Bellamkonda. 2003. Tissue-Engineered Scaffolds Are Effective Alternatives to Autografts for Bridging Peripheral Nerve Gaps. *Tissue Engineering* 9: 421–430.

Yu, X., G.P. Dillon, and R.V. Bellamkonda. 1999. A Laminin and Nerve Growth Factor-Laden Three-Dimensional Scaffold for Enhanced Neurite Extension. *Tissue Engineering* 5: 291–304.

Yurchenco, P.D., and Y. Cheng. 1994. Laminin Self-Assembly: A Three-Arm Interaction Hypothesis for the Formation of a Network in Basement Membranes. *Contributions to Nephrology* 107: 47–56.

Zhang, Z., M. Rouabhia, Z. Wang, C. Roberge, G. Shi, P. Roche, J. Li, and L.H. Dao. 2007. Electrically Conductive Biodegradable Polymer Composite for Nerve Regeneration: Electricity-Stimulated Neurite Outgrowth and Axon Regeneration. *Artificial Organs* 31: 13–22.

Zhong, Y., and R.V. Bellamkonda. 2008. Biomaterials for the Central Nervous System. *Journal of the Royal Society Interface* 5: 957–975.

Zimmermann, D.R., and M.T. Dours-Zimmermann. 2008. Extracellular Matrix of the Central Nervous System: From Neglect to Challenge. *Histochemistry and Cell Biology* 130: 635–653.

Zumwalt, M., and A. Wooldridge. 2014. Brachial Plexus Injury Accompanying Glenohumeral Instability Case Report and Literature Review. *Austin Journal of Orthopedics & Rheumatology* 1: 4.

Chapter 7
Cell Sources and Nanotechnology for Neural Tissue Engineering

Wei Zhu, Nathan Castro, Brent Harris, and Lijie Grace Zhang

7.1 Introduction

Neural injures, including central nervous system (CNS; brain and spinal cord) and peripheral nervous systems (PNS), resulting in the loss of sensory and motor as well as autonomic dysfunction, still present unique challenges regarding the full-functional recovery. Current clinical interventions are less than ideal and limited to relatively small defects. For peripheral nerve injury, typical treatment methods involve the end-to-end surgical connection of the severed ends (Schmidt and Leach 2003). However, current FDA-approved devices, such as NeuraGen Nerve Guide and SaluMedica's SaluBridge Nerve Cuff, only address small transections and fail

W. Zhu • N. Castro
Department of Mechanical and Aerospace Engineering, The George Washington University, Washington, DC 20052, USA

B. Harris
Departments of Neurology and Pathology, Georgetown University Medical Center, Washington, DC 20057, USA

L.G. Zhang (✉)
Department of Mechanical and Aerospace Engineering, The George Washington University, Washington, DC 20052, USA

Department of Medicine, The George Washington University, Washington, DC 20052, USA

Department of Biomedical Engineering, The George Washington University, Washington, DC 20052, USA

800 22nd Street, NW Science and Engineering Hall, Room 3590, Washington, DC 20052, USA
e-mail: lgzhang@gwu.edu

L.G. Zhang, D.L. Kaplan (eds.), *Neural Engineering*,
DOI 10.1007/978-3-319-31433-4_7

to regenerate larger injures. For CNS injures, clinical treatment options are far less than promising, the PNS-CNS transections are challenging to reconnect. Particularly, when bone fragmentation occurs with spinal cord injury, surgery may reduce the risk of secondary injury, but fails to restore nerve function. One of the greatest challenges in CNS regeneration is attributed to the inhibitory environment of the injured site where the axonal outgrowth is blocked by the formation of a glial scar, composed of astrocytes and microglia (Scheib and Hoke 2013).

These challenges provide fertile ground to incite researchers toward the development of new therapies to structurally and functionally restore the nervous system, especially for large defects which traverse the PNS and CNS transition zone. Neural tissue engineering is considered a promising method. It employs biocompatible materials and cells with the aim of regenerating injured neural tissues with functional recovery. Unlike conventional neural prosthesis which solely provides a direct framework to bridge the gap and guide cells within the recipients' body to regenerate injured tissues, neural tissue engineering scaffolds integrate autologous cells with biomaterials. The scaffolds' microenvironment allows autologous cells to secrete more inductive/supportive factors for axonal elongation and reestablishment of neural networks in the defective site(s) improving the tissue "neighborhood" for successful regeneration.

Cells incorporated within tissue engineered scaffolds can help replace damaged neural cells by serving as "relays" to reestablish axonal connections for functional recovery (Sandner et al. 2012). In order to fulfill this objective, numerous cell sources have been investigated for neural tissue engineering. Stem cells are basic cell lines that hold the potential to differentiate into neural phenotypes. Additionally, glial cells which aid in promoting axon regrowth and enhanced myelination are also popularly used.

In addition to cell sources, the intimate microenvironment which can improve the regenerative capacity of cells is crucial for successful regeneration. Therefore, numerous strategies for stimulating axonal growth are under development. Among them, nanomaterials have attracted increasing interests due to their unique properties in regulating cell behavior at the molecular level. When compared to bulk materials, nanomaterials exhibit a drastic increase in surface area, effective stiffness, and surface area to volume ratio, leading to scaffolds exhibiting favorable physiochemical properties (Padmanabhan and Kyriakides 2015). Nanomaterials can be tuned to respond to specific cell microenvironment and interact with cells at the molecular and supra-molecular level (Gilmore et al. 2008).

In the next section, we will begin our discussion by examining multiple stem cells sources and glial cells that are currently being investigated as promising cell sources for neural tissue engineering. In addition, the review will highlight biomimetic nanomaterials, including electrospun and self-assembling nanofibers and carbon-based nanomaterials used in regulating neural cell growth and function.

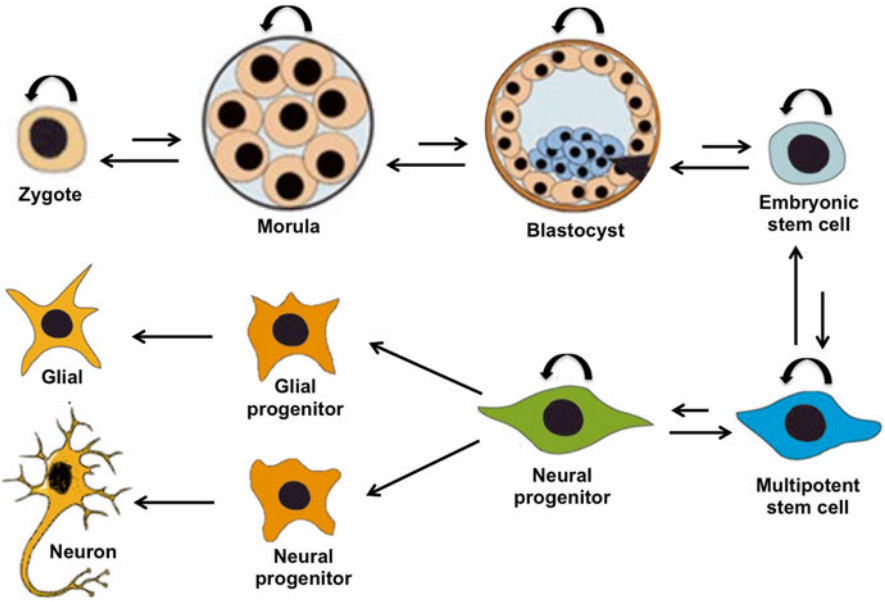

Fig. 7.1 Neural stem cell as a model to illustrate various developmental stages of stem cell differentiation. Adapted from Sandner et al. (2012)

7.2 Cell Sources for Neural Tissue Engineering

7.2.1 Stem Cells

Stem cells can be classified into the following: embryonic, fetal, neonatal, and adult stem cells based on the developmental stage (Fig. 7.1) (Sandner et al. 2012). Among them, embryonic stem cells (ESCs) are obtained from a 5 to 6-day embryo exhibiting pluripotency. Fetal and neonatal stem cells which are isolated from fetuses or newborn babies, respectively, hold multipotency. Adult stem cells including adult neural stem cells, hematopoietic stem cells, and mesenchymal stem cells (MSCs) exhibit multipotent capacity. In addition, induced pluripotent stem cells (iPSCs), reprogrammed somatic cells, are also explored for the application of neural regeneration.

7.2.1.1 Embryonic Stem Cells

ESCs inherently contain a high capacity of continuous self-renew and differentiation. Even when cultured in vitro, ESCs can retain their differentiation potential (Evans and Kaufman 1981). Pluripotent ESCs have drawn considerable interest for

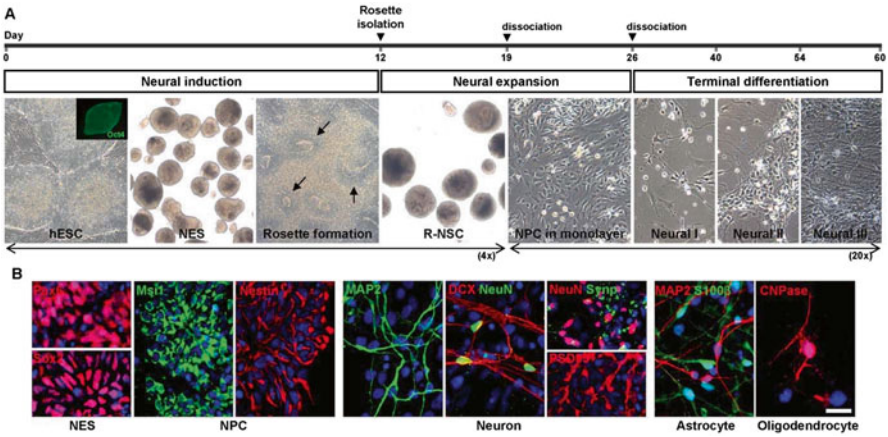

Fig. 7.2 Neural differentiation of human ESCs. (**a**) Phase-contrast images showed the various stages of differentiation in vitro. (**b**) Immunochemistry staining illustrated the differentiation progression and specific makers expression (For neural progenitor cells: musashi 1 and Nestin. For neurons: DCX, MAP2, NeuN, synaptophysin, and PSD95. For astrocytes: S100b. For oligodendrocytes: CNPase. DNA stained with DAPI (*blue*)). Adapted from Cho et al. (2011)

the repair of nervous system injury. It has been documented that ESCs are able to differentiate into neurons, astrocytes, and oligodendrocytes when implanted into the brain, spinal cord, and peripheral nerves (Cui et al. 2008; McDonald et al. 1999; Liu et al. 2000). Cho et al. successfully induced human ESC-derived neural stem/progenitor cells to generate neurons in vitro using myocyte enhancer factor 2C as a neurogenic and anti-apoptotic transcription factor (Fig. 7.2) (Cho et al. 2011). McDonald et al. utilized neural differentiated mouse ESCs to restore partial function after transection of rat spinal cord 9 days after trauma (McDonald et al. 1999). Results showed the transplanted ESCs maintained survivability, differentiated into neurons, astrocytes, and oligodendrocytes as well as migrated 8 mm away from the lesion edge. Importantly, a modest functional recovery was observed for the injured spinal cord. When ESC-derived neural progenitor cells were implanted into a severe peripheral nerve transection (rat sciatic nerve), it was found that the transplanted cells survived and differentiated into myelination cells (Cui et al. 2008). A uniform connection exhibiting near normal nerve diameter and densely packed Schwann cell-like phenotype was established between the proximal and distal stumps. In addition, functional activity recovery was observed over the regenerated injured gap. In another report, Xie et al. investigated the interaction between mouse ESCs and electrospun biodegradable polymer scaffolds (Xie et al. 2009). ESC growth and differentiation were evaluated when seeded upon poly(ε-caprolactone) (PCL) nanofibers with random or aligned orientation. In both cases, ESCs were induced toward neural lineages (neurons, oligodendrocytes, and astrocytes). Most importantly, aligned nanofibers produced the greatest neural differentiation with enhanced directed neurite outgrowth, suggesting the combination of ESC-derived neural progenitor cells and tissue engineered scaffolds holds high potential for nerve injury repair.

7.2.1.2 Fetal and Neonatal Stem Cells

Multipotent fetal stem cells are less adaptable than ESCs with regard to differentiation potential. Studies demonstrated fetal stem cells isolated from developing embryos give rise to differentiated neurons when cultured in vitro (Goslin et al. 1988). Like ESCs, the application of fetal stem cells is limited by ethical concerns and the use of immunosuppressive drugs.

Umbilical cords containing umbilical cord blood-derived stem cells is the only clinical source for harvesting neonatal stem cells. Umbilical cord blood-derived stem cells can be easily isolated without donor side effects and ethical concerns (Rogers et al. 2007). In addition, umbilical cord blood-derived stem cells present less immunogenicity when compared to other stem cells (Sanberg et al. 2005). Cui et al. studied the influence of human umbilical cord blood-derived mesenchymal stem cell transplantation on the functional restoration of spinal cord injury (Cui et al. 2014). They found that rats undergoing stem cell transplantation showed significant different recovery of spinal cord nerve function, suggesting this cell source is promising for neural regeneration. Brain repair using umbilical cord blood-derived stem cells can be also found (Sanberg et al. 2005). Although some exciting results have been obtained, umbilical cord can only provide a very limited number of stem cells which impair its wide application for tissue engineering (Tse and Laughlin 2005).

7.2.1.3 Adult Stem Cells

In addition to embryo, fetuses, and newborns cell sources, stem cells can be also acquired from adult tissues and classified in terms of tissue origin. Neural stem cells are the most popular type of adult stem cell utilized in neural regeneration. Neural stem cells can self-renew and give rise to both neurons and glia. They can be isolated from neurogenic regions including the hippocampus and subventricular zone, or some non-neurogenic regions, such as the spinal cord (Temple 2001).

The interaction between neural stem cells and tissue engineered scaffolds has been extensively studied both in vitro and in vivo. Nisbet et al. found neural stem cells grown on electrospun scaffolds can be induced to differentiate into oligodendrocytes in the presence of 10 % fetal bovine serum (Nisbet et al. 2008). In another report by Leipzig et al., the scaffolds' stiffness influenced neural stem cell proliferation and differentiation (Leipzig and Shoichet 2009). They fabricated a photopolymerizable methacrylamide chitosan scaffold with Young's modulus ranging from less than 1 kPa to greater than 30 kPa. Herein, neural stem cell proliferation was observed on scaffolds with less than 10 kPa Young's modulus and the maximal cell proliferation was noted on a 3.5 kPa scaffold. Oligodendrocyte differentiation is preferred on stiffer surfaces with Young's modulus greater than 7 kPa. However, softer surfaces (<1 kPa) can promote oligodendrocyte maturation and myelination as well as mature neuron growth. Astrocyte differentiation represented less than 2 % of the total cell population and only took place upon <1 kPa and 3.5 kPa surfaces.

These results suggest that mechanical properties play a crucial role in regulating proliferation and differentiation of adult neural stem cells; thus they should be carefully considered when designing scaffolds for nerve repair.

In addition to adult neural stem cells, adult MSCs are also used in neural tissue engineering. MSCs can be easily harvested; therefore, they are a rich autologous cell source for this application. When undergoing stimulation by environment or chemical cues, MSCs are capable of trans-differentiating into neuronal phenotypes. For instance, Tohill et al. found that MSCs can give rise to glial differentiation when stimulated by glial growth factor. Following transplantation of MSCs into a 1 cm neural conduit for a rat sciatic nerve, MSCs without any growth factor stimulation started to express glial cell markers, indicating that MSC glial differentiation can be induced by local cytokines and growth factors in vivo. Additionally, some reports illustrated that MSCs have anti-inflammatory capabilities, promoting axonal extension, as well as improving functional recovery after spinal cord injury and stroke (Hofstetter et al. 2002; Cho et al. 2009).

7.2.1.4 Induced Pluripotent Stem Cell

iPSCs can be derived from differentiated somatic cells by reprogramming a limited number of genes (Oct3/4, Sox2, c-Myc and Klf4, or Oct3/4, Sox2, Nanog and Lin28) (Park et al. 2008; Takahashi and Yamanaka 2006; Yu et al. 2007). There are many advantages which render iPSCs a valuable cell source for neural tissue engineering: (a) unlimited expansion potential; (b) easily bypassing immune rejection; (c) no ethical issues. Wang et al. applied iPSCs to derive neural crest stem cells for neural tissue engineering (Wang et al. 2011a). They found that the derived cells can differentiate into mesodermal and ectodermal lineages, including neural cells (Fig. 7.3). Then they seeded the cells into nanofibrous tubular scaffolds and implanted scaffolds into transected sciatic nerves in a rat model. The scaffolds enabled to promote axonal myelination and accelerate neural regeneration. In another study performed by Uemura et al., functional recovery was observed when iPSCs were combined with a nerve conduit to bridge a 5 mm mouse sciatic nerve gap. In their study, neurospheres derived from mouse iPSCs were seeded on nerve conduits showing significant recovery of sensory and motor function when compared to nerve conduits alone. Although great progress has been obtained using iPSCs as a neural regeneration cell source, the issue of non-uniformed differentiation to the cell type of interest needs to be further evaluated and addressed.

7.2.2 Glial Cells

Glial cells comprise the largest population of cells in the brain, which play an essential role in the nervous system as illustrated by their diverse function. Glial cells can be classified as microglia which are located in the CNS and macroglia which exist

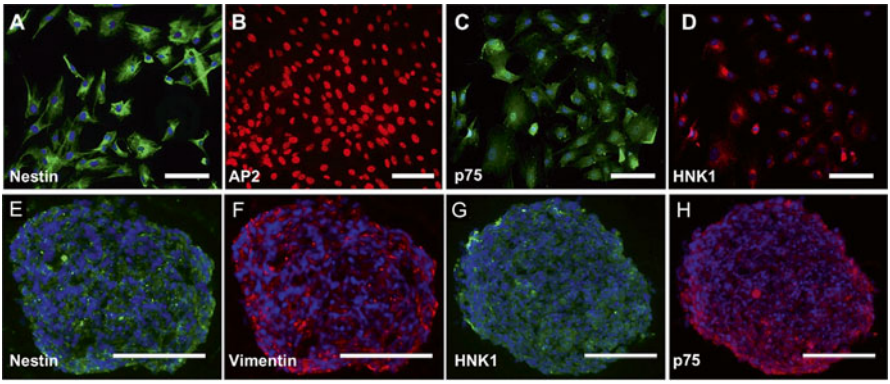

Fig. 7.3 iPSCs-derived neural crest stem cells can be cultured in ether monolayer (**a**)–(**d**) and identified by markers (**a**) nestin, (**b**) AP2, (**c**) p75, and (**d**) HNK1, or floating spheres maintained uniform expression of markers (**e**) nestin, (**f**) Vimentin, (**g**) HNK1, and (**h**) p75. *Blue* represents nuclei. Adapted from Wang et al. (2011a)

in both the CNS and PNS (Doetsch 2003). Microglia are derived from hematopoietic stem cells and play an important role in inflammation associated with damage (Welberg 2014). Macroglia are a group of cells within the nervous system mainly composed of oligodendrocytes and astrocytes (CNS) and Schwann cells (PNS).

Oligodendrocytes are myelinating cells undergoing a complex progression of proliferation, migration, differentiation, and myelination to eventually form the insulating sheath of axons (Bradl and Lassmann 2010). The sheath facilitates the conduction of neuronal impulses along the axon. Star-shaped astrocytes not only provide metabolic and structural support to neurons but also directly contribute to many aspects of brain function (Whalley 2014). In particular, astrocytes are involved in the maintenance of extracellular ion homeostasis and secretion of growth factors, cytokines, and other extracellular matrix components (Doetsch 2003). In addition, they also take part in the formation of glial scars and modulate synaptic efficacy. Schwann cells of the PNS are primarily responsible for the support and myelination of axons. At the injured site, Schwann cells proliferate, facilitate debris elimination, and upregulate localized secretion of trophic and tropic factors (RodríGuez et al. 2000).

Considering the importance of glial cells in regulating nervous system function, the use of tissue engineered scaffolds consisting of nerve guides seeded with isolated glial cells has been widely investigated. Weightman et al. incorporated astrocytes, oligodendrocyte precursor cells, and oligodendrocytes within a 3D nanofibrous construct and investigated its potential for neural tissue regeneration (Weightman et al. 2014). They found that highly aligned nanofibers are capable of inducing astrocyte elongation. Strikingly, oligodendrocyte precursor cells cultured alone upon aligned nanofibers exhibited limited survival and the absence of elongation, while cell survival, elongation, and maturation were observed when cells were seeded upon pre-aligned astrocytes. It was hypothesized that multiple glial populations on oriented 3D scaffolds could be an effective option to rebuild glial circuitry

in damaged nerves. When compared to oligodendrocytes and astrocytes, Schwann cells are a more popular cell source used in repairing both PNS and CNS injuries. Rodríguez evaluated the ability of Schwann cells seeded on nerve guides to regenerate and reinnervate a 6 mm sciatic nerve gap in a mouse model (RodríGuez et al. 2000). They isolated Schwann cells from pre-degenerated adult sciatic nerves as an autologous cell source and cultured cells with nerve constructs prior to 4-month implantation. Quicker and greater levels of reinnervation and myelination were achieved in the group containing autologous Schwann cell-seeded constructs when compared to the group that underwent tubulization alone. In addition to PNS repair, research by Olson et al. demonstrated the effectiveness of Schwann cell-seeded nerve guidance conduits for CNS regeneration (Olson et al. 2009). They found significantly improved axon regeneration when using Schwann cell-seeded scaffolds to bridge transected spinal cord relative to scaffold-only controls.

7.3 Nanotechnology for Neural Tissue Engineering

Nanotechnology refers to materials with functional organization of 100 nm or less in at least one dimension. This unique size feature enables them to interact with biological substances at the molecular level, thus holding high potential in biomedical applications. Advances in nanotechnology have allowed the selection of numerous nanomaterials for neural tissue engineering, which alters the way we approach nerve repair. It is expected that nanomaterials are capable of preventing the activity of astrocytes, stimulating axon growth as well as restoring synaptic connections (Fraczek-Szczypta 2014). In this section, we will focus on the application of various nanomaterials involved in neural tissue regeneration. In particular, we will discuss carbon-based nanomaterials, including carbon nanotubes, carbon nanofibers, and graphene, which are currently considered as promising candidates for the regeneration and stimulation of nerve tissue due to their unmatched physical, chemical, and biological properties.

7.3.1 Carbon-Based Nanomaterials

7.3.1.1 Carbon Nanotubes

Carbon nanotubes (CNTs) are hollow cylinders made by rolling one layer (single-walled CNTs, SWCNTs) or several layers (multiple-walled CNTs, MWCNTs) of graphene. They can be synthesized by a variety of methods, such as chemical vapor deposition, electric arc discharge, and laser ablation. Among these techniques, chemical vapor deposition is most popular due to its simple operation and easily achievable processing conditions. CNT thin films directly grow upon a catalyst-seeded substrate by hydrocarbon gas carrier (Hu et al. 2010). Electric arc discharge

employs two graphite electrodes under an inert environment of helium or argon. When a high level current passes through the electrodes, carbon atoms are evacuated from the positive electrode and deposited upon the negative electrode resulting in the formation of CNTs on the cathode (Ajayan 1999). Laser ablation was introduced to produce CNTs by Guo et al. in 1995 (Guo et al. 1995). In this method, a heated graphite target was ablated by a powerful laser to allow carbon evaporation on the target. Then, the carbon atoms are swept to a cold copper collector where they are condensed into nanotubes.

CNTs have been extensively investigated in the design and fabrication of nanostructured neural scaffolds by virtue of their excellent mechanical, electrical, and biological properties. With regard to mechanical properties, CNTs have shown extraordinary mechanical strength because the covalent bond between carbon atoms in CNTs is known to be extremely strong (Falvo et al. 1997). The electrical properties of CNTs are determined by geometric parameters, including diameter and chiral angle (Dai 2002). SWCNTs can be classified as metals or semiconductors, while MWCNTs only exhibit metallic behavior. Their extraordinary electrical properties are expected to contribute to signal transformation in neural interface; therefore, numerous attempts targeting neural tissue regeneration have been explored based on CNTs. Both SWCNTs and MWCNTs attracted great interest as potential scaffolds for restoring interconnections between neurons. Mattson et al., for the first time, reported the application on MWCNTs for neural tissue engineering (Mattson et al. 2000). When embryonic rat-brain neurons were cultured on unmodified nanotubes, limited neurite extension and branching was observed. In contrast, bioactive molecule 4-hydroxynonenal-coated nanotubes supported greater neurite outgrowth and extensive branching, indicating that CNTs could be suitable substrates for neural cell growth.

Jan et al. prepared layer-by-layer assembled SWCNTs and polyelectrolyte substrates and investigated mouse embryonic neural stem cell growth and differentiation (Jan and Kotov 2007). The biocompatibility of SWCNTs is comparable to that of poly-L-ornithine which is one of the most popularly used growth substrates for neural stem cells. Also, it was demonstrated that neural stem cells were enabled to give rise to neurons, astrocytes, and oligodendrocytes with well-defined neurite formation on a SWCNT-based substrate.

Although great progress has been made with regard to CNTs' biomedical application, clinical trials are still limited due to cytotoxicity reports (Firme Iii and Bandaru 2010). Functionalization of CNTs with chemical or biological cues is one possible solution to address this concern (Fig. 7.4). The CNTs' cytotoxicity can be rectified by altering surface charge. Positively, negatively, or neutrally charged CNTs can be obtained by covalently conjugating various reactive groups, including $–NH_2$, –SH, and –COOH. It has been documented that surface charge is able to influence nerve response, including length, number of neurites, as well as branching and number of synaptic connections (Fraczek-Szczypta 2014). Hu et al. revealed CNTs functionalized to be positively charged were more effective in promoting neurite outgrowth and branching when compared with negatively charged CNTs (Hu et al. 2005). In addition to simple surface modification, CNTs could also be

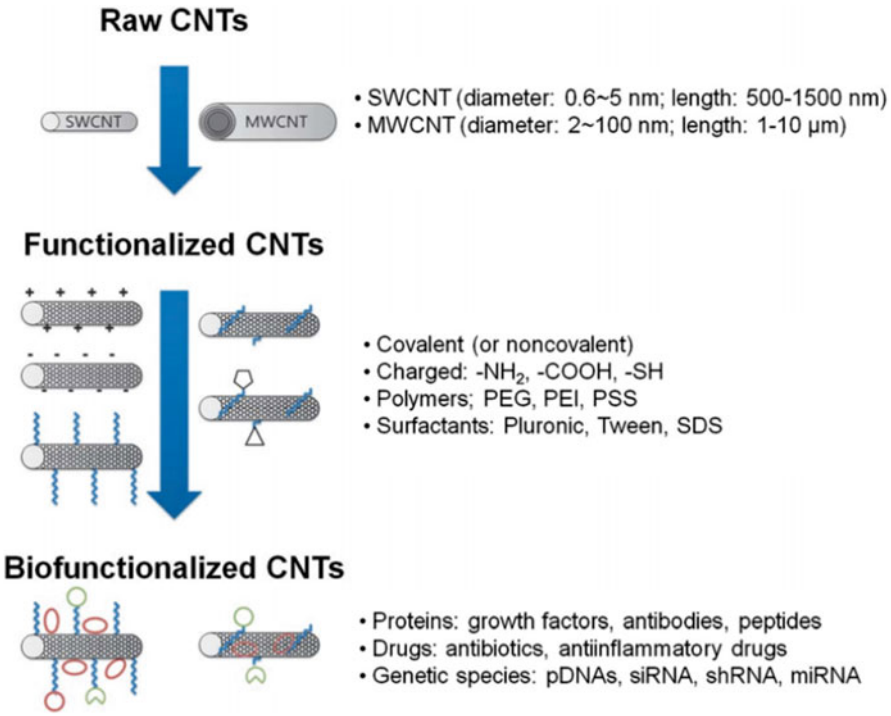

Fig. 7.4 Schematic illustration of various functionalization processes of CNTs. Adapted from Hwang et al. (2012)

conjugated with biologically relevant molecules for biofunctionalization. During biofunctionalization, biological factors of interest, such as growth factors and peptides, may be conjugated to CNTs, which not only solve the problems of cytotoxicity but also improve functionality of the target neural cell(s) (Hwang et al. 2012). In a report by Gaillard et al., MWCNTs were functionalized by conjugating cell adhesion peptides and the growth of neurons on modified CNTs was investigated (Gaillard et al. 2009). Results demonstrated RGD-based sequences functionalized CNT-aided cell adhesion and neurite outgrowth. Similarly, peptides derived from different domains of laminin also simulated neural growth and axon regeneration. Additionally, integrin regulation of neural gene expression was also intervened by CNTs modified with RGD-containing peptides.

7.3.1.2 Carbon Nanofibers

Like CNTs, carbon nanofibers (CNFs) possess attractive features, but the lower cost of fabrication and easier scale-up process make CNFs a more attractive option. CNFs can be produced by vapor growth and spinning followed by stabilization and carbonization (Kim et al. 2006; Tibbetts et al. 2007). For the preparation of CNFs

by vapor growth, carbon is first dissolved in metal or alloys as catalysts to form metal carbide. Iron, chromium, vanadium, cobalt, and nickel are commonly used metal or alloy catalysts, the carbon source generally provided by methane, ethyne, ethene, carbon monoxide or synthesis gas (H_2/CO) at high temperature ranging from 700 to 1200 K (Feng et al. 2014; De Jong and Geus 2000). Finally, CNFs grow upon the metal surface via deposition of hydrocarbons dissolved in the catalytic particle. Electrospinning approaches to produce CNFs require the use of precursor polymer nanofibers. Popular precursors include polyacrylonitrile, poly(vinyl alcohol), polyimides, polybenzimidazol, poly(vinylidene fluoride), phenolic resin, and lignin (Inagaki et al. 2012). CNFs form by heating polymer nanofibers to induce carbonization. Properties of the resultant CNFs including morphology, purity, crystallinity, diameters, and porosity are governed by the type of polymer and processing conditions which further influence the biological performance of synthesized CNFs. McKenzie et al. first reported the adherent preference of astrocyte on carbon fibers with large diameters and low surface energy (McKenzie et al. 2004). This further demonstrated that the nanostructured CNTs may limit astrocytes functions. But positive interaction between neurons and astrocytes was observed with limited astrocyte function resulting in decreased glial scare tissue formation.

7.3.1.3 Graphene

Graphene is a single atom layer of carbon atoms arranged into a two-dimensional honeycomb lattice (Soldano et al. 2010). Extensive research interest in graphene is a result from its exotic properties including a large theoretical specific surface area (2630 $m^2\ g^{-1}$), high electron mobility at room temperature (200,000 $cm^2\ v^{-1}\ s^{-1}$), high Young's modulus (~1.0 TPa), and thermal and electrical conductivity (Zhu et al. 2010). Owing to these interesting properties, graphene has shown potential applications in a vast majority of areas, including neural tissue engineering. Park et al. investigated human neural stem cell behavior when seeded upon graphene substrates (Park et al. 2011). They found that nanostructured graphene can promote long-term neural stem cell adhesion and differentiation. More importantly, graphene is able to induce neural stem cell differentiation toward neurons instead of glial cells, which is critical and beneficial toward the overall success of neural regeneration. The same result was observed when neural stem cells were cultured on 3D graphene foams (Li et al. 2013). When compared to 2D graphene cultures, cells grown on 3D graphene foams tend to maintain an active proliferation state. Furthermore, phenotype analysis demonstrated 3D graphene can enhance neural stem cell differentiation into neurons. When electrical stimulation was applied, good coupling between neural stem cells and 3D graphene was observed.

Graphene is robust yet flexible which allows modification of its carbon backbone for improved biocompatibility, solubility, and selectivity (Wang et al. 2011b). Therefore, a variety of graphene-based materials including graphene oxide, reduced graphene oxide, and exfoliated graphite have also been investigated for biomedical applications. It was found that the cytotoxicity of these graphene derivatives exhibit

dose, size, and shape dependent responses (Zhang et al. 2013). In general, the biocompatibility of graphene derivatives is superior to other carbon-based materials such as CNTs (Yan et al. 2011). Lower concentrations and smaller sizes of graphene derivatives usually display more favorable biocompatibility. In addition, the surface charge also influences the biological properties of graphene derivatives. In a study performed by Tu et al., graphene oxide was carboxylated and then treated to exhibit different surface charges by chemical functionalization with amino- ($–NH_2$), poly-m-aminobenzene sulfonic acid- (–PABS), or methoxyl- ($–OCH_3$) terminated functional groups (Tu et al. 2014). Their findings suggested positively charged graphene oxide to be more beneficial for neurite outgrowth and branching of primary rat hippocampal neurons relative to neutrally, zwitterionic, or negatively charged graphene oxide (Fig. 7.5).

7.3.2 Engineered Nanostructured Neural Scaffolds

In addition to nanomaterials with nanoscale dimension(s), a majority of tissue engineering strategies have been used in neural tissue engineering whereby conventional materials are used in combination with nanomaterials or promoted to display nanostructures by nanofabrication techniques. Popular nanofabrication approaches involve electrospinning and self-assembly which enable the fabrication of nanofibrous scaffolds for neural regeneration. These nanofibrous scaffolds have intrinsic merits due to the physical similarity of the resultant structure to that of native fibrous extracellular matrix (Zhang and Webster 2009). Furthermore, bioactive factors including peptides, proteins, neurotrophic factors, and even living cells can be incorporated into the nanofibers for synergetic neural repair (Cunha et al. 2011).

7.3.2.1 Electrospinning Nanofibrous Scaffolds

Electrospinning is a simple and versatile technique for processing polymeric solutions into nanofibers. More than 100 polymers derived from natural and synthetic origins have been electrospun (Burger et al. 2006) resulting in fiber diameters as thin as tens of nanometers (Tan et al. 2005). Although a lot of parameters such as polymer viscosity, working distance, applied voltage, and flow rate influence the electrospinning process, the small size of electrospun fibers is considered as a result of whipping motion that provides a strong axial force (Yarin et al. 2001). The whipping instability results from the electrostatic interaction between the charged polymer and external electric field. Polymer viscosity should be accurately adjusted to withstand the whipping process. Another intriguing advantage of electrospinning is to have control over fiber orientation by modifying the collector. For this purpose, a rotating mandrel is employed to collect nanofibers in aligned orientation. In this method, the speed of the mandrel must be precisely controlled to mechanically stretch and align nanofibers. Because a higher rotating speed might break the fibers

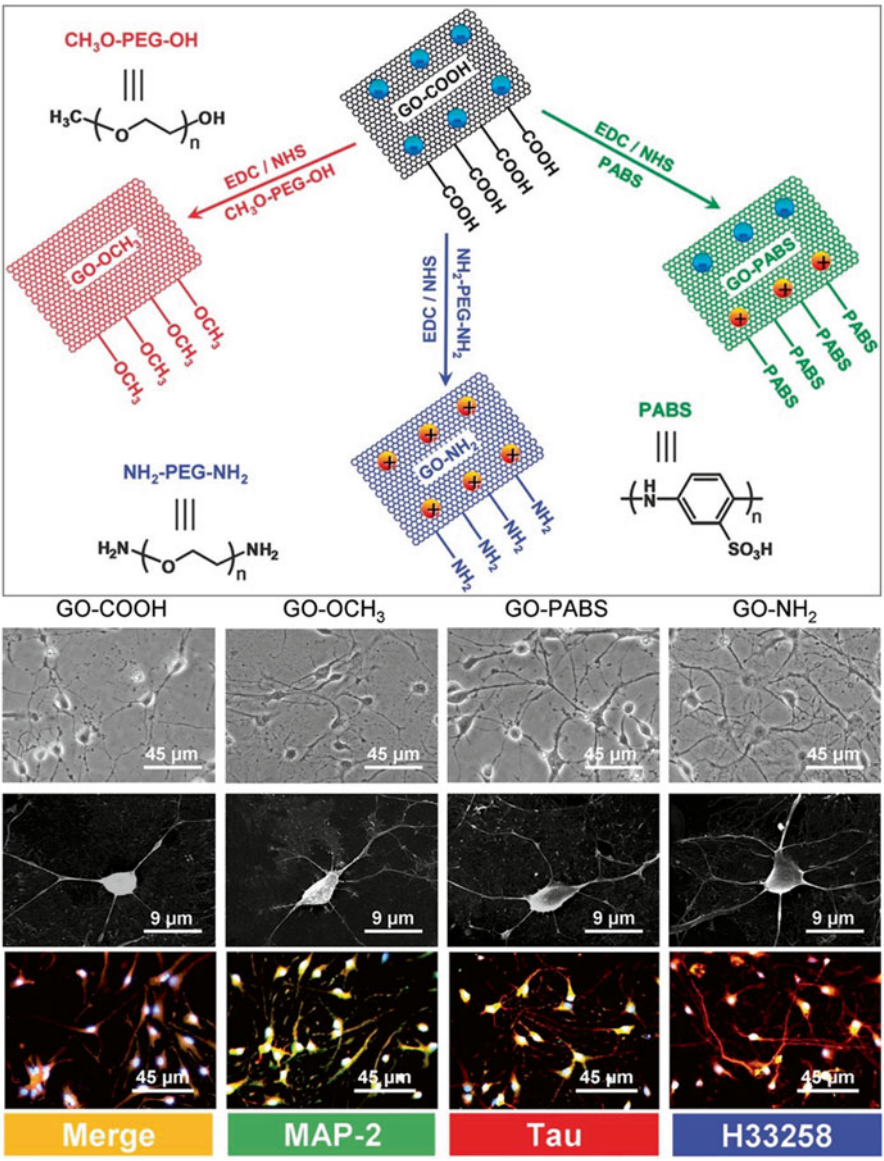

Fig. 7.5 Scheme of chemical functionalization of graphene to form graphene (GO) –COOH, GO–OCH_3, GO–PABS, and GO–NH_2 that exhibit negatively, neutrally, zwitterionic, and positively charged surfaces, and optical and immunochemistry staining images of hippocampal neurons grew on them for 7 days. Adapted from Tu et al. (2014)

during deposition, lower speeds will lead to less alignment (Xie et al. 2010). In addition to this conventional approach, Li et al. developed a new collector to generate uniaxially aligned nanofibrous arrays (Li et al. 2004). As shown in Fig. 7.6, the key of this method is the collector composed of two conductive strips that are

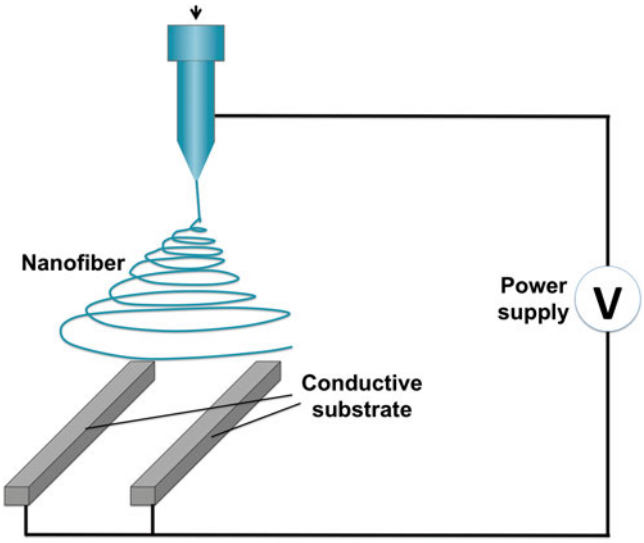

Fig. 7.6 Scheme of the setup of electrospinning with a collector composed of two separate conductive substrates for fabrication of aligned nanofibrous mat

separated by an insulating gap. The charged nanofibers are capable of spanning the gap and producing aligned arrays under electrostatic interactions.

Due to the ease of manipulation and controllable aligned orientation, electrospinning has attracted great interest in various fields, especially neural tissue engineering. In general, it is expected that aligned nanofibers provide better contact for neurite outgrowth along the fiber's direction, which would benefit the eventual restoration of nerve function. However, in a recent study, Xie et al. found that contact cues provided by electrospun nanofibers are more complicated than only guiding neurite elongation (Xie et al. 2014). For the first time, they demonstrated that neurites are not only directed by the contact nanofibers but also project along a direction perpendicular to the aligned fibers (Fig. 7.7). This influence is related to the density of nanofibers, protein deposition on the scaffold surface, and surface properties of the substrate which supports the nanofibers. This finding provides new insight for the design of nanofibrous neural scaffolds and construction of neural network.

7.3.2.2 Self-Assembling Nanofiber Scaffolds

Self-assembly is a process wherein components autonomously organize into ordered structures without external stimulation. The components can range in size from the molecular to planetary scale (George and Bartosz 2002). Molecular self-assembly involves the specific association of molecules via non-covalent interactions such as ionic bonds, hydrogen bonds, and van der Waals interactions (Kyle et al. 2009). This is a very practical strategy for producing ensembles of nanostructures, thereby

offering a novel approach to engineer nanostructured scaffolds for tissue regeneration. Since native extracellular matrix is an environment produced through the self-assembly of cell-derived materials, these self-assembling nanostructures hold great potential in biological applications.

Peptides are the most investigated self-assembling blocks by virtue of their unique biological and self-assembly characteristics. Self-assembling peptides also have other intriguing properties including a sol–gel transition under physiological conditions. In addition, peptide sequences can be modified by conjugating additional functional motifs to enhance bioactive properties. These advantages of self-assembling peptide nanofibrous hydrogels make them one of the most popular biomaterials for CNS repair.

In a report by Iwasaki et al., they injected K2(QL)6K2 self-assembling peptides into the lesion epicenter of a bilateral clip compression-induced cervical spinal cord injury, combined with simultaneous transplantation of neural stem/progenitor cells into the adjacent area (Iwasaki et al. 2014). They found that the self-assembling peptides reduced the volume of cystic cavitation, preserved motor neurons of neural stem/progenitor cells, as well as attenuated perilesional inflammation. In the meantime, forelimb neurobehavioral recovery was observed associated with dramatically improved forelimb print area and stride length. In addition to spinal cord repair, self-assembling peptides have also shown promise for brain regeneration. Cheng et al. functionalized self-assembling peptide RADA16 by linking laminin-derived IKVAV motif (RADA16-IKVAV) and investigated its potential in brain reconstruction (Cheng et al. 2013). Results demonstrated RADA16-IKVAV enabled to self-assembly into nanofibrous hydrogels with similar stiffness to brain tissue. The linked IKVAV served as a molecular cue to enable directly encapsulated neural stem cell adhesion and promote neuronal differentiation. More importantly, the peptide solution could be injected into the brain and immediately form a 3D hydrogel in situ to fill the injured cavity and eventually improve brain tissue regeneration.

7.4 Conclusions and Prospects

Neural tissue engineering has emerged as an excellent strategy for injured nerve repair and functional recovery, with the advantages circumventing limitations of traditional autografts. However, despite the great progress made, the source of cells remains challenging toward the realization of a successful tissue engineered neural graft. Despite the fact that autologous adult stem cells have illustrated robust differentiation potential toward neural lineages, their limited life span and/or ethical concerns have hampered their application. Future research should focus on developing alternative, easily accessible, and more efficient processing of stem cells that minimize or eliminate ethical concerns. In this regard, iPSCs obtained from the patient's own cells with greater life span hold great promise to serve as an effective cell source for neural tissue engineering. Notwithstanding, issues about chromosomal aberrations, incomplete differentiation, and oncogenic potential (Bajpai and

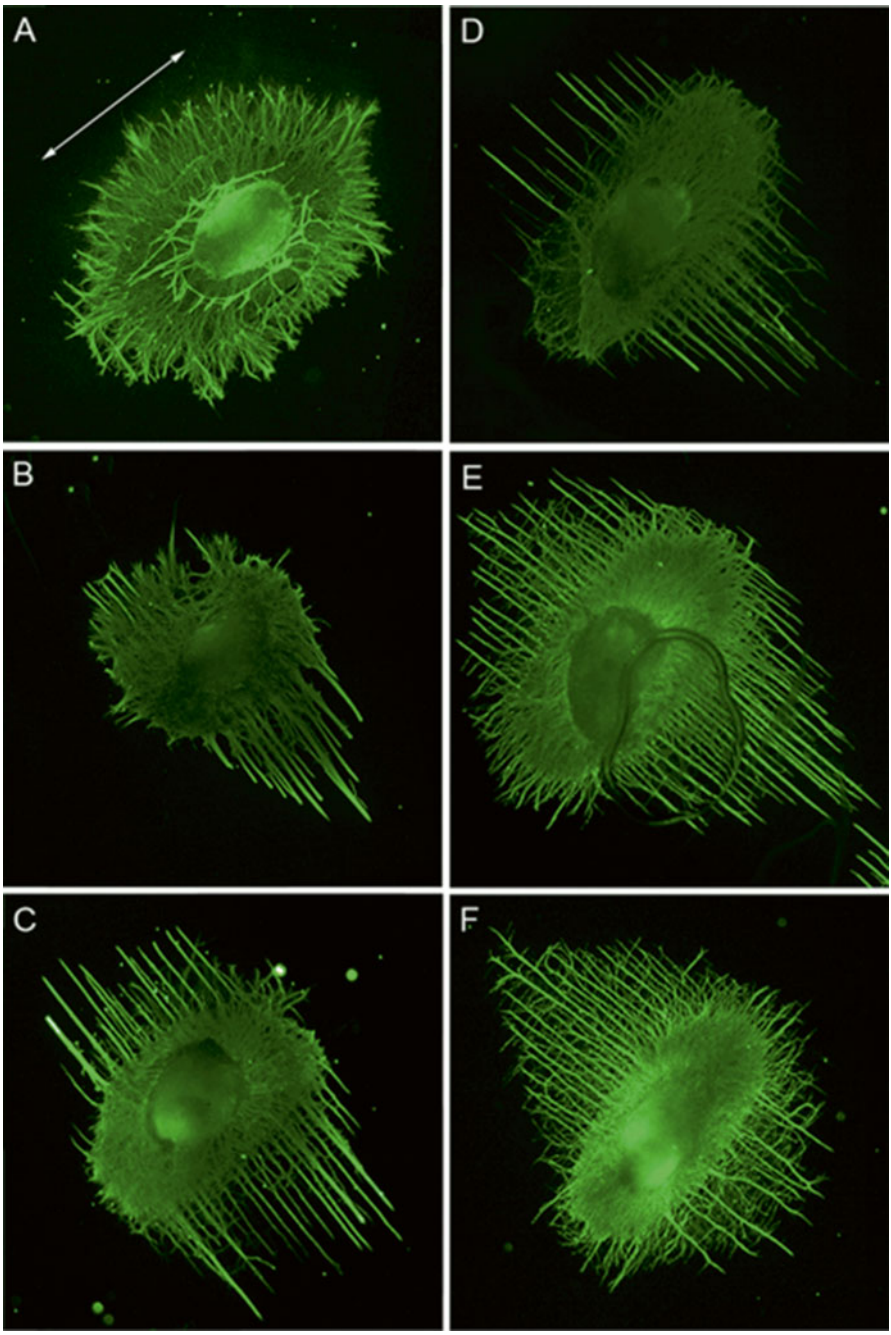

Fig. 7.7 Fluorescence micrographs illustrating the neurite extension was guided to grow along a direction perpendicular to the aligned nanofibers. The nanofibers were collected with different time duration: (**a**) 1, (**b**) 2, (**c**) 4, (**d**) 8, (**e**) 15, and (**f**) 30 min, respectively. The *arrow* in (**a**) indicates the direction of aligned nanofibers which also applies to all other samples. Adapted from Xie et al. (2014)

Andreadis 2012) should be addressed. Another crucial aspect will be controlling appropriate glial and neuronal phenotype to better control structural and functional repair while inhibiting scar formation.

The development of nanomaterials has enhanced the scope of neural scaffold fabrication toward the generation of mimetic structures closely matching native human extra cellular matrix at the nanometer scale and particularly interacting with cells at the molecular level. Despite numerous studies about the interaction between nanomaterials and nervous system, in vivo studies remain few and challenging. Nanomaterials aimed at promoting cellular function and facilitating neural signal reconstruction in vivo will contribute significantly to clinical care and prevention. However, although many positive reports exist for the treatment of neural injures using nano-based scaffolds, a number of concerns related to toxicity of nanomaterials as well as an underdeveloped understanding of the underlying mechanisms that nanomaterials influence on stimulating neural cells should be better resolved and understood.

References

Ajayan, P.M. 1999. Nanotubes from Carbon. *Chemical Reviews* 99: 1787–1799.

Bajpai, V.K., and S.T. Andreadis. 2012. Stem Cell Sources for Vascular Tissue Engineering and Regeneration. *Tissue Engineering, Part B: Reviews* 18: 45–425.

Bradl, M., and H. Lassmann. 2010. Oligodendrocytes: biology and pathology. *Acta Neuropathologica* 119: 37–53.

Burger, C., Hsiao, B. S. & Chu, B. Nanofibrous materials and their applications. 2006 PALO ALTO. ANNUAL REVIEWS, 333–368.

Cheng, T.-Y., M.-H. Chen, W.-H. Chang, M.-Y. Huang, and T.-W. Wang. 2013. Neural stem cells encapsulated in a functionalized self-assembling peptide hydrogel for brain tissue engineering. *Biomaterials* 34: 2005–2016.

Cho, E.-G., S.A. Lipton, J.D. Zaremba, S.R. Mckercher, M. Talantova, S. Tu, E. Masliah, S.F. Chan, N. Nakanishi, and A. Terskikh. 2011. MEF2C enhances dopaminergic neuron differentiation of human embryonic stem cells in a parkinsonian rat model. *PLoS ONE* 6, e24027.

Cho, J.-S., S.-K. Park, H.-W. Park, S. Roh, S.-K. Kang, K.-S. Paik, and M.-S. Chang. 2009. Transplantation of mesenchymal stem cells enhances axonal outgrowth and cell survival in an organotypic spinal cord slice culture. *Neuroscience Letters* 454: 43–48.

Cui, B., E.N. Li, B.O. Yang, and B.O. Wang. 2014. Human umbilical cord blood-derived mesenchymal stem cell transplantation for the treatment of spinal cord injury. *Experimental and Therapeutic Medicine* 7: 1233–1236.

Cui, L., J. Jiang, L. Wei, X. Zhou, J.L. Fraser, B.J. Snider, and S.P. Yu. 2008. Transplantation of Embryonic Stem Cells Improves Nerve Repair and Functional Recovery After Severe Sciatic Nerve Axotomy in Rats. *Stem Cells* 26: 1356–1365.

Cunha, C., S. Panseri, and S. Antonini. 2011. Emerging nanotechnology approaches in tissue engineering for peripheral nerve regeneration. *Nanomedicine: Nanotechnology, Biology, and Medicine* 7: 50–59.

Dai, H. 2002. Carbon nanotubes: opportunities and challenges. *Surface Science* 500: 218–241.

De Jong, K.P., and J.W. Geus. 2000. Carbon Nanofibers: Catalytic Synthesis and Applications. *Catalysis Reviews—Science and Engineering* 42: 481–510.

Doetsch, F. 2003. The glial identity of neural stem cells. *Nature Neuroscience* 6: 1127–1134.

Evans, M.J., and M.H. Kaufman. 1981. Establishment in culture of pluripotential cells from mouse embryos. *Nature* 292: 154–156.

Falvo, M.R., G.J. Clary, R.M. Taylor, V. Chi, F.P. Brooks, S. Washburn, and R. Superfine. 1997. Bending and buckling of carbon nanotubes under large strain. *Nature* 389: 582–584.

Feng, L.C., N. Xie, and J. Zhong. 2014. Carbon Nanofibers and Their Composites: A Review of Synthesizing, Properties and Applications. *Materials* 7: 3919–3945.

Firme Iii, C.P., and P.R. Bandaru. 2010. Toxicity issues in the application of carbon nanotubes to biological systems. *Nanomedicine: Nanotechnology, Biology and Medicine* 6: 245–256.

Fraczek-Szczypta, A. 2014. Carbon nanomaterials for nerve tissue stimulation and regeneration. *Materials Science & Engineering C-Materials for Biological Applications* 34: 35–49.

Gaillard, C., A. Bianco, G. Celiot, S. Li, F.M. Toma, H. Dumortier, G. Spaliuto, B. Cacciari, M. Prato, and L. Ballerini. 2009. Carbon nanotubes carrying cell-adhesion peptides do not interfere with neuronal functionality. *Advanced Materials* 21: 2903–2908.

George, M.W., and G. Bartosz. 2002. Self-Assembly at All Scales. *Science* 295: 2418–2421.

Gilmore, J.L., X. Yi, L. Quan, and A.V. Kabanov. 2008. Novel Nanomaterials for Clinical Neuroscience. *Journal of Neuroimmune Pharmacology* 3: 83–94.

Goslin, K., D.J. Schreyer, J.H.P. Skene, and G. Banker. 1988. Development of neuronal polarity: GAP-43 distinguishes axonal from dendritic growth cones. *Nature* 336: 672–674.

Guo, T., P. Nikolaev, A. Thess, D.T. Colbert, and R.E. Smalley. 1995. Catalytic Growth of Single-Walled Nanotubes by Laser Vaporization. *Chemical Physics Letters* 243: 49–54.

Hofstetter, C.P., E.J. Schwarz, D. Hess, J. Widenfalk, A. El Manira, D.J. Prockop, and L. Olson. 2002. Marrow Stromal Cells Form Guiding Strands in the Injured Spinal Cord and Promote Recovery. *Proceedings of the National Academy of Sciences of the United States of America* 99: 2199–2204.

Hu, H., Y. Ni, S.K. Mandal, V. Montana, B. Zhao, R.C. Haddon, and V. Parpura. 2005. Polyethyleneimine functionalized single-walled carbon nanotubes as a substrate for neuronal growth. *The Journal of Physical Chemistry, B* 109: 4285–4289.

Hu, L., D.S. Hecht, and G. Grüner. 2010. Carbon nanotube thin films: Fabrication, properties, and applications. *Chemical Reviews* 110: 5790–5844.

Hwang, J.-Y., U.S. Shin, W.-C. Jang, J.K. Hyun, I.B. Wall, and H.-W. Kim. 2012. Biofunctionalized carbon nanotubes in neural regeneration: a mini-review. *Nanoscale* 5: 487–497.

Inagaki, M., Y. Yang, and F. Kang. 2012. Carbon nanofibers prepared via electrospinning. *Advanced Materials* 24: 2547.

Iwasaki, M., J.T. Wilcox, Y. Nishimura, K. Zweckberger, H. Suzuki, J. Wang, Y. Liu, S.K. Karadimas, and M.G. Fehlings. 2014. Synergistic effects of self-assembling peptide and neural stem/progenitor cells to promote tissue repair and forelimb functional recovery in cervical spinal cord injury. *Biomaterials* 35: 2617–2629.

Jan, E., and N.A. Kotov. 2007. Successful Differentiation of Mouse Neural Stem Cells on Layer-by-Layer Assembled Single-Walled Carbon Nanotube Composite. *Nano Letters* 7: 1123–1128.

Kim, C., K.S. Yang, M. Kojima, K. Yoshida, Y.J. Kim, Y.A. Kim, and M. Endo. 2006. Fabrication of electrospinning-derived carbon nanofiber webs for the anode material of lithium-ion secondary batteries. *Advanced Functional Materials* 16: 2393–2397.

Kyle, S., A. Aggeli, E. Ingham, and M.J. Mcpherson. 2009. Production of self-assembling biomaterials for tissue engineering. *Trends in Biotechnology* 27: 423–433.

Leipzig, N.D., and M.S. Shoichet. 2009. The effect of substrate stiffness on adult neural stem cell behavior. *Biomaterials* 30: 6867–6878.

Li, D., Y. Wang, and Y. Xia. 2004. Electrospinning Nanofibers as Uniaxially Aligned Arrays and Layer-by-Layer Stacked Films. *Advanced Materials* 16: 361–366.

Li, N., G. Cheng, Q. Zhang, S. Gao, Q. Song, R. Huang, L. Wang, L. Liu, J. Dai, and M. Tang. 2013. Three-dimensional graphene foam as a biocompatible and conductive scaffold for neural stem cells. *Scientific Reports* 3: 1604.

Liu, S., Y. Qu, T.J. Stewart, M.J. Howard, S. Chakrabortty, T.F. Holekamp, and J.W. Mcdonald. 2000. Embryonic Stem Cells Differentiate into Oligodendrocytes and Myelinate in Culture and

after Spinal Cord Transplantation. *Proceedings of the National Academy of Sciences of the United States of America* 97: 6126–6131.

Mattson, M.P., R.C. Haddon, and A.M. Rao. 2000. Molecular functionalization of carbon nanotubes and use as substrates for neuronal growth. *Journal of Molecular Neuroscience* 14: 175–182.

Mcdonald, J.W., X.-Z. Liu, Y. Qu, S. Liu, S.K. Mickey, D. Turetsky, D.I. Gottlieb, and D.W. Choi. 1999. Transplanted embryonic stem cells survive, differentiate and promote recovery in injured rat spinal cord. *Nature Medicine* 5: 1410–1412.

Mckenzie, J.L., M.C. Waid, R. Shi, and T.J. Webster. 2004. Decreased functions of astrocytes on carbon nanofiber materials. *Biomaterials* 25: 1309–1317.

Nisbet, D.R., L.M.Y. Yu, T. Zahir, J.S. Forsythe, and M.S. Shoichet. 2008. Characterization of neural stem cells on electrospun poly(ε-caprolactone) submicron scaffolds: evaluating their potential in neural tissue engineering. *Journal of Biomaterials Science, Polymer Edition* 19: 623–634.

Olson, H.E., G.E. Rooney, L. Gross, J.J. Nesbitt, K.E. Galvin, A. Knight, B. Chen, M.J. Yaszemski, and A.J. Windebank. 2009. Neural stem cell- and Schwann cell-loaded biodegradable polymer scaffolds support axonal regeneration in the transected spinal cord. *Tissue Engineering—Part A* 15: 1797–1805.

Padmanabhan, J., and T.R. Kyriakides. 2015. Nanomaterials, Inflammation, and Tissue Engineering. *Wiley Interdisciplinary Reviews: Nanomedicine and Nanobiotechnology* 7: 355–370.

Park, I.-H., R. Zhao, J.A. West, A. Yabuuchi, H. Huo, T.A. Ince, P.H. Lerou, M.W. Lensch, and G.Q. Daley. 2008. Reprogramming of human somatic cells to pluripotency with defined factors. *Nature* 451: 141–146.

Park, S.Y., J. Park, S.H. Sim, M.G. Sung, K.S. Kim, B.H. Hong, and S. Hong. 2011. Enhanced differentiation of human neural stem cells into neurons on graphene. *Advanced Materials* 23: H263–H267.

RodríGuez, F.J., E. Verdú, D. Ceballos, and X. Navarro. 2000. Nerve Guides Seeded with Autologous Schwann Cells Improve Nerve Regeneration. *Experimental Neurology* 161: 571–584.

Rogers, I., N. Yamanaka, R. Bielecki, C.J. Wong, S. Chua, S. Yuen, and R.F. Casper. 2007. Identification and analysis of in vitro cultured CD45-positive cells capable of multi-lineage differentiation. *Experimental Cell Research* 313: 1839–1852.

Sanberg, P.R., A.E. Willing, S. Garbuzova-Davis, S. Saporta, G. Liu, C.D. Sanberg, P.C. Bickford, S.K. Klasko, and N.S. El-Badri. 2005. Umbilical Cord Blood-Derived Stem Cells and Brain Repair. *Annals of the New York Academy of Sciences* 1049: 67–83.

Sandner, B., P. Prang, F.J. Rivera, L. Aigner, A. Blesch, and N. Weidner. 2012. Neural stem cells for spinal cord repair. *Cell and Tissue Research* 349: 349–362.

Scheib, J., and A. Hoke. 2013. Advances in peripheral nerve regeneration. *Nature Reviews Neurology* 9: 668–676.

Schmidt, C.E., and J.B. Leach. 2003. Neural Tissue Engineering: Strategies for Repair and Regeneration. *Annual Review of Biomedical Engineering* 5: 293–347.

Soldano, C., A. Mahmood, and E. Dujardin. 2010. Production, properties and potential of graphene. *Carbon* 48: 2127–2150.

Takahashi, K., and S. Yamanaka. 2006. Induction of Pluripotent Stem Cells from Mouse Embryonic and Adult Fibroblast Cultures by Defined Factors. *Cell* 126: 663–676.

Tan, S.H., R. Inai, M. Kotaki, and S. Ramakrishna. 2005. Systematic parameter study for ultra-fine fiber fabrication via electrospinning process. *Polymer* 46: 6128–6134.

Temple, S. 2001. The development of neural stem cells. *Nature* 414: 112–117.

Tibbetts, G.G., M.L. Lake, K.L. Strong, and B.P. Rice. 2007. A review of the fabrication and properties of vapor-grown carbon nanofiber/polymer composites. *Composites Science and Technology* 67: 1709–1718.

Tse, W., and M.J. Laughlin. 2005. Umbilical cord blood transplantation: a new alternative option. *Hematology/The Education Program of the American Society of Hematology* 1: 377–383.

Tu, Q., L. Pang, Y. Chen, Y.R. Zhang, R. Zhang, B.Z. Lu, and J.Y. Wang. 2014. Effects of surface charges of graphene oxide on neuronal outgrowth and branching. *Analyst* 139: 105–115.

Wang, A., Z. Tang, I.-H. Park, Y. Zhu, S. Patel, G.Q. Daley, and S. Li. 2011a. Induced pluripotent stem cells for neural tissue engineering. *Biomaterials* 32: 5023–5032.

Wang, Y., J. Wang, J. Li, Z. Li, and Y. Lin. 2011b. Graphene and graphene oxide: biofunctionalization and applications in biotechnology. *Trends in Biotechnology* 29: 205–212.

Weightman, A., S. Jenkins, M. Pickard, D. Chari, and Y. Yang. 2014. Alignment of multiple glial cell populations in 3D nanofiber scaffolds: Toward the development of multicellular implantable scaffolds for repair of neural injury. *Nanomedicine: Nanotechnology, Biology and Medicine* 10: 291–295.

Welberg, L. 2014. A synaptic role for microglia. *Nature Reviews Neuroscience* 15: 68–69.

Whalley, K. 2014. A dynamic role for astrocytes. *Nature Reviews Neuroscience* 15: 566.

Xie, J., W. Liu, M.R. Macewan, P.C. Bridgman, and Y. Xia. 2014. Neurite outgrowth on electrospun nanofibers with uniaxial alignment: the effects of fiber density, surface coating, and supporting substrate. *ACS Nano* 8: 1878–1885.

Xie, J., M.R. Macewan, A.G. Schwartz, and Y. Xia. 2010. Electrospun nanofibers for neural tissue engineering. *Nanoscale* 2: 35.

Xie, J., S.M. Willerth, X. Li, M.R. Macewan, A. Rader, S.E. Sakiyama-Elbert, and Y. Xia. 2009. The differentiation of embryonic stem cells seeded on electrospun nanofibers into neural lineages. *Biomaterials* 30: 354–362.

Yan, L., F. Zhao, S. Li, Z. Hu, and Y. Zhao. 2011. Low-toxic and safe nanomaterials by surface-chemical design, carbon nanotubes, fullerenes, metallofullerenes, and graphenes. *Nanoscale* 3: 362–382.

Yarin, A.L., S. Koombhongse, and D.H. Reneker. 2001. Bending instability in electrospinning of nanofibers. *Journal of Applied Physics* 104: 3018–3026.

Yu, J., R. Stewart, I.I. Slukvin, J.A. Thomson, M.A. Vodyanik, K. Smuga-Otto, J. Antosiewicz-Bourget, J.L. Frane, S. Tian, J. Nie, G.A. Jonsdottir, and V. Ruotti. 2007. Induced Pluripotent Stem Cell Lines Derived from Human Somatic Cells. *Science* 318: 1917–1920.

Zhang, H., G. Grüner, and Y. Zhao. 2013. Recent advancements of graphene in biomedicine. *Journal of Materials Chemistry B* 1: 2542–2567.

Zhang, L., and T.J. Webster. 2009. Nanotechnology and nanomaterials: Promises for improved tissue regeneration. *Nano Today* 4: 66–80.

Zhu, Y., S. Murali, W. Cai, X. Li, J.W. Suk, J.R. Potts, and R.S. Ruoff. 2010. Graphene and graphene oxide: Synthesis, properties, and applications. *Advanced Materials* 22: 3906–3924.

Chapter 8
Brain-Machine Interfaces: Restoring and Establishing Communication Channels

Charlie Rodenkirch, Brian Schriver, and Qi Wang

The idea of a cybernetic organism–a being with both organic and biomechatronic parts–is a hallmark of modern science fiction, with iconic characters such as Darth Vader, Robocop, and The Terminator being prime examples. Yet novel medical technologies are turning this fiction into reality, allowing an alternative to treating diseased organs and limbs, simply replace them. This image of a new medical revolution, which promises permanent solutions for once unsolvable health problems, has inspired a generation of researchers to further the field's knowledge.

This chapter will provide a brief background on some recent progress in the field of brain-machine interfaces (BMIs), starting with overviews of select, highly developed neuroprostheses. In particular, it will discuss how BMIs allow for the creation of communication channels between the brain and prosthesis. The chapter highlights the communication channel as it presents the greatest difficulty in seamlessly integrating neuroprostheses with their users. To elaborate, the necessary electronic peripherals, such as robotic arms and cameras, are now well defined, leaving interfacing these peripherals with the brain as the current limiting factor in performance.

The chapter will start by reviewing the simplest efferent communication channel: a one-way connection, which reads from the brain, translates the signal into motor intent, and uses the results to control a robotic arm. Next, it will cover afferent communication channels: interfaces which acquire signals from electronic sensory prosthetics, convert these signals into a neural code, and finally write them into the brain in an attempt to create desired perceptions. Last, it will discuss the establishment of a communication channel directly between two brains, wherein it is necessary to read information from one brain and write it to another.

C. Rodenkirch • B. Schriver • Q. Wang (✉)
Department of Biomedical Engineering, Columbia University, Manhattan, NY, USA
e-mail: qi.wang@columbia.edu

L.G. Zhang, D.L. Kaplan (eds.), *Neural Engineering*,
DOI 10.1007/978-3-319-31433-4_8

8.1 A Neuroprosthetic Arm

The loss of the ability to control one's limbs commonly stems either from complete limb amputation or from nerve damage, such as spinal cord injury or brainstem stroke, which prevents the brain from communicating with the limb. There are nearly two million people living with limb loss in the United States alone, a statistic, which is expected to exceed three-and-a-half million by 2050 (Ziegler-Graham et al. 2008). Although non-lethal, limb loss presents a permanent disability for these individuals, often compromising their ability to live independently. Even more individuals—around six million in the United States—are paralyzed, with completely unusable limbs (The Reeve Foundation 2009). Biomechanical engineering has provided some solutions, such as mechanical prosthetic arms, for these individuals. However, it is apparent that these mechanical solutions could never fully restore the dexterity of a natural arm. Whereas a natural arm receives a multitude of signals from the brain and decodes them into muscle movements, a mechanical prosthesis receives its driving commands from a limited number of muscles, thereby vastly constraining its potential as a proper replacement.

Decades ago, science fiction writers were already thinking of a more elegant solution, even before the existence of the necessary technology to implement it. This solution involved combining a robotic arm with a human body in such a way that the final result would mimic the performance of a natural limb. In the 1980s, fans of Star Wars received a glimpse of how this technology may one day be implemented: after losing his hand in combat, Luke Skywalker has it replaced with a robotic hand. Post-procedure, this artificial hand works flawlessly and its performance and outer appearance are indistinguishable from his natural hand. Even today, such seamless integration remains a dream, a goal toward which many researchers are making important steps.

The past several decades have seen amazing advancements in robotics, driven by mainstream adoption of the technology by the manufacturing industry. Seeing how well robotic arms on an assembly line work, one may wonder why a neuroprosthetic arm has not already been perfected. The difficulty stems from the limited understanding of the motor system. The neural signal theoretically provides all the instructions the arm needs, but from where and how should this signal be read? Additionally, once acquired, how can spike trains be translated into precise movements? Finally, how can the robotic arm provide feedback, such as proprioception and tactile sensation, to the brain? This section will look at how several research groups have approached these problems, and how their groundbreaking results helped further advance the field along the path to developing a neuroprosthetic arm.

8.1.1 Rats Can Control Robotic Arms Using Only Their Minds

Although the technology to read signals from the brain had existed for many years, it wasn't until the rapid improvement in computer technology during the 1990s that researchers were provided with the capability to digitally process these signals.

Toward the end of the decade, it became feasible to process, in real time, many signals simultaneously recorded from multiple neurons. These advancements in digital signal processing facilitated the creation of a BMI, a direct communication channel between the brain and an electronic device. It was hypothesized that by using this new interface technology, it would be possible to decode an animal's desired limb movement at any moment (Chapin et al. 1999). One of the most commonly used laboratory animals, the rat, was chosen as the first animal model on which to test this hypothesis. In theory, the hypothesis could be tested by reading and attempting to decode neural signals from the primary motor cortex (M1), which neuroscientists had long ago identified as a region fundamentally involved in volitional control of body movements. However, converting signals from multiple neurons in the M1 region into quantifiable movement of a robotic arm in a particular direction proves to be a complex task.

To investigate this hypothesis, multi-electrode arrays (MEAs) were implanted into M1 and the ventrolateral thalamus of the rats. Initially, the researchers wanted to learn what types of signals appear in the motor cortex when a rat moves its forelimb (Chapin et al. 1999). To record these signals, the rats were water deprived and then placed within a behavioral training box, which contained a joystick that the rats could manipulate to control a robotic arm to deliver water. Recordings were performed until enough data was collected to allow for the mapping of neural signals to the forelimb, and consequently, joystick movements. A diagram of the behavioral training box and recorded signals can be seen above in Fig. 8.1. Sophisticated decoding algorithms combining principal component analysis and artificial neural networks were applied to the neural data to convert spike trains from simultaneously recorded neurons into a neuronal population function, which represented the desired direction of arm movement. Amazingly, when this decoder was applied to the MEA recording in real time and used to direct the robotic arm's movement, the rats were able to control the robotic arm with their minds, without physically manipulating the joystick. These results proved the feasibility of a neuroprosthetic arm, if only in its most basic sense.

8.1.2 Monkeys Are Able to Use Neural Interfaces to Manipulate Computer Cursors

Encouraged by the success of creating an interface between a rat's brain and a robotic arm, many labs began to pursue BMI-related research. To further assess the feasibility of ultimately using this technology in humans, a more humanistic model was necessary. Thus, many labs adopted a primate model as their primary interface-testing platform. Not only is the primate's body and brain much more analogous to a humans, their higher intelligence allows researchers to test the interface's performance under more demanding tasks. This provides us a better sense of how well these interfaces would function in a human patient performing real-world tasks. Also around this time, an MEA, commonly referred to as the Utah array, was developed and deemed a large step toward an MEA suitable for human implantation

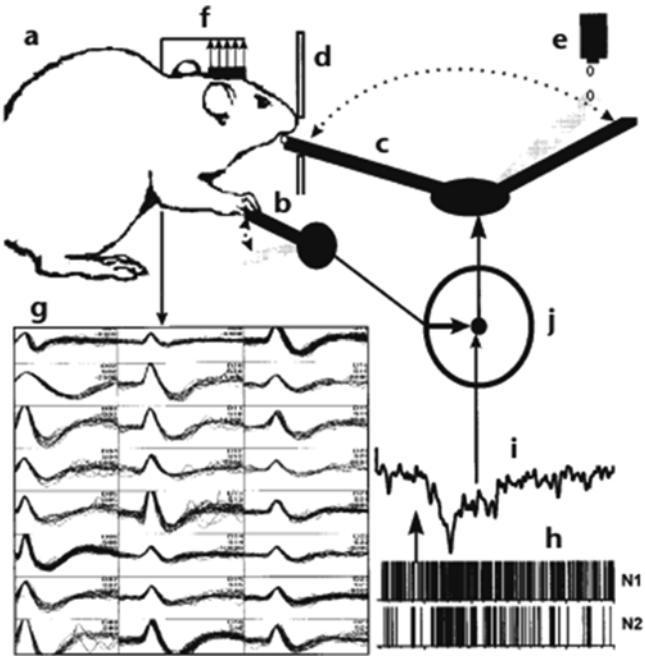

Fig. 8.1 A rat uses its forearm to manipulate a lever, which controls a robotic arm, to bring a water reward. During some trials, neural signals from M1, which encode the movements of the rat's forearm, are recorded and used to successfully control the robotic arm. Adopted from Chapin et al. 1999 with permission

(Maynard et al. 1997). When implanted into the motor cortex of monkeys, this array allowed for the reliable, simultaneous recording of multiple neurons over many months (Serruya et al. 2002).

One of the first trials in primates involved the implantation of an MEA into the left dorsal premotor cortex of two owl monkeys (Wessberg et al. 2000). Using data recorded during the monkeys' movement of a joystick allowed the researchers to create a decoder, which translated neural activity to directional movement. More complex nonlinear decoders, such as artificial neural networks, were also shown to provide adequate decoding. Finally, this research showed that a decoder, which continuously optimizes its parameters while in use, will have a much higher performance than a decoder whose parameters remain static.

Another study taught monkeys implanted with a Utah array to use a joystick to move a computer cursor along a pseudorandom path on the computer screen (Serruya et al. 2002). A linear filter system, constructed using 1 minute of continuous recording and hand tracking data, was then applied as a decoder to determine intended cursor position. When applied to subsequent data, this decoder allowed for the recovery of hand trajectory. The monkeys were then given the option to use the neural interface to directly control the cursor, and were presented with visual feedback to close the loop. The monkeys quickly learned how to use the neural interface

with only visual feedback and no formal training, and, as previously seen in the rat model, stopped using the joystick altogether.

These initial results were quite promising, showing that a BMI in primates could be used to control the position of an object. However, there was still an issue with the developed system preventing its use by disabled humans. In all of the previous animal models, the decoding algorithm, which translates the neural activity into intended limb movement, was created using data recorded while the animals moved their working arms. Unfortunately, many parapelegics does not have this capability; therefore training data could not be collected. To solve this problem, attempts were made to create adaptive decoders, which required no initial training data. It was found that if a monkey was given visual feedback, it will be able to learn how to use a neural interface which employed an arbitrary decoding scheme (Taylor et al. 2002). After learning how to manipulate their neural signals to properly fit this decoder, monkeys were able to use the neural interface to guide a digital cursor to its target. Further analysis of the resulting data showed that the neurons in the monkeys' motor cortex were actually shifting their tuning functions during the experiment so as to better interface with the decoder. This showed that a closed-loop neural interface could induce neural plasticity, allowing for adaptive improvements in performance. This suggests that providing the brain feedback from the neuroprosthetic arm may be just as important as reading information from the motor cortex.

Indeed, more recent advancements in decoding schemes support the idea that the optimal neural interface for controlling a neuroprosthetic arm may be fundamentally different than the natural interface between the brain and an organic arm. If this is true, then research should focus less on replicating natural communication and more on establishing a completely new communication protocol. In line with this, it was proposed that the decoder's adaptation and neural adaptation do not need to be separated; instead, algorithms that capitalize on using both mechanisms to improve communication produce the most robust total systems for neuroprosthetic control (Shenoy and Carmena 2014). Therefore, a better understanding of the interaction between biomimetic designs and both user and decoder adaption could greatly improve the quality of motor BMIs (Bensmaia and Miller 2014).

All the neural interfaces described thus far have used the M1 region as their interface site. Due to the multitude of complex motions a hand can perform, it was estimated that signals from hundreds of motor cortex neurons would be necessary to precisely replicate the natural kinematics of reaching and grasping using a neuroprosthetic arm. Although decoding intended limb movement from neural activity in M1 was the most straightforward approach, some researchers hypothesized that there may be other brain regions whose neural activity might be valuable to consider when decoding arm movement intent. Certainly, neuroscientists had already shown that many other brain regions encode information related to limb movement. One such region is the parietal reach region (PRR), a subregion of the posterior parietal cortex. The PRR is located earlier along the sensory-motor pathway than the motor cortex, and does not encode movement, but rather the desire to move and movement planning information such as the final target toward which the movement is made (Shenoy et al. 2003). Since trajectory planning is a trivial task for modern robotics,

these earlier signals, if decodable, offer different possibilities for neuroprosthetic limb control. Maximum likelihood estimation was applied to neural recordings from the PRR to estimate what reach parameters could be resolved. From these recordings, a finite-state, machine-decoding algorithm was created. This algorithm was shown to be effective in determining when an animal is planning to reach and in which direction the animal will execute this reach. In addition to the intended target of the movements, other higher-level cognitive signals, such as the expected magnitude or probability of a reward upon the successful grasp of an object, were encoded in neural activity in this region (Musallam et al. 2004). This allows an interface into the PRR to read not only the desire of arm movement but also the preferences and motivation of the individual as the movement is carried out.

Although much progress had been made, the performance of neural interfaces at this time was still too slow and inaccurate to offer a real solution; eye tracking systems, which used pupil movement for control, still outperformed the cutting-edge neural interfaces. However, it was still widely thought that a direct neural interface, when optimally implemented, should be able to outperform these eye tracking systems. As researchers continued to look for ways to improve the performance of the neural interface, the dorsal premotor cortex (PMd) was investigated as a possible interface location (Santhanam et al. 2006). The PMd encodes information about the final target of desired arm movement. Instead of decoding every detail of movement necessary to move the arm and grasp an object from signals in the motor cortex, the desired object could be determined from PMd recordings, and standard robotic arm control algorithms, already commonly used in factories, could be easily applied to direct the arm to grasp that object. Monkeys with a neural interface in the PMd confirmed not only that this approach worked, but also that motions were executed many times faster than previous BMIs (Santhanam et al. 2006). Monkeys were then taught to use this interface to type on a digital keyboard with a digital cursor and were able to achieve rates of approximately 15 words per minute, although no works of Shakespeare were reproduced.

With neural interfaces and decoding systems becoming more defined, research continued to move toward preparing the system for real-world tasks. To this end, neural interfaces were designed through which monkeys could control two on-screen avatar arms. Research using this interface produced surprising results: it was found more effective to consider the two avatar limbs together than independently when decoding motor cortex signals in predicting movements (Ifft et al. 2013). A single fifth-order, unscented Kalman filter, instead of two independent filters and cortical networks, was found to allow for faster adaptation in the frontal and parietal cortical areas, resulting in better neural interface performance.

8.1.3 Monkeys Feed Themselves Using Neuroprosthetic Arms

Although the studies discussed above have shown that neural interfaces worked well in the digital world, it was important to consider how well they would perform in the physical world. Toward this goal, monkeys were trained to use a neural

interface to manipulate a robotic arm. A more complex decoder, which used ensemble neural recordings from several brain regions, was able to extract several kinematic parameters, such as hand position, velocity, and gripping force (Carmena et al. 2003). It was found that by recording from these large neuronal ensembles, high accuracy arm movements could be resolved. This allowed monkeys to use a robotic arm, in conjunction with visual feedback, to perform reach and grasp tasks. Continuous use of this BMI led to significant improvements in performance as well as functional reorganization in multiple cortical areas. Recent work has further confirmed that cortical adaptation occurs during use of a BMI, which results in better performance of the BMI's decoder (Rouse et al. 2013). In fact it has been shown that large-scale modifications of the cortical network and changes in directional tuning occur when an implanted monkey learns to proficiently use its BMI (Ganguly et al. 2011).

The ability to feed oneself is often taken for granted, but for individuals with tetraplegia this task is impossible, leading to reduced quality of life and necessitating daily assistance. Researchers thought that if monkeys could successfully perform reach and grasp tasks with a robotic arm and neural interface, perhaps they could then use this interface to feed themselves. This may seem like a simple extension of the previous tasks; however, feeding oneself requires more complex motor skills. During the study, the monkeys used a five-degrees-of-freedom robotic arm to interact with physical objects. Undeterred by the complexity of their new task, the monkeys were able to consistently grasp food placed at arbitrary positions and bring it to their mouths (Velliste et al. 2008). The results were promising, showing monkeys could successfully move the arm in three dimensions as well as open and close a gripper at the end of the arm. This suggests that one day humans could use neuroprosthetic devices to achieve dexterous functions at near-natural levels.

8.1.4 The Disabled Are Finally Getting a Hand as Motor Neuroprostheses Enter Clinical Trials

Today, the cutting edge of neuroprostheses exists within the world of clinical trials, and MEAs have been successfully implanted into the motor cortices of human patients. As research in primates suggested, humans could use associated neural signals to control a digital cursor. A quadriplegic, who had been paralyzed 3 years earlier by a spinal cord injury, was implanted with a neural interface that would allow him to manipulate a robotic arm (Hochberg et al. 2006). The interface, shown in Fig. 8.2, successfully recorded signals from the M1 region and decoded these signals into intended hand motions. The patient used the neural interface and decoder to manipulate the movements of a computer cursor, to type e-mails, control his television, and play video games. This achievement is quite wonderful when considering that the ability to control a cursor is much more meaningful for a human than a monkey. Long-term monitoring of these neural interfaces has shown sustained viability, addressing a classic concern with implantation of foreign material

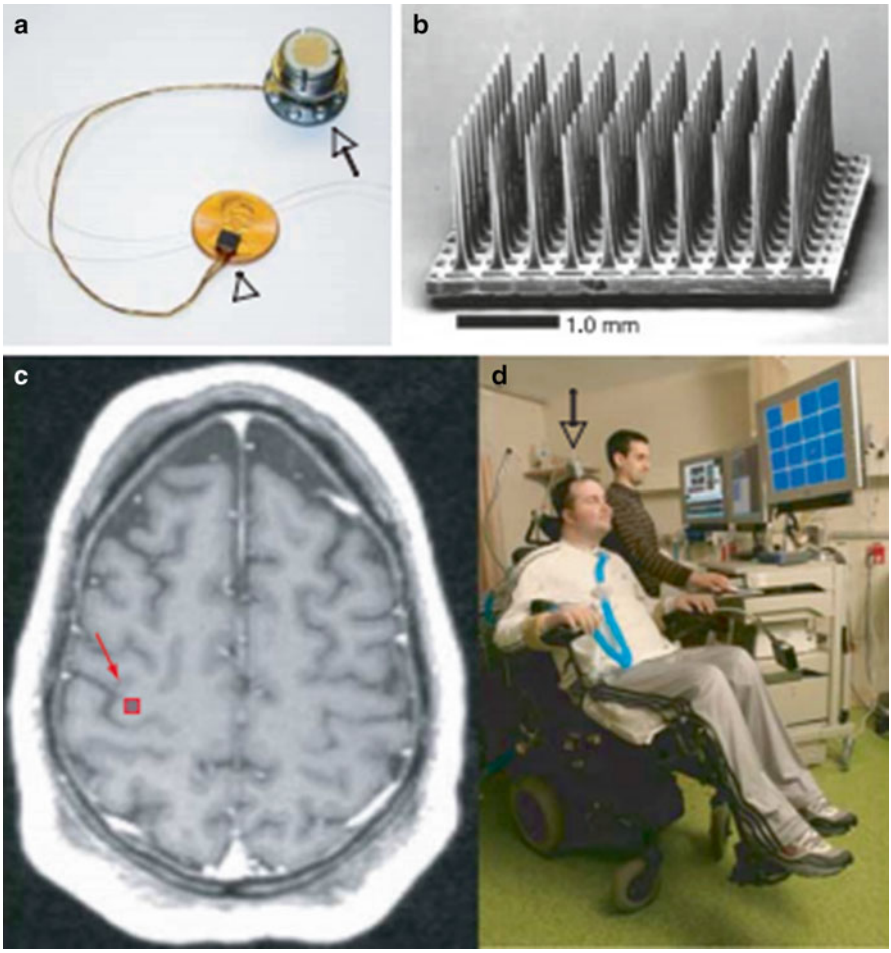

Fig. 8.2 This small MEA, when implanted into the M1 region of paraplegic patients, allows for the recording and decoding of the patient's neural signals into movement intent which can be used to control a variety of peripherals, such as robotic arms and computer cursors (Hochberg et al. 2006)

(Simeral et al. 2011). Several years after implantation, patients have still been able to accurately perform cursor point-and-click tasks.

The last step left toward full implantation of a motor neuroprosthesis was the addition of the robotic arm. Following the success of humans using neurally controlled prosthetic devices, researchers began new clinical trials, hoping to help patients accomplish even more complex tasks. Quadriplegics with neural interfaces were shown to be able to control advanced robotic arms and perform reach and grasp tasks. It was also found that simple visual feedback worked well toward helping individuals learn to use their new, neurally interfaced robotic arm. Adopted from Hochberg et al. 2012 with permission.

8.1.5 *Researchers Give the Disabled More than a Hand, for Example, an F-35 Fighter Jet*

The ability to restore motor function in disabled individuals provided more than enough reason to expand neural interface research. Now that the technology has moved beyond its infancy, new and more diverse uses of the interfaces are being proposed. One example of an alternative use comes from the University of Pittsburgh's Human Engineering Research Laboratories. In 2012, researchers implanted a neural interface into a quadriplegic, and over the course of the next 2 years, she was taught to control a robotic arm. DARPA, the research branch of the military, was closely involved in this project, as many veterans suffer from limb loss or paralysis due to combat injuries. Once the patient had mastered the use of the arm, DARPA wondered what else she might be able to control. One proposal was an F-35 jet, a stealth multi-role fighter only recently introduced into the air force. After an interface was created between the patient and a flight simulator, the patient could successfully control the F-35's altitude, pitch, and roll purely using her mind (Stockton 2015)!

8.1.6 *Brain-Controlled Stimulation of Muscles Presents an Alternative Pathway to Regaining Mobility*

Completely replacing a damaged arm with a neuroprosthetic arm provides a solution to almost any type of circumstance preventing individuals from using their current arm, particularly for amputees. However, a large subset of handicapped individuals has lost control of their limbs due to a spinal cord injury. In these instances, the limbs remain fully intact and functional, but the damaged spinal cord prevents signals from traveling between the brain and the limbs, thereby precluding the individual from moving them. In these situations, it is apparent that replacing the healthy limb with a neuroprosthetic arm is an unnecessarily drastic approach. Instead, recent research has focused on reestablishing the communication channel between the brain and the healthy organic limb (Moritz et al. 2008).

As previously outlined in this chapter, BMIs can convert brain signals from the motor cortex into a desired movement of a robotic arm. It was proposed that perhaps these same, recorded signals could be used to control a healthy, organic limb. Functional electrical stimulation (FES) of the muscles was used to achieve this goal (Moritz et al. 2008). Electrically stimulating muscles in the arm causes them to contract, much as they would in response to an innervating nerve firing. The feasibility of restoring the communication channel between the brain and healthy limb, while bypassing the damaged spinal cord, was tested in a monkey model. Not only did these trials show that neuronal activity could be translated into muscle movement via a BMI-to-FES interface, it was also found that the monkeys were able to quickly adapt their neural signals so as to better utilize the new communication channel. Specifically, it was not necessary to match neurons with the same muscles

they were associated with prior to the injury. This shows the monkeys were able to quickly learn the new mapping between the neurons and the muscles connected to the FES system, and adapt their neural activity to be able to best utilize these new connections.

Clinical trials have shown that FES can be used in patients with tetraplegia to regain control of hand movement. These trials use residual, proximal limb movements to trigger a preprogrammed hand grasp induced by an FES system (Keith et al. 1989). Due to the inability to perform any unique grasping gestures besides those that are preprogrammed, this system does not allow for nuanced or precise grasping motions, thereby limiting its usefulness. To remedy this problem, it was proposed that a BMI could be used to translate neuron signals into FES stimulation of muscles in the hand, allowing for the return of more natural grasping ability. This idea was tested in a primate model, where a BMI recording from 100 motor cortex neurons was used to control an FES system implanted in a primate's hand (Ethier et al. 2012). To train the interface, both the motor cortex neurons and their corresponding muscles within the hand and forearm were recorded while the primate performed a task which involved picking up a rubber ball and placing it at a target location. Once the different neural activity patterns had been mapped to corresponding muscle contractions, the primate's forearms and hands were temporarily paralyzed by a peripheral nerve block in the elbow. The primates were then asked to perform the same task again, but this time they could only move their hand and forearm using an FES system controlled by their neural interface. Using this system, the primates were able to grasp and move the ball reliably with movements that seemed natural to a casual observer.

8.2 A Somatosensory Neuroprosthesis

We've already covered, in depth, how BMIs can be used to control the motion of a robotic arm. However, besides allowing mechanical interaction with the environment, natural limbs serve another purpose, providing somatosensory feedback. Somatosensory feedback includes feedback from a wide variety of receptors, which encode senses such as nociception, proprioception, mechanoreception, and thermoception. The addition of somatosensory feedback has the potential to make the neuroprosthetic arm feel as it if is the patient's own, natural limb. Even more importantly, efficient, natural limb movement is better achieved by using a closed-loop neuroprosthetic arm, thereby necessitating implementation of an artificial afferent system.

8.2.1 Adding Feedback to Neuroprosthetic Arms Is a Touching Story

As sensory and motor systems are inextricably linked, somatosensory feedback is essential in motor control. Removing or blocking sensory feedback via anesthetics or lesions dramatically impairs motor abilities in otherwise healthy subjects.

Proprioception, or the ability to sense the relative position of body parts and the forces needed to maintain or move them, has been found to be essential in movement planning, especially during complex tasks (Sainburg et al. 1995). Expectedly, when deprived of any sense of mechanoreception, commonly referred to as the sense of touch, a human's ability to interact with or even hold objects correctly goes awry (Monzee et al. 2003), and inactivation of the primary somatosensory cortex (S1), the brain area responsible for processing and relaying somatosensory information, results in severe loss of coordination and exaggerated movements in monkeys (Brochier et al. 1999).

While touch and proprioception are the most necessary senses for proper limb control, they are by no means the only senses that provide valuable feedback. While other senses, such as temperature and pain, are less critical to movement, a full gamut of senses is necessary to make neuroprosthetic limbs feel like a natural body part. Multiple robotic hands have been developed toward this purpose, with the latest models incorporating numerous sensors for encoding a broad range of information including measures of joint angle, tendon tension, temperature, vibration, and skin deformation (Hellman et al. 2015). These robotic hands employ numerous, novel techniques to produce these senses. For instance, one design employs a conductive liquid chamber enclosed between a synthetic elastomeric skin and an electrode array-covered artificial finger skeleton (Su et al. 2012). Hydraulic pressure measured and encoded by the electrode array provides a more natural, even sense of touch when pressure is applied to the hand. Other design features include an artificial fingerprint imprinted onto the skin, which allows a user to gauge surface texture by measuring the vibrations created by the friction between the fingerprint and the surface. Unfortunately, current neural interfaces cannot yet take advantage of these cutting-edge peripherals, and therefore the peripherals have not been tested in clinical trials. The first problem with providing somatosensory feedback is determining how to convert the signals collected from the sensors within the neuroprosthetic arm to a neural code, which can be understood by the brain. The second problem is finding the best brain location and stimulation techniques to effectively deliver this neural code.

8.2.2 Electrical Stimulation of the Primary Somatosensory Cortex Provides a Substitute for Natural Tactile Stimuli

The well-known cortical homunculus—a pictorial representation of the anatomical divisions of the M1 and S1 brain regions—was created using electrical stimulation to map each region, and provides the first example of artificial somatosensory perception (Penfield 1937). It was later demonstrated that focal stimulation of the cortical surface resulted in specific, localized tactile sensations on corresponding body parts (Rasmussen and Penfield 1947). It was not until the 1990s that a seminal work showed that intracortical microstimulation (ICMS) pulses delivered to S1 would result in tactile sensations that were indistinguishable from the sensations evoked by tactile stimuli applied to monkeys' fingers (Romo et al. 1998).

Monkeys were trained to discriminate the difference in frequencies between mechanical vibrations sequentially applied to their fingertips. On random trials, ICMS were delivered to S1 in place of the second mechanical stimuli. It was found that the animals were able to reliably determine the frequency change regardless of whether the second stimulus was mechanically delivered or simulated via ICMS stimulation. This was the first experiment to systematically show that animals could not distinguish between natural and ICMS induced sensations, thereby demonstrating the capability of ICMS for delivering varying somatosensory percepts (Romo et al. 1998). Several years later, it was shown that a rat's movements could be remotely controlled, similar to how a radio-controlled toy car is steered (Talwar et al. 2002). This was accomplished by implanting electrodes into the barrel cortex, allowing for the delivery of signals, which the rat would perceive as a whisker deflection. The rat was then outfitted with a backpack containing the necessary electronics to wirelessly control the stimulation delivered to these electrodes. Using this system, "Robo-Rats" were successfully guided by stimulating the barrel cortex in different hemispheres. These influential works solidified the idea that ICMS could be used to write meaningful somatosensory information to the brain.

To minimize mental load during use, and to decrease the necessary training time, the ideal somatosensory neuroprosthesis would deliver sensations similar, if not identical, to those delivered via afferent neurons from a healthy limb. In practice, this would require the conversion of signals from multiple sensors into their representative pattern of neural activation, and their delivery to the correct brain regions using ICMS. Unfortunately, due to the current limited understanding of the somatosensory system, this biomimetic approach remains a challenge. Instead, most current systems rely on brain plasticity, which allows patients to adaptively learn and recognize the new input signals (Bensmaia and Miller 2014).

In order to construct a somatosensory neuroprosthesis, parameters for inducing these sensations via ICMS must be established. Work from several groups demonstrated that rats were an acceptable model for ICMS testing, as head-fixed rats could readily detect ICMS delivered to the barrel cortex (Bari et al. 2013). Moreover, it was shown that it was possible to convince rats of the presence of virtual objects in their environment by using ICMS to deliver a sensation that matches that of object-detecting whisking, a rat's method of sweeping its whiskers to explore its environment (Venkatraman and Carmena 2011; O'Connor et al. 2013). Applying computer-simulated models to neural data recorded during behavioral tasks, researchers have begun to map certain neural activity patterns with specific sensory features. With this, researchers have shown that perceived intensity is primarily attributed to spatiotemporal integration of action potentials. For example, increased amplitude may be linked to increased size of the firing neuronal population, while increased frequency may be linked to greater firing rates (Fridman et al. 2010).

8.2.3 *Closing the Sensorimotor Loop Allows for more Naturalistic Control of Neuroprostheses*

As stated in the section on neuroprosthetic arms, a primate model is often necessary to prepare a design for human implantation. This is also true when considering a somatosensory neuroprosthesis. To create a primate model, researchers first successfully trained monkeys to discriminate spatial and temporal patterns of ICMS delivered to S1 (Fitzsimmons et al. 2007). Subsequently, it was shown that the delivery of these same ICMS patterns could be used to instruct a monkey about where to move a BMI-controlled computer cursor (O'Doherty et al. 2009). In another experiment, multiple somatosensory features, including contact location, pressure, and timing, were conveyed to monkeys through ICMS of the S1 region (Tabot et al. 2013). Monkeys were first trained to discriminate between mechanical stimuli differing in location and pressure, which were sequentially delivered to their palms. When the mechanical stimuli were randomly replaced with ICMS of S1, the monkeys were still able to properly gauge the target location and pressure of the ICMS-simulated stimuli. This resulted in the monkeys showing equivalent task performance with mechanical and artificial stimuli. The group was also able to mimic on- and off-responses associated with first and last contact with object, respectively. This mimicry was achieved by delivering phasic ICMS at the onset and offset of contact, while using tonic ICMS during contact to encode varying pressure and location.

A groundbreaking study was recently completed, which showcased the successful development of the first closed-loop, sensorimotor neuroprosthesis (O'Doherty et al. 2011). The system, outlined in Fig. 8.3, coupled a BMI, which allowed a monkey to move an on-screen cursor, with a sensorimotor neuroprosthesis, which delivered ICMS to the monkey's S1 so as to evoke the sensation of the texture of whatever digital object the cursor was hovering over at any given time. Using these two BMIs, monkeys were able to identify a target digital object out of a group of digital objects simply by comparing the objects' corresponding textures, proving the feasibility of bidirectional neuroprostheses.

While most of the research has focused on mechanoreception, proprioception remains of great importance to neuroprosthetic limbs. However, proprioception is a more complicated sensation than mechanoreception and has proven more difficult to parameterize due, primarily, to the lack of a well-structured topographic map of associated encoding locations in the brain. One group demonstrated that a monkey could discriminate between different ICMS patterns delivered to the S1 sub-region, 3A (an area concerned with proprioception), suggesting proprioception could be restored using ICMS (London et al. 2008). In a subsequent experiment, S1 activity was recorded in monkeys carrying out both active and passive movements to determine how different proprioception is represented in S1. Neural data were recorded while monkeys directed a cursor using a manipulandum that allowed researchers to

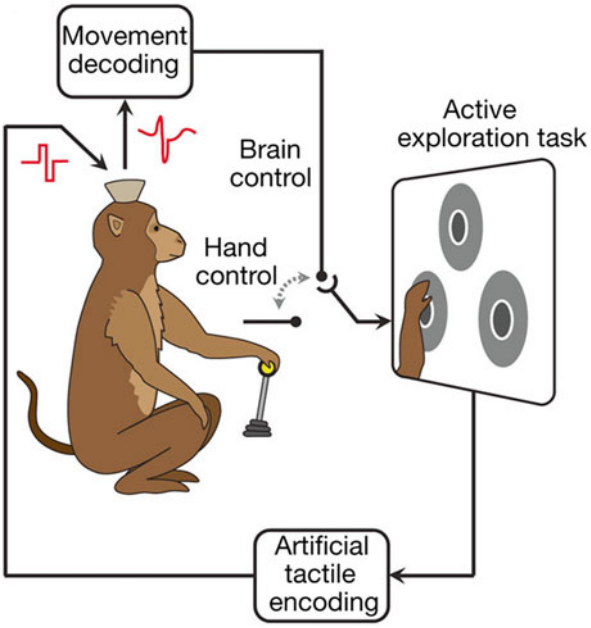

Fig. 8.3 A monkey outfitted with a BMI is able to use the interface to move a cursor on screen, while simultaneously using a virtual tactile sensation induced by patterned microstimulation of the S1 region to distinguish the texture of the object below the cursor. Adopted from O'Doherty et al. 2011 with permission

deliver pulses of force through its handle. The monkeys were then tasked with using the direction of these force pulses to determine which movements to make (Zaaimi et al. 2013). The mechanical forces were then replaced with their representative neural activity patterns, delivered to the S1 region by ICMS, which simulated a force from the manipulandum. The monkeys were found to treat the ICMS-delivered sensation as if it were an actual force through the manipulandum. Though still a simplified representation of proprioception, this study opened the door to conveying a complicated spectrum of sensations. Other approaches include using an MEA to interface with nerve stumps in the remaining section of the limb, instead of with the brain, to provide both tactile and proprioceptive feedback (Chapin 2004; Horch et al. 2011).

Somatosensory neuroprostheses have only recently been implemented in animal models, so it is quite amazing that they have already been introduced into the humans as well. However, due to the high-risk nature of electrode implantations, initial clinical trials have focused on less invasive means of delivering stimulation to the S1 region. One technique utilizes an electrocorticography array along the surface of the cortex to deliver ICMS. Using this system, patients were able to readily distinguish the presentation of different stimulation patterns, proving that direct cortical stimulation can offer unique sensory feedback in humans (Johnson et al. 2013).

Transcranial focused ultrasound (tFUS) is another, even less invasive technique, which is a promising option for activating S1. tFUS has the ability to modulate sensory-evoked brain oscillations, thereby enhancing performance on sensory discrimination tasks (Legon et al. 2014). Furthermore, tFUS, targeted at areas corresponding to mechanoreception in the hand, has been shown capable of eliciting tactile sensations with precision on the individual-finger level (Lee et al. 2015). These early successes make it likely that future innovative techniques and a further understanding of the somatosensory system will lead to somatosensory neuroprostheses as successful as the auditory and visual neuroprostheses described in the following sections.

8.3 An Auditory Neuroprosthesis

Auditory neuroprostheses are designed to deliver audio signals to the brain while bypassing any damaged peripheries of the auditory pathway. The auditory nervous system is well defined, and there are many options along its pathway for a viable interface location. Cochlear implants (a type of auditory neuroprosthesis) represent the most widely adopted and commercially successful neuroprostheses. Implantable models are capable of restoring useful auditory perception to the 360 million individuals suffering from disabling hearing loss worldwide (Olusanya et al. 2014). Although communication with the cochlea is not direct communication with the brain, for completeness and given the commercial success of cochlear implants, this section will briefly review their history and development, before moving on to discuss auditory neuroprostheses that interface directly with the brain.

8.3.1 The Cochlear Implant Emerges as the First Commercially Successful Neuroprosthesis

Initial attempts at improving hearing using electronic stimulation began as early as 1748 when it was found that the hearing of a deafened woman could be improved by applying an electric potential across her temples using a Leyden jar, a rudimental type of battery (Wilson 1752). This concept remained untouched until 1930, when recordings from the cochlear nerves of cats showed that the nerve encoded both the frequency and amplitude of speech waveforms (Wever and Bray 1930). As hearing loss is commonly caused by damaged hair cells within the ear, it was proposed that one could bypass these damaged cells and interface directly with the healthy cochlear nerve. A couple decades later, it was confirmed that stimulating the cochlear nerve of a human patient caused that patient to perceive a noise (Gisselson 1950).

The first instance of a deaf human's hearing being augmented by an intra-auricular implanted electrode was unplanned. While performing a surgery to treat cholesteatoma, a destructive growth within the middle ear, doctors implanted an electrical stimulation device within the cholesteatoma in the hopes that they could use electric current to treat it (Djourno et al. 1957). Due to the location of the cholesteatoma, the implantation location of the stimulation device was in close proximity to the internal auditory canal. Upon activation of the stimulation device, it was found that the patient had some of his hearing restored. Later, this was understood to be due to the stimulation device activating acoustic nerve fibers in the patient's inner ear (Djourno and Eyries 1957). These accidental findings encouraged otologists to begin designing a cochlear implant for hearing restoration. The first models of such a device were single-channel interfaces, which electrically stimulated the acoustic nerve fibers. Due to their simplicity, these cochlear implants allowed their users to hear rhythms of speech but not to recognize the words being spoken (House and Owens 1973). However, the return of any hearing—no matter how distorted—was trailblazing, and unveiled the potential of a cochlear implant.

Many of the improvements made to the initial cochlear implant stemmed from research which provided an in-depth understanding of how the inner ear's shape affects sound processing. One particularly important achievement was the demonstration that external sound is transduced into a traveling wave within the cochlea (Békésy 1928; Olson et al. 2012). The interface between the electronic stimulator and auditory receptors was also better defined to allow for optimal excitation (Davis 1968; Kiang and Moxon 1972). Another breakthrough came when researchers discovered that hair cells within the cochlea respond to unique frequencies, and that their corresponding cochlear nerves encoded those frequencies (Evans 1975). Current devices capitalize on this frequency specificity by splitting audio signals into their frequency components and then feeding these individual frequency components to their corresponding sections of the cochlear nerve. A six-channel electrode array served as the first multichannel implant to successfully transmit multiple frequency components to multiple nerve sites (Simmons et al. 1965). The basic design principles of these early devices remain the mainstay of modern cochlear implants.

8.3.2 Competition Within the Commercial Market Improves the Cochlear Implant

Once the performance of the cochlear implant had been proven in an academic setting, the device soon began to attract the attention of commercial investors, with the first patent for a multi-electrode cochlear implant submitted in 1977 (Chourard 1977). Production of the patented device was entrusted to the French company Bertin. The fact that this company held the patent until 1999 influenced the development of the cochlear implant by forcing competitors to try alternative designs.

One example of such an idea was using only specific, high-frequency bands, which were known to convey acoustic information important for speech processing. These innovative ideas led competitors to ultimately surpass Bertin, leading the company to abandon the field.

Around this time, the company Cochlear Limited entered the scene, producing a multi-electrode cochlear implant (Clark et al. 1979). This implant—FDA approved in 1984—was the first successful, commercialized, multichannel cochlear implant. Concurrent research led to the development of the first microelectronic, multichannel cochlear implant (Hochmair et al. 1979) which lead to the formation of another cochlear neuroprosthetics company, Med-EL, in 1982. In 1993, an additional production company, Advanced Bionics, joined the competition to create the perfect auditory neuroprosthesis.

The market's competition generated a large push for increased cochlear implant performance. At this time, it was thought that improving the electrode array interface offered the best hope for improving signal clarity and transmission. The first devices used a single conduit implanted into the cochlea with multiple electrode channels located along its length. This system was championed by companies like Cochlear Limited and was shown to allow for speech discrimination by a previously deaf individual (Michelson and Schindler 1981). However, it was also shown that multiple wire arrays inserted into the scala tympani of the cochlea offered higher performance by offering more channels and more options for the spatial placement of those channels (Clark and Tong 1982). This led all three companies to focus on increasing the amount of channels, postulating that more channels would allow for a higher-fidelity encoding of audio into neural signals.

However, researchers quickly found that further increasing the number of channels led to decreasing returns. This is due to the fact that the electrode array is not in direct contact with the cochlear nerve, but is separated from the nerve by the boney, medial wall of the cochlea. This small fluid filled space between the electrodes and the cochlear nerve causes the electrode's current to spread. An increased density of electrodes corresponds with a decreased distance between neighboring electrodes, and at a certain density current spread will cause interference between the signals of these electrodes. Present research looks to overcome this issue by focusing on the design of new electrodes and implantation surgeries, which would allow for the insertion of the array directly into the nerve trunk in the modiolus of the cochlea (Middlebrooks and Snyder 2008). If successful, these arrays could make it possible for more electrodes to yield higher spectral and temporal resolution, without signal corruption due to current leak (Middlebrooks and Snyder 2010). Another attempt, referred to as current field focusing, seeks to reduce the effects of current spread with current fields that sum spatially in a predefined, beneficial manner. Therefore, instead of focusing on the current emitted directly from the electrode, and allowing the overlapping current regions to be sources of noise, overlapping current fields are used to create a three-dimensional electric field, which correctly targets sites along the cochlear nerve (Srinivasan et al. 2010).

Beyond the interfacing electrode array, other aspects of cochlear implants have also been improved. In particular, the shift from using an analog audio processing

system to a discrete digital one has allowed for devices to present far more complex patterns to their electrodes. Instead of presenting continuous analog waveforms simultaneously to all electrodes, devices can employ a discrete interleaved sampling strategy, which presents brief pulses to each electrode in non-overlapping sequences (Wilson et al. 1991). Using this advanced audio processing, it was found that by extracting temporal envelopes of speech information from a limited number of broad frequency bands, higher performance could be achieved. This is because these envelopes can be designed to modulate noises of the same bandwidths, thus preserving the temporal envelope cues in each band. These band-limited temporal envelopes can then be non-simultaneously delivered to the electrodes (Shannon et al. 1995; Galvin et al. 2015).

Although cochlear implant performance may seem nearly optimal—especially as compared to other sensory neuroprostheses—there are still areas of the design that can be improved upon. For example, cochlear implants still perform poorly when faced with "the cocktail party problem," a problem describing any auditory situation analogous to that of an individual that must distinguish the voice of their conversation partner from the plethora of voices at a cocktail party. To combat this issue, efficient techniques to bolster signal-to-noise ratio during times of high background noise are still highly sought after (Carroll et al. 2011). Another deficiency in cochlear neuroprostheses is their lack of tone perception when listening to music (McDermott 2004; Peng et al. 2004). Techniques such as bilateral implantation (van Hoesel et al. 1993; Laske et al. 2009) and the use of cochlear implants in combination with hearing aids for low-frequency amplification attempt to alleviate these issues (Francart and McDermott 2013).

8.3.3 Interfaces in the Cochlear Nucleus or Inferior Colliculus Deliver Audio Signals Directly to the Brain

Many separate research groups have taken steps toward developing auditory neuroprostheses that directly interface with the brain. This is, in part, because many individuals lack a functioning cochlear nerve, rendering a cochlear implant useless and necessitating an interface location further along the pathway. The next potential interface site along the auditory pathway is the cochlear nucleus, which exists within the dorsolateral side of the brainstem and receives direct input from the cochlear nerve. Since demonstration of this site as a successful interface (Edgerton et al. 1982), several multichannel systems implanted into patients' cochlear nuclei were developed and carried through clinical trials (Nevison et al. 2002). Stimulating electrodes within the cochlear nucleus are able to successfully transfer auditory information; however, this information is not well received and decoded by the cochlear nucleus, making it difficult for patients to comprehend speech without concurrent lip-reading (Otto et al. 2002). While, as before, this may be due to distortion from overlapping electrical fields, it is also likely that the neurons encoding

high frequencies, typical of normal conversation, are located below the surface of the brainstem and are therefore not easily accessible or well stimulated by the surface electrodes (Shannon et al. 1993).

In an attempt to reach these inaccessible neurons, an auditory, brainstem implant was designed which used surface electrodes in conjunction with electrodes that penetrate a couple millimeters into the cochlear nucleus. While this new electrode array improved some aspects of performance, overall speech understanding did not significantly increase (Otto et al. 2008). One confounding variable in the initial studies of these implants was that nearly all of the patients who qualified for clinical trials had lost their hearing from neurofibromatosis type II (NF2), a disease characterized by tumorigenesis along the auditory pathway between the inner ear and the brainstem. After restricting testing to patients without NF2, greater levels of speech comprehension than with a cochlear implant were found, as expected (Colletti et al. 2009). While this suggested that NF2 renders the cochlear nucleus a poor interface site, some studies have shown that improved surgical approach and procedure may allow for the cochlear nucleus implant to deliver better speech recognition in patients with NF2 (Behr et al. 2007).

Researchers are also working on additional, possible interface sites, such as the higher-level inferior colliculus within the auditory midbrain. An electrode array was successfully implanted into the midbrain of six patients, but unfortunately yielded unsatisfactory results in speech recognition (Lim et al. 2007). That said, these midbrain implants will continue to be developed and improved as they offer the only option for patients with damage to lower sites along the auditory pathway, such as the cochlear nucleus. More importantly, even small successes in restoration of speech recognition are still helpful as they provide sound awareness and discrimination to support lip-reading.

8.4 A Visual Neuroprosthesis

Worldwide approximately 285 million are visually impaired, worldwide, and another 40 million people are blind (Pascolini and Mariotti 2012). Early medical treatment centered on drugs which only slowed the onset of blindness, leaving no options for those who had already lost their vision. In light of this obvious need for an effective solution, researchers have become very interested in designing an implantable, visual neuroprosthesis that reproduces natural functionality. Approaches to the creation of such a device vary, but the underlying goal is the same: convey visual information about the user's surroundings in an intuitive manner. To accomplish this, the implanted visual neuroprosthesis must capture the incoming light, process it into a representative signal compatible with the neural region it interfaces with, and convey the signal to the targeted region through patterned electrical microstimulation.

Possible interface locations are limited by the status of the patient's visual system, as the location must be intact and healthy. Highly studied stimulation targets

include the retina, optic nerve, and visual cortex. Each of these locations encode the visual signal differently, necessitating uniquely encoded input signals, which leads to different locations performing better in different qualitative review tasks such as contrast, brightness, edge detection, and depth of vision. Device design is also dependent on the process of translating light into an electrical signal, which dictates the bandwidth and type of available information that will be processed and transmitted through the rest of the system.

8.4.1 Interfaces in the Visual Cortex Deliver Visual Signals Directly to the Brain

Shockingly, just like the auditory neuroprosthesis, the first iteration of a visual neuroprosthesis came as early as 1748, when it was shown that a voltage potential across the eyes of a blind patient caused him to perceive a flame passing in front of his eyes (Leroy 1755). Significant advancement would not come again until the 1920s when the capacity to induce visual percepts via electrical stimulation of the occipital cortex was formally shown (Culver 1929). Then, in 1968, the first successful implantation of an electronic stimulation device into the visual cortex took place when a pair of doctors connected an array of radio receivers to electrodes implanted in the occipital pole of the right hemisphere of a blind patient (Brindley and Lewin 1968). Certain radio signals were found to cause the patient to experience sensations of flashes of light, known as phosphenes. Even more promising was the amount of distinguishable phosphene patterns they could produce: the patient was able to resolve the difference between stimulation from electrodes placed only a couple millimeters apart from one another.

The effectiveness of this solution for patients who were blind for a long period of time was still unproven, and researchers worried that such patients' visual pathway may degenerate and become unresponsive to stimulus (Brindley et al. 1972). However, further studies showed that implanted electrodes allowed for successful production of phosphenes in individuals who were blind for many years (Dobelle et al. 1974). In 1978, a team of researchers implanted a square array of platinum electrodes on the surface of a patient's primary visual cortex. At the turn of the century, after two decades of monitoring this patient and tweaking their interface, the group published their research, unveiling the first visual neuroprosthesis capable of restoring vision by feeding a processed digital signal from a digital video camera into the visual cortex (Dobelle 2000).

The initial success of this device encouraged many other researchers to pursue the idea of a visual neuroprosthesis. At the same time, it also set an archetypical design for future devices. A CCD array, similar to those found in simple black and white cameras, was mounted to glasses and used to capture incoming light and convert it into a digital signal, which was sent to a small processing unit worn in a beltpack, which converted the image into its representative neural signal. The output from the processing unit was then sent to a microcontroller, which delivered stimu-

lation to electrodes in the visual cortex via a percutaneous pedestal. It was found that by delivering certain stimulation patterns, this system could produce phosphene-based images. Researchers also hypothesized that they could interface with other cortical locations in addition to the occipital lobes, allowing for greater information transfer and increased resolution (Dobelle 2000).

It is interesting to consider what these phosphene-based images may look like to a patient. Currently, it is though that they may look similar to simple, low-resolution images produced by the large light bulbs in older stadium scoreboards. Continued implantations of these visual neuroprosthesis were associated with high success rates and limited negative effects. After implantation, patients took only 10 days of training to become comfortable with the system and quickly progressed to routine, high performance on common eyesight tests, such as letter recognition and finger counting. The users were even able to achieve visual acuity scores of around 20/400 on standardized eye tests (Dobelle 2000). From these results, it was evident that visual neuroprostheses could dramatically improve quality of life and provide recipients with independence, including the ability to navigate alone (Dobelle 2000). Even more impressively, one of the implanted patients would go on to demonstrate that he could drive a car using only the visual data provided by the implant (Naumann 2012). In addition to spatial navigation tasks, it was found that the camera interface could be adapted to allow the user to watch television and control their computer.

Although Dobelle's project was kept secret, others were concurrently expanding research in this field. One group, in particular, had shown the feasibility of using ICMS to deliver high-resolution visual percepts by utilizing higher-density, penetrating MEAs with reduced power requirements (Schmidt et al. 1996). Using this concept, a rival visual neuroprosthesis was developed, which is now in clinical trials (Srivastava et al. 2009). This new system is very similar to Dobelle's but with several dramatic improvements (Lane et al. 2011). Instead of using flat, surface electrodes, a custom intracortical array of penetrating electrodes was created. The small footprint of this array permits for numerous arrays to be implanted into a patient's occipital lobe, allowing for as many as one thousand unique intracortical stimulation sites. It is hoped that this increase in spatial resolution of stimulation would allow for effective transmission of higher resolution images. To increase the feasibility of this approach, a wireless telemetry system was developed, which uses a subminiature, autonomous, wireless stimulator module to communicate with the electrode arrays and power them wirelessly (Rush and Troyk 2012). In addition to making multiple, autonomous arrays possible, this system will prove crucial in promoting the development of devices that employ intracortical stimulation techniques, whose early safety concerns limited their entrance on the market (Srivastava et al. 2009).

Although now facing competition from visual neuroprostheses that interface with the retina, cortical-based implants still offer many benefits. The devices have reduced power requirements, more predictable phosphene production with less flicker and blur (Brindley and Lewin 1968), and the capability of higher resolution with the increased room for electrodes available on the cortex (Nordhausen et al. 1996). Cortical implants also remain a necessity for those with extensive damage to both the retina and optic nerve, thereby preventing the use of a retinal implant.

8.4.2 *Interfacing with the Retina May Allow for Less Complex Encoding of the Visual Signal*

Retinal implants, which interface with the retina of the eye, cannot be considered a BMI in the strictest sense, as the retina is actually part of the central nervous system. However, the retina offers a promising interface site for visual neuroprosthesis for those with diseases solely affecting the eye's photoreceptor cells. For example, in the two million individuals, globally, that face blindness due to retinitis pigmentosa (Busskamp et al. 2012) and the 50 million that are blind due to age-related macular degeneration (Stanton and Wright 2014), it is still possible to directly interface with the retinal bipolar and ganglion cells. This interface location, at the beginning of the visual pathway, allows for minimal preprocessing of the signal by taking advantage of the visual system's own processing circuitry. This inclusion of significant, natural processing helps shape the neural response at the visual cortex into a more instinctively familiar pattern, while providing a less invasive option than direct interfacing with the visual cortex.

The Argus II retinal implant manufactured by Second Sight Medical Products (SSMP) became the first approved retinal implant on the European market, in 2011, and in the United States, in 2013. Its predecessor, the Argus I, had completed the first successful clinical trial of an active epiretinal implant (Humayun et al. 2003). The design of the Argus II used the same image capture and processing scheme as seen in previous visual neuroprostheses, differing only with its interface. In the Argus II, this interface consists of an extraocular electronic case, attached to the temporal region of the skull, which produces and delivers stimulation signals via a subcutaneous cable into an intraocular electrode array placed on the epiretinal surface. The array contains a square arrangement of 16 flat platinum electrodes, allowing for its placement on the epiretinal surface (Piyathaisere et al. 2003). Interestingly, the design also utilizes the vitreous as a sink for heat dissipation of the device (Piyathaisere et al. 2003). However, arrays placed in this location were found to have difficulty maintaining prolonged attachment (Majji et al. 1999) and necessitated increased image processing to mimic the output of ganglion cells (Becker et al. 1999). When creating the Argus II, an array with 60 electrodes was used to allow for higher resolution; after a clinical trial, the device gained FDA approval (Humayun et al. 2012). Today, more than 80 patients have been implanted with the Argus II and Second Sight is working on developing a future model, employing a 200-electrode array (Fernandes et al. 2012).

Though the first to gain approval, Second Sight is not the only company to produce retinal implant-based visual neuroprosthetic systems. Bionic Vision Australia (BVA) has also been developing two implants. However, instead of implanting the electrode array into the epiretinal space, their first system is designed to be implanted into the suprachoroidal space, between the sclera and choroid. BVA believes this space offers a safer location for implantation allowing the visual neuroprosthesis to work in tandem with preoperative residual vision, increasing acuity. The device is undergoing clinical trials using a 22-electrode array, while BVA works on upgrading

to a 98-electrode array (Ayton et al. 2014). The second system BVA is developing is a high-acuity epiretinal implant-based device that uses artificial diamond electrodes and casing for the implanted chip, replacing the standard platinum and silicon hardware (Hadjinicolaou et al. 2012). They believe this unique material could allow for over a 1000 electrodes in one array, while a model with 256 electrodes has already been developed (Smith et al. 2014).

It is thought that subretinal placement of an implant, between the photoreceptor layer and the retinal-pigment epithelium, may allow for normal processing by the middle and inner retinal layers. The subretinal space may also provide a more stable location for array fixation, allowing for longer-lasting functionality (Chow et al. 2004). While proximity to the retina is advantageous for many reasons, it provides added obstacles such as limited implant space (Volker et al. 2004) and increased likelihood of thermal injury to the retina. The use of a photodiode array, instead of a traditional MEA, is another reason some visual neuroprostheses utilize early stage interface locations along the visual pathway. A photodiode array takes the entire system, including the camera and imaging processing and places it within the implantable chip. Light enters the eye and is absorbed by the outer-facing photodiodes on the array. These photodiodes are then able to convert this light into an electrical current, which is sent through microelectrodes to stimulate the ganglion cells. A visual neuroprosthesis company, Optobionics, developed and successfully implanted a model with 5000 micro-photodiodes, becoming the first company to develop a subretinal implant evaluated in clinical trials (Chow et al. 2004). The initial study implanted the devices into six patients suffering from retinitis pigmentosa. After implantation, all of the subjects reported improved perception of contrast and motion detection, sharper resolution, and an increased visual field. However, current micro-photodiodes are unable to receive enough incident light from realistic environments to generate adequate currents for stimulation of the remaining retinal cells (Zrenner 2002). To counter this shortcoming, several other groups have developed designs that incorporate external power sources to amplify the effects of incident light. Recently, Retina Implant AG developed a chip suitable for subretinal implantation, which housed 15,000 independent micro-photodiode-amplifier-electrode elements, which were powered via transdermal current induction. This implant underwent clinical testing in nine patients, with most patients reporting improvements in light perception, light localization, motion and angular speed detection, grating acuity measurement, and visual acuity. Unfortunately, trials were eventually put on hold due to repeated failure of the implant (Stingl et al. 2013).

Much of the development of visual neuroprostheses has centered on improving the hardware used to interface with the visual system. While this has yielded good results, one must also consider optimizing the code that controls these implants. With this thought in mind, researchers have been working on mimicking the natural processesing performed by the retina on incoming light. This is important as it is thought that incorporation of the retina's neural code is essential for creating stimulation patterns comprehensible by the visual cortex. Recent research has shown that an encoder—designed to convert incoming light into code—that mimics naturally

occurring neural signals can be incorporated into the design of visual neuroprostheses to improve performance. (Nirenberg and Pandarinath 2012).

8.5 A Brain-to-Brain Interface

These last few sections have showcased the amazing modularity of the brain, which allows it to interface with a wide variety of man-made devices ranging from robotic arms to sensor arrays. In this context, it is easy to imagine the brain as a computer, and these neuroprostheses as connected peripheral devices. Yet today's computers have moved beyond just computer-peripheral interfaces to a new type of interface: the worldwide web, a network enabling billions of computers to interface directly. It is thus easy to wonder about the possibility of creating a similar network using neural interfaces, a network of connected brains. Certainly, the technology exists to both read and write neural information; but, what would the actual network look like and what kind of data transfer could it actually support? Although anything close to a network of brains remains solidly within the realm of science fiction, within the last few years researchers have started to lay the groundwork for this concept by creating and testing its simplest configuration: a direct brain-to-brain interface.

8.5.1 Telepathically Linked Rats Are Able to Cooperatively Complete Tasks While in Separate Locations

Many variables were associated with creating the first brain-to-brain interface, including, what information to transmit. In the first proof-of-concept, brain-to-brain interface, researchers turned to a familiar neural interface location: the sensorimotor brain region in rats. To test the feasibility of this interface, two rats, identified as the encoder and decoder, were paired (Pais-Vieira et al. 2013). The encoder rat was placed in a cage and given a two-alternative-forced-choice task, such as that of pressing the correct lever when presented with two options. In one experiment, the encoder rat was tasked with choosing a lever based on an LED cue. While the encoder rat received this cue and performed the task, sensorimotor information was recorded from the rat's M1 via an MEA. This information was transmitted to the decoder rat, where ICMS was employed to write the same neural signal into its M1. The decoder rat was then given the same selection task, but with the ICMS signals replacing the LED cue. Amazingly, the transmission of information via the brain-to-brain interface allowed the decoder rat to select the correct lever. Finally, feedback was introduced so that the encoder rat received additional reward if the decoder rat performed well. This created a dyad, with each rat dependent on the other for high task performance. The resulting data showed that the rats coordinated, using their real-time, brain-to-brain interface to achieve the highest performance and corresponding, highest possible reward rate.

After successfully sending signals between motor regions of two different rats using this brain-to-brain interface, the researchers wondered if they could also transmit sensory information (Pais-Vieira et al. 2013). To test this, a second experiment, very similar to the first, was performed. In this experiment, the encoder rat was given a tactile clue to indicate which lever to press. The encoder rat received this cue by poking its nose into an aperture, gauging the width of the opening with its whiskers, and then choosing the correct lever based on that width. The tactile signal produced by the encoder rat's whiskers when measuring the aperture was recorded from the encoder rat's S1 and transmitted into the decoder rat's S1. Again, it was found that the decoder rat was able to use this transmitted sensory information to successfully determine which lever to press.

8.5.2 An Interspecies Brain-To-Brain Interface Allows a Human to Twitch a Rat's Tail

Proof-of-concept of a brain-to-brain interface generated excitement about porting the technology to human subjects. EEG was selected as a noninvasive method of reading neural information and was used in an attempted, interspecies, brain-to-brain interface between a human volunteer and anesthetized rat (Yoo et al. 2013). Steady-state visually evoked potentials were used to identify whether the human volunteer was looking at a flashing light bar. Researchers then linked these potentials to an MEA within the rat's motor cortex, causing the rat's tail to move for each time the human viewed the flashing bar. This interface achieved a transmission success rate of over 90 %, with an approximate, two-second delay in transmission.

8.5.3 A Brain-to-Brain Interface in Humans Can Be Used to Cooperatively Play Video Games or Send Morse Code

After solving the problem of reading neural signals nonivasively, the next challenge to completing a human brain-to-brain interface was to successfully and noninvasively write neural signals. Research suggested that transcranial magnetic stimulation (TMS) could be a viable option for this task. TMS uses a magnetic field generator to produce small electric currents within a targeted brain region, but is limited by poor temporal and spatial resolution. To test the feasibility of using TMS to create a brain-to-brain interface, an experiment was set up consisting of a human encoder wearing an EEG-based BMI and a human decoder wearing a TMS-based BMI (Rao et al. 2014). These two human subjects, connected via the brain-to-brain interface, were separated in different rooms and then tasked to play a computer game cooperatively. The goal of the game was to identify incoming planes as friend or enemy, and then fire a cannon only at enemy planes. The encoder was able to view the game screen and identify the planes, but had no ability to fire the cannon.

The decoder had a button for firing the cannon, but no knowledge of when to fire it. When the encoder identified an enemy plane and wished to fire a rocket, he/she would engage in right hand motor imagery. This motor imagery signal could be detected through the EEG, translated into a signal representing finger movement, and then transmitted into the receiving individual's motor cortex, causing his or her finger to twitch and press the button, therefore firing the cannon at a correct time. Although performance with the brain-to-brain interface was not perfect, it was still statistically significant, with transmission latency of only 650 ms.

All aforementioned brain-to-brain interfaces were designed to transfer motor and sensory information. Could more abstract information, like words, be transferred? To test this theory, a similar EEG-TMS-based brain-to-brain interface was used, detailed in Fig. 8.4. However, instead of monitoring the motor cortex, the EEG monitored the encoder's responses to motor imagery tasks and the TMS stimulated the decoder's occipital cortex, creating a phosphene (Grau et al. 2014). On screen, the encoder was shown a flashing, Morse code representation of a word. The brain-to-brain interface then transferred this same Morse code signal to the decoder by delivering a phosphene whenever the EEG registered the encoder seeing a flash of code. Using this set up, simple words such as "hola" and "ciao" where transmitted between individuals in different cities with an error rate of less than 20 %.

There is no question that the development of these brain-to-brain interfaces is an incredible achievement. While many work to transform today's technologies into complex brain networks, others have begun to postulate about the possible dangers

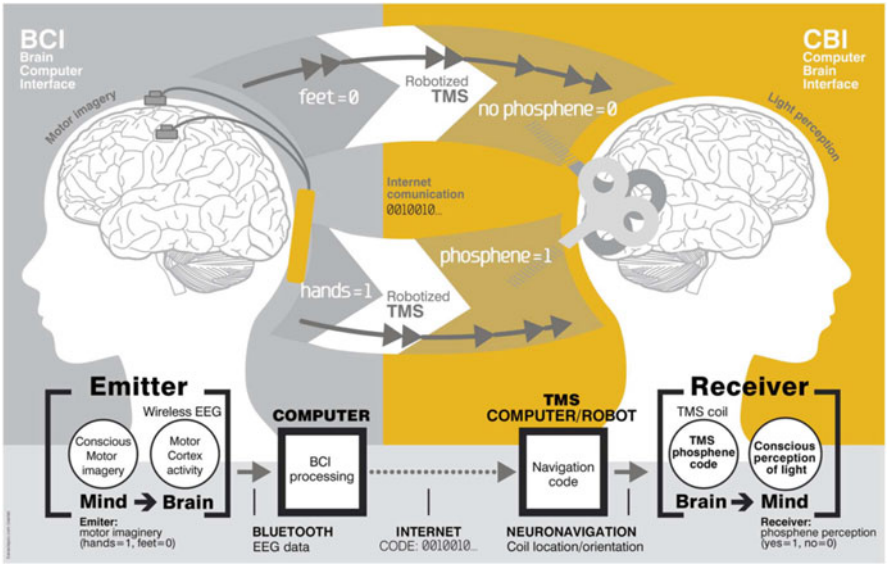

Fig. 8.4 A schematic overview shows how information from the motor cortex of one individual can be collected using EEG and transmitted to another individual using TMS. Using this interface and an internet connection, two individuals were able to communicate simple Morse code (Grau et al. 2014)

of using such technologies. In particular, there is a fear that individual minds could be assimilated into a group mind or hive mind (Trimper et al. 2014; Hildt 2015; Kyriazis 2015). Although some believe this could usher in an era of higher intelligence (Kyriazis 2015), others believe it could eliminate the aspect of individuality (Hildt 2015). Another issue raised is neural privacy: some are afraid that sensitive thoughts could be read and exposed to the public without the thinker's consent (Trimper et al. 2014). If and when noninvasive, high-throughput, neural interface technologies become commercially feasible, these concerns will undoubtedly need to be addressed. However, current neural interfaces pose no immediate ethical danger and continue to provide us with novel and beneficial information about the brain. For those still concerned that others may be reading their mind, it is widely known that a thin layer of tin foil does an excellent job of preventing an EEG signal from being acquired.

8.6 Closing Words

The BMIs which were discussed in this chapter serve as some of the pillars behind this growing field of medical devices. Beyond the few applications touched on in this chapter exist many others, which can be read about in Moxon and Foffani (2015). Within the next century, researchers hope to develop a neuroprosthetic arm, which allows a user to effortlessly drink a glass of water and feel the glass' temperature. In sensory neuroprosthetics, it is hoped that devices can improve so that instead of hearing electronic voices or seeing blurry contrast, users can indulge in symphonies and enjoy gazing upon works of art. On the biological side, these achievements will necessitate an increased understanding of the circuits of the brain: how they encode and process information, and how to best interface with them. On the technological side, it will require advances in computing power, wireless communication, electronic sensors, and material sciences.

Although this chapter serves only as a brief review of the field of BMIs, it is hoped that it piques the reader's interest. As a growing field, on the cusp of bringing many different products to clinical trial, the industry will need many promising future scientists and engineers to contribute to the research. Beyond the products emerging from academia and being brought to clinical trial, there is another exciting expansion in the field of BMIs occurring right now: for the first time, noninvasive BMI technologies are available on the open consumer market. Within the last couple years, brain interface technologies have gone from prohibitively expensive and technically challenging to inexpensive plug-and-plays. Now, the public is able to order their own EEG recording equipment and use it by simply plugging it into their personal computer. For example, the bioinformatics company, Emotiv, produces a range of EEG headsets, which it markets to the general public. The availability of this equipment, coupled with the current generation's love of technology and passion for hacking and improving electronic devices, will undoubtedly bring forth innovative ideas and exciting new uses for neural interfaces. Already, individuals

are using the equipment to play videos games with their minds and track their stress levels. It is with much anticipation that the field looks forward to seeing what other uses will be discovered.

References

Ayton, L.N., P.J. Blamey, R.H. Guymer, C.D. Luu, D.A. Nayagam, N.C. Sinclair, M.N. Shivdasani, J. Yeoh, M.F. McCombe, R.J. Briggs, N.L. Opie, J. Villalobos, P.N. Dimitrov, M. Varsamidis, M.A. Petoe, C.D. McCarthy, J.G. Walker, N. Barnes, A.N. Burkitt, C.E. Williams, R.K. Shepherd, P.J. Allen, and Bionic Vision Australia Research C. 2014. First-in-Human Trial of a Novel Suprachoroidal Retinal Prosthesis. *PLoS One* 9, e115239.

Bari, B.A., D.R. Ollerenshaw, D.C. Millard, Q. Wang, and G.B. Stanley. 2013. Behavioral and Electrophysiological Effects of Cortical Microstimulation Parameters. *PLoS One* 8, e82170.

Becker, M., R. Eckmiller, and R. Hunerman. 1999. Psychophysical Test of Tunable Retina Encoder for Retinal Implants. *IEEE Transactions on Neural Networks* 1: 192–195.

Béḱésy G. 1928. Zur Theorie des Hörens; die Schwingungsform der Basilarmembran. *Phys Zeits*, 29:793–810.

Behr, R., J. Muller, W. Shehata-Dieler, H.P. Schlake, J. Helms, K. Roosen, N. Klug, B. Holper, and A. Lorens. 2007. The High Rate CIS Auditory Brainstem Implant for Restoration of Hearing in NF-2 Patients. *Skull Base* 17: 91–107.

Bensmaia, S.J., and L.E. Miller. 2014. Restoring Sensorimotor Function Through Intracortical Interfaces: Progress and Looming Challenges. *Nature Reviews Neuroscience* 15: 313–325.

Brindley, G.S., P.E. Donaldson, M.A. Falconer, and D.N. Rushton. 1972. The Extent of the Region of Occipital Cortex that When Stimulated Gives Phosphenes Fixed in the Visual Field. *The Journal of Physiology* 225: 57P–58P.

Brindley, G.S., and W.S. Lewin. 1968. The Sensations Produced by Electrical Stimulation of the Visual Cortex. *The Journal of Physiology* 196: 479–493.

Brochier, T., M.J. Boudreau, M. Pare, and A.M. Smith. 1999. The Effects of Muscimol Inactivation of Small Regions of Motor and Somatosensory Cortex on Independent Finger Movements and Force Control in the Precision Grip. *Experimental Brain Research* 128: 31–40.

Busskamp, V., S. Picaud, J.A. Sahel, and B. Roska. 2012. Optogenetic Therapy for Retinitis Pigmentosa. *Gene Therapy* 19: 169–175.

Carmena, J.M., M.A. Lebedev, R.E. Crist, J.E. O'Doherty, D.M. Santucci, D.F. Dimitrov, P.G. Patil, C.S. Henriquez, and M.A. Nicolelis. 2003. Learning to Control a Brain-Machine Interface for Reaching and Grasping by Primates. *PLoS Biology* 1, E42.

Carroll, J., S. Tiaden, and F.G. Zeng. 2011. Fundamental Frequency is Critical to Speech Perception in Noise in Combined Acoustic and Electric Hearing. *The Journal of the Acoustical Society of America* 130: 2054–2062.

Chapin, J.K. 2004. Using Multi-Neuron Population Recordings for Neural Prosthetics. *Nature Neuroscience* 7: 452–455.

Chapin, J.K., K.A. Moxon, R.S. Markowitz, and M.A. Nicolelis. 1999. Real-Time Control of a Robot Arm Using Simultaneously Recorded Neurons in the Motor Cortex. *Nature Neuroscience* 2: 664–670.

Chourard, C.H. 1977. French 77 07824; US 4 207 441.

Chow, A.Y., V.Y. Chow, K.H. Packo, J.S. Pollack, G.A. Peyman, and R. Schuchard. 2004. The Artificial Silicon Retina Microchip for the Treatment of Vision Loss from Retinitis Pigmentosa. *Archives of Ophthalmology* 122: 460–469.

Clark, G.M., B.C. Pyman, and Q.R. Bailey. 1979. The Surgery for Multiple-Electrode Cochlear Implantations. *The Journal of Laryngology & Otology* 93: 215–223.

Clark, G.M., and Y.C. Tong. 1982. A Multiple-Channel Cochlear Implant. A Summary of Results for Two Patients. *Archives of Otolaryngology* 108: 214–217.

Colletti, V., R. Shannon, M. Carner, S. Veronese, and L. Colletti. 2009. Outcomes in Nontumor Adults Fitted with the Auditory Brainstem Implant: 10 years' Experience. *Otology & Neurotology* 30: 614–618.

Culver, G.D. 1929. Painful Ear Nodule of Winkler and Foerster: Report of Cases. *California and Western Medicine* 31: 414–418.

Davis, H. 1968. Mechanisms of the Inner Ear. *The Annals of Otology, Rhinology, and Laryngology* 77: 644–655.

Djourno, A., and C. Eyries. 1957. Auditory Prosthesis by Means of a Distant Electrical Stimulation of the Sensory Nerve with the Use of an Indwelt Coiling. *Presse Med* 65: 1417.

Djourno, A., C. Eyries, and P. Vallancien. 1957. Preliminary Attempts of Electrical Excitation of the Auditory Nerve in Man, by Permanently Inserted Micro-Apparatus. *Bulletin Academy of National Medicine* 141: 481–483.

Dobelle, W.H. 2000. Artificial Vision for the Blind by Connecting a Television Camera to the Visual Cortex. *ASAIO Journal* 46: 3–9.

Dobelle, W.H., M.G. Mladejovsky, and J.P. Girvin. 1974. Artificial Vision for the Blind: Electrical Stimulation of Visual Cortex Offers Hope for a Functional Prosthesis. *Science* 183: 440–444.

Edgerton, B.J., W.F. House, and W. Hitselberger. 1982. Hearing by Cochlear Nucleus Stimulation in Humans. *Annals of Otology, Rhinology, Laryngology Supplement* 91: 117–124.

Ethier, C., E.R. Oby, M.J. Bauman, and L.E. Miller. 2012. Restoration of Grasp Following Paralysis Through Brain-Controlled Stimulation of Muscles. *Nature* 485: 368–371.

Evans, E.F. 1975. The Sharpening of Cochlear Frequency Selectivity in the Normal and Abnormal Cochlea. *Audiology* 14: 419–442.

Fernandes, R.A., B. Diniz, R. Ribeiro, and M. Humayun. 2012. Artificial Vision Through Neuronal Stimulation. *Neuroscience Letters* 519: 122–128.

Fitzsimmons, N.A., W. Drake, T.L. Hanson, M.A. Lebedev, and M.A. Nicolelis. 2007. Primate Reaching Cued by Multichannel Spatiotemporal Cortical Microstimulation. *The Journal of Neuroscience: The Official Journal of the Society for Neuroscience* 27: 5593–5602.

Francart, T., and H.J. McDermott. 2013. Psychophysics, Fitting, and Signal Processing for Combined Hearing Aid and Cochlear Implant Stimulation. *Ear and Hearing* 34: 685–700.

Fridman, G.Y., H.T. Blair, A.P. Blaisdell, and J.W. Judy. 2010. Perceived Intensity of Somatosensory Cortical Electrical Stimulation. *Experimental Brain Research* 203: 499–515.

Galvin 3rd, J.J., S. Oba, D. Baskent, and Q.J. Fu. 2015. Modulation Frequency Discrimination with Single and Multiple Channels in Cochlear Implant Users. *Hearing Research* 324: 7–18.

Ganguly, K., J.D. Wallis, and J.M. Carmena. 2011. Reversible Large–Scale Modification of Cortical Networks During Neuroprosthetic Control. *Nature Neuroscience* 14: 662–667.

Gisselson, L. 1950. Evidence Favouring a Possible Humoral Transmission in the Inner Ear. *Acta Otolaryngology* 38: 9–23.

Grau, C., R. Ginhoux, A. Riera, T.L. Nguyen, H. Chauvat, M. Berg, J.L. Amengual, A. Pascual-Leone, and G. Ruffini. 2014. Conscious Brain-to-Brain Communication in Humans Using Non-invasive Technologies. *PLoS One* 9, e105225.

Hadjinicolaou, A.E., R.T. Leung, D.J. Garrett, K. Ganesan, K. Fox, D.A. Nayagam, M.N. Shivdasani, H. Meffin, M.R. Ibbotson, S. Prawer, and B.J. O'Brien. 2012. Electrical Stimulation of Retinal Ganglion Cells with Diamond and the Development of an All Diamond Retinal Prosthesis. *Biomaterials* 33: 5812–5820.

Hellman, R.B., E. Chang, J. Tanner, S.I. Helms Tillery, and V.J. Santos. 2015. A Robot Hand Test bed Designed for Enhancing Embodiment and Functional Neurorehabilitation of Body Schema in Subjects with Upper Limb Impairment or Loss. *Frontiers in Human Neuroscience* 9: 26.

Hildt, E. 2015. What Will this Do to Me and My Brain? Ethical Issues in Brain-to-Brain Interfacing. *Frontiers in Systems Neuroscience* 9: 17.

Hochberg, L.R., D. Bacher, B. Jarosiewicz, N.Y. Masse, J.D. Simeral, J. Vogel, S. Haddadin, J. Liu, S.S. Cash, P. van der Smagt, and J.P. Donoghue. 2012. Reach and Grasp by People with Tetraplegia Using a Neurally Controlled Robotic Arm. *Nature* 485: 372–375.

Hochberg, L.R., M.D. Serruya, G.M. Friehs, J.A. Mukand, M. Saleh, A.H. Caplan, A. Branner, D. Chen, R.D. Penn, and J.P. Donoghue. 2006. Neuronal Ensemble Control of Prosthetic Devices by a Human with Tetraplegia. *Nature* 442: 164–171.

Hochmair, E.S., I.J. Hochmair-Desoyer, and K. Burian. 1979. Investigations Towards an Artificial Cochlea. *International Journal of Artificial Organs* 2: 255–261.

Horch, K., S. Meek, T.G. Taylor, and D.T. Hutchinson. 2011. Object Discrimination with an Artificial Hand Using Electrical Stimulation of Peripheral Tactile and Proprioceptive Pathways with Intrafascicular Electrodes. *IEEE Transactions on Neural Systems and Rehabilitation Engineering: A Publication of the IEEE Engineering in Medicine and Biology Society* 19: 483–489.

House, W.F., and F.D. Owens. 1973. Long-Term Results of Endolymphatic Subarachnoid Shunt Surgery in Meniere's Disease. *Journal of Laryngology and Otology* 87: 521–527.

Humayun, M.S., J.D. Dorn, L. da Cruz, G. Dagnelie, J.A. Sahel, P.E. Stanga, A.V. Cideciyan, J.L. Duncan, D. Eliott, E. Filley, A.C. Ho, A. Santos, A.B. Safran, A. Arditi, L.V. Del Priore, R.J. Greenberg, and I.I.S.G. Argus. 2012. Interim Results from the International Trial of Second Sight's Visual Prosthesis. *Ophthalmology* 119: 779–788.

Humayun, M.S., J.D. Weiland, G.Y. Fujii, R. Greenberg, R. Williamson, J. Little, B. Mech, V. Cimmarusti, G. Van Boemel, G. Dagnelie, and E. de Juan. 2003. Visual Perception in a Blind Subject with a Chronic Microelectronic Retinal Prosthesis. *Vision Research* 43: 2573–2581.

Ifft, P.J., S. Shokur, Z. Li, M.A. Lebedev, and M.A. Nicolelis. 2013. A Brain-Machine Interface Enables Bimanual Arm Movements in Monkeys. *Science Translational Medicine* 5: 210ra154.

Johnson, L.A., J.D. Wander, D. Sarma, D.K. Su, E.E. Fetz, and J.G. Ojemann. 2013. Direct Electrical Stimulation of the Somatosensory Cortex in Humans Using Electrocorticography Electrodes: A Qualitative and Quantitative Report. *Journal of Neural Engineering* 10: 036021.

Keith, M.W., P.H. Peckham, G.B. Thrope, K.C. Stroh, B. Smith, J.R. Buckett, K.L. Kilgore, and J.W. Jatich. 1989. Implantable Functional Neuromuscular Stimulation in the Tetraplegic Hand. *Journal of Hand Surgery* 14: 524–530.

Kiang, N.Y., and E.C. Moxon. 1972. Physiological Considerations in Artificial Stimulation of the Inner Ear. *The Annals of Otology, Rhinology, and Laryngology* 81: 714–730.

Kyriazis, M. 2015. Systems Neuroscience in Focus: From the Human Brain to the Global Brain? *Frontiers in Systems Neuroscience* 9: 7.

Lane, F.J., M.H. Huyck, and P. Troyk. 2011. Looking Ahead: Planning for the First Human Intracortical Visual Prosthesis by Using Pilot Data from Focus Groups of Potential Users. *Disability and Rehabilitation Assistive Technology* 6: 139–147.

Laske, R.D., D. Veraguth, N. Dillier, A. Binkert, D. Holzmann, and A.M. Huber. 2009. Subjective and Objective Results After Bilateral Cochlear Implantation in Adults. *Otology & Neurotology* 30: 313–318.

Lee, W., H. Kim, Y. Jung, I.U. Song, Y.A. Chung, and S.S. Yoo. 2015. Image-Guided Transcranial Focused Ultrasound Stimulates Human Primary Somatosensory Cortex. *Scientific Reports* 5: 8743.

Legon, W., T.F. Sato, A. Opitz, J. Mueller, A. Barbour, A. Williams, and W.J. Tyler. 2014. Transcranial Focused Ultrasound Modulates the Activity of Primary Somatosensory Cortex in Humans. *Nature Neuroscience* 17: 322–329.

Leroy, C. 1755. Où l'on rend compte de quelques tentatives que l'on a faites pour guérir plusieurs maladies par l'électricité. *History Academy Roy Sciences (Paris), Mémoires Math Phys* 60: 87–95.

Lim, S.N., S.T. Lee, Y.T. Tsai, I.A. Chen, P.H. Tu, J.L. Chen, H.W. Chang, Y.C. Su, and T. Wu. 2007. Electrical Stimulation of the Anterior Nucleus of the Thalamus for Intractable Epilepsy: A Long-Term Follow-Up Study. *Epilepsia* 48: 342–347.

London, B.M., L.R. Jordan, C.R. Jackson, and L.E. Miller. 2008. Electrical Stimulation of the Proprioceptive Cortex (Area 3a) Used to Instruct a Behaving Monkey. *IEEE Transactions on Neural Systems and Rehabilitation Engineering: A Publication of the IEEE Engineering in Medicine and Biology Society* 16: 32–36.

Majji, A.B., M.S. Humayun, J.D. Weiland, S. Suzuki, S.A. D'Anna, and E. de Juan Jr. 1999. Long-Term Histological and Electrophysiological Results of an Inactive Epiretinal Electrode Array Implantation in Dogs. *Investigative Ophthalmology & Visual Science* 40: 2073–2081.

Maynard, E.M., C.T. Nordhausen, and R.A. Normann. 1997. The Utah Intracortical Electrode Array: A Recording Structure for Potential Brain-Computer Interfaces. *Electroencephalography and Clinical Neurophysiology* 102: 228–239.

McDermott, H.J. 2004. Music Perception with Cochlear Implants: A Review. *Trends in Amplification* 8: 49–82.

Michelson, R.P., and R.A. Schindler. 1981. Multichannel Cochlear Implant. Preliminary Results in Man. *Laryngoscope* 91: 38–42.

Middlebrooks, J.C., and R.L. Snyder. 2008. Intraneural Stimulation for Auditory Prosthesis: Modiolar Trunk and Intracranial Stimulation Sites. *Hearing Research* 242: 52–63.

Middlebrooks, J.C., and R.L. Snyder. 2010. Selective Electrical Stimulation of the Auditory Nerve Activates a Pathway Specialized for High Temporal Acuity. *The Journal of Neuroscience: The Official Journal of the Society for Neuroscience* 30: 1937–1946.

Monzee, J., Y. Lamarre, and A.M. Smith. 2003. The Effects of Digital Anesthesia on Force Control Using a Precision Grip. *Journal of Neurophysiology* 89: 672–683.

Moritz, C.T., S.I. Perlmutter, and E.E. Fetz. 2008. Direct Control of Paralysed Muscles by Cortical Neurons. *Nature* 456: 639–642.

Moxon Karen, A., and G. Foffani. 2015. Brain-Machine Interfaces Beyond Neuroprosthetics. *Neuron* 86: 55–67.

Musallam, S., B.D. Corneil, B. Greger, H. Scherberger, and R.A. Andersen. 2004. Cognitive Control Signals for Neural Prosthetics. *Science* 305: 258–262.

Naumann, J. 2012. *Search for Paradise: A Patient's Account of the Artificial Vision Experiment*. Bloomington, IN: Xlibris.

Nevison, B., R. Laszig, W.P. Sollmann, T. Lenarz, O. Sterkers, R. Ramsden, B. Fraysse, M. Manrique, H. Rask-Andersen, E. Garcia-Ibanez, V. Colletti, and E. von Wallenberg. 2002. Results from a European Clinical Investigation of the Nucleus Multichannel Auditory Brainstem Implant. *Ear and Hearing* 23: 170–183.

Nirenberg, S., and C. Pandarinath. 2012. Retinal Prosthetic Strategy with the Capacity to Restore Normal Vision. *Proceedings of the National Academy of Sciences of the United States of America* 109: 15012–15017.

Nordhausen, C.T., E.M. Maynard, and R.A. Normann. 1996. Single Unit Recording Capabilities of a 100 Microelectrode Array. *Brain Research* 726: 129–140.

O'Connor, D.H., S.A. Hires, Z.V. Guo, N. Li, J. Yu, Q.Q. Sun, D. Huber, and K. Svoboda. 2013. Neural Coding During Active Somatosensation Revealed Using Illusory Touch. *Nature Neuroscience* 16: 958–965.

O'Doherty, J.E., M.A. Lebedev, T.L. Hanson, N.A. Fitzsimmons, and M.A. Nicolelis. 2009. A Brain-Machine Interface Instructed by Direct Intracortical Microstimulation. *Frontiers in Integrative Neuroscience* 3: 20.

O'Doherty, J.E., M.A. Lebedev, P.J. Ifft, K.Z. Zhuang, S. Shokur, H. Bleuler, and M.A. Nicolelis. 2011. Active Tactile Exploration Using a Brain-Machine-Brain Interface. *Nature* 479: 228–231.

Olson, E.S., H. Duifhuis, and C.R. Steele. 2012. Von Bekesy and Cochlear Mechanics. *Hearing Research* 293: 31–43.

Olusanya, B.O., K.J. Neumann, and J.E. Saunders. 2014. The Global Burden of Disabling Hearing Impairment: A Call to Action. *Bulletin of the World Health Organization* 92: 367–373.

Otto, S.R., D.E. Brackmann, W.E. Hitselberger, R.V. Shannon, and J. Kuchta. 2002. Multichannel Auditory Brainstem Implant: Update on Performance in 61 Patients. *Journal of Neurosurgery* 96: 1063–1071.

Otto, S.R., R.V. Shannon, E.P. Wilkinson, W.E. Hitselberger, D.B. McCreery, J.K. Moore, and D.E. Brackmann. 2008. Audiologic Outcomes with the Penetrating Electrode Auditory Brainstem Implant. *Otology & Neurotology* 29: 1147–1154.

Pais-Vieira, M., M. Lebedev, C. Kunicki, J. Wang, and M.A.L. Nicolelis. 2013. A Brain-to-Brain Interface for Real-Time Sharing of Sensorimotor Information. *Scientific Reports* 3: 1319.

Pascolini, D., and S.P. Mariotti. 2012. Global Estimates of Visual Impairment: 2010. *British Journal of Ophthalmology* 96: 614–618.

Penfield, B. 1937. Somatic Motor and Sensory Representation in the Cerebral Cortex of Man as Studied by Electrical Stimulation. *Brain: A Journal of Neurology* 60: 389–443.

Peng, S.C., J.B. Tomblin, H. Cheung, Y.S. Lin, and L.S. Wang. 2004. Perception and Production of Mandarin Tones in Prelingually Deaf Children with Cochlear Implants. *Ear and Hearing* 25: 251–264.

Piyathaisere, D.V., E. Margalit, S.J. Chen, J.S. Shyu, S.A. D'Anna, J.D. Weiland, R.R. Grebe, L. Grebe, G. Fujii, S.Y. Kim, R.J. Greenberg, E. De Juan Jr., and M.S. Humayun. 2003. Heat Effects on the Retina. *Ophthalmic Surgery, Lasers & Imaging* 34: 114–120.

Rao, R.P.N., A. Stocco, M. Bryan, D. Sarma, T.M. Youngquist, J. Wu, and C.S. Prat. 2014. A Direct Brain-to-Brain Interface in Humans. *PLoS One* 9, e111332.

Rasmussen, T., and W. Penfield. 1947. The Human Sensorimotor Cortex as Studied by Electrical Stimulation. *Federation Proceedings* 6: 184.

Romo, R., A. Hernandez, A. Zainos, and E. Salinas. 1998. Somatosensory Discrimination Based on Cortical Microstimulation. *Nature* 392: 387–390.

Rouse, A.G., J.J. Williams, J.J. Wheeler, and D.W. Moran. 2013. Cortical Adaptation to a Chronic Micro-Electrocorticographic Brain Computer Interface. *The Journal of Neuroscience* 33: 1326–1330.

Rush, A.D., and P.R. Troyk. 2012. A Power and Data Link for a Wireless-Implanted Neural Recording System. *IEEE Transactions on Bio-Medical Engineering* 59: 3255–3262.

Sainburg, R.L., M.F. Ghilardi, H. Poizner, and C. Ghez. 1995. Control of Limb Dynamics in Normal Subjects and Patients Without Proprioception. *Journal of Neurophysiology* 73: 820–835.

Santhanam, G., S.I. Ryu, B.M. Yu, A. Afshar, and K.V. Shenoy. 2006. A High-Performance Brain-Computer Interface. *Nature* 442: 195–198.

Schmidt, E.M., M.J. Bak, F.T. Hambrecht, C.V. Kufta, D.K. O'Rourke, and P. Vallabhanath. 1996. Feasibility of a Visual Prosthesis for the Blind Based on Intracortical Microstimulation of the Visual Cortex. *Brain: A Journal of Neurology* 119(Pt 2): 507–522.

Serruya, M.D., N.G. Hatsopoulos, L. Paninski, M.R. Fellows, and J.P. Donoghue. 2002. Instant Neural Control of a Movement Signal. *Nature* 416: 141–142.

Shannon, R.V., J. Fayad, J. Moore, W.W. Lo, S. Otto, R.A. Nelson, and M. O'Leary. 1993. Auditory Brainstem Implant: II. Postsurgical Issues and Performance. *Otolaryngology—Head and Neck Surgery* 108: 634–642.

Shannon, R.V., F.G. Zeng, V. Kamath, J. Wygonski, and M. Ekelid. 1995. Speech Recognition with Primarily Temporal Cues. *Science* 270: 303–304.

Shenoy, K.V., and J.M. Carmena. 2014. Combining Decoder Design and Neural Adaptation in Brain-Machine Interfaces. *Neuron* 84: 665–680.

Shenoy, K.V., D. Meeker, S. Cao, S.A. Kureshi, B. Pesaran, C.A. Buneo, A.P. Batista, P.P. Mitra, J.W. Burdick, and R.A. Andersen. 2003. Neural Prosthetic Control Signals from Plan Activity. *Neuroreport* 14: 591–596.

Simeral, J.D., S.P. Kim, M.J. Black, J.P. Donoghue, and L.R. Hochberg. 2011. Neural Control of Cursor Trajectory and Click by a Human with Tetraplegia 1000 Days After Implant of an Intracortical Microelectrode Array. *Journal of Neural Engineering* 8: 025027.

Simmons, F.B., J.M. Epley, R.C. Lummis, N. Guttman, L.S. Frishkopf, L.D. Harmon, and E. Zwicker. 1965. Auditory Nerve: Electrical Stimulation in Man. *Science* 148: 104–106.

Smith, L.H., T.A. Kuiken, and L.J. Hargrove. 2014. Real-Time Simultaneous and Proportional Myoelectric Control Using Intramuscular EMG. *Journal of Neural Engineering* 11: 066013.

Srinivasan, A.G., D.M. Landsberger, and R.V. Shannon. 2010. Current Focusing Sharpens Local Peaks of Excitation in Cochlear Implant Stimulation. *Hearing Research* 270: 89–100.

Srivastava, N.R., P.R. Troyk, and G. Dagnelie. 2009. Detection, Eye-Hand Coordination and Virtual Mobility Performance in Simulated Vision for a Cortical Visual Prosthesis Device. *Journal of Neural Engineering* 6: 035008.

Stanton, C.M., and A.F. Wright. 2014. Inflammatory Biomarkers for AMD. *Advances in Experimental Medicine and Biology* 801: 251–257.

Stingl, K., K.U. Bartz-Schmidt, D. Besch, A. Braun, A. Bruckmann, F. Gekeler, U. Greppmaier, S. Hipp, G. Hortdorfer, C. Kernstock, A. Koitschev, A. Kusnyerik, H. Sachs, A. Schatz, K.T. Stingl, T. Peters, B. Wilhelm, and E. Zrenner. 2013. Artificial Vision with Wirelessly Powered Subretinal Electronic Implant Alpha-IMS. *Proceedings of Biological Science* 280: 20130077.

Stockton, N. 2015. Woman Controls a Fighter Jet Sim Using Only Her Mind. In: *WIRED*.

Su, Z., J.A. Fishel, T. Yamamoto, and G.E. Loeb. 2012. Use of Tactile Feedback to Control Exploratory Movements to Characterize Object Compliance. *Frontiers in Neurorobotics* 6: 7.

Tabot, G.A., J.F. Dammann, J.A. Berg, F.V. Tenore, J.L. Boback, R.J. Vogelstein, and S.J. Bensmaia. 2013. Restoring the Sense of Touch with a Prosthetic Hand Through a Brain Interface. *Proceedings of the National Academy of Sciences of the United States of America* 110: 18279–18284.

Talwar, S.K., S. Xu, E.S. Hawley, S.A. Weiss, K.A. Moxon, and J.K. Chapin. 2002. Rat Navigation Guided by Remote Control. *Nature* 417: 37–38.

Taylor, D.M., S.I. Tillery, and A.B. Schwartz. 2002. Direct Cortical Control of 3D Neuroprosthetic Devices. *Science* 296: 1829–1832.

The Reeve Foundation. 2009. One Degree of Separation: Paralysis and Spinal Cord Injury in the United States. Christopher & Dana Reeve Foundation.

Trimper, J.B., P.R. Wolpe, and K.S. Rommelfanger. 2014. When "I" Becomes "We": Ethical Implications of Emerging Brain-to-Brain Interfacing Technologies. *Frontiers in Neuroengineering* 7: 4.

van Hoesel, R.J., Y.C. Tong, R.D. Hollow, and G.M. Clark. 1993. Psychophysical and Speech Perception Studies: A Case Report on a Binaural Cochlear Implant Subject. *Journal of the Acoustical Society of America* 94: 3178–3189.

Velliste, M., S. Perel, M.C. Spalding, A.S. Whitford, and A.B. Schwartz. 2008. Cortical Control of a Prosthetic Arm for Self-Feeding. *Nature* 453: 1098–1101.

Venkatraman, S., and J.M. Carmena. 2011. Active Sensing of Target Location Encoded by Cortical Microstimulation. *IEEE Transactions on Neural Systems and Rehabilitation Engineering: A Publication of the IEEE Engineering in Medicine and Biology Society* 19: 317–324.

Volker, M., K. Shinoda, H. Sachs, H. Gmeiner, T. Schwarz, K. Kohler, W. Inhoffen, K.U. Bartz-Schmidt, E. Zrenner, and F. Gekeler. 2004. In Vivo Assessment of Subretinally Implanted Microphotodiode Arrays in Cats by Optical Coherence Tomography and Fluorescein Angiography. *Graefe's Archive for Clinical and Experimental Ophthalmology=Albrecht von Graefes Archiv fur klinische und experimentelle Ophthalmologie* 242: 792–799.

Wessberg, J., C.R. Stambaugh, J.D. Kralik, P.D. Beck, M. Laubach, J.K. Chapin, J. Kim, S.J. Biggs, M.A. Srinivasan, and M.A.L. Nicolelis. 2000. Real-Time Prediction of Hand Trajectory by Ensembles of Cortical Neurons in Primates. *Nature* 408: 361–365.

Wever, E.G., and C. Bray. 1930. The Nature of Acoustic Response: The Relation Between Sound Frequency and Frequency of Impulse in the Auditory Nerve. *Journal of Experimental Psychology* 13: 373–387.

Wilson, B. 1752. *Treatise on Electricity*, 202–208. London, England: Davis.

Wilson, B.S., C.C. Finley, D.T. Lawson, R.D. Wolford, D.K. Eddington, and W.M. Rabinowitz. 1991. Better Speech Recognition with Cochlear Implants. *Nature* 352: 236–238.

Yoo, S.-S., H. Kim, E. Filandrianos, S.J. Taghados, and S. Park. 2013. Non-Invasive Brain-to-Brain Interface (BBI): Establishing Functional Links Between Two Brains. *PLoS One* 8, e60410.

Zaaimi, B., R. Ruiz-Torres, S.A. Solla, and L.E. Miller. 2013. Multi-Electrode Stimulation in Somatosensory Cortex Increases Probability of Detection. *Journal of Neural Engineering* 10: 056013.

Ziegler-Graham, K., E.J. MacKenzie, P.L. Ephraim, T.G. Travison, and R. Brookmeyer. 2008. Estimating the Prevalence of Limb Loss in the United States: 2005 to 2050. *Archives of Physical Medicine and Rehabilitation* 89: 422–429.

Zrenner, E. 2002. Will Retinal Implants Restore Vision? *Science* 295: 1022–1025.

Chapter 9
In Vitro Modeling of Nervous System: Engineering of the Reflex Arc

Xiufang Guo, Frank Sommerhage, Christopher McAleer, Candace Martin, Christopher Long, Ying Wang, Navaneetha Santhanam, Alisha Colon, Carlota Oleaga Sancho, and James Hickman

Abbreviations

Ach	Acetyl choline
AchR	Acetyl choline receptor
ASC	Adult stem cells
ALS	Amyotrophic lateral sclerosis
Bio-MEMs	Biomedical or biological microelectromechanical systems
BBB	Blood–brain barrier
BMECs	Brain microvascular endothelial cells
CNS	Central nervous system
CSF	Cerebral spinal fluid
CMOS	Complementary-metal-oxide-semiconductor
CFD	Computational fluid dynamics
CMS	Congenital myasthenic syndromes
DETA	*N*-1(3-(trimethoxysilyl) propyl) diethylenetriamine
DRG	Dorsal root ganglia
ESCs	Embryonic stem cells
ECM	Extracellular matrix
FTD	Frontotemporal dementia
iPSC	Induced pluripotent stem cells
LTP	Long-term potentiation
MEA	Microelectrode array

X. Guo • F. Sommerhage • C. McAleer • C. Martin • C. Long
Y. Wang • N. Santhanam A. Colon • C.O. Sancho • J. Hickman (✉)
Hybrid Systems Lab, NanoScience Technology Center, University of Central Florida,
12424 Research Parkway, Suite 400, Orlando, FL 32826, USA
e-mail: jhickman@ucf.edu

L.G. Zhang, D.L. Kaplan (eds.), *Neural Engineering*,
DOI 10.1007/978-3-319-31433-4_9

MNs	Motoneurons
NMJ	Neuromuscular junction
NVU	Neurovascular unit
PDMS	Polydimethylsiloxane
PEG	Polyethylene glycol
PCB	Printed circuit board
SAM	Self-assembled monolayers
SKM	Skeletal muscles
SMA	Spinal muscular atrophy
TEER	Trans-endothelial electrical resistance

9.1 Introduction

9.1.1 Importance of In Vitro Engineering of Neural System

Neural models are invaluable for understanding the physiology and pathology of the nervous system as well as for developing therapeutic strategies targeting relevant injury and diseases. Numerous models have been developed and utilized for the nervous system. In general, they are categorized into four classes (Hopkins et al. 2015): in vivo, ex vivo, in vitro, and in silico. In vivo work typically involves the study of primates for cognitive and behavioral neuroscience (Goldman-Rakic 1988; Ridderinkhof et al. 2004), rodents for disease modeling and regenerative/pharmacology investigation (Vandamme 2014; Swanborg 1995) and other vertebrates and invertebrates for genetic dissection and disease modeling (Shimohama et al. 2003; Alexander et al. 2014; Markaki and Tavernarakis 2010; Pandey and Nichols 2011). Ex vivo models utilize slices of brain/spinal cord tissue which preserves most of the 2D complexity (Humpel 2015; Cho et al. 2007; Timme et al. 2014). In vitro models are cell-based systems which most commonly involve culturing cells on modified surfaces to reproduce the connections/interactions of neurons. This requires coculture of multiple components, either in physically connected configurations or separated in various devices (Millet and Gillette 2012a; Halldorsson et al. 2015; Zweifel et al. 2005). Increasingly, 3D models are being developed with the incorporation of advances in biomaterials (Choi et al. 2014; Kim et al. 2015; Kaneko and Sankai 2014). In silico models computationally generate predictions based on experimental data sets, for example predicting likely pharmacological effects of untested compounds in a specific physiological system (Focus on Computational and Systems Neuroscience 2011; Brette et al. 2007; Welberg 2009). This review will focus on in vitro modeling of a subset of components of the central nervous system (CNS) and peripheral nervous system (PNS) portions of the nervous system and its ultimate integration with other organ systems.

9.1.2 *Major Neural Systems that Have Been Engineered In Vitro*

Traditional in vitro models have revealed extensive information about many neural cell types. This information includes biological markers for each cell type; basic electrophysiological properties; cell attachment properties for adhesion and migration; axonal guidance mechanisms; spontaneous network formation; essential factors for viability, regeneration, and functionality; and essential molecules (soluble and insoluble) for synaptic targeting. Prevalent research topics in the field of in vitro neural modeling include neurobiology of nerve regeneration, repair, myelination, extracellular matrix (ECM) modification, and target identification (Marquardt and S.E. Sakiyama-Elbert 2013); modeling brain circuits for measuring signal transduction and processing (Timme et al. 2014; Spira and Hai 2013) (e.g., functional circuits for long-term potentiation (LTP) (Liu et al. 2012; Liu et al. 2013), reward system modeling (Russo and Nestler 2013), and spinal motor circuits (Goulding 2009; Catela et al. 2015)); and in vitro models of the blood–brain barrier (BBB) (Naik and Cucullo 2012) and drug delivery to the CNS (Pardridge 2002).

To meet the technological demands required for these in vitro nervous system models, the development of interdisciplinary technologies has been a major research focus. Some of the more notable technological areas that have been employed include brain-device interfaces and surface technologies (Aregueta-Robles et al. 2014; Helmke and Minerick 2006; El-Ali et al. 2006; Cooke et al. 2008; Edwards et al. 2013); biomaterials such as synthetic extracellular matrices (Maclean et al. 2016; Tibbitt and Anseth 2009; Theocharidis et al. 2014); cell sources, particularly from stem cells (Merkle Florian and K. Eggan 2013); microfluidic systems (Bhatia and Ingber 2014; Harink et al. 2013; Barata et al. 2015); and biomedical or biological microelectromechanical systems (Bio-MEMS). This chapter will focus on the in vitro modeling of the reflex arc.

9.2 Establishment of In Vitro Biologically Based Neural Models

9.2.1 *Cell Sources for Neural Engineering*

Primary cells: Originally, primary neurons and glia from animals were the major cell sources for developing in vitro models. Primary neurons from various species have been utilized, with the rodent as the most popular source for neural culture (Chen et al. 2013; Hollenbeck and Bamburg 2003). By integrating advances in genetics, primary neurons with various genetic modifications have become available to model the nervous system with genetic defects, providing a powerful tool for understanding basic biology, neurological diseases, and therapeutic investigation

(Dawson et al. 2010; McGoldrick et al. 2013; Philips and Rothstein 2015; Serikawa et al. 2015). The main disadvantages of using primary cultures are that procurement of these cells relies on the sacrifice of animals (Levy 2012), and the species gap between animals and humans presents a substantial hurdle for translating the findings to clinical usage (Sterneckert et al. 2014). While primary human neurons eliminate the species gap, it is next to impossible to consistently access primary human neurons. Although some studies tried to recover neural elements from postmortem human tissues, most of the cells recovered from cadavers were stem cells or proliferative cells with non-neuronal properties (Wolozin et al. 1992; Schwartz et al. 2003; Valente et al. 2014).

Cell lines: Since mature neurons are nonproliferative and thus cannot be expanded to make them widely available, multiple secondary cell lines have been derived from neuronal tumors and have become immortalized. For example, NG108-15, a hybrid of mouse neuroblastoma and rat glioma, and the human neuroblastoma cell line SH-SY5Y have been utilized in various in vitro neurological research investigations (Xie et al. 2010; Tojima et al. 2000). Cell lines have the advantage of being easy to grow in cell culture to generate unlimited cell numbers and have limited variability. The availability of cell lines also provides an opportunity to work with human-derived cells. The primary disadvantage of cell lines is that these cells often cannot fully reproduce the physiological or functional properties of their source cells. Therefore, these cell lines are often induced to display a more specific phenotype via additional manipulations, such as gene transfection or the addition of specific trophic factors in the culture (Doležal et al. 2001; Duhr et al. 2014; Dwane et al. 2013; Karra and Dahm 2010).

Stem cells: Due to the increasing demand for human-based in vitro systems in translational studies, primary cell cultures and transformed cell lines are far from sufficient. Fortunately, current stem cell research now provides a potentially unlimited source for generating specific and fully functional human cells. Advantages of stem cells are that they can self-renew, implying an infinite cell source, and that they are pluri/multipotent, implying the potential of generating various cell types with mature phenotypes as in vivo. Depending on the source, stem cells are categorized into adult stem cells (ASC), embryonic stem cells (ESCs), and induced pluripotent stem cells (iPSCs). ESCs are isolated from primordial germ cells (Shamblott et al. 1998) or the inner cell mass of blastocysts (Thomson et al. 1998). ASCs, tissue-specific stem cells present in developmental stages beyond the embryo, can only give rise to progenies restricted to the tissue of origin (Fortier 2005). IPSCs are generated by extracellular or intracellular induction as described below. Both ESCs and iPSCs are pluripotent, where they have the potential of differentiating into all somatic cell types as well as germ cells when injected into a blastocyst, and form mature progeny of all three embryonic germ layers in vitro. All of these stem cell types have been utilized for in vitro modeling and investigation of the nervous system (NS), especially for the human NS (Johnson et al. 2007; Sharp et al. 2010; Abranches et al. 2009; Selvaraj et al. 2012; Hunsberger et al. 2015; Guo et al. 2010a; Davis et al. 2012). As for limitations of stem cell utilization, ethical issues may be the biggest hurdle (Lo and Parham 2009). Any work performed with ESCs, especially the isolation of ESCs, must be

done under strict regulation (Klitzman 2010; Robertson 2001). ASCs are typically easier to work with, though availability depends on the tissue source. Working with iPSCs has even more flexibility since the source is usually skin, blood, or other easily accessible adult tissues.

iPSCs (Yamanaka 2012; Hu et al. 2010): The development and maturation of iPSC technology provides a novel source for NS research, especially for disease modeling. This technology theoretically can generate pluripotent stem cells similar to ESCs from *any* adult or terminally differentiated cell. The reprogramming is accomplished through nuclear transfer or employment of master transcription factors through virus-mediated gene transfer, with or without integration, or even nonviral reprogramming (Malik and M.S. Rao 2013). Despite some concerns about iPSCs, such as aberrations in their epigenetic landscape, gene expression array, and differentiation potential compared to ESCs and even induced genomic mutation load (Hu et al. 2010; Bilic and Belmonte 2012), they have been faithful in giving rise to many types of cells after differentiation. Examples include motoneurons (Guo et al. 2010a; Li et al. 2005), midbrain dopamine neurons (Kim 2002; Schulz et al. 2004; Perrier et al. 2004), cortical neurons (Nat 2011; Shi et al. 2012), sensory neurons (Pomp et al. 2005; Brokhman et al. 2008), oligodendrocytes (Davis et al. 2012; Nistor et al. 2005), and astrocytes (Davies et al. 2011; Emdad et al. 2012). Even the differentiation of blood–brain barrier (BBB) components such as pericytes, brain endothelial cells, and smooth muscle cells have been performed (Chaudhury et al. 2012; Dore-Duffy 2008; Dore-Duffy et al. 2006; Cheung and Sinha 2011).

To recapitulate human diseases in vitro, several stem cell technologies have been developed or are emerging. Currently, the most prosperous approach is through patient-derived iPSCs. Neurons differentiated from these iPSCs have recapitulated phenotypes of not only monogenic diseases but also late-onset polygenic diseases, such as Parkinson's disease (Sánchez-Danés et al. 2012), Alzheimer's disease (Israel et al. 2012), Amyotrophic Lateral Sclerosis (ALS) and Frontotemporal Dementia (FTD) (Lee and Huang 2015), Schizophrenia (Brennand et al. 2011), and autism spectrum disorder (Kim et al. 2014). ESCs are also being investigated for disease modeling but are not as promising as iPSCs, primarily due to their limited accessibility and ethical considerations (Sterneckert et al. 2014; Song et al. 2010; Halevy and Urbach 2014). Another technology that is triggering increased interest is genome editing, which can precisely change the genome sequence at a desired location (Sander and Joung 2014; Ran et al. 2013), allowing for the creation of desired mutations in iPSC lines or ESCs. The advantage of this approach is the generation of isogenic pairs of control and mutant cell lines, which eliminates genetic variations during mutant analysis. However, the major drawbacks are low efficiency and the difficulty of generating homozygous mutations. In general, stem cell technology holds great promise for generating nervous system models for pathological studies, therapeutic screening, and autologous transplantation (Sterneckert et al. 2014).

The media for nervous system cultures have also undergone dramatic progression toward more physiologically relevant conditions. Original systems nearly universally included serum (Walsh et al. 2005). However, serum introduces undesirable and unaccountable variability because it contains a large number of undefined biomolecules

such as growth factors, hormones, RNA, antibodies, and other biological molecules, which vary from source to source. To produce defined media, more and more serum-free media systems have been developed (Brewer 1995; Brewer et al. 2008; Guo et al. 2011). These defined systems have higher reproducibility and are easier to analyze, which is essential for their application in either drug or biological screenings. There are two major approaches to defined media development. The first is the specification of media for individual neurobiological systems in order to recapitulate the system's in vivo properties or functions. The other approach is the development of common media for the coculture of multiple cellular types to reproduce the in vivo complexity and to study interactions among the systems.

9.2.2 In Vitro Engineering of the Reflex Arc

9.2.2.1 Overview of the Reflex Arc

The reflex arc refers to a circular neural pathway that controls reflex actions, and can involve the autonomous (inner organs) or somatic (skeletal muscles) systems, and is the interface between the PNS and CNS systems. It consists of the sensation pathway that carries the signals from sensory organs to the spinal cord, the motor pathway that transmits commands from motoneurons (MNs) to effector organs, and the connection between sensory neurons and motoneurons in the spinal cord. Minimally, four types of cells are required to form a simplistic somatic reflex arc (monosynaptic): sensory neuron, motoneuron, and extrafusal and intrafusal skeletal muscle fibers. In some cases, interneurons are involved to modulate the communication of sensory neurons and motoneurons, which would form a polysynaptic reflex arc.

The reflex arc has been a popular model system for studying neural regulation and circuit modulation, due to its high accessibility, relative simplicity compared to other neural circuits, and clinical importance. The monosynaptic circuit's cellular components have a clearly defined identity and function and consequently, this circuit has also been the focus of numerous neural modeling and computation investigations (Kawato 1999; Guo et al. 2012). However, the most important reason for interest in the reflex arc is that many diseases and injuries are associated with this system. Compared to other circuits of the CNS, which are protected by the BBB, the peripheral components of the reflex arc are more susceptible to insults such as traumatic injury (Fernandez-Valle et al. 1995), infection, toxin exposure, metabolic abnormalities, immune system disorders, cancer, and chemotherapy (Sheikh and Amato 2010). Particularly, in the motoneuron disease amyotrophic lateral sclerosis (ALS), where about 90 % of the incidences are caused by nongenetic or unidentified reasons, no cure has been identified for this lethal condition (Swarup and Julien 2011). In addition, spinal cord dysfunction, predominantly from sports injuries and car accidents, mostly disables lower motor circuit function due to disruption of the reflex arc. Therefore, the reflex arc represents a significant system for studying neural function deficits and is a primary target for understanding disease and for investigating spinal cord repair treatments.

To develop in vitro reflex arc models, a number of studies have focused on the efferent pathway: innervation of skeletal muscles (SKM) by motoneurons (MN-SKM) and subsequent neuromuscular junction (NMJ) formation (Guo et al. 2011; Das et al. 2010; Guo et al. 2010b), due to this pathway's essential role in motor diseases, spinal cord injuries, and synapse modeling. Fewer studies have been conducted on the afferent sensory pathway (Rumsey et al. 2009; Rumsey et al. 2010) with very few on the sensory neuron to MN connection (Guo et al. 2012). Also of importance, myelination models have been developed by employing MNs or sensory neurons cocultured with Schwann cells or Oligodendrocytes (Rumsey et al. 2009; Davis et al. 2014).

9.2.2.2 In Vitro Models of the Neuromuscular Junction

The vertebrate Neuromuscular Junction (NMJ) is a highly specialized biochemical synapse whose function is to transmit action potentials at a 1:1 ratio from motoneurons to skeletal muscle, leading to muscle contractile activity (Tintignac et al. 2015). The NMJ is the primary route for the control and regulation of skeletal muscle activity by the central nervous system. The key components of a functional NMJ consists of (a) the presynaptic motor nerve terminal, (b) the 50–80 nm wide gap between the nerve ending and muscle known as the synaptic cleft, and (c) the post-synaptic muscle membrane directly under the motor axon terminal in the form of a motor end plate. Normally in vivo, this terminal is capped by three to five specialized glia known as terminal Schwann cells.

Dysfunction of the NMJ usually results in the weakening of muscle or paralysis, which can be induced by both traumatic injuries and many diseases. NMJ function is directly affected by genetic disorders such as congenital myasthenic syndromes (CMS) (Hughes et al. 2006) and Charcot-Marie-Tooth disease; autoimmune diseases such as myasthenia gravis and Lambert-Eaton myasthenic syndrome (Engel et al. 2003; Punga and Ruegg 2012); and by various forms of poisoning such as botulism. The loss of presynaptic input due to the death of motoneurons is another leading cause of neuromuscular diseases such as spinal muscular atrophy (SMA) and ALS (Tintignac et al. 2015). The importance of the NMJ as a therapeutic target has been highlighted by the finding that MNs' survival in ALS is not sufficient to slow down the degradation of NMJs and progression of the disease (Gould et al. 2006; Chipman et al. 2014). This suggests that NMJ function rather than MN viability is a more sensitive and crucial marker for ALS diagnosis and treatment than motoneuron viability. In vitro NMJ models are in high demand for addressing NMJ-related diseases/injuries, for early diagnosis, in therapeutic design and for drug screening (Guo et al. 2011).

The need for high-content screening with in vitro NMJs has long been recognized and addressed by systems involving Xenopus (Lu et al. 1996), chick (Fischbach 1972; Fischbach and Cohen 1973), mouse (Harper et al. 2004), rat (Daniels et al. 2000; Dutton et al. 1995), and human cells (Guo et al. 2011) as well as cross-species experiments with mouse MN and chick muscle (Soundararajan et al. 2007). However, all of these in vitro motoneuron-muscle coculture systems use serum containing media and a biological substrate (Fischbach 1972; Fischbach

and Cohen 1973; Daniels et al. 2000; Dutton et al. 1995; Frank and Fischbach 1979). As previously mentioned, serum introduces unknown variables and is not amenable for reproducible assays. Moreover, serum contains many factors which can confound the elucidation of a drug's effect on single cell analysis or on functional constructs. For example, a report suggested inhibition of full functional in vitro development of myelination by serum (Rumsey et al. 2009). Thus, a small number of serum-free NMJ systems have been developed in an attempt to eliminate the inherent variability present with serum (Walsh et al. 2005). NMJ formation in serum-free media has been demonstrated in rat (Das et al. 2010) and cross-species between human MN and rat muscle (Guo et al. 2010b) as well as in human (Guo et al. 2011; Guo et al. 2010b). In general, in vitro systems composed of animal-derived components have provided the scientific community with readily available models for understanding NMJ synaptogenesis and NMJ-related diseases. However, due to the species gap, there are frequent discrepancies when extrapolating the findings from animals to humans. This discrepancy is especially pronounced for drug discovery and toxicology that could lead to clinical applications.

Fortunately, dramatic advancements in stem cell biology in recent years provide a solution to the problem of translating results from animal models to human systems. Human MNs have been successfully differentiated in vitro from ESCs (Li et al. 2005; Li et al. 2008), neural progenitors (Guo et al. 2010a), and iPSCs (Dimos et al. 2008). In addition, human ESC-derived MNs have been investigated for their capability of innervating the murine muscle cell line, C2C12 cells, in a serum-containing system (Gajsek et al. 2008; Guettier-Sigrist et al. 2000; Kobayashi et al. 1987; Mars et al. 2003; Mars et al. 2001). MNs derived from human fetal spinal cord stem cells successfully formed functional NMJs with rat myotubes derived from embryonic skeletal muscles in a defined serum-free system (Guo et al. 2010b). Separately, human satellite cells, the ASCs isolated from muscle biopsies, have been used extensively for the generation of human muscle myocytes and for the development of in vitro NMJ models by combining the ACSs with rat spinal explants or dissociated MNs in serum-containing systems (Gajsek et al. 2008; Guettier-Sigrist et al. 2000; Kobayashi et al. 1987; Mars et al. 2003; Mars et al. 2001). A human-based functional in vitro NMJ system was first reported by the Hybrid Systems Laboratory, by the coculture of MNs derived from human spinal cord stem cells and skeletal muscle cells derived from human satellite cells. Functional NMJ formation was demonstrated by the blockage of muscle contraction by Curare, a blocker of acetylcholine receptors (Guo et al. 2011). The coculture of hiPSC-derived MNs and myotubes has recently been described by (Demestre et al. 2015), with potential NMJ formation demonstrated by immunocytochemistry (Demestre et al. 2015). In order to model the early NMJ phenotype of spinal muscular atrophy, patient-derived iPSCs were introduced to the coculture with C2C12s by (Yoshida et al. 2015).

The formation of NMJs in vitro has been typically characterized by two avenues: morphological characterization primarily via phase microscopy or immunocytochemistry (Fig. 9.1), and functional testing. For functional testing, several approaches have been utilized in demonstrating the activity of NMJs in vitro. The first is by applying blockers of acetylcholine receptors (AchRs), such as Curare and

α-Bungarotoxin, and demonstrating a resultant decrease in muscle contraction (Guo et al. 2011). The second is the induction of muscle contraction by exciting MNs with the neurotransmitter glutamate (Guo et al. 2010b; Umbach et al. 2012). However, a fundamental limitation of the mixed culture is the difficulty in identifying particular MN-SKM pairs and therefore the inability to analyze the strength of the synapse. Several studies successfully performed dual patch clamp electrophysiology of MN-SKM pairs in a coculture by dramatically reducing the MN density to the point that individual axons could be traced to identify MN-SKM pairs (Guo et al. 2010b; Umbach et al. 2012). The primary problem with this system is that only very few MN-SKM pairs can be analyzed in each culture and the efficiency is low. Recently, compartmentalized Bio-MEMs chambers have been utilized for in vitro NMJ systems so that the soma of MNs can be physically separated from the SKM, in effect modernized Campenot chambers. This physical separation gives more flexibility in enabling the excitation of MNs and the monitoring of subsequent SKM contraction (Park et al. 2013; Southam et al. 2013). The integration of other interdisciplinary technologies is currently advancing in vitro NMJ systems with increasing efficiency and content. This topic will be further investigated in Sect. 9.3.

9.2.2.3 In Vitro Modeling of Other Components of the Reflex Arc

Three other synaptic connections are important for the function of the intact reflex arc: (a) intrafusal muscle fiber—sensory neurons, (b) sensory neurons—motoneurons, and (c) γ-MNs—intrafusal muscle fibers. The majority of muscle tissue is composed of extrafusal fibers, the elongated and multinucleated cells that contract and relax in response to MN stimulation. Deep within the muscle tissue are muscle spindles that are responsible for the sensory portion of muscle function. Spindles are collagen-encapsulated clusters of intrafusal fibers, containing 1–2 nuclear bag fibers and 5–7 nuclear chain fibers in each spindle. Intrafusal muscle fibers are innervated by both afferent sensory nerve terminals and efferent γ-motor nerve terminals. Innervation by sensory nerve terminals is responsible for sending information from the muscle to the CNS concerning the muscle length (both static and rate of change) and muscle position. Innervation by γ-MNs is responsible for controlling the sensitivity of the muscle spindle. The combination of these two intrafusal fiber-related circuits keeps the CNS constantly informed concerning a muscle's contraction state as verification that a motion command from the CNS is being properly accomplished. The circuit of a sensory neuron—MN connection is responsible for transmitting the information on muscle state generated by the muscle spindle to MNs in the spinal cord. For example, in the case of the monosynaptic reflex arc, elongation of the muscle by stretching will first be detected by the muscle spindle, and will then be communicated to the CNS neurons in the spinal cord via afferent sensory nerves. Synapses onto α-MNs will cause the excitation of these MNs, which then triggers contraction of extrafusal muscle fibers, completing one cycle of excitation of the reflex arc. Meanwhile, sensory inputs synapse onto interneurons that regulate γ-MN activity such that the sensitivity of intrafusal muscle fibers is adjusted to accommodate the change of muscle length.

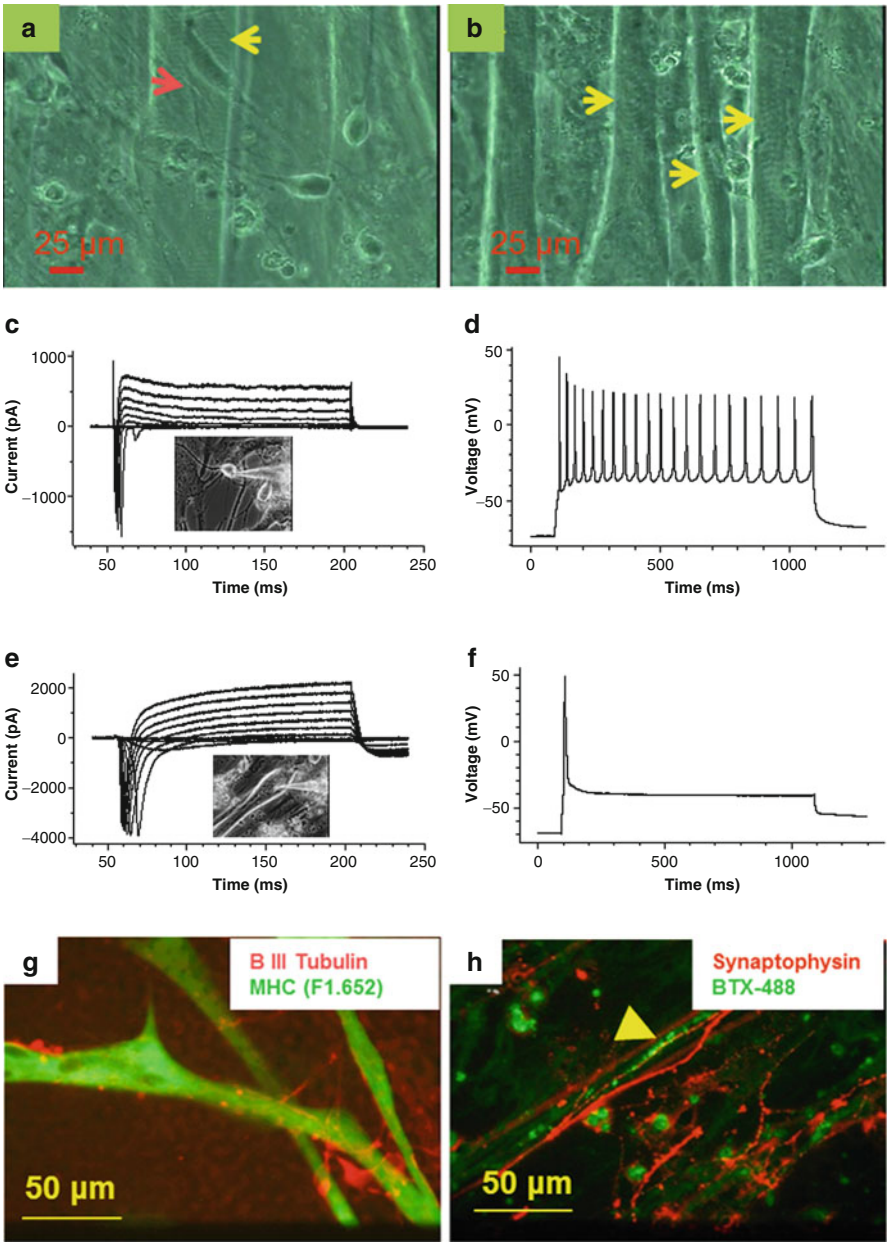

Fig. 9.1 A defined system that supports human-based NMJ formation. (**a**) and (**b**), Phase images demonstrate the mature morphology of generated myotubes and motoneurons. (**c**)–(**f**) Representative patch clamp recording traces from hMNs (**c**) and (**d**) and myotubes (**e**) and (**f**) in the coculture. (**c**) and (**e**) demonstrate sodium and potassium currents under voltage clamp. (**d**) and (**f**) demonstrate Action potential firing(s) under current clamp. (**g**) Co-staining of MHC and β III Tubulin revealed intensive connections between axons with myotubes in the coculture. (**h**) Potential synaptic sites were indicated by the co-localization of Synaptophysin and BTX (adapted from Guo et al. (2011))

In vitro modeling of these reflex arc circuits is not as extensive as for the NMJ segment, largely due to the fact that the malfunction of the sensory portion of the reflex arc is not as lethal or serious and thus has lower public visibility. A number of advancements in these parts of the circuit have been made recently with the in vitro reflex arc. Intrafusal muscle fibers have been induced in vitro from rat embryonic muscle cells (Rumsey et al. 2008), and the establishment of their connection with rat sensory neurons from dorsal root ganglia (DRG) in a defined in vitro system has been demonstrated (Rumsey et al. 2010). In vitro induction of intrafusal fibers from human myoblasts has also been reported, though by utilizing serum-containing system and with a focus on the molecular mechanism of signal transduction (Jacobson et al. 2004). Hickman's group has successfully differentiated functional proprioceptive sensory neurons from human neural progenitors (Guo et al. 2013). The differentiation of human intrafusal muscle fibers and their connection with human sensory neurons is currently under investigation in our laboratory. A serum-free culture system has been developed that supports the synaptic connection between rat DRG sensory neurons and rat α-motoneurons (Guo et al. 2012). Currently, there are no in vitro models of γ-MNs—intrafusal muscle fibers.

9.3 Interdisciplinary Technologies Utilized for Engineering of the Reflex Arc

9.3.1 Surface Modification for Directing Neural Circuit Formation

The earliest attempt to create systems to monitor NMJ function were developed by Campenot in the 1970s (Campenot 1977) and refined by Nelson and Fields and other researchers in the following decades (Wheeler and Brewer 2010; Kleinfeld et al. 1988; Corey et al. 1996; Wheeler et al. 1999; Fields et al. 1990). Several methods for surface modification have also been developed to control the neurite outgrowth of neurons so as to direct circuit formation between neurons, or between neurons and another cell types such as skeletal muscle. These methods include direct covalent attachment of cytophilic and cytophobic molecules to a surface, adsorptive modification of these molecules, and topographical patterning/microfluidic devices. The examples discussed here are a small sampling of the literature available on this topic.

9.3.1.1 Topographical Patterning/Microfluidic Devices

In vitro studies using compartmentalized "Campenot" systems have long been used to investigate axonal biology by separating neuronal cell bodies from their axons (Campenot 1977; Skaper 2012). The past decade has seen the development of microfluidic devices that efficiently allow spatial and temporal control of cellular microenvironments (Taylor et al. 2005; Millet and Gillette 2012b). The advantages

of compartmentalized systems when applied to the study of NMJs have recently been exploited by several research groups to model the fluidic isolation of motoneuron cell bodies from skeletal muscle (Park et al. 2013; Southam et al. 2013) and to reveal spatial aspects of GDNF function (Zahavi et al. 2015).

Topographical methods are typically used to physically guide neuronal axons in a particular direction. Shi et al. used PDMS microtunnels to isolate axons from the cell bodies, and then further used PDMS stamps to print proteins in specific patterns. Their results showed axons passing through the microtunnels and following specific protein patterns depending upon functionality (Shi et al. 2010). Claverol-Tinture et al. formed PDMS microchannels on planar microelectrode arrays and coated the channels with poly L-lysine prior to cell seeding (Claverol-Tinture et al. 2005). Finally, Millet and Gillette presented a review of current work concerned with microfluidic patterning and the study of neuronal microenvironments and development (Millet and Gillette 2012b).

9.3.1.2 Direct Chemical Modification of Surfaces

Hickman's group has made significant contributions to the field of surface patterning by utilizing self-assembled monolayers (SAM) of silane molecules that contain different functional groups (Stenger et al. 1993; Ravenscroft et al. 1998; Stenger et al. 1998; Hickman et al. 1994). One major type of SAM utilized to encourage cell attachment and growth is a monolayer of *N*-1(3-(trimethoxysilyl) propyl) diethylenetriamine (DETA). The DETA-modified surface supports neuronal growth as well as biological surfaces, if not better (Varghese et al. 2009; Das et al. 2003), and it has been shown to support the growth of both rat and human MNs (Das et al. 2007; Das et al. 2005). Surface patterning is achieved by coating the desired cell growth area with cytophilic functional groups such as DETA, interspersed with cytophobic functional groups in the area in which cells are undesired. Typically, two types of patterns have been employed to generate surface patterns for the development of neural circuits. One is the pairing of DETA with cytophobic polyethylene glycol (PEG)-functionalized silanes. Specifically, the PEG molecules are deposited as a blanket layer first and the desired pattern for cell attachment is ablated away by exposing the surface to deep UV laser radiation through a quartz mask (Stenger et al. 1992). The ablation makes the patterned area amenable to further silane modification, and the DETA-functional molecules are back-filled onto the ablated regions of the surface (Wilson et al. 2011). Another pairing for silane surface modification is DETA with highly fluorinated silanes, which work in much the same way as the DETA/PEG pair but where the fabrication protocol is reversed. In this pairing, the DETA is deposited first, the surface regions to prevent cell attachment are ablated, and the fluorinated silane is back-filled onto the surface (Ravenscroft et al. 1998; Stenger et al. 1998; Hickman et al. 1994). The demonstrated success of both methods indicates the usefulness of silane surface chemistry for creating patterned neuronal circuits and other groups have adopted this methodology (Liu et al. 2000). Examples of the application of this silane-based surface technology in neural

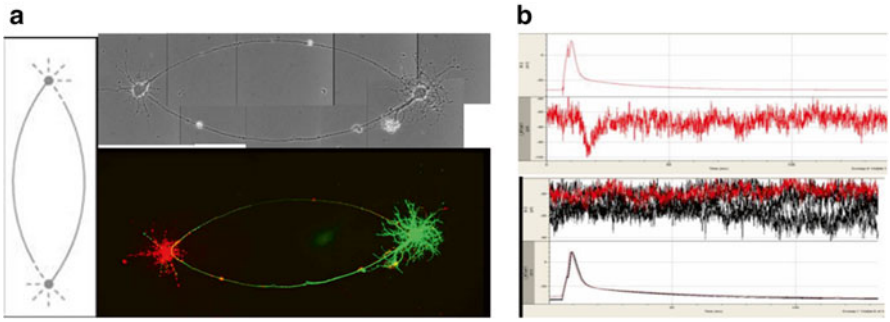

Fig. 9.2 Controlled growth of hippocampal neurons and functional synapse formation on a two-cell circuit pattern created by geometric surface manipulation with DETA/13F. (**a**) The design of the pattern and conformed distribution of embryonic hippocampal neurons on the pattern. (**b**) EPSCs were recorded from one of the neurons when stimulating the other neuron, but not vise versa, indicating a one-way functional synapse formation on the patterned surface (adapted from Molnar et al. (2007a))

engineering include two-cell circuit patterns of hippocampal neurons (Edwards et al. 2013; Molnar et al. 2007a) (Fig. 9.2) and feed-forward patterns for mimicking signal propagation in the nervous system (Natarajan et al. 2013) (Fig. 9.3). Surface engineering approaches to micropattern surfaces for cell culture are reviewed by Falconnet et al. (2006), Ito (1999), and Ni et al. (2009).

Patterning has also been achieved with the use of photoresist, functional polymers used to repel cell growth, and UV light (Wheeler and Brewer 2010; Kleinfeld et al. 1988; Corey et al. 1996). Wyart et al. coated a glass substrate with a fluorinated silane, applied photoresist, performed conventional photolithography, and ablated patterns using water plasma with a photoresist mask. Cells adhered to polylysine which was applied after the plasma ablation (Wyart et al. 2002). Leclair et al. used a photoresist to create fluorinated regions applied with plasma on glass coverslips, and mouse cortical neurons and C2C12 cells were cultured on the clean glass regions at the end of the modification process (Leclair et al. 2011). Matsuda et al. applied a hydrophilic polymer, *N*, *N*-dimethyl-acrylamide, to tissue culture dishes and used photoresist and UV irradiation to remove sections of the polymer. The clear regions were then coated with collagen and cells were cultured onto the collagen (Matsuda et al. 1992).

9.3.1.3 Adsorptive Modification of Surfaces

The method described in the preceding section involving the use of photoresist is often coupled with adsorptive modification of surfaces. Two of the previous examples included adsorption of proteins after the initial patterning (Wyart et al. 2002; Matsuda et al. 1992). The cytophobic region was chemisorbed while the cytophilic region was physadsorbed. Two other methods for adsorptive modification include

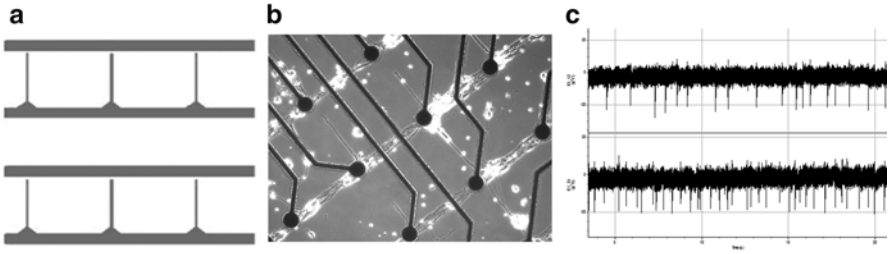

Fig. 9.3 Electrophysiological activity from patterned hippocampal neurons. (**a**) Pattern design, a line/gap topology was used to promote neuronal polarity in a feed-forward architecture between horizontal layers of soma interconnected by vertical segments. The mask consisted of four 50 μm wide lines that were oriented over every other row of electrodes on an MEA to provide a primary attachment point for neural soma. Each line contained eight vertical 5 μm wide narrow extensions that terminated 10 μm before the next layer in the series to guide neuronal polarity and produce directional connectivity proceeding from the bottom layer upward in this feed-forward architecture. (**b**) Phase contrast images of a patterned neuronal network on a Multichannel Systems microelectrode array (image is at 7 days in vitro, Electrode distance 200 μm) consisting of cellular interconnected layers. (**c**) Sample traces of neuronal firing recorded from the MEA electrodes demonstrated in (**b**) ((**a**) and (**b**) were adapted from Natarajan et al. (2013))

printing and stamping (Wheeler et al. 1999; Branch et al. 1998). In these methods, it is required that the transferred material, the ink, should stick to the culture surface but not the machinery used to transfer the ink.

Xu et al. used an HP inkjet printer and a cell suspension solution to print lines and circles onto a collagen gel "bio-paper" (Xu et al. 2006). The authors noted that the cell print exhibited "strong compliance" to the desired pattern. This particular example involves direct printing of cells onto a protein-coated surface to create the pattern. Additionally, the authors in previous work have also printed proteins such as collagen/poly D-lysine and laminin onto a cell-repulsive surface in order to pattern cells (Roth et al. 2004).

The process for creating a stamp involves several fabrication steps, including the production of molds. Vogt et al. used a photolithographically created mold to construct polydimethylsiloxane (PDMS) stamps that were inked with ECM proteins and applied to culture dishes. Cells were then grown on the transferred proteins in the pattern of the stamp (Vogt et al. 2005). Branch et al. formed polyimide layers onto glass slides and then reactive ion etched the stamp mold. The authors created PDMS stamps using this mold, functionalized the stamps with silanes, and coated the stamp with protein for patterning the substrate (Branch et al. 1998).

9.3.2 MEA System for Controlling/Monitoring Neuronal Activation

The field of Bio-MEMs (biomedical or biological microelectromechanical systems) is another fast-growing area that has already greatly impacted the development of in vitro models. One representative Bio-MEMs technology that has driven in vitro

biological neural cultures into high throughput territory is the microelectrode array (MEA). The first *miniature microelectrode array to monitor the bioelectric activity of cultured cells*' was reported by Thomas et al. (Thomas et al. 1972) and had 30 platinized gold electrodes of 7×7 μm^2 in a 2 by 15 array. The MEA system records the electric potential of cells cultured directly on top of the electrodes, which can be used to measure the electrical activity of the cells. Since then, a plethora of modifications and extensions have been devised to improve the recording and stimulation quality, the experimental throughput, and the production cost of microelectrode arrays (MEAs). MEA improvements are ongoing and include modern Bio-MEMS processes, new materials and geometries, intricate surface modifications, and alternative methods of fabrication. This section will provide a broad overview of the latest and most significant developments in MEA technology.

The most noticeable improvement in the field is the increase in spatial resolution. While the first reported MEA provided 30 electrodes, the latest research indicates up to 16,384 electrodes (128×128) in one device are possible (Hutzler et al. 2006; Berdondini et al. 2009; Frey et al. 2009). Thus, these high-resolution systems can collect a tremendous amount of data within seconds and the investigation of variables and parameters, such as information pathways in random neuronal networks or slices, can be a matter of analyzing (video) frames rather than individual traces (Ferrea et al. 2012). Currently, the data must be analyzed manually after recordings are completed, and real-time evaluation of this high-resolution system will require software that has yet to be developed.

On the other end of the spectrum, long-term investigations with fewer electrodes can be used to continuously stimulate neurons and record data, sometimes for months at a time, and occasionally directly from within an incubator (Esposti et al. 2009). There are advantages to having fewer electrodes, such as the ability to transmit the data (sometimes wirelessly) to a dedicated server for real-time analysis (Franke et al. 2012). In this case, several clients can have access to the data for monitoring and further examination (Zordan et al. 2015). While the commercial MEAs were limited to 60 or at most 64 electrodes for decades, recent developments have enabled commercially available MEAs with 128 or 256 electrodes. Many vendors of MEAs as well as the accompanying amplification, stimulation, and recording systems offer solutions in which the electrodes are divided into individual wells, allowing for a stream-lined investigation of multiple drugs or drug concentrations in parallel experiments (Wallace et al. 2015; McConnell et al. 2012).

Alternative materials and geometries for the individual electrodes in arrays have been the most investigated area for MEA improvement, and the variety deserves a separate review. However, a small number of advancements are of particular importance in the framework of this section. The classic electrode materials are gold and platinum (Bieberich and Anthony 2004). While some research aimed to change the geometry of usually planar metal electrodes to utilize pillars, pyramids, "mushrooms,, nails, or needles (Huys et al. 2012), other investigations experimented with entirely different materials to increase the signal-to-noise ratio of recordings and impedance for stimulation of attached cells (Brüggemann et al. 2011; Motlagh 2014; Hai and Spira 2012). Today, titanium nitride and the transparent indium tin oxide are the most abundantly used materials, as they create rough films, which

increase the surface area of an electrode for better recording and stimulation (Heer et al. 2004; Gross et al. 1985). A more recently investigated material is carbon in the form of nanotubes, graphene, or diamonds and the results are very promising (Pagels et al. 2005). Another interesting approach is to replace the electrode by moving the primary amplifier to where the electrode once was located, directly under the cell culture (Fromherz et al. 1991). These field-effect transistor arrays have been investigated almost as long as MEAs and have progressed significantly since their inception (Offenhäusser et al. 1997; Dankerl et al. 2010; Livi et al. 2013). Research on cell stimulation has advanced also and now can be completely independent from the electrode layout if target cells are genetically equipped with channel rhodopsin (Zhang et al. 2009). This light-sensitive ion channel allows for a selective stimulation with lasers (optogenetic stimulation).

Overall, MEAs are now commercially available from several competing manufacturers with different fabrication approaches. Besides conventional clean-rooms in larger research facilities, stream-lined complementary metal-oxide semiconductor (CMOS) processes, widely used in the computer industry, are now employed for new MEA designs to reduce cost (Huys et al. 2012). Printable MEAs are also now available on nearly any surface (Pickard 1979). However, some labs are building their own hybrid solutions with commercially available parts as well as custom electrode materials, electrode geometries, surface substrates, amplifier circuits, stimulators, recording systems, and software. The application of MEA technology, combined with surface patterning and compartmentalization techniques, potentially could map out the surface distribution of MNs and achieve specific stimulation of them in an in vitro NMJ system, which is one of the major challenges for interrogating NMJ function in vitro.

9.3.3 Cantilever Systems and Their Application in Monitoring Muscle Contraction

Another Bio-MEMs technology that advanced quantification of in vitro muscle contraction and NMJ function is the cantilever system (Fig. 9.4). The formation of NMJs between motoneurons and skeletal muscle in vitro has been primarily identified and quantified via immunocytochemistry (Guo et al. 2011; Guo et al. 2010b; Southam et al. 2015). While co-localization of pre- and post-synaptic markers such as SV2 and AchR indicates proximity of the motoneuron synaptic cleft to skeletal muscle motor end plates, a functional readout of muscle response to motoneuron stimulation provides a definitive confirmation of NMJ formation. However, the assessment of in vitro NMJs has been limited to visual inspection, which lacks a high degree of accuracy and repeatability, or dual patch clamp electrophysiology, which is highly invasive and labor intensive (Li et al. 2015; Liou and Wu 2015; Song and Jin 2015). A more simplified system utilizing cantilever arrays to measure the physical displacement of the muscle and subsequent force output in response to stimuli from motoneurons provides an ideal method for NMJ interrogation (Fig. 9.4).

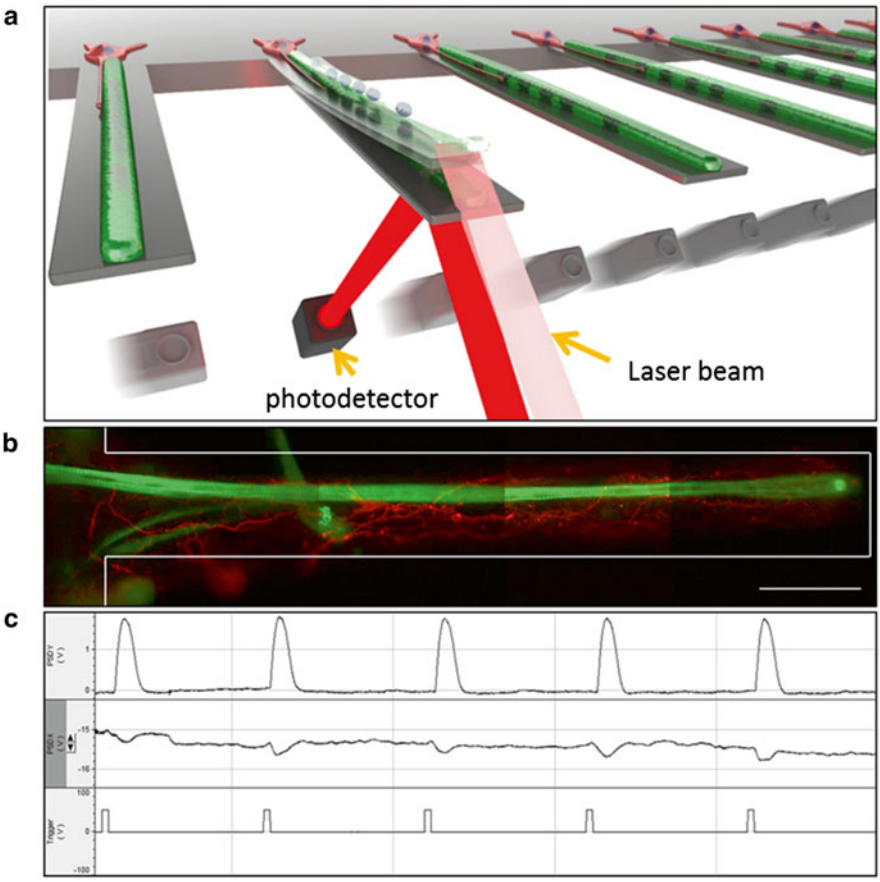

Fig. 9.4 Cantilever system for monitoring NMJ function. (**a**) Idealized schematic representation of the scanning system used to measure cantilever deflection in response to myotube contraction. Controlled movement of the laser and photo detector was used to align the laser beam with the tip of each cantilever in turn. (**b**) Composite image of an example of a primary rat myotube cocultured with primary rat motoneurons on a cantilever for 13 DIV and immunostained for Myosin Heavy Chain (*green*) and β-III Tubulin (*red*). Cantilever edges in this image were added to the image to give an indication of their scale in relation to the cultured cells. Scale bar ¼ 100 μm. (**c**) Example of a trace recording from a myotube (illustrated in (**b**)) stimulated using broad field electrical pulses. Top trace ¼ laser deflection (in Volts) in the *x*-axis, indicating lengthwise strain on the cantilever. Middle trace ¼ laser deflection (in Volts) in the *y*-axis, indicating torsional strain across the cantilever. Bottom trace ¼ indication of the temporal position of electrical pulses used to elicit myotube contraction in this system (adapted from Smith et al. (2013))

In general, these cantilever arrays have varying degrees of form and feasibility of readout. Silicon and PDMS-based devices to measure in vitro physiological parameters of muscle are the most widely used, including cantilever-based (Wilson et al. 2007; Shimizu et al. 2009; Defranchi et al. 2005) and post-based designs (Vandenburgh et al. 2008; Supinski et al. 2000). Each technique possesses inherent

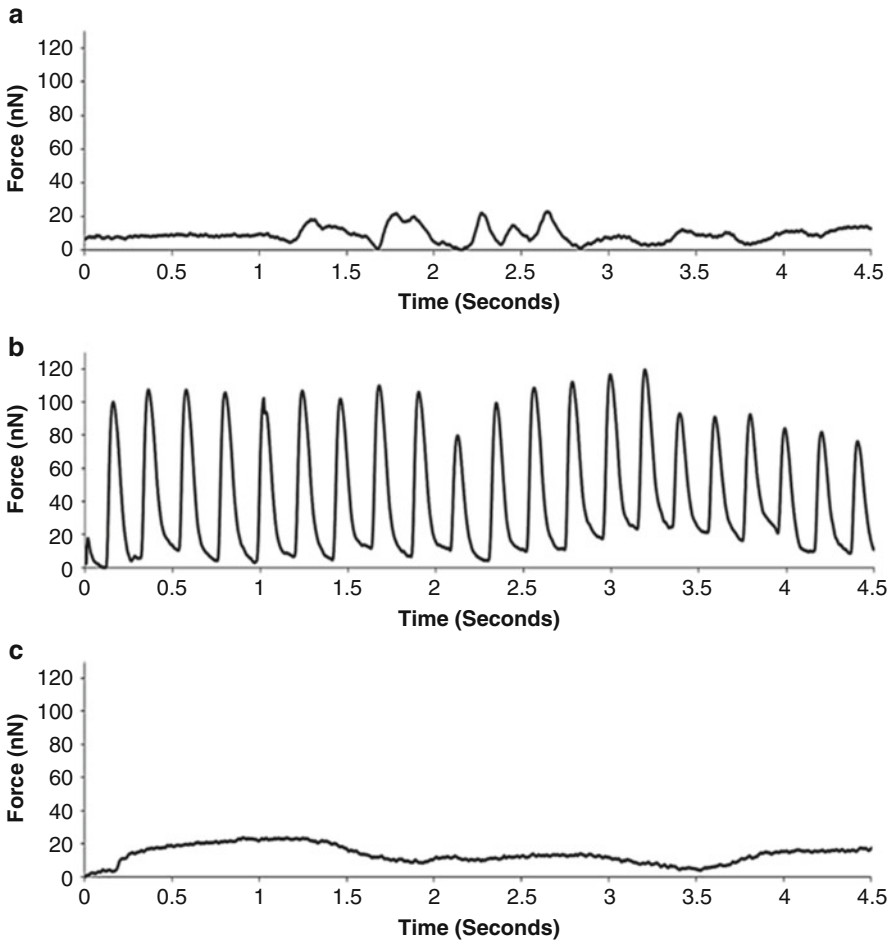

Fig. 9.5 Representative traces from analysis of the muscle-motoneuron coculture cantilever system, demonstrating the functional effects of motoneuron stimulation with and without addition of an NMJ blocker. Raw data (in Volts) was converted to a measurement of myotube force (in nano Newtons) and replotted. (**a**) Measurement of spontaneous contractions by the cultured myotubes without neuronal stimulation. (**b**) Measurement of myotube contraction following neuronal stimulation via the addition of 200 μM glutamate. (**c**) Measurement of myotube contraction following glutamate and 12.5 μM curare treatment (adapted from Smith et al. (2013))

advantages and limitations in fabrication, ease of measurement, overall cost, and capacity to be incorporated into multi-organ culture systems. PDMS and post-based designs are readily and easily fabricated but primarily rely on optical imaging for analysis of muscle displacement, which would be difficult to accomplish in the three-dimensional nature of a multi-organ system. The use of micro-fabricated silicon cantilevers enables the assessment of myotube contraction through measurement of cantilever deflection via a laser and photo-detector system and can be

stimulated by either electrical or chemical means (Vandenburgh et al. 2008; Duffy and Feinberg 2014; Neal et al. 2015; Vandenburgh et al. 2009) (Fig. 9.4). In addition, although being relatively expensive in terms of fabrication cost, silicon-based cantilever strategies are noninvasive allowing for the incorporation of recording and stimulating electrodes, providing the possibility of integrating MEA technology for specific MN stimulation while monitoring myofiber contraction, leading to the potential of developing high-content NMJ screening systems. In a representative study from the HSL, a rat NMJ culture was integrated with silicon cantilever chips, and the function of NMJs was monitored in real time by recording laser beam deflections noninvasively with the MNs were stimulated by glutamate (Smith et al. 2013) (Figs. 9.4 and 9.5). Other advantages of the presented system include: (a) allowing for simultaneous monitoring of multiple MN-SKM pairs by periodic scanning though the cantilevers and (b) allowing for measurement of the force of myotube contraction.

In addition to MEA and cantilever technologies, surface patterning applications are also available to promote myotube alignment and fusion (Li et al. 2014; Molnar et al. 2007b) and to guide axonal movement. Compartmentalization via a PDMS chamber system will allow coculture of multiple cell populations, each with an individualized excitation and monitoring capability. Overall, the integration of these interdisciplinary technologies with biological NMJ cultures as well as the whole reflex arc components will generate high content models that have important implications for the study of motor regulation and neuromuscular disorders such as ALS and Myasthenia Gravis as well as testing of novel therapeutic agents.

9.4 Addition of Systematic Complexity to Nervous System Models to Mimic In Vivo Conditions

In vivo, the CNS is isolated from all the other systems by a biological barrier: the blood–brain barrier (BBB). This barrier provides extra protection for the CNS, but also generates undesired obstacles for drug targeting. Furthermore, the nervous system is in constant direct or indirect interactions with all the other organ systems in the body. All of these complexities need to be considered when developing in vitro neurological models, especially those utilized for drug development.

9.4.1 Blood–Brain Barrier

9.4.1.1 The Relationship Between the PNS, CNS, and the BBB

The Blood–Brain Barrier (BBB) is composed of a layer of highly specialized brain microvascular endothelial cells (BMECs) covering the cerebral vascular system, in close contact with neighboring pericytes and glial cells which reside on the cerebral

side. The CNS and the BBB are structurally and functionally interconnected. The BBB forms a dynamic physical and metabolic barrier that strictly regulates molecular exchange between the blood and the brain, protecting the CNS from systematic variations and potentially harmful substances carried in the blood. Disruption of the BBB impairs brain homeostasis and coincides with many CNS disorders. Yet the neuroprotective BBB also poses a formidable challenge for CNS drug development. Inadequate delivery of therapeutic candidates across the BBB remains a major cause of failure for a majority of CNS disorders, including brain cancer, stroke, autism and Alzheimer's disease (Pardridge 2005; Pardridge 2012). Any integrated system for the reflex arc will eventually require the incorporation of the BBB into the platform.

9.4.1.2 Concept of the Neurovascular Unit

The increasingly acknowledged importance of the coupling between the CNS and the BBB give rise to an evolving perception of the neurovascular unit (NVU) (Neuwelt et al. 2011; Muoio et al. 2014; Abbott et al. 2006), which has caused substantial research efforts toward developing integrated in vitro models of the CNS and the BBB (Alcendor et al. 2013; Achyuta et al. 2013; Palmiotti et al. 2014; Brown et al. 2015). This would also establish a link to the PNS components of the reflex arc as well. Desirable characteristics of an effective in vitro model of the human NVU include: (a) high-fidelity human brain cells (brain microvascular endothelial cells, neurons, and glial cells) from expandable sources; (b) bio-mimetic spatial and functional organization of multicellular elements and extracellular matrix; (c) physiologically relevant perfusion of blood surrogates to achieve realistic bio-metabolism; and (d) on-line analytical capabilities of monitoring BBB properties and CNS responses.

9.4.1.3 Current Development and Future Directions of In Vitro NVU Models

Recent progress in stem cell technologies provides promising potential for unlimited cell sources for creating realistic and even patient-specific NVU models. Derivation of NVU cells from human pluripotent or embryonic stem cells has been described, including human brain microvascular cells (Lippmann et al. 2012), astrocytes (Shaltouki et al. 2013; Juopperi et al. 2012), and neurons (Guo et al. 2010a; Perrier et al. 2004). Incorporation of these cells in a Transwell® system, the most commonly used setup for dual or triple cell coculture, has generated encouraging outcomes in mimicking in vivo BBB integrity and permeability (Lippmann et al. 2014; Chou et al. 2014). The integrity of the tight junctions formed between cells can be measured by trans-endothelial electrical resistance (TEER) (Srinivasan et al. 2015; Wilhelm and Krizbai 2014). However, Transwell®-based models have limited ability to replicate physiological neurovascular bio-metabolism due to a large liquid-to-cell volume ratio, and often have limited analytical capability for neuron responses.

Microfluidic platforms have intrinsic advantages of precise control over microscale feature patterning and fluid delivery, which offer great promise for recreating in vivo like multicellular structural hierarchy of the NVU, as well as physiologically relevant metabolism and transport of nutrients, metabolites, and exogenous substances within the neurovascular environment. In addition, microfluidics-based models are versatile in integrating in situ measurements, such as the MEA technology (Nam and Wheeler 2011), for barrier integrity monitoring and CNS functional analysis (Booth and Kim 2012). A prototype neurovascular unit-on-a-chip was constructed as a multilayered vertical stack of a perfusable vascular channel and a neural compartment (Achyuta et al. 2013). This simple modular microfluidic model effectively reduced the gap between neurons and the brain endothelial barrier to 100 μm, which allowed the neuroglial mixed culture to reside within the oxygen diffusion distance and this model also substantially decreased the liquid-to-cell volume ratio. A recent model further reduced this ratio by encapsulating neurons in a 3D collagen gel, which also created spatial gradients within the neural chamber (Brown et al. 2015). All of these microfluidic models of the NVU, however, have not progressed beyond the proof-of-concept stage. Future development includes incorporation of 3D cell culture technology with current nanotechnology to recreate multicellular NVU structure on chip, as well as integration of microelectrodes for real-time recording of neuronal responses and monitoring BBB properties.

9.4.2 Organ-on-a-Chip Systems Under Microfluidic Circulation to Mimic In Vivo Conditions

Ultimately, the reflex arc platform would benefit from integration with other organs such as the liver and circulatory systems. However, these systems are already under development with body-on-a-chip or human-on-a-chip systems, which gives promise for the creation of complex systems in a reasonable time frame (Oleaga et al. 2016). In vivo, the localized environments for tissues are rarely the static conditions that typical cell culture methods produce. Specific examples include: endothelial cells lining blood vessels experience large shear stresses in pulsatile flow patterns, lung alveoli exist in the interface between inhaled air and capillary blood, and many other tissues have areas of specific shear stresses that influence development of the functional structures. Specifically, cerebral-spinal fluid (CSF), the bath that nurtures the CNS, is in continuous exchange with the cerebral blood stream through the BBB such that the microenvironment for the nervous system is constantly refreshed.

Traditional cell culture environments, such as multi-well plates, tissue culture flasks, or petri dishes, have major limitations in the physiological conditions they can mimic. The cell culture medium in these configurations is usually static or sometimes slightly rocked or swirled to create some internal fluid mixing. If several tissues are cocultured together, the multi-well plates, flasks, and dishes produce similar conditions on all of the tissues, making the creation of tailored microenvironments for each tissue extremely difficult to achieve. Transwell® tissue culture inserts and

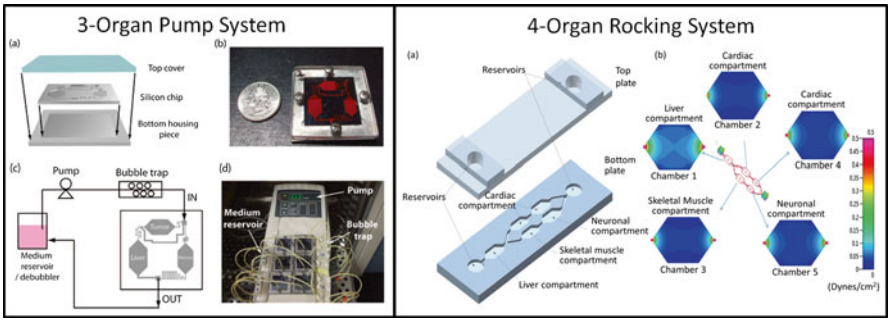

Fig. 9.6 Examples of multi-organ flow systems: A 3-organ system utilizing a pump-based system (*Left*) (Sung and Shuler 2009) and a 4-organ system utilizing a rocking platform to produce flow (Oleaga et al. 2016). In the 3-organ system on the *left*, a schematic diagram showing system assembly (**a**), picture of an assembled system (**b**), a schematic diagram of operation setup (**c**), and a picture of the system in operation with multiple chips (**d**) are shown. In the 4-organ system, a schematic layout of the system (**a**) and shear stresses in each chamber as determined with computational fluid dynamic modeling (**b**) are shown

similar products provide two separate volumes, separated by a permeable support. This configuration allows for using two different media, especially with barrier tissues, or for the creation of an air-liquid interface for tissues that require contact with air on one side and liquid on the other. Culture inserts also allow for the study of active and passive transport across barrier tissues. However, similar to the multi-well plate configuration, medium in the standard format is limited to static culture or a slight rocking or swirling.

To improve physiological relevance, a common method is to incorporate the tissue constructs into a fabricated housing and produce a dynamic microfluidic environment (Sung and Shuler 2009) (Fig. 9.6). Housings enable the use of microfluidic structures to engineer and control micro-environmental conditions. Simple microfluidic housings control perfusion rates into the tissues using various pump systems, with syringe pumps and peristaltic pumps being the most common, and can provide a continuous supply of fresh culture medium while removing waste compounds from the system. When coupled with even basic fluidic modeling, simple microfluidic housings can be used to produce desired shear stresses on cultured tissues (Ferrell et al. 2010). By expanding the complexity of the housings and the fluidic modeling, multiple tissue compartments with different shear stresses and flow rates can be created to produce tailored microenvironments for each tissue (Sung et al. 2010) (Fig. 9.6a). Computational fluid dynamics (CFD) enables the modeling of even more complex shapes and microstructures for the control of the fluidic environment for body-on-a-chip tissue components and supporting structures (Long et al. 2012). Other pump systems have been created to enhance the benefits of housing-based systems for body-on-a-chip studies and to address disadvantages of peristaltic and syringe pumps. Osmotic pumps, which are driven with osmotic pressure, eliminate the need for mechanical components and enable smaller systems (Park et al. 2007). On-chip peristaltic pumps driven by pressure-driven valves

require external tubing and control systems, but allow much smaller liquid volumes to be used to enable buildup of metabolites and signaling molecules for studying organ interactions (Maschmeyer et al. 2015). A rocking system (Fig. 9.6b), which uses gravity-driven flow to move fluid between two reservoirs in an alternating pattern, allows many systems on a single rocker. Housing-based body-on-a-chip systems engineered for this rocking pump allow minimal liquid volume to be used with recirculating flow, while allowing for in situ sampling. The use of housings for body-on-a-chip systems enables a wide variety of pumping mechanisms to suit the needs of the individual system, in addition to local control of cellular environments and multiple organ coculture.

9.4.3 Inclusion of Other Tissues to Reproduce Systemic Interactions

The nervous system manages body responses to both external and internal signals. The nervous system is in constant communication with other organs by direct innervations (Lisman 2015) or homeostasis regulation (Ulrich-Lai and Herman 2009; Betley et al. 2015; Mimee et al. 2013). Therefore, inclusion of cells of other organs is an obligatory improvement to better reproduce the in vivo condition for neural modeling. It is even more crucial from the perspective of drug development. On one hand, the presence of cells from other organs can affect the kinetics or dynamics or even the effects of drugs targeting nervous system due to the effects of physical barrier (i.e., BBB), specific or nonspecific absorption, endocytosis, or metabolism. For example, hepatocytes may metabolize the drug, producing compounds that have dramatically different effects than the parent drug. On the other hand, inclusion of other tissues/cells in the in vitro neural models also allows for the examination of off-target effects of the drugs. In general, the inclusion of other organ cells in neural modeling and the investigation of their interactions with neural cells are important for the understanding of the physiology and pathology of the nervous system, especially for drug development (Nikoletseas 2010). Recent development has already shown multi-organ systems composed of muscle, motoneurons, cardiomyocytes, and hepatocytes, and their response to toxins (Oleaga et al. 2016).

9.5 Summary and Perspectives

Highlighted by the efforts made by the combination of neuroscience and engineering, the gold standard for in vitro neural modeling is to recreate defined functional innervation models that are quantifiable, noninvasive, efficient, and with necessary complexity to match their applications. These models should provide essential tools for the study of not only physiology and pathology but also pharmacology and toxicology for future human therapies. The in vitro reflex arc systems introduced in this

chapter provide good examples of neural modeling toward this standard. The increased expansion of stem cell technologies, especially iPSCs, provides a growing pool of cell resources to choose from when building human-based in vitro biological systems. The integration of interdisciplinary technologies such as surface patterning for circuit mapping, MEAs for defined neural stimulation and recording, and microchip-based cantilevers for noninvasive monitoring of muscle contraction endows these in vitro systems with high resolution, efficiency, as well as the capability for long-term noninvasive testing. In vitro modeling of the whole reflex arc will provide an invaluable model for the dissection of motor circuit regulation, disease studies, and drug development. The inclusion of the BBB as well as multi-organs-on-a-chip and the application of microfluidic components will significantly upgrade the isolated static systems into complex dynamic models that more closely reproduce in vivo conditions. Prospectively, the expeditious development of stem cell technology and other interdisciplinary technologies and their integrated applications will culminate in the development of high content phenotypes of well-defined biological modules. The advancement of the multi-organ-on-a-chip field is expected to add complexity to these modules to better approximate in vivo conditions so that their biological function and the efficacy for different therapeutics can be better evaluated. Progress in neural modeling will accelerate our understanding of this crucial biological system and its diseased conditions, which reversely will continue to guide the development of more relevant in vitro neurological models.

References

Abbott, N.J., L. Ronnback, and E. Hansson. 2006. Astrocyte-Endothelial Interactions at the Blood-Brain Barrier. *Nature Review Neuroscience* 7(1): 41–53.

Abranches, E., M. Silva, L. Pradier, H. Schulz, O. Hummel, D. Henrique, and E. Bekman. 2009. Neural Differentiation of Embryonic Stem Cells *In Vitro*: A Road Map to Neurogenesis in the Embryo. *PloS One* 4(7), e6286. doi:10.1371/journal.pone.0006286.

Achyuta, A.K.H., A.J. Conway, R.B. Crouse, E.C. Bannister, R.N. Lee, C.P. Katnik, A.A. Behensky, J. Cuevas, and S.S. Sundaram. 2013. A Modular Approach to Create a Neurovascular Unit-On-a-Chip. *Lab on a Chip* 13: 542–553. doi:10.1039/c2lc41033h.

Alcendor, D.J., F.E. Block Iii, D.E. Cliffel, J.S. Daniels, K.L.J. Ellacott, C.R. Goodwin, L.H. Hofmeister, D. Li, D.A. Markov, J.C. May, L.J. McCawley, B. McLaughlin, J.A. McLean, K.D. Niswender, V. Pensabene, K.T. Seale, S.D. Sherrod, H.-J. Sung, D.L. Tabb, D.J. Webb, and J.P. Wikswo. 2013. Neurovascular Unit on a Chip: Implications for Translational Applications. *Stem Cell Research & Therapy* 4(1): 1–5. doi:10.1186/scrt379.

Alexander, A.G., V. Marfil, and C. Li. 2014. Use of C. Elegans as a Model to Study Alzheimer's Disease and Other Neurodegenerative Diseases. *Frontiers in Genetics* 5: 279. doi:10.3389/fgene.2014.00279.

Aregueta-Robles, U.A., A.J. Woolley, L.A. Poole-Warren, N.H. Lovell, and R.A. Green. 2014. Organic Electrode Coatings for Next-Generation Neural Interfaces. *Frontiers in Neuroengineering* 7: 15. doi:10.3389/fneng.2014.00015.

Barata, D., C. van Blitterswijk, and P. Habibovic. 2015. High-Throughput Screening Approaches and Combinatorial Development of Biomaterials Using Microfluidics. *Acta Biomaterialia* doi:http://dx.doi.org/10.1016/j.actbio.2015.09.009.

Berdondini, L., K. Imfeld, A. Maccione, M. Tedesco, S. Neukom, M. Koudelka-Hep, and S. Martinoia. 2009. Active Pixel Sensor Array for High Spatio-Temporal Resolution Electrophysiological Recordings from Single Cell to Large Scale Neuronal Networks. *Lab on a Chip* 9(18): 2644–2651. doi:10.1039/b907394a.

Betley, J.N., S. Xu, Z.F.H. Cao, R. Gong, C.J. Magnus, Y. Yu, and S.M. Sternson. 2015. Neurons for Hunger and Thirst Transmit a Negative-Valence Teaching Signal. *Nature* 521(7551): 180–185. doi:10.1038/nature14416.

Bhatia, S.N., and D.E. Ingber. 2014. Microfluidic Organs-on-Chips. *Nature Biotechnology* 32(8): 760–772. doi:10.1038/nbt.2989.

Bieberich, E., and G.E. Anthony. 2004. Neuronal Differentiation and Synapse Formation of PC12 and Embryonic Stem Cells on Interdigitated Microelectrode Arrays: Contact Structures for Neuron-to-Electrode Signal Transmission (NEST). *Biosensors & Bioelectronics* 19(8): 923–931.

Bilic, J., and J.C.I. Belmonte. 2012. Concise Review: Induced Pluripotent Stem Cells Versus Embryonic Stem Cells: Close Enough or Yet Too Far Apart? *Stem Cells* 30(1): 33–41. doi:10.1002/stem.700.

Booth, R., and H. Kim. 2012. Characterization of a Microfluidic In Vitro Model of the Blood-Brain Barrier (μBBB). *Lab on a Chip* 12: 1784–1792. doi:10.1039/c2lc40094d.

Branch, D.W., J.M. Corey, J.A. Weyhenmeyer, G.J. Brewer, B.C. Wheeler. 1998. Microstamp Patterns of Biomolecules for High-Resolution Neuronal Networks. *Medical & Biological Engineering & Computing* 36(1): 135–141. doi:10.1007/Bf02522871.

Brennand, K.J., A. Simone, J. Jou, C. Gelboin-Burkhart, N. Tran, S. Sangar, Y. Li, Y. Mu, G. Chen, D. Yu, S. McCarthy, J. Sebat, and F.H. Gage. 2011. Modelling Schizophrenia Using Human Induced Pluripotent Stem Cells. *Nature* 473(7346): 221–225. doi:http://www.nature.com/nature/journal/v473/n7346/abs/10.1038-nature09915-unlocked.html#supplementary-information.

Brette, R., M. Rudolph, T. Carnevale, M. Hines, D. Beeman, J.M. Bower, M. Diesmann, A. Morrison, P.H. Goodman, F.C. Harris, M. Zirpe, T. Natschläger, D. Pecevski, B. Ermentrout, M. Djurfeldt, A. Lansner, O. Rochel, T. Vieville, E. Muller, A.P. Davison, S. El Boustani, and A. Destexhe. 2007. Simulation of Networks of Spiking Neurons: A Review of Tools and Strategies. *Journal of Computational Neuroscience* 23(3): 349–398. doi:10.1007/s10827-007-0038-6.

Brewer, G.J. 1995. Serum-Free B27/Neurobasal Medium Supports Differentiated Growth of Neurons from the Striatum, Substantia Nigra, Septum, Cerebral Cortex, Cerebellum, and Dentate Gyrus. *Journal of Neuroscience Research* 42(5): 674–683.

Brewer, G.J., M.D. Boehler, T.T. Jones, and B.C. Wheeler. 2008. NbActiv4 Medium Improvement to Neurobasal/B27 Increases Neuron Synapse Densities and Network Spike Rates on Multielectrode Arrays. *Journal of Neuroscience Methods* 170(2): 181–187.

Brokhman, I., L. Gamarnik-Ziegler, O. Pomp, M. Aharonowiz, B.E. Reubinoff, and R.S. Goldstein. 2008. Peripheral Sensory Neurons Differentiate from Neural Precursors Derived from Human Embryonic Stem Cells. *Differentiation* 76(2): 145–155.

Brown, J.A., V. Pensabene, D.A. Markov, V. Allwardt, M.D. Neely, M. Shi, C.M. Britt, O.S. Hoilett, Q. Yang, B.M. Brewer, P.C. Samson, L.J. McCawley, J.M. May, D.J. Webb, D. Li, A.B. Bowman, R.S. Reiserer, and J.P. Wikswo. 2015. Recreating Blood-Brain Barrier Physiology and Structure on Chip: A Novel Neurovascular Microfluidic Bioreactor. *Biomicrofluidics* 9(5): 054124. doi:http://dx.doi.org/10.1063/1.4934713.

Brüggemann, D., B. Wolfrum, V. Maybeck, Y. Mourzina, M. Jansen, and A. Offenhäusser. 2011. Nanostructured Gold Microelectrodes for Extracellular Recording from Electrogenic Cells. *Nanotechnology* 22(26): 265104. doi:10.1088/0957-4484/22/26/265104.

Campenot, R.B. 1977. Local Control of Neurite Development by Nerve Growth Factor. *Proceedings of the National Academy of Sciences of the United States of America* 74(10): 4516–4519.

Catela, C., M.M. Shin, and J.S. Dasen. 2015. Assembly and Function of Spinal Circuits for Motor Control. *Annual Review of Cell and Developmental Biology* 31: 669–698.

Chaudhury, H., E. Raborn, L.C. Goldie, and K.K. Hirschi. 2012. Stem Cell-Derived Vascular Endothelial Cells and Their Potential Application in Regenerative Medicine. *Cells, Tissues, Organs* 195(1–2): 41–47. doi:10.1159/000331423.

Chen, Z., H. Lee, S.J. Henle, T.R. Cheever, S.C. Ekker, and J.R. Henley. 2013. Primary Neuron Culture for Nerve Growth and Axon Guidance Studies in Zebrafish. *PloS One* 8(3), e57539. doi:10.1371/journal.pone.0057539.

Cheung, C., and S. Sinha. 2011. Human Embryonic Stem Cell-Derived Vascular Smooth Muscle Cells in Therapeutic Neovascularisation. *Journal of Molecular and Cellular Cardiology* 51(5): 651–664. doi:10.1016/j.yjmcc.2011.07.014.

Chipman, P.H., Y. Zhang, and V.F. Rafuse. 2014. A Stem-Cell Based Bioassay to Critically Assess the Pathology of Dysfunctional Neuromuscular Junctions. *PloS One* 9(3), e91643. doi:10.1371/journal.pone.0091643.

Cho, S., A. Wood, and M.R. Bowlby. 2007. Brain Slices as Models for Neurodegenerative Disease and Screening Platforms to Identify Novel Therapeutics. *Current Neuropharmacology* 5(1): 19–33.

Choi, S.H., Y.H. Kim, M. Hebisch, C. Sliwinski, S. Lee, C. D'Avanzo, H. Chen, B. Hooli, C. Asselin, J. Muffat, J.B. Klee, C. Zhang, B.J. Wainger, M. Peitz, D.M. Kovacs, C.J. Woolf, S.L. Wagner, R.E. Tanzi, and D.Y. Kim. 2014. A Three-Dimensional Human Neural Cell Culture Model of Alzheimer's Disease. *Nature* 515(7526): 274–278. doi:10.1038/nature13800; http://www.nature.com/nature/journal/v515/n7526/abs/nature13800.html#supplementary-information.

Chou, C.-H., J.D. Sinden, P.-O. Couraud, and M. Modo. 2014. In Vitro Modeling of the Neurovascular Environment by Coculturing Adult Human Brain Endothelial Cells with Human Neural Stem Cells. *PloS One* 9(9), e106346. doi:10.1371/journal.pone.0106346.

Claverol-Tinture, E., M. Ghirardi, F. Fiumara, X. Rosell, and J. Cabestany. 2005. Multielectrode Arrays with Elastomeric Microstructured Overlays for Extracellular Recordings from Patterned Neurons. *Journal of Neural Engineering* 2(2): L1–L7.

Cooke, M.J., S.R. Phillips, D.S. Shah, D. Athey, J.H. Lakey, and S.A. Przyborski. 2008. Enhanced Cell Attachment Using a Novel Cell Culture Surface Presenting Functional Domains from Extracellular Matrix Proteins. *Cytotechnology* 56(2): 71–79. doi:10.1007/s10616-007-9119-7.

Corey, J.M., B.C. Wheeler, and G.J. Brewer. 1996. Micrometer Resolution Silane-Based Patterning of Hippocampal Neurons: Critical Variables in Photoresist and Laser Ablation Processes for Substrate Fabrication. *IEEE Transactions on Biomedical Engineering* 43(9): 944–955. doi:10.1109/10.532129.

Daniels, M.P., B.T. Lowe, S. Shah, J. Ma, S.J. Samuelsson, B. Lugo, T. Parakh, and C.S. Uhm. 2000. Rodent Nerve-Muscle Cell Culture System for Studies of Neuromuscular Junction Development: Refinements and Applications. *Microscopy Research and Technique* 49(1): 26–37.

Dankerl, M., M.V. Hauf, A. Lippert, L.H. Hess, S. Birner, I.D. Sharp, A. Mahmood, P. Mallet, J.-Y. Veuillen, M. Stutzmann, and J.A. Garrido. 2010. Graphene Solution-Gated Field-Effect Transistor Array for Sensing Applications. *Advanced Functional Materials* 20(18): 3117–3124. doi:10.1002/adfm.201000724.

Das, M., P. Molnar, H. Devaraj, M. Poeta, and J.J. Hickman. 2003. Electrophysiological and Morphological Characterization of Rat Embryonic Motoneurons in a Defined System. *Biotechnology Progress* 19(6): 1756–1761. doi:10.1021/bp034076l.

Das, M., N. Bhargava, C. Gregory, L. Riedel, P. Molnar, and J.J. Hickman. 2005. Adult Rat Spinal Cord Culture on an Organosilane Surface in a Novel Serum-Free Medium. *In Vitro Cellular & Developmental Biology—Animal* 41(10): 343–348. doi:10.1007/s11626-005-0006-2.

Das, M., J.W. Rumsey, C.A. Gregory, N. Bhargava, J.F. Kang, P. Molnar, L. Riedel, X. Guo, and J.J. Hickman. 2007. Embryonic Motoneuron-Skeletal Muscle Co-culture in a Defined System. *Neuroscience* 146(2): 481–488.

Das, M., J.W. Rumsey, N. Bhargava, M. Stancescu, and J.J. Hickman. 2010. A Defined Long-Term In Vitro Tissue Engineered Model of Neuromuscular Junctions. *Biomaterials* 31(18): 4880–4888. doi:10.1016/j.biomaterials.2010.02.055.

Davies, S.J., C.H. Shih, M. Noble, M. Mayer-Proschel, J.E. Davies, and C. Proschel. 2011. Transplantation of Specific Human Astrocytes Promotes Functional Recovery After Spinal Cord Injury. *PloS One* 6(3), e17328. doi:10.1371/journal.pone.0017328.

Davis, H., X. Guo, S. Lambert, M. Stancescu, and J.J. Hickman. 2012. Small Molecule Induction of Human Umbilical Stem Cells into MBP-Positive Oligodendrocytes in a Defined Three-Dimensional Environment. *ACS Chemical Neuroscience* 3(1): 31–39. doi:10.1021/cn200082q.

Davis, H., M. Gonzalez, M. Stancescu, R. Love, J.J. Hickman, and S. Lambert. 2014. A Phenotypic Culture System for the Molecular Analysis of CNS Myelination in the Spinal Cord. *Biomaterials* 35(31): 8840–8845. doi:http://dx.doi.org/10.1016/j.biomaterials.2014.07.007.

Dawson, T.M., H.S. Ko, and V.L. Dawson. 2010. Genetic Animal Models of Parkinson's Disease. *Neuron* 66(5): 646–661. doi:10.1016/j.neuron.2010.04.034.

Defranchi, E., E. Bonaccurso, M. Tedesco, M. Canato, E. Pavan, R. Raiteri, and C. Reggiani. 2005. Imaging and Elasticity Measurements of the Sarcolemma of Fully Differentiated Skeletal Muscle Fibres. *Microscopy Research and Technique* 67(1): 27–35. doi:10.1002/jemt.20177.

Demestre, M., M. Orth, K.J. Föhr, K. Achberger, A.C. Ludolph, S. Liebau, and T.M. Boeckers. 2015. Formation and Characterisation of Neuromuscular Junctions Between hiPSC Derived Motoneurons and Myotubes. *Stem Cell Research* 15(2): 328–336. doi:http://dx.doi.org/10.1016/j.scr.2015.07.005.

Dimos, J.T., K.T. Rodolfa, K.K. Niakan, L.M. Weisenthal, H. Mitsumoto, W. Chung, G.F. Croft, G. Saphier, R. Leibel, R. Goland, H. Wichterle, C.E. Henderson, and K. Eggan. 2008. Induced Pluripotent Stem Cells Generated from Patients with ALS can be Differentiated into Motor Neurons. *Science* 321(5893): 1218–1221.

Doležal, V.R., V. Lisá, M.-F. Diebler, J. Kašparová, and S. Tuček. 2001. Differentiation of NG108-15 Cells Induced by the Combined Presence of dbcAMP and Dexamethasone Brings About the Expression of N and P/Q Types of Calcium Channels and the Inhibitory Influence of Muscarinic Receptors on Calcium Influx. *Brain Research* 910(1–2): 134–141. doi:http://dx.doi.org/10.1016/S0006-8993(01)02701-9.

Dore-Duffy, P. 2008. Pericytes: Pluripotent Cells of the Blood Brain Barrier. *Current Pharmaceutical Design* 14(16): 1581–1593.

Dore-Duffy, P., A. Katychev, X. Wang, and E. Van Buren. 2006. CNS Microvascular Pericytes Exhibit Multipotential Stem Cell Activity. *Journal of Cerebral Blood Flow & Metabolism* 26(5): 613–624. doi:10.1038/sj.jcbfm.9600272.

Duffy, R.M., and A.W. Feinberg. 2014. Engineered Skeletal Muscle Tissue for Soft Robotics: Fabrication Strategies, Current Applications, and Future Challenges. *Wiley Interdisciplinary Reviews: Nanomedicine and Nanobiotechnology* 6(2): 178–195. doi:10.1002/wnan.1254.

Duhr, F., P. Déléris, F. Raynaud, M. Séveno, S. Morisset-Lopez, C. Mannoury la Cour, M.J. Millan, J. Bockaert, P. Marin, and S. Chaumont-Dubel. 2014. Cdk5 Induces Constitutive Activation of 5-HT6 Receptors to Promote Neurite Growth. *Nature Chemical Biology* 10(7): 590–597. doi:10.1038/nchembio.1547. http://www.nature.com/nchembio/journal/v10/n7/abs/nchembio.1547.html#supplementary-information.

Dutton, E.K., C.S. Uhm, S.J. Samuelsson, A.E. Schaffner, S.C. Fitzgerald, and M.P. Daniels. 1995. Acetylcholine Receptor Aggregation at Nerve-Muscle Contacts in Mammalian Cultures: Induction by Ventral Spinal Cord Neurons is Specific to Axons. *The Journal of Neuroscience* 15(11): 7401–7416.

Dwane, S., E. Durack, and P. Kiely. 2013. Optimising Parameters for the Differentiation of SH-SY5Y Cells to Study Cell Adhesion and Cell Migration. *BMC Research Notes* 6(1): 366.

Edwards, D., M. Stancescu, P. Molnar, and J.J. Hickman. 2013. Two Cell Circuits of Oriented Adult Hippocampal Neurons on Self-Assembled Monolayers for Use in the Study of Neuronal Communication in a Defined System. *ACS Chemical Neuroscience* 4(8): 1174–1182. doi:10.1021/cn300206k.

El-Ali, J., P.K. Sorger, and K.F. Jensen. 2006. Cells on Chips. *Nature* 442(7101): 403–411.

Emdad, L., S.L. D'Souza, H.P. Kothari, Z.A. Qadeer, and I.M. Germano. 2012. Efficient Differentiation of Human Embryonic and Induced Pluripotent Stem Cells into Functional Astrocytes. *Stem Cells and Development* 21(3): 404–410. doi:10.1089/scd.2010.0560.

Engel, A.G., K. Ohno, and S.M. Sine. 2003. Sleuthing Molecular Targets for Neurological Diseases at the Neuromuscular Junction. *Nature Review Neuroscience* 4(5): 339–352.

Esposti, F., M.G. Signorini, S.M. Potter, and S. Cerutti. 2009. Statistical Long-Term Correlations in Dissociated Cortical Neuron Recordings. *IEEE Transactions on Neural Systems and Rehabilitation Engineering* 17(4): 364–369. doi:10.1109/TNSRE.2009.2022832.

Falconnet, D., G. Csucs, H. Michelle Grandin, and M. Textor. 2006. Surface Engineering Approaches to Micropattern Surfaces for Cell-Based Assays. *Biomaterials* 27(16): 3044–3063. doi:http://dx.doi.org/10.1016/j.biomaterials.2005.12.024.

Fernandez-Valle, C., R.P. Bunge, and M.B. Bunge. 1995. Schwann Cells Degrade Myelin and Proliferate in the Absence of Macrophages: Evidence from In Vitro Studies of Wallerian Degeneration. *Journal of Neurocytology* 24(9): 667–679. doi:10.1007/bf01179817.

Ferrea, E., A. Maccione, L. Medrihan, T. Nieus, D. Ghezzi, P. Baldelli, F. Benfenati, and L. Berdondini. 2012. Large-Scale, High-Resolution Electrophysiological Imaging of Field Potentials in Brain Slices with Microelectronic Multielectrode Arrays. *Frontiers in Neural Circuits* 6: 80. doi:10.3389/fncir.2012.00080.

Ferrell, N., R.R. Desai, A.J. Fleischman, S. Roy, H.D. Humes, and W.H. Fissell. 2010. A Microfluidic Bioreactor with Integrated Transepithelial Electrical Resistance (TEER) Measurement Electrodes for Evaluation of Renal Epithelial Cells. *Biotechnology and Bioengineering* 107(4): 707–716. doi:10.1002/bit.22835.

Fields, R.D., E.A. Neale, and P.G. Nelson. 1990. Effects of Patterned Electrical-Activity on Neurite Outgrowth from Mouse Sensory Neurons. *The Journal of Neuroscience* 10(9): 2950–2964.

Fischbach, G.D. 1972. Synapse Formation Between Dissociated Nerve and Muscle Cells in Low Density Cell Cultures. *Developmental Biology* 28(2): 407–429.

Fischbach, G.D., and S.A. Cohen. 1973. The Distribution of Acetylcholine Sensitivity Over Uninnervated and Innervated Muscle Fibers Grown in Cell Culture. *Developmental Biology* 31(1): 147–162.

Focus on Computational and Systems Neuroscience. 2011. *Nature Neuroscience* 14(2): 121–121.

Fortier, L.A. 2005. Stem Cells: Classifications, Controversies, and Clinical Applications. *Veterinary Surgery* 34(5): 415–423. doi:10.1111/j.1532-950X.2005.00063.x.

Frank, E., and G.D. Fischbach. 1979. Early Events in Neuromuscular Junction Formation In Vitro: Induction of Acetylcholine Receptor Clusters in the Postsynaptic Membrane and Morphology of Newly Formed Synapses. *The Journal of Cell Biology* 83(1): 143–158. doi:10.1083/jcb.83.1.143.

Franke, F., D. Jäckel, J. Dragas, J. Müller, M. Radivojevic, D. Bakkum, and A. Hierlemann. 2012. High-Density Microelectrode Array Recordings and Real-Time Spike Sorting for Closed-Loop Experiments: An Emerging Technology to Study Neural Plasticity. *Frontiers in Neural Circuits* 6: 105. doi:10.3389/fncir.2012.00105.

Frey, U., U. Egert, F. Heer, S. Hafizovic, and A. Hierlemann. 2009. Microelectronic System for High-Resolution Mapping of Extracellular Electric Fields Applied to Brain Slices. *Biosensors & Bioelectronics* 24(7): 2191–2198. doi:10.1016/j.bios.2008.11.028.

Fromherz, P., A. Offenhäusser, T. Vetter, and J. Weis. 1991. A Neuron-Silicon Junction: A Retzius Cell of the Leech on an Insulated-Gate Field-Effect Transistor. *Science* 252(5010): 1290–1293.

Gajsek, N., M. Jevsek, T. Mars, K. Mis, S. Pirkmajer, J. Brecelj, and Z. Grubic. 2008. Synaptogenetic Mechanisms Controlling Postsynaptic Differentiation of the Neuromuscular Junction are Nerve-Dependent in Human and Nerve-Independent in Mouse C2C12 Muscle Cultures. *Chemico-Biological Interactions* 175(1–3): 50–57.

Goldman-Rakic, P.S. 1988. Topography of Cognition: Parallel Distributed Networks in Primate Association Cortex. *Annual Review of Neuroscience* 11: 137–156.

Gould, T.W., R.R. Buss, S. Vinsant, D. Prevette, W. Sun, C.M. Knudson, C.E. Milligan, and R.W. Oppenheim. 2006. Complete Dissociation of Motor Neuron Death from Motor Dysfunction by Bax Deletion in a Mouse Model of ALS. *The Journal of Neuroscience* 26(34): 8774–8786. doi:10.1523/jneurosci.2315-06.2006.

Goulding, M. 2009. Circuits Controlling Vertebrate Locomotion: Moving in a New Direction. *Nature Review Neuroscience* 10(7): 507–518.

Gross, G.W., W.Y. Wen, and J.W. Lin. 1985. Transparent Indium-Tin Oxide Electrode Patterns for Extracellular, Multisite Recording in Neuronal Cultures. *Journal of Neuroscience Methods* 15(3): 243–252.

Guettier-Sigrist, S., G. Coupin, J.M. Warter, and P. Poindron. 2000. Cell Types Required to Efficiently Innervate Human Muscle Cells In Vitro. *Experimental Cell Research* 259(1): 204–212. doi:10.1006/excr.2000.4968.

Guo, X., K. Johe, P. Molnar, H. Davis, and J. Hickman. 2010a. Characterization of a Human Fetal Spinal Cord Stem Cell Line, NSI-566RSC, and Its Induction to Functional Motoneurons. *Journal of Tissue Engineering and Regenerative Medicine* 4(3): 181–193. doi:10.1002/term.223.

Guo, X., M. Das, J. Rumsey, M. Gonzalez, M. Stancescu, and J. Hickman. 2010b. Neuromuscular Junction Formation Between Human Stem-Cell-Derived Motoneurons and Rat Skeletal Muscle in a Defined System. *Tissue Engineering. Part C, Methods* 16(6): 1347–1355. doi:10.1089/ten.TEC.2010.0040.

Guo, X., M. Gonzalez, M. Stancescu, H.H. Vandenburgh, and J.J. Hickman. 2011. Neuromuscular Junction Formation Between Human Stem Cell-Derived Motoneurons and Human Skeletal Muscle in a Defined System. *Biomaterials* 32(36): 9602–9611. doi:10.1016/j.biomaterials.2011.09.014.

Guo, X., J.E. Ayala, M. Gonzalez, M. Stancescu, S. Lambert, and J.J. Hickman. 2012. Tissue Engineering the Monosynaptic Circuit of the Stretch Reflex Arc with Co-culture of Embryonic Motoneurons and Proprioceptive Sensory Neurons. *Biomaterials* 33(23): 5723–5731. doi:http://dx.doi.org/10.1016/j.biomaterials.2012.04.042.

Guo, X., S. Spradling, M. Stancescu, S. Lambert, and J.J. Hickman. 2013. Derivation of Sensory Neurons and Neural Crest Stem Cells from Human Neural Progenitor hNP1. *Biomaterials* 34(18): 4418–4427. doi:http://dx.doi.org/10.1016/j.biomaterials.2013.02.061.

Hai, A., and M.E. Spira. 2012. On-Chip Electroporation, Membrane Repair Dynamics and Transient In-Cell Recordings by Arrays of Gold Mushroom-Shaped Microelectrodes. *Lab on a Chip* 12(16): 2865–2873. doi:10.1039/c2lc40091j.

Halevy, T., and A. Urbach. 2014. Comparing ESC and iPSC-Based Models for Human Genetic Disorders. *Journal of Clinical Medicine* 3(4): 1146–1162.

Halldorsson, S., E. Lucumi, R. Gómez-Sjöberg, and R.M.T. Fleming. 2015. Advantages and Challenges of Microfluidic Cell Culture in Polydimethylsiloxane Devices. *Biosensors and Bioelectronics* 63: 218–231. doi:http://dx.doi.org/10.1016/j.bios.2014.07.029.

Harink, B., S. Le Gac, R. Truckenmuller, C. van Blitterswijk, and P. Habibovic. 2013. Regeneration-on-a-Chip? The Perspectives on Use of Microfluidics in Regenerative Medicine. *Lab on a Chip* 13(18): 3512–3528. doi:10.1039/C3LC50293G.

Harper, J.M., C. Krishnan, J.S. Darman, D.M. Deshpande, S. Peck, I. Shats, S. Backovic, J.D. Rothstein, and D.A. Kerr. 2004. Axonal Growth of Embryonic Stem Cell-Derived Motoneurons In Vitro and in Motoneuron-Injured Adult Rats. *Proceedings of the National Academy of Sciences of the United States of America* 101(18): 7123–7128. doi:10.1073/pnas.0401103101.

Heer, F., W. Franks, A. Blau, S. Taschini, C. Ziegler, A. Hierlemann, and H. Baltes. 2004. CMOS Microelectrode Array for the Monitoring of Electrogenic Cells. *Biosensors & Bioelectronics* 20(2): 358–366. doi:10.1016/j.bios.2004.02.006.

Helmke, B.P., and A.R. Minerick. 2006. Designing a Nano-Interface in a Microfluidic Chip to Probe Living Cells: Challenges and Perspectives. *Proceedings of the National Academy of Sciences of the United States of America* 103(17): 6419–6424. doi:10.1073/pnas.0507304103.

Hickman, J.J., S.K. Bhatia, J.N. Quong, P. Shoen, D.A. Stenger, C.J. Pike, and C.W. Cotman. 1994. Rational Pattern Design for In Vitro Cellular Networks Using Surface Photochemistry. *Journal of Vacuum Science & Technology A* 12(3): 607–616. doi:http://dx.doi.org/10.1116/1.578844.

Hollenbeck, P.J., and J.R. Bamburg. 2003. Comparing the Properties of Neuronal Culture Systems: A Shopping Guide for the Cell Biologist. *Methods in Cell Biology* 71: 1–16.

Hopkins, A.M., E. DeSimone, K. Chwalek, and D.L. Kaplan. 2015. 3D In Vitro Modeling of the Central Nervous System. *Progress in Neurobiology* 125: 1–25. doi:http://dx.doi.org/10.1016/j.pneurobio.2014.11.003.

Hu, B.-Y., J.P. Weick, J. Yu, L.-X. Ma, X.-Q. Zhang, J.A. Thomson, and S.-C. Zhang. 2010. Neural Differentiation of Human Induced Pluripotent Stem Cells Follows Developmental Principles But with Variable Potency. *Proceedings of the National Academy of Sciences of the United States of America* 107(9): 4335–4340. doi:10.1073/pnas.0910012107.

Hughes, B.W., L.L. Kusner, and H.J. Kaminski. 2006. Molecular Architecture of the Neuromuscular Junction. *Muscle & Nerve* 33(4): 445–461.

Humpel, C. 2015. Organotypic Brain Slice Cultures: A Review. *Neuroscience* 305: 86–98. doi:http://dx.doi.org/10.1016/j.neuroscience.2015.07.086.

Hunsberger, J.G., A.G. Efthymiou, N. Malik, M. Behl, I.L. Mead, X. Zeng, A. Simeonov, and M. Rao. 2015. Induced Pluripotent Stem Cell Models to Enable In Vitro Models for Screening in the Central Nervous System. *Stem Cells and Development* 24(16): 1852–1864. doi:10.1089/scd.2014.0531.

Hutzler, M., A. Lambacher, B. Eversmann, M. Jenkner, R. Thewes, and P. Fromherz. 2006. High-Resolution Multitransistor Array Recording of Electrical Field Potentials in Cultured Brain Slices. *Journal of Neurophysiology* 96(3): 1638–1645. doi:10.1152/jn.00347.2006.

Huys, R., D. Braeken, D. Jans, A. Stassen, N. Collaert, J. Wouters, J. Loo, S. Severi, F. Vleugels, G. Callewaert, K. Verstreken, C. Bartic, and W. Eberle. 2012. Single-Cell Recording and Stimulation with a 16k Micro-Nail Electrode Array Integrated on a 0.18 μm CMOS Chip. *Lab on a Chip* 12(7): 1274–1280. doi:10.1039/c2lc21037a.

Israel, M.A., S.H. Yuan, C. Bardy, S.M. Reyna, Y. Mu, C. Herrera, M.P. Hefferan, S. Van Gorp, K.L. Nazor, F.S. Boscolo, C.T. Carson, L.C. Laurent, M. Marsala, F.H. Gage, A.M. Remes, E.H. Koo, and L.S.B. Goldstein. 2012. Probing Sporadic and Familial Alzheimer's Disease Using Induced Pluripotent Stem Cells. *Nature* 482(7384): 216–220. doi:http://www.nature.com/nature/journal/v482/n7384/abs/nature10821.html#supplementary-information.

Ito, Y. 1999. Surface Micropatterning to Regulate Cell Functions. *Biomaterials* 20(23–24): 2333–2342. doi:http://dx.doi.org/10.1016/S0142-9612(99)00162-3.

Jacobson, C., D. Duggan, and G. Fischbach. 2004. Neuregulin Induces the Expression of Transcription Factors and Myosin Heavy Chains Typical of Muscle Spindles in Cultured Human Muscle. *Proceedings of the National Academy of Sciences of the United States of America* 101(33): 12218–12223. doi:10.1073/pnas.0404240101.

Johnson, M.A., J.P. Weick, R.A. Pearce, and S.-C. Zhang. 2007. Functional Neural Development from Human Embryonic Stem Cells: Accelerated Synaptic Activity Via Astrocyte Coculture. *The Journal of Neuroscience* 27(12): 3069–3077. doi:10.1523/jneurosci.4562-06.2007.

Juopperi, T.A., W.R. Kim, C.-H. Chiang, H. Yu, R.L. Margolis, C.A. Ross, Ming G-l, and H. Song. 2012. Astrocytes Generated from Patient Induced Pluripotent Stem Cells Recapitulate Features of Huntington's Disease Patient Cells. *Molecular Brain* 5(1): 1–14. doi:10.1186/1756-6606-5-17.

Kaneko, A., and Y. Sankai. 2014. Long-Term Culture of Rat Hippocampal Neurons at Low Density in Serum-Free Medium: Combination of the Sandwich Culture Technique with the Three-Dimensional Nanofibrous Hydrogel PuraMatrix. *PloS One* 9(7), e102703.

Karra, D., and R. Dahm. 2010. Transfection Techniques for Neuronal Cells. *The Journal of Neuroscience* 30(18): 6171–6177. doi:10.1523/jneurosci.0183-10.2010.

Kawato, M. 1999. Internal Models for Motor Control and Trajectory Planning. *Current Opinion in Neurobiology* 9(6): 718–727.

Kim, J. 2002. Dopamine Neurons Derived from Embryonic Stem Cells Function in an Animal Model of Parkinson's Disease. *Nature* 418: 50–56.

Kim, D.-S., P.J. Ross, K. Zaslavsky, and J. Ellis. 2014. Optimizing Neuronal Differentiation from Induced Pluripotent Stem Cells to Model ASD. Frontiers in Cellular Neuroscience 8: 109. doi:10.3389/fncel.2014.00109.

Kim, Y.H., S.H. Choi, C. D'Avanzo, M. Hebisch, C. Sliwinski, E. Bylykbashi, K.J. Washicosky, J.B. Klee, O. Brustle, R.E. Tanzi, and D.Y. Kim. 2015. A 3D Human Neural Cell Culture System for Modeling Alzheimer's Disease. *Nature Protocols* 10(7): 985–1006. doi:10.1038/nprot.2015.065. http://www.nature.com/nprot/journal/v10/n7/abs/nprot.2015.065.html#supplementary-information.

Kleinfeld, D., K. Kahler, and P. Hockberger. 1988. Controlled Outgrowth of Dissociated Neurons on Patterned Substrates. *The Journal of Neuroscience* 8(11): 4098–4120.

Klitzman, R. 2010. The Use of Eggs and Embryos in Stem Cell Research. *Seminars in Reproductive Medicine* 28(4): 336–344. doi:10.1055/s-0030-1255182.

Kobayashi, T., V. Askanas, and W.K. Engel. 1987. Human Muscle Cultured in Monolayer and Cocultured with Fetal Rat Spinal Cord: Importance of Dorsal Root Ganglia for Achieving Successful Functional Innervation. *The Journal of Neuroscience* 7(10): 3131–3141.

Leclair, A.M., S.S.G. Ferguson, and F. Lagugne-Labarthet. 2011. Surface Patterning Using Plasma-Deposited Fluorocarbon Thin Films for Single-Cell Positioning and Neural Circuit Arrangement. *Biomaterials* 32(5): 1351–1360. doi:10.1016/j.biomaterials.2010.10.051.

Lee, S., and E.J. Huang. 2015. Modeling ALS and FTD with iPSC-Derived Neurons. *Brain Research* doi:http://dx.doi.org/10.1016/j.brainres.2015.10.003.

Levy, N. 2012. The Use of Animal as Models: Ethical Considerations. *International Journal of Stroke* 7(5): 440–442. doi:10.1111/j.1747-4949.2012.00772.x.

Li, X.-J., Z.-W. Du, E.D. Zarnowska, et al. 2005. Specification of Motoneurons from Human Embryonic Stem Cells. *Nature Biotechnology* 23(2): 215–221.

Li, X.J., B.Y. Hu, S.A. Jones, Y.S. Zhang, T. LaVaute, Z.W. Du, and S.C. Zhang. 2008. Directed Differentiation of Ventral Spinal Progenitors and Motor Neurons from Human Embryonic Stem Cells by Small Molecules. *Stem Cells* 26(4): 886–893. doi:10.1634/stemcells.2007-0620.

Li, Y., G. Huang, X. Zhang, L. Wang, Y. Du, T.J. Lu, and F. Xu. 2014. Engineering Cell Alignment In Vitro. *Biotechnology Advances* 32(2): 347–365. doi:http://dx.doi.org/10.1016/j.biotechadv.2013.11.007.

Li, Y.T., S.H. Zhang, X.Y. Wang, X.W. Zhang, A.I. Oleinick, I. Svir, C. Amatore, and W.H. Huang. 2015. Real-Time Monitoring of Discrete Synaptic Release Events and Excitatory Potentials Within Self-Reconstructed Neuromuscular Junctions. *Angewandte Chemie (International ed in English)* 54(32): 9313–9318. doi:10.1002/anie.201503801.

Liou, J.-C., and Y.-C. Wu. 2015. Studies on the Synaptic Facilitation Effect of Hydrogen Peroxide in the Developing Neuromuscular Synapse. *The FASEB Journal* 29 (1 Supplement).

Lippmann, E.S., S.M. Azarin, J.E. Kay, R.A. Nessler, H.K. Wilson, A. Al-Ahmad, S.P. Palecek, and E.V. Shusta. 2012. Derivation of Blood-Brain Barrier Endothelial Cells from Human Pluripotent Stem Cells. *Nature Biotechnology* 30(8): 783–791. http://www.nature.com/nbt/journal/v30/n8/abs/nbt.2247.html#supplementary-information.

Lippmann, E.S., A. Al-Ahmad, S.M. Azarin, S.P. Palecek, and E.V. Shusta. 2014. A Retinoic Acid-Enhanced, Multicellular Human Blood-Brain Barrier Model Derived from Stem Cell Sources. *Scientific Reports* 4: 4160. doi:10.1038/srep04160. http://www.nature.com/articles/srep04160#supplementary-information.

Lisman, J. 2015. The Challenge of Understanding the Brain: Where We Stand in 2015. *Neuron* 86(4): 864–882. doi:10.1016/j.neuron.2015.03.032.

Liu, Q.Y., M. Coulombe, J. Dumm, K.M. Shaffer, A.E. Schaffner, J.L. Barker, J.J. Pancrazio, D.A. Stenger, and W. Ma. 2000. Synaptic Connectivity in Hippocampal Neuronal Networks Cultured on Micropatterned Surfaces. *Brain Research. Developmental Brain Research* 120(2): 223–231.

Liu, M.-G., X.-F. Chen, T. He, Z. Li, and J. Chen. 2012. Use of Multi-Electrode Array Recordings in Studies of Network Synaptic Plasticity in Both Time and Space. *Neuroscience Bulletin* 28(4): 409–422. doi:10.1007/s12264-012-1251-5.

Liu, M.-G., S.J. Kang, T.-Y. Shi, K. Koga, M.-M. Zhang, G.L. Collingridge, B.-K. Kaang, and M. Zhuo. 2013. Long-Term Potentiation of Synaptic Transmission in the Adult Mouse Insular Cortex: Multielectrode Array Recordings. *Journal of Neurophysiology* 110(2): 505–521. doi:10.1152/jn.01104.2012.

Livi, P., M. Wipf, A. Tarasov, R. Stoop, K. Bedner, J. Rothe, Y. Chen, A. Stettler, C. Schonenberger, and A. Hierlemann. 2013. Silicon Nanowire Ion-Sensitive Field-Effect Transistor Array Integrated with a CMOS-Based Readout Chip. In *Solid-State Sensors, Actuators and Microsystems (TRANSDUCERS & EUROSENSORS XXVII)*, 2013 Transducers & Eurosensors

XXVII: The 17th International Conference on, 16–20 June 2013. pp 1751–1754. doi:10.1109/Transducers.2013.6627126.

Lo, B., and L. Parham. 2009. Ethical Issues in Stem Cell Research. *Endocrine Reviews* 30(3): 204–213. doi:10.1210/er.2008-0031.

Long, C., C. Finch, M. Esch, W. Anderson, M. Shuler, and J. Hickman. 2012. Design Optimization of Liquid-Phase Flow Patterns for Microfabricated Lung on a Chip. *Annals of Biomedical Engineering* 40(6): 1255–1267. doi:10.1007/s10439-012-0513-8.

Lu, B., A.J. Czernik, S. Popov, T. Wang, M.M. Poo, and P. Greengard. 1996. Expression of Synapsin i Correlates with Maturation of the Neuromuscular Synapse. *Neuroscience* 74(4): 1087–1097.

Maclean, F.L., A.L. Rodriguez, C. Parish, R.J. Williams, and D.R. Nisbet. 2016. Integrating Biomaterials and Stem Cells for Neural Regeneration. *Stem Cells and Development* 25(3): 214–226. doi:10.1089/scd.2015.0314.

Malik, N., and M.S. Rao. 2013. A Review of the Methods for Human iPSC Derivation. *Methods in Molecular Biology* (*Clifton, NJ*) 997: 23–33. doi:10.1007/978-1-62703-348-0_3.

Markaki, M., and N. Tavernarakis. 2010. Modeling Human Diseases in Caenorhabditis Elegans. *Biotechnology Journal* 5(12): 1261–1276.

Marquardt, L.M., and S.E. Sakiyama-Elbert. 2013. Engineering Peripheral Nerve Repair. *Current Opinion in Biotechnology* 24(5): 887–892. doi:http://dx.doi.org/10.1016/j.copbio.2013.05.006.

Mars, T., K.J. Yu, X.-M. Tang, A.F. Miranda, Z. Grubic, F. Cambi, and M.P. King. 2001. Differentiation of Glial Cells and Motor Neurons During the Formation of Neuromuscular Junctions in Cocultures of Rat Spinal Cord Explant and Human Muscle. *Journal of Comparative Neurology* 438(2): 239–251.

Mars, T., M.P. King, A.F. Miranda, W.F. Walker, K. Mis, and Z. Grubic. 2003. Functional Innervation of Cultured Human Skeletal Muscle Proceeds by Two Modes with Regard to Agrin Effects. *Neuroscience* 118(1): 87–97.

Maschmeyer, I., A.K. Lorenz, K. Schimek, T. Hasenberg, A.P. Ramme, J. Hubner, M. Lindner, C. Drewell, S. Bauer, A. Thomas, N.S. Sambo, F. Sonntag, R. Lauster, and U. Marx. 2015. A Four-Organ-Chip for Interconnected Long-Term Co-culture of Human Intestine, Liver, Skin and Kidney Equivalents. *Lab on a Chip* 15(12): 2688–2699. doi:10.1039/c5lc00392j.

Matsuda, T., T. Sugawara, and K. Inoue. 1992. Two-Dimensional Cell Manipulation Technology. An Artificial Neural Circuit Based on Surface Microphotoprocessing. *American Society for Artificial Internal Organs: 1992* 38(3): M243–M247.

McConnell, E.R., M.A. McClain, J. Ross, W.R. Lefew, and T.J. Shafer. 2012. Evaluation of Multi-Well Microelectrode Arrays for Neurotoxicity Screening Using a Chemical Training Set. *Neurotoxicology* 33(5): 1048–1057. doi:10.1016/j.neuro.2012.05.001.

McGoldrick, P., P.I. Joyce, E.M.C. Fisher, and L. Greensmith. 2013. Rodent Models of Amyotrophic Lateral Sclerosis. *Biochimica et Biophysica Acta* 1832(9): 1421–1436.

Merkle Florian, T., and K. Eggan. 2013. Modeling Human Disease with Pluripotent Stem Cells: From Genome Association to Function. *Cell Stem Cell* 12(6): 656–668. doi:10.1016/j.stem.2013.05.016.

Millet, L.J., and M.U. Gillette. 2012a. Over a Century of Neuron Culture: From the Hanging Drop to Microfluidic Devices. *The Yale Journal of Biology and Medicine* 85(4): 501–521.

Millet, L.J., and M.U. Gillette. 2012b. New Perspectives on Neuronal Development Via Microfluidic Environments. *Trends in Neurosciences* 35(12): 752–761.

Mimee, A., P.M. Smith, A.V. Ferguson. 2013. Circumventricular Organs: Targets for Integration of Circulating Fluid and Energy Balance Signals? *Physiology Behavior* 121: 96–102. doi:http://dx.doi.org/10.1016/j.physbeh.2013.02.012.

Molnar, P., J.F. Kang, N. Bhargava, M. Das, and J.J. Hickman. 2007a. Synaptic Connectivity in Engineered Neuronal Networks. Patch Clamp Methods and Protocols. *Methods in Molecular Biology Series* 403: 165–173. doi:10.1007/978-1-59745-529-9_10.

Molnar, P., W. Wang, A. Natarajan, J.W. Rumsey, and J.J. Hickman. 2007b. Photolithographic Patterning of C2C12 Myotubes Using Vitronectin as Growth Substrate in Serum-Free Medium. *Biotechnology Progress* 23(1): 265–268. doi:10.1021/bp060302q.

Motlagh, B.G. 2014. High-Density 3D Pyramid-Shaped Microelectrode Arrays for Brain-Machine Interface Applications. In *Biomedical Circuits and Systems Conference (BioCAS)*, 2014 IEEE. pp 364–367. doi:10.1109/BioCAS.2014.6981738.

Muoio, V., P.B. Persson, and M.M. Sendeski. 2014. The Neurovascular Unit—Concept Review. *Acta Physiologica (Oxford, England)* 210(4): 790–798. doi:10.1111/apha.12250.

Naik, P., and L. Cucullo. 2012. In Vitro Blood–Brain Barrier Models: Current and Perspective Technologies. *Journal of Pharmaceutical Sciences* 101(4): 1337–1354. doi:10.1002/jps.23022.

Nam, Y., and B.C. Wheeler. 2011. In Vitro Microelectrode Array Technology and Neural Recordings. *Critical Reviews in Biomedical Engineering* 39(1): 45–61. doi:10.1615/CritRevBiomedEng.v39.i1.40.

Nat, R. 2011. Cortical Network from Human Embryonic Stem Cells. *Journal of Cellular and Molecular Medicine* 15(6): 1429–1431. doi:10.1111/j.1582-4934.2011.01309.x.

Natarajan, A., T.B. DeMarse, P. Molnar, and J.J. Hickman. 2013. Engineered In Vitro Feed-Forward Networks. *Biotechnology & Biomaterials* 3(1): 153.

Neal, D., M.S. Sakar, R. Bashir, V. Chan, and H.H. Asada. 2015. Mechanical Characterization and Shape Optimization of Fascicle-like 3D Skeletal Muscle Tissues Contracted with Electrical and Optical Stimuli. *Tissue Engineering. Part A* 21(11–12): 1848–1858. doi:10.1089/ten.tea.2014.0317.

Neuwelt, E.A., B. Bauer, C. Fahlke, G. Fricker, C. Iadecola, D. Janigro, L. Leybaert, Z. Molnár, M.E. O'Donnell, J.T. Povlishock, N.R. Saunders, F. Sharp, D. Stanimirovic, R.J. Watts, and L.R. Drewes. 2011. Engaging Neuroscience to Advance Translational Research in Brain Barrier Biology. *Nature Reviews Neuroscience* 12(3): 169–182. http://www.nature.com/nrn/journal/v12/n3/suppinfo/nrn2995_S1.html.

Ni, M., W.H. Tong, D. Choudhury, N.A.A. Rahim, C. Iliescu, and H. Yu. 2009. Cell Culture on MEMS Platforms: A Review. *International Journal of Molecular Sciences* 10(12): 5411–5441. doi:10.3390/ijms10125411.

Nikoletseas, M. 2010. Behavioral and Neural Plasticity. CreateSpace Independent Publishing Platform (August, 2010).

Nistor, G.I., M.O. Totoiu, N. Haque, et al. 2005. Human Embryonic Stem Cells Differentiate into Oligodendrocytes in High Purity and Myelinate After Spinal Cord Transplantation. *Glia* 49(3): 385–396.

Offenhäusser, A., C. Sprössler, M. Matsuzawa, and W. Knoll. 1997. Field-Effect Transistor Array for Monitoring Electrical Activity from Mammalian Neurons in Culture. *Biosensors and Bioelectronics* 12(8): 819–826. doi:http://dx.doi.org/10.1016/S0956-5663(97)00047-X.

Oleaga, C., C. Bernabini, A.S.T. Smith, B. Srinivasan, W. McLamb, V. Platt, L.R. Bridges, Y. Cai, S. Najjar, C. Martin, G. Ekman, J. Langer, G. Ouedraogo, J. Cotovio, L. Breton, M.L. Shuler, and J.J. Hickman. 2016. Multi-Organ Toxicity Demonstration in a Functional Human In Vitro System Composed of Four Organs. *Sci Rep* 6: 20030.

Pagels, M., C.E. Hall, N.S. Lawrence, A. Meredith, T.G. Jones, H.P. Godfried, C.S. Pickles, J. Wilman, C.E. Banks, R.G. Compton, and L. Jiang. 2005. All-Diamond Microelectrode Array Device. *Analytical Chemistry* 77(11): 3705–3708. doi:10.1021/ac0502100.

Palmiotti, C.A., S. Prasad, P. Naik, K.M.D. Abul, R.K. Sajja, A.H. Achyuta, and L. Cucullo. 2014. In Vitro Cerebrovascular Modeling in the 21st Century: Current and Prospective Technologies. *Pharmaceutical Research* 31(12): 3229–3250. doi:10.1007/s11095-014-1464-6.

Pandey, U.B., and C.D. Nichols. 2011. Human Disease Models in Drosophila Melanogaster and the Role of the Fly in Therapeutic Drug Discovery. *Pharmacological Reviews* 63(2): 411–436. doi:10.1124/pr.110.003293.

Pardridge, W.M. 2002. Drug and Gene Delivery to the Brain: The Vascular Route. *Neuron* 36(4): 555–558. doi:http://dx.doi.org/10.1016/S0896-6273(02)01054-1.

Pardridge, W.M. 2005. The Blood-Brain Barrier: Bottleneck in Brain Drug Development. *NeuroRx* 2(1): 3–14.

Pardridge, W.M. 2012. Drug Transport across the Blood–Brain Barrier. *Journal of Cerebral Blood Flow & Metabolism* 32(11): 1959–1972. doi:10.1038/jcbfm.2012.126.

Park, J.Y., C.M. Hwang, S.H. Lee, and S.H. Lee. 2007. Gradient Generation by an Osmotic Pump and the Behavior of Human Mesenchymal Stem Cells Under the Fetal Bovine Serum Concentration Gradient. *Lab on a Chip* 7(12): 1673–1680. doi:10.1039/b710777c.

Park, H.S., S. Liu, J. McDonald, N. Thakor, and I.H. Yang. 2013. Neuromuscular Junction in a Microfluidic Device. In *Engineering in Medicine and Biology Society (EMBC)*, 2013 35th Annual International Conference of the IEEE, 3–7 July 2013. pp 2833–2835. doi:10.1109/EMBC.2013.6610130.

Perrier, A.L., V. Tabar, T. Barberi, M.E. Rubio, J. Bruses, N. Topf, N.L. Harrison, and L. Studer. 2004. Derivation of Midbrain Dopamine Neurons from Human Embryonic Stem Cells. *Proceedings of the National Academy of Sciences of the United States of America* 101(34): 12543–12548. doi:10.1073/pnas.0404700101.

Philips, T., and J.D. Rothstein. 2015. Rodent Models of Amyotrophic Lateral Sclerosis. in: editorial board, S J Enna (editor-in-chief) [et al] *Current Protocols in Pharmacology* 69:5.67.61–65.67.21.

Pickard, R.S. 1979. A Review of Printed Circuit Microelectrodes and Their Production. *Journal of Neuroscience Methods* 1(4): 301–318.

Pomp, O., I. Brokhman, I. Ben-Dor, B. Reubinoff, and R.S. Goldstein. 2005. Generation of Peripheral Sensory and Sympathetic Neurons and Neural Crest Cells from Human Embryonic Stem Cells. *Stem Cells* 23(7): 923–930. doi:10.1634/stemcells.2005-0038.

Punga, A.R., and M.A. Ruegg. 2012. Signaling and Aging at the Neuromuscular Synapse: Lessons Learnt from Neuromuscular Diseases. *Current Opinion in Pharmacology* 12(3): 340–346. doi:http://dx.doi.org/10.1016/j.coph.2012.02.002.

Ran, F.A., D. Hsu Patrick, C.-Y. Lin, S. Gootenberg Jonathan, S. Konermann, A.E. Trevino, A. Scott David, A. Inoue, S. Matoba, Y. Zhang, and F. Zhang. 2013. Double Nicking by RNA-Guided CRISPR Cas9 for Enhanced Genome Editing Specificity. *Cell* 154(6): 1380–1389. doi:http://dx.doi.org/10.1016/j.cell.2013.08.021.

Ravenscroft, M.S., K.E. Bateman, K.M. Shaffer, H.M. Schessler, D.R. Jung, T.W. Schneider, C.B. Montgomery, T.L. Custer, A.E. Schaffner, Q.Y. Liu, Y.X. Li, J.L. Barker, and J.J. Hickman. 1998. Developmental Neurobiology Implications from Fabrication and Analysis of Hippocampal Neuronal Networks on Patterned Silane-Modified Surfaces. *Journal of the American Chemical Society* 120(47): 12169–12177.

Ridderinkhof, K.R., M. Ullsperger, E.A. Crone, and S. Nieuwenhuis. 2004. The Role of the Medial Frontal Cortex in Cognitive Control. *Science* 306(5695): 443–447.

Robertson, J.A. 2001. Human Embryonic Stem Cell Research: Ethical and Legal Issues. *Nature Reviews Genetics* 2(1): 74–78.

Roth, E.A., T. Xu, M. Das, C. Gregory, J.J. Hickman, and T. Boland. 2004. Inkjet Printing for High-Throughput Cell Patterning. *Biomaterials* 25(17): 3707–3715.

Rumsey, J.W., M. Das, J.F. Kang, R. Wagner, P. Molnar, and J.J. Hickman. 2008. Tissue Engineering Intrafusal Fibers: Dose- and Time-Dependent Differentiation of Nuclear Bag Fibers in a Defined In Vitro System Using Neuregulin 1-Beta-1. *Biomaterials* 29(8): 994–1004. doi:10.1016/j.biomaterials.2007.10.042.

Rumsey, J.W., M. Das, M. Stancescu, M. Bott, C. Fernandez-Valle, and J.J. Hickman. 2009. Node of Ranvier Formation on Motoneurons In Vitro. *Biomaterials* 30(21): 3567–3572.

Rumsey, J.W., M. Das, A. Bhalkikar, M. Stancescu, and J.J. Hickman. 2010. Tissue Engineering the Mechanosensory Circuit of the Stretch Reflex Arc: Sensory Neuron Innervation of Intrafusal Muscle Fibers. *Biomaterials* 31(32): 8218–8227. doi:10.1016/j.biomaterials.2010.07.027.

Russo, S.J., and E.J. Nestler. 2013. The Brain Reward Circuitry in Mood Disorders. *Nature Review Neuroscience* 14(9): 609–625. doi:10.1038/nrn3381.

Sánchez-Danés, A., Y. Richaud-Patin, I. Carballo-Carbajal, S. Jiménez-Delgado, C. Caig, S. Mora, C. Di Guglielmo, M. Ezquerra, B. Patel, A. Giralt, J.M. Canals, M. Memo, J. Alberch, J. López-Barneo, M. Vila, A.M. Cuervo, E. Tolosa, A. Consiglio, and A. Raya. 2012. Disease-Specific Phenotypes in Dopamine Neurons from Human iPS-Based Models of Genetic and Sporadic Parkinson's Disease. *EMBO Molecular Medicine* 4(5): 380–395. doi:10.1002/emmm.201200215.

Sander, J.D., and J.K. Joung. 2014. CRISPR-Cas Systems for Editing, Regulating and Targeting Genomes. *Nature Biotechnology* 32(4): 347–355. doi:10.1038/nbt.2842. http://www.nature.com/nbt/journal/v32/n4/abs/nbt.2842.html#supplementary-information.

Schulz, T.C., S.A. Noggle, G.M. Palmarini, D.A. Weiler, I.G. Lyons, K.A. Pensa, A.C.B. Meedeniya, B.P. Davidson, N.A. Lambert, and B.G. Condie. 2004. Differentiation of Human Embryonic Stem Cells to Dopaminergic Neurons in Serum-Free Suspension Culture. *Stem Cells* 22(7): 1218–1238. doi:10.1634/stemcells.2004-0114.

Schwartz, P.H., P.J. Bryant, T.J. Fuja, H. Su, D.K. O'Dowd, and H. Klassen. 2003. Isolation and Characterization of Neural Progenitor Cells from Post-Mortem Human Cortex. *Journal of Neuroscience Research* 74(6): 838–851. doi:10.1002/jnr.10854.

Selvaraj, V., P. Jiang, O. Chechneva, U.G. Lo, and W. Deng. 2012. Differentiating Human Stem Cells into Neurons and Glial Cells for Neural Repair. *Frontiers in Bioscience* 17: 65–89.

Serikawa, T., T. Mashimo, T. Kuramoro, B. Voigt, Y. Ohno, and M. Sasa. 2015. Advances on Genetic Rat Models of Epilepsy. *Experimental Animals* 64(1): 1–7.

Shaltouki, A., J. Peng, Q. Liu, M.S. Rao, and X. Zeng. 2013. Efficient Generation of Astrocytes from Human Pluripotent Stem Cells in Defined Conditions. *Stem Cells* 31(5): 941–952. doi:10.1002/stem.1334.

Shamblott, M.J., J. Axelman, S. Wang, E.M. Bugg, J.W. Littlefield, P.J. Donovan, P.D. Blumenthal, G.R. Huggins, and J.D. Gearhart. 1998. Derivation of Pluripotent Stem Cells from Cultured Human Primordial Germ Cells. *Proceedings of the National Academy of Sciences of the United States of America* 95(23): 13726–13731. doi:10.1073/pnas.95.23.13726.

Sharp, J., J. Frame, M. Siegenthaler, G. Nistor, and H.S. Keirstead. 2010. Human Embryonic Stem Cell-Derived Oligodendrocyte Progenitor Cell Transplants Improve Recovery After Cervical Spinal Cord Injury. *Stem Cells* 28(1): 152–163. doi:10.1002/stem.245.

Sheikh, S.I., and A.A. Amato. 2010. The Dorsal Root Ganglion Under Attack: The Acquired Sensory Ganglionopathies. *Practical Neurology* 10(6): 326–334. doi:10.1136/jnnp.2010.230532.

Shi, P., S. Nedelec, H. Wichterle, and L.C. Kam. 2010. Combined Microfluidics/Protein Patterning Platform for Pharmacological Interrogation of Axon Pathfinding. *Lab on a Chip* 10(8): 1005–1010. doi:10.1039/b922143c.

Shi, Y., P. Kirwan, and F.J. Livesey. 2012. Directed Differentiation of Human Pluripotent Stem Cells to Cerebral Cortex Neurons and Neural Networks. *Nature Protocols* 7(10): 1836–1846. doi:10.1038/nprot.2012.116.

Shimizu, K., H. Sasaki, H. Hida, H. Fujita, K. Obinata, M. Shikida, and E. Nagamori. 2009. Integration of Skeletal Muscle Cell onto Si-MEMS and Its Generative Force Measurement. In *Micro Electro Mechanical Systems, 2009*. IEEE 22nd International Conference. pp 403–406. doi:10.1109/MEMSYS.2009.4805404.

Shimohama, S., H. Sawada, Y. Kitamura, and T. Taniguchi. 2003. Disease Model: Parkinson's Disease. *Trends in Molecular Medicine* 9(8): 360–365. doi:http://dx.doi.org/10.1016/S1471-4914(03)00117-5.

Skaper, S.D. 2012. Compartmented Chambers for Studying Neurotrophic Factor Action. In *Neurotrophic Factors: Methods and Protocols*, ed. D.S. Skaper, 213–222. Totowa, NJ: Humana Press. doi:10.1007/978-1-61779-536-7_19.

Smith, A., C.J. Long, and J.J. Hickman. 2013. A Functional System for High-Content Screening of Neuromuscular Junctions In Vitro. *Technology* 1(1): 37–48.

Song, W., and X.A. Jin. 2015. Brain-Derived Neurotrophic Factor Inhibits Neuromuscular Junction Maturation in a cAMP-PKA-Dependent Way. *Neuroscience Letters* 591: 8–12. doi:http://dx.doi.org/10.1016/j.neulet.2015.02.019.

Song, H., S.-K. Chung, and Y. Xu. 2010. Modeling Disease in Human ESCs Using an Efficient BAC-Based Homologous Recombination System. *Cell Stem Cell* 6(1): 80–89.

Soundararajan, P., B.W. Lindsey, C. Leopold, and V.F. Rafuse. 2007. Easy and Rapid Differentiation of Embryonic Stem Cells into Functional Motoneurons Using Sonic Hedgehog-Producing Cells. *Stem Cells* 25(7): 1697–1706. doi:10.1634/stemcells.2006-0654.

Southam, K.A., A.E. King, C.A. Blizzard, G.H. McCormack, and T.C. Dickson. 2013. Microfluidic Primary Culture Model of the Lower Motor Neuron–Neuromuscular Junction Circuit. *Journal of Neuroscience Methods* 218(2): 164–169. doi:http://dx.doi.org/10.1016/j.jneumeth.2013.06.002.

Southam, K.A., A.E. King, C.A. Bliszzard, G.H. McCormack, and T.C. Dickson. 2015. A Novel In Vitro Primary Culture Model of the Lower Motor Neuron—Neuromuscular Junction Circuit. *Microfulidic and Compartmentalized Platforms for Neurobiological Research Neuromethods* 103: 181–193.

Spira, M.E., and A. Hai. 2013. Multi-Electrode Array Technologies for Neuroscience and Cardiology. *Nature Nanotechnology* 8(2): 83–94.

Srinivasan, B., A.R. Kolli, M.B. Esch, H.E. Abaci, M.L. Shuler, and J.J. Hickman. 2015. TEER Measurement Techniques for In Vitro Barrier Model Systems. *Journal of Laboratory Automation* 20(2): 107–126. doi:10.1177/2211068214561025.

Stenger, D.A., J.H. Georger, C.S. Dulcey, J.J. Hickman, A.S. Rudolph, T.B. Nielsen, S.M. McCort, and J.M. Calvert. 1992. Coplanar Molecular Assemblies of Amino- and Perfluorinated Alkylsilanes: Characterization and Geometric Definition of Mammalian Cell Adhesion and Growth. *Journal of the American Chemical Society* 114(22): 8435–8442. doi:10.1021/ja00048a013.

Stenger, D.A., C.J. Pike, J.J. Hickman, and C.W. Cotman. 1993. Surface Determinants of Neuronal Survival and Growth on Self-Assembled Monolayers in Culture. *Brain Research* 630(1–2): 136–147.

Stenger, D.A., J.J. Hickman, K.E. Bateman, M.S. Ravenscroft, W. Ma, J.J. Pancrazio, K. Shaffer, A.E. Schaffner, D.H. Cribbs, and C.W. Cotman. 1998. Microlithographic Determination of Axonal/Dendritic Polarity in Cultured Hippocampal Neurons. *Journal of Neuroscience Methods* 82(2): 167–173.

Sterneckert, J.L., P. Reinhardt, and H.R. Scholer. 2014. Investigating Human Disease Using Stem Cell Models. *Nature Reviews Genetics* 15(9): 625–639. doi:10.1038/nrg3764.

Sung, J.H., and M.L. Shuler. 2009. A Micro Cell Culture Analog ([Small Micro]CCA) with 3-D Hydrogel Culture of Multiple Cell Lines to Assess Metabolism-Dependent Cytotoxicity of Anti-cancer Drugs. *Lab on a Chip* 9(10): 1385–1394. doi:10.1039/B901377F.

Sung, J.H., C. Kam, and M.L. Shuler. 2010. A Microfluidic Device for a Pharmacokinetic-Pharmacodynamic (PK-PD) Model on a Chip. *Lab on a Chip* 10(4): 446–455. doi:10.1039/b917763a.

Supinski, G., D. Nethery, T.M. Nosek, L.A. Callahan, D. Stofan, and A. DiMarco. 2000. Endotoxin Administration Alters the Force Vs. pCa Relationship of Skeletal Muscle Fibers. *American Journal of Physiology—Regulatory Integrative Comparative Physiology* 278(4): R891–R896.

Swanborg, R.H. 1995. Animal Models of Human Disease—Experimental Autoimmune Encephalomyelitis in Rodents as a Model for Human Demyelinating Disease. *Clinical Immunology and Immunopathology* 77(1): 4–13. doi:http://dx.doi.org/10.1016/0090-1229(95)90130-2.

Swarup, V., and J.P. Julien. 2011. ALS Pathogenesis: Recent Insights from Genetics and Mouse Models. *Progress in Neuro-Psychopharmacology & Biological Psychiatry* 35(2): 363–369. doi:10.1016/j.pnpbp.2010.08.006.

Taylor, A.M., M. Blurton-Jones, S.W. Rhee, D.H. Cribbs, C.W. Cotman, and N.L. Jeon. 2005. A Microfluidic Culture Platform for CNS Axonal Injury, Regeneration and Transport. *Nature Methods* 2(8): 599–605. http://www.nature.com/nmeth/journal/v2/n8/suppinfo/nmeth777_S1.html.

Theocharidis, U., K. Long, C. ffrench-Constant, and A. Faissner. 2014. Chapter 1—Regulation of the Neural Stem Cell Compartment by Extracellular Matrix Constituents. In *Progress in Brain Research*, eds. B.W.-H. Alexander Dityatev, P. Asla, vol. 214. pp 3–28. Amsterdam: Elsevier. doi:http://dx.doi.org/10.1016/B978-0-444-63486-3.00001-3.

Thomas, C.A., P.A. Springer, G.E. Loeb, Y. Berwald-Netter, and L.M. Okun. 1972. A Miniature Microelectrode Array to Monitor the Bioelectric Activity of Cultured Cells. *Experimental Cell Research* 74(1): 61–66.

Thomson, J.A., J. Itskovitz-Eldor, S.S. Shapiro, M.A. Waknitz, J.J. Swiergiel, V.S. Marshall, and J.M. Jones. 1998. Embryonic Stem Cell Lines Derived from Human Blastocysts. *Science* 282(5391): 1145–1147. doi:10.1126/science.282.5391.1145.

Tibbitt, M.W., and K.S. Anseth. 2009. Hydrogels as Extracellular Matrix Mimics for 3D Cell Culture. *Biotechnology and Bioengineering* 103(4): 655–663. doi:10.1002/bit.22361.

Timme, N., S. Ito, M. Myroshnychenko, F.-C. Yeh, E. Hiolski, P. Hottowy, and J.M. Beggs. 2014. Multiplex Networks of Cortical and Hippocampal Neurons Revealed at Different Timescales. *PloS One* 9(12), e115764. doi:10.1371/journal.pone.0115764.

Tintignac, L.A., H.-R. Brenner, and M.A. Rüegg. 2015. Mechanisms Regulating Neuromuscular Junction Development and Function and Causes of Muscle Wasting. *Physiological Reviews* 95(3): 809–852. doi:10.1152/physrev.00033.2014.

Tojima, T., Y. Yamane, M. Takahashi, and E. Ito. 2000. Acquisition of Neuronal Proteins During Differentiation of NG108-15 cells. *Neuroscience Research* 37(2): 153–161. doi:http://dx.doi.org/10.1016/S0168-0102(00)00110-3.

Ulrich-Lai, Y.M., and P. Herman. 2009. Neural Regulation of Endocrine and Autonomic Stress Responses. *Nature Reviews Neuroscience* 10(6): 397–409. http://www.nature.com/nrn/journal/v10/n6/suppinfo/nrn2647_S1.html.

Umbach, J.A., K.L. Adams, C.B. Gundersen, and B.G. Novitch. 2012. Functional Neuromuscular Junctions Formed by Embryonic Stem Cell-Derived Motor Neurons. *PLoS One* 7(5): e36049. doi:10.1371/journal.pone.0036049.

Valente, S., F. Alviano, C. Ciavarella, M. Buzzi, F. Ricci, P. Tazzari, P. Pagliaro, and G. Pasquinelli. 2014. Human Cadaver Multipotent Stromal/Stem Cells Isolated from Arteries Stored in Liquid Nitrogen for 5 Years. *Stem Cell Research & Therapy* 5(1): 8.

Vandamme, T.F. 2014. Use of Rodents as Models of Human Diseases. *Journal of Pharmacy and Bioallied Sciences* 6(1): 2–9. doi:10.4103/0975-7406.124301.

Vandenburgh, H., J. Shansky, F. Benesch-Lee, V. Barbata, J. Reid, L. Thorrez, R. Valentini, and G. Crawford. 2008. Drug-Screening Platform Based on the Contractility of Tissue-Engineered Muscle. *Muscle & Nerve* 37(4): 438–447. doi:10.1002/mus.20931.

Vandenburgh, H., J. Shansky, F. Benesch-Lee, K. Skelly, J.M. Spinazzola, Y. Saponjian, and B.S. Tseng. 2009. Automated Drug Screening with Contractile Muscle Tissue Engineered from Dystrophic Myoblasts. *The FASEB Journal* 23(10): 3325–3334. doi:10.1096/fj.09-134411.

Varghese, K., M. Das, N. Bhargava, M. Stancescu, P. Molnar, M.S. Kindy, and J.J. Hickman. 2009. Regeneration and Characterization of Adult Mouse Hippocampal Neurons in a Defined In Vitro System. *Journal of Neuroscience Methods* 177(1): 51–59. pii:S0165-0270(08)00565-7; doi:10.1016/j.jneumeth.2008.09.022.

Vogt, A.K., G. Wrobel, W. Meyer, W. Knoll, and A. Offenhausser. 2005. Synaptic Plasticity in Micropatterned Neuronal Networks. *Biomaterials* 26(15): 2549–2557. doi:10.1016/j.biomaterials.2004.07.031.

Wallace, K., J.D. Strickland, P. Valdivia, W.R. Mundy, and T.J. Shafer. 2015. A Multiplexed Assay for Determination of Neurotoxicant Effects on Spontaneous Network Activity and Viability from Microelectrode Arrays. *Neurotoxicology* 49: 79–85. doi:10.1016/j.neuro.2015.05.007.

Walsh, K., J. Megyesi, and R. Hammond. 2005. Human Central Nervous System Tissue Culture: A Historical Review and Examination of Recent Advances. *Neurobiology of Disease* 18(1): 2–18.

Welberg, L. 2009. Computational Neuroscience: Model Behaviour. *Nature Review Neuroscience* 10(10): 696–697.

Wheeler, B.C., and G.J. Brewer. 2010. Designing Neural Networks in Culture: Experiments are Described for Controlled Growth, of Nerve Cells Taken from Rats, in Predesigned Geometrical Patterns on Laboratory Culture Dishes. *Proceedings of the IEEE Institute of Electrical and Electronics Engineers* 98(3): 398–406. doi:10.1109/JPROC.2009.2039029.

Wheeler, B.C., J.M. Corey, G.J. Brewer, and D.W. Branch. 1999. Microcontact Printing for Precise Control of Nerve Cell Growth in Culture. *Journal of Biomechanical Engineering* 121(1): 73–78.

Wilhelm, I., and I.A. Krizbai. 2014. In Vitro Models of the Blood–Brain Barrier for the Study of Drug Delivery to the Brain. *Molecular Pharmaceutics* 11(7): 1949–1963. doi:10.1021/mp500046f.

Wilson, K., P. Molnar, and J. Hickman. 2007. Integration of Functional Myotubes with a Bio-MEMS Device for Non-invasive Interrogation. *Lab on a Chip* 7(7): 920–922. doi:10.1039/b617939h.

Wilson, K., M. Stancescu, M. Das, J. Rumsey, and J. Hickman. 2011. Direct Patterning of Coplanar Polyethylene Glycol Alkylsilane Monolayers by Deep-Ultraviolet Photolithography as a General Method for High Fidelity, Long-Term Cell Patterning and Culture. *Journal of Vacuum Science & Technology B* 29(2): 21020. doi:10.1116/1.3549127.

Wolozin, B., T. Sunderland, B.-b. Zheng, J. Resau, B. Dufy, J. Barker, R. Swerdlow, and H. Coon. 1992. Continuous Culture of Neuronal Cells from Adult Human Olfactory Epithelium. *Journal of Molecular Neuroscience* 3(3): 137–146. doi:10.1007/BF02919405.

Wyart, C., C. Ybert, L. Bourdieu, C. Herr, C. Prinz, and D. Chatenay. 2002. Constrained Synaptic Connectivity in Functional Mammalian Neuronal Networks Grown on Patterned Surfaces. *Journal of Neuroscience Methods* 117(2): 123–131.

Xie, H., L. Hu, and G. Li. 2010. SH-SY5Y Human Neuroblastoma Cell Line: In Vitro Cell Model of Dopaminergic Neurons in Parkinson's Disease. *Chinese Medical Journal* 123(8): 1086–1092.

Xu, T., C.A. Gregory, P. Molnar, X. Cui, S. Jalota, S.B. Bhaduri, and T. Boland. 2006. Viability and Electrophysiology of Neural Cell Structures Generated by the Inkjet Printing Method. *Biomaterials* 27(19): 3580–3588. doi:10.1016/j.biomaterials.2006.01.048.

Yamanaka, S. 2012. Induced Pluripotent Stem Cells: Past, Present, and Future. *Cell Stem Cell* 10(6): 678–684. doi:10.1016/j.stem.2012.05.005.

Yoshida, M., S. Kitaoka, N. Egawa, M. Yamane, R. Ikeda, K. Tsukita, N. Amano, A. Watanabe, M. Morimoto, J. Takahashi, H. Hosoi, T. Nakahata, H. Inoue, and K. Saito Megumu. 2015. Modeling the Early Phenotype at the Neuromuscular Junction of Spinal Muscular Atrophy Using Patient-Derived iPSCs. *Stem Cell Reports* 4(4): 561–568. doi:10.1016/j.stemcr.2015.02.010.

Zahavi, E.E., A. Ionescu, S. Gluska, T. Gradus, K. Ben-Yaakov, and E. Perlson. 2015. A Compartmentalized Microfluidic Neuromuscular Co-culture System Reveals Spatial Aspects of GDNF Functions. *Journal of Cell Science* 128(6): 1241–1252. doi:10.1242/jcs.167544.

Zhang, J., F. Laiwalla, J. Kim, H. Urabe, R. Van Wagenen, S. Yoon-Kyu, B.W. Connors, and A.V. Nurmikko. 2009. A Microelectrode Array Incorporating an Optical Waveguide Device for Stimulation and Spatiotemporal Electrical Recording of Neural Activity. In *EMBC 2009*. Annual International Conference of the IEEE. pp 2046–2049. doi:10.1109/IEMBS.2009.5333947.

Zordan, S., M. Zanotto, T. Nieus, S. Di Marco, H. Amin, A. Maccione, and L. Berdondini. 2015. A Scalable High Performance Client/Server Framework to Manage and Analyze High Dimensional Datasets Recorded by 4096 CMOS-MEAs. In *Neural Engineering (NER)*, 2015 7th International IEEE/EMBS Conference. pp 968–971. doi:10.1109/NER.2015.7146787.

Zweifel, L.S., R. Kuruvilla, and D.D. Ginty. 2005. Functions and Mechanisms of Retrograde Neurotrophin Signalling. *Nature Review Neuroscience* 6(8): 615–625.

Index

L.G. Zhang, D.L. Kaplan (eds.), *Neural Engineering*,
DOI 10.1007/978-3-319-31433-4